UNIVERSITÉ DE STRASBOURG

ÉCOLE DOCTORALE DES SCIENCES DE LA VIE ET DE LA SANTE

ICUBE – CNRS UMR 7357- LE LABORATOIRE DES SCIENCES DE l'INGENIEUR, DE l'INFORMANTIQUE ET DE l'IMAGERIE

THÈSE présentée par :

Anil Ufuk BATMAZ

Soutenue le : **03 Juillet 2018**

pour obtenir le grade de : **Docteur de l'université de Strasbourg**

Discipline/ Spécialité : Biomedical Engineering

Speed, precision and grip force analysis of human manual operations with and without direct visual input

THÈSE dirigée par :

Dr Birgitta DRESP	PhD, HDR, CNRS Strasbourg (Supervisor)
Pr Michel DE MATHELIN	Professor of Robotics, University of Strasbourg (Co-supervisor)

RAPPORTEUR-E-S :

Pr Daniel OBERFELD	Professor of Psychology, Mainz University
Pr Christophe JOUFFRAIS	DR2, CNRS Singapore

AUTRES MEMBRES DU JURY :

Pr Jean-Christophe CASSEL	Professor of Neuroscience, University of Strasbourg
Dr Evelyne KLINGER	Eng, PhD, HDR, ESIEA Laval

INVITEE :

Pr Dominique BECHMANN	Professor of Informatics, University of Strasbourg

To my family... Aileme...

Preface

I would like to express my sincere and deepest gratitude to,

- **Dr. Birgitta Dresp** who provided me with a fully operational laboratory to conduct the experiments. She constantly supported me with all the knowledge, background, and information I needed about the behavioral science and statistics. She showed me the way out whenever I was stuck. I owe her my profound gratitude for her support and tremendous contribution to this research.
- **Prof. Michel de Mathelin** who provided his invaluable biomedical engineering, signal processing, modeling, and data processing knowledge, regardless of his tight schedule. I owe him my deepest appreciation for his valuable comments and suggestions through this research.
- My sister, **Isik Batmaz** who believed in me and encouraged me to have an academic career since the beginning. She always helped me without any hesitation. You will see her in most of the pictures.

I also would like to thank İlkem Karaaslan, who motivated, supported and helped me in my darkest hours, my friends from PDI (*Programme doctoral international*), my neighbors in INRIA-MIMESIS team, residents of CDE *(College Doctoral Europeen),* surgeons at IHU and IRCAD, and many others, who attended my experiments without any hesitations and questions. Most of the research data here belong to their voluntary participation to the scientific progress.

I also would like to thank ICube AVR team members such as Prof. Pierre Renaud, Prof. Bernard Bayle, Florent Nageotte and Muhammed Amin Falek for their contributions.

Moreover, Vincent Durel (his wisdom, support and trust in me), Emmanuel Garcia (French translation), Bruno Marques and Agnes Münch (technical support), and Patrick Muller, Marcel Heine, Pilar Garcia, Andrea Rojas, Özel family, Müzeyyen Uğur and Gökşen Acar (social support) are the other people who helped me with this study.

And last but not the least … My family. There are no words or descriptions that I can use to emphasize their importance in this research.

Index

List of Figures

List of Tables

Publications and corresponding chapters

Chapter 1	Batmaz AU, de Mathelin M, Dresp-Langley B (2016). Effects of indirect screen vision and tool-use on the time and precision of object positioning on real-world targets. Perception, 45(ECVP Supplement), 196. http://journals.sagepub.com/doi/full/10.1177/0301006616671273
Study 1	Batmaz AU, de Mathelin M, Dresp-Langley B (2016) Getting nowhere fast: trade-off between speed and precision in training to execute image-guided hand-tool movements. BMC Psychology, 4(1), 55. https://doi.org/10.1186/s40359-016-0161-0
Study 2 (Speed-Precision)	Batmaz AU, de Mathelin M, Dresp-Langley B (2017) Seeing virtual while acting real: Visual display and strategy effects on the time and precision of eye-hand coordination. PLoS ONE 12(8): e0183789. https://doi.org/10.1371/journal.pone.0183789
(Trajectory)	Batmaz AU, de Mathelin M, Dresp-Langley B (2018) Effects of 2D and 3D image views on hand movement trajectories in the surgeon's peri-personal space in a computer-controlled simulator environment Cogent Medicine, 5(1), 1426232. https://doi.org/10.1080/2331205X.2018.1426232
Chapter 2	Batmaz AU, de Mathelin M, Dresp-Langley B (2017). Inside the Virtual Brain: using Oculus Dk2 for Surgical Planning. NeuroTalk, Barcelona Spain
Study 3	Batmaz AU, de Mathelin M, Dresp-Langley B (2017) Effects of relative target position on ipsilateral and contralateral manual operations in head-mounted virtual reality. European Conference on Visual Perception (ECVP), Berlin Germany. http://journals.sagepub.com/page/pec/collections/ecvp-abstracts/index/ecvp-2017
Study 4	Batmaz AU, de Mathelin M, Dresp-Langley B (2018) Effects of image size and structural complexity on time and precision of hand movements in head mounted virtual reality. IEEE VR Reutlingen Germany.
Chapter 3	Batmaz AU, Falek MA, Zorn L, Nageotte F, Zanne P, de Mathelin M, Dresp-Langley B (2017) Novice and expert haptic behaviours while using a robot-controlled surgery system. In 13th IASTED International Conference on Biomedical Engineering (BioMed) (pp. 94-99). IEEE. https://doi.org/10.2316/P.2017.852-022

Introduction

Emerging computer-controlled technologies in the biomedical and healthcare domains have created new needs for research on intuitive interactions and design control in the light of human behavior strategies. Collecting users' views on system requirements may be a first step towards understanding how a given design or procedure needs to be adapted to better fit user needs, but is insufficient as even experts may not have complete insight into all aspects of task-specific constraints [1]. Cross-disciplinary studies focused on interface design in the light of display ergonomics and, in priority, human psychophysics are needed to fully understand specific task environments and work domain constraints. Being able to decide what should be improved in the development and application of emerging technologies requires being able to assess how changes in design or display may facilitate human information processing during task execution. Human error [2] is a critical issue here as it is partly controlled by display properties, which may be more or less optimal under circumstances given [3]. Although there is general agreement that human cognitive processes from an integrative component of computer-assisted interventional technologies, how human performance and decision making is affected by these technologies are still no well-known enough [4]. The pressing need for research in this domain reaches far beyond the realms of workflow analysis and task models (e.g. [5]), as was made clear here with the example of these experimental studies, which addresses the problem of individual performance variations in novices learning to execute image-guided hand movements in a computer controlled simulator environment.

Key point: precision assessment

Surgical simulator training for image-guided interventions is currently facing the problem of defining reliable performance standards [6]. This problem partly relates to the fact that task execution time is often used as the major, or the sole criterion for establishing individual learning curves. Faster times are readily interpreted in terms of higher levels of proficiency (e.g. [7]), especially in extensive simulator training programs hosting a large number of novice trainees. Novices are often moved from task to task in rapid succession and train by themselves in different tasks on different workstations. Times are counted by computers which generate the learning curves while the relative precision of the skills the novices are training for is, if at all, only qualitatively assessed, generally by a senior expert surgeon who himself moves from

workstation to workstation. The quantitative assessment of precision requires pixel-by-pixel analyses of video image data showing hand-tool and tool-object interactions during task execution; sometimes the mechanical testing of swiftly tied knots may be necessary to assess whether they are properly tied or come apart easily. Such analyses are costly to implement, yet, they are critically important for reasons that should become clear in the light of the findings produced in this thesis.

One of the major research topics of this thesis is the precision assessment in surgical simulator training. Importance of the precision and precision assessment is highlighted several times in the thesis. In the first and second chapter, importance of the precision assessment and why precision should be included to the motor performance and skill assessment is discussed in detail.

Experimental setups

In this thesis, three experimental setups were used. The first experimental setup was called “Excalibur”, the second experimental setup was called “NoTouch” and the third experimental setup was called glove for STRAS. The “Excalibur” system was designed with Lego bricks. Previous research on image guided surgical simulators have used Lego boards and bricks to create a controlled environment to execute a complex task [8–17]. These designed complex task environments resemble the surgical task execution environment complexity. Moreover, novices can easily earn near-body space eye-hand coordination experience in these complex tasks and they can move on to the moderately complex tasks with training [18–20]. Considering this approach in surgical training, the “Excalibur” system was designed for complete beginners.

In the “NoTouch” system, an OCULUS DK2 head-mounted display was used with a Leap Motion sensor as an experimental setup. These two systems were used together to detect human hand movements and project them to the immersive virtual reality display. This headset setup has been used in recent medical studies [21–25] as well as in other studies [26–29].

The glove system was completely built-up from scratch and designed according to handles of the STRAS, a surgical robotic system that was developed by ICube

Laboratories, Strasbourg, University of Strasbourg. Twelve Force Sensitive Resistors (FSRs) were used to measure the grip force applied to STRAS handles.

First Chapter – Comparison of real-world manual operations under 2D and 3D image guidance

In the first chapter of thesis, different methods used in the surgical environments to create better surgical training systems and how they affect the motor performance of the subjects are studied [30–32]. For this purpose, “EXCALIBUR” experimental platform was designed with specific hardware and software components for novices.

Image guided procedures and 2D visual feedback

In the first chapter, speed and precision analysis of real-world manual operations are inspected under different visual and tactile feedbacks in an environment close to a surgical operation. Image-guided interventional procedures constrain the human operator to process critical information about what his/her hands are doing in a 3D real-world environment by looking at a 2D screen representation of that environment [33]. In addition to this problem, the operator or surgeon often has to cope with uncorrected 2D visual feedback from a single camera with a fisheye lens [34,35], providing a hemispherical focus of vision with poor off-axis resolution and aberrant shape contrast effects at the edges of the objects viewed on the screen. The information provided by natural view with eyes is not the same as looking through a 2D monitor screen. This information limitation also affects the perception of users and disturbs the actions and movements in the real-world application. Previous research on this topic [3,36,37] shows that subjects are slower, less precise and make more errors under 2D screen conditions. Effects of the 2D image guidance on time and precision of the complete novices was the research topic of the first chapter.

Stereoscopic 3D displays

Recently developed 3D visualization technology may represent a possibility for overcoming the drawbacks of 2D views, yet, whether different 3D imaging solutions all significantly improve task performance has remained a controversial issue. While some authors have reported that 3D viewing significantly improves task performance in both novices and experts [38–44], others have found equivalent task performance

comparing 2D viewing to 3D viewing systems [45–48]. It has been suggested that differences in task complexity and inherent affordance levels [49,50], or inter-individual differences in adaptive goal-setting strategies of novices [32] may account for differences in results between studies using similar 3D viewing systems. In the second and third studies of chapter 1, how stereoscopic 3D viewing affects the complete novices' 'time' and 'precision' is studied in detail with a stereoscopic head-mounted display. One of the major outcomes of this thesis is the conclusion regarding comparison between the 2D image guidance and stereoscopic display using complete novices' motor performance evaluation in surgical skill training.

Tool Manipulation and glove

During a surgical procedure, the surgeon must use a tool to perform surgery. Tool manipulation disables the direct haptic feedback between the surgeon and the object: the information about the object has to be transferred by the tool to the surgeon. In this case, the surgeon has to perform movements, maneuvers, and actions according to the tactile information transferred by the surgical tool. Furthermore, during the image guided surgical operation, a surgeon has to wear a glove and the sensation of touch [51] is altered due to lack of haptic feed-back from the object that is being manipulated. There is no direct tactile feed-back from the object to the sensory receptors in the hand [52], which communicate with cortical neurons driven by multisensory input [53–55]. Visual-haptic mapping for cross-modal sensory integration [56] is affected by such lack of direct sensory feed-back. Understanding how haptic feedback variations affect the novices' performance during complex task execution was one of the major research topics of the first chapter.

Individual preferences

Conditional accuracy trade-offs occur spontaneously when novices train to perform a motor task as swiftly and as precisely as possible in a limited number of sessions [57], as is the case in laparoscopic simulator training. Conditional accuracy functions relate the duration of trial or task execution to a precision index reflecting the accuracy of the performance under conditions given [58,59]. This relationship between speed and precision reflects hidden functional aspects of learning, and delivers important information about individual strategies the learner, especially if he/she is a beginner, is

not necessarily aware of [60]. In the first study of chapter 1, the importance of the precision and precision assessment is investigated with individual preferences. Furthermore, the results of the individual preferences are used show that why a tutor or skill evaluator should intervene at the earliest phases of learning and is essential for effective skill monitoring and for making sure that the trainee progresses in the right direction. Individual preferences and relationship between speed and precision are studied in the first and second chapter.

Expertise leveling

In the literature, there is no systematical expertise leveling for surgical experience, which makes it difficult to render novice groups from a population consisting of professional surgeons homogenous with respect to eye-hand coordination expertise. All surgeons are experts in this regard, yet, they are more or less proficient at different specific tasks. This variability may not be easy to track down. While some of the latest studies divide the participants into the groups according to their given titles by institutions (e.g. [61]) or years of experience (e.g. [62]), some of them give expertise titles according to number of laparoscopic cases performed (e.g. Park et al. [63], Mashiach et al [64], Curro et al [65] ,Leite et al [66], etc.). Some studies do not specify any quantitative experience information about the participants (e.g. [67]). While each group has to represent homogeneous certain level of skills (such as eye-hand coordination, spatial performance, etc.), mixing surgeons into these groups and creating so-called “novices” and “experts” can affect the experiment results. In the last study of chapter 1, how expertise leveling can affect the visual feedback research on the surgical simulation studies is investigated in detail with three different expertise groups.

Color cues

One of the stereoscopic depth information feature is the color cues [61] and color cues can provide additional information on important medical structures. [63]. Studies in image-guided neurosurgery [62] have previously shown that adding color to specific locations in 2D images produces strong and self-sufficient cues to visual depth for interventional guidance, especially in novices, potentially making 3D viewing unnecessary. On the other hand, surgeons can adjust the screen brightness and

contrast to eliminate distracting visual information on the screen [64]. How subjects' 'time' and 'precision' is affected by color and grayscale screen representations and the relation between the color cues and expertise level are also other research topics discussed in first chapter.

Second Chapter – Human-computer interaction in head mounted virtual reality

In the second chapter of thesis, novice motor performance in virtual reality (VR) medical training applications with manual hand operations is studied in the context of human computer interactions [68–70]. Medical and non-medical virtual objects are inspected with the "NoTouch" system, the experimental platform designed with a motion sensor and immerse virtual reality headset.

Learning in virtual environments

Previous research on learning in virtual environments showed that using interactive learning in virtual environments increased cognitive gains, work-related skills and learning outcomes compared to the traditional teaching methods [71]. For instance, Sitzmann [72] showed that when the virtual training and comparison group compared, subjects' declarative knowledge was %11 higher, procedural knowledge was %14 higher, self-efficacy was %20 higher and retention was %9 higher in simulations. Similarly, in surgical simulation research, Seymour et al. [73] showed that subjects were making less errors and more steady progress with surgical simulators.

If trainees are motivated and guided well to use the knowledge and skills acquired from the simulations, learning can be enhanced. Since virtual reality headsets became easy-to-use and easy-to-access, different disciplines can use VR simulations to improve trainees' skills. This leads to a more and detailed research on VR simulators that designed for specific needs. In the second chapter, the "NoTouch" system is designed to collect data from the novices in VR and asses their spatial and temporal performance with several virtual reality experimental setups.

Motor performance assessment in VR

To fully understand human motor behavior in VR applications, several complementary behavioral indicators should be taken into consideration, operationalized

experimentally in terms of different related dependent variables. To be able to choose accurate assessment criteria according to the requirements of the task, motor performance of the individuals has to be studied and examined. For this reason, in the second chapter, three different precision criteria were used to evaluate the subjects: ‘average number of finger out’, ‘motor performance index’ and ‘average accumulated distance away from the object surface’.

Handedness in simulation environments

In VR environments, a designer can design a simulation that might require both hands to interact with environments. For example, in aviation simulations, individuals have to use their both hands to interact with the virtual objects in all over the cockpit. Similarly, in virtual medical simulation applications, according to target position, individuals might need to choose between their dominant or non-dominant hand to interact with the object. Thus, subjects’ time and precision performance variation according to the hand they are using also needs to be investigated in VR environments.

Movement direction

In 2D and 3D pointing tasks execution time is significantly affected by the movement direction [74–76]. For example, Murata and Iwase [76], showed that subjects were slower with upward movements. Grossman and Balakrishnan [77], and Scheme and Englehart [78] showed that movements in the depth also affects the task execution time. Apart from human-computer interaction studies on the movement time, how movement direction affects subjects’ precision also needs to be explored for an effective skill learning in VR environments. Extending these studies with the precision assessment and inspecting handedness and movement interaction can provide more information about the surgical skill simulation designs in VR.

VR among the simulation environments

Emerging technologies on different visual feedback systems helped surgeons to train themselves in different environments. Among these environments, VR became more popular in the last decade and new simulator applications on surgical training have started to develop since VR became easy-to-access and easy-to-develop. Moreover, the same surgical simulation application can be used for training in different

environments. For instance, a similar training application about a specific topic can be found on a desktop application, a VR application and even in the real life with different input devices. The major downside of these applications is they do not perform any cognitive or psychomotor assessment experiments and they only take execution time into account for performance assessment (e.g. [79,80]). The lack of how-to-assess-performance-of-the-novice knowledge on different surgical training systems can negatively affect the evaluation of the participants who use the same or similar surgical training environment systems: beginners' motor performance results may vary due to the task environment and prefrontal motor cortex has to learn the same tasks in different environments. This limitation creates a drawback in understanding the psychophysics behind the applications and VR itself. In the first study of second chapter, differences between VR and other simulation environments are inspected by using time and precision dependent variables.

Objects size in VR

One of the biggest advantages of VR systems is the ability to create virtual objects in any size, dimension, and scale. On the other hand, the human interaction with the virtual objects in the VR is not going to be the same as with the real world object interactions. Especially, when the tactile and auditory feedbacks are used to assist novices to focus in VR, human performance and decision making are going to be affected. Effects of these non-real-world feedbacks on human motor performance are still not well known. Different size, orientation, scale and even the position of the designed virtual object can affect the motor performance of the subjects and their assessments.

Fitts's law

Object size and the individual's interaction with this object have been a very attractive research topic since the "Fitts's law" [57]. Especially, after the implementation of the "Fitts's law" into the computer systems and expansion of this research area to the human-computer interactions, length and width of the targeted objects became more important for designers [81–84]. For the tunnel shaped objects, Accot and Zhai [85] developed the "Steering Law", which is derived from the "Fitts's Law". The effects of different size and width of objects in VR with an immersive head-mounted display

needs to be explored with “Steering Law” for time. Furthermore, applying index of difficulty to the different precision criteria results can reveal how to use these criteria according to different task requirements and task designs.

How motor performance of subjects is affected by the object size (length and width variation) and application of the “Steering Law” to the VR environments is the topic of the second study of chapter 2.

Depth perception and movements in the depth

In the three-dimensional real world, individuals can interact with objects including the depth perception. On the other hand, grabbing, reaching or extending goal-directed hand movements cannot be executed in the two-dimensional visual feedback systems, such as tv monitors, screens, and projectors. This limitation affects the movements of the subjects [86,87]. Immersive VR systems can provide this depth perception and the movement information using the depth cues such as perception, relative motion, occlusion, shadows, etc. [88,89]. The literature lacks a systematic target position effect on subject’s time and precision assessment for depth movements. The target interaction in the immerse VR environments is still needed to be examined with a particular focus on the ipsilateral and confraternal hand movements for depth perception.

How subjects’ performance affected by goal-directed manual operations in the depth is the main research topic of the third study of chapter 2.

Structural complexity

Structural complexity of objects should also be considered, as it may affect human skills and motor performance depending on the context. Although previous authors have addressed the problem of structural complexity and its possible effects on reaching for objects in virtual reality environments (e.g. [90,91]), there is still a need for deeper research into the effects of structural complexity on the time and the precision of hand movements towards or along the borders of virtual objects and other motor skill indicators.

The fourth study of chapter 2 addresses why structural complexity must be included among the independent variables. Furthermore, this study focuses on the unexpected results on subjects' handedness results and tries to explain the possible causes of this results.

Auditory feedback

In surgical simulator research, it was found that active learning (when a subject interacts with the object) leads to better motor performance in VR than passive learning (when a subject just observes the virtual scene) [92]. Moreover, the motor skills of subjects increase when they are provided with additional tactile [93] or auditory feedback [94]. For example, Swapp and his colleagues [95] showed that tactile feedback improved the speed of subjects in a 3D VR stereo environment. While haptic feedback is a larger research area, auditory feedback also increases the motor performance of subjects in the virtual reality environment [96,97]. The positive effect of additional feedbacks and the positive effect of auditory feedback has been studied by different researchers and started to be used in different applications [98–100]. Additional research is required to understand the effects of different sound feedback frequencies in an immersive VR head-mounted display environment,

In the last study of second chapter, the effects of auditory feedback on the "NoTouch" system are studied. In this experiment two different topics are explored: 1) which frequencies improve the motor performance of the subjects and 2) which frequencies should be used for multisensory feedback mechanisms.

Third Chapter – Grip-force analysis in the tele-manipulated operations

In the third chapter of the thesis, hand grip force analysis is performed during a surgical robotic task execution. In the first two chapters, effects of different visual and tactile feedbacks used in medical training applications were studied. In the last chapter of the thesis, studies are extended into a minimally invasive surgical robot system, STRAS [101]. To be able to measure the grip force variations on the STRAS, a special glove is designed to collect data. The aim of this glove is to record grip-force signals from different *loci* of measurement in the palm, the fingers, and the fingertips of the dominant and non-dominant hand.

Haptic information on surgical robotic systems

When the surgeon loose haptic information caused by reduced-access conditions in robot-assisted surgery, it may compromise the safety of the procedure. This limitation must be overcome through practice and, in particular, surgical simulator training for specific hand-tool interactions. Using biosensors for the measurement of grip force variations during surgical simulator training with hand-tool interaction provides valuable insight into surgical skill evolution.

Training in teleoperation systems

In minimally invasive teleoperation systems, surgeons need to operate master interfaces to manipulate the endoscope. Subjects need to master the system and its user interface to fully dominate the slave system because of the remote control and the complexity of the design. Such expertise can only be reached by getting used to the control mechanism, by practicing in vivo or using robotic surgical systems [102]. Previous studies were more focused on the tool-tip pressure and tactile feedback than the force applied on the grab sticks [103]. STRAS [104–106] is designed without force feedback and the control is therefore based on the visual feedback from the endoscope only.

All three chapters focus on not only the task execution time but also the precision criteria which affect the motor performance of the subjects and their progress assessment during the skill acquisition of the targeted task. In all studies, different visual, tactile and auditory feedbacks used in the surgical environment and skill training simulations are explored. Thus, visual, somatosensory and auditory cortex and the complex cross-talks between these cortexes are also inspected by using the results of each study.

In the first chapter, the effects of 2D and 3D image guidance and tool manipulation are studied with a surgical training setup. In the second chapter, the human-computer interaction in the immersive VR head-mounted display is explored. In the last chapter, hand grip force differences between a novice and an expert during a surgical robotic system task execution are investigated. In general, the results and conclusions of each study/chapter can be used to improve the training and simulation environments.

Chapter 1
Comparison of Real-World Manual Operations Under 2D and 3D Image Guidance

Introduction

In the first chapter, speed and precision analysis of real world manual operations are inspected under different visual and tactile feedbacks. When a surgeon performs a minimally invasive surgery, he/she must look at another source of visual feedback that is provided by a digital camera. The information provided by the natural view with eyes is not the same as looking through a 2D screen. This limitation also affects the perception of users and disturbs the actions and movements in real-world application. Previous research on this topic [3,36,37] shows that subjects are slower, less precise and make more task errors under 2D screen conditions.

Furthermore, during a surgical procedure, the surgeon must use a tool to perform the surgery. This tool manipulation disables the direct haptic feedback between the touch sensation of the surgeon and the manipulated object. In this case, the surgeon has to perform movements, maneuvers and actions according to the tactile information transferred by the surgical tool.

To overcome these major visual and tactile feedback challenges, different approaches have been tried such as: training novices in the use of surgical simulators, trying to find the best screen position for the surgeon to perform surgery, and using different visual feedbacks including stereoscopic 3D vision to create an artificial visual feedback.

In the first chapter of this thesis, different methods used in surgical environments to create a better surgical training system are studied. For this purpose, the “EXCALIBUR” experimental platform was designed with specific hardware and software components.

Materials and Methods

The “Excalibur” experimental platform was used to collect data from human subjects. The main frame of the hardware of “Excalibur” was the same for all of the studies in chapter 1. In the following section, the general system utilization was explained. In each particular study, specific conditions of the experiment were explained in more detail.

Handedness and spatial ability

In chapter 1, participants’ handedness was assessed using the Edinburgh inventory for handedness designed by [107] to confirm that they were all true right-handers. They were screened for spatial ability on the basis of the PTSOT (Perspective Taking Spatial Orientation Test) developed by Hegarty and Waller [108]. This test permits evaluating the ability of individuals to form three-dimensional mental representations of objects and their relative localization and orientation on the basis of merely topological (i.e. non-axonometric) visual data displayed two-dimensionally on a sheet of paper or a computer screen. All participants scored successful on 10 or more of the 12 items of the test, which corresponds to performances well above average, corresponds to spatial ability above average, as would be required for surgery.

Research ethics

The study was conducted in conformity with the Helsinki Declaration relative to scientific experiments on human individuals with the full approval of the ethics board of the corresponding author’s host institution (CNRS). All participants were volunteers and provided written informed consent. Their identities were not revealed.

Experimental platform: “Excalibur” hardware

The “Excalibur” experimental platform is a combination of hardware and software components designed to test the effectiveness of varying visual environments for image-guided actions in the real world.

The main body of the “Excalibur” contains adjustable horizontal and vertical aluminum bars connected to a stable but adjustable wheel-driven sub-platform. The main body can be resized along two different axes in height and in width, and has two USB cameras (ELP, Fisheye Lens, 1080p, Wide Angle) fitted into the structure for monitoring the real-world action field from a stable vertical height, which was at 60 cm for the experiments. The distance between the two cameras was 6.4 cm, which was also the same with the Oculus DK2 system. No head tracking system was used during the experiments.

Two different approaches were used to create the experimental environment. At the beginning of the experiments, there was an idea to use a cardboard box to cover the experimental setup. To select the most suitable experimental setup, two different approaches were tested by virtual simulation in Unreal Engine 4.0 (Figure 1(a) for no box and Figure 1(b) for box) and constructed in real life (Figure 1(c) for no box and Figure 1(d) for box) to see the differences.

During the experimental setup selection trials, it was observed that the cardboard was not stable. Each time the 2D visual feedback conditions were executed, the box had to be moved in to the experimental platform which thus caused the camera to become unstable. This was not a problem for open-box condition. Furthermore, the cardboard box was not flexible enough for moving, and the future experiments were planned in several different places. As a result, it was decided to no longer use the box system, as shown in Figure 1(e).

Computer used in experiments

The video input received from the cameras was processed by a DELL Precision T5810 model computer equipped with an Intel Xeon CPU E5-1620 with 16 Giga bytes memory (RAM) capacity at 16 bits and an NVidia GeForce GTX980 graphics card. This

computer was also equipped with three USB 3.0 ports, two USB 2.0 SS ports and two HDMI video output generators. The operating system was Windows 7. The computer was connected to a high-resolution full HD color monitor (EIZO LCD 'Color Edge CG275W') with an in-built color calibration device (colorimeter), which uses the Color Navigator 5.4.5 interface for Windows. The colors of objects viewed on the screen can be matched to LAB or RGB color space, fully compatible with Photoshop 11 and similar software tools. The color coordinates for RGB triples can be retrieved from a look-up table at any moment in time after running the auto-calibration software.

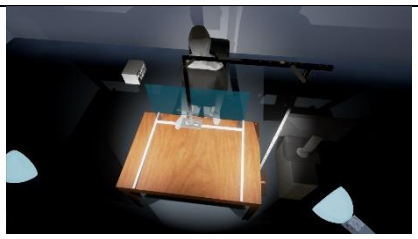

(a)

(b)

(c)

(d)

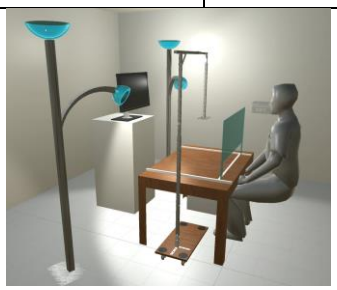

(e)

Figure 1 – Different approaches tested for Excalibur hardware. (a) No box and (b) with box solutions in simulations. (c) No box and (d) with box solutions in real life. (e) simulation of final experimental setup.

Software design in experiments

Experiments were programmed in Python 2.7 using the Open CV computer vision software library. The basic algorithm of the software is shown here in Figure 2.

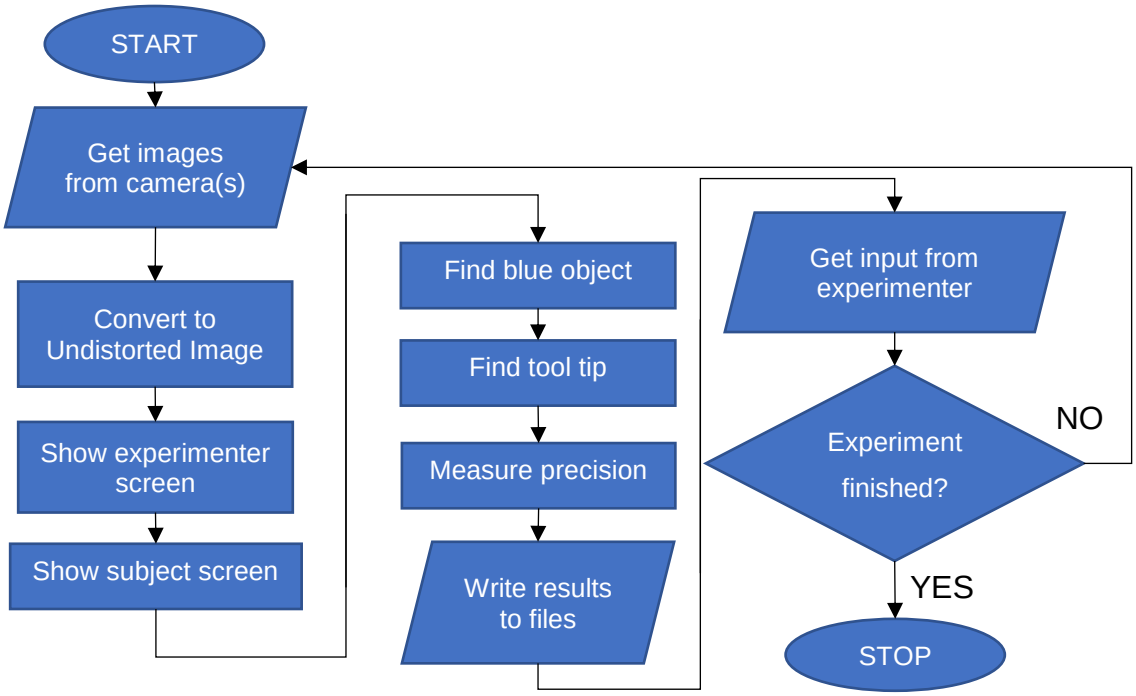

Figure 2 – General algorithm flowchart. For each different experiment, codes are given in the particular study file.

The main software algorithm of the system was running on an infinite loop. After acquiring the image(s) from the camera(s), the left eye camera fisheye view was converted into the undistorted vision for image processing. A copy of the undistorted vision image was shown to the experimenter for the information with the set number, trial number and experimental conditions. The image shown to the subject changed according to the experimental condition; fisheye vision, undistorted vision or Oculus 3D vision. After the undistorted image conversion, the algorithm found the blue object and green tool tips on the screen. The precision measurement was done after counting the number of blue pixels on the screen. More information about the precision analysis can be found in Figure 5 and in the section concerning Data generation. The results of the experiments were written to a file and at the end of the algorithm and the loop continued until an input was received from the experimenter. If there was an input from the experimenter, such as a change in the experimental conditions, start trial, etc. the

next loop continued with the given instructions. The time of one loop execution was between 30-40 milliseconds, which corresponds to 33-25 FPS (frame per second). In other words, the delay between the real-world action and the image of that action shown to subject on the screen was about 30-40 milliseconds.

Objects in the real-world action field

The Real-world Action Field (as of now referred to as the RAF) consisted of a classic square shaped (45 cm × 45 cm) light grey LEGO© board available worldwide in the toy sections of large department stores. Six square-shaped (4.5 cm × 4.5 cm) target areas (as of no referred to as the TAs), were painted on the board at various locations in a medium grey tint (acrylic). The cube object that had to be placed on the target areas in a specific order was a small (3 cm × 3 cm × 3 cm) cube made of very light plastic foam but resistant to deformation in all directions. Five sides of the cube were painted in the same medium grey tint (acrylic) as the target areas. One side, which was always pointing upwards in the task (Figure 3), was given an ultramarine blue tint (acrylic) to permit tracking object positions.

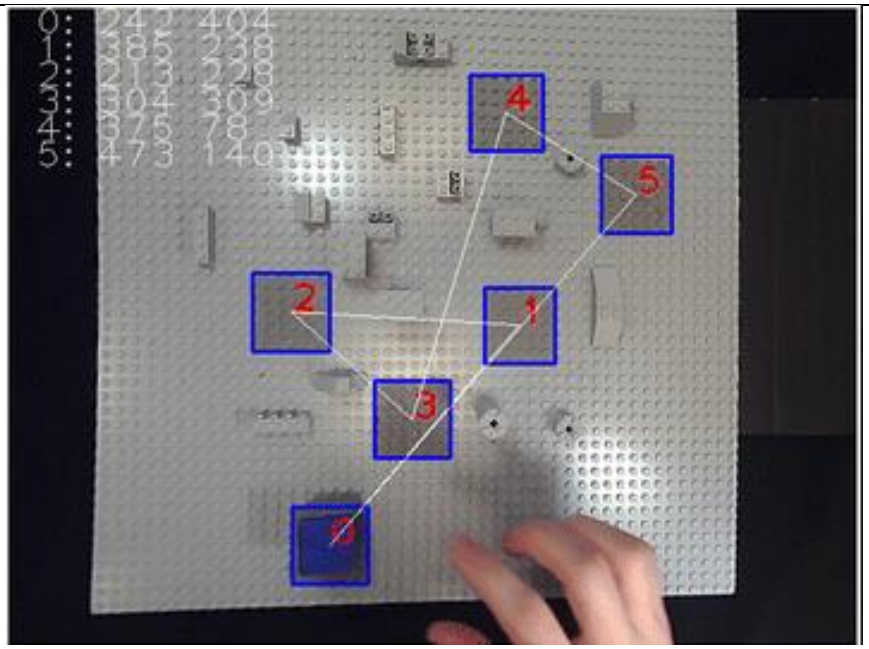

Figure 3 – Screenshot view of the RAF, with the reference trajectory, indicated here by the white line. The red numbers show the successive target locations on which the object was to be placed, from the starting point zero to positions one, two, three, four, five, and then back to zero.

In-between the TAs, small LEGO© pieces of varying shapes and heights were placed to add a certain level of complexity to both the visual configuration and the task and to reduce the likelihood of getting performance ceiling effects. Trajectory segments were named after the targeted TA number, e.g. if the subject was moving from TA0 to TA1, this trajectory segment was named as X1. According to this classification, rest of the trajectory segments were also named as X2, X3, X4, X5 and X0. There were no obstacles on X1 TAs. Subjects had to be careful as they approached the end of the X1 trajectory, where two-cylinder towers 2 cm below TA1 had been placed (4 cm and 1 cm high, on the left and right of X1 respectively). These two small cylinder towers were moved in the color cues study, study 3. In X2, there was a 1 cm high, 2 cm wide, and 3 cm long obstacle. This obstacle was raised above the RAF by a 3 cm long cylinder tower of 1 cm radius. The cylinder was placed underneath the obstacle, not in the middle but on its right side, which rendered the obstacle unstable. In X3, there was a 4-cm high triangular obstacle which was placed slightly on the trajectory. In X4, there were no obstacles, but subjects had to be careful because of the obstacle placed between TA1-TA2. This segment was also used to reach the farthest point in the experimental setup. In X5, there was a 1 cm high cylindrical tower of 1 cm radius. This segment was used to maneuver between the two TAs that were the furthest away. X0, the last and longest trajectory segment, had no obstacles. Several other obstacles were distributed on the LEGO© board to create a visual complexity in the design (Figure 4).

The aim of designing a RAF with such obstacles and segments was to create a complex environment, not a simplified one with a single-trajectory-no-obstacles goal directed movement trajectory as in previous studies. As a result, the goal-directed movements are closer to surgical gestures.

A medium sized forceps-like gripping instrument with straight ends was used for manipulating the object in the conditions ‘with tool’. The tool-tips were given a matte fluorescent green tint (acrylic) to allow tool-tip tracking.

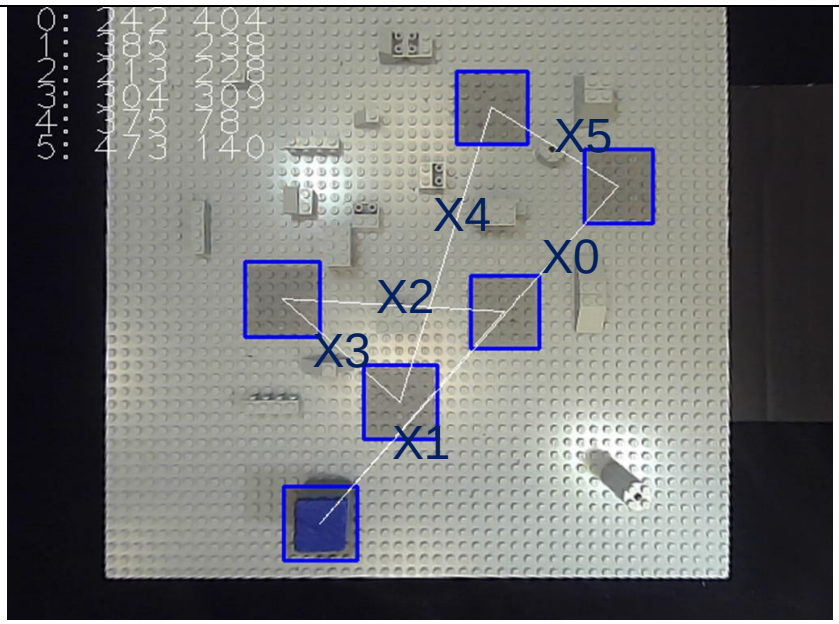

Figure 4 – Trajectory Segments. Between TA0-TA1 is X1, between TA1-TA2 is X2, Between TA2-TA3 is X3, between TA3-TA4 is X5, Between TA4-TA5 is X5, Between TA5-TA0 is X0.

Objects viewed on 2D screen

The video input received by the computer from the USB camera generated a raw image data within a viewing frame of the dimensions of 640 pixels (width) × 480 pixels (height). These data were processed to generate shown image data in a viewing frame of the dimensions 1280 pixels (width) × 960 pixels (height), the size of a single pixel on the screen being 0.32 mm. The size of the RAF (grey LEGO© board) viewed on the computer screen was identical to that in the real world (45 cm × 45 cm), and so were the size of the target areas (4.5 cm × 4.5 cm) and of the object manipulated (3 cm × 3 cm). A camera output matrix with image distortion coefficients using the Open CV image library in Python was used to correct the fisheye effects for the 2D corrected viewing conditions of the experiment. This did not affect the size dimensions of the visual objects given here above. The luminance (***L***) of the light grey RAF viewed on the screen was 33.8 cd/m^{2}and the luminance of the medium grey target areas was 15.4 cd/m^2, producing a target/background contrast (Weber contrast: (($\boldsymbol{L}_{foreground}$-$\boldsymbol{L}_{background}$)/$\boldsymbol{L}_{background}$)) of -0.54. The luminance of the blue (x = 0.15, y = 0.05, z = 0.80 in CIE color space) object surface viewed on the screen was 3.44 cd/m^2, producing Weber contrasts of −0.90 with regard to the RAF, and −0.78 with regard to the target

areas. The luminance (29,9 cd/m^2) of the green (x = 0,20, y = 0,70, z = 0,10 in CIE color space) tool-tips produced Weber contrasts of −0,11 with regard to the RAF, and 0,94 with regard to the target areas. All luminance values for calculating the object contrasts viewed on the screen were obtained on the basis of standard photometry using an external photometer (Cambridge Research Instruments) with the adequate interface software. These calibrations were necessary to ensure that the image conditions matched the direct vision condition as closely as possible.

Actions viewed in stereoscopic 3D through a head-mounted device

The video input received by the computer from two HD USB cameras was fed into the Excalibur software in Figure 2 (which concatenates two camera inputs into a stereoscopic 3D image) and was displayed on the head-mounted screen of the OCULUS DK2 (https://www.oculus.com/). Real-world data and visual display data were scaled psychophysically for each observer, i.e. the image size was adjusted for each subject to ensure that the visual display subjectively matched the scale of the RAF seen in the real world as closely as possible. OCULUS DK2 had a fixed inter-ocular distance.

Experimental environment

The experiments were run under conditions of free viewing, with general illumination levels that could be assimilated to daylight conditions. The RAF was illuminated by two lamps (40Watt, 6500 K), constantly lit during the whole duration of the experiment. Participants were comfortably seated on an adjustable chair. The experimental setup table was covered by a black velvet curtain. On the 2D screen monitor, the background was completely black to not distract the subject. Next to the experimental setup, a second DELL screen was positioned to observe the experiment. The experimenter was able to watch the experimental setup and RAF from this screen and interfere when it was necessary. The experimenter was able to change the experimental independent conditions from the keyboard in front of him.

Procedure

A printout of the targets-on-RAF (Figure 3) configuration was handed out to the participant at the beginning of each experiment. White straight lines on the printout indicates the object reference trajectory, and red numbers indicates the order in which the small blue cube object has to be placed on the light grey targets in a given trial set. The pick-and-place sequence was always from position zero to position one, then to two, to three, to four, to five, then back to position zero. Participants were instructed to position the cube with their dominant hand “as precisely as possible and as swiftly as possible on the center of each target, in the right order as indicated on the printout. They were also informed that they were going to perform this task under different conditions of object manipulation: with and without a tool, while viewing the RAF (and their own hands) directly in front of them, and while viewing the RAF (and their own hands) on a computer screen. In the direct viewing condition, participants saw the RAF and what their hands were doing through a glass window, which was covered by a black velvet curtain. In the 2D video conditions, subjects saw an image of the RAF on the computer screen. All participants grasped the object with the thumb and the index of their right hand, from the same angle, when no tool was used. When using the tool, they all had to approach the object from the front to grasp it with the two tool-tips. Before starting the first trial set, participants could look at the printout of the task trajectory for as long as they wanted. When they felt confident that they remembered the target order well enough to do the task, the printout was taken away from them. An individual experiment was always started with a “warm-up” run in each of the different conditions. Data were collected from the moment a participant was able to produce a trial sequence without missing the target area or dropping the object. An experimental session always began with the easiest (cf. [3]) condition of direct viewing.

Data generation

Data from fully completed trial sets only were recorded. A fully complete trial set consists of a set of positioning operations starting from zero, then going to one, to two, to three, to four, to five, and back to position zero without dropping the object accidentally and without errors in the positioning order. Whenever such an error occurred the trial set was aborted immediately, and the participant started from scratch in that specific condition.

Ten fully completed trial sets were recorded for each combination of factor levels. For each of such ten trial sets, the computer program generated data relative to the dependent variables ‘time’ and ‘precision’. For ‘time’, the computer program counts the CPU time (in milliseconds) from the moment the blue cube object is picked up by the participant to the time it is reached back to position zero again. For ‘precision’, the computer program counts the number of blue object pixels at positions “off” the 3 cm × 3 cm central area of each of the five 4.5 cm × 4.5 cm target areas (see Figure 5) whenever the object is positioned on a target. The standard error of these positional estimates, determined in the video-image calibration procedure, was always smaller than 10 pixels. “Off”-center pixels were not counted for object positions on the square labeled ‘zero’ (the departure and arrival square). Individual ‘time’ and ‘precision’ data were written to an excel file by the computer program, with labeled data columns for the different conditions, and stored in a directory for subsequent analysis. TA0 could be seen under the velvet curtain, so precision calculation for this TA was not included in the precision data. Subjects were also informed that TA0 was not going to be counted in the precision calculation and they could stop at the TA0 to rest.

Three different dependent variables were used to analyze object trajectory data. For the trajectory data analysis, the center of the blue cube position data in all TAs were deleted when the object was not moving. Only the data when the object was moving were analyzed, which focuses on movements in the different trajectories with different obstacles. The first dependent variable was called ‘“mean distance” from the reference trajectory’ (in pixels). A virtual reference trajectory was created as shown in (Figure 3), connecting the centers of two consecutive TAs. The perpendicular pixel distance between this virtual reference line and the center of the foam cube was measured in natural numbers for each segment. Afterwards, mean of this distance data for each individual segment was calculated and used as the ‘“mean distance” from the reference trajectory’ dependent variable. The second dependent variable was the ‘mean “dispersion” in the object movement’ (in pixels) which refers to the mean standard deviation in the undulated movement of the foam cube. The standard deviation of the perpendicular pixel distance from the reference line data of each segment was used for this dependent variable. The third dependent variable was the ‘from-target-to-target duration’ (in seconds) for each segment. A software timer started when the center of the blue-cube entered each TAs and it stopped when the center of

the blue-cube reached the next TA. The time difference between these two TAs is called the ‘from-target-to-target duration’. In this dependent variable, time spend to place the object at the center of the TA was not included in the analysis.

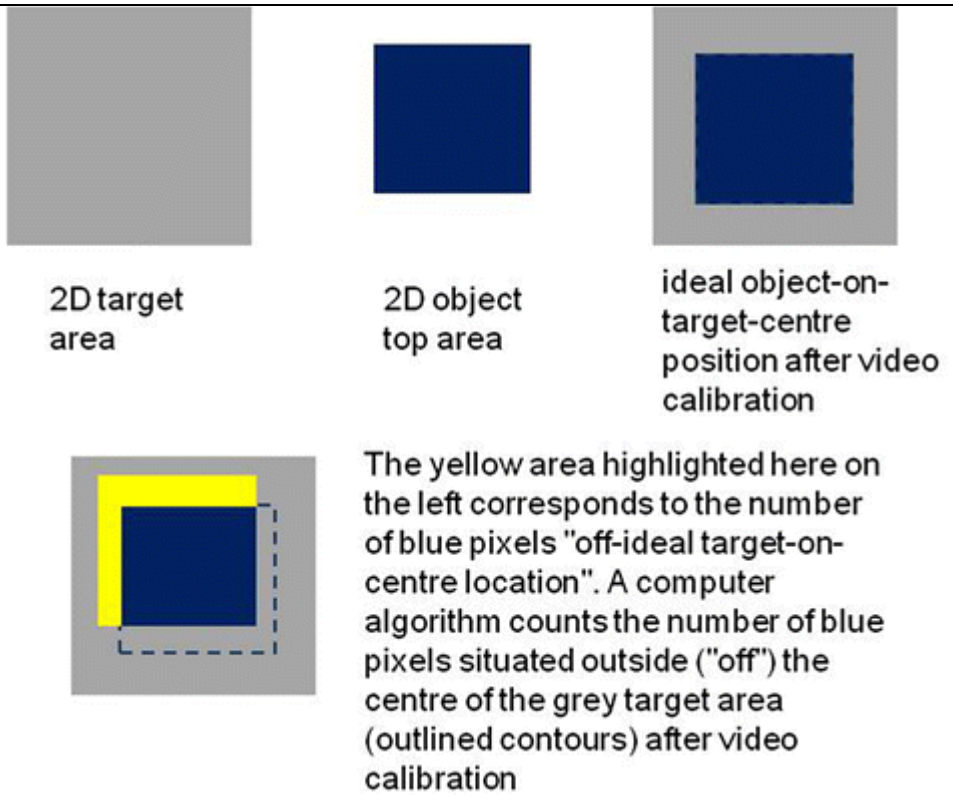

Figure 5 – Schematic illustration showing how the computer counts *number of pixels “off” target center* in the video-images

The other important key point in the experiment was the way of obtaining data of the individuals from the start point. It is important to keep in mind that the Excalibur was designed to measure ‘time’ and ‘precision’ of a pick-and-place task. The data started to be recorded after the subject said “GO” at TA0 and it lasted until the blue object center returned back to the TA0, the start point. Each segment data was recorded until the object center reached to the TA. In this case, during the placement of the object on TAs, subjects spent time putting the object in the center of each TA, except TA0. This created a bias for the X1 segment.

Study 1 - Individual Speed-Precision Trade-offs from Training Sessions

In the first study of chapter 1, the learning process of the individuals is studied to explore image guided feedback effects on ‘time’, ‘precision’ and ‘trajectory’. Subjects were slower and made more task errors in image guided visual feedback [3,36,37]. In this study, tool manipulation and session progression are investigated on complete beginners to understand the evaluation of motor performance with 2D visual feedback task executions.

Study Goal and Hypotheses

Image-guided interventional procedures constrain the human operator to process critical information about what his/her hands are doing in a 3D real-world environment by looking at a 2D screen representation of that environment [33]. In addition to this problem, the operator or surgeon often has to cope with uncorrected 2D visual feedback from a single camera with a fisheye lens [34,35], providing a hemispherical focus of vision with poor off-axis resolution and aberrant shape contrast effects at the edges of the objects viewed on the screen. Novices have to learn to adapt to whatever viewing conditions, postural demands or task sequences may be imposed on them in a simulator training environment. Loss of three-dimensional vision has been pointed out as the major drawback of image-guided procedures (see [109], for a review). Compared with direct (“natural”) action field viewing, 2D image viewing slows down tool-mediated task execution significantly, and also significantly affects the precision with which the task is carried out (e.g. [3,36]).

The operator or surgeon’s postural comfort during task execution partly depends on where the monitor displaying the video images is placed, and there is a general consensus that it should be positioned as much as possible in line with the forearm-instrument motor axis to avoid fatigue due to axial rotation of the upper body during task execution (e.g. [109]). An off-motor-axis viewing angle of up to 45° seems to be the currently adopted standard [110].

In tool-mediated eye-hand coordination, the sensation of touch [51] is altered due to lack of haptic feed-back from the object that is being manipulated. There is no direct tactile feed-back from the object to the sensory receptors in the hand [52], which communicate with cortical neurons driven by multisensory input [53–55]. Visual-haptic mapping for cross-modal sensory integration [56] is affected by such lack of direct sensory feed-back. Repeated tool-use engenders dynamic changes in cognitive hand and body schema representations (e.g. [111–113]), reflecting the processes through which highly trained experts are ultimately able to adapt to both visual and tactile constraints of image-guided interventions. as in laparoscopic interventions.

Image-guided hand movements, whether mediated by a tool or not, require sensorimotor learning, an adaptive process that leads to improvement in performance through practice. This adaptive process consists of multiple distinct learning processes [114]. Hitting a target, or even getting closer to it, may generate a form of implicit reward where the trainee increasingly feels in control and where successful error reduction, which is associated with specific commands relative to the specific motor task [115], occurs naturally without external feed-back. In this process, information from multiple senses (vision, touch, audition, proprioception) is integrated by the brain to generate adjustments in body, arm, or hand movements leading to faster performance with greater precision. Subjects are able to make use of error signals relative to the discrepancy between the desired and the actual movement, and the discrepancy between visual and proprioceptive estimates of body, arm, or hand positions [116,117]. Under conditions of image-guided movement execution, real-world (direct) visual feed-back is not provided, and with the unfamiliar changes in critical sensory feed-back this engenders, specific sensory integration processes may no longer be effective (see the study by [118], on the cost of expecting events in the wrong sensory modality, for example).

Here, in the light of what is summarized above, the problem of conditional accuracy functions in individual performance learning were addressed [119]. Conditional accuracy trade-offs occur spontaneously when novices train to perform a motor task as swiftly and as precisely as possible in a limited number of sessions [57], as is the case in laparoscopic simulator training. Conditional accuracy functions relate the duration of trial or task execution to a precision index reflecting the accuracy of the

performance under conditions given [58,59]. This relationship between speed and precision reflects hidden functional aspects of learning, and delivers important information about individual strategies the learner, especially if he/she is a beginner, is not necessarily aware of [60]. For the tutor or skill evaluator, performance trade-offs allow assessing whether a trainee is getting better at the task at hand, or whether he/she is simply getting faster without getting more precise, for example. The tutor's awareness of this kind of individual strategy problem permits intervention if necessary in the earliest phases of learning and is essential for effective skill monitoring and for making sure that the trainee progresses in the right direction.

In the first study of first chapter, the evolution of the speed, the precision and trajectory movements were investigated in tool-mediated (or not) and image-guided (or not) object manipulation in an object positioning task (sometimes referred to as "pick-and-place task", as for example in [4]). The task was performed by complete novices during a limited number of training sessions. In the light of previously reported data (e.g. [3,36]), longer task execution times and lesser precision under conditions of 2D video image viewing when compared with direct ("natural") vision were expected. Since the experiments were run with novices, tool-mediated object manipulation was expected to be slower and less precise (e.g. [120]) when compared with bare-handed object manipulation. Previous research had shown that wearing a glove does not significantly influence task performance (e.g. [36,121]), but viewing conditions and tool-use were not included in these analyses. Here, whether or not wearing a glove may add additional difficulty to the already complex conditions of indirect viewing and tool-use with learning was aimed to tested. Furthermore, it was expected to observe trade-offs between task execution times and precision that are specific for each individual and can be expected to occur spontaneously (e.g. [57]) in all the training conditions, which are run without external feed-back on performance scores. The individual data of the trainees were analyzed to bring these trade-offs to the fore and to generate conclusions relative to individual performance strategies. The implications for skill evaluation and supervised versus unsupervised simulator training was made clear.

Materials and Methods

Subjects

Two healthy right-handed men, 25 (Subject 3) and 27 (Subject 4) years old, and two healthy right-handed women, 25 (Subject 2) and 55 (Subject 1) years old, participated in this study. None had any experience in image-guided activities such as laparoscopic surgery training or other. Three of them stated that they did “not play videogames”, one of them (Subject 4) stated to “play videogames every now and again”.

Experimental platform

In this study, direct vision, undistorted vision and fisheye vision shown in Figure 6 are used for the experiments. Figure 6(a) is used as direct vision, Figure 6(b) is used for 2D undistorted vision Figure 6 (c) is used for 2D fisheye vision.

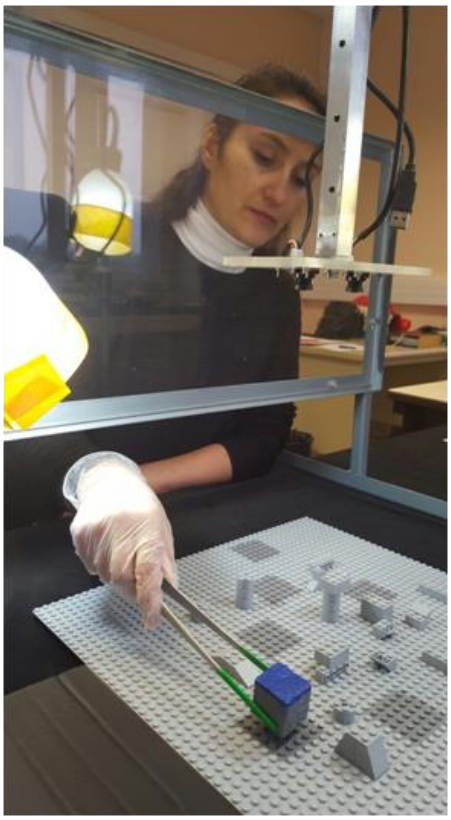

(a)

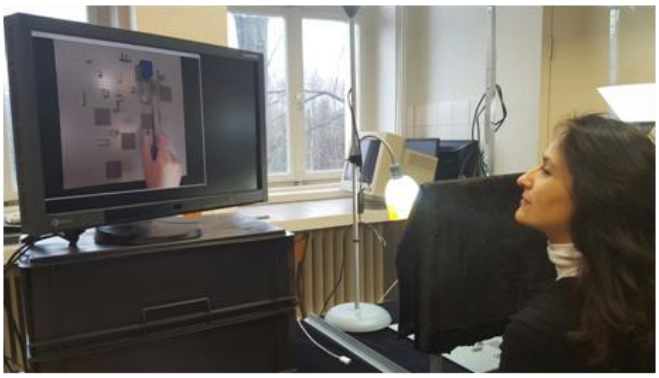

(b)

(c)

Figure 6 – Experimental conditions used in the first study. (a) Direct view with tool manipulation with glove (b) Undistorted vision (c) Fisheye vision

As mentioned in Materials and Methods section, Excalibur hardware had two cameras. In this experiment, only left camera was active to process images on RAF.

Objects in the real-world action field

In the first study, apart from the tool manipulation, subjects used examination gloves for ‘glove’ condition in the experiments. The gloves used in the *‘with glove’* conditions (in Figure 26(a), a glove donned by subject is visualized) were standard, medium size (7/8) non-sterile, ambidexter, sensitive vinyl glove was donned by the subjects for the touch conditions. Subjects’ hands were suitable for medium size gloves.

Procedure

Participants were comfortably seated at a distance of approximately 75 cm from the RAF in front of them, and from the screen, which was positioned at an angle of slightly less than 45° to their left. As explained in the introduction, this monitor position is within the range of currently accepted standards for comfort. A printout of the targets-on-RAF configuration was handed out to the participant at the beginning.

Subjects were instructed that they were going to perform this task under different conditions of object manipulation: with and without a tool, with their bare hands and wearing a surgical glove under three different visual feedback conditions, direct, fisheye and undistorted.

An experimental session always began with the easiest condition of direct vision. Thereafter the order of the two 2D visual feedback conditions (undistorted and fisheye) was counterbalanced, between sessions and between participants, to avoid order specific habituation effects. For the same reason, the order of the tool-use conditions (with and without tool) and the touch conditions (with and without glove) was also counterbalanced, between sessions and between participants. No performance feedback was given. At the end of training, each participant was able to see his/her learning curves from the eight sessions, for both ‘time’ and ‘precision’. No specific comments were communicated to them, and no questions were asked at this stage. Subject 4 spontaneously wanted to run in twelve additional sessions to see whether he could produce any further evolution in his performance.

Cartesian Design Plan and Data Generation

Experimental design

A Cartesian design plan $S_4 x T_2 x V_3 x M_2 x S_8$ was adopted for testing the expected effects of training, viewing modality, and object manipulation mode on inter-individual variations in time and precision during training, specified here above in the last paragraph of the introduction. To this purpose, four participant subjects (P_4) performed the experimental task in three vision conditions (V_3: direct vision, fisheye vision and undistorted vision) with two conditions of object manipulation (M_2: with tool and without tool), and two modalities of touch (T_2: Bare hand and glove) in eight successive training sessions (S_8).

Data generation

The data recorded from each of the subjects were analyzed as a function of the different experimental conditions, for each of the five dependent variables ('time', 'precision', 'from-target-to-target duration', 'average distance from the reference trajectory' and 'dispersion in trajectory').

$S_4 x T_2 x V_3 x M_2 x S_8$ Cartesian design plan is used with ten repeated trial sets for each combination of conditions within a session, yielding a total of 3840 experimental observations for 'time' and for 'precision'. The same approach was used to perform trajectory performance analysis. As mentioned in the chapter 1 materials and methods, each movement of the subjects were divided into to six segments and averages of each experimental level was used in the data analysis yielding total of 2304 experimental observations for $S_4 x V_3 x M_2 x S_8 x X_6$. Touch condition is removed from the analysis to reduce degrees of freedom and to reduce the computational complexity.

Results

Time and precision results

The data recorded from each of the subject were analyzed as a function of the different experimental conditions, for each of the two dependent variables ('time' and

‘precision’). Medians and scatter of the individual distributions relative to ‘time’ and ‘precision’ for the different experimental conditions were computed first. Box-and-whiskers plots were generated to visualize these distributions. Means and their standard errors for ‘time’ and ‘precision’ were computed in the next step, for each subject and experimental condition. The raw data were submitted to analysis of variance (ANOVA) and conditional plots of means and standard errors as a function of the rank number of the trial sessions were generated for each subject to show the evolution of ‘time’ and ‘precision’ with training.

Medians and extremes

Medians and extremes of the individual data relative ‘time’ and ‘precision’ for the different experimental conditions were analyzed first. The results of these analyses are represented graphically as box-and-whiskers plots in Figure 7 and Figure 8.

Figure 7 shows distributions around the medians of data from the manipulation modality with tool in the three different viewing conditions. Figure 8 shows distributions around the medians of data from the manipulation modality without tool in the three different viewing conditions. The distributions around the medians, with upper and lower extremes, for the data relative to ‘time’ show that Subject 1 was the slowest in all conditions, closely followed by Subject 2. Subjects 3 and 4 were noticeably faster in all conditions and their distributions for ‘time’ generally display the least scatter around the median. All subjects took longer in the tool-mediated manipulation modality (see graphs on left in Figure 8) compared with the by-hand manipulation modality without tool. The shortest times are displayed in the distributions from the direct viewing condition and the longest times in the distributions from the fisheye image viewing condition.

Medians, upper and lower quartiles and extremes for ‘precision’ (graphs on right) show that subject 1 is the most precise in all conditions, with distributions displaying the smallest number of pixels “off” target center and the least scatter around the medians. Subject 2 was the least precise, with distributions displaying the largest number of pixels “off” target center and the most scatter around the medians in most conditions except in the direct viewing conditions without tool, where subject 3′s distribution displays the largest “off” center values and the most scatter around the median. All

other subjects were the most precise in the direct viewing conditions, excluding the two outlier data points at the upper extremes of the distributions of subject 3 and 4. Subject 2 was the least precise in the fisheye image viewing conditions, and the three other subjects were the least precise in the 2D corrected image viewing conditions.

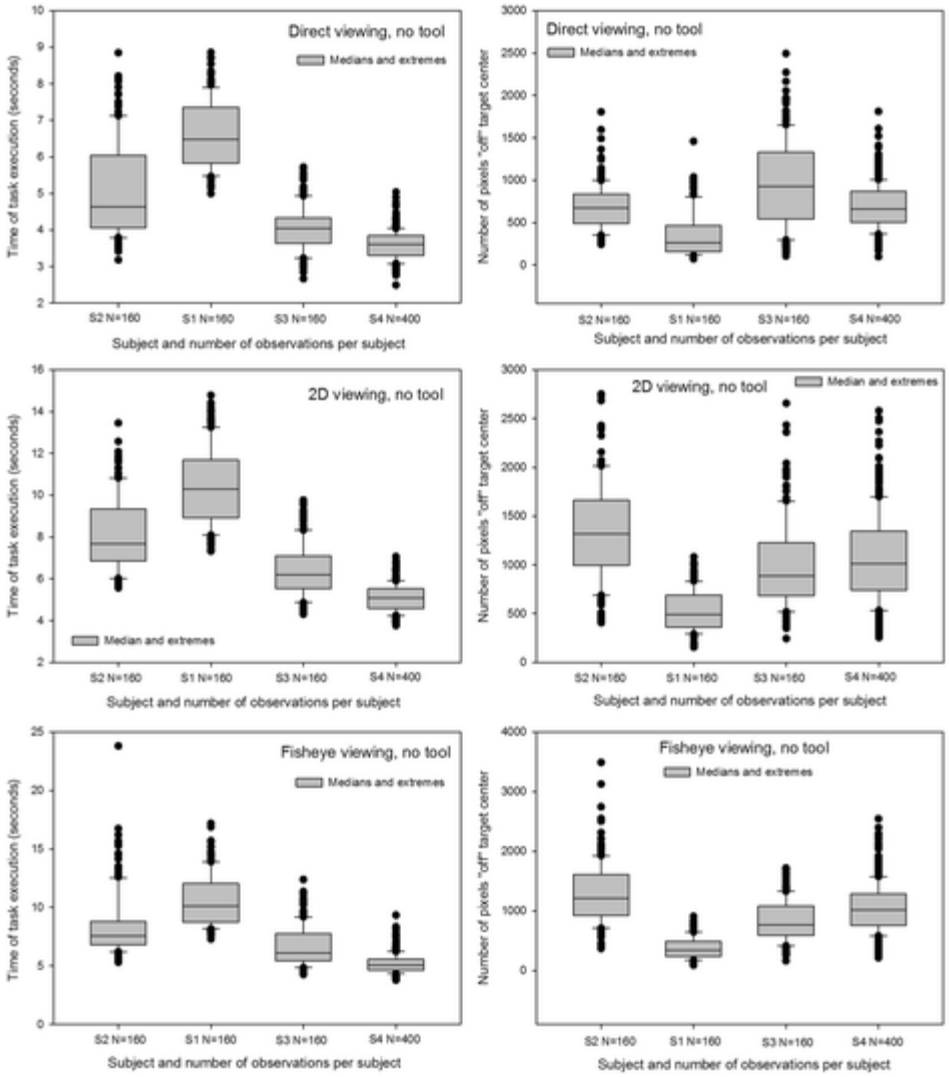

Figure 7 - Box-and-whiskers plots with medians and extremes of the individual distributions for 'time' (*left*) and 'precision' (*right*) in the manipulation modality without tool. Data for the direct viewing (panel on top), the 2D corrected image viewing (middle panel), and the fisheye image viewing (lower panel) conditions are plotted here.

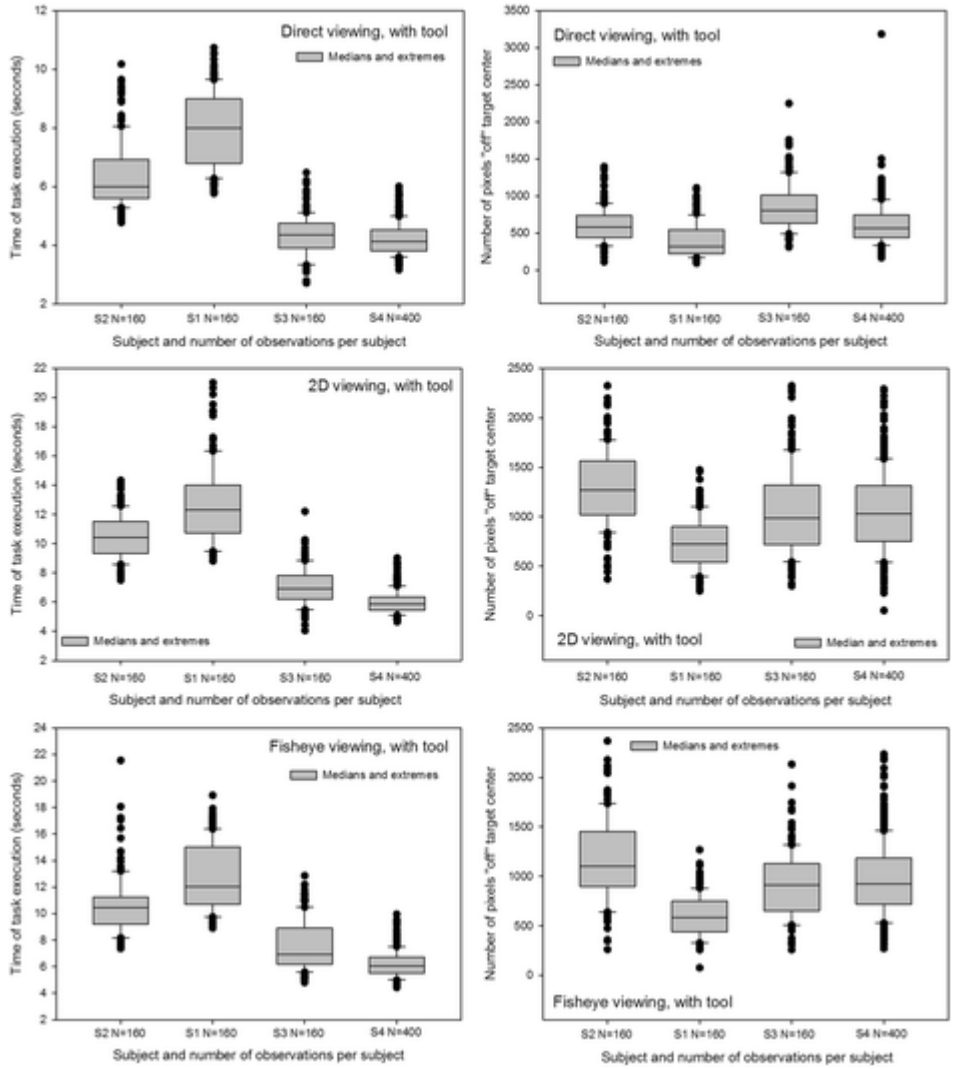

Figure 8 - Box-and-whiskers plots with medians and extremes of the individual distributions for 'time' (*left*) and 'precision' (*right*) in the manipulation modality with tool, for the direct viewing (*upper panel*), the 2D corrected image viewing (*middle panel*), and the fisheye image viewing (*lower panel*) conditions.

Analysis of variance

3840 raw data for 'time' and 3840 raw data for 'precision' were submitted to Analysis of Variance (ANOVA). The distributions for 'time' and 'precision' satisfy general criteria for parametric testing (independence of observations, normality of distributions and equality of variance). Five-Way ANOVA was performed for a design plan $P_4 \times T_2 \times V_3 \times M_2 \times S_8$ with four levels of the *'participant'* factor P_4, which is analyzed as a main experimental factor here because the differences between

individuals were the priority of this research, as explained earlier in the introduction paragraph.

Principal variables

The differences between means for 'time' (Annex 1- Figure 1) and 'precision' (Annex 1- Figure 2) of the different levels of each factor were statistically significant for almost all experimental factors except for effects of *'touch'* (T_2) on 'time' and effects of *'manipulation'* (M_2) on 'precision'. Means (M) and standard errors (SEM) for each level of each principal variable, and the ANOVA results, with *F* values and the associated degrees of freedom and probability limits, are summarized in Batmaz et al [32] Table 1. The differences between means for 'time' and 'precision' of the three levels of the *'vision'* (V_4) factor displayed in the table show that participants were significantly slower and significantly less precise in the image guided conditions compared with the direct viewing condition. Comparing the means for the two levels of *'manipulation'* (M_2) shows that tasks were executed significantly faster when no tool was used, with no significant difference in precision. The 'touch' factor (T_2) had no effect on task execution times, but participants were significantly less precise when wearing a glove. The most critical factors for the learning study here, the *'session'* (S_8) and *'participant'* (P_4) factors, produced significant effects on 'time' and on 'precision'. These can, however, not be summarized without taking into account their interaction, which was significant for 'time' $F(21, 3839) = 162.88$; $p < 0.001$ and for 'precision' $F(21, 3839) = 35.21$; $p < 0.001$.

Interactions

The *'participant'* and *'session'* factors produced significant interactions with the *'viewing'* factor: ($F(14, 3839) = 104.67$ $p < 0.001$ for *'session' x 'vision'* on 'time' and $F(6, 3839) = 267.74$ $p < 0.001$ for *'participant' x 'vision'* on 'time'; ($F(14, 3839) = 3.86$ $p < 0.001$ for *'session' x 'vision'* on 'precision' and $F(6,3839) = 81.32$ $p < 0.001$ for *'participant' x 'vision'* on 'precision'. To further quantify these complex interactions, *post-hoc* comparisons (Holm-Sidak procedure, the most robust for this purpose) for the three levels of *'vision'* (V_3) and the eight levels of *'session'* (S_8) in each level (p1, p2, p3, and p4) of the *'participant'* factor (P_4) were carried out for both

dependent variables. The degrees of freedom (*df*) of these step-down tests are *N-k*, where *N* is the sample size (here 3840/4 = 960) and *k* the number of factor levels (here 3 + 8 = 12) compared in each test. The results of these *post-hoc* comparisons are displayed in Tables between 2 to 9 in Batmaz et al [32], which give effect sizes in terms of differences in means, for 'time' and 'precision', between the viewing conditions for each participant and session, *t* values, and the corresponding unadjusted probabilities. According to these tables, the effect sizes do not evolve in the same way in the different participants as the sessions progress.

In the next step of the analysis, the conditional data for 'time' and 'precision' were represented graphically. Figure 9 shows the effects of *'session'* (S_8) on 'time' (left) and on 'precision' (right). Figure 10 shows the effects of *'participant'* (P_4) on 'time' (left) and 'precision' (right). For further insight into differences between participants, their individual functions (means and standard errors of the conditional performance scores) were plotted as a function of the rank number of the sessions. These functions permit tracking the evolution of individual performance with training.

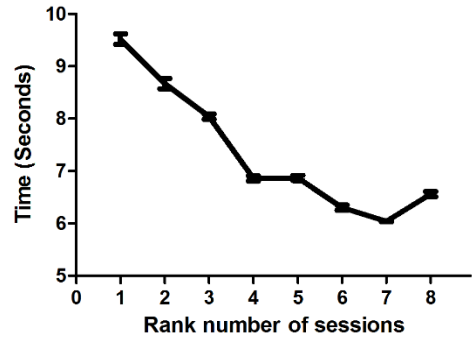

(a)

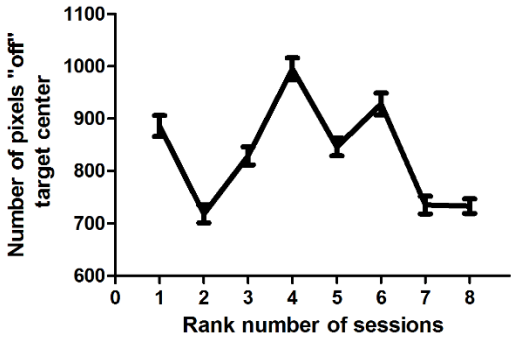

(b)

Figure 9 - Average data for 'time' (a) and 'precision' (b) and their standard errors (SEMs), plotted as a function of the rank number of the experimental session. The effect of the 'session' factor is significant for both performance variables (see *'Analysis of variance'* in the Results section)

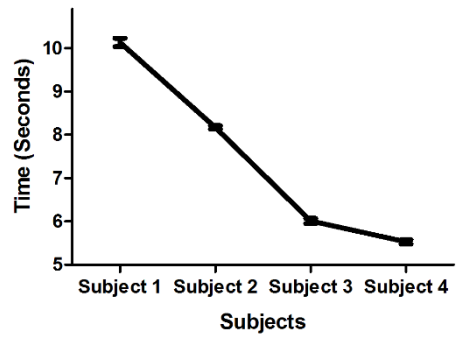

(a)

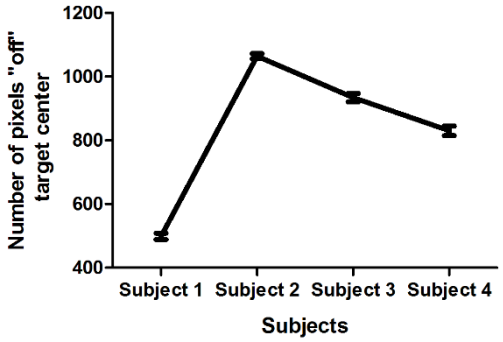

(b)

Figure 10 - Average data for 'time' (a) and 'precision' (b) and their standard errors (SEMs), plotted for the four different participants. The effect of the 'participant' factor is significant for both performance variables and significantly interacts with the 'session' factor (see *'Analysis of variance'* in the Results section)

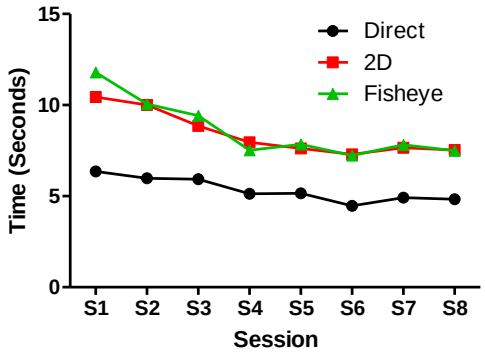

(a)

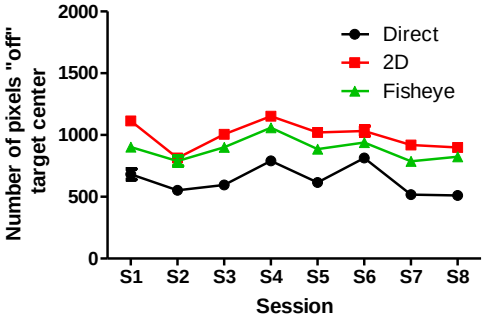

(b)

Figure 11 - Average data for 'time' (a) and 'precision' (b) and their standard errors (SEMs), plotted for the eight session and each visual feedback. The effect of the 'vision' and 'session' interaction is significant for both performance variables and significantly interacts with the 'session' factor (see *'Analysis of variance'* in the Results section).

In Figure 10, significant 'session' (S8) and 'vision' (V3) interaction on 'time' ($F(14,3839) = 140.67$ $p < 0.001$) and 'precision' ($F(14,3839) = 3.86$ $p < 0.001$) are shown. According

to these results, all the visual feedbacks lines were parallel to each other, so ‘vision’ (V3) conditions did not affect the training effect.

Individual performance evolution with training

These individual data are plotted in Figure 12(data of subject 1, female), Figure 13 (subject 2′s data, female), Figure 14 (subject 3′s data, male) and Figure 15 (subject 4′s data, male). The upper figure panels show average data for ‘time’ and ‘precision’ as a function of the rank number of the training session, the lower panels show the corresponding standard errors (SEM).

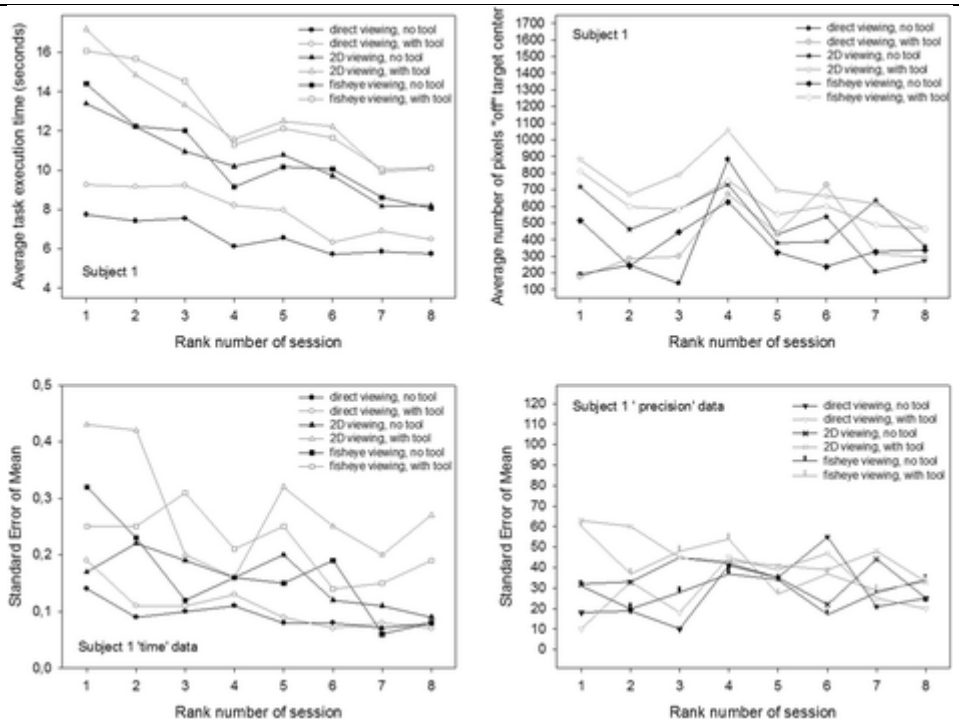

Figure 12 - Conditional performance curves for ‘time’ and ‘precision’ for the second participant (subject 2, female). Means (*upper panel*) and standard errors (*lower panel*) are plotted as a function of the rank number of the experimental training session.

Comparisons between individuals show that subject 1 starts with the slowest times, while the other three participants start noticeably faster, especially subjects 3 and 4, with subject 4 being the fastest of all. Subject 1, while being the slowest of all, starts with the best performance in precision, with the smallest “off” target pixel score, and keeps getting more precise with training while getting faster at the same time. Her

precision levels in the last of her eight training sessions are the best compared with the three others, with the smallest standard errors in all the training sessions. Her times at the end of training are comparable with the times of subject 2 at the beginning of the sessions, who gets faster thereafter but, at the same time, is the least accurate and does not get any better in the eight training sessions.

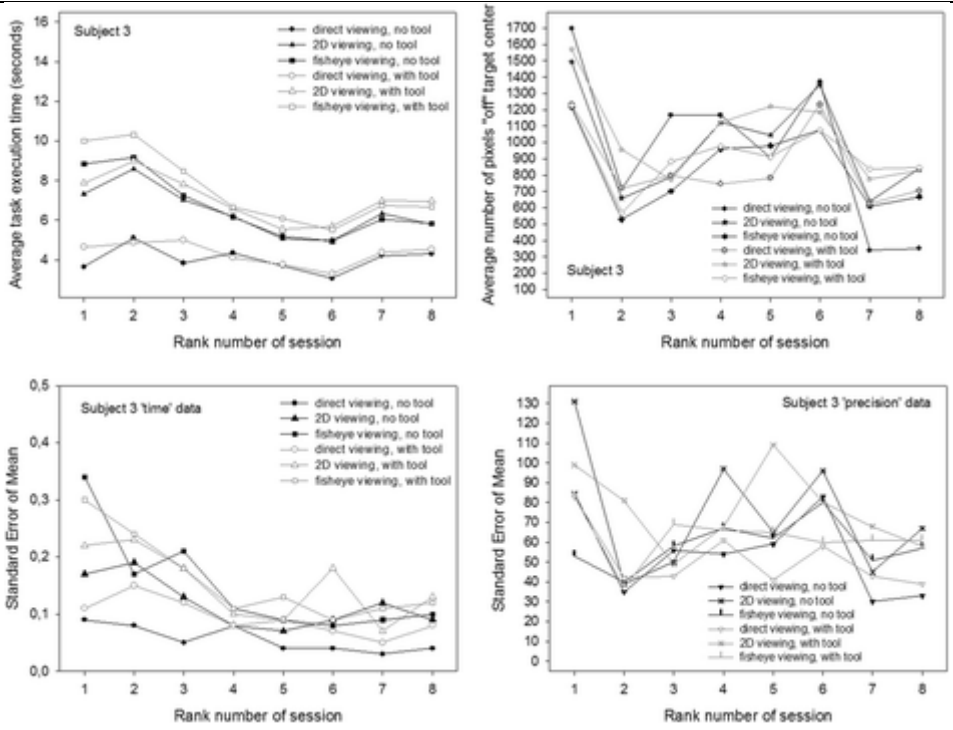

Figure 13 - Conditional performance curves for ‘time’ and ‘precision’ of the third participant (subject 2, female). Means (*upper panel*) and standard errors (*lower panel*) are plotted as a function of the rank number of the experimental training session.

Subjects 3 and 4 both start with the fastest times. Subject 3′s precision first improves drastically in the first session, then gets worse again as he is getting faster. In the last sessions, this subject’s performance improves with regard to precision while the times and their standard errors remain stable.

Subject 4 is the fastest performer. His average times and their standard errors decrease steadily with training and level off at the lowest level after his eight first training sessions. Precision, however, does not evolve, but varies considerably in all the training sessions, with the highest standard errors. Adding another 12 training

sessions for this subject results in even faster performances in all conditions with even lower standard errors, however, precision does not improve noticeably in any of the image viewing conditions, it improves a little in the direct viewing condition when a tool is used to execute the object positioning task. All subjects perform best and improve to a greater or lesser extent in time and precision of task execution in the direct viewing conditions. In the fisheye image viewing and the corrected 2D viewing conditions, only the performances of subject 1 and subject 3 become more accurate with training. Subject 2′s precision gets worse rather than better with training in the image viewing conditions. Subject 4′s precision remains unstable, with highs and lows up to the last of his twenty training sessions, where his average times and their standard errors have leveled out at the best possible performance score for ‘time’ under the task conditions given.

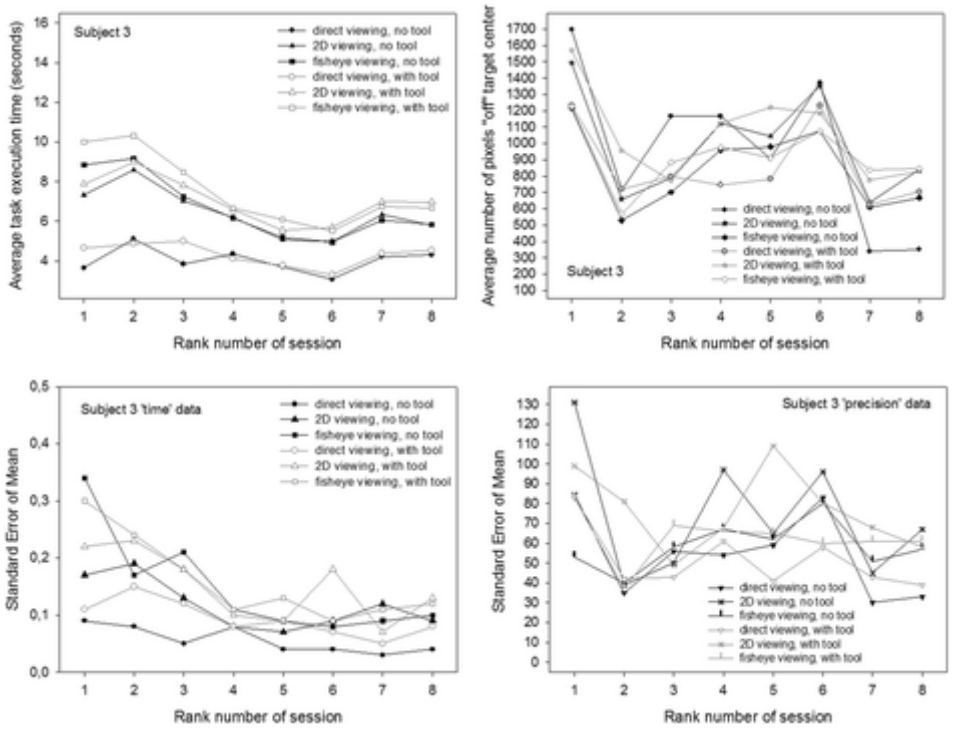

Figure 14 - Conditional performance curves for ‘time’ and ‘precision’ of the third participant (subject 3, male). Means (*upper panel*) and standard errors (*lower panel*) are plotted as a function of the rank number of the experimental training session.

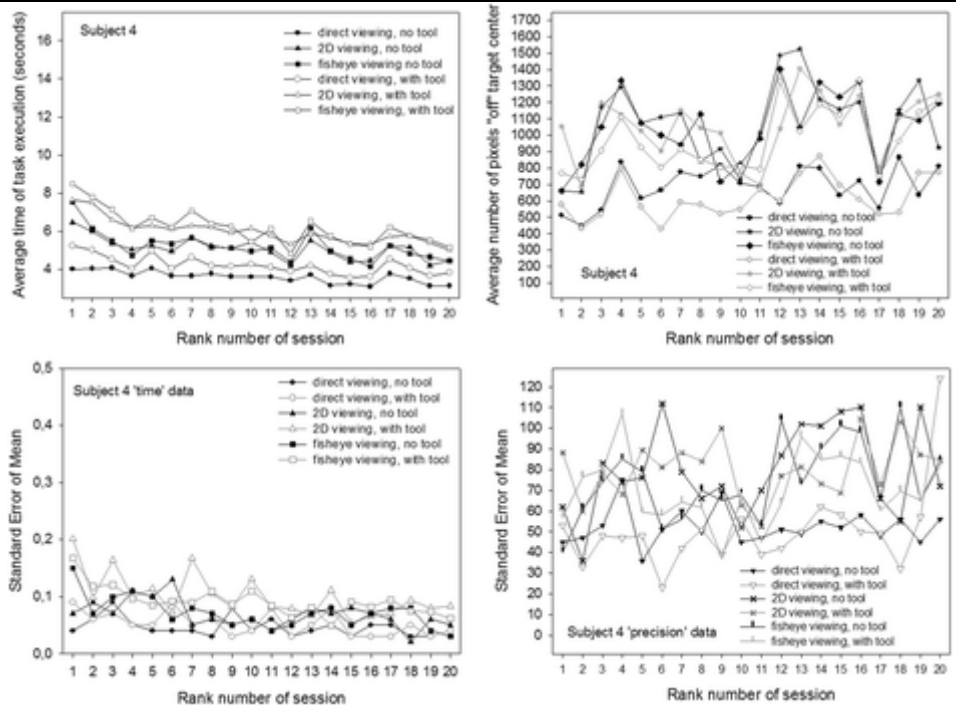

Figure 15 - Conditional performance curves for 'time' and 'precision' of the fourth participant (subject 4, male). Means (*upper panel*) and standard errors (*lower panel*) are plotted as a function of the rank number of the experimental training session. This participant was run in twelve additional training sessions, producing a total of 20 sessions instead of eight

Trajectory results

In the following results section, the trajectory data of the subjects were inspected in detail. The 'average distance from the reference trajectory' data was not inspected here because the ANOVA result for the session condition was not significant for this dependent variable, which was shown in the *Analysis of Variance* section.

The medians and scatter of the individual distributions relative to 'from-target-to-target duration' and 'dispersion in trajectory' for the different experimental conditions were computed first. Box-and-whiskers plots were generated to visualize these distributions. The mean data were submitted to analysis of variance (ANOVA) and conditional plots of means and standard errors as a function of the rank number of the trial sessions were generated for each subject to show the evolution of 'from-target-to-target duration' and 'dispersion in trajectory' with training.

Medians and extremes

Medians and extremes of the individual data relative ‘from-target-to-target duration’ and ‘dispersion in trajectory’ for the different experimental conditions were analyzed first as in [32]. The results of this analysis are represented graphically as box-and-whiskers plots here in Figure 16 and Figure 17. Figure 16 shows distributions around the medians of data from the manipulation modality with the tool in the three different vision conditions. Figure 17 shows distributions around the medians of data from the manipulation modality without the tool in the three different vision conditions.

The distributions around the medians, with upper and lower extremes, for the data relative to ‘from-target-to-target duration’ show that Subject 1 was the slowest in all conditions, closely followed by Subject 2. Subjects 3 and 4 were noticeably faster in all conditions and their distributions for ‘from-target-to-target duration’ generally display the least scatter around the median. These results also support the ‘time’ results in [32].

All subjects took longer in the tool-mediated manipulation modality (see graphs on left in Figure 17) compared to the by-hand manipulation modality without the tool. The shortest times are displayed in the distributions from the direct viewing condition and the longest times in the distributions from the fisheye image viewing condition.

Analysis of variance

In the first stage of ANOVA analysis, 2304 average data for ‘from-target-to-target duration’(Annex 1- Figure 4), 2304 average data for ‘average distance from the reference trajectory’(Annex 1- Figure 5), and 2304 average data for ‘dispersion in trajectory’(Annex 1- Figure 6) were submitted to Analysis of Variance (ANOVA) for *‘session’* (S_8), *‘vision’* (V_3), *‘participant’* (P_4), *‘manipulation’* (M_2), *‘touch*‘(T_2) conditions. The results of the ‘average distance from the reference trajectory’ did not perform any significant session interaction (Annex 1- Figure 5), so this dependent variable was not inspected further here.

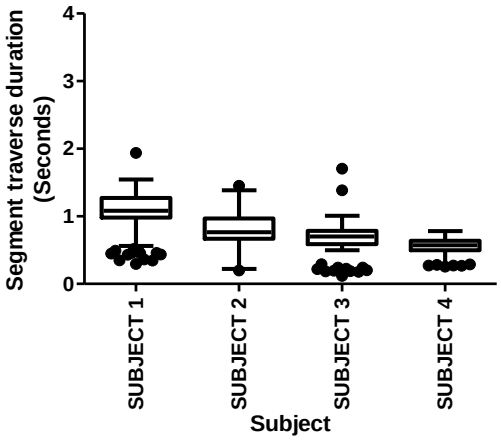

(a)

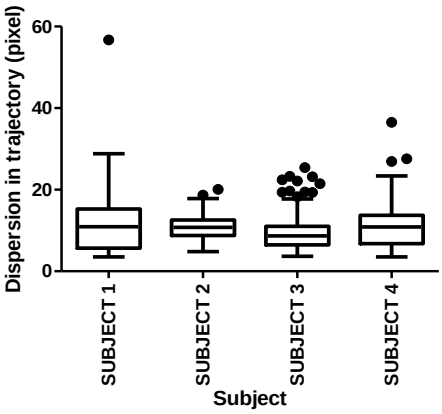

(b)

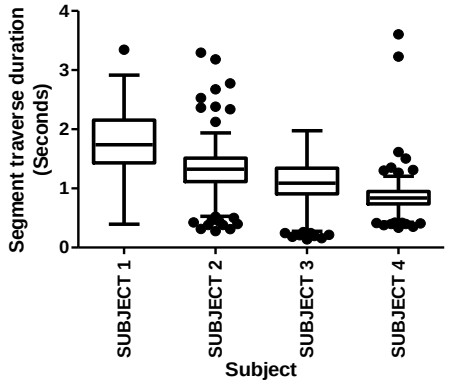

(c)

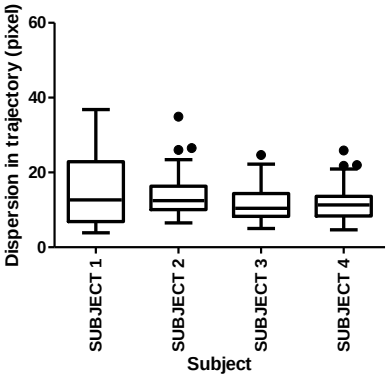

(d)

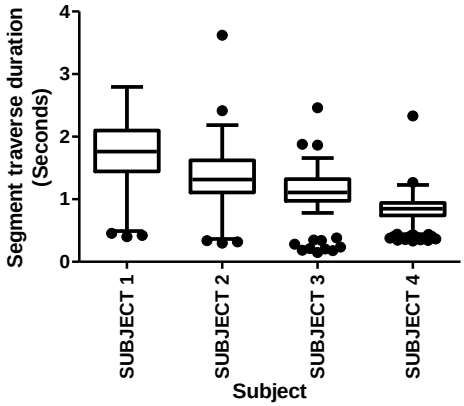

(e)

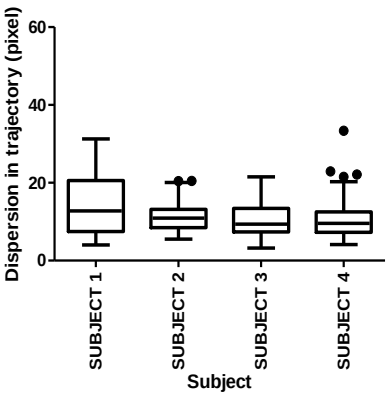

(f)

Figure 16 – Box-and-whiskers plots with medians and extremes of the individual distributions in manipulation modality without tool. (a) ‘from-target-to-target duration’ for direct vision (b) ‘Dispersion’ for direct vision (c) ‘from-target-to-target duration’ for undistorted vision (d) Dispersion’ for undistorted vision (e) ‘from-target-to-target duration’ for fisheye vision and (f) ‘Dispersion’ for undistorted vision.

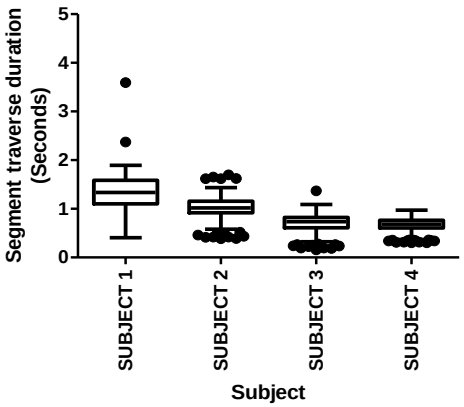

(a)

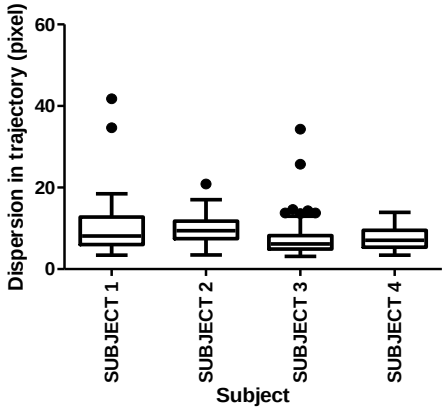

(b)

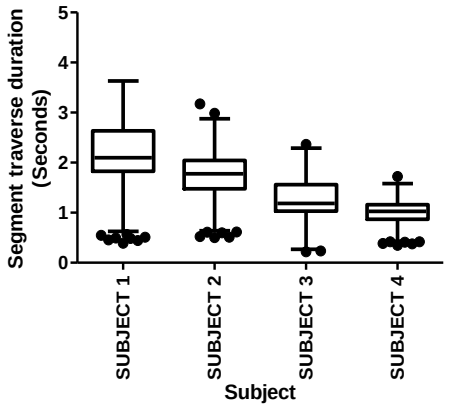

(c)

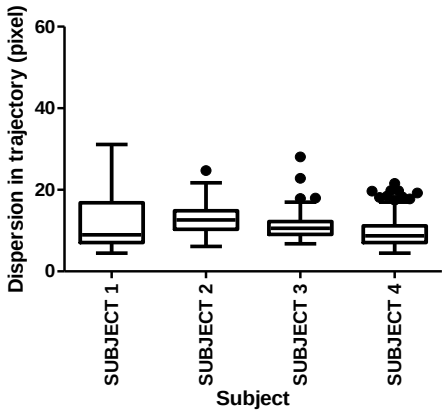

(d)

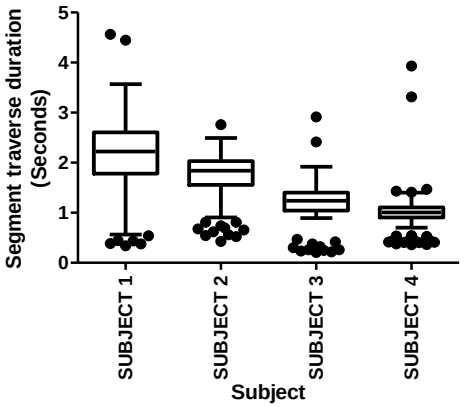

(e)

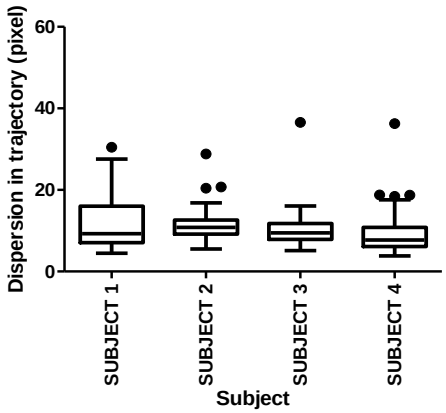

(f)

Figure 17 – Box-and-whiskers plots with medians and extremes of the individual distributions in manipulation modality with tool. (a) ‘from-target-to-target duration’ for direct vision (b) ‘Dispersion’ for direct vision (c) ‘from-target-to-target duration’ for undistorted vision (d) Dispersion’ for undistorted vision (e) ‘from-target-to-target duration’ for undistorted vision and (f) ‘Dispersion’ for undistorted vision.

In the second stage of ANOVA analysis, 2304 average data for 'from-target-to-target duration' and 2304 average data for 'dispersion in trajectory' were submitted to Analysis of Variance (ANOVA) for *'session'* (S_8), *'vision'* (V_3), *'participant'* (P_4), *'manipulation'* (M_2), *'segment'*(X_6). The distributions for 'from-target-to-target duration' and 'dispersion in trajectory' satisfy the general criteria for parametric testing (independence of observations, normality of distributions and equality of variance). Five-Way ANOVA was performed for a design plan $P_4xV_3xM_2\ xS_8xX_6$ with four levels of the *'participant'* factor P_4, which was analyzed as a main experimental factor here. Touch condition was removed from independent variables to focus on the main variables, the *'session'* (S_8), *'participant'* (P_4) and *'segment'* (X_6).

Principal variables

The differences between means for 'from-target-to-target duration' (Annex 1- Figure 7) and 'dispersion in trajectory' (Annex 1- Figure 8) of the different levels of each factor were statistically significant. Means and standard errors (SEM) for each level of each principal variable, and the ANOVA results are summarized in Annex 4-Table 1. For additional information, the 'average distance from the reference trajectory' results are also shown in Annex 4-Table 1.

Annex 4-Table 1 shows that the participants were significantly slower and significantly less stable in object movement in the image guided conditions compared with the direct vision condition. Comparing the means for the two levels of *'manipulation'* (M_2) shows that tasks were executed significantly faster when no tool was used, but they were scattering more in the trajectory movement. The most critical factors for the learning study here, the *'session'* (S_8), *'participant'* (P_4) and *'segment'* (X_6) factors, produced significant effects on 'from-target-to-target duration' and 'dispersion in trajectory'. These can, however, not be summarized without taking into account their interaction, which was significant for 'from-target-to-target duration' ($F(105, 2303) = 2.45$ $p < 0.001$) and for ''dispersion in trajectory' ($F(105, 2303) = 2.33$ $p < 0.001$). The differences between means for 'from-target-to-target duration' and 'dispersion in trajectory' of the three levels of the *'vision'* factor were displayed in Annex 4-Table 1.

Interactions

The *'participant', 'session'* and *'segment'* factors produced significant interactions with the *'vision'* factor, $F(6, 2303) = 53.68$ $p < 0.0001$ for *'participant' x 'vision*' on 'from-target-to-target duration', $F(10, 2303) = 56.82$ $p < 0.0001$ for *'segment' x 'vision'* on 'from-target-to-target duration'; $F(14, 2303) = 23.95$ $p < 0.0001$ for *'session' x 'vision'* on 'from-target-to-target duration'; $F(6, 2303) = 5.3$ $p < 0.0001$ for *'participant' x 'vision on* 'dispersion in trajectory'; $F(10, 2303) = 12.5$ $p < 0.0001$ for *'segment' x 'vision on* 'dispersion in trajectory' and $F(14, 2303) = 2.15$ $p < 0.01$ for *'session' x 'vision'* on 'dispersion in trajectory'.

To further quantify these complex interactions, *post-hoc* comparisons (Holm-Sidak procedure, the most robust for this purpose) for the three levels of *'vision'* (V_3) and the six levels of *'segments'* (X_6) in each level (Subject 1, Subject 2, Subject 3, and Subject 4) of the *'participant'* factor (P_4) were carried out for both dependent variables. The degrees of freedom (*df*) of these step-down tests are *N-k*, where *N* is the sample size (here 2304/4 = 576) and *k* the number of factor levels (here 3 + 6 = 9) compared in each test. The results of these post-hoc comparisons are displayed in Figure 18 for both conditions. Annex 4-Table 2, Annex 4-Table 3, Annex 4-Table 4, and Annex 4-Table 5 show 'from-target-to-target duration' results and Annex 4-Table 6, Annex 4-Table 7, Annex 4-Table 8, and Annex 4-Table 9 show 'dispersion in trajectory' results – only the significant results of these *post-hoc* comparisons, which give effect sizes in terms of differences in means, for 'from-target-to-target duration' and 'dispersion in trajectory', between the viewing conditions for each participant and session, *t* values, and the corresponding unadjusted probabilities. In these tables it was observed that the effect sizes do not evolve in the same way in the different participants as the sessions progress.

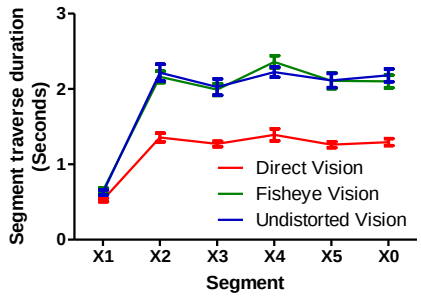

(a)

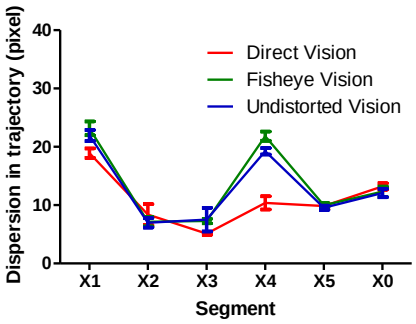

(b)

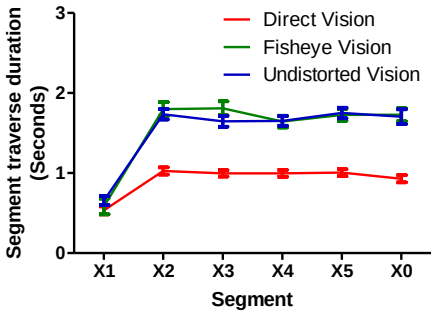

(c)

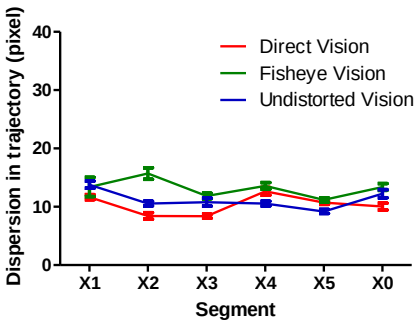

(d)

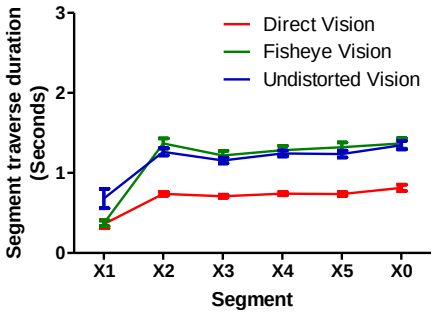

(e)

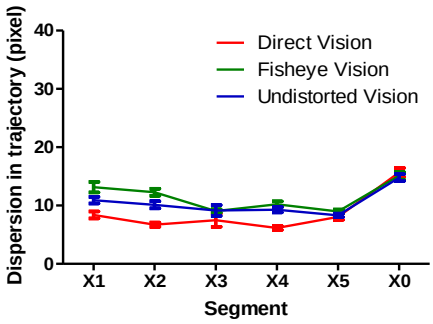

(f)

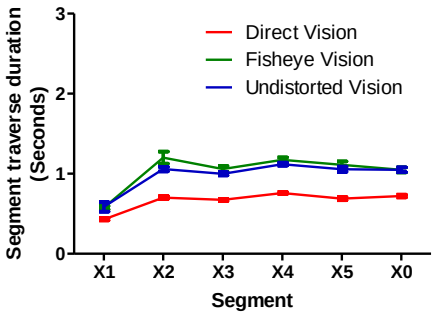

(g)

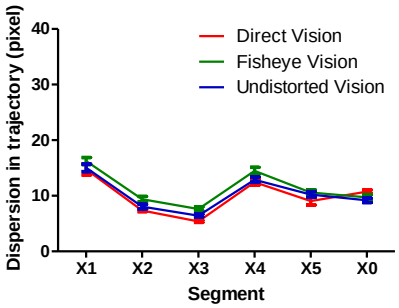

(h)

Figure 18 – Average data for ‘from-target-to-target duration’ and ‘dispersion in trajectory’ for Subject 1 ((a) and (b), respectively), Subject 2 ((a) and (b), respectively), Subject 3 ((a) and (b), respectively), and Subject 4 ((a) and (b), respectively) for segment and vision.

In the next step of the analysis, the conditional data for ‘from-target-to-target duration’ and ‘dispersion in trajectory’ were represented graphically. Figure 19 shows the effects of *‘session’* (S_8) on ‘from-target-to-target duration’ (a) and on ‘dispersion in trajectory’ (b). Figure 20 shows the effects of *‘participant’* (P_4) on ‘from-target-to-target duration’ (a) and ‘dispersion in trajectory’ (b). Figure 21 shows the effects of *‘segment’* (X_6) on ‘from-target-to-target duration’ (a) and ‘dispersion in trajectory’ (b). For further insight into the differences between participants, their individual functions (means and standard errors of the conditional performance scores) were plotted as a function of the rank number of the sessions. These functions permitted tracking the evolution of individual performance with training.

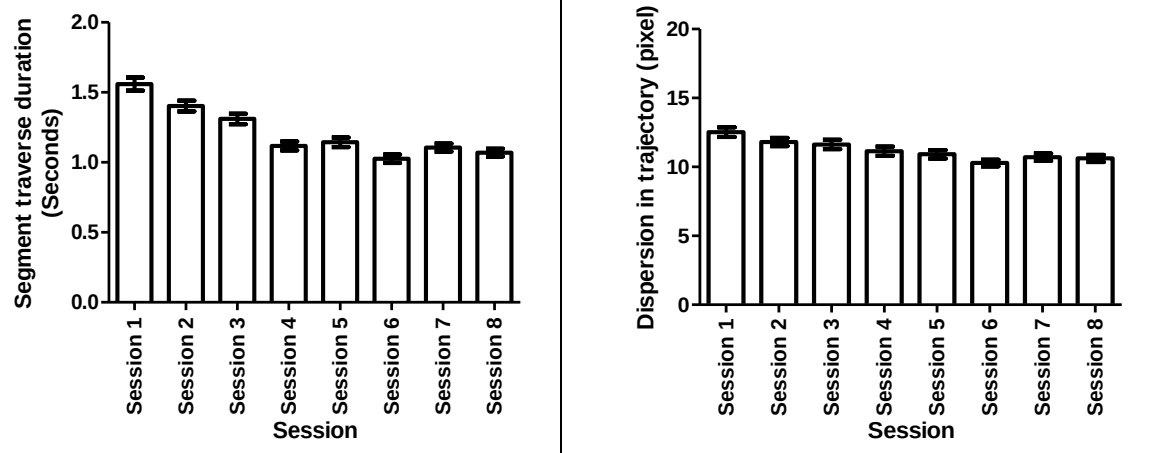

(a) (b)

Figure 19 – Average data for ‘from-target-to-target duration’ (*a*) and ‘dispersion in trajectory’ (b) and their standard errors (SEMs), plotted as a function of the rank number of the experimental session. The effect of the ‘session’ factor is significant for both performance variables

All subjects performed best and improved to a greater or lesser extent in ‘from-target-to-target duration’ in the direct vision conditions except for X1 segment. Visual feedbacks had different effects on each subject for each segment on ‘dispersion in trajectory’. All subjects were more precise in direct vision with X1 segment, except subject 4; there was no difference between direct vision and 2D visual feedback in X1 segment for subject 4. While there was no difference between 2D visual feedback and direct vision for X2 segment with subject 1, the rest of the subjects were more precise

in direct vision in X2 segment. Similarly, X3 segment only affects subject 2 and 4, where they were more precise with direct vision compared to 2D visual feedbacks. In X4 segment, all subjects were more precise with direct vision compared to 2D visual feedbacks. X5 and X0 segments only affected subject 2 in which she was more precise in undistorted vision in segment X5 and in direct vision in segment X0.

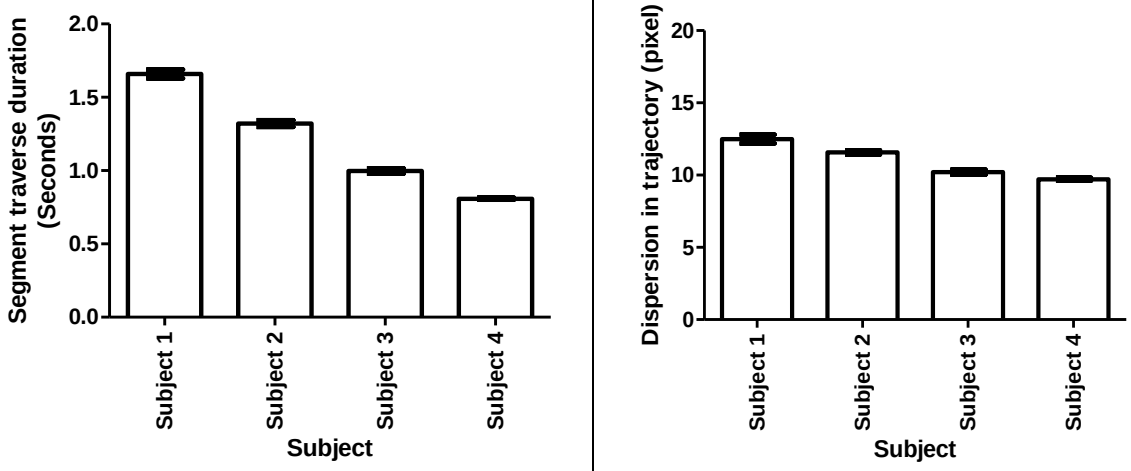

(a) (b)

Figure 20 – Average data for 'from-target-to-target duration' (a) and 'dispersion in trajectory' (b) and their standard errors (SEMs), plotted for the four different participants. The effect of the 'participant' factor is significant for both performance variables and significantly interacts with the 'session' factor (see *'Analysis of variance'* in the Results section).

Individual performance evolution with training

Individual data are plotted in Figure 22 (data of Subject 1, female), Figure 23 (Subject 2′s data, female), Figure 24 (Subject 3′s data, male) and Figure 25 (Subject 4′s data, male). The left side of the figures shows the 'from-target-to-target duration' and right sides for 'dispersion in trajectory' as a function of the rank number of the training session.

The 'from-target-to-target duration' results in individual performance evaluation figures shows similarities with Batmaz et al. [32]. While subject 1 starts with the slowest times, the other three participants start noticeably faster, especially subjects 3 and 4, with subject 4 being the fastest of all. Her times at the end of training are comparable with the times of subject 2 at the beginning of the sessions, who gets faster thereafter.

Subject 4 is the fastest performer like the ‘time’ results. His average times and their standard errors decrease steadily with training and level off at the lowest level after his eight first training sessions. His average times and their standard errors decrease steadily with training and level off at the lowest level after his eight first training sessions.

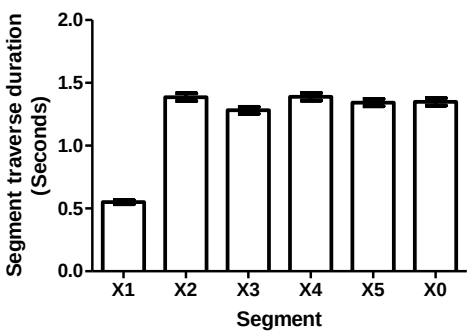

(a)

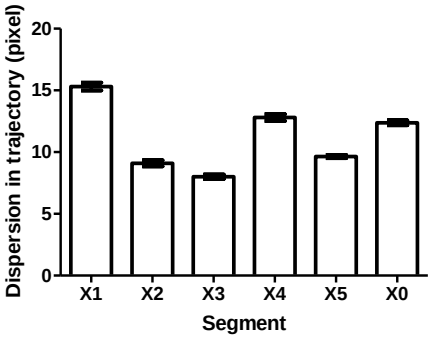

(b)

Figure 21 – Average data for ‘from-target-to-target duration’ (*a*) and ‘dispersion in trajectory’ (b) and their standard errors (SEMs), plotted as a function of segments. The effect of the ‘segment’ factor is significant for both performance variables

The trajectory data on the dispersion shows another important key point for individuals. Subject 1 has the most scattered trajectory within all subjects. However, she also has the only distinguishable learning curves on the trajectory data. She gets more stable in her movements after the eight training sessions. She kept getting more stable with training and faster at the same time [32]. The other subjects also moved more stable in their object movements, but these results were not as apparent as Subject 1.

The other important point in the trajectory dispersion data was the segments and their effect on the object movement of the individuals. For example, subject 1 considerably scattered object movements X1 and X4 segments in fisheye vision and undistorted vision. A similar result can be seen in subject 4’s first eight sessions, but this effect does not exist in the other subjects’ trajectory data. While subject 2’s trajectory data evolved after 8 sessions and got more stable in all segments, subject 3 is negatively affected by the X0 segment, he did not get any better in X0 segment and he gets even worse in the undistorted vision. Modalities in the trajectory complexity affect the

subjects' movements differently. This topic is further discussed in the second study of this chapter.

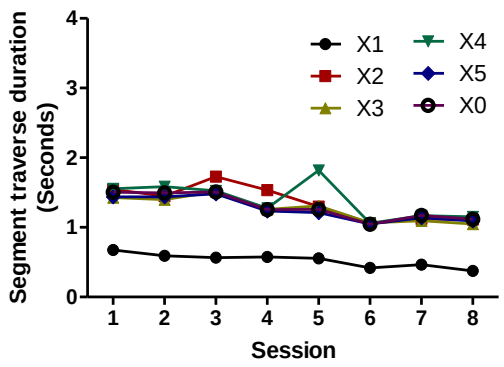

(a)

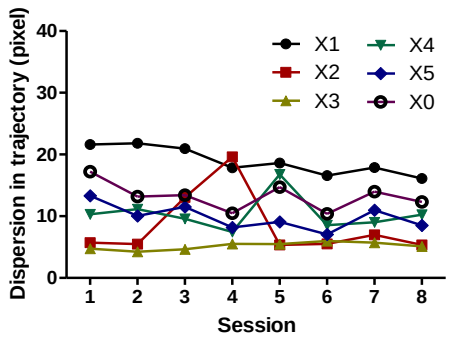

(b)

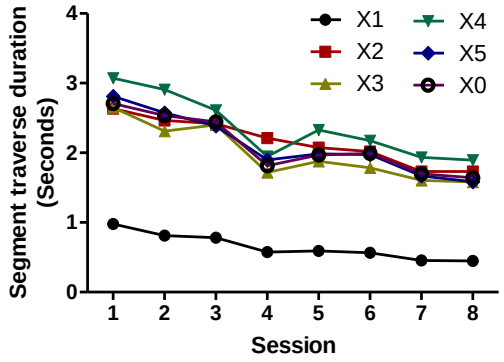

(c)

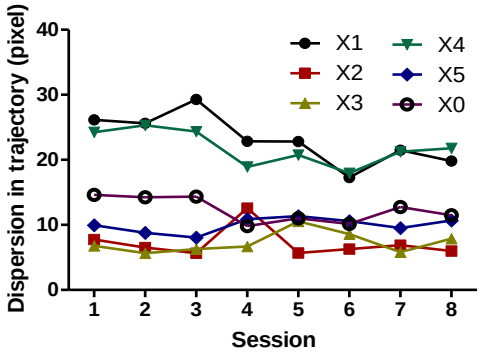

(d)

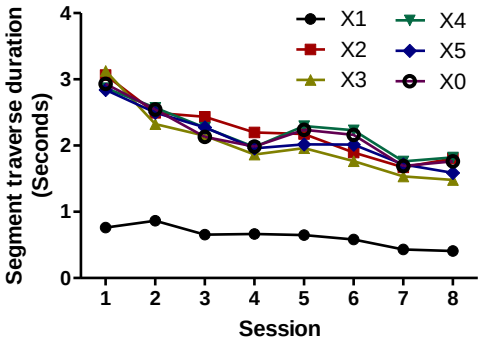

(e)

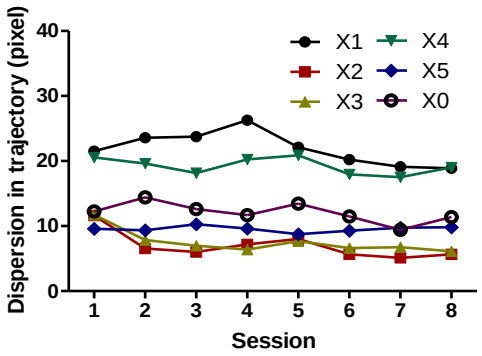

(f)

Figure 22 – Average segment data for 'from-target-to-target duration' and 'dispersion in trajectory' for direct vision ((a) and (b), respectively), fisheye vision ((c) and (d), respectively) and undistorted vision ((e) and (f), respectively) of Subject 1 plotted as a function of training session.

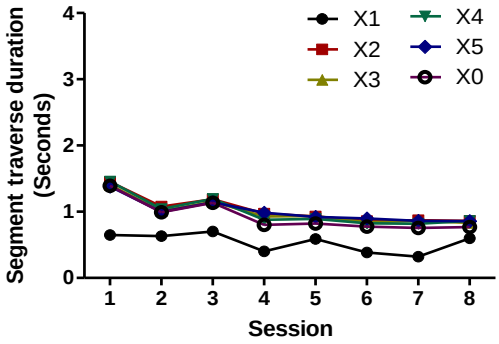

(a)

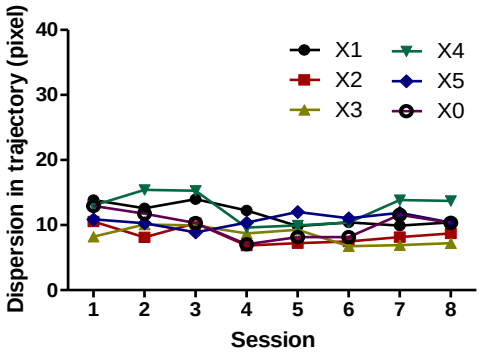

(b)

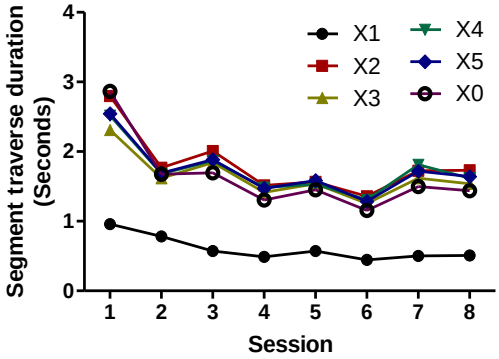

(c)

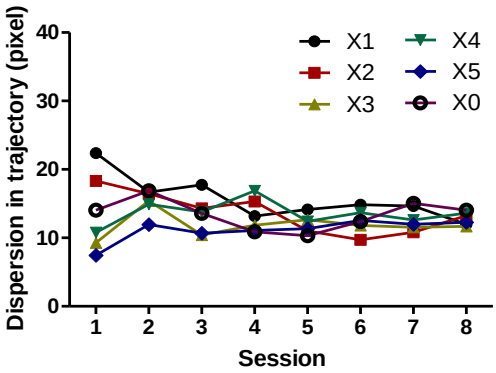

(d)

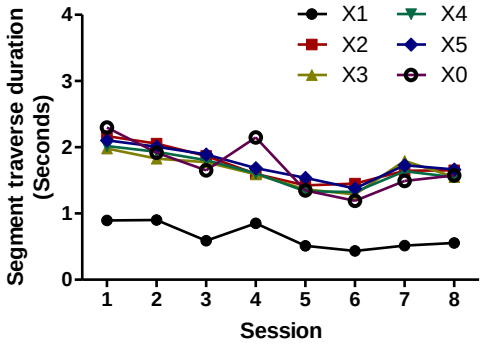

(e)

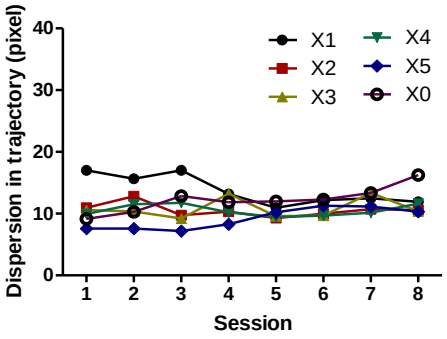

(f)

Figure 23 – Average segment data for ‘from-target-to-target duration’ and ‘dispersion in trajectory’ for direct vision ((a) and (b), respectively), fisheye vision ((c) and (d), respectively) and undistorted vision ((e) and (f), respectively) of Subject 2 plotted as a function of training session.

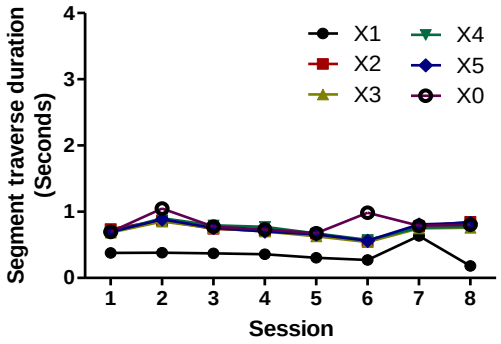

(a)

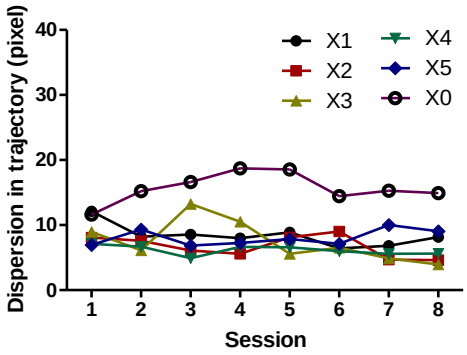

(b)

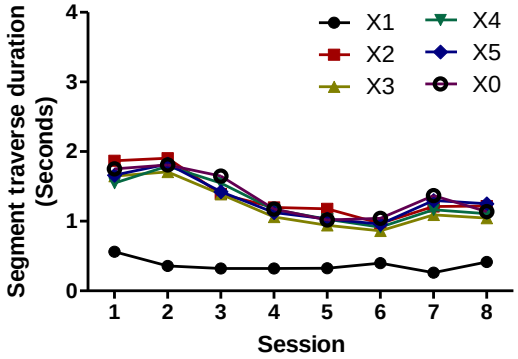

(c)

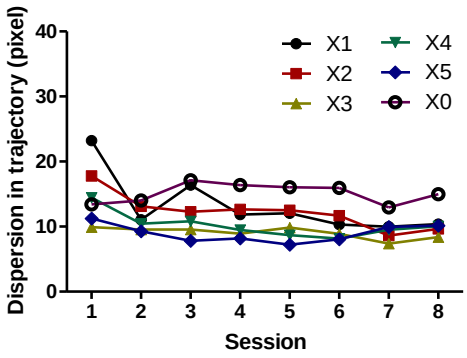

(d)

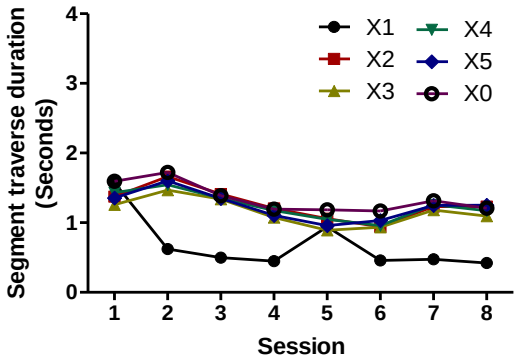

(e)

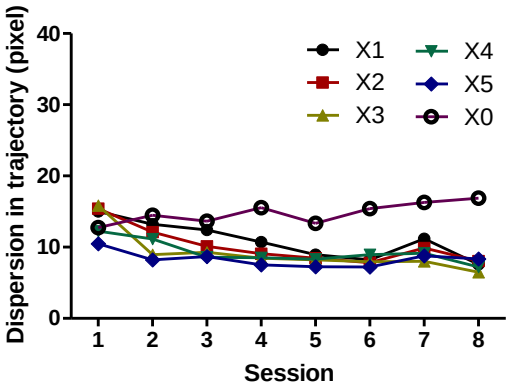

(f)

Figure 24 – Average segment data for ‘from-target-to-target duration’ and ‘dispersion in trajectory’ for direct vision ((a) and (b), respectively), fisheye vision ((c) and (d), respectively) and undistorted vision ((e) and (f), respectively) of Subject 3 plotted as a function of training session.

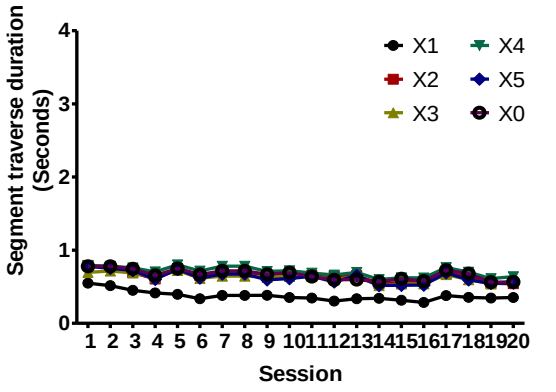

(a)

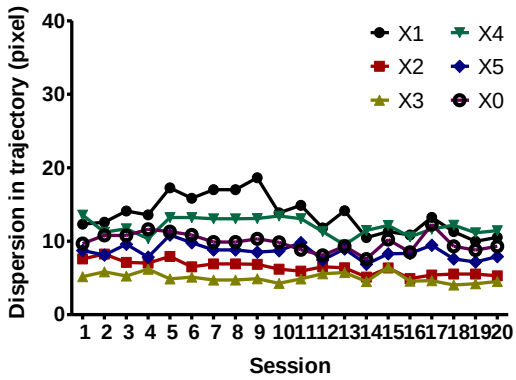

(b)

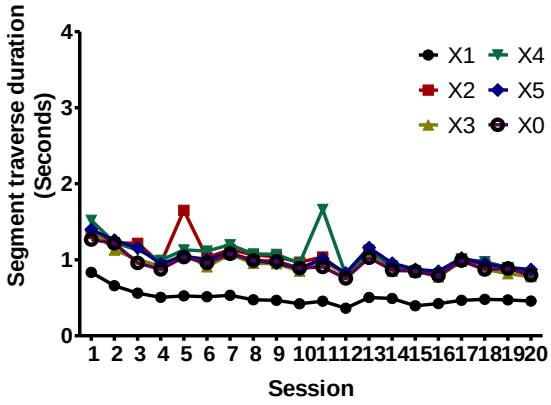

(c)

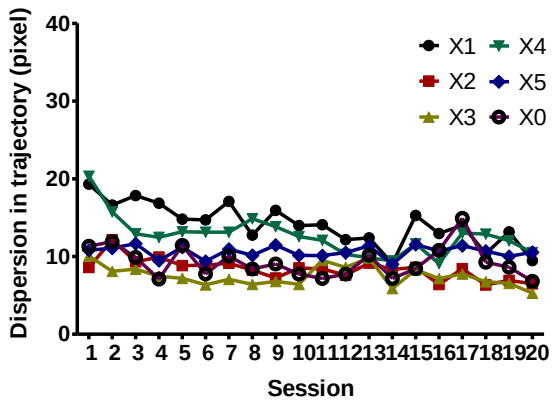

(d)

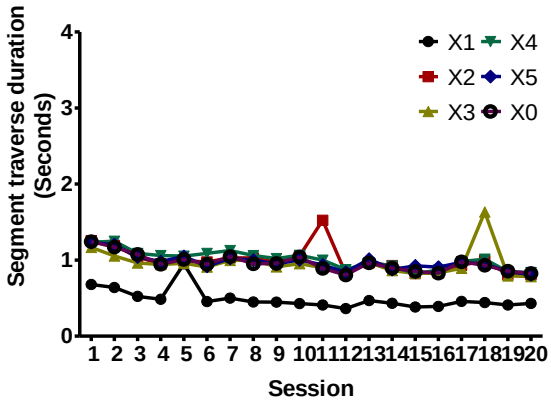

(e)

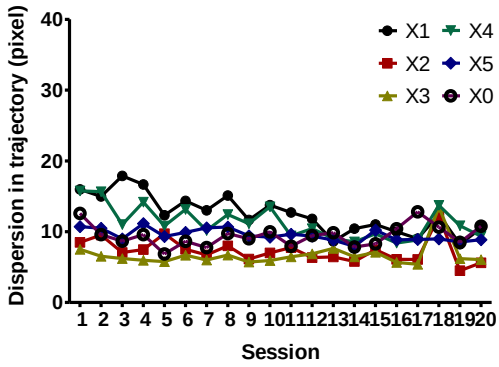

(f)

Figure 25 – Average segment data for ‘from-target-to-target duration’ and ‘dispersion in trajectory’ for direct vision ((a) and (b), respectively), fisheye vision ((c) and (d), respectively) and undistorted vision ((e) and (f), respectively) of Subject 4 plotted as a function of training session.

Discussion

As would be expected on the basis of previous observations [3,36,109] the results confirm that 2D video-image viewing negatively affects time, precision and goal-directed trajectory movement compared with direct action viewing (control). This performance loss is statistically significant. Although the disadvantage of image-guidance may diminish with training and eventually level off, none of the individuals gets to perform as well as in the direct viewing condition in the last training sessions. In fact, the effects of the viewing conditions vary significantly between individuals as a function of the training session, as shown by the two-by-two interactions between these factors. The results of the relevant *post-hoc* comparisons, summarized in Batmaz et al [32] Tables from 1 to 8 and Annex 4-Table 2 to Annex 4-Table 9 here give a quantitative overview of these variations, which are difficult to interpret in terms of any simple explanation or model.

Low-level explanations in terms of vision-proprioception conflict during task execution in the indirect viewing conditions would be a possible candidate. It has been shown that visual-proprioceptive matching, which is optimal in “natural” direct action viewing, is important for feeling in control of one’s actions during the visual observation of one’s own hand movements in eye-hand coordination tasks. This feeling of control, sometimes also referred to as *agency*, influences both the timing and the accuracy of hand movements [122]. Moreover, badly matched visual and proprioceptive inputs may reduce tactile sensitivity significantly [123].

However, this explanation is not a likely candidate here. Firstly, although, compared with direct viewing, image viewing was not perfectly aligned with the forearm motor axis, it did not exceed the recommended maximal offset angle of 45°, beyond which performance may not be optimal (e.g. [110]). Moreover, previous work has shown that the direction of arm movements (vertical *vs* horizontal) matters critically in image-guided performance. Tasks requiring arm movements mostly in the vertical direction (as in the experimental task here) were performed faster and with more precision than tasks requiring essentially movements in the horizontal direction, regardless of where the monitor for viewing the video images was placed [124]. Secondly, the video images received from the camera in the experiment were professionally calibrated for both

time and space. Spatial matching of the image conditions with the direct viewing condition was controlled by making sure the size of real-world action field parameters such as target, object, and tool sizes, were identical when viewed from the participants sitting position. Temporal matching was controlled by the algorithm driving the internal clock of the CPU, ensuring that the video-images where synchronized with the real-world actions, as specified in *Materials and Methods* of this chapter. In the software, delay between the captured image from cameras on top of the experimental setup and displaying the same image on the screen was less than 25 millisecond. In other words, there was no perceptible mismatch or misalignment in either time or space between actions represented in the video-images and actions viewed directly. In motor learning, both low-level and high-level processes contribute to the evolution of performance with training (e.g. [125,126]). High-level action intentions, which are closely linked to psychological factors such as response strategy preferences, were deliberately not controlled or selectively manipulated (no performance feed-back of any sort was given) in the experiment. “Natural” variations in high-level action intentions are therefore the most likely source of the inter-individual differences in the performances observed here. These typically occur spontaneously during training, are independent of low-levels task constraints, and reflect individual goal setting strategies predicted decades ago by results from seminal work in the field (e.g. [57]) and consistent with current neurophysiological models involving top-down decision control by the frontal lobe (e.g. [127]).

Wearing a glove does not significantly affect speed of execution, but does affect precision. This observation was not expected in the light of previous data (see [121]), but is explained by a reduction of tactile sensitivity to physical objects when no direct finger contact with the object is possible, which may be detrimental to feedback signaling from hand to cortex for eye-hand coordination. This interpretation relates to earlier findings showing that the direct manipulation of objects by hand is combined with the visual and tactile integration of physical object parameters for action planning, gestural programming, and motor control ([53,56,128,129]). This possibly involves cortical neurons with non-classic receptive field structures in the brain [54,55]. It can be assumed that under conditions of touch with direct contact between the physical object and the fingers of the hands, the finely tuned mechanoreceptors under the skin

which control both fingertip forces and grasp kinematics [52] send stronger feed-back signals to these cortical neurons [130].

Tool-mediated object positioning was as precise as by-hand direct object positioning, but task execution was slower, as expected in the light of previous observations on novices (e.g.[120]). Tool-specific motor requirements (e.g. [53,111,131–134]), such as having to grab and hold the handle of the tool, or having to adjust one's hand movements to the shape and the size of the tool, readily account for this effect. The effect of tool use on execution times is present throughout all the training sessions as shown in the conditional performance curves of the four individuals here.

The most important results in the light of the study goal are the significant inter-individual differences in performance strategies during training found here in this image-guided pick-and-place task. These differences are reflected by strategy specific trade-offs between speed of task execution and the precision with which the object is placed on the targets. As predicted, these trade-offs occur spontaneously and without performance feedback (e.g. [57]). The observations lead to understand why monitoring only execution times for learning curve analysis in simulator training is not a viable option. Some trainees may get faster, but not necessarily better in the task, as shown here. Yet, in a majority of simulator training programs for laparoscopic surgery, the relative precision of image-guided hand maneuvers based on a conditional pixel-by-pixel analysis of hand or tool-movements from the video image data is not taken into account in the individual's learning curve. Neglecting the functional relationship between the time and the precision of task execution highlighted by the results from this study here is likely to have a cost. Individuals start the training sessions with different goals on their minds. Some place their effort on performing the object positioning task as fast as possible while others place their effort on being as precise as possible. The conditional performance curves reveal that the choice to privilege one strategy goal (either speed or precision) at the beginning has measurable consequences on the individual performance evolution at further stages of training. One trainee, who privileges precision at the outset (subject 1), becomes even more precise with further training, and also gets faster. Two other trainees (subjects 2 and 3) start fast, and re-adjust their execution times in mid-training, possibly because they realize that they may not perform with enough precision. One of them (subject 3)

manages, indeed, to become more precise by adjusting his speed strategy to a slightly slower temporal performance level. One trainee, the fastest performer here (subject 4), starts fast and gets faster steadily with training in all conditions, yet, his precision never stabilizes. Even with twelve additional sessions, there was no measurable improvement in the precision score of this trainee.

Study 2- Effects of 2D Monitor Position and Image Viewing Conditions

In the first study described in this chapter, the learning effect under conditions of direct vision and image guidance is studied in different manipulation modalities. In short, results showed that image guidance makes subjects slower and less precise and even after eight learning sessions, subjects do not get as fast or as precise as direct vision in image guidance. To overcome the disadvantages of the image guidance, several methods are proposed for use in surgical theaters. One of them is enhancing ergonomic factors in the operating rooms and another one is developing new ways to present the real world in image guidance systems. In the second chapter, these two different methods are explored using the “Excalibur” experimental setup.

Study Goal and Hypotheses

In image-guided processes for decision and action, as in laparoscopic surgical interventions, the human operator has to process critical information about what his/her hands are doing in a real-world environment while looking at a two-dimensional (2D) or three-dimensional (3D) representation of that environment displayed on a monitor. This virtual information needs to be correctly interpreted by the brain to ensure safe and effective human intervention [1,135–137]. In comparison with direct observation and action, image-guided eye-hand coordination represents a disadvantage [3,138], for essentially three reasons. First, veridical information about real-world depth is missing from the image representations. Second, the operator is looking sideways or straight ahead at a monitor, or at an image displayed by a head-mounted device, instead of looking down on his/her hands. Third, due to a variety of camera and image calibration problems, the hand or tool movements displayed virtually may not match the real-world movements in time and space.

Recently developed 3D visualization technology may represent a possibility for overcoming the drawbacks of 2D views, yet, whether different 3D imaging solutions all significantly improve task performance has remained a controversial issue. While

some authors have reported that 3D viewing significantly improves task performance in both novices and experts [38–44], others have found equivalent task performance comparing 2D viewing to 3D viewing systems [45–48]. It has been suggested that differences in task complexity and inherent affordance levels [49,50], or inter-individual differences in adaptive goal-setting strategies of novices [32] may account for differences in results between studies using similar 3D viewing systems.

The most recent results available in the dedicated literature come from the study by Sakata and colleagues. These authors [44] used a laparoscopic (Olympus Endoeye Flex) HD camera system that can be switched from 2D to 3D stereoscopic viewing mode. This system gets rid of problems relative to viewing position and viewing distance [139], and it is reported that under such conditions, the 3D viewing mode produces better depth judgments and faster task execution in both novice and expert surgeons.

Monitor position [109] matters in as far as a considerable misalignment of the eye-hand-target axis during task execution, caused by a sub-optimal monitor position constraining the operator to turn his/her head sideways during an intervention, significantly affects measures of postural comfort [110,140], and interventional safety[141]. A monitor placed straight ahead of the operator, in line with the forearm-instrument motor axis and at a height lower than the eye-level when looking straight ahead, is recognized as the recommended optimal standard [109]. Previously reported effects of monitor position on fatigue levels or speed of task execution [47,140,141] point towards complex interactions between viewing angle, height of the image in the field of observation, expertise or training, and task sequencing. Varying the task sequences and allow operators to change posture between tasks, for example, was found to have significantly beneficial effects on fatigue levels of novices in simulator training for pick-and-place tasks [4].

Spatial and/or temporal mismatches between images and real-world data may occur in monitor views generated by different camera types. Surgical fisheye lens cameras, for example, provide a hemispherical focus of vision with poor off-axis resolution and aberrant shape contrast effects at the edges of the objects viewed [34]. Current prototype research struggles to find camera solutions which provide a larger, corrected

focus of vision compared with that of commonly used laparoscopic cameras [35]. Whether fisheye image views affect eye-hand coordination performance to a greater extent than undistorted 2D views is not known. Furthermore, spatial as well as temporal mismatches between movements viewed on the monitor and the corresponding real-world movements may occur as a consequence of specific constraints for placing the camera. In the case of endoscopic surgery, for example, the camera moves with the tool used to perform the intervention, and movements represented visually are not aligned with the surgeon's real arm and hand movements. Another problem with camera-monitor systems for technology-driven visuo-motor tasks consists of temporal asynchronies between frames of reference for vision and action [114,142]. These are known to produce a cognitive phenomenon called visual-proprioceptive mismatch, which negatively affects task performance [123]. Cognitive mismatch of relative distances in virtual reality representations of large-scale environments to their real-world counterparts produce wrong turns in navigation tasks [143]. To overcome this drawback, the operator needs to work out a way of compensating for the mismatched cues and, as a consequence, feels less in control of his/her actions [125,126]. Experienced surgeons learn to cope with this problem through training, but the cognitive mechanisms of this adaptation are not understood.

When a tool is used to manipulate physical objects dynamic changes in cognitive hand and body schema representations [112,113,132–134] occur as a consequence, and these cognitive changes are consolidated by repeated tool-use [111]. For lack of experience in laparoscopic interventions of tool-mediated eye-hand coordination, the performances of novices can be expected to be slower and less precise in tool-mediated object manipulation compared with the "natural" situation where they are using their hands directly and their skin receptors are in touch with the manipulated object.

Reaching operations in peri-personal space are encoded topologically in terms of step-by-step representations of hand or hand-tool trajectories (e. g. [127,144]). Movements constrained by the use of a tool [145] and unconstrained movements of the bare hand (e.g. [145]) produce different trajectory shapes, with greater or lesser angles of curvature, and are affected to a greater or lesser extent by the eccentricity of targets in the action field (e.g. [145,146]). Moreover, reaching movements executed with and

without a tool are known to extend visual-tactile perceptual interaction for eye-hand coordination to locations further away in peri- personal space compared with unconstrained reaching [111–113,133]. It can therefore be expected that the effects of 2D and 3D viewing modes on constrained versus unconstrained hand movements are not be the same across target locations in the subjects' peri-personal space.

In this study here, the same five-step pick-and-place-task is executed by complete novices using their bare dominant hand or a tool as in study 1 of chapter 1 except for glove wearing. Individuals with no surgical experience at all scoring high in spatial 3D perspective taking ability [108] to eliminate, as much as possible, hidden sources of potentially relevant eye-hand coordination skill variations in surgical study populations were selected. A large majority of previous findings in this field were obtained with populations of surgeons with or without laparoscopic training, divided into "novices" and "experts" on that basis. Some relevant hidden sources of skill variability may have been left unaccounted for given that all surgeons share expertise in surgical eye-hand coordination procedures. The homogeneity of such experience in a "novice" study group may be difficult if not impossible to control. In novice population here, all individuals are absolute beginners in image-guided eye-hand coordination and, in addition, they have no other potentially relevant surgical eye-hand coordination expertise. Here, the effects of 2D image viewing with near-optimally and sub-optimally positioned monitors to the effects of direct "natural" 3D and to the effects of stereoscopic 3D viewing through a head-mounted display were compared. Effects on both the time the precision and the trajectory of task execution are assessed. The head-mounted 3D system gets rid of problems relative to both viewing position and viewing distance.

On the basis of results from study 1 and previous work [3,32,36], it is predicted that "natural" top-down direct viewing produces the best task performance for time and precision compared with top-down 2D image views (fisheye or corrected). As predicted by other [109,47], a sub-optimal monitor position, where the subject has to look sideways to perform the task, is predicted to affect task performance negatively compared with a near-optimal viewing position, where the monitor is aligned with the fore-arm motor task execution axis and the subject is looking straight ahead. The head-mounted 3D system used here presenting the same advantage of controlling for effects

of viewing angle and distance as the 3D stereo system in Sakata et al [44], faster task execution times compared with 2D views from a near-optimally placed monitor were expected. In the system here, the stereo view is generated by two HD fisheye cameras at fixed locations, while in the display used by Sakata et al [44], the endoscopic HD camera producing the images for left and right moves along with the tool.

Materials and Methods

Participants

Eight healthy right-handed men ranging in age between 25 and 45, and eight healthy right-handed women ranging in age between 25 and 45 participated in this study. They were all highly achieved professionals in administrative careers, with normal or corrected-to normal vision, and naive to the scientific hypotheses underlying the experiments. Pre-screening interviews were conducted to make sure that none of the selected participants had any particular experience in knitting, eating with chopsticks, tool-mediated mechanical procedures, or surgery.

Study groups

After pre-screening, subjects were divided at random into two groups of four men and four women each. Both groups performed the same tasks under the same conditions with the exception of that of the 2D monitor position, which varied between groups. The monitor was placed sideways for one group, and straight ahead for the other.

Experimental platform

In this study, direct vision, undistorted vision, fisheye vision and Oculus 3D vision shown in Figure 26 are used for the experiments. Figure 26 (a) represents Direct Vision, Figure 26 (b) represents Oculus 3D Vision, Figure 26 (c) and Figure 26 (d) represents fisheye vision with sideways and straight ahead views, respectively, Figure 26 (e) and Figure 26 (f) represents undistorted vision with sideways and straight ahead views, respectively.

(a)

(b)

(c)

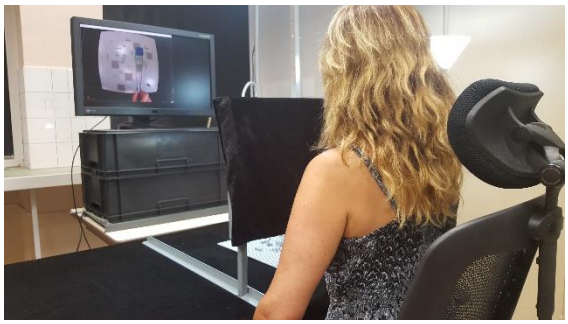

(d)

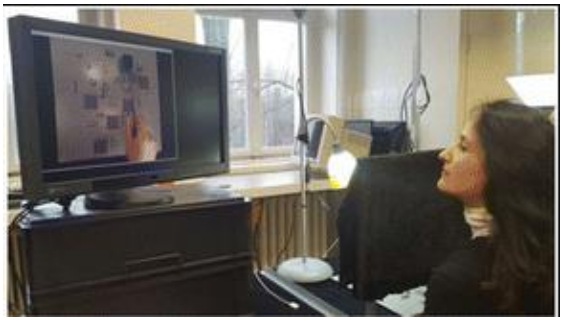

(e)

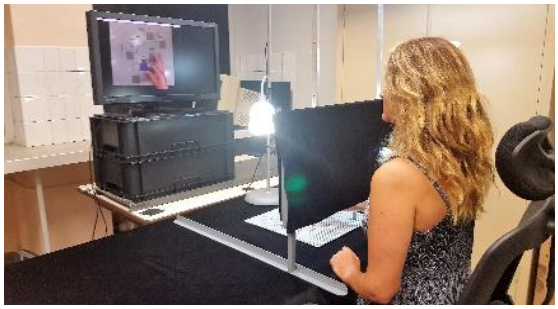

(f)

Figure 26 – Different visual feedback systems used in the first chapter second study. (a) Direct vision-no tool, (b) Oculus vision no tool (c) side view, fisheye vision, tool manipulation, (d) straight ahead view, fisheye vision, tool manipulation, (e) side view, undistorted vision, tool manipulation (f) straight ahead view, undistorted vision, no-tool manipulation.

Procedure

In the second study of first chapter, two different view modalities were used, as explained in introduction. For the group who performed the 2D image-guided conditions with the monitor placed sideways, there was a lateral angle of offset from

the forearm motor axis of about 45° to the left (sub-optimal monitor position, see introduction), and the screen was about 75-cm away from their eyes Figure 26(c) and Figure 26(e) used as in study 1. For the group who performed the 2D image-guided conditions with the monitor placed straight ahead of them, there was no lateral offset from the forearm motor axis, and the screen was about 150 cm away from their eyes (Figure 26(e) and Figure 26(f)). To compensate for the change in image size on the screen with the change in body-to-screen distance, the image on the screen was adjusted, ensuring that the perceived scale of the RAF displayed in an image subjectively matched the perceived scale of the RAF when viewed directly.

Participants were instructed that they were going to be asked to perform this task under different conditions of object manipulation: with their bare right hand or using a tool, while viewing the RAF (and their own hand) directly in front of them, on a computer screen, or through the head-mounted Oculus device rendering a 3D image.

An experimental session always began with the easiest condition of direct viewing like the first chapter, the order of two 2D and 3viewing conditions (2D undistorted, 2D fisheye, 3D OCULUS) was counterbalanced, between sessions and between participants, to avoid order specific habituation effects. For the same reason, the order of the tool-use conditions (with and without tool) was also counterbalanced, between sessions and between participants.

Cartesian Design Plan and Data Generation

Experimental design

Given the four levels of the vision factor (V_4: direct, fisheye, undistorted and Oculus 3D) combined with the two levels of the manipulation factor (M_2: no tool *vs* tool), the two levels of the gender factor (G_2: men, women) and the two levels of the session factor (S_2: first session *vs* second session), and with ten repeated trial sets per condition for four individuals of each gender in the two study groups, which leads to Cartesian design plan with four principal design variables $V_4 \times M_2 \times G_2 \times S_2$ and ten repeated trial sets in each condition and for each of the eight individuals from each of the two study groups with the two different monitor positions. The monitor position

factor (P_2: sideways *vs* straight ahead) is the fifth principal design variable (*between-groups factor*).

Data generation

The data recorded from each of the subjects were analyzed as a function of the different experimental conditions, for each of the four dependent variables ('time', 'precision', 'from-target-to-target duration' and 'average distance from the trajectory').

In a first step, the data from the two study groups with the different 2D monitor positions were grouped together to assess the effects of the inter-group factor P_2 (monitor position). A five-way analysis of variance (ANOVA) was run on raw data for 'time' and 'precision'. This analysis took into account only the two 2D conditions of the viewing factor (2D undistorted *vs* 2D fisheye) in combination with the two levels of the monitor position factor (straight ahead *vs* sideways), the two levels of the manipulation factor (tool *vs* no tool), the two levels of the gender factor (men *vs* women), and the two levels of the session factor (first session *vs* second session). Given ten repeated trial sets per condition with four men and four women in each of the two study groups, the following five-factor analysis was acquired: $V_2 \times P_2 \times M_2 \times G_2 \times S_2$ combined with 10 repeated sets for the four individuals per gender and a total of 1280 raw data for 'time' and for 'precision'.

In a second step, the data from each study group were analyzed separately. Descriptive analyses were performed first, and boxplots showing the data distributions around the medians in the four different viewing conditions, for each study group separately, were generated (Batmaz et al [31] -Figure 3). Outliers in the data were indeed rare and given the large amount of data collected for each condition, correcting these few by replacing them by averages would not have changed the statistical analyses. The raw data for each group were therefore submitted to ANOVA as shown in Batmaz et al [31] - table 1.

The second step analyses took into account all four conditions of the viewing factor (direct *vs* 2D *vs* 2D fisheye *vs* 3D head-mounted) for each study group in combination with the two levels of the manipulation factor (tool *vs* no tool), the two levels of the gender factor (men *vs* women), and the two levels of the session factor (first

session *vs* second session). Given ten repeated trial sets per condition with four men and four women in each of the two study groups, the following four-factor analysis was used: V_4 x M_2 x G_2 x S_2 combined with 10 repeated sets for the four individuals per gender and a total of 1280 raw data for 'time' and for 'precision'.

Furthermore, an additional repeated measures ANOVA used for *straight ahead* group including all four conditions of the viewing factor (direct *vs* 2D *vs* 2D fisheye *vs* 3D head-mounted) with the two levels of the manipulation factor (tool *vs* no tool) for eight subjects for 2 sessions. Given 20 repeated trial sets per condition (both session one and session two are included), the following two-factor analysis was used for ANOVA: V_4 x M_2 combined with 20 repeated sets for eight subjects and a total of 1280 raw data for 'time' and for 'precision'. For repeated measures (RM) ANOVA, average execution time and average precision for each combination of participant was calculated and the following two-factor analysis was used for RM ANOVA: V_4 x M_2 combined with eight subjects' average data and a total of 64 data for 'time' and for 'precision'. Only for this analysis, SPSS 18 was used to get Huynh-Feldt correction.

For the trajectory analysis, only straight-ahead conditions were considered because of the ergonomic results mentioned in the introduction. For each x, y coordinate sampled in trajectory, its lateral offset from the reference trajectory was calculated, which is indicated by the straight green lines in the graphs in Batmaz et al [30] Figure 4. The average individual data from each experimental condition were committed to five-way analysis of variance (ANOVA) on the basis of a Cartesian design plan $P_8 \times V_3 \times M_2 \times T_6 \times S_2$, with eight participants (P_8), three levels of viewing (V_3:Direct, Undistorted, Oculus 3D, two levels of movement (M_2: constrained vs unconstrained), six levels of the trajectory segment location factor (X_6), and two levels of the session factor (S_2). With this design plan, a total of 576 means for the dependent variable lateral trajectory offset (precision), and 576 means for the dependent variable movement time were used.

Results

‘Time’ and ‘precision’ results

Means and standard errors for each of the two dependent variables ('time' and 'precision') were computed for a first scrutiny, and then the raw data were submitted to analysis of variance (ANOVA).

Batmaz et al [31] - Table 1 summarizes the results of this first analysis, showing means and standard errors for the different experimental conditions (effect sizes), and F and p values signaling the statistical significance of the effect of each principal design variable (factor) on the dependent variables ‘time’ and ‘precision’. ANOVA results for raw ‘time’ and ‘precision’ data can be found in Annex 1- Figure 9 and Annex 1- Figure 10. Annex 1- Figure 15 and Annex 1- Figure 16 show the mean data analysis for replacing ‘time’ and ‘precision’ data. In these tables, averages of ten successfully executed trials were submitted to ANOVA.

The results for ‘time’ show no effect of 2D undistorted *vs* 2D fisheye, but significant effects of monitor position, manipulation, session, and gender. Subjects were significantly faster in the group where the monitor was placed straight ahead of them. They were significantly faster when no tool was used to perform the task. Times are significantly shorter in the second session compared with the first (training effect). Results for ‘precision’ show a significant effect of viewing where 2D fisheye viewing yields a significantly better precision score than 2D undistorted viewing. Subjects were significantly more precise in the group where the monitor was positioned sideways. Neither the manipulation mode, nor the session factor (training), had any significant effect on ‘precision’ in this analysis. There were no significant two-way interactions between factors.

Four-way ANOVA was performed on raw data for ‘time’ and ‘precision’ from each of the two study groups independently. These results can be found in Annex 1- Figure 11 and Annex 1- Figure 12 for ‘time’ and ‘precision’ in straight ahead monitor position, and Annex 1- Figure 13 and Annex 1- Figure 14 ‘time’ and ‘precision’ for sideway monitor positions, respectively. Results for mean data ANOVA for ‘time’ and ‘precision’ from each of the two study groups independently can be found in Annex 1- Figure 17 and

Annex 1- Figure 18 for straight ahead monitor position and Annex 1- Figure 19 and Annex 1- Figure 20 for sideway monitor position, respectively. Batmaz et al [31] Tables 2 and 3 summarize the results of these analyses, showing means and standard errors for the different experimental conditions (effect sizes), and *F* and *p* values signaling the statistical significance of the effect of each principal design variable (factor) on the dependent variables 'time' and 'precision'.

Results for 'time' from the group with the monitor positioned straight ahead (Batmaz et al [31] - Table2) and from the group with the monitor positioned sideways (Batmaz et al [31] - Table 3) show quite clearly and consistently that subjects in both groups performed significantly faster in the direct viewing condition, and took significantly more time in all the four image viewing conditions, which produced roughly equivalent data for 'time' in each of the two groups. The sideways group (Batmaz et al [31] - Table 3) took on average two seconds longer than the *straight ahead* group (Batmaz et al [31]- Table2) in all the experimental conditions. The manipulation factor also affected both study groups in the same way, as subjects from both groups performed significantly faster when they did not have to use a tool. Subjects from both study groups were significantly faster in the second session compared with the first (i.e. a training effect on 'time'). Results for 'precision' from the group with the monitor positioned straight ahead (Batmaz et al [31] - Table2) and from the group with the monitor positioned sideways (Batmaz et al [31] - Table 3) show quite clearly and consistently that subjects in both groups were significantly more precise in the direct viewing condition than in any of the image viewing conditions, which produced roughly equivalent data for 'precision' in each of the two groups. The *sideways* group (Batmaz et al [31] - Table 3) was more precise than the *straight ahead* group (Batmaz et al [31] - Table2) Table 3 in all the experimental conditions. The manipulation factor also affected both study groups in the same way, as subjects from both groups were significantly more precise when they did not have to use a tool. Subjects from neither study group were more precise in the second session compared with the first (i.e. no training effect on 'precision'). Significant interactions were found between the viewing and the manipulations factors in each of the two study groups (Figure 27).

In the *straight ahead* group, there was no significant interaction between viewing and tool-use in their effects on 'time' $F(3,1279) = 2.06$ NS. Such an interaction in

the *sideways* group was found F(3,1279)=4.17; p<0.01, independent of the change in 2D monitor position (Figure 27). The interaction only involves the head-mounted 3D viewing condition, where the tool-use has a more detrimental effect on times than in any of the other viewing conditions. In both study groups, significant interactions between viewing and tool-use in their effects on 'precision' were found (F(3,1279) = 7.30 p < 0.001 in the *straight ahead* group and F(3,1279)=5.15; p<0.01 in the *sideways* group), involving the head-mounted 3D and the 2D fisheye viewing conditions (Figure 27).

Moreover, the results for comparison of ANOVA and RM ANOVA are shown in only for this experiment, a repeated measures ANOVA was run in SPSS 18 to analyze the data of the *straight ahead* group. According to the RM ANOVA Huynh-Feldt correction 'time' results in Annex 1- Figure 21, significant differences were found for 'vision' (F(1.435,10.043)= 59.29; p<0.001) and 'manipulation' F(1,7)= 26.345; p<0.001). There was no significant interaction between vision and manipulation conditions (F(3,21)=2.27; NS). Similarly, in the ANOVA 'time' results in Annex 1- Figure 23 significant differences were found for 'vision' (F(3,1279)= 298.56; p<0.001) and 'manipulation' F(1,1279)= 75.67; p<0.001). There was no significant interaction between vision and manipulation conditions (F(3,1297)=1.91; NS). In the Annex 1- Figure 22 precision RM ANOVA Huynh-Feldt correction 'precision' results, significant differences were found for 'vision' (F(2.85,19.95)= 27.99; p<0.001), 'manipulation' F(1,7)= 30.81; p<0.001) and 'vision' and 'manipulation' interaction F(2.782,19.48)= 7.278; p<0.01). In the Annex 1- Figure 24 precision ANOVA results, significant differences were found for 'vision' (F(3,1279)= 196.29; p<0.001), 'manipulation' F(1,1279)= 36.21; p<0.001) and 'vision' and 'manipulation' interaction F(1,1279)= 7.13; p<0.001). These results show that there are no major differences between RM ANOVA and ANOVA Fisher's test result. They both give the same significance level.

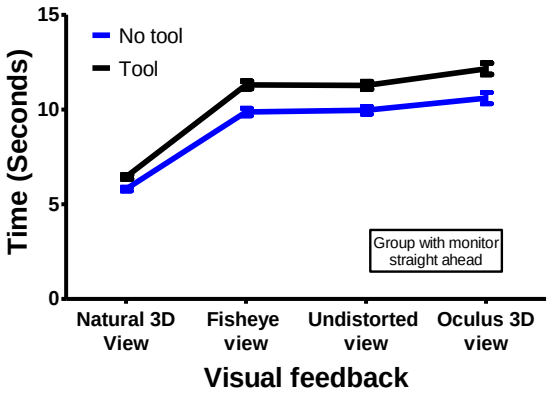

(a)

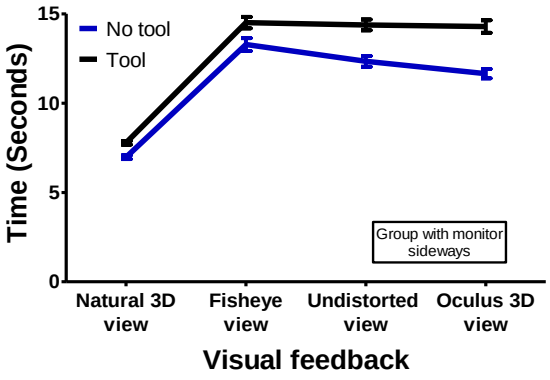

(b)

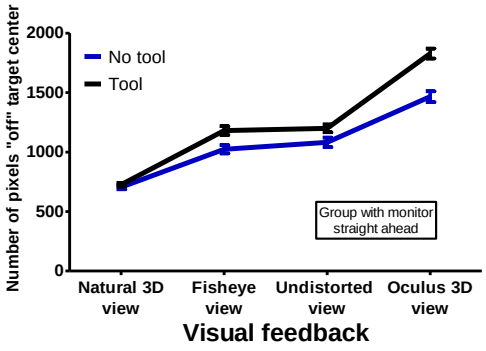

(c)

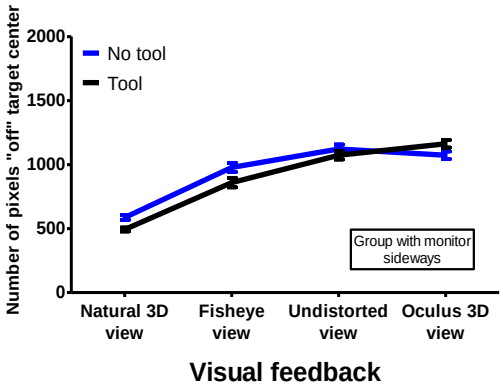

(d)

Figure 27 – 'Time' (a) and 'precision' (c) results for straight ahead monitor position and 'time' (b) and 'precision' (d) results for sideway monitor positions.

Trajectory Results

In a first step of trajectory results, point-by-point discrete sampling of spatial coordinates (x, y) of individual object movement trajectories in the different experimental conditions were performed. These were then plotted against the reference trajectory line to graphically represent real-world object movement trajectory offsets in terms of planar (x, y) plots (Batmaz et al [30] Figure 4). The sampled real-world object trajectories across the different segments of the RAF are indicated by the blue points in the graphs in Batmaz et al [30] Figure 4, which shows trajectory data for constrained and unconstrained object movements in the different visual feedback conditions. The blue trajectory points in the graphs on the left of Batmaz et al [30]

Figure 4 exhibit the expected curved shapes of unconstrained hand movements, when no tool is used to displace the object.

Batmaz et al [30] Figure 4 also shows that constrained movements with use of a tool (graphs on right) do not necessarily follow the expected straight line path. The variations in shape of the sampled real-world trajectories for constrained and unconstrained movements in the subject's peri-personal space suggest complex effects of the type of visual feed-back given, type of object movement to be realized, and target position or eccentricity on the RAF. The results also point toward critical interactions between viewing conditions and target-to-target trajectory positions.

In the second step of trajectory analysis, five-way Analysis of Variance (ANOVA) was performed on the 'from-target-to-target duration' (Annex 1- Figure 26) and 'average distance from the reference trajectory' (Annex 1- Figure 29) to check where significant interactions occur in the data. Batmaz et al [30] Tables 1 shows the means, standard errors (SEM), F statistics and probability limits (p) from this ANOVA. In Annex 4-Table 10below, 'from-target-to-target duration'(Annex 1- Figure 25), 'average distance from the reference trajectory' (Annex 1- Figure 28) and 'dispersion in trajectory' (Annex 1- Figure 27) results are given by their means and standard errors (SEM). According to similarity between fisheye and undistorted vision(for 'from-target-to-target duration' R=0.898, for 'average distance from the reference trajectory' R=0.821 and 'dispersion in trajectory' R=0.511), only undistorted vision is used a 2D visual feedback condition in Batmaz et al [30]. Likewise, according to similarity between 'average distance from the reference trajectory' and 'dispersion in trajectory' (R=0.814), only 'average distance from the reference trajectory' is used a 2D visual feedback condition in Batmaz et al [30].

Significant effects of vision modality on movement 'from-target-to-target duration' and 'average distance from the reference trajectory' were found in the trajectory movement. Subjects were fastest and getting closer to the reference trajectory under conditions of direct vision, where the shortest movement times (Batmaz et al [30] Table 1, left) and the smallest lateral offsets from the ideal movement trajectory (Batmaz et al [30] Table 1, right) were observed. *Post-hoc* paired comparisons using the Holm-Sidak method were performed to check which of the differences between the three levels of the vision

factor were significant. For ‘from-target-to-target duration’, the difference in means between 2D and virtual 3D (d=130 msec) signaled non-significant. The differences in means between direct and 2D vision (d=660 msec) and between direct and Oculus 3D vision (d=890 msec) signaled significant with $t(1,1)=11.37$; $p<.001$ and $t(1,1)=13.18$; $p<.001$ respectively for ‘from-target-to-target duration’. For ‘average distance from the reference trajectory’, the difference in means between direct and 2D (d=2 pixel) signaled non-significant. The differences in means between 2D and 3D (d=18 pixel) and between direct and virtual 3D (d=20 pixel) signaled significant with $t(1,1)=13.74$; $p<0.001$ and $t(1,1)=15.33$; $p<0.001$ respectively for ‘average distance from the reference trajectory’. ANOVA signaled statistically significant interactions between the vision factor and the trajectory location factor on ‘from-target-to-target duration’ ($F(10,575)=4.33$; $p<0.01$), and on ‘average distance from the reference trajectory’ ($F(10, 575)=14.46$; $p<0.001$).

A significant effect of the manipulation factor or type of hand movement on ‘from-target-to-target duration’ was found, where subjects were significantly faster (Batmaz et al [30] Table 1, left) when no tool was used (unconstrained hand movements). The effect of the manipulation factor on ‘average distance from the reference trajectory’ signaled non-significant (Batmaz et al [30] Table 1, right). Significant interactions between type of hand movement and any of the other factors were not found.

A significant effect of the session factor on ‘from-target-to-target duration’ was also found, where subjects were significantly faster (Batmaz et al [30] Table 1, left) in the first session. The effect of session on ‘average distance from the reference trajectory’ signaled non-significant (Batmaz et al [30] Table 1, right). Significant interactions between the session factor and any of the other factors were not found.

Significant effects of the location of trajectories in the surgeon's peri-personal space (within the limits of the RAF) on ‘from-target-to-target duration’ (Batmaz et al [30] Table 1, left) and ‘average distance from the reference trajectory’ (Batmaz et al [30] Table 1, right) were found. Subjects were faster and getting closer to the reference line across specific locations, depending on the viewing modality as signaled by the significant interactions between the vision and trajectory location factors, with probability limits ($p<.0001$ for time and precision), as stated above. To find out which differences in

mean scores for time and precision between trajectory locations were significant for a given level of the viewing factor, *post-hoc* paired comparisons were performed using the Holm-Sidak method. Comparisons that signaled a statistically significant difference are summarized in Batmaz et al [30] Table 2 for each of the three levels of the vision factor, with effect sizes, t-statistics, and the corresponding probability limits.

The viewing modality producing the largest number of significant differences in 'from-target-to-target duration' and 'average distance from the reference trajectory' across trajectory segment locations is the Oculus 3D condition (see Batmaz et al [30] Table 2). The 2D visual feedback and the direct vision conditions produced fewer significant differences between locations. More importantly, the trajectory segment locations producing significant differences in 'from-target-to-target duration' and 'average distance from the reference trajectory' are not same in the different vision modalities. These results point toward a complex interdependency between visual feed-back conditions, the direction and shape of the hand movements from target to target, bearing in mind that some target-to-target trajectories contained small obstacles, and the spatial position of the targets. To gather further insight into this complexity the individual means for 'average distance from the reference trajectory' in the different conditions as function of the trajectory segment location were plotted. These individual data are shown in Batmaz et al [30] Figure 5, with average lateral deviations from the reference trajectory as a function of trajectory segment locations on the RAF, in the different experimental conditions and sessions.

The data of the male are shown in Figure 5a, the data of the female in Figure 5b Batmaz et al [30]. The data curves reveal consistent shapes across subjects, with almost invariably the worst 'average distance from the reference trajectory' scores across the trajectory segments X1 and X4, especially under conditions of Oculus 3D vision. Both trajectory segments involve target-to-target movements across a small obstacle in the sideways direction (from left to right) in the peri-personal space of the subject. X4 segment variations were also observed in the first study of chapter 1. Hand movements of each subject varied in segment X4 in the first study and subjects were more stable in the Segment X4 in direct vision compared to 2D screen vision.

The longest ‘segment traverse durations’ were observed across the trajectory segment X4, which involves the target-to-target ‘from-target-to-target duration’ the furthest away in the subject's peri-personal space. This result is shown in Batmaz et al [30] Figure 6, with the ‘from-target-to-target duration’ in the different conditions plotted as a function of the trajectory segment location.

Discussion

The results show that, compared with the direct viewing condition, the three image viewing conditions had significantly detrimental effects on the time and the precision with which the participants placed the small cube object on the target centers in the specific order. The negative effects of 2D image views compared with “natural” direct action viewing was previously discussed in the first study of Chapter 1. The same effect of 2D image-guided performance on motor performance is also observed in this study, and in the previous studies [3,138]. The absence of a superiority effect of head-mounted 3D viewing compared with 2D viewing from different monitor positions in this study is consistent with previous findings by some authors [45–47], and in seeming contradiction with data from studies published by others showing such a superiority effect [38–43]. The major implications of these findings were discussed in detail in the following paragraphs.

The effects of 2D and 3D viewing modes on the precision and timing of surgical hand movements, whether constrained by tool-use or not, are not the same across target locations in the surgeon's peri-personal space, as clearly shown by the results of the simulator study here.

2D fisheye *vs* undistorted 2D vision

Although the 2D fisheye vision condition would have been expected to affect performances more negatively than undistorted 2D screen vision, the opposite was observed. Given the task instruction to place the cube as precisely as possible on the target centers, the 2D fisheye version of the RAF may have generated a task-specific facilitation effect on precision. In fact, in the top-down 2D fisheye vision, the targets

appear dome-like rather than flat, as in top-down undistorted 2D vision, which makes the target centers perceptually more distinguishable from the image background.

Monitor position

The between-groups factor monitor position affected performances significantly, but in opposite directions for task execution times and the pixel-based precision score: while subjects performed significantly faster in the two 2D vision conditions in the group with the monitor positioned straight ahead, they were also significantly less precise in that group. This is an important finding because it suggests that subjective comfort factors need to be considered in tight relation to individual goal-setting strategies [32,36,49]. Subjects in the straight ahead group experienced less strain on the neck during task execution, as previously reported [109], and therefore felt more comfortable and fully disposed to go as fast as they could, while the subjects in the other group felt less comfortable [110,140] and therefore paid more attention to the precision of their maneuvers. Trade-off effects between speed and precision of task execution are an important aspect of the performances of novices and well-known to reflect individual strategy variations [57,119,58–60,147,148]. These strategy variations are difficult to predict in complex tasks because they do not depend on any single parameter, or clearly identified factor combination. They result from a multitude of internal and external constraints. State-of-the-art research in the neurosciences of goal-related strategies and decision making suggests that they are top-down controlled by the temporal lobes of the human brain [115,127].

Interactions between viewing and tool-use

The performances of both the men and the women were significantly impaired when they had to use a tool to perform the positioning task compared with the conditions where they used their bare hand. Tool-specific motor requirements [131,133], such as having to grab and hold the handle of the tool, or having to adjust one’s hand movements to the shape and the size of the tool, would readily account for this effect. However, given the significant interaction of this effect with the effects of the different viewing conditions found here, there is a need for further research about how different viewing modalities affect so-called near-body space. The latter is defined as the space around one’s own body within arm’s reach and its perceived extent affects

performance by drawing attention to regions of space that are not paid attention to when the same task is performed with the hands directly [132]. Body space extension through the tool explains why it is easier to position an object with a tool in far-away space, but how this space scales in different 2D and 3D viewing conditions is still unknown.

Gender effect or inter-individual strategy differences?

The gender effect showing that men performed significantly faster than the women has to be interpreted with much caution. First, other studies have shown effects in the opposite direction, reporting faster performance in women compared with men [149,150]. Second, temporal performance scores must not be considered without taking into account the precision scores, for reasons already pointed out here above and explained in terms of individually specific goal-related speed-accuracy trade-offs. These depend on the type of task, and on other, physiological and psychological, factors which need to be identified. In this study here, it is shown that the men were significantly faster but, at the same time, also significantly less precise than the women in the sideways group. This apparent gender effect is absent in the straight-ahead group but cannot be explained away by the mere difference in monitor position. Monitor position affects subjective comfort levels [4,109,47], and subjective comfort levels affect individual goal-setting, which involves criteria for timing and precision strategies [116,122]. More research is clearly needed to understand these complex processes.

Trajectory movements in peri-personal space

Hand movements away from or back to the body in a pick-and-place simulator task appear less affected by image guidance compared with direct action viewing. Hand movements in a sideways direction in the subject's peri-personal space are markedly less precise with image guidance, especially with stereoscopic 3D viewing. Moreover, at target locations further away in peri-personal space, sideways movements are considerably slowed down with image guidance, especially under conditions of 3D stereoscopic viewing. These results suggest that goal-directed hand movements, whether constrained or not, are affected by both the direction of movement and the spatial position (or eccentricity) of target locations in peri-personal space (e.g.

[145,151]). Small obstacles on the target-to-target trajectories affect precision and timing of hand movements, as shown here, and this drawback is not compensated for by a 3D image view, supposed to convey three-dimensional cues to the subjects to a greater extent than a 2D image view.

3D stereoscopic viewing does not help to compensate for the effects of variations in hand movement direction and position in peri-personal space, which are known to affect the control of human arm movements [114,152]. Neuropsychological evidence suggests that action influences spatial perception [132]; the latter, during hand movements in particular, is known to determine an individual's sense of agency, or feeling in control [122]. It can be assumed that the type of tool used for action, and the way in which a camera system captures the movements seen on the screen would have a critical impact on both. When the surgical camera system is part of the surgical tool itself and moves along with the tool in peri-personal space as in a recent study by Sakata et al. [44], a positive effect of stereoscopic viewing on surgical task execution times was, indeed, found. A state-of-the-art endoscopic 2D/3D camera system (EndoEye Flexlens) built into the tip of the surgical tool was used in that study.

Stereoscopic 3D *vs* 2D viewing

Stereoscopic 3D vision through the head-mounted device did not represent a performance advantage compared with the 2D image vision conditions in this study here. In some of the earlier studies, authors concluded that novice and expert users with normal capacity for spatial perception can work faster and safer under 3-D vision, especially in complicated surgical tasks [40,44,139]. Several explanations may account for the difference between these and the results here.

First, most of the previous studies were run on surgeons with different levels of expertise, from so-called novices to so-called experts. It is difficult to render novice groups from a population consisting of professional surgeons homogenous with respect to eye-hand coordination expertise. All surgeons are experts in this regard, yet, they are more or less proficient at different specific tasks. This variability may not be easy to track down. For this reason, the experiment here was run on complete novices, all scoring high in spatial ability, without any surgical experience at all.

Second, high resolution 2D/3D surgical camera systems, as the one used in one of the most recent studies [44], not only control for viewing angle and distance like the camera display here, but these cameras also move along with the tools during task execution. The cameras in this study had fixed locations. When the cameras are moving along with the tool, the movements represented visually are not aligned with the surgeon's real arm and hand movements. Thus, when such a system is switched into 3D mode, the stereoscopic information conveyed could help overcome this problem, which would explain why task execution is easier, especially for the less trained surgeons, compared with the 2D mode [44].

Third, in the display here, the tool-tips and a critical part of the manipulated object (the top) were selectively colored for tracking. These colors may have provided particularly powerful visual cues for task execution in 2D [33,153], cancelling the major advantage of stereoscopic viewing. Studies in image-guided neurosurgery [153] have previously shown that adding color to specific locations in 2D images produces strong and self-sufficient cues to visual depth for interventional guidance, especially in novices, potentially making 3D viewing unnecessary.

Finally, the absence of a 3D superiority effect here in this study may be partly be due to the complex interactions between viewing and manipulation modalities, i.e. the tool-use factor, affecting subjectively extended near-body space [112,113]. Absolute beginners from possibly heterogeneous general training backgrounds have to learn to adjust to extended near-body space when using a tool, especially when confronted with different viewing modalities. These complex processes of adjustment have not yet been studied in the context of image-guided eye-hand coordination, and more research oriented in that direction is needed.

Study 3- Effects of Local Color Cues in the Images

In the first study of this chapter, the learning effect on direct vision and image guidance systems were studied under different manipulation conditions. In short, results showed that image guidance makes subjects slower and less precise and even after eight learning sessions, subjects do not get as fast or as precise as direct vision in image guidance. In the second study of this chapter, two different methods, stereoscopic 3D vision and monitor position, were studied. These methods are used to enhance the motor performance of the surgeons in surgical theaters for novices. Monitor position modalities affect the motor performance of beginners, as expected in previous studies. Stereoscopic 3D vision, on the other hand, did not provide any superiority over 2D image guidance as in previous studies Four different explanations were given in the Batmaz et al. study [31] to explain the possible reasons for this difference. In the last and third study of chapter 1, these different explanations are studied with the 'Excalibur' experimental setup.

Study Goal and Hypotheses

At the end of the second study of first chapter, the possible explanations of the absence of stereoscopic 3D display superiority was given. These were: subject expertise heterogeneity, color cues, subject background heterogeneity, and camera position. In the last study of chapter 1, these effects were inspected with a color cues experiment with the "Excalibur" system on different participant groups.

The participant expertise heterogeneity is caused by unclear boundaries of given titles to the surgeons in each research. While some of the latest studies divide the participants into the groups according to their given titles by institutions (e.g. [61]) or years of experience (e.g. [62]), some of them give expertise titles according to number of laparoscopic cases performed (e.g. Park et al. [63] defines *novices* as "surgeons who have performed less than 20 cases", *intermediates* as "surgeons who have performed between 20 and 99 laparoscopic cases" and *experts* as "surgeons who have performed laparoscopic surgery more than 100 cases". Mashiach et al [64] defines *novices* as "surgeons who have assisted in less than 10 laparoscopic procedures", and

experts as “surgeons who have performed more than 50 laparoscopic procedures”, Curro et al [65] defines *novices* as “surgeons who had performed around 200 laparoscopic surgical procedures as the assistant or camera operator, and around 40 laparoscopic procedures as the first operator during the last 2 years” and *experts* as those “who have performed more than 500 laparoscopic procedures”, Leite et al [66] defines *novices* as “surgeons who have performed laparoscopic procedures less than 50 times” and *experts* as “more than 50 times”, Sanchez-Margallo et al [154] study does not define novices but defines *intermediates* as “performed between 1 and 50 laparoscopic cases” and *experts* as “more than 50 cases”). Some studies do not specify any quantitative experience information about the participants (e.g. [67]). These expertise group divisions are usually made according to sample size and the surgical experience of the participants. In this case, an surgeon can be considered an intermediate surgeon or an expert surgeon in different experiments.

Studies 1 and 2 on chapter 1 related to the learning, and 2D and 3D visual feedback competition were entirely performed with complete beginners coming from heterogeneous backgrounds. Complete novices had to learn near-body space movements with a tool under different visual feedbacks that they had not experience before. Previous studies on novice and experienced surgeons show that while surgeons experienced in image-guided interventions tend to focus their attention on target locations, novices split their attention between trying to focus on targets and, at the same time, trying to track the tools [120]. This reflects a common strategy for controlling goal-directed hand movements in non-trained subjects and affects task execution times [151]. Surgeons who have this kind of training complete image-guided tasks significantly faster than novices, with significantly fewer tool movements, shorter tool paths, and fewer grasp attempts [120]. These complex processes of adjustment have been studied in the context of image-guided eye-hand coordination for complete beginners in the first two studies of this chapter, but their comparison with the surgeons and expert surgeon have not yet been studied.

Color cues have an important role during surgical procedures; they can both disturb or assist user according to the subject’s expertise level. An important key point during a surgery is focusing on a region of interest on 2D visual system during the operation. Surgeons can be exposed to a variety of colors *in-vivo* during the surgery and current

cameras, and visual feedback systems allow surgeons to adjust color and brightness of the feedback to concentrate on that precise region [155]. While these adjustments help surgeons to focus on a distinct area, it can cause loss of information such as color cues, shadows, and even depth perception [156]. The loss of higher order (cortical) depth cues in image-guided manual tasks has been identified as a major drawback, significantly affecting performances of novices compared with task execution in direct binocular or monocular vision [3,36] as shown in study 1 [32] and 2 [31] of this chapter. Adapting to this constraint is possible through a long period of training to optimize indirect eye-hand coordination [1,136,137]. Developing this expertise requires significant adjustments in individual goal-control strategies [32,120,49]. Nonetheless, for novices, it is a better option to highlight a specific region to provide more information and help them to track that region [153,157]. Studies in image-guided surgery [153] have previously shown that adding color to specific locations in 2D images produces strong and self-sufficient cues to visual depth for interventional guidance, especially in novices, potentially making 3D viewing unnecessary.

In the Excalibur experimental setup, the tool-tips and a critical part of the manipulated object (the top) were selectively colored for tracking. These colors may have provided particularly powerful visual cues for task execution in 2D [33,153]. In the minimally invasive surgeries, instrument tips can be easily identified by their dominant achromatic color. Furthermore, the instruments tips reflect the light coming from the endoscope, which can whiten the tool-tips [158]. The matte fluorescent green tinted tool-tips inhibit visual cues of the feedback and could be distracting the user.

Camera position alignment with the tool movement has been a research topic for a long time. It is an important key point during surgery and provides an important advantage for the surgeon. The Excalibur experimental setup does not allow changing camera(s) position(s) according to the manipulated object or to tool-tips. This creates a problem on RAF for subjects, because they have to consider the distortion on the image during the object movement. For instance, when the blue object has to be positioned at the center of a particular TA, the subject has to consider the shift caused by the height of the object due to the camera. Participants have to use visual clues in the image to correctly place the blue object.

For the last study described in this first chapter, an experiment was designed to explore these four possible explanations to further investigate the difference between 3D stereoscopic vision and 2D image guidance found in the second study. For this purpose, an experiment was designed to measure the effects of color cues and perform the second study experiment only with the straight ahead monitor position with three different groups; complete novices, surgeons and an expert surgeon. In the previous studies of this chapter, the importance of precision was highlighted several times. This study also strengthens the importance of the precision assessment by comparing an experienced surgeon's data to other participants.

Materials and Methods

Participants

In the last study of chapter 1, participants were divided into the three different groups. The first group was called, '*novices'*; 12 healthy right-handed men ranging in age between 25 and 45, participated in this study. They were all highly achieved professionals in administrative careers, with normal or corrected-to normal vision, and naive to the scientific hypotheses underlying the experiments. Pre-screening interviews were conducted to make sure that none of the selected participants had any particular experience in knitting, eating with chopsticks, tool-mediated mechanical procedures, or surgery.

The second group was called *'surgeons'*. Six surgeons ranging in age between 29 and 41 participated in the experiment. Their age and experiences are given in Table 1 in detail. They had all performed more than 500 laparoscopic surgical cases, so their experiences were given in hours to be more precise. All of the surgeons were fellow-surgeons who were working at IRCAD (Institut de Recerche contre les Cancers de l'appareil Digestif), Strasbourg, France. They also highlighted that they never had a stereoscopic 3D display experience before this experiment; they had only performed image guided surgeries with 2D visual feedbacks.

Table 1 – Age and hours of experience of participant surgeons

Surgeon	Age	Hours of experience on image guided procedure
Surgeon 1	30	>5000
Surgeon 2	32	>3500
Surgeon 3	44	>5000
Surgeon 4	44	>6500
Surgeon 5	31	>3500
Surgeon 6	32	>3700

The last experimental group was called *'expert surgeon'.* An expert surgeon who was 62 years old with more than 25 years of expertise in image guided surgical applications participated in this study. The expert surgeon had a worldwide recognized career on digestive and endocrine surgery. As well as being a member of many international surgical societies, he also received prestigious awards from surgical institutions, including the EXCEL award from the Society of Laparoendoscopic Surgeons. He was also one of the pioneer surgeons in minimally invasive surgery; for instance, he co-partnered the first transvaginal cholecystectomy. He was also co-author of more than 250 scientific publications. His expertise on the 2D image guided procedures developed an excessive level of eye-hand coordination and his exclusive background on endoscopic surgery was unique for this study.

Experimental platform

In this study, four different visual feedbacks are used as in the second study of chapter 1. The same experimental condition on study 2's straight ahead condition was used in this experiment. To study the color cues effects, image guided visual feedbacks were shown to subjects in gray scale and in color, which is called *'color feedback'* condition. The experimental visual feedbacks used in this experiment are shown in Figure 28.

Procedure

In the third study of first chapter, the screen was about 150 cm straight ahead away from participants eyes with no lateral offset from the forearm motor axis. To

compensate for the change in image size on the screen with the change in body-to-screen distance, the image on the screen was adjusted, ensuring that the perceived scale of the RAF displayed in an image subjectively matched to the perceived scale of the RAF when viewed directly.

(a)

(b)

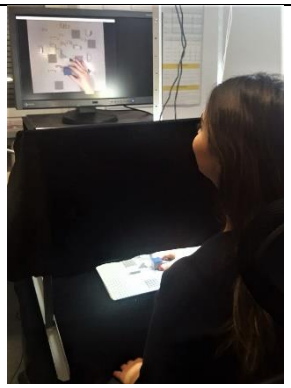

(c)

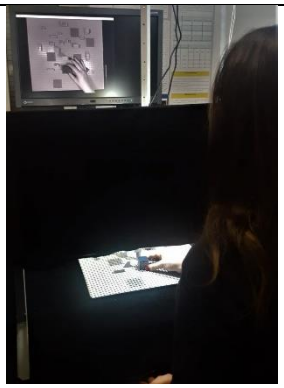

(d)

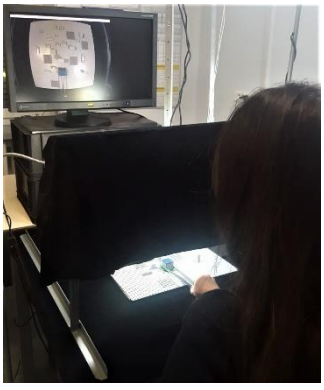

(e)

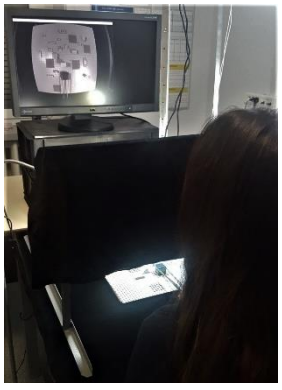

(f)

Figure 28 – Visual feedbacks used in the third study. (a) Direct vision (b) Oculus 3D vision, (c) fisheye vision in color (d) fisheye vision in grayscale (e) undistorted vision in color (f) undistorted vision in grayscale.

Participants were instructed that they were going to be asked to perform this task under different conditions of object manipulation: with their bare right hand or using a tool, while viewing the RAF (and their own hand) directly in front of them, on a computer screen with and without color, or through the head-mounted Oculus device rendering a 3D image with and without color.

An experimental session always began with the easiest condition of direct viewing like the previous studies in the first chapter, the order of two 2D and 3D viewing conditions (2D undistorted, 2D fisheye, 3D OCULUS) was counterbalanced between participants, to avoid order specific habituation effects. Expert surgeon, on the other hand, did the experiment in the following order: direct vision, fisheye vision, undistorted vision and Oculus 3D vision. The order of the tool-use conditions (with and without the tool) and screen color conditions were also counterbalanced between participants.

Cartesian Design Plan and Data Generation

Experimental design

Given the four levels of the vision factor (V_4: direct, fisheye, undistorted and Oculus 3D) combined with the two levels of the manipulation factor (M_2: no tool *vs* tool), the two levels of the screen color factor (C_2: color, grayscale) for image guided feedbacks, and with ten repeated trial sets per condition for twelve novices, six surgeons and expert surgeon, a Cartesian design plan with four principal design variables $V_4 \times M_2 \times C_2$ and ten repeated trial sets in each condition was used to perform the experiments.

Data generation

The data recorded from each of the subjects were analyzed as a function of the different experimental conditions, for each of the five dependent variables (‘time’, ‘precision’, ‘from-target-to-target duration’, ‘average distance from the trajectory’ and ‘from-target-to-target duration’). Just for this study, the ‘number of total error’ dependent variable was used to inspect the differences between *novices, surgeons* and *expert surgeon*. As explained in the materials and method section of the first chapter, the experiment stopped and restarted when the blue cube fell down, when

subjects missed the order of the sequence or when subjects hit one of the Lego towers and the tower rolled over. This was called an ‘error’.

In a first step of the data analysis, the data from each study group were analyzed separately for ‘time’ and ‘precision’. In each analysis, the data of the subjects were assessed individually and with two different analysis for variance (ANOVA); a two-way ANOVA) to compare *visual feedbacks* which took into account all visual feedbacks (direct vision, fisheye vision, undistorted vision and Oculus 3D vision) in combination with the two levels of the manipulation M_2 factor (tool *vs* no tool) for ‘time’ and ‘precision’, and a three-way ANOVA to compare *color feedback* effect which took into account indirect visual feedbacks (fisheye vision, undistorted vision and Oculus 3D vision) in combination with the two levels of the manipulation M_2 factor (tool *vs* no tool), the two levels of the screen color C_2 factor (color *vs* gray scale) for ‘time’ and ‘precision’. Given ten repeated trial sets per condition, following factor analyses for three groups were acquired:

For twelve novices, *visual feedback* analysis: $V_4 \times M_2$ combined with 10 repeated sets including all the color factor levels, a total of 1680 raw data for ‘time’ and for ‘precision’, *color feedback* analysis: $V_3 \times M_2 \times C_2$ combined with 10 repeated sets, a total of 1440 raw data for ‘time’ and for ‘precision’;

For six surgeons, *visual feedback* analysis: $V_4 \times M_2$ combined with 10 repeated sets including all the color factor levels, a total of 840 raw data for ‘time’ and for ‘precision’, *color feedback* analysis: $V_3 \times M_2 \times C_2$ combined with 10 repeated sets, a total of 720 raw data for ‘time’ and for ‘precision’;

For the expert surgeon, *visual feedback* analysis $V_4 \times M_2$ combined with 10 repeated sets including all the color factor levels, a total of 140 raw data for ‘time’ and for ‘precision’, *color feedback* analysis: $V_3 \times M_2 \times C_2$ combined with 10 repeated sets, a total of 120 raw data for ‘time’ and for ‘precision’.

In the second step of the analysis, three expertise levels were grouped together to assess *visual feedback* effects for ‘time’ and ‘precision’. A three-way ANOVA was run on all vision factors V_4 (direct vision, fisheye vision, undistorted vision and Oculus 3D vision) in combination with the two levels of the manipulation factor M_2 (tool *vs* no tool)

including both *color feedback* factor levels. Given ten repeated trial sets per condition with twelve novices, six surgeons and one expert in each of the three study groups, the following three-factor analysis was used*:* $V_4 \times E_3 \times M_2$ combined with 10 repeated sets for the four individuals per gender and a total of 2660 raw data for 'time' and for 'precision'.

In the last step of the analysis, trajectory data of the all three groups were assessed together with a four-way ANOVA for *visual feedbacks* and a five-way ANOVA for *color feedback*. These analyses took into account four vision factors V_4 (direct vision, fisheye vision, undistorted vision and Oculus 3D vision) for *visual feedback* analysis and three vision factors V_3 (fisheye vision, undistorted vision and Oculus 3D vision) for *color feedback*, in combination with the two levels of the manipulation factor M_2 (tool *vs* no tool), the two levels of the color cues factor C_2 (color *vs* grayscale) for only *color feedback effect* and three levels of expertise E_3 (novice, surgeon and expert surgeon), with six levels of segments X_6 . Given the average of ten repeated trial sets per condition in each of the three study groups, the following four-factor analysis for *visual feedback* was used: $V_4 \times M_2 \times E_3 \times S_6$ and a total of 1596 mean data for ''average distance from the reference trajectory', 'dispersion in the trajectory' and for 'from-target-to-target duration'; for the *color feedback* effect: $V_3 \times M_2 \times C_2 \times E_3 \times S_6$ and a total of 1368 mean data for ''average distance from the reference trajectory', 'dispersion in the trajectory' and for 'from-target-to-target duration'

Results

Individual group results for 'time' and 'precision'

In a first step, the data from each study group were analyzed separately. The data recorded from each of the group were analyzed as a function of the different experimental conditions, for each of the two dependent variables ('time' and 'precision'). First, individuals' data were plotted relative to 'time' and 'precision' for the different experimental conditions. Means and their standard errors for 'time' and 'precision' were computed in the next step, for each subject and experimental condition. The raw data were submitted to analysis of variance (ANOVA).

Novice results

Medians and extremes of the individual data relative ‘time’ and ‘precision’ for the different experimental conditions were analyzed first. The results of this analysis are represented graphically as box-and-whiskers plots in Figure 29 and Figure 30 for with or without tool manipulation, respectively. Figure 29 shows ‘time’ distributions and Figure 30 shows ‘precision’ distributions around the medians of data from the manipulation modality with tool in the four different vision conditions.

Results show that novices are slower and less precise in 3D Oculus vision compared to 2D image guidance and there is a direct vision superiority for ‘time’ and ‘precision’. These results show similarity with the previous studies in chapter 1 [31,32] and the previous research in the literature [3,36] for novices.

In further analysis, subjects time-precision curves are plotted for first six subject (Figure 31) and for the next six subject Figure 32.In Figure 32 and Figure 33, each point represents a trial and the lines represents the linear regression results of the factor level results. As it can be seen from Figure 32 and Figure 33, novices pay attention to their speed results but not their precision. For example, while Subject 1 (Figure 32(a)) prefers to go faster without progressing in precision, Subject 7 (Figure 28(a)) choses to get faster while she gets less precise. On the other hand, when Subject 6 (Figure 32(f)) gets faster, s/he also gets more precise with the stereoscopic 3D display.

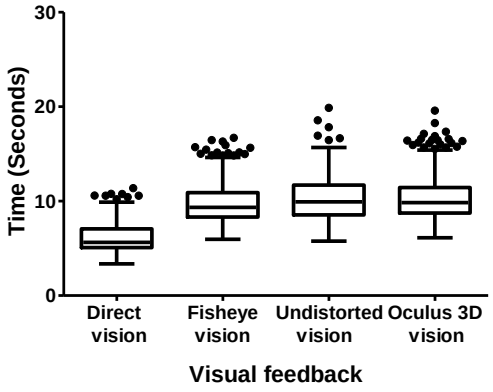

(a)

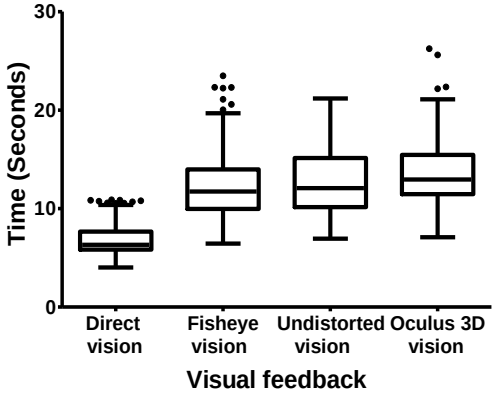

(b)

Figure 29 – Data distributions around the medians in the four different viewing conditions for novice no tool (a) and tool (b) manipulation for 'time' dependent variable for all visual and color feedbacks.

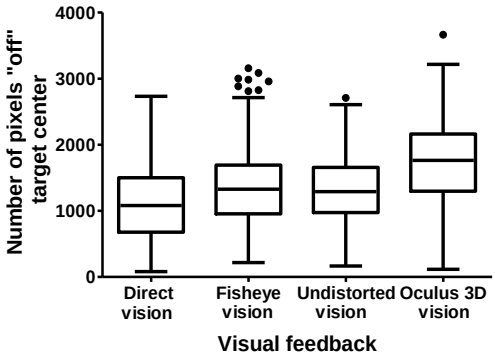

(a)

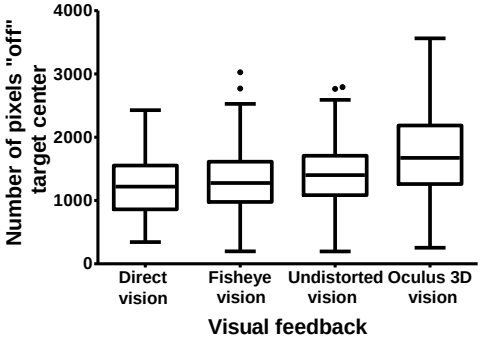

(b)

Figure 30 – Data distributions around the medians in the four different viewing conditions for novice no tool (a) and tool (b) manipulation for ''precision' dependent variable for all visual and color feedbacks.

Two two-way ANOVA were performed on raw data for 'time' (Annex 1- Figure 30) and 'precision' (Annex 1- Figure 32) independently to compare the effects of visual feedbacks. Similarly, two three-way ANOVA were performed on raw data for 'time' (Annex 1- Figure 31) and 'precision' (Annex 1- Figure 33) independently to compare the effects of visual feedbacks. Annex 4-Table 10 summarizes the results of these analyses, showing means and standard errors for the different experimental conditions

of each principal design variable (factor) on the dependent variables ‘time’ and ‘precision’.

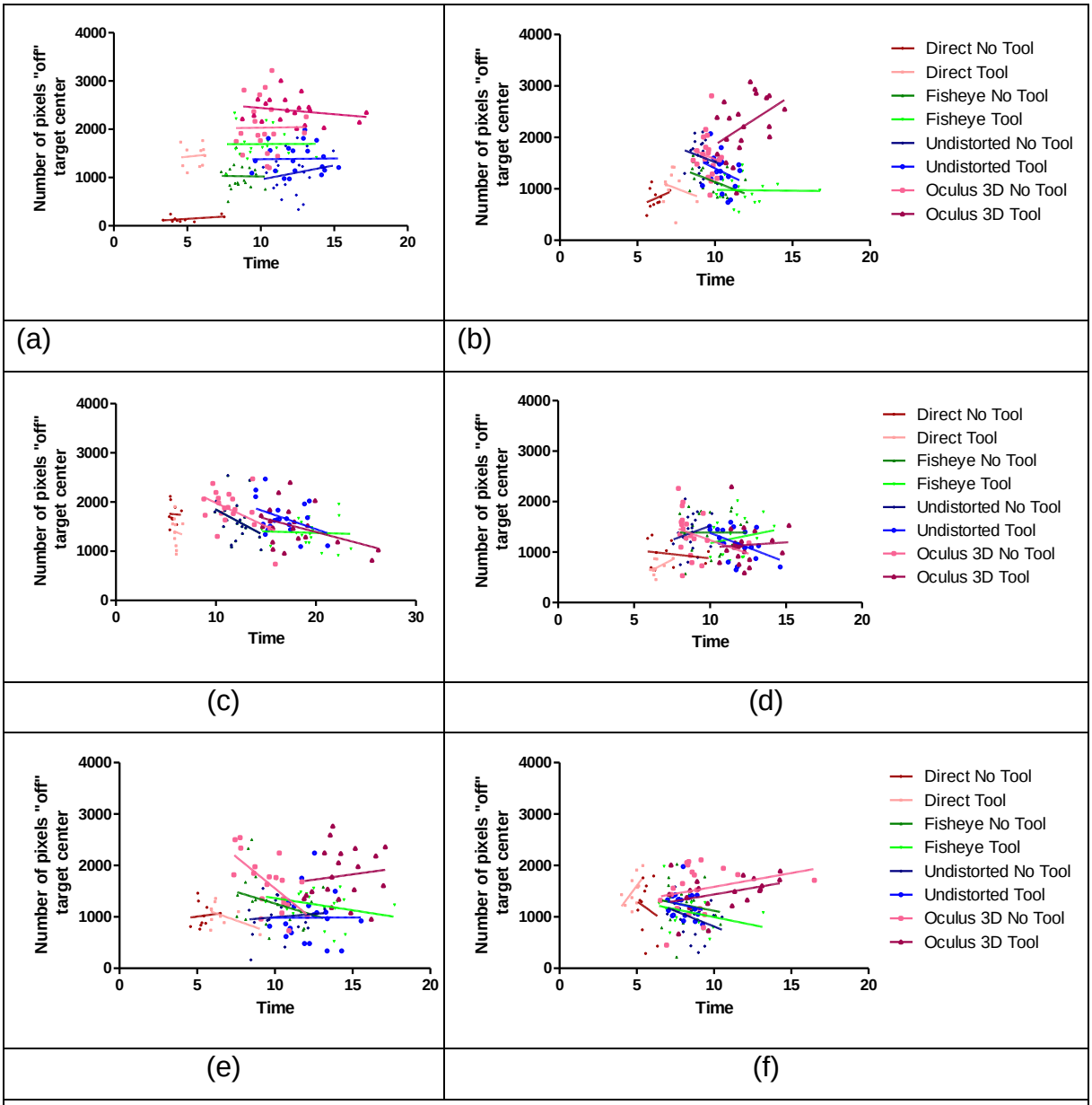

Figure 31 – Individual speed-precision curves for each subject. (a) Subject 1 (b) Subject 2 (c) Subject 3 (d) Subject 4 (e) Subject 5 (f) Subject 6 results for ‘time’ and ‘precision’. Legends of the left panel figures are deleted to enlarge figures. Legends on the right panel are also valid for the legend on the left panel.

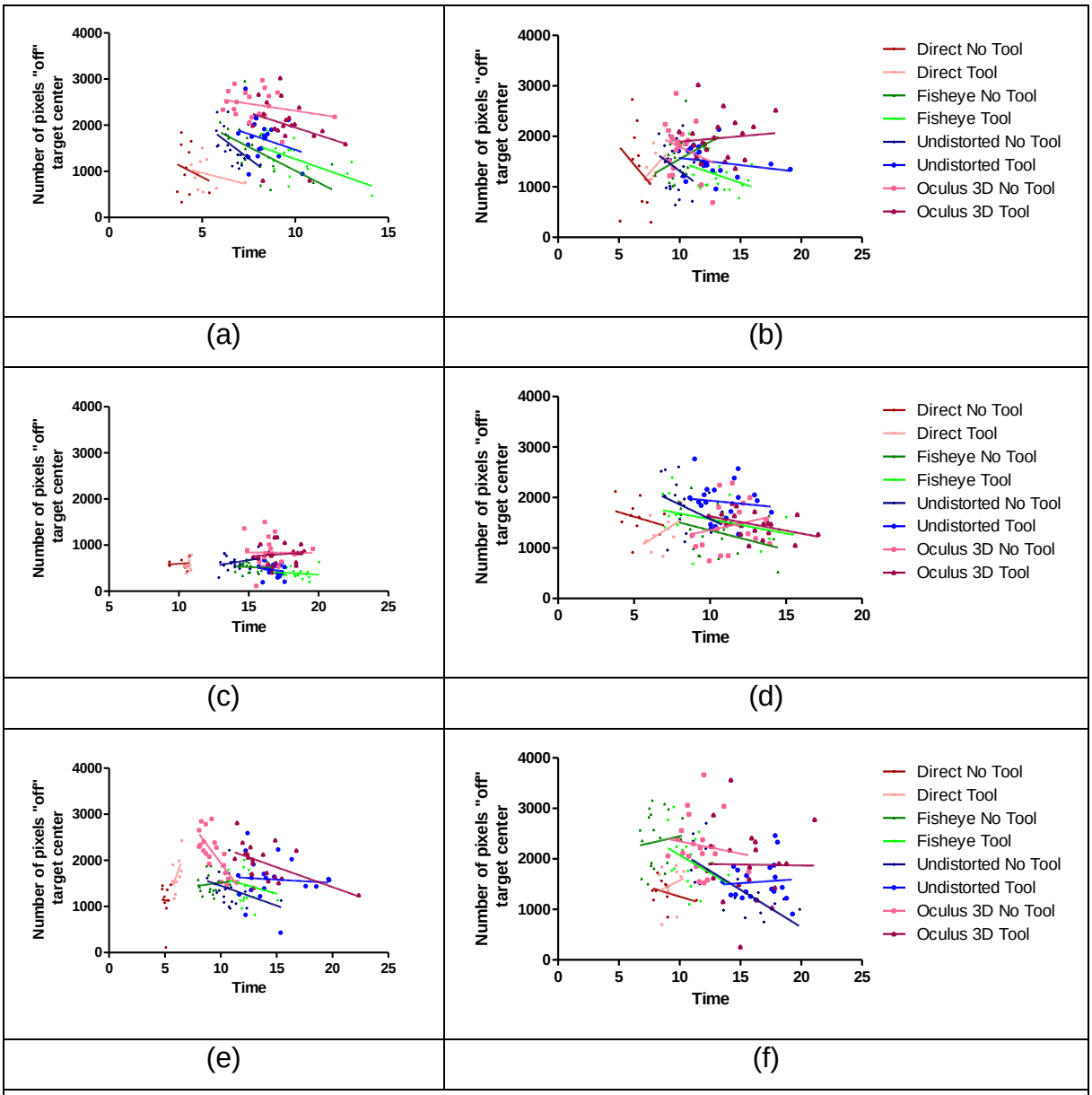

Figure 32 – Individual speed-precision curves for each subject. (a) Subject 7 (b) Subject 8 (c) Subject 9 (d) Subject 10 (e) Subject 11 (f) Subject 12 results for 'time' and 'precision'. Legends of the left panel figures are deleted to enlarge figures. Legends on the right panel are also valid for the legend on the left panel.

The results for 'time' show no effect of 'color' vs 'grayscale' $F(1,1439)=0.44$; NS, but significant effect of manipulation $F(1,1679)=220.21$; $p<0.0001$ and vision $F(3,1679)=223.07$; $p<0.0001$. Subjects were significantly faster without tool and they were faster with direct vision (Figure 33(a)) such as study 1 and study 2. Results for 'precision' show a significant effect of vision $F(3,1679)= 78.96$; $p<0.0001$ where direct vision yields a significantly better score than other visual feedbacks and Oculus 3D

yields significantly the worst score (Figure 33(b)). Neither the manipulation modality F(1.1679)= 0.41; NS, nor the color factor F(1,1439)=0.99; NS had any significant effect on ‘precision’ in novice data analysis.

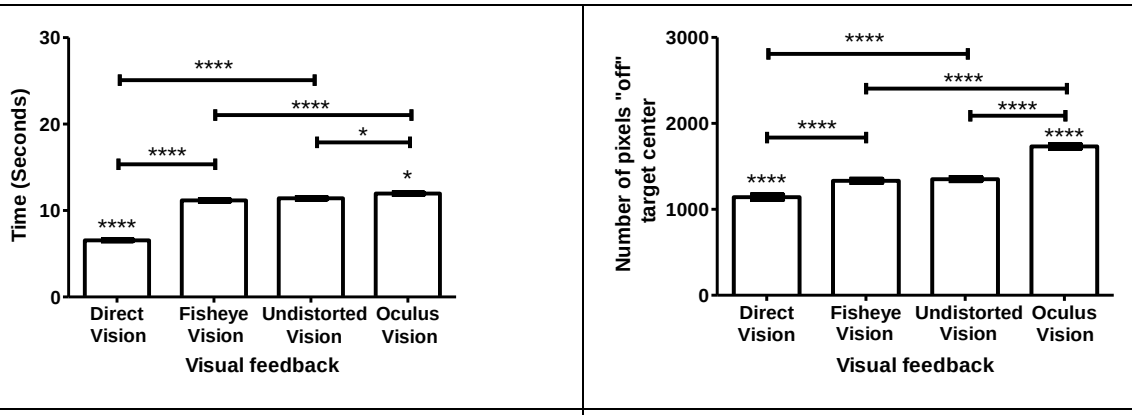

(a) (b)

Figure 33 – Twelve novice (a) ‘time’ and (b) ‘precision’ results for visual feedbacks in study 3. * is for p<0.05, ** for p<0.01, *** for p<0.001, **** for p<0.0001.

Surgeon results

The individual surgeon data are plotted in Figure 34 (Surgeon 1, 5000 hours of image guided operation experience), Figure 35 (Surgeon 2, 3000 hours of image guided operation experience), Figure 36 (Surgeon 3, 5000 hours of image guided operation experience) and Figure 37 (Surgeon 4, 7500 hours of image guided operation experience), Figure 38 (3000 hours of image guided operation experience) and Figure 39 (3700 hours of image guided operation experience). The upper figure panels show data for ‘time’ for no tool (on left) and tool (on right) and the lower panels show the corresponding ‘precision’ data.

Surgeon 1, 3 and 6 ‘time’ results on direct vision were closer to image guided feedbacks results. While surgeon 4 was the slowest surgeon, surgeon 3 was the least precise among them all. The learning effect on ‘time’ results can be seen in all the surgeons, but their precision results were not improving. Such trade-offs were already observed and discussed for individuals during the first study of this chapter and in the Batmaz et al study [32].

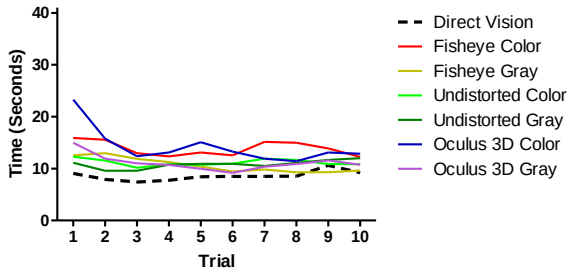

(a)

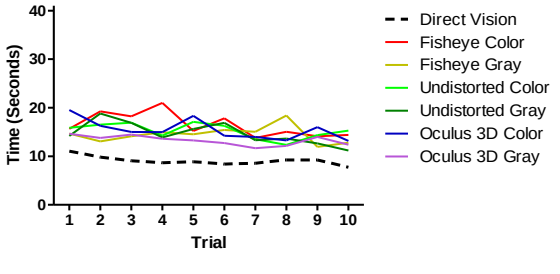

(b)

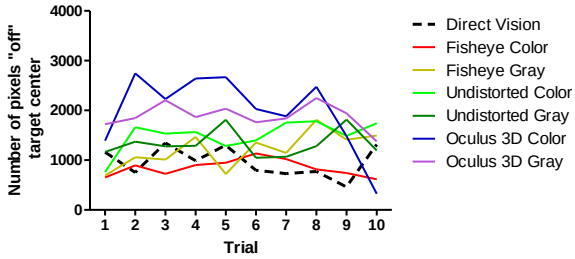

(c)

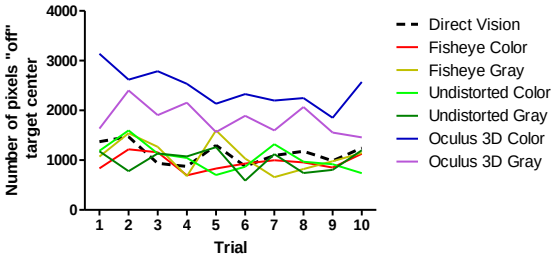

(d)

Figure 34 – Surgeon 1 no tool (a) and tool (b) manipulation on ‘time’ and (c) no tool and (d) tool manipulation on ‘precision’.

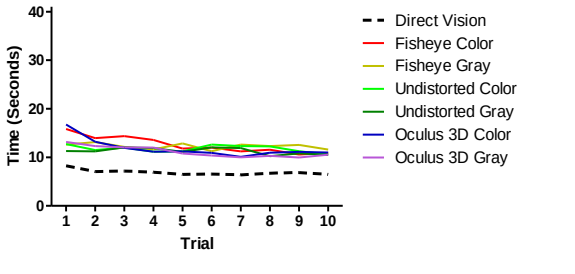

(a)

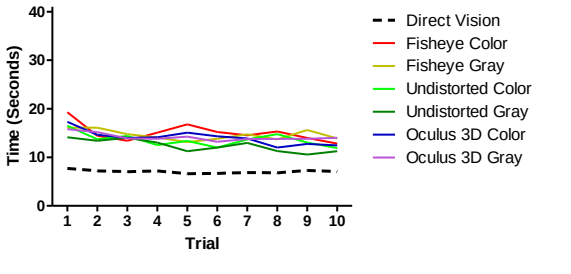

(b)

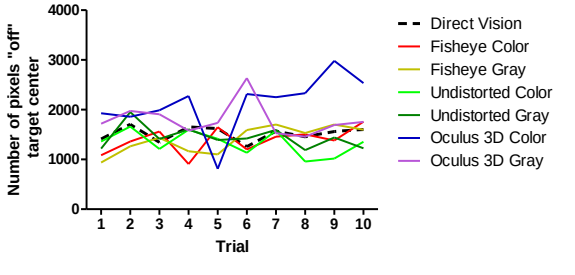

(c)

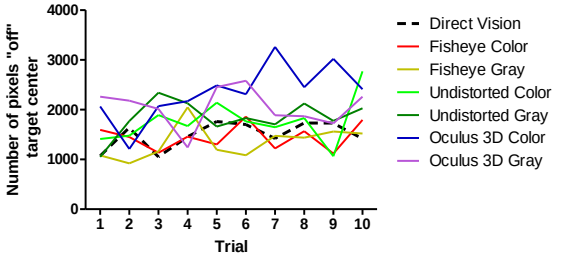

(d)

Figure 35 – Surgeon 2 no tool (a) and tool (b) manipulation on ‘time’ and (c) no tool and (d) tool manipulation on ‘precision’.

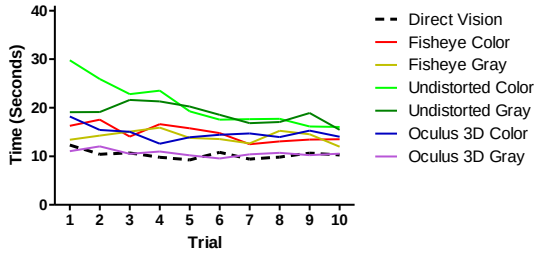

(a)

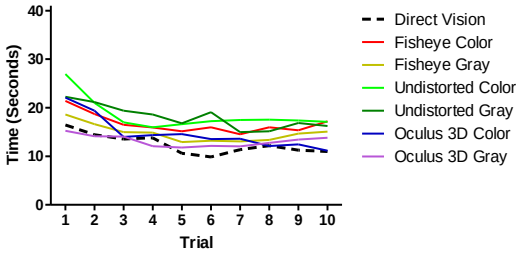

(b)

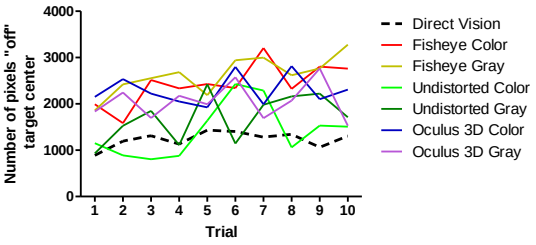

(c)

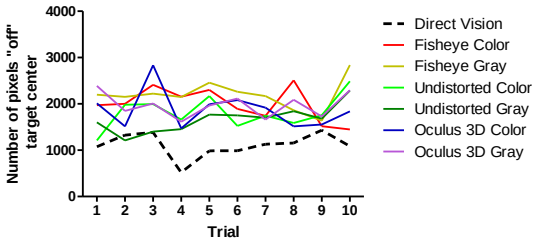

(d)

Figure 36 – Surgeon 3 no tool (a) and tool (b) manipulation on 'time' and (c) no tool and (d) tool manipulation on 'precision'.

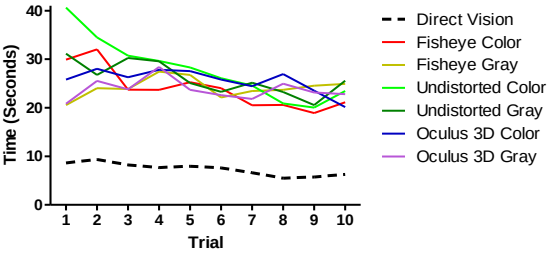

(a)

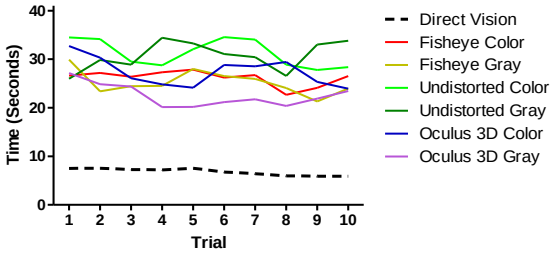

(b)

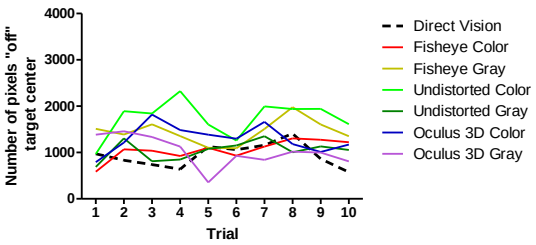

(c)

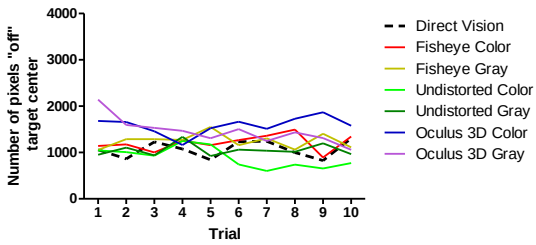

(d)

Figure 37 – Surgeon 4 no tool (a) and tool (b) manipulation on 'time' and (c) no tool and (d) tool manipulation on 'precision'.

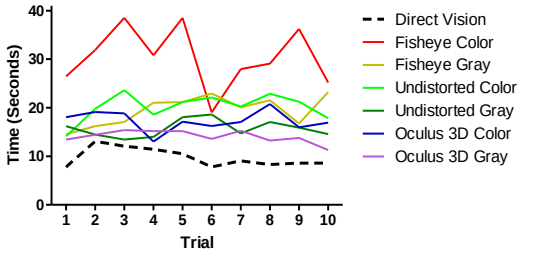

(a)

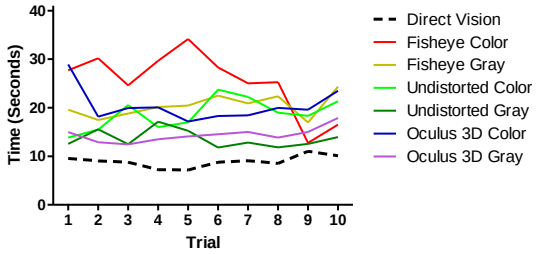

(b)

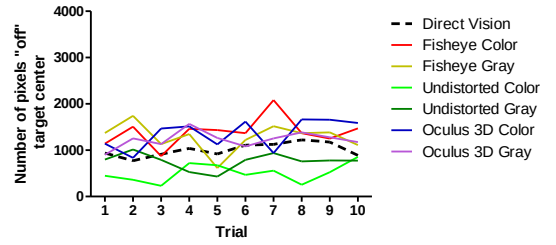

(c)

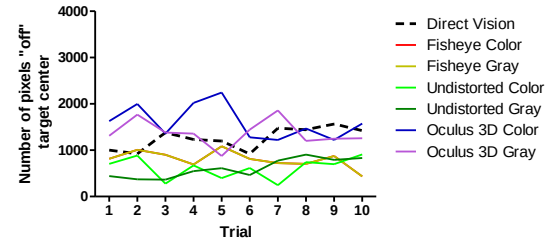

(d)

Figure 38 – Surgeon 5 no tool (a) and tool (b) manipulation on ‘time’ and (c) no tool and (d) tool manipulation on ‘precision’.

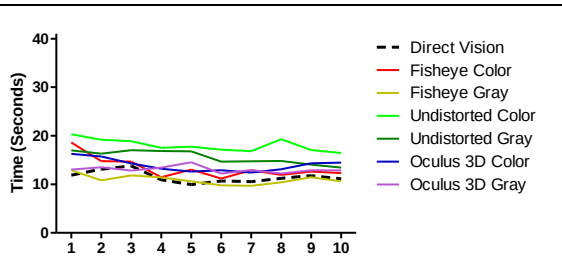

(a)

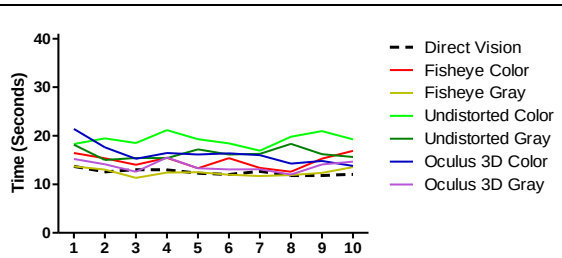

(b)

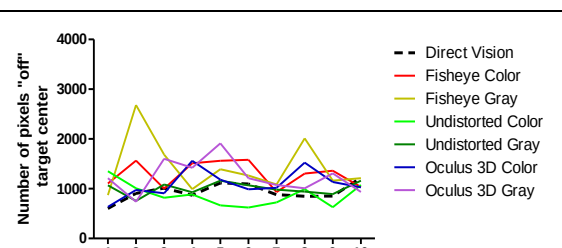

(c)

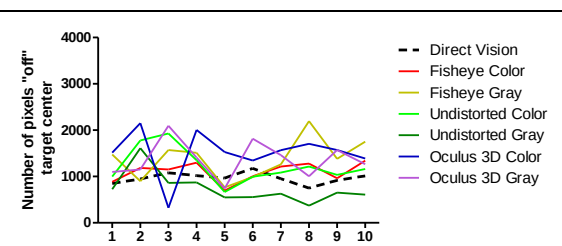

(d)

Figure 39 – Surgeon 6 no tool (a) and tool (b) manipulation on ‘time’ and (c) no tool and (d) tool manipulation on ‘precision’.

Two two-way ANOVA's were performed on raw data for 'time' (Annex 1- Figure 34) and 'precision' (Annex 1- Figure 36) independently to compare the effects of *visual feedbacks* on surgeons. Similarly, two three-way ANOVA's were performed on raw data for 'time' (Annex 1- Figure 35) and 'precision' (Annex 1- Figure 37) independently to compare the effects of *color feedback* on surgeons. Annex 4-Table 12 summarizes the results of these two analyses, showing means and standard errors for the different experimental conditions of each principal design variable (factor) on 'time' and 'precision' dependent variables.

The results for 'time' show significant effect of vision $F(3,839)=78.09$; $p<0.0001$, manipulation $F(1,839)=8.16$; $p<0.01$ and color $F(2,719)=30.11$; $p<0.0001$ in Annex 4-Table 12. Surgeons were significantly faster when no tool was used to perform the task and they were faster with direct vision (Figure 40(a)) like in the previous studies in chapter 1 and novices. Surgeons were also faster with Oculus 3D vision compared to the 2D visual image guided systems and with grayscale feedback compared to color feedback. Results for 'precision' show a significant effect of vision $F(3,839)=51.49$; $p<0.0001$ where direct vision yields a significantly better score than other visual feedbacks and Oculus 3D yields significantly the worst score (Figure 40(b)). Neither the manipulation modality $F(1,839)=0.01$; NS, nor the color factor $F(1,719)= 0.74$; NS had any significant effect on 'precision' in surgeon data analysis, such as with the novices.

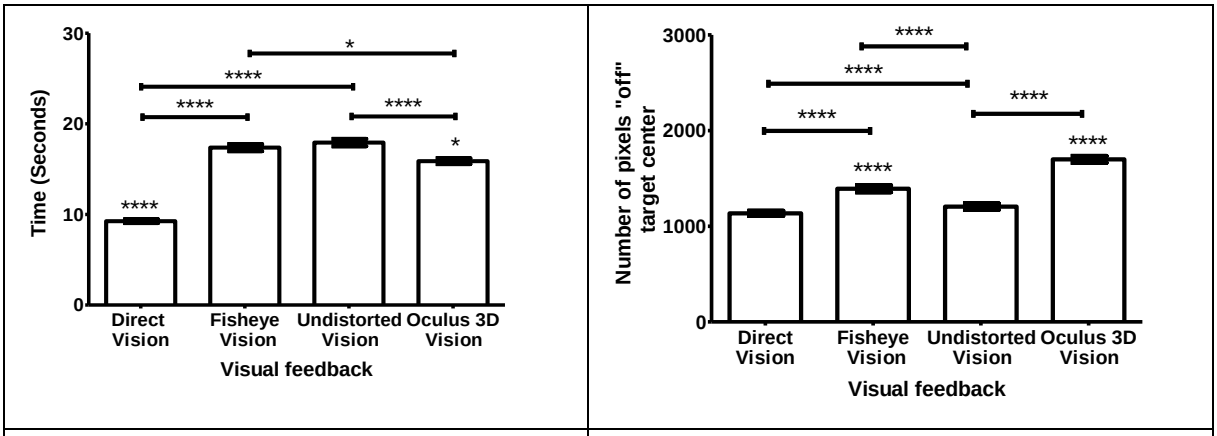

(a) (b)

Figure 40 – Six surgeon (a) 'time' and (b) 'precision' results for visual feedbacks in study 3. * is for $p<0.05$, ** for $p<0.01$, *** for $p<0.001$, **** for $p<0.0001$.

Expert surgeon results

The individual expert surgeon's data are shown in Figure 41. The upper figure panels show data for 'time' for no tool (on left) and tool (on right) manipulation and the lower panels show the corresponding 'precision' data, respectively. Expert surgeon was slower with tool and no tool manipulation in fisheye color view. His image guided visual feedback 'time' results are as fast as his direct vision results.

Two two-way ANOVA's were performed on raw data for 'time' (Annex 1- Figure 38) and 'precision' (Annex 1- Figure 40) independently to compare the effects of *visual feedbacks* on expert surgeon. Similarly, two three-way ANOVA's were performed on raw data for 'time' (Annex 1- Figure 39) and 'precision' (Annex 1- Figure 41) independently to compare the effects of *color feedbacks* on expert surgeon. Annex 4- Table 12 summarizes the results of this analysis, showing means and standard errors for the different experimental conditions of each principal design variable (factor) on the dependent variables 'time' and 'precision'.

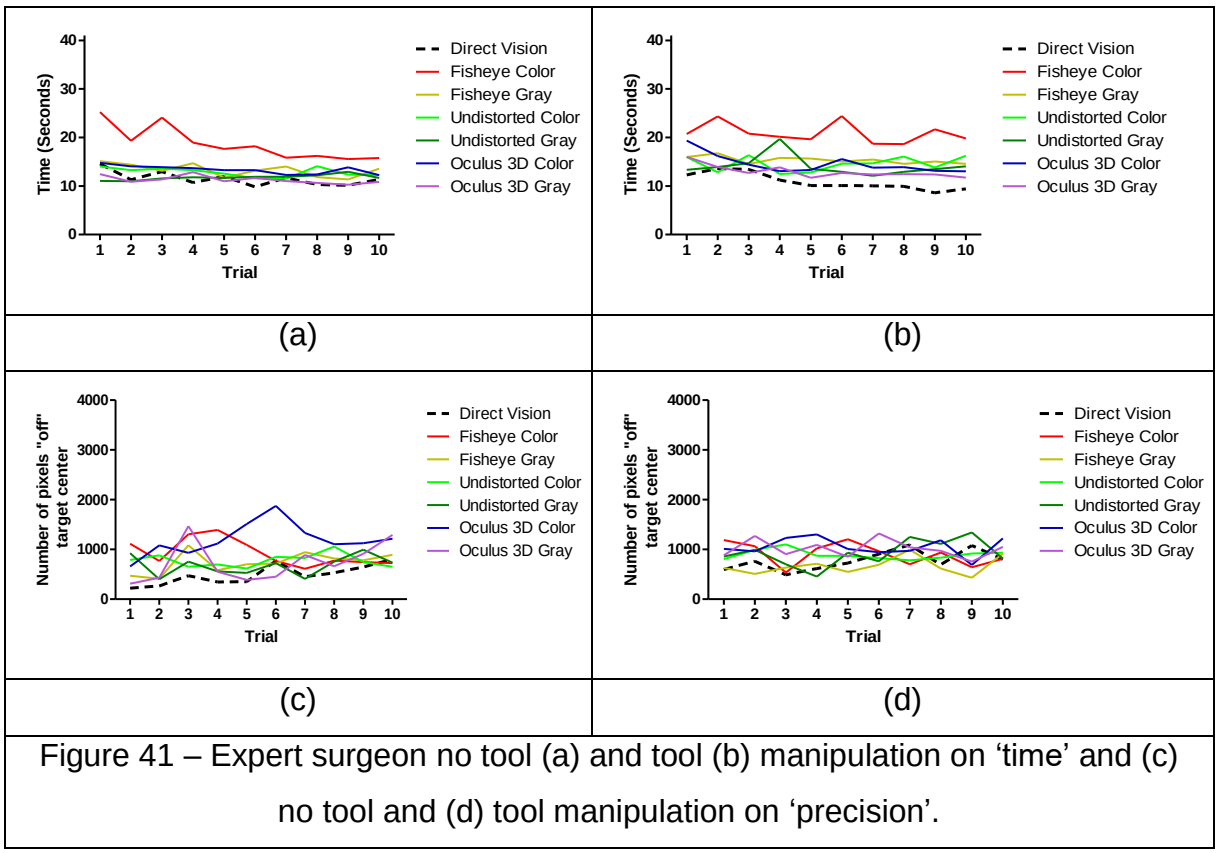

Figure 41 – Expert surgeon no tool (a) and tool (b) manipulation on 'time' and (c) no tool and (d) tool manipulation on 'precision'.

The results for ‘time’ show significant effect of vision F(3,139)=37.74; p<0.0001, manipulation F(1,139)=9.54; p<0.01 and color F(1,119)=78.49; p<0.0001 in Annex 4- Table 13. Expert surgeon was significantly faster with no tool condition and he was faster with direct vision like the novices (Figure 42(a)). There was no significant difference between the Oculus 3D stereo vision and undistorted 2D visual feedback. Expert surgeon was also faster with grayscale feedback compared to color feedback. Results for ‘precision’ show a significant effect of vision F(1,139)=10.3; p<0.0001 where direct vision yields a significantly better score than other visual feedbacks and Oculus 3D yields significantly the worst score, such as novices and surgeons (Figure 42(b)). Expert surgeon was also more precise without the tool in manipulation condition F(1,139)= 7.67; p<0.01 and he was more precise with the gray scale compared to color feedback on color condition F(1,119)=14.78; p<0.001.

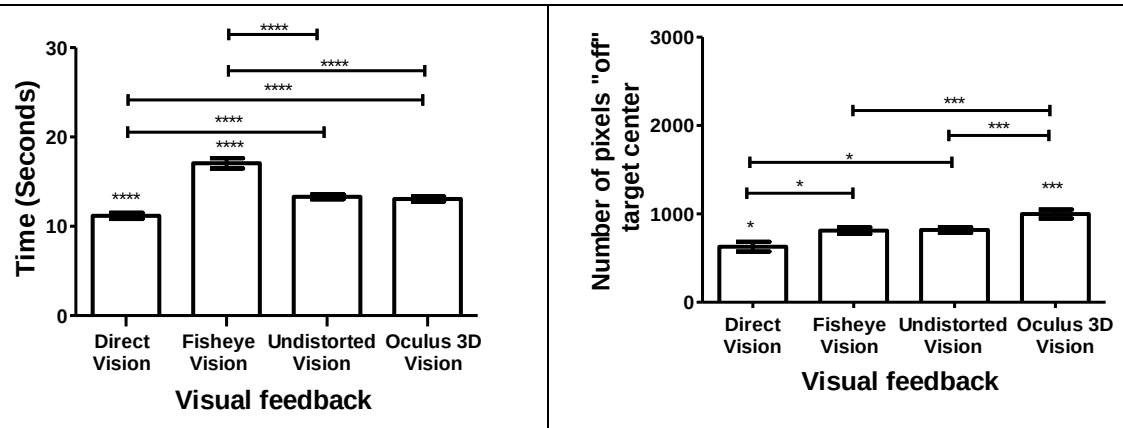

(a) (b)

Figure 42 – Expert surgeon (a) ‘time’ and (b) ‘precision’ results for visual feedbacks in study 3. * is for p<0.05, ** for p<0.01, *** for p<0.001, **** for p<0.0001.

Novices, Surgeons and Expert Surgeon motor performance on visual feedback

After the individual participant results, a comparison between the three groups (novices, surgeons and expert surgeon) was performed to understand expertise level modality on motor performance. Two three-way ANOVA was performed on raw data for ‘time’ (Annex 1- Figure 42) and ‘precision’ (Annex 1- Figure 44) independently to compare the effects of *visual feedbacks* on three different groups. Similarly, two four-

way ANOVA was performed on raw data for 'time' (Annex 1- Figure 43) and 'precision' (Annex 1- Figure 45) independently to compare the effects of *color feedbacks* on three groups, but because these results can be observed from the individual group results, they were not inspected here in detail. Only the interaction between ***expertise'*** (E_3) and *'color'* (C_2) conditions was investigated in detail for time ($F(2,2279)=21.85$; $p<0.001$) and 'precision' ($F(2,2279)= 0.11$; NS). These results are shown in Figure 43. According to the results in Figure 43, novices were the fastest compared to the surgeons and expert surgeon in both *color feedbacks*. Moreover, surgeons and expert surgeon were faster with the grayscale *color feedback.* On the other hand, expert surgeon was the most precise in both *color feedbacks.*

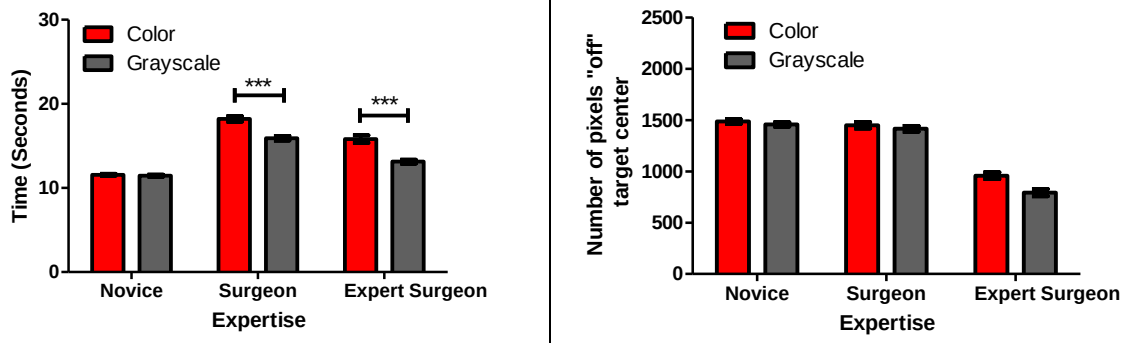

(a) (b)

Figure 43 – Novices, surgeons and expert surgeon trajectory color feedback analysis on (a) 'time' and (b) 'precision' in study 3. * is for $p<0.05$, ** for $p<0.01$, *** for $p<0.001$, **** for $p<0.0001$.

Moreover, a three-way ANOVA was performed for the 'error' independent variable to compare the effects of visual feedbacks (Annex 1- Figure 46) and color feedbacks (Annex 1- Figure 47) independently. The results of novices, surgeons, and expert surgeon are shown in Figure 44 for 'time', 'precision' and 'error'. Results of 'error' dependent variable are summarized in Annex 4-Table 14, showing means and standard errors for the different experimental conditions.

The results for 'time' in Figure 44(a) shows significant interaction between expertise E_3 and vision V_4 conditions $F(6,2659)=19.53$; $p<0.0001$ that novices were faster in each visual feedback condition. Expert surgeon was the slowest in the direct vision and he

was faster in undistorted and Oculus 3D conditions compared to the surgeons. Surgeons were the slowest group for undistorted and Oculus 3D conditions. The results for 'precision' in Figure 44(b) show significant interaction between expertise E_3 and vision V_4 conditions F(6,2659)=2.88; p<0.001 where expert surgeon was more precise in each vision condition level. There was no precision difference between novices and surgeons in visual feedbacks except for undistorted vision where surgeons were more precise compared to novices. Results for 'error' Figure 44(c) F(2,263)=5.35 p>0.001 show that surgeons made less errors compared to the novices and there is no error difference between novices and expert surgeon for 'error' dependent variable.

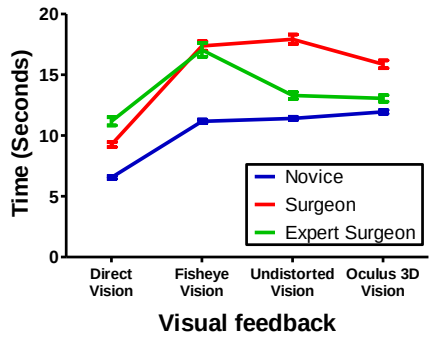

(a)

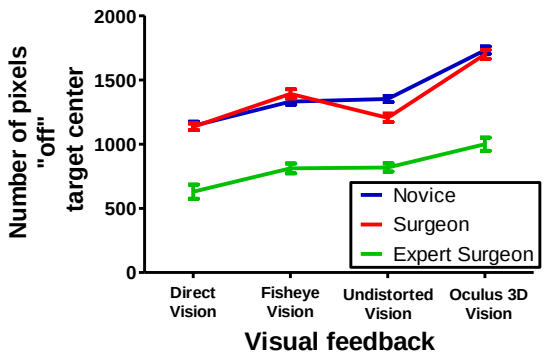

(b)

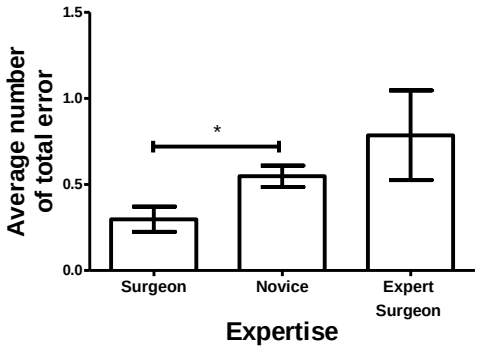

(c)

Figure 44 – Novice, surgeon and expert surgeon (a) 'time' and (b) 'precision' and (c) 'error' results for visual feedbacks in study 3. * is for p<0.05, ** for p<0.01, *** for p<0.001, **** for p<0.0001.

Novices, Surgeons and Expert Surgeon trajectory results on visual feedback

Medians and extremes of the individual data relative ‘from-target-to-target duration’, ‘average distance from the reference trajectory’ and ‘from-target-to-target duration’ for the different experimental conditions were analyzed first for novices, surgeons and expert surgeon. The results of this analysis are represented graphically as box-and-whiskers plots in Figure 45 for with or without tool manipulation with the four different vision conditions.

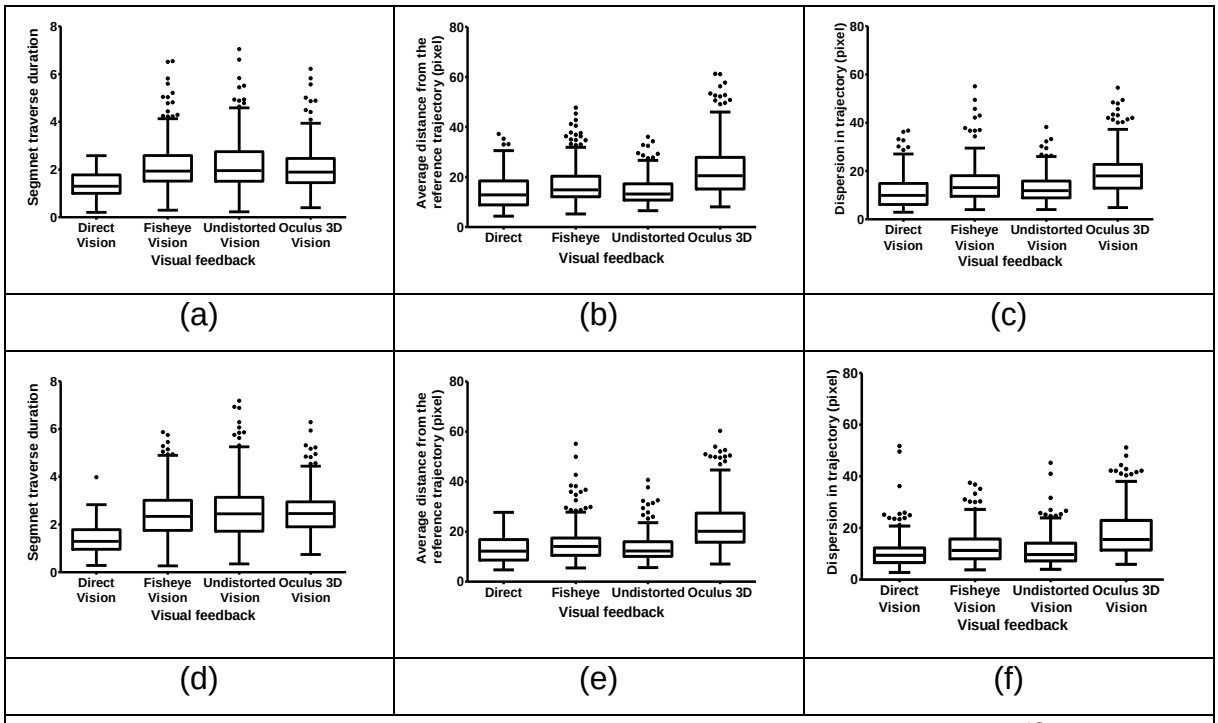

Figure 45 – Novices, surgeons and expert surgeon trajectory no tool (a) ‘from-target-to-target duration’, (b) ‘average distance from the reference trajectory’, (c) ‘dispersion in trajectory’ and tool (d) ‘from-target-to-target duration’, (e) ‘average distance from the reference trajectory’, (f) ‘dispersion in trajectory’ results for visual feedbacks in study 3.

Three three-way ANOVA were performed on mean data for ‘from-target-to-target duration’ (Annex 1- Figure 48), ‘average distance from the reference trajectory’(Annex 1- Figure 50) and ‘dispersion in trajectory’ (Annex 1- Figure 52) independently to compare the effects of visual feedbacks on novices, surgeons, and expert surgeon. Similarly, three four-way ANOVA were performed on mean data for ‘from-target-to-target duration’ (Annex 1- Figure 49), ‘average distance from the reference trajectory’

(Annex 1- Figure 51) and ‘dispersion in trajectory’ (Annex 1- Figure 53) independently to compare the effects of color feedbacks on novices, surgeons, and expert surgeon.

Annex 4-Table 15 summarizes the results of these analyses, showing means and standard errors for the different experimental conditions of each principal design variable (factor) on the dependent variables ‘from-target-to-target duration’, ‘average distance from the reference trajectory’ and ‘dispersion in trajectory’

The results for ‘from-target-to-target duration’ show significant effect for all factors for both color and visual feedback analysis. In expertise condition $F(2,1595)= 147.79$; $p<0.001$ novices were faster compared to the surgeons and expert surgeon (which also supports ‘time’ results), and all participants were faster in the direct vision compared to the other visual feedbacks in vision condition $F(3,1595)= 36.98$; $p<0.001$. Participants were also slower with tool manipulation $F(1,1595)=14.98$; $p<0.0001$ and faster with color feedback of the screen $F(1,1367)=18.46$; $p<0.0001$. The results for ‘average distance from the reference trajectory’ were not significant for both color feedback $F(2,1367)=2.8$; NS and visual feedback $F(2,1595)=0.45$; NS analyses on expertise factor. In vision conditions, $F(2,1595)= 106.3$; $p<0.001$ subjects moved away from the reference line with Oculus 3D vision and they moved closer with direct vision. Subjects also moved away from the reference line with the no tool manipulation condition $F(1,1595)= 19.79$; $p<0.0001$ and color feedback condition $F(1.1367)=3.90$; $p<0.05$. The results for ‘dispersion in trajectory’ show a significant effect for all factors in visual feedback and color feedback, except the expertise factor in the visual feedback condition $F(2,1367)=2.48$; NS. According to these results, expert surgeon was less stable in the trajectory movements $F(2,1595)= 7.87$; $p<0.001$. Subjects were more stable in direct vision and least in the Oculus 3D $F(3,1595)= 52.37$; $p<0.001$. Similarly, subjects were dispersing less when tool was used to perform the task $F(1,1595)=22.05$; $p<0.001$ and they were more precise with the grayscale visual feedback $F(1,1367)=4.53$; $p<0.05$.

The most critical factors for the study here, the *‘expertise’* (E_3) and *‘color’* (C_2) factors, produced significant effects on *color feedback* analysis for ‘from-target-to-target duration’ and on *visual feedback* analysis for ‘from-target-to-target duration’ and ‘dispersion in trajectory’. These can, however, not be summarized without taking into

account their interaction, which was significant on color feedback for 'from-target-to-target duration' for *'color'* (C_2) and *'expertise'* (E_3) (Annex 1- Figure 49 F(2,1367)=10.81; p<0.0001), and on *visual feedback* for 'from-target-to-target duration' (Annex 1- Figure 48 F(6,1367)=9.91; p<0.0001) and 'dispersion in trajectory' (Annex 1- Figure 52 F(6,1595)= 3.43; p<0.01) for *'vision'* (V_3) and *'expertise'* (E_3). The results for *'color'* (C_2) and *'expertise'* (E_3) are shown in Figure 46 and the results for 'from-target-to-target duration' and *'vision'* (V_3), and *'expertise'* (E_3) are shown in Figure 47(a) for 'from-target-to-target duration' and Figure 47(b) for 'dispersion in trajectory'.

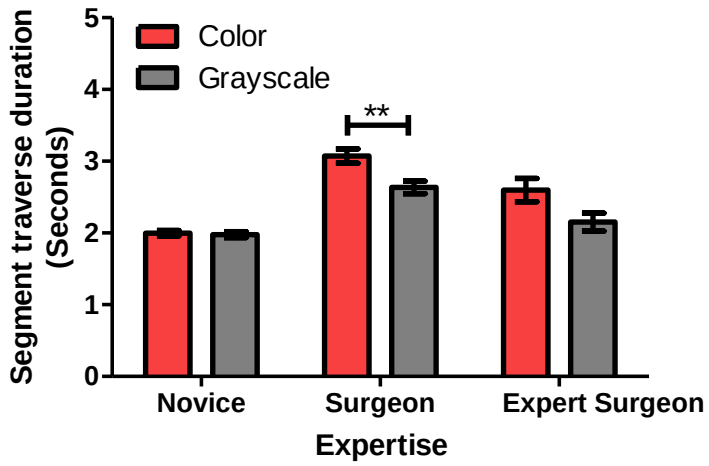

Figure 46 – Novices, surgeons and expert surgeon trajectory color feedback analysis on 'from-target-to-target duration' in study 3. * is for p<0.05, ** for p<0.01, *** for p<0.001, **** for p<0.0001.

The *'color'* (C_2) and *'expertise'* (E_3) interaction results in Figure 46 show a significant difference in surgeon's fisheye *color feedback* factor level, where surgeons were faster with grayscale feedback on 'from-target-to-target duration'. Expert surgeon was also faster with grayscale *color feedback* but this difference is not significant in the post-hoc analysis. These results also show a similarity with the 'time' results in the previous analysis on novices, surgeons and expert surgeon.

The results of *'vision'* (V_4) and *'expertise'* (E_3) interaction in Figure 47 (a) show a significant difference in surgeons' undistorted vision and Oculus 3D vision, and novices' fisheye vision of 'from-target-to-target duration'. Surgeons were slower in the undistorted vision compared to expert surgeon and novices undistorted vision and

surgeon were also slower in the Oculus 3D vision compared to novices. Novices were faster in each visual feedback and this result was significantly different in fisheye vision. The results of *'vision'* (V_4) and *'expertise'* (E_3) interaction in 'dispersion in trajectory' Figure 47 (b) shows significant differences for expert surgeon in direct vision and Oculus 3D vision. Expert surgeon was less stable in direct vision and Oculus 3D vision compared to surgeons and novices in Figure 47 (b).

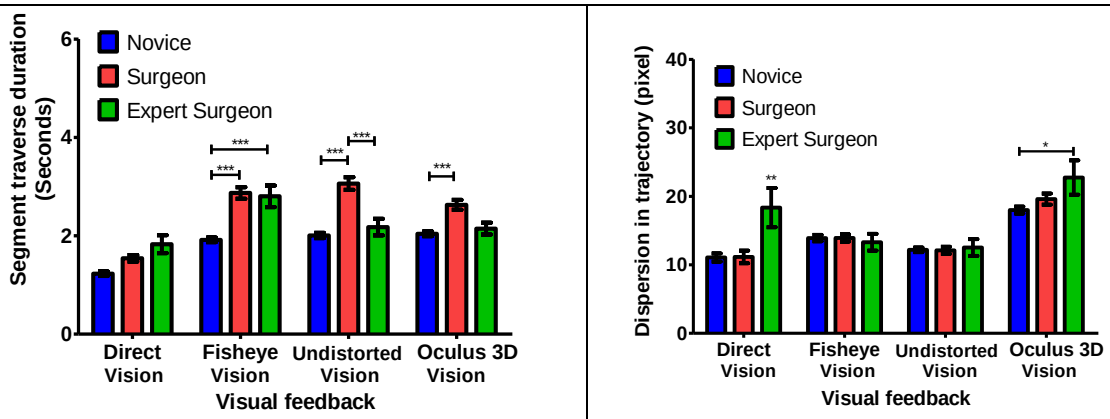

(a) (b)

Figure 47 – Novices, surgeons and expert surgeon trajectory *visual feedback* vision and expertise analysis on (a) 'from-target-to-target duration' and (b) 'dispersion in trajectory' in study 3. * is for p<0.05, ** for p<0.01, *** for p<0.001, **** for p<0.0001.

Discussion

In the last study of chapter 1, color cues on the Excalibur experimental setup for novices, surgeons and expert surgeon were analyzed with the same direct and indirect visual feedbacks used in the second study of first chapter.

In the previous studies of chapter 1, direct vision was always superior to the 2D image guidance during the pick-and-place task on the Excalibur system. The same result was also found in this study; novices, surgeons and the expert surgeon were faster and more precise with the direct vision compared to the fisheye vision. On the other hand, the 2D image guidance and stereoscopic 3D vision results of this study explain the differences between the previous research on this topic and the current study on Excalibur system.

The importance of precision

Precision is an important assessment factor, and this has been highlighted several times in the study 1, study 2 and the results here, in study 3. In this study, individual speed-precision curves were shown for novices and it was observed that novices were giving preference to their speed results more than their precision results. On the other hand, expert surgeon was always the most precise participant compared to novices and surgeons in each visual feedback, including direct vision. Batmaz et al. [31,32,36] showed the importance of the precision and why it has to be used as an assessment criterion. In conclusion, to develop motor performance of the subjects with a better visuo-motor experience in an image guided visual feedback and to reach the level of an expert surgeon, precision should be taken into account as an assessment criterion. For instance, in the latest review on 2D vs 3D Laparoscopic Cholecystectomy [159], writers focused on the execution time as the primary outcome, but not on the precision. The precision criterion should be included as an assessment method for future studies on the image guided surgical skill evaluation.

Stereoscopic 3D vs 2D on subject expertise

Previous studies from different researchers showed that stereoscopic 3D displays are superior to 2D visual feedback systems, however there was no advantage of stereoscopic 3D vision over the 2D visual feedback systems in the study 2 with novices. On the other hand, in this study, 3D display superiority was found only in the surgeons results among the all three of the participant groups - novices, surgeons and the expert surgeon. Surgeons were faster with the Oculus 3D vision compared to the 2D fisheye and undistorted vision, and this result was significant. This 3D stereoscopic display result shows similarity with previous research on visual feedbacks (e.g. [40,44,139]), especially taking time analysis into account (e.g. [64,65]) on surgeons.

The results for expert surgeon show that undistorted vision and stereoscopic 3D vision had similar execution times and that he was slower with the fisheye vision. Expert surgeon’s this result was an expected outcome due to the previous studies such as Curro et al [65] or Van Bergen et al [40]. According to Storz et al. [42] the difference between stereoscopic 3D vision and 2D visual feedbacks only occurs when expert surgeons are performing difficult tasks such as suturing or stitching.

Expert surgeon began his 2D visual feedback experiments with the fisheye vision. As he was the only expert among the surgeons, this fisheye execution time result created a bias between fisheye vision and other 2D visual feedbacks. The difference between fisheye image and other image guided visual feedbacks should disappear with the counter-balanced experiments on vision condition.

Results on novices show a similar outcome like previous studies in chapter 1 for image guided visual feedbacks; there was no superiority of stereoscopic 3D display either for time or precision.

As mentioned in the introduction, different studies divide their subjects into different groups according to the expertise level of participating subjects and there are no limits or boundaries for this grouping. This results in different groups with different experience levels in different studies which analyze image guided applications. Novices are usually defined as the group with the least number of laparoscopic case experiences, but this does not make them absolute beginners (examples of so-called novices are given in the introduction). On the other hand, the “Excalibur” experimental setup was designed for the complete beginners with no surgical experience in order to understand psychophysics behind the image guided procedures with tool manipulation executed in a pick-and-place task. To understand the complex interactions between different expertise levels and feedback systems, more subjects from heterogeneous backgrounds are needed (for more information, please look at the research of Ercikan and Roth [160]). This research derives the results for the initial learning process for novices from different backgrounds who have no previous experience on complex near-body space movements which can be used at the beginning of the training for surgeons.

Strategy preferences

Background homogeneity of the participants does not solely affect the results of the visio-motor performance analysis. A discussion with the surgeons took place after the results of the experiment were shared with them. Surgeons said that they were trying to be careful not to make any task errors during the experiment, even though they knew that they had to place the object “as fast as and as swiftly as possible” at the center of

each TA. When commenting on the trials, they stated that they were “trained to be careful and pay attention in order to make less errors” during the surgical procedures. Their attempt to avoid making any task error can be seen in their results in Figure 44(c); surgeons made significantly less errors compared to novices and expert surgeon. This result shows the importance of response strategy preferences, which is discussed in the first study of this chapter. ‘Errors’ are also used as an assessment criterion (e.g. [159]), but in this experiment, it was not an assessment criterion. However, surgeons tried to be careful to not to make any mistakes and it affected their performance measurements: it took longer for them to execute tasks compared to novices and expert surgeon. In this case, not only should the homogeneity of the participants be observed during the research, but also their “natural” variations in high-level action intentions during the execution of the task.

Color cues in image guidance

Results indicate that there was no ‘time’ and ‘precision’ difference between color and grayscale visual feedbacks on novices, but *surgeons* and *expert surgeon* were faster with the grayscale color feedback. Furthermore, *expert surgeon* was more precise with grayscale color feedback. This color visual feedback result shows that colored objects in the experimental setup distracts participants with experience on image guidance and affects their motor performance on ‘time’ and ‘precision’. The grayscale feedback affected the color of the blue top of the object and green tool-tips and turned them into grayscale colors. *Surgeons* and *expert surgeon* are used to bright achromatic tool reflections and screen color/brightness adjustments on the 2D visual feedback. These results could not be tracked on the *novices* because they were not used to performing complex near-body space movements with image guidance. Moreover, they had no experience on the color adjusted screens to focus on a particular region, so their actions were not affected by this color feedbacks.

Camera position

As explained in the introduction, the camera position of the “Excalibur” system could not be changed to follow the tool-tip or manipulated object. The current studies on 2D/3D visual feedback systems have this feature: a surgeon can move the camera to

the particular region of interest during the surgery. The camera position alignment and tool tracking have been studied for a long time (e.g. [141,154,161–165]) and it has been concluded that the camera position has a significant effect on visio-spatial performance of the subjects.

During the discussions with the surgeons, all the surgeons (the six members of surgeons and the one expert surgeon) were surprised by the fixed cameras of the Excalibur system. While the regular laparoscopic cameras allow them to move on a selected region, *surgeons* and the *expert surgeon* had to pay attention to the distortion in the Excalibur experimental systems to focus on each TA. This unusual feedback created a time and precision bias on *surgeons* and *expert surgeon*. This is potentially another possible explanation for the direct vision superiority compared to other 2D and 3D visual feedbacks.

Peri-personal space trajectory movements for novices, surgeons, and expert surgeon

Segment difficulty and its effect on peri-personal space with movement direction has been discussed in the second study of this chapter and in previous research [57,166–177]. In this study, expert surgeon came markedly closer to the reference trajectory line, but he deviated more compared to surgeons and novices. In the interaction results, it was observed that expert surgeon scattered more only in direct vision and Oculus 3D vision compared to surgeons and novices. In the image guided feedback, there was no difference between novices, surgeons, and expert surgeon for dispersion dependent variable.

During the interview with expert surgeon, he claimed that his performance results would be worse with the direct vision compared to other image guided feedbacks. In the results shown here in study 3, his direct vision task execution time was slower for segment traverse duration. Furthermore, his direct vision dispersion results were considerably more scattered compared to novices and surgeons. His assumption of direct vision was correct for ‘time’ and ‘dispersion in trajectory’, but it is still important to keep in mind that he was the most precise participant amongst the groups, which is an important assessment criterion.

Conclusions

The results from this chapter reveal complex and spontaneously occurring trade-offs between time and precision in the performance of individuals, for absolute beginners in visual spatial learning of an image-guided object positioning task. These trade-offs reflect cognitive strategy variations that need to be monitored individually to ensure effective skill learning. Collecting only time data to establish learning curves is not an option, as getting faster does not straightforwardly imply getting better at the task. Training procedures should include skill evaluation by expert psychologists and procedures for the adaptive control of speed-accuracy trade-offs in the performances of novices.

In consistency with earlier findings, image-guidance significantly slows down and significantly reduces the precision of goal-directed manual operations of novices, with all non-surgeons scoring high in spatial ability. In seeming contradiction with some of the results reported previously, 3D viewing systems do not straightforwardly produce better surgical eye-hand coordination in image guided procedures. The relative effectiveness of 3D technology for the precision and timing of surgical hand movements depends on the type and direction of hand movement required for the intervention, the participant’s (surgeon's) individual training, their division into the homogenous groups, color cues, and on the flexibility of the camera system generating the image views across target locations in the surgeon's peri-personal space.

The complex interactions between viewing, tool-use, ergonomics and individual strategy factors [117,118,178] open new and important perspectives for further research on novices in image-guided eye-hand coordination.

Chapter 2
Human-Computer Interaction in Head Mounted Virtual Reality

Introduction

In the second chapter, speed and precision analysis of real-world manual operations is investigated using immersive virtual reality (VR) and VR head mounted display. Emerging technologies on different visual feedback systems help surgeons to train themselves in different environments. Among these environments, VR became more popular in the last decade thanks to technological and industrial support. New simulator applications on surgical training are starting to develop in VR, but the major downside of these applications is their evaluation techniques. These applications do not perform any cognitive or psychomotor assessment experiments and they only take the execution time into account for performance assessment. This limitation creates a drawback in understanding the psychophysics behind the applications and VR itself.

One of the biggest advantages of the VR system is the ability to create virtual objects in any size, dimension or scale, and giving individual's an ability to interact with these objects using different input devices. Different size, orientation, scale, and even the position of the designed virtual objects can affect the motor performance of the individuals and the effects of these features on human cognition need to be studied within the framework of psychophysics. On the other hand, the human interaction with these virtual objects in the VR is not the same as real-world real target interactions since the feedbacks are artificially created. To overcome this problem, designers and engineers work on the visual, tactile, and auditory feedbacks to enhance the perception and to assist users to focus in VR, which causes variations in human performance and decision. Nevertheless, the effects of these non-real-world feedbacks and pseudo-feedbacks on human motor performance are still not well known.

In the first chapter, the importance of the precision assessment in surgical training and effects of different methods used to enhance motor performance of the novices in image guidance systems were studied. In the second chapter, motor performance of novices in VR medical training applications with manual hand operations [68–70] are analyzed by using human-computer interactions. For his purpose, the "NoTouch" system is developed to collect data from the complete novices.

Materials and Methods

The “NoTouch” experimental platform with its software was designed to collect data from human subjects in the second chapter. The computer hardware and main software “NoTouch” system were the same for all studies in chapter 2. In this following section below, the general system specifications are explained. In each particular study, explicit conditions and further improvements in the software regarding the experiment are explained in detail.

Handedness and spatial ability

In the experiments from this chapter, like for those described in chapter 1, participants’ handedness was assessed using the Edinburgh inventory for handedness designed by [107] to confirm that they were all true right-handers. They were screened for spatial ability on the basis of the PTSOT (Perspective Taking Spatial Orientation Test) developed by Hegarty and Waller [108]. This test permits evaluating the ability of individuals to form three-dimensional mental representations of objects and their relative localization and orientation on the basis of merely topological (i.e. non-axonometric) visual data displayed two-dimensionally on a sheet of paper or a computer screen. All participants scored successfully on 10 or more of the 12 items of the test, which corresponds to performances well above average, corresponds to spatial ability above average, as would be required for surgery.

Research ethics

All the studies were conducted in conformity with the Helsinki Declaration relative to scientific experiments on human individuals with the full approval of the ethics board of the corresponding author’s host institution (CNRS). All participants were volunteers and provided written informed consent. Their identity is not revealed.

Experimental platform – “NoTouch”

The experimental platform was a combination of hardware and software components designed to test the effectiveness of varying visual environments and VR for image-guided manual hand operations.

For the immerse VR headset, Oculus DK2 headset was used with the Leap Motion “hand and finger” Motion Sensor (from now on referred as ‘MS’). Oculus DK2 system head movement tracking was disabled during the experiments, only head orientation was enabled.

The MS was placed at the center of the front of the VR headset which enables simultaneous hand and finger tracking from the headset’s perspective. The instructions for the MS mounting on VR headset can be found on MS’s website [179]. The same exact procedure was also followed in the “NoTouch” system.

This MS and VR Headset setup has been used in recent medical studies [21–25] as well as in other studies [26–29].

Computer used in experiments

The same computer used in chapter 1 was also used in this study. A DELL Precision T5810 model computer equipped with an Intel Xeon CPU E5-1620 with 16 Giga bytes memory (RAM) capacity at 16 bits and an NVidia GeForce GTX980 graphics card. This computer was also equipped with three USB 3.0 ports, two USB 2.0 SS ports and two HDMI video output generators. The operating system was Windows 7. The computer was connected to a high-resolution full HD color monitor (EIZO LCD ‘Color Edge CG275W’) with an in-built color calibration device (colorimeter), which uses the Color Navigator 5.4.5 interface for Windows. The colors of objects viewed on the screen can be matched to LAB or RGB color space, fully compatible with Photoshop 11 and similar software tools. The color coordinates for RGB triples can be retrieved from a look-up table at any moment in time after running the auto-calibration software.

To perform the experiments, a Unity 3D 5.3.4 64-bit game engine was used with the Leap Motion Orion Software Development Kit and Oculus 0.8 Software Development Kit. 3D virtual objects were created with Blender 2.79 3D animation software.

Software design in experiments

Experiments were programmed in Unity 3D Game Engine using C#. The basic algorithm of the software is given here in Figure 48.

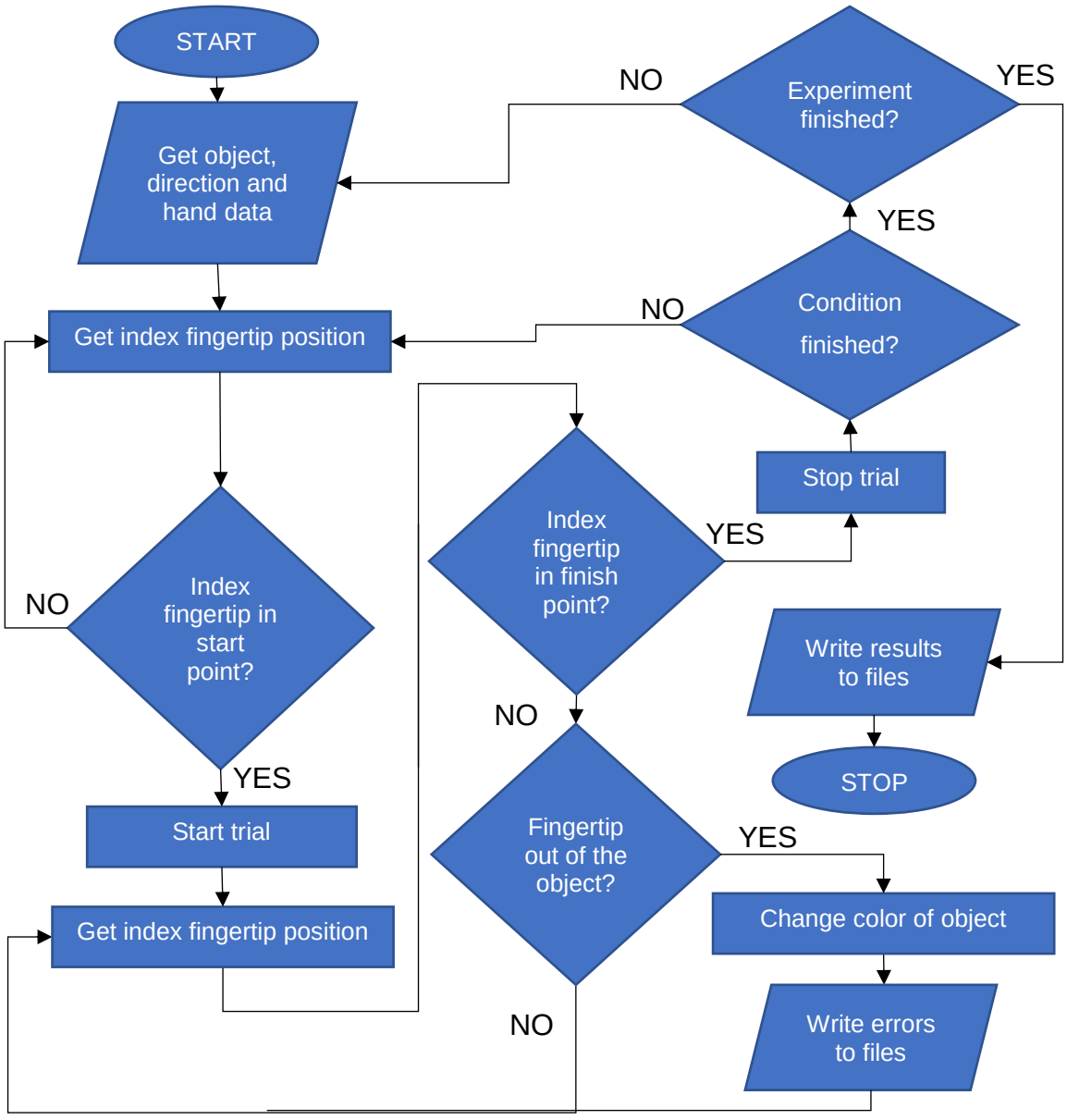

Figure 48 – General algorithm flowchart for second chapter studies. For each different experiment, codes are given in the particular study file.

The main software algorithm of the system was running on an infinite loop. At the beginning of the experiment, the experimenter had to choose the experimental factor levels for each experimental factor such as the size (small, medium, large), hand (dominant hand, non-dominant hand), hand movement direction (left-to-right or right-

to-left, up-to-down or down-to-up, clockwise or counter-clockwise), object (horizontal, vertical, torus), etc. After entering the chosen factor level, the subject had to place his/her index fingertip inside the ‘start point’. When the subject’s fingertip left the ‘start point’, the software checked if the subject’s index fingertip was outside the virtual object. If the subject’s index fingertip went out from the object surface, it was recorded as the precision criteria (more detailed experimental procedure was given in the Procedure and Data generation section of Materials and Methods). As soon as the subject’s fingertip reached back to the inside of the object, error recording was stopped. Once the subject’s index fingertip reached the ‘finish point’, a trial of the set was completed. After ten successful trials, the specific condition was completed and with the help of the experimenter, the experimental condition was changed to another and subject continued the experiment in that other experimental condition.

The index fingertip position was provided by the Orion Software Development Kit of MS and detection of the fingertip going out from the object surface, ‘start point’ and ‘finish point’ was detected by the object colliders of Unity 3D. All the objects in the experiment were placed at the scene of the Unity 3D which allowed virtual objects to drag-and-drop, position, scale and orientate. The time of one loop execution was between 10-20 milliseconds, which corresponds to a margin of 100-50 FPS (frame per second) of the image shown between frames. The average frame per second of the software was about 80 FPS.

Objects viewed on VR Scene

During the experiments, subjects saw two different objects in the virtual reality scene; their virtual skeleton hand and virtual images to follow. The skeleton hand was selected particularly for the experimental procedure; the joints of the subjects were highlighted by spheres in Figure 49. The whole hand was shown to subjects to help them to understand the direction and rotation of their own hand and to get the full spatial coordination reference in 3D virtual space. The fingertip estimation between the real index fingertip and the virtual index fingertip was bounded within 3.5 mm.

According to the study of Dankedar and colleagues [180], the average human index fingertip width varies between 1.6 cm and 2 cm. In the chapter 2 experiments, virtual

design of the objects used in the experiments were done according to the Dankedar et al. results; the narrowest cross-sectional diameter of the objects was 2 cm. Before each experiment, the index fingertips of the subjects were measured and it was assured that they were in the limits of the Dankedar et al. research.

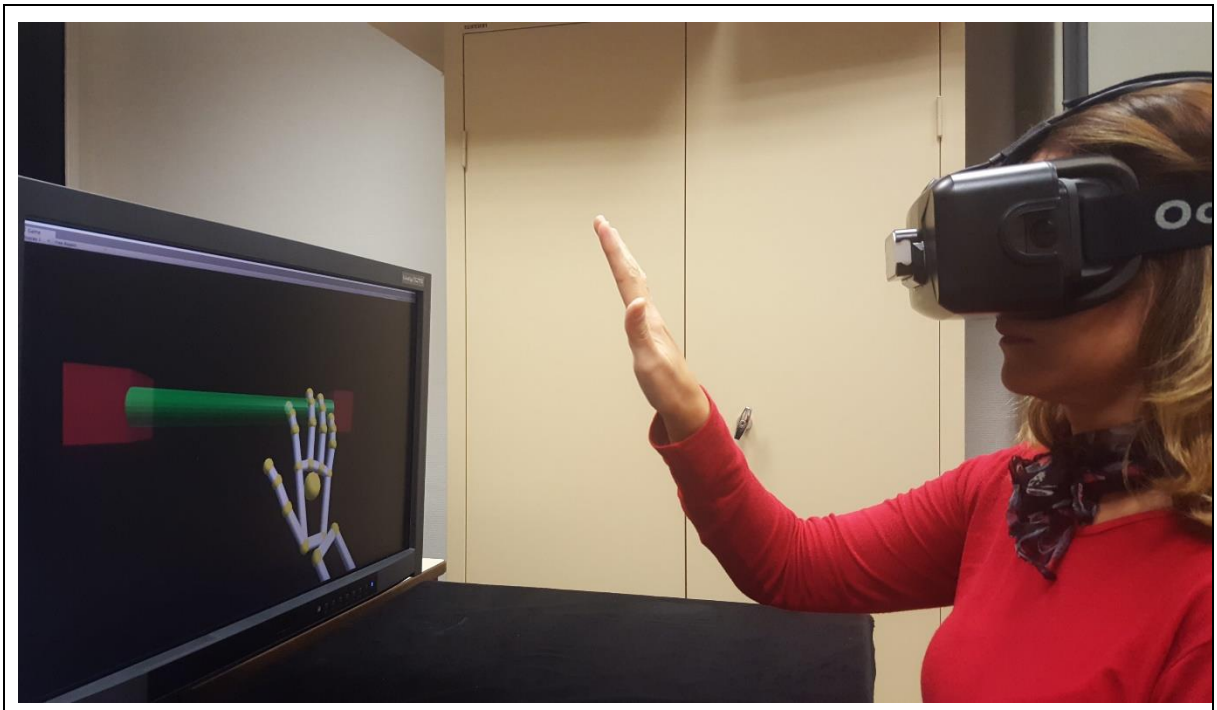

Figure 49 – An example scene from the left-eye-view of the subject with VR head mounted display and MS.

Two cylindrical objects (28 cm long with 3 cm cross sectional diameter) and a torus (25 cm major diameter and 3 cm minor diameter) were used to perform the experiments, as seen in Figure 50. The center of the all virtual objects in the VR was aligned with the eye level of the participants and the objects were 30 cm away from the eyes in VR. The position of the center of the VR objects were also at the center of the subjects two eyes.

One of the cylindrical objects was placed horizontally and the other one vertically. From this point on, the horizontally placed cylindrical object is called ‘Horizontal’ (Figure 50(a)) and the vertically placed cylindrical object is called ‘Vertical’ (Figure 50(b)). The third object, which is a torus, is called ‘Torus’(Figure 50(c)).

Six 5 cm x 5 cm x 5 cm cubes were used to “start” and “finish” the trials. At each side of the ‘Vertical’ and ‘Horizontal’ objects, two cubes were placed to indicate start and stop areas, positioning at the center of the two end points of each cylindrical object. For ‘Torus’, the start and finish cubes were placed on the left and right side of the object as shown in Figure 50(c). These cubes were called the ‘start point’ and the ‘finish point’, according to the direction of the hand movement (these cubes are shown in red in Figure 49).

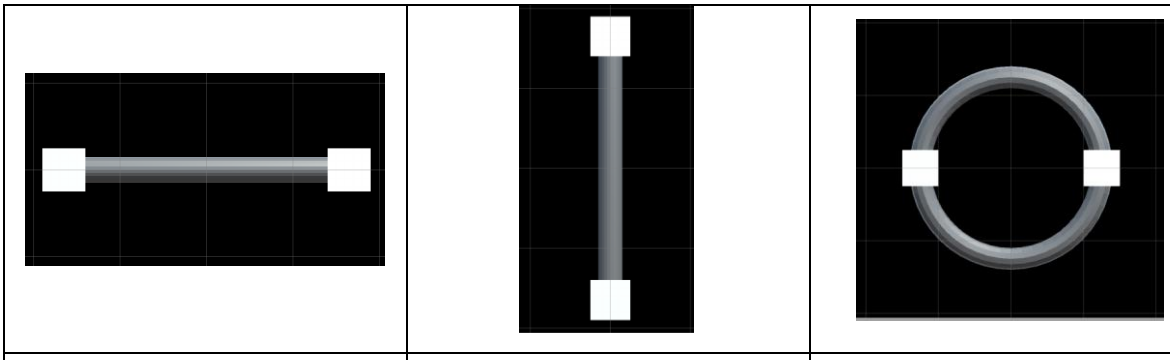

(a)	(b)	(c)

Figure 50 – VR objects used in the NoTouch. (a) ‘Horizontal’ virtual object, (b) ‘Vertical’ virtual object and (c) ‘Torus’ virtual object. Isometric perception of the objects turned cylinders into rectangles and torus into a circle.

‘Vertical’ and ‘Horizontal’ had cylindrical colliders on them for a collision detection algorithm. These colliders were the same size of the objects. ‘Torus’ was divided into 12 sub-parts and each part was containing less than 255 vertices. 255 vertices was the limit for the maximum number of vertices supported by the game engine for the collision detection.

Experimental environment

The experimental setup table was covered by a black velvet curtain. On the 2D screen monitor, the background was completely black so not to distract the subject. The virtual scene view of the left eye of the subject was projected to the 2D screen for the experimenter. Next to the experimental setup, a second DELL monitor was positioned. The experimenter was able to observe the experiment from the isometric view for depth perception. The experimenter was also able to change the experimental independent

conditions from the keyboard in front of him. A Dell mouse with a “SteelSeries” mousepad (40 cm x 44.5 cm) was used to move the cursor on the screen.

Procedure

Participants were comfortably seated at an adjustable chair. Before starting the experiments, they were instructed by the experimenter and shown how to perform the experiment correctly. The subjects were asked to strictly comply with the following rules:

- The outer side of the active hand had to always face the subject
- Subjects had to open their active hand and spread their fingers in order to show the outer side of all fingers to the motion sensor. The whole active hand had to be visible to the motion sensor on the virtual reality display.

During the experiments, the subjects were reminded of these rules which were necessary to collect stable index finger tip data from the motion sensors.

In all virtual objects, subjects had to start from the ‘start point’ and follow the structure with their index fingertip until the ‘finish point’. The ‘start point’ turned green when subject’s index fingertip was placed at the ‘start point’. At the same time the virtual object turned gray. Data collection started when the tip of the subject’s index finger left the ‘start point’ which then turned back to red.

For ‘Torus’, in particular, when the fingertip of the subject left the ‘start point’, this point turned into the ‘finish point’. The second cube used as ‘finish point’ in ‘Vertical’ and ‘Horizontal’ was turned into a gateway for the subject in ‘Torus’, so that subject had to go inside the cube to validate the trial. This approach was used to prevent the subjects making smaller circular movements and to prevent task fatigue.

For the trials of the studies, the whole of the virtual object turned into red color (R=255, G=0, B=0, A=100) whenever the subject’s fingertip left the structures inner surface at any moment during the experiment. Once the fingertip was back inside the object, the color of the object changed back to green color (R=0, G=255, B=0, A=100) (In Figure

49, the ‘Horizontal’ is green as the subject’s fingertip was inside the structure). The error visual feedback was provided to the subject with this color change, [181].

In each trial, only the virtual object to be followed was visualized; the other virtual objects were not shown to the subject (e.g. if the subject was performing experiment on ‘Horizontal’, she/he was not able to see ‘Vertical’ and ‘Torus’ objects. When the subject was not performing the experiment, the color of the object changed to gray color (R=100, G=100, B=100, A=100).

When the index fingertip of the subject reached the finish point, the given structure turned into red and the finish point turned into green to indicate the end of the trial set.

Every individual experiment always started with a “warm-up” run for each of the different conditions. Participants were instructed to “retrace the central axis of alignment of the objects as precisely and swiftly as possible”.

Data generation

During the experiments, all data were recorded in real time for each of the trial sets. Subjects had to perform the experiment starting at the “start point” and ending at the “finish point”. The data relative to time and precision of finger movements were recorded between these two points. There was no trial abortion or trial repetition in case of any errors. Subjects had to fully complete ten trial sets to validate the sets for each condition.

Four different dependent variables were used to analyze a subject’s motor performance. The first dependent variable was called ‘time’. Timing by the computer started when the index fingertip of the subject left the “start point” and it stopped when the index finger tip reached the “finish point”. For data analysis, an average of 10 repetitive trial set execution times was taken for each condition of the experimental design.

The second dependent variable was called ‘average number of finger-outs’. Whenever a subject’s fingertip went out of a virtual object’s inner surface, an error was recorded. For each trial, the total number of finger-outs was counted. This dependent variable was also used in the previous research, such as [182]. The average number of total

errors for 10 repetitive trials was computed at the end of each trial set and used for data analysis.

The third dependent variable was called ‘motor performance index”. This variable dependent is found by dividing the total time spent out of the virtual object to the execution time. The equation of this dependent variable is given in Equation (1). For data analysis, the average of 10 repetitive trial sets motor performance index was taken for each condition of the experimental design.

$$Motor\ performance\ index = \frac{Total\ out\ time}{Execution\ Time}$$	(1)

The last dependent variable was called “average accumulated distance away from the object surface” in cm. In this variable, the distance between the center of the index finger tip and the surface of virtual object was summed in every frame. This dependent variable was also used in previous research such as Williams et al [183]. The average number of accumulated distance away from the object surface for 10 repetitive trials was computed at the end of each trial set and used for data analysis.

All Post-hoc analyses are done by Sidak method. * is used for $p<0.05$, ** is used for $p<0.01$, *** is used for $p<0.001$ and **** is used for $p<0.0001$.

Study 1 – Effects of Different Levels of Virtual Rendering

In the first study of chapter two, different levels of virtual rendering were studied. Before working on VR and how it affects the motor performance of the subjects, the differences between various surgical simulation environments are investigated. The previous studies performed several comparisons between different simulator environment (e.g. [84,184,185]). In this study, these simulation environments are investigated further with time and precision dependent variables. Exclusively in this study head mounted display based immersive environments are compared to the conventional simulation environments.

Study Goal and Hypotheses

Since the accessibility and availability of different simulator environments have started to increase, various new simulation applications are starting to develop, which have the same goal but different methods to perform the task. Novices might need to use these similar surgical training systems in different environments. For instance, similar training applications for a topic can be found on desktop applications, VR applications, and even in the real life. Focusing on creating a variety of these applications leads to insufficient methods of motor performance assessment. The lack of how-to-assess-performance-of-the-novice knowledge on different surgical training systems can negatively affect the evaluation of the participants who use the same or similar surgical training environment systems: beginners' motor performance results may vary due to the task environment and prefrontal motor cortex and therefore have to learn the same tasks in different environments.

Virtual reality (VR) is an example of surgical training environments and it is frequently used in simulators to save on time and the cost of learning [25,180,186,187]. VR simulators became even more popular with the recent increase in the market availability and accessibility of immersive virtual reality headsets [22]. This opportunity also prompted VR designers to create powerful applications in different environments

and fields of application, and one of these is the biomedical field. Different types of virtual reality training applications and simulators are in use for different purposes with a variety of methods [22,188–190]. Although these systems are widespread, too little is still known to fully understand the cognitive feedback effects of immersive virtual reality and its influence on human perception and action.

Spatial performance analysis for 3D immersive virtual reality head-mounted displays usually exploits the task execution times to assess a subject's motor performance. Analysis based on a single dependent variable is, however, not enough to evaluate the full scope of motor performances of subjects and to assess their progress on simulators and applications [31,32]. For beginners, especially, action-specific hand movements can be affected by several factors, such as the head position, the overall environmental complexity, the color context, and so on [181,191]. To fully understand human motor behavior in surgical training applications, several complementary behavioral indicators should be taken into consideration and, operationalized experimentally in terms of different related dependent variables.

In the first experiment of the second chapter, motor performance of novices in different surgical training environments were studied. Subjects followed two cylindrical sticks positioned horizontally and vertically and a circular object as a torus in different simulator environments and their motor performance were assessed with task execution time and three different precision criteria.

Materials and Methods

Subjects

Eighteen right-handed subjects (seven male) ranging in ages between 25 and 33 (average = 27.35) participated in this study. None had any experience in VR and image-guided activities such as laparoscopic surgery training or other. Before starting the experiments, each subject's index fingertip width was measured as an average of 1.64 cm with the maximum of 1.9 cm. To be able to follow the objects in the virtual reality, the minimum distance between the shoulder and the fingertip was calculated

as 40 cm. Before starting the experiments, each subject's shoulder to fingertip distance was measured and the minimum distance was 62 cm.

Experimental platform

In this study, six different simulation environments used as different visual feedbacks were compared to see the advantages and disadvantages of the VR. These different environments are shown in Figure 51. Each experimental condition is named according to the study of Milgram et al [192].

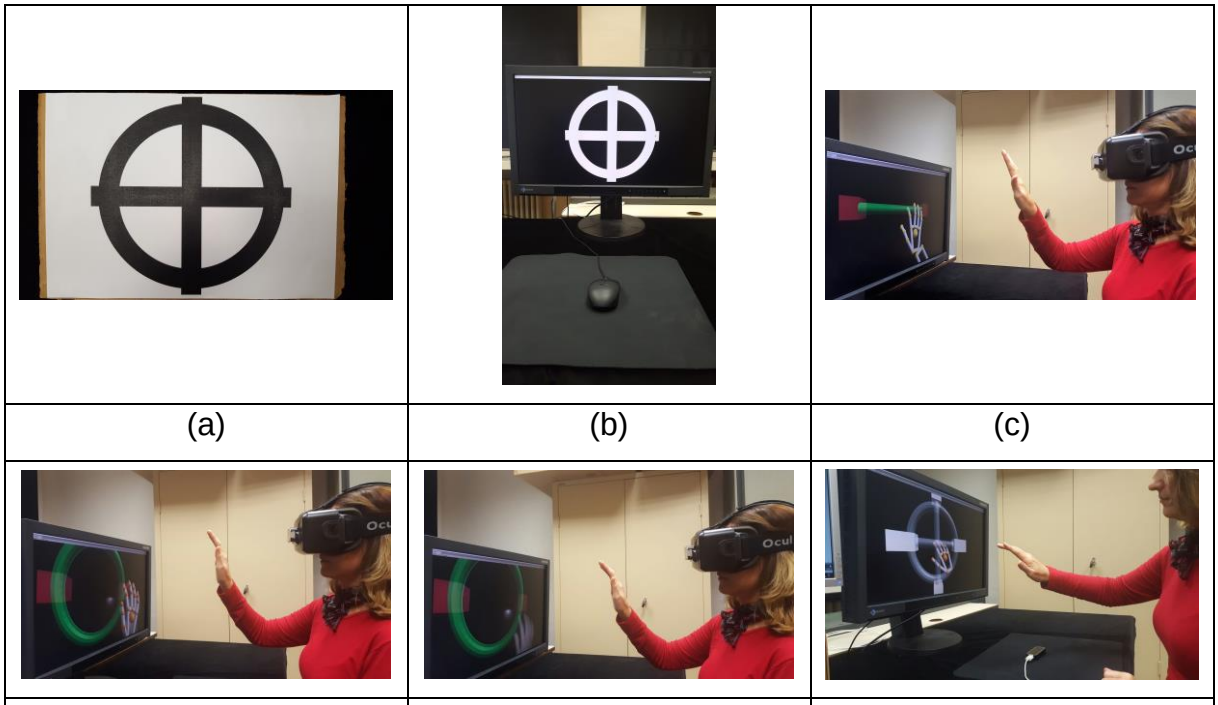

Figure 51 – Different experimental conditions used in the first study of chapter 2. (a) Natural View with Direct Touch (b) 2D Screen View (c) Virtual Reality (VR) (d) Augmented Reality (AR) (e) Mixed Reality (MR) (f) 2D Screen view with MS.

Real world view with direct touch

In this experimental setup, a size of A3 paper (297mm x 420 mm) was used on a carton board (Figure 51(a)). The same 'Horizontal', 'Vertical' and 'Torus' used in the "NoTouch" system were also drawn here in the same sizes ('Horizontal' and 'Vertical' virtual objects were 28 cm long and 3 cm wide and 'Torus' had a 25 cm major diameter and 3 cm minor diameter). 'Horizontal' and 'Vertical' virtual objects were extended 0.5

cm from each side to highlight the ‘start point’ and ‘finish point’ of the virtual objects. The dimensions of ‘Horizontal’, ‘Vertical’ and ‘Torus’ were checked with a tape.

2D Screen view

Similar to the *Real world view with direct touch* condition, the same ‘Horizontal’, ‘Vertical’ and ‘Torus’ used in the “NoTouch” system were also drawn here in the same sizes (‘Horizontal’ and ‘Vertical’ virtual objects were 28 cm long and 3 cm wide and ‘Torus’ had a 25 cm major diameter and 3 cm minor diameter) on the EIZO 2D screen monitor (Figure 51(b)). ‘Horizontal’ and ‘Vertical’ virtual objects were extended 1 cm from each side to highlight the ‘start point’ and ‘finish point’ of the virtual objects. Dimensions of ‘Horizontal’, ‘Vertical’ and ‘Torus’ were checked with a tape measure for fine adjustments.

Virtual Reality (VR)

The “NoTouch” system was used for the experiments in VR (Figure 51(c)). The size of the ‘Horizontal’, ‘Vertical’ and ‘Torus’ are given in the Materials and Methods section of chapter 2. The sizes of the ‘Horizontal’, ‘Vertical’ and ‘Torus’ were checked with a tape measure from the real world to ensure that image conditions matched the *real world view with direct touch* and *2D screen view* condition.

Augmented Reality (AR)

The “NoTouch” system was also used for the experiments in the *AR* condition. For this purpose, two-infrared cameras of the MS were used as camera inputs in the background of the virtual scene. This allowed subjects to see around their immediate space, such as their hands or the border of the table in front of them. The virtual skeleton hands were used in the *VR* condition and an image of the hands of the subjects were superimposed onto the virtual skeleton. This let subjects see their whole real hand and virtual skeleton hand at the same time (Figure 51(d)). The sizes of the ‘Horizontal’, ‘Vertical’ and ‘Torus’ are given in the Materials and Methods section of chapter 2. The sizes of the ‘Horizontal’, ‘Vertical’ and ‘Torus’ were checked with a tape measure in the real world to ensure that image conditions matched the previous experimental conditions.

Mixed Reality (MR)

In the *MR* condition, the “NoTouch” system was also used like the *VR* and *AR* conditions. Similar to the *AR* condition, two-infrared cameras of the MS were used as camera inputs for background images of virtual scene in the VR environment. Apart from the *AR* condition, the virtual skeleton was not used in this experiment. Subjects saw their own hands in the VR. The virtual skeleton used in the previous experiments was still used for data acquisition for index fingertip positions, but they were not visible on the scene (Figure 51(e)). The size of the ‘Horizontal’, ‘Vertical’ and ‘Torus’ used in the experiment are given in the Materials and Methods section of chapter 2. The sizes of the ‘Horizontal’, ‘Vertical’ and ‘Torus’ were checked with a tape measure in the real world to be ensured that image conditions matched the previous experimental conditions.

2D Screen view with Motion Sensor (MS)

2D Screen view with MS was a composition of VR and 2D screen view experiments in “NoTouch”. Within this condition, an immersive VR headset was not used. Instead, the EIZO Full HD screen was used for visual feedback. The MS in front of the immersive VR headset was positioned at the front of the subject, looking upwards as in Figure 51(f). This setup allowed the subject to perform 3D hand movement in free-space while she/he was looking at a 2D screen. The size of the ‘Horizontal’, ‘Vertical’ and ‘Torus’ used in the experiment were given in the Materials and Methods section of chapter 2. The sizes of the ‘Horizontal’, ‘Vertical’ and ‘Torus’ were checked with a tape measure in the real world to ensure that image conditions matched the previous experimental conditions.

Computer used in the experiments

In the first experiment of the second chapter, subjects used the same computer with the VR headset and the MS for *VR, AR, MR* conditions mentioned in the Materials and Methods section of chapter 2. In *Real world view with direct touch* condition, no computer or VR headset with MS was used to perform the experiments. In the *2D screen view* and *2D Screen view with MS* conditions, instead of the VR headset, 2D EZIO Full HD screen was used in the experiments with the computer. In *2D Screen*

view condition, a Dell mouse was used to retrace the objects on a SteelSeries mousepad. The software for the *2D Screen view* condition was written in Python 2.7 with OpenCV and the average Frame Per Second (FPS) of the screen was about 60 FPS.

Procedure

In *VR, AR, MR,* and *2D Screen view with MS* conditions, subjects performed the tasks with the “NoTouch” system.

In *Real world view with direct touch* condition, subjects placed their index fingertip between the end of the ‘Horizontal’ or ‘Vertical’ and the ‘Torus’ as ‘start point’. Subjects started to retrace ‘Horizontal’ or ‘Vertical’ with the ‘ready, GO!’ command of the experimenter and at the same time, the experimenter started the chronometer. When the index fingertip of participants reached the place between the other end of ‘Horizontal’ or ‘Vertical’ and ‘Torus’, subjects reached the ‘finish point’ and the experimenter stopped the chronometer to measure the execution time. For ‘Torus’, subjects placed their index fingertip into the intersection of ‘Torus’ and ‘Horizontal’ as ‘start point’. As the experimenter gave the ‘ready, GO!’ command, the chronometer of the execution time was started, and subjects began to retrace the ‘Torus’. When subjects reached back to the same intersection of ‘Torus’ and ‘Horizontal’, this point turned into the ‘finish point’ and chronometer was stopped to measure the execution time.

Similarly, for the *2D screen view* condition, subjects placed the cross cursor of the mouse between the end of the ‘Horizontal’ or ‘Vertical’ and the ‘Torus’ as the ‘start point’. Subjects started to retrace ‘Horizontal’ or ‘Vertical’ with the ‘ready, GO!’ command of the experimenter and at the same time, the experimenter started the chronometer from the computer keyboard. When cursor of the mouse reached the place between the other end of ‘Horizontal’ or ‘Vertical’ and ‘Torus’, subjects reached the ‘finish point’. The experimenter stopped the chronometer to measure the execution ‘time’ by using the computer keyboard. For ‘Torus’, subjects placed the mouse cursor to the intersection of ‘Torus’ and ‘Horizontal’ as ‘start point’. As experimenter gave the ‘ready, GO!’ command, the chronometer of the execution ‘time’ was started by using a

computer keyboard and the subject started to retrace the ‘Torus’. When subjects returned back to the same intersection of ‘Torus’ and ‘Horizontal’, this point turned into the ‘finish point’ and chronometer was stopped to measure the execution time by using the computer keyboard.

Cartesian Design Plan and Data Generation

Experimental design

Each experiment consisted of 10 successive trial sets per experimental condition for 18 subjects (P_{18}) and there were 144 experimental conditions: each subject followed ‘Vertical’, ‘Horizontal’ and ‘Torus’ in six different visual feedbacks (V_6: Real world view with direct touch, VR, AR, MR, 2D screen view, 2D screen view with MS), with three conditions of object parts (OP_3: ‘Vertical’, ‘Horizontal’ and ‘Torus’), with two conditions of handedness (H_2: dominant-hand and non-dominant hand) and with two conditions of finger movements direction for each individual object part (D_2: up to down-down to up for ‘Vertical’, left to right-right to left for ‘Horizontal’ and clockwise and counterclockwise for ‘Torus’. The order of visual feedback condition was counterbalanced between subjects and structures to avoid specific habituation effects. For the same reason, the order of the handedness and direction of finger movement conditions was also counterbalanced between subjects. Each subject performed 720 trials. In total, 12960 trials were performed. The Cartesian design plan of the experiment can be presented as V_6 x OP_3 x D_2 x H_2 x P_{18} x 10 trial sets.

Data generation

The data recorded from each of the subjects were analyzed as a function of the different experimental conditions, for each of the four dependent variables (‘time’, ‘average number of finger outs’, ‘motor performance index’ and ‘average accumulated distance away from the object surface’).

In *Real world view with direct touch* condition, execution ‘time’ was measured by a chronometer and number of finger outs were measured by naked eye. Thus, the total time spent out of the object surface was not able to be measured and ‘motor performance index’ was not used as a dependent variable in the results section. For

the same reason, the distance away from the object surface was not able to be measured and ‘average accumulated distance away from the object surface’ was not used as a dependent variable. In the ‘Results’ section, # is used to indicate *Real world view with direct touch* condition significant difference for $p<0.001$ with other visual feedback conditions.

Because of different direction movements, it was not possible to perform a full factorial ANOVA including all three object parts and all movement directions in the same ANOVA with full factorial analysis. For this reason, a three-way ANOVA was performed for each object part, separately for each dependent variable.

Three three-way ANOVA were run on the average data for each ‘time’ and ‘average number of finger outs’ dependent variables. V_6 x D_2 x H_2 x P_{18} Cartesian design plan was used with average of ten repeated trial sets for each combination of conditions within a session, yielding a total of 432 experimental observations for each Object part (OP_3.), ‘Horizontal’, Vertical and ‘Torus’ for each ‘time’ and ‘average number of finger outs’.

A similar Cartesian design plan was used for ‘motor performance index’ and ‘average accumulated distance away from the object’, but in these dependent variable analyses, *Real world view with direct touch* condition was not included into the Visual Feedback condition V_6. In this case, V_5 x D_2 x H_2 x P_{18} Cartesian design plan is used with average of ten repeated trial sets for each combination of conditions within a session, yielding a total of 360 experimental observations for each Object part (OP_3.), ‘Horizontal’, Vertical and ‘Torus’ for each ‘‘motor performance index’ and ‘average accumulated distance away from the object surface’.

Results

‘Time’ ANOVA results on ‘Horizontal’, ‘Vertical’ and ‘Torus’ object parts with r*eal world view with direct touch* condition

The object parts three-way ANOVA ‘time’ results are shown in Annex 2-Figure 1 for ‘Horizontal’, in Annex 2-Figure 2 for ‘Vertical’ and in Annex 2-Figure 3 for ‘Torus’.

ANOVA results showed that there were significant differences in “Visual feedback” on ‘Horizontal’ $F(5,431) = 30.97$; $p<0.0001$, on ‘Vertical ’$F(5,431)=79,786$; $p<0.0001$ and on ‘Torus’ $F(5, 431)= 39.86$; $p<0.0001$. Means and Standard Error of Means (SEM) are shown in Figure 52 and Annex 4-Table 16. In Figure 52, dashed line for each individual virtual stick show the Real-world view with direct touch condition as the benchmark condition.

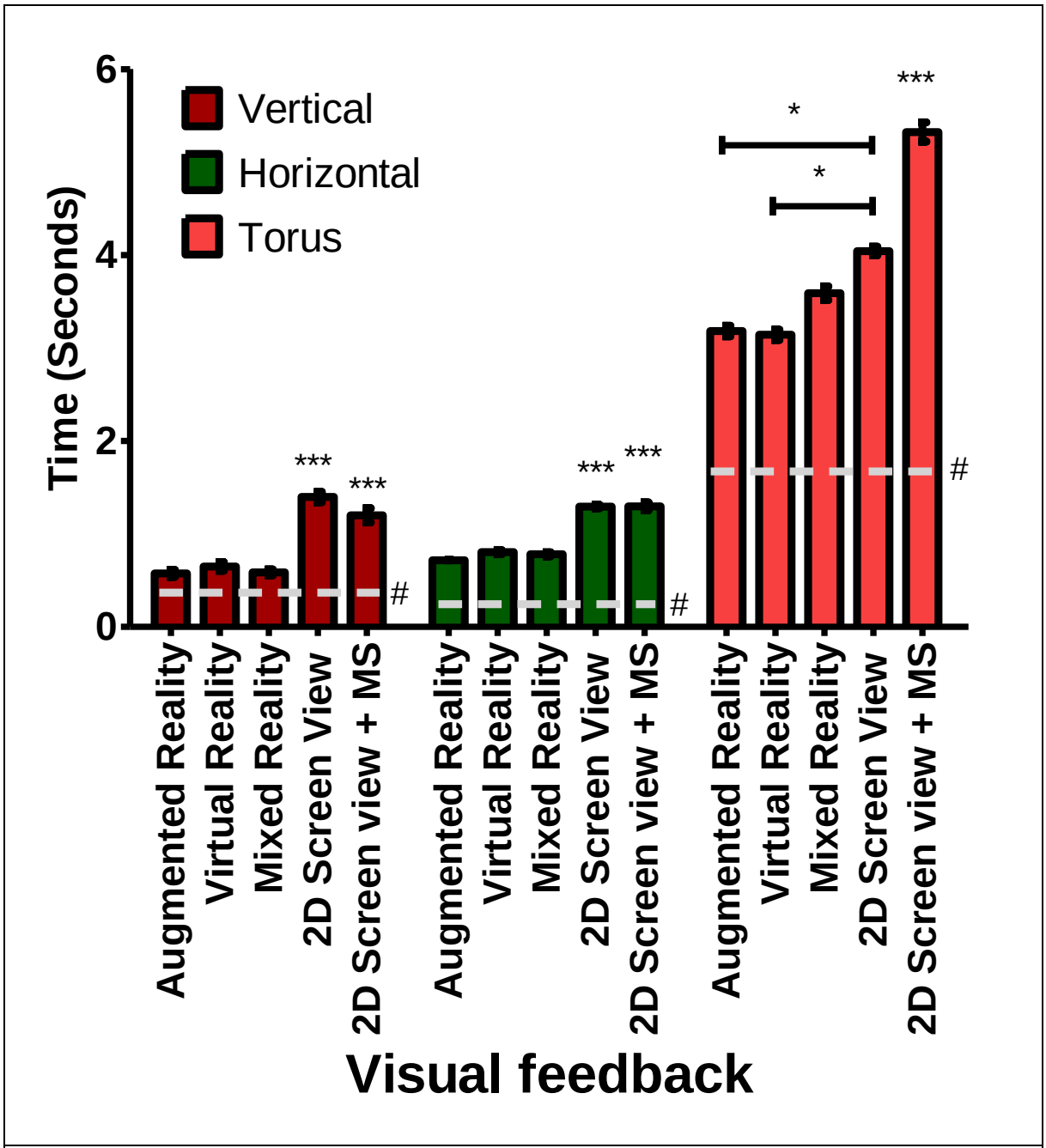

Figure 52 – Visual feedback results for different visual feedback on ‘time’

Furthermore, significant differences were found in ‘Torus’ for Handedness independent variable $F(1,431)= 4.752$; $p<0.05$ (Annex 4-Table 17) and in ‘Vertical’ for Visual feedback and Handedness interaction with $F(5,431)= 2.85$; $p<0.05$ (Annex 4-Table 18 and Figure 53).

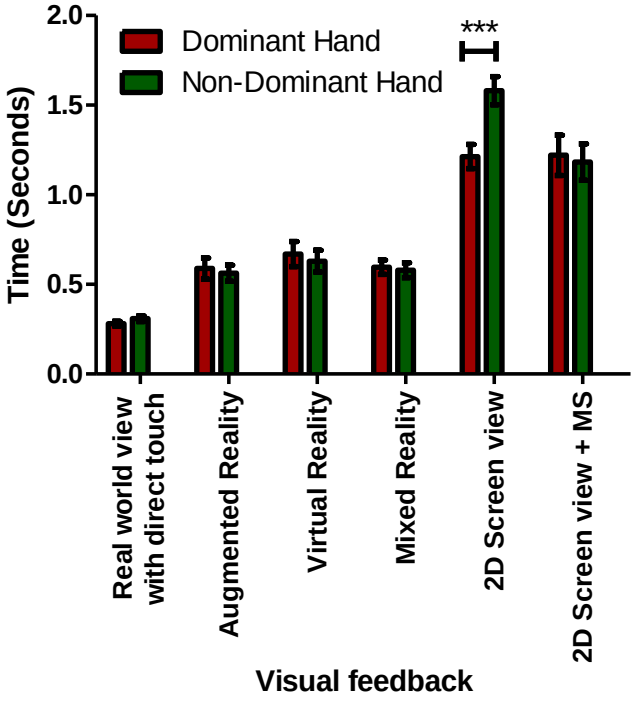

Figure 53 – Visual feedback and handedness results for ‘Horizontal’ for ‘time’ dependent variable

These results show that subjects were faster with the *Real-world view with direct touch* condition and there was no major significant difference between *VR, AR,* and *MR*. Moreover, when subjects were using *2D screen view* and *2D screen view with MS*, they were slower when compared to other visual feedback conditions. Moreover, subjects were faster with their dominant hand and these results were especially significantly different in *2D Screen view*.

‘Average number of finger outs’ ANOVA results on ‘Horizontal’, ‘Vertical’ and ‘Torus’ object parts with *real world view with direct touch* condition

The object parts three-way ANOVA results are shown in Annex 2-Figure 4 for ‘Horizontal’, in Annex 2-Figure 5 for ‘Vertical’ and in Annex 2-Figure 6 for ‘Torus’.

ANOVA results showed that there were significant differences in “Visual feedback” in ‘Horizontal’ $F(5,431) = 8.737$; $p<0.0001$, in ‘Vertical’ $F(5,431) =12.609$; $p<0.0001$ and in ‘Torus’ $F(5, 431) = 154.53$; $p<0.0001$. Moreover, handedness condition was also significant for ‘Horizontal’ $F(5,431) = 6.679$; $p<0.0001$, ‘Vertical’ $F(5,431) =6.296$; $p<0.015$ and on ‘Torus’ $F (5, 431) = 154.53$; $p<0.0001$ and means and SEMs are shown in Figure 54 and Annex 4-Table 19. In Figure 54, dashed lines for each individual virtual stick show the *Real-world view with direct touch* condition as the benchmark condition. The results for ‘Horizontal’ and ‘Vertical’ in *Real-world view with direct touch* are not available to see in Figure 54 because of its small value.

Apart from results in Figure 54 and Annex 4-Table 19, ‘Vertical’ showed significant difference on Visual feedback and Handedness interaction (Annex 4-Table 21 and Figure 55) with $F(5,431) = 2.28$; $p<0.05$; ‘Horizontal’ showed significant difference on movement direction $F(2,431)= 8.306$; $p<0.01$ (Annex 4-Table 20) and visual feedback and movement direction interactions $F(5,431) = 3.285$; $p<0.01$ (Annex 4-Table 22 and Figure 56) and ‘Torus’ showed significant difference on handedness and movement direction interaction $F(1,431)=11.355$; $p<0.001$ (Annex 4-Table 23 and Figure 57).

These ‘average number of finger outs’ results showed that there is no major differences between *VR, AR,* and *MR* on the ‘average number of finger outs’. Furthermore, while subjects were slower on *2D screen view* condition compared to *VR, AR,* and *MR*, conditions, they were more precise in ‘average number of finger outs’ results on *2D screen view* condition compared to *VR, AR,* and *MR*. While the *real-world view with direct touch* was the most precise condition, *2D screen view with MS* showed the worst results in all visual feedbacks.

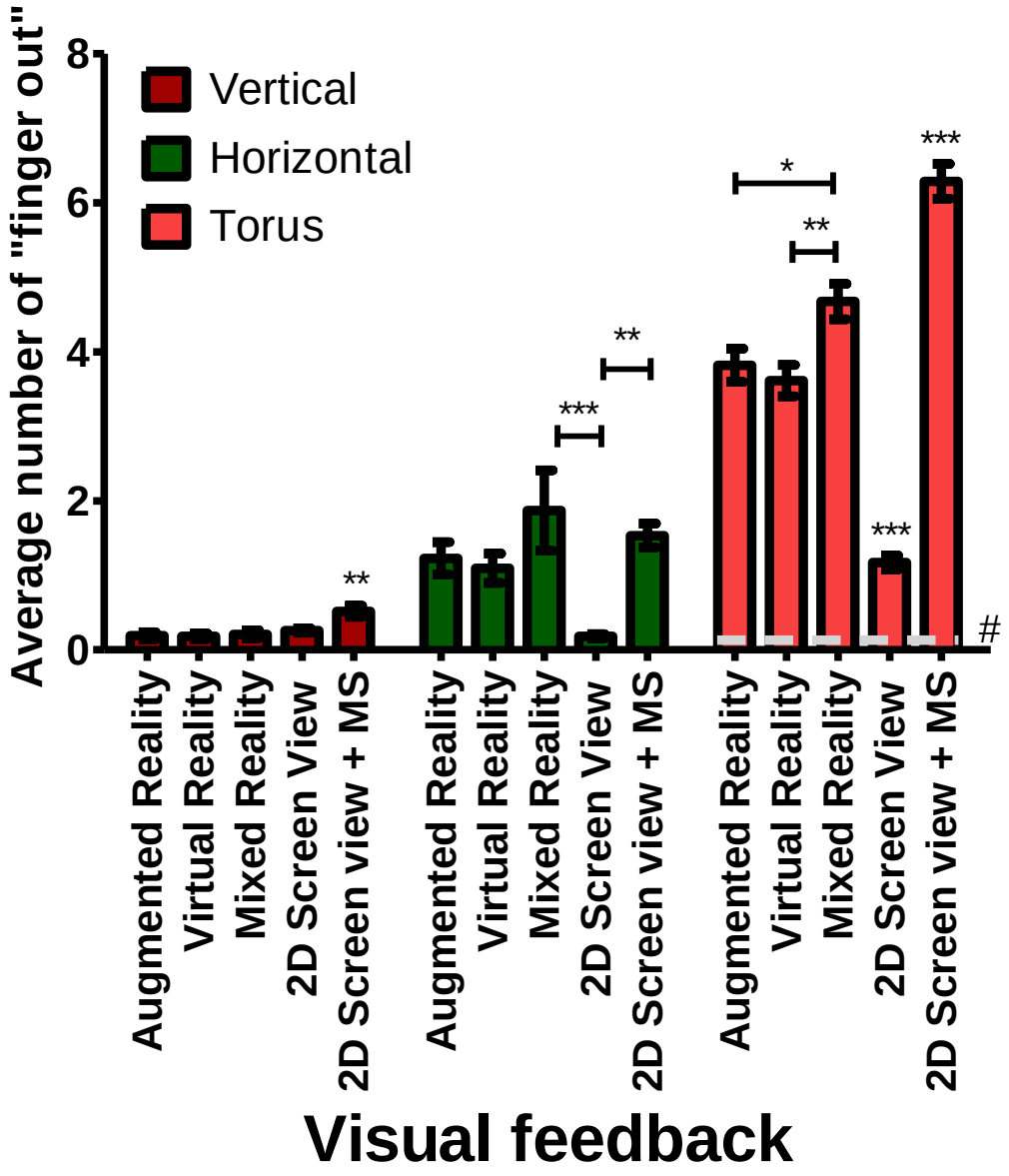

Figure 54 – Visual feedback results for different visual feedback of rendering on ‘average number of finger outs’ dependent variable

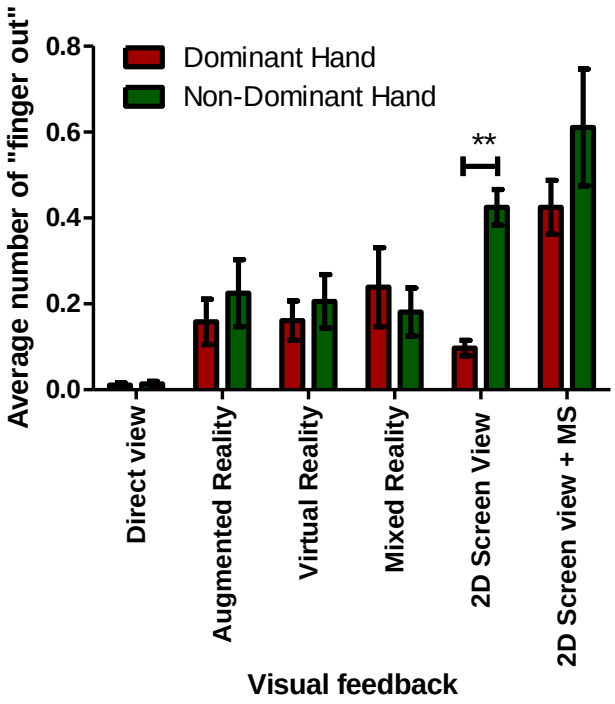

Figure 55 – Visual feedback and handedness results for 'Vertical' on 'average number of finger outs' dependent variable

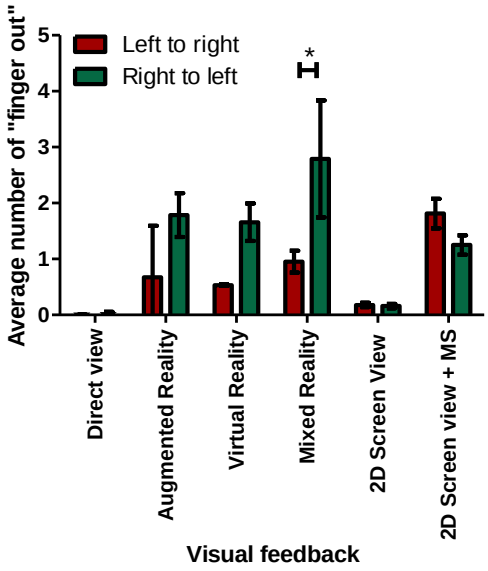

Figure 56 – Visual feedback and handedness results for 'Vertical' on 'average number of finger outs' dependent variable

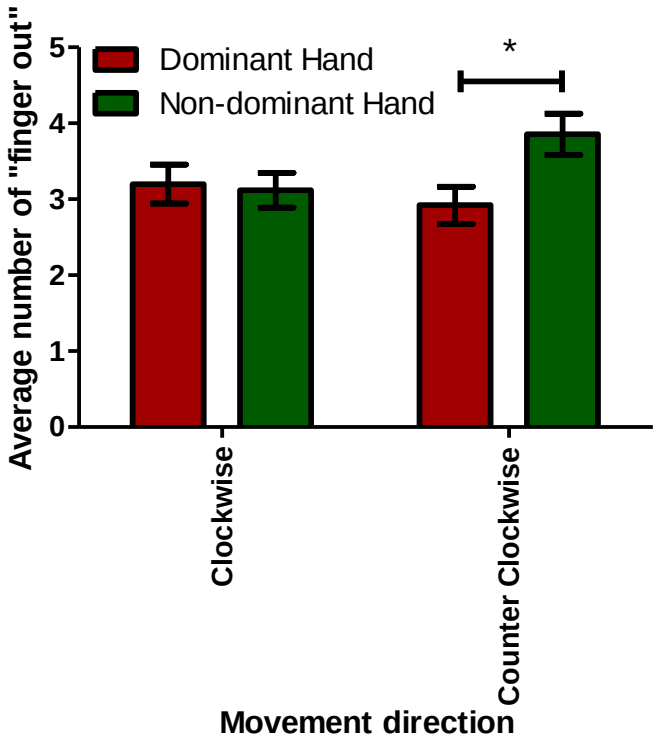

Figure 57 – Visual feedback and handedness results for 'Vertical' on 'average number of finger outs' dependent variable

'Motor performance index' ANOVA results on 'Horizontal', 'Vertical' and 'Torus' Object Parts without *Real world view with direct touch* condition

The object parts three-way ANOVA results for 'motor performance index' are shown in Annex 2-Figure 4 for 'Horizontal', in Annex 2-Figure 5 for 'Vertical' and in Annex 2-Figure 6 for 'Torus'.

ANOVA results showed that there were significant differences in visual feedback on 'Horizontal' $F(4,359) = 13.205$; $p<0.0001$, on 'Vertical' $F(4,359) = 9.651$; $p<0.0001$ and on 'Torus' $F(4, 359) = 49.526$; $p<0.0001$. Means and Standard Error of Means (SEM) are shown in Figure 58 and Annex 4-Table 24.

Furthermore, 'Horizontal' had a significant difference on movement direction condition $F(1,359) = 7.695$; $p<0.001$ (Annex 4-Table 25), visual feedback and hand interaction $F(4,359)= 5.205$; $p<0.0001$ (Annex 4-Table 26 and Figure 59) handedness and

movement direction interaction F(1,359)= 5.546; p <0.05 (Annex 4-Table 27 and Figure 60). 'Torus' also had significant differences on Handedness F(1,359) = 7.437; p<0.01 (Annex 4-Table 28), visual feedback and handedness F(4,359)= 6.071; p<0.0001 (Annex 4-Table 29 and Figure 61), and handedness and movement direction conditions F(4,359)= 4.237; p<0.05 (Annex 4-Table 30 and Figure 62).

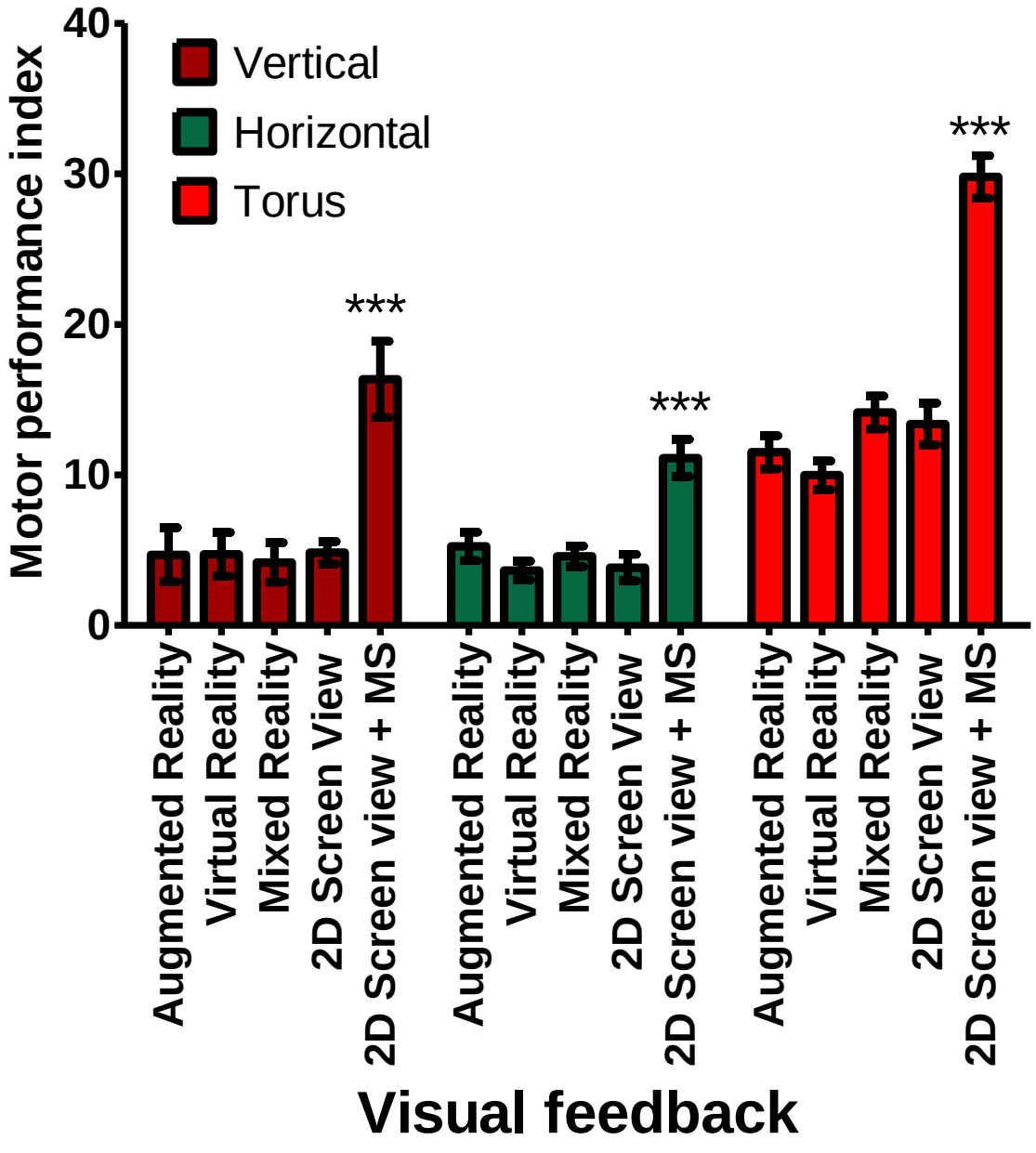

Figure 58 – Visual feedback results for different visual feedbacks of rendering 'motor performance index' dependent variable

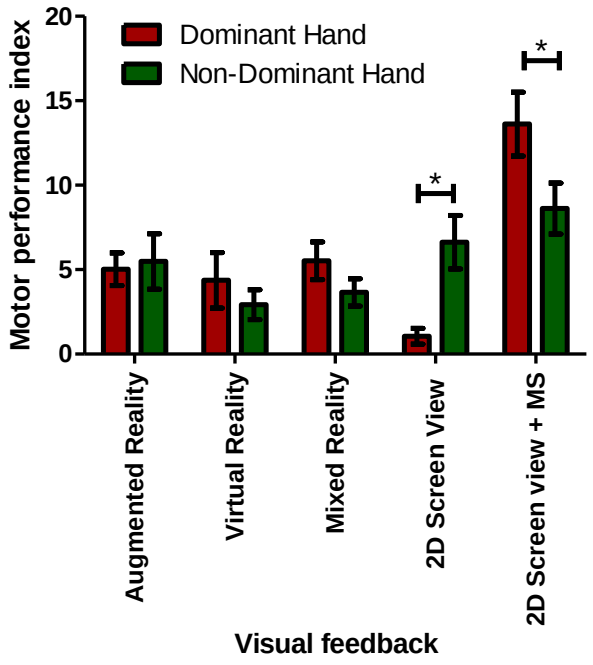

Figure 59 – Visual feedback and handedness interaction 'motor performance' index results on 'Horizontal'

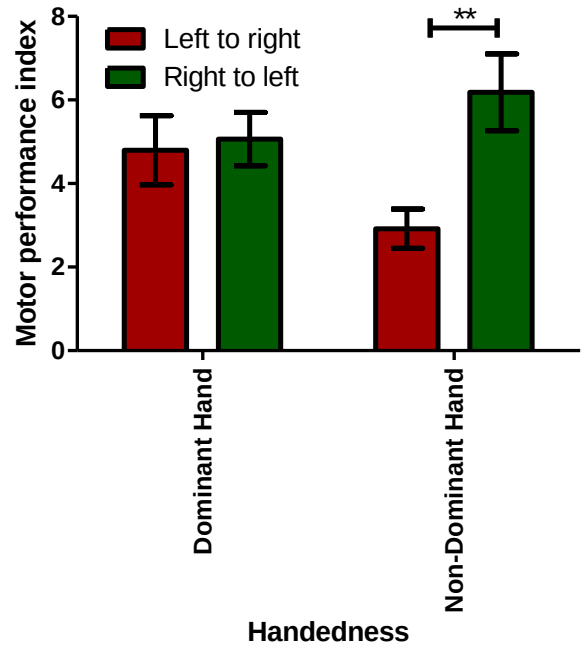

Figure 60 – Handedness and movement direction interaction 'motor performance index' results on 'Horizontal'

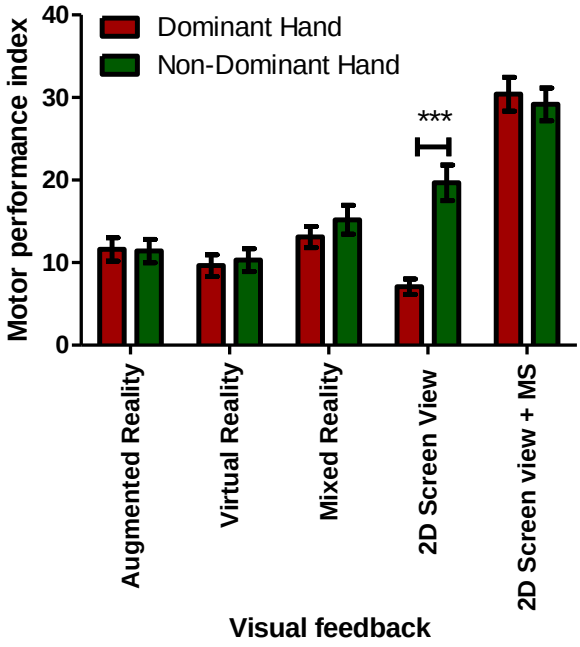

Figure 61 – Handedness and movement direction interaction 'motor performance index' results for 'Torus'

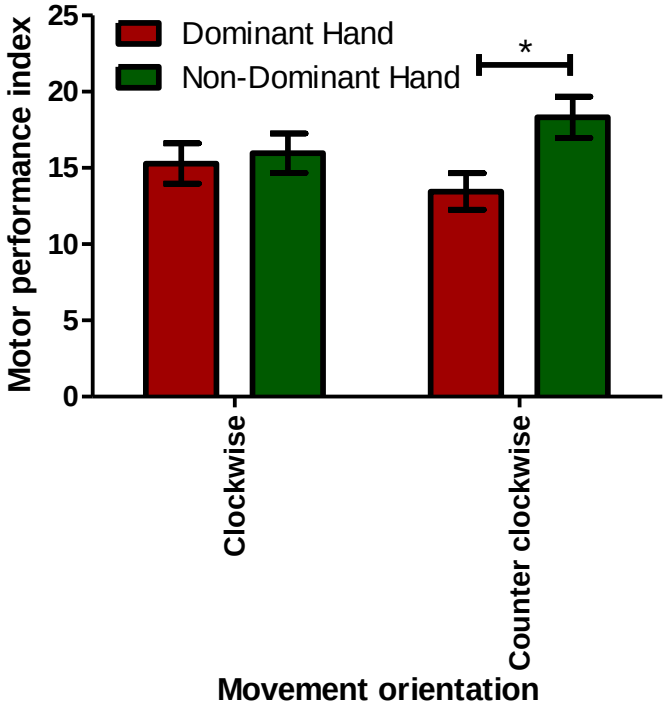

Figure 62 – Handedness and movement direction interaction results on 'motor performance index' for 'Torus'

According to these results, there is no significant difference between AR, VR, MR and 2D screen view. On the other hand, 2D screen view with MS showed the worst results for the 'motor performance index'.

'Average accumulated distance away from the object surface' ANOVA results on 'Horizontal', 'Vertical' and 'Torus' object parts without *real world view with direct touch* condition

The object parts three-way ANOVA results are shown in Annex 2-Figure 10 for 'Horizontal', in Annex 2-Figure 11 for 'Vertical' and in Annex 2-Figure 12 for 'Torus' for 'average accumulated distance away from the object surface'.

ANOVA results showed that there were significant differences in "Visual feedback" in 'Horizontal' $F(4,359) = 4.356$; $p<0.01$, on 'Vertical' on $F(4,359) =14.024$; $p<0.0001$ and on 'Torus' $F(4, 359) = 33.445$; $p<0.0001$. Means and SEMs are shown in Figure 63 and Annex 4-Table 31.

Furthermore, 'Horizontal' had a significant difference in movement direction condition $F(1,359) = 13.647$; $p<0.0001$(Annex 4-Table 32), visual feedback and hand interaction $F(4,359)= 4.044$; $p<0.001$(Annex 4-Table 33 and Figure 64) hand and movement direction interaction $F(1,359)= 8.671$; $p<0.001$ (Annex 4-Table 34 and Figure 65). 'Torus' also had significant differences in visual feedback and handedness $F(4,359)= 5.872$; $p<0.0001$ (Annex 4-Table 35band Figure 66) and handedness and movement direction conditions $F(4,359)= 8.329$; $p<0.001$ (Annex 4-Table 36 and Figure 67).

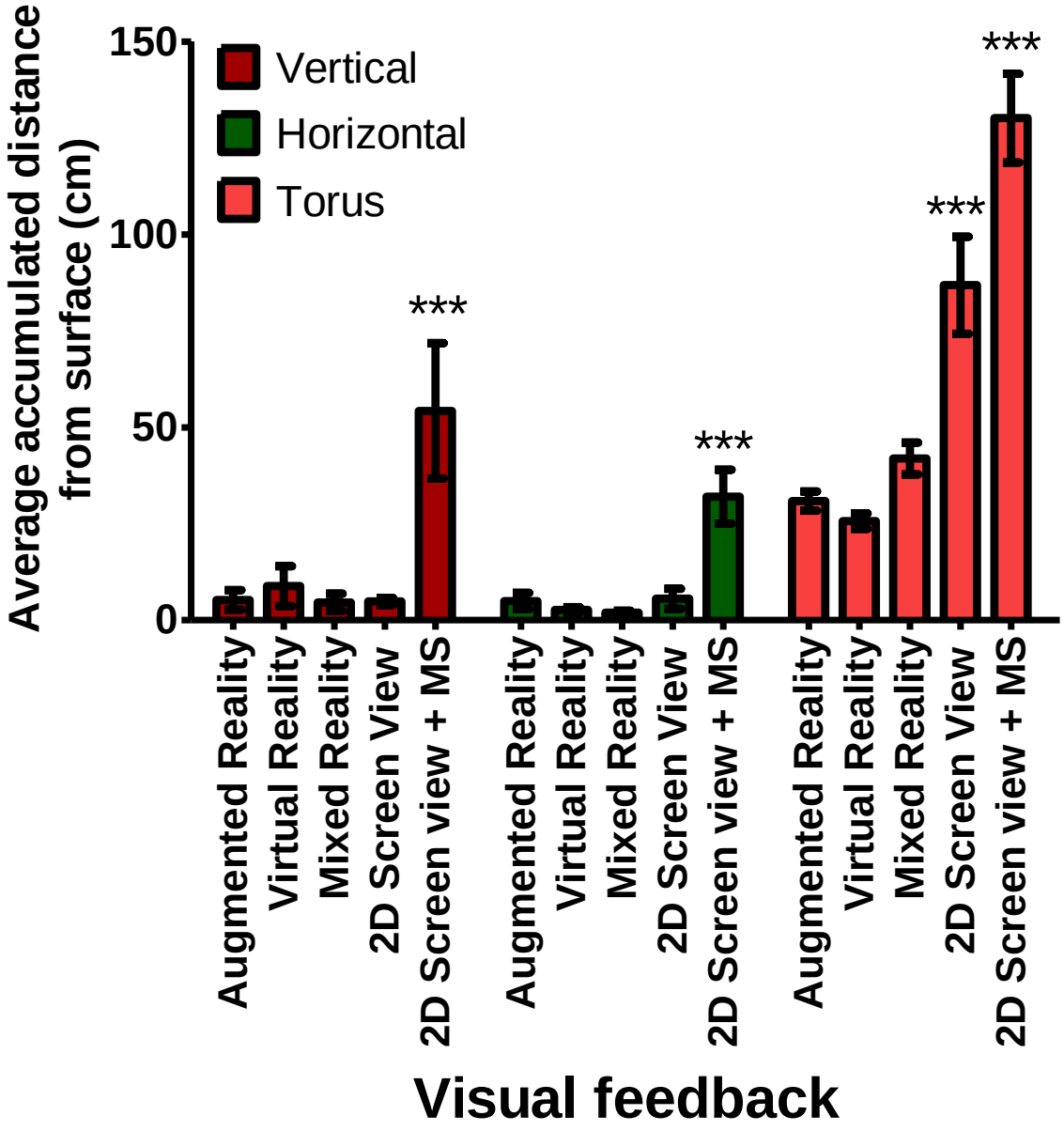

Figure 63 – Visual feedback results for different visual feedback of 'average accumulated distance away from the object surface' dependent variable

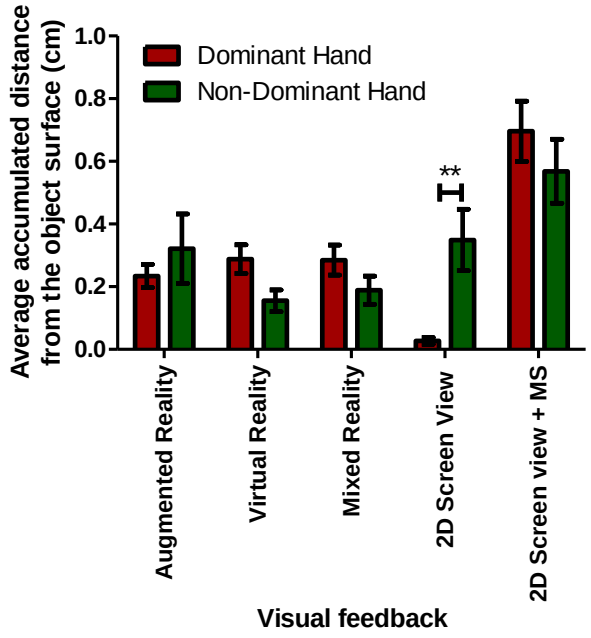

Figure 64 – Handedness and visual feedback interaction results for 'average accumulated distance away from the object surface' on 'Horizontal'

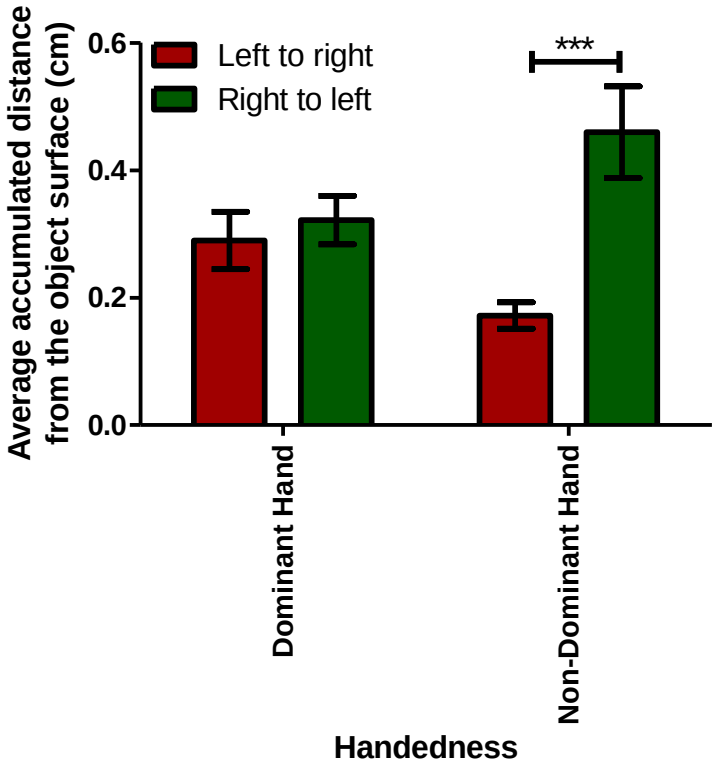

Figure 65 – Handedness and movement direction interaction results for 'average accumulated distance away from the object surface' for 'Horizontal'

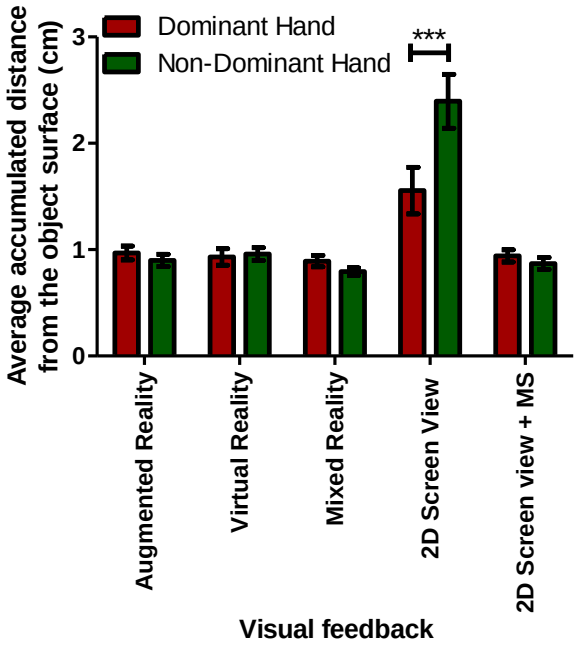

Figure 66 – Handedness and movement direction interaction results for 'average accumulated distance away from the object surface' for 'Torus'

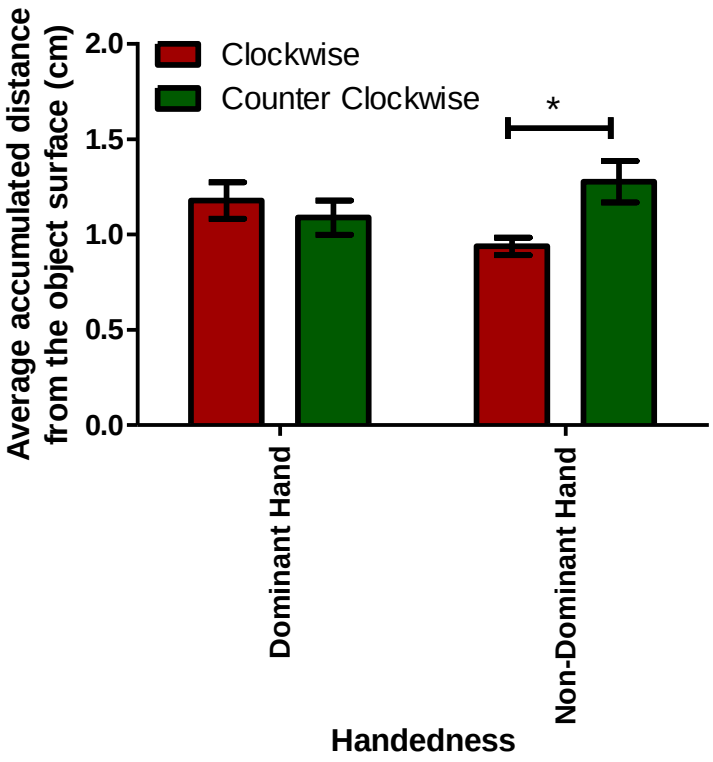

Figure 67 – Handedness and movement direction results for 'average accumulated distance away from the object surface' on 'Torus'

Discussion

In study one, effects of different visual feedbacks were inspected on time and precision of the finger movements for ‘Horizontal’, Vertical’ and ‘Torus ‘objects for both the dominant and non-dominant hand in all possible movement directions for each and every virtual object.

Results indicate that subjects were faster and more precise in *real world view with direct touch* condition compared to other types of different visual feedbacks used in this experiment. These results also show similarity with previous studies such as Morris et al [193], King et al.[103], Lou and Vogel [194]. Touching an object provides an additional feedback and including a tactile feedback increases the motor performance of the subjects.

Subjects were slower with the *2D screen view* condition compared to *VR, AR,* and *MR.* This result highlights the importance of the covered space during the action. During the experiments, to move the cursor from ‘start point’ to ‘finish point’, subjects had to move the mouse for 5-10 cm for ‘Horizontal’ and ‘Vertical’ and they were following a smaller circular movement with their hands when compared to *VR, AR, MR* and *2D screen view with MS* conditions. In a digitalized environment, mouse movements do not represent a linear action (e.g. when the user moves the mouse 3 cm in the real world, the cursor on 2D monitor does not always move 3 cm). This is called control-to-display ratio and it affects the error results and execution time of the individuals [195]. The control-to-display ratio does not always have to be a linear and constant value [196]. This creates a need for a visual feedback loop to execute the tasks in the 2D screen conditions.

The other result found in this experiment is that there were no major differences for *VR, AR,* and *MR* on time and precision. This result was valid for each individual object part (‘Horizontal’, ‘Vertical’ and ‘Torus’) for four dependent variables.

On the other hand, even though subjects had to cover less space with their hand movements with a mouse in 2D screen view with MS condition and they were slower compared to *VR, AR* and *MR* conditions where they were covering a larger distance, they were more precise. ‘Average number of finger outs’ dependent variable results

give a better precision after the natural view with direct touch results in ‘Horizontal’ and ‘Torus’. Furthermore, subjects were going out of the virtual object less in the ‘Vertical’ with their dominant hand in the ‘Horizontal’. In the ‘motor performance index’ dependent variable, there was no difference between *VR, AR, MR* and *2D screen view* condition for all virtual objects. Moreover, the subject had a better score with their dominant hand in the ‘Torus’ and with the ‘average distance away from the object surface’ variable, subjects showed a similar performance in *VR, AR, MR* and *2D screen view* conditions with ‘Horizontal’ and ‘Vertical’ and subjects got closer to the object while their fingers were outside of the virtual object with their dominant hand in *2D screen view*. These results show that subjects performed better results in *2D screen view* with their dominant hand. These results can be explained by the daily habits of the subjects. *2D screen view* was the condition in which the subjects had to follow the object on a 2D screen monitor with a mouse. All the participants were educated people who came from different backgrounds. These participants already had previous experience using a mouse and they used their computers in their daily lives with their dominant hand.

In addition, *2D screen view with MS* shows the worst performance results in all dependent variables. This can be caused by several reasons. First, subjects had to move their index fingertip in 3D space while they were looking at a 2D screen that provided only monocular cues of the virtual object. The lack of depth information caused longer execution time with less precise results. In *VR, AR*, *MR* and *2D screen view with MS* conditions an error could occur when the finger left the object in depth plane but, providing the depth information with stereoscopic head-mounted display created time and precision differences between *VR, AR,* and *MR* and *2D screen view with MS* conditions. This result can be explained by the fact that the computer detected errors in the depth plane while the display did not provide the depth information. A similar result was also observed in the previous chapter when the 2D screen vision was compared to the direct vision. Secondly, subjects had no previous experience using a desktop application with a motion sensor. Their motor skills had to adapt to this new input device during the experiments Moreover, subjects were not able to see the virtual hand on the 2D monitor as they saw in the *VR, AR* and *MR* conditions. In *VR, AR* and *MR,* immersive virtual reality helped subjects to perceive the virtual hand as their own hand because virtual hands were overlapped with their own hands. In the *2D*

screen vision with MS, subjects saw both their real hand and their virtual hand on a 2D screen which reduced the telepresence and affected the motor performance of the subjects.

In the 'average number of finger outs' results, *2D screen view* condition was the second most precise visual feedback condition. In the 'motor performance index' results, there was no major difference between *VR, AR*, *MR* and *2D screen view* conditions. In the 'average accumulated distance away from the object surface' results, there was no major difference between *VR, AR*, *MR* and *2D screen view* conditions for 'Horizontal' and 'Vertical', but for 'Torus' subjects were less precise with *2D screen view* condition compared to the *VR, AR* and *MR.* In the *2D screen view* condition and *real world view with direct touch* condition, subjects had to perform the experiment in 2D space. On the other hand, in other conditions subjects had to perform the experiment in 3D space. The third dimension mentioned here (depth) did not always show an advantage or a disadvantage for subjects' time and precision results except for *real world view with direct touch* condition. The motor performance of the subjects varied according to designed object complexity and used visual feedback.

Furthermore, subjects were more precise with their dominant hand compared to their non-dominant hand during the counter-clockwise movement direction. The interaction with 'Torus' was uniform for both hands, for both movement directions, and required symmetric muscle movements. Research on upper extremity on continuous steering movement experiments for clockwise and counterclockwise directions [197] and research on shoulder muscles can explain this differences. For example, the Lee et al. [197] study shows that even torque of the steering direction varies with the clockwise and counter-clockwise direction and relates their results to intra-limb and inter-limb coordination. In the circle drawing experiments with dominant hand non-dominant hand, it is observed that the maxima and minima of the hand movement trajectory varies with the handedness and active hand [198], with the movement direction [199] and these results are especially significant with non-dominant hand with less accurate interactions [200]. For instance, Hora et al. study explains these results as the "disadvantages of intersegmental dynamics during movement planning for non-dominant hand" [201].

In this study, effects of different simulation environments on time and precision of the individuals were investigated. Results showed that subjects were faster and more precise in natural view and direct touch and there was no major difference between VR, AR, and MR. In the following studies, virtual object aspects, such as length, width, position, and object complexity and their effect on subjects' interactions were explored with human computer interactions.

Study 2 – Effects of Virtual Object Length and Width

In the first study of chapter 2, six different visual feedbacks and their manual hand operation effects on ‘Horizontal’, ‘Vertical’ and ‘Torus’ were studied. In short, results showed that subjects were faster and more precise when they were interacting with the object in the *real-world view with direct touch* condition and there was no major motor performance difference between *VR, AR,* and *MR*. In the second study of chapter 2, effects of length and width of virtual objects are inspected with “NoTouch”. The results are studied further with “Steering Law” which is a derivation of “Fitts’s law”.

Study Goal and Hypotheses

Size of an object and individual’s interaction with this object have been a very attractive research topic since the Fitts’s law [57]. Especially, after the implementation of “Fitts’s Law” into the computer systems and expansion of this research area to the human-computer interactions, length and width of the targeted objects become more important for designers [81–84]. In further research, the relation between length and width of the objects was investigated in stereo-vision [202] and in VR [203] and showed that “Fitts’s Law” is also valid for these environments. In this study, this literature was extended with the movements in VR headsets by using the “NoTouch” system.

As explained in the previous chapter, “Fitts’s Law” revealed the trade-off between time and precision: faster execution times means less precise movements. Similarly, in tough or precision-required conditions, individuals perform slower task executions.

According to “Fitts’s Law” [57], there is a linear relationship between task execution time and the placement, which is given in (2).

$Time = a + blog_2\left(\frac{A}{W} + 1\right)$	(2)

In the equation (2), a and b are empirically determined values, W is the target width and A is the target distance. The reciprocal of b, which is the logarithmic term, indicates the index of difficulty (ID) [82] or index of performance (IP) [85].

Accot and Zhai's research on the continuous trajectories showed that "Fitts's Law" is not enough to model trajectory-based interactions [85,204–206]. Instead, Accot and Zhai enhanced to "Fitts's Law" for steering movements. For this, they descried "Fitts's Law" for curvilinear shapes as in equation for (3), by integrating path width along the trajectory as index of difficulty of the task.

$$Time = a + b\ x \int_C \frac{ds}{W(s)}$$	(3)

In the equation (3), a and b are empirically determined values, C is the path and W is the width of the path. W(s) is the width of the path at point s. In a tunnel with a constant width, this equation can be simplified as shown in (4).

$$Time = a + b\left(\frac{A}{W}\right)$$	(4)

In the equation (4), W is the target width and A is the length of the path. These terms and variables are also used as the same in Accot's study [85]. For the circular objects with a constant width, A becomes circle circumference of the circle: 2πr, where r is the radius of the circular object [85]. This equation is shown in (5).

$$Time = a + b\left(\frac{2\pi r}{W}\right)$$	(5)

The important point in this equation is the constant cross-sectional area width. If the width of the objects had changed, this equation could not be used in this study for 'Torus'.

Another derivation of the "Fitts's Law" is the "Stevens' power law" [207] adaptation, which is shown in (6). Liu [208] used this equation to model 3-D steering task performance of the users in VR environment instead of 2-D "Steering Law".

$$Time = a\left(\frac{A}{W}\right)^{b}$$	(6)

After getting both sides logarithm of (6), the following equation in (7) was obtained which gives a non-linear approach to find a relation between the execution time and length-width ratio of the objects.

$$\log(Time) = \log(a) + \ b\log\left(\frac{A}{W}\right)$$	(7)

In this study here, time and precision effects on length and width of the virtual objects are explored by using the “NoTouch” system. Furthermore, by applying “Steering Law” to the “NoTouch” system, correlation between motor performance of the subjects and the human computer interaction is investigated. Apart from the previous research on “Steering Law”[85,204,209], precision dependent variable is explored by applying “Fitts’s Law” to the results.

Materials and Methods

Subjects

Eighteen right-handed subjects (11 female) ranging in age between 20 and 33 (average = 26.33) participated in this study. None had any experience in VR and image-guided activities such as laparoscopic surgery training or other. Before starting experiments, each subject’s index fingertip width was measured with an average of 1.7 cm and a maximum of 2 cm. To be able to follow the objects in the virtual reality, the minimum distance between the shoulder and the fingertip was calculated as 55 cm. Before starting the experiments, each subject’s shoulder to fingertip distance was measured and the minimum distance was 62 cm.

Experimental platform

In the second study of chapter 2, effects of virtual object size on time and precision was inspected by the “NoTouch” system only in the VR environment. The length and the width of the ‘Horizontal’, ‘Vertical’ and ‘Torus’ were changed as shown in Figure 68 and Table 2.

When the object width changed in this experiment, the cross-sectional area of the circular objects was changed, which also changed the object size in the depth. The ratio between the length and width of the objects was calculated separately for each ‘Horizontal’ and ‘Vertical’, and ‘Torus’. This ratio and the results of this equation (4) and (5) are shown in Table 2. ‘Horizontal’, ‘Vertical’ and ‘Torus’ in Figure 68(c) had the same dimensions as the first study virtual objects, thus the virtual object parts in Figure 68(c) with ID=8.3 for ‘Horizontal and ‘Vertical’ and ID=26.17 for ‘Torus’ ratios are used as benchmark conditions.

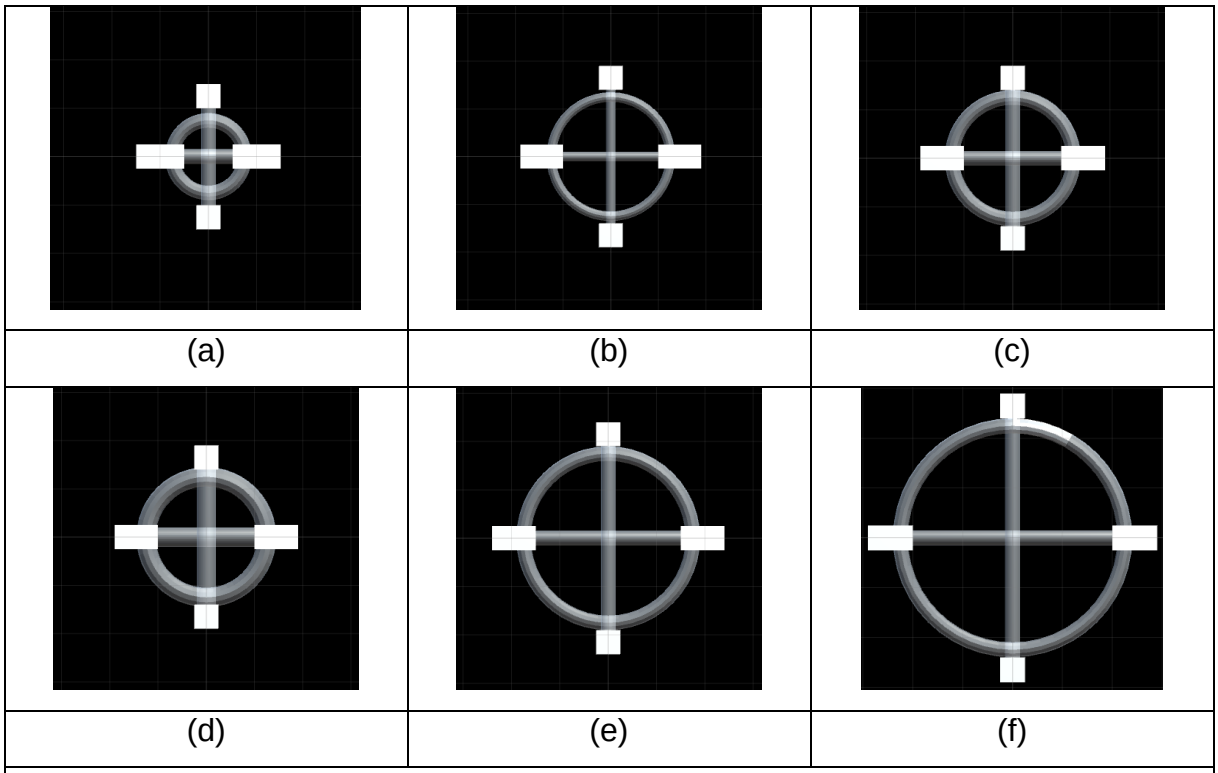

Figure 68 – Different ‘Horizontal’, ‘Vertical’ and ‘Torus’ used in the second experiment.

Cartesian Design Plan and Data Generation

Experimental design

Each experiment consisted of 10 successive trial sets per experimental condition for 18 subjects (P_{18}) and there were 144 experimental conditions: each subject followed ‘Vertical’, ‘Horizontal’ (S_6: ‘5’,’12.5’,’8.3’,’6.25’, ’11.6’,’15’), and ‘Torus’ (S_6: ’15.7’, ’39.26’,’26.17’,’19.63’, ’36.65’,’47.12’) in six different sizes, with three conditions of

object parts (OP_3: 'Vertical', 'Horizontal' and 'Torus), with two conditions of handedness (H_2: dominant-hand and their non-dominant hand) and with two conditions of finger movements direction for each individual object part (D_2: up to down-down to up for 'Vertical', left to right-right to left for 'Horizontal' and clockwise and counterclockwise for 'Torus'. The order of visual feedback condition was counterbalanced between subjects and structures to avoid specific habituation effects. For the same reason, the order of the handedness and direction of finger movement conditions were also counterbalanced between subjects. Each subject performed 720 trials. In total, 12960 trials were performed. The Cartesian design plan of the experiment can be presented as S_6 x OP_3 x D_2 x H_2 x P_{18} x 10 trial sets.

Table 2 – Length and width of the objects used in the second experiment with their difficulty index (ID)

Length(cm)	**Width(cm)**	**Figure**	**ID** $_{\text{Horizontal, Vertical}}$	**ID** $_{\text{Torus}}$
15	3	Figure 68 (a)	5	15.7
25	2	Figure 68 (b)	12.5	39.26
25	3	Figure 68 (c)	8.3	26.17
25	4	Figure 68 (d)	6.25	19.63
35	3	Figure 68 (e)	11.6	36.65
45	3	Figure 68 (f)	15	47.12

Data generation

The data recorded from each of the subjects were analyzed as a function of the different experimental conditions, for each of the four dependent variables ('time', 'average number of finger outs', 'motor performance index' and 'average accumulated distance away from the object surface'). In this study, all experimental conditions were applied to ANOVA without exception.

Because of different movement directions, it was not possible to perform an ANOVA analysis including all three objects parts and all movement directions in the same ANOVA with full factorial analysis. For this reason, a three-way ANOVA was performed for each object part, separately for each dependent variable.

Six three-way ANOVA was run on the average data for each ‘time’, ‘average number of finger outs’, ‘motor performance index’ and ‘average accumulated distance away from the object surface’ dependent variables. S_6 x D_2 x H_2 x P_{18} Cartesian design plan was used with average of ten repeated trial sets for each combination of conditions within a session, yielding a total of 432 experimental observations for each Object part (OP_3.), ‘Horizontal’, ‘Vertical’ and ‘Torus’ for each ‘time’, ‘average number of finger outs’, ‘motor performance index’ and ‘average accumulated distance away from the object surface’.

Results

‘Time’ ANOVA results on ‘Horizontal’, ‘Vertical’ and ‘Torus’ object parts on object size

Three-way ANOVA results on object size are shown in Annex 2-Figure 13 for ‘Horizontal’, in Annex 2-Figure 14 for ‘Vertical’ and in Annex 2-Figure 15 for ‘Torus’ for ‘time’.

‘Time’ was significantly different for ‘Vertical’ $F(5,431)=50.943$; $p<0.0001$, ‘Horizontal’ $F(5,431)=49.736$; $p<0.0001$ and ‘Torus’ $F(5,431)= 68.969$; $p<0.0001$ for size condition. These results are shown in Figure 69 and Annex 4-Table 37. Furthermore, movement direction in ‘Horizontal’ $F(1,431)=5.943$; $p<0.05$ (Annex 4-Table 38) and in ‘Vertical’ $F(1,431)= 5.708$; $p<0.05$ (Annex 4-Table 38) was significantly different. These results are also shown in Annex 4-Table 38. There was no other significant interaction or difference between the conditions.

According to the results in Figure 69 and Annex 4-Table 37, subjects got faster when the object length got smaller or the object width got larger. Furthermore, subjects were faster in up-to-bottom movements compared to bottom-to-up movements in ‘Vertical’ and they were faster in right-to-left compared to the left-to-right movements in ‘Horizontal’.

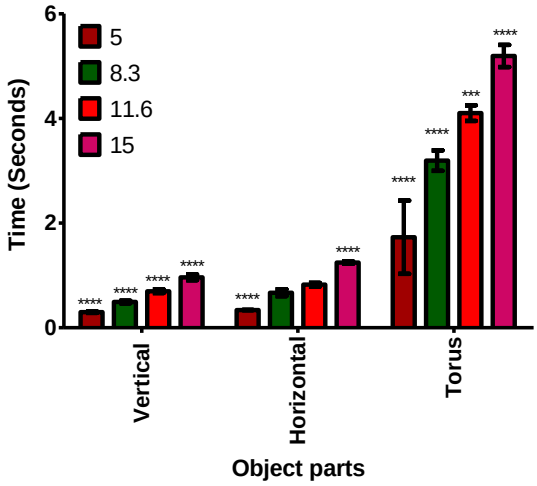

(a)

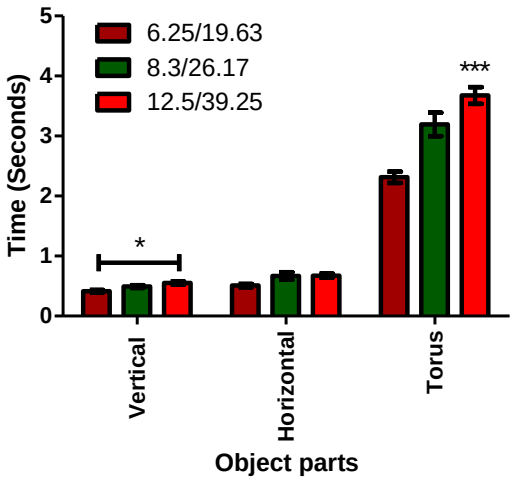

(b)

Figure 69 – Results for time dependent variable. (a) 3D image length change (b) 3D image with change results. In both figures, green column (Ratio: 8.3 for 'Horizontal' and 'Vertical' and 26.17 for 'Torus') is used as benchmark.

'Average number of finger outs' ANOVA results on 'Horizontal', 'Vertical' and 'Torus' object parts on object size

Three-way ANOVA results on object size are shown in Annex 2-Figure 16 for 'Horizontal', in Annex 2-Figure 17 for 'Vertical' and in Annex 2-Figure 18 for 'Torus' for 'average number of finger outs'.

"Average number of finger outs" was significantly different for 'Vertical' $F(5,431)=11.25$;$p<0.0001$, 'Horizontal' $F(5,431)=5.229$; $p<0.0001$ and 'Torus' $F(5,431)= 69.215$; $p<0.0001$ for size condition. These results are shown in Figure 70 and Annex 4-Table 39. Furthermore, movement direction in 'Horizontal' $F(1,431)=8.631$; $p<0.01$ (Annex 4-Table 40), and handedness and movement direction interaction in 'Torus' $F(1,431)=8.077$; $p<0.01$ (Annex 4-Table 41 and Figure 71) were significantly different.

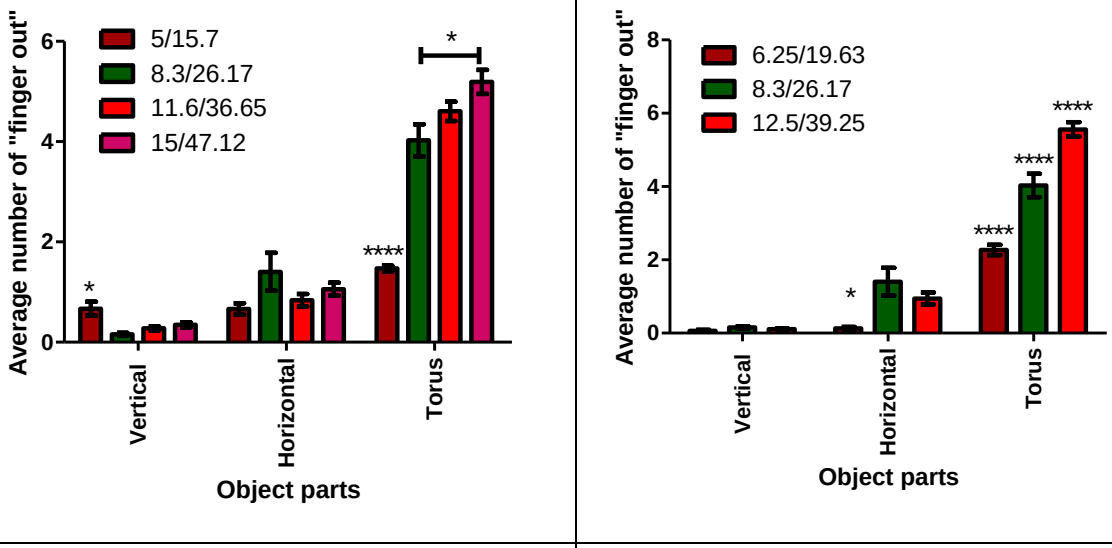

(a) (b)

Figure 70 – Results for 'average number of finger outs'. (a) 3D image length change (b) 3D image width change results. In both figures, green column (Ratio: 8.3 for 'Horizontal' and 'Vertical' and 26.17 for 'Torus') is used as benchmark.

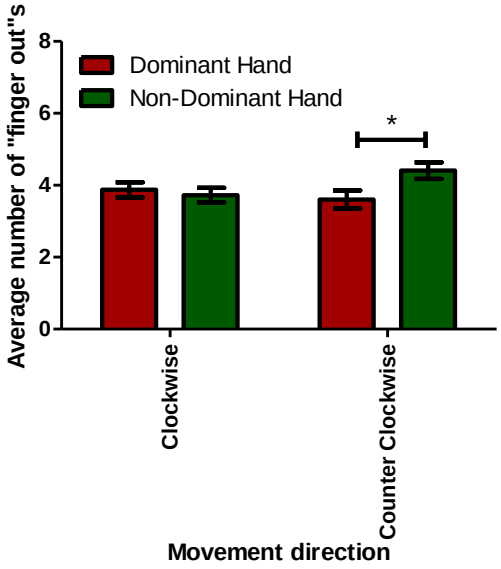

Figure 71 – Results for handedness and movement direction interaction for 'average number of "finger out" in Torus.

The 'Average number of finger outs' results show that in 'Horizontal' and 'Vertical' there was no major difference. On the other hand, subjects made more errors when the major radius of 'Torus 'was increased, or the minor radius of 'Torus' was decreased.

Furthermore, subjects were more precise with their dominant hand in the clockwise direction.

‘Motor performance index’ ANOVA results on ‘Horizontal’, ‘Vertical’ and ‘Torus’ object parts on object size

Three-way ANOVA results on object size are shown in Annex 2-Figure 19 for ‘Horizontal’, in Annex 2-Figure 20 for ‘Vertical’ and in Annex 2-Figure 21 for ‘Torus’ for ‘motor performance index’.

‘Motor performance index’ was significantly different for ‘Vertical’ $F(5,431)=4.697$; $p<0.0001$, ‘Horizontal’ $F(5,431)=15.182$; $p<0.0001$ and ‘Torus’ $F(5,431)= 33.488$; $p<0.0001$ for size condition. These results are shown in Annex 4-Table 42 and Figure 72. Furthermore, handedness on ‘Vertical’ $F(1,431)= 4.202$; $p<0.05$ (Annex 4-Table 43) and ‘Horizontal’ $F(1,431)= 4.131$; $p<0.05$ (Annex 4-Table 43), movement direction in ‘Horizontal’ $F(1,431)= 18.326$; $p<0.0001$(Annex 4-Table 44) and on ‘Torus’ $F(1,431)=8.896$; $p<0.01$ (Annex 4-Table 44), object size and movement direction interactions on ‘Horizontal’ $F(5,431)=3.858$; $p<0.01$ (Annex 4-Table 45 and Figure 74(a) and (b)) and ‘Torus’ $F(5,431)= 10.774$; $p<0.0001$(Annex 4-Table 45 and Figure 74(c) and (d)), and handedness and movement direction interaction on ‘Torus’ $F(1,431)=7.446$; $p<0.01$(Annex 4-Table 46 and Figure 73) were significantly different.

According to these results, there is no major difference between increasing object length or width in VR for ‘Horizontal’ and ‘Vertical’. On the other hand, on ‘Torus’, when the object minor radius was increased, ‘motor performance index’ was also increased, which means that finger tip of the subjects was more inside of the ‘Torus’ during the task execution. This result was valid for clockwise and counterclockwise movement directions. Furthermore, subjects stayed inside of the virtual stick more when they were following counter clockwise movement with their dominant hand.

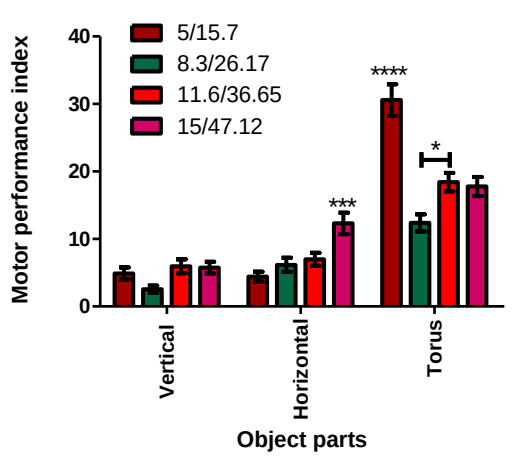

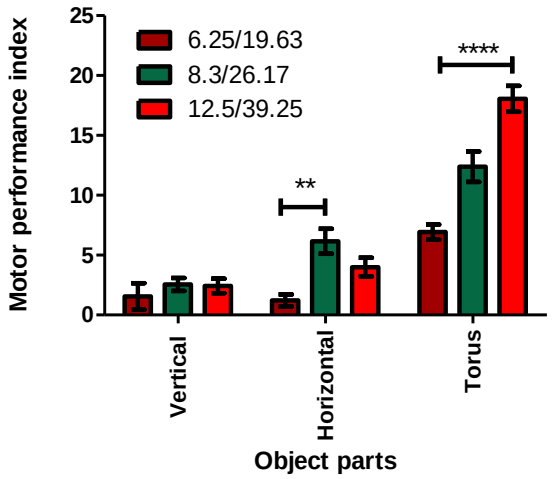

(a) (b)

Figure 72 – Results for 'motor performance index'. (a) 3D image length and (b) width change. In both figures, green column (Ratio: 8.3 for 'Horizontal' and 'Vertical' and 26.17 for 'Torus') is used as benchmark.

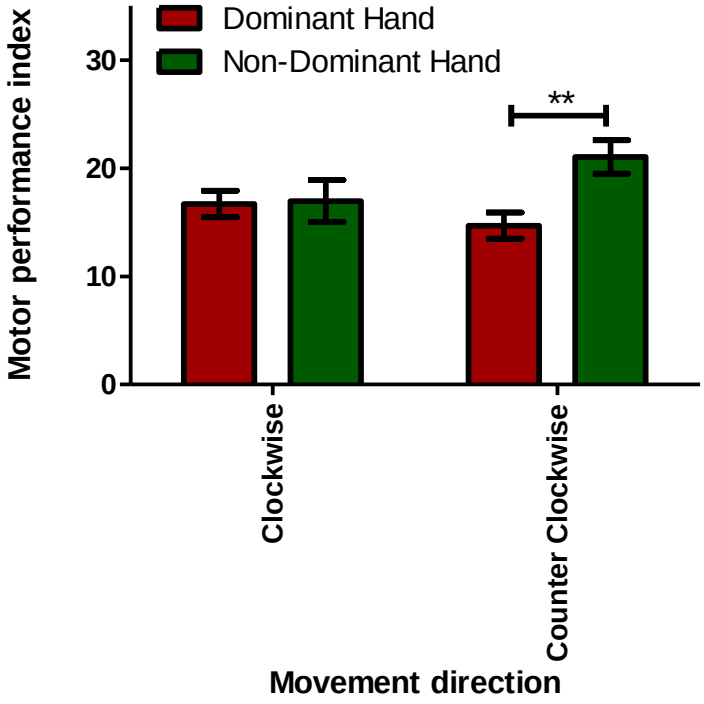

Figure 73 – Results for handedness and movement direction interaction for 'motor performance index' in 'Torus'.

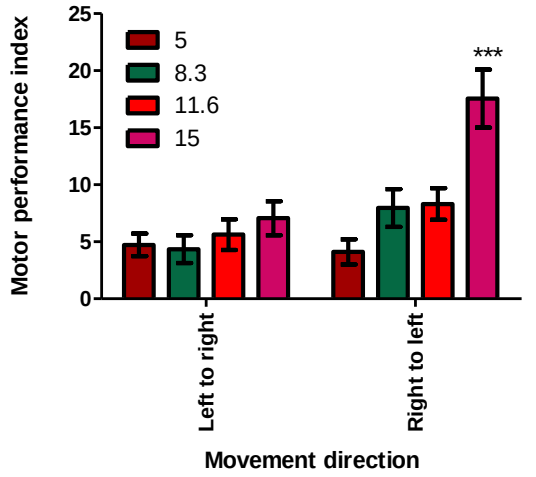

(a)

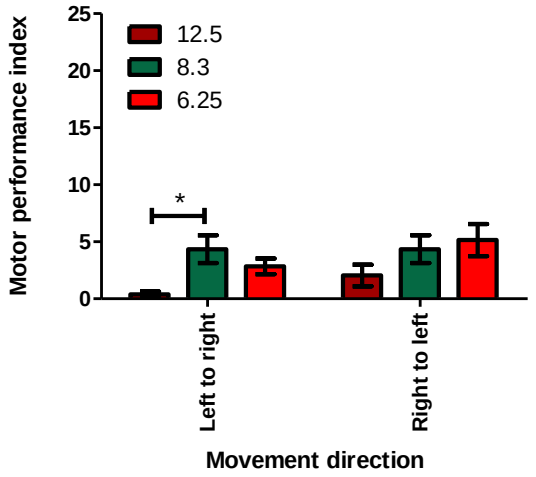

(b)

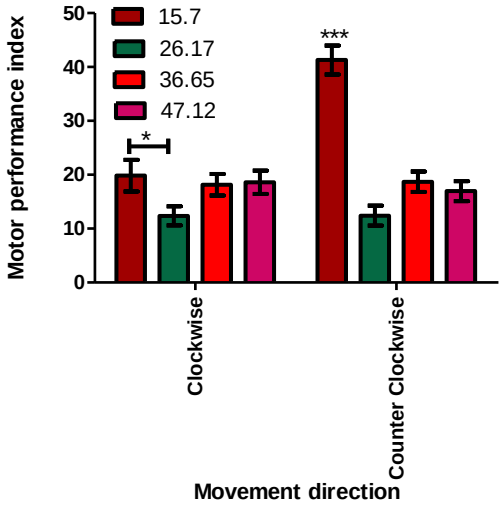

(c)

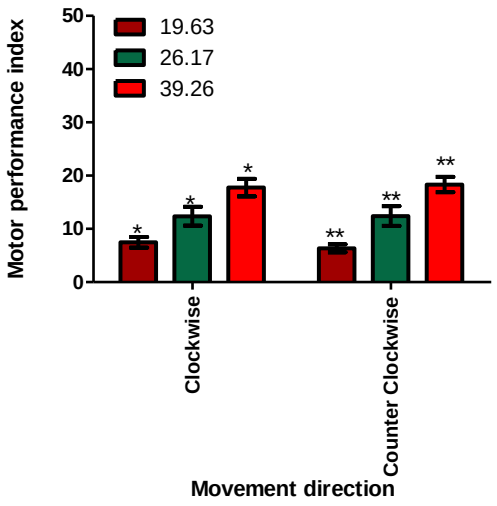

(d)

Figure 74 – Results for ‘motor performance index’ dependent variable for object size and movement direction interaction. (a) 3D image length change and (b) width change results for ‘Horizontal’. (c) 3D image length change and (d) width change results for ‘Torus’. In both figures, green column (Ratio: 0.282) is used as benchmark.

‘Average accumulated distance away from the object surface’ ANOVA results on ‘Horizontal’, ‘Vertical’ and ‘Torus’ object parts on object size

Three-way ANOVA results on object size are shown in Annex 2-Figure 22 for ‘Horizontal’, in Annex 2-Figure 23 for ‘Vertical’ and in Annex 2-Figure 24 for ‘Torus’ for ‘average accumulated distance away from the object surface’.

‘Average accumulated distance away from the object surface’ was significantly different for ‘Horizontal’ $F(5,431)=10.413$; $p<0.0001$ and ‘Torus’ $F(5,431)= 9.863$; $p<0.0001$ for size condition. These results are shown in Annex 4-Table 47 and Figure 75. Furthermore, movement direction in ‘Horizontal’ $F(1,431)= 12.001$; $p<0.001$ (Annex 4-Table 48) and ‘Torus’ $F(1,431)= 4.131$; $p<0.05$ (Annex 4-Table 48), object size and movement direction interaction in ‘Horizontal’ $F(5,431)= 2.559$; $p<0.05$ (Annex 4-Table 49 and Figure 76) and handedness and movement direction interaction on ‘Horizontal’ $F(1,431)=3.932$; $p<0.05$ (Annex 4-Table 50 and Figure 77) were significantly different.

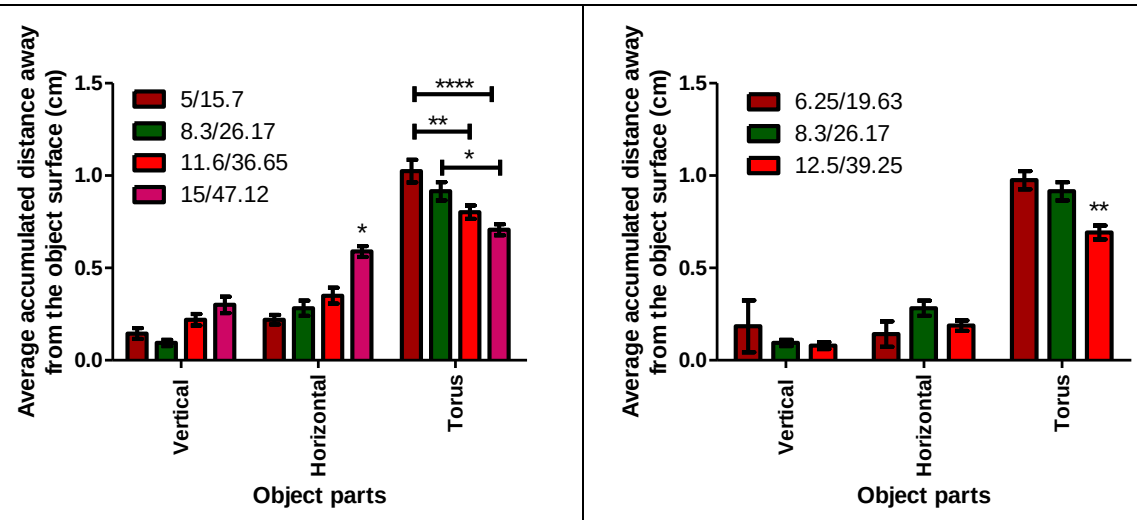

(a) (b)

Figure 75 – Results for ‘average accumulated distance away from the object surface’ dependent variable. 3D image (a) length and (b) width change results. In both figures, green column (Ratio: 8.3 for ‘Horizontal’ and ‘Vertical’ and 26.17 for ‘Torus’) is used as benchmark.

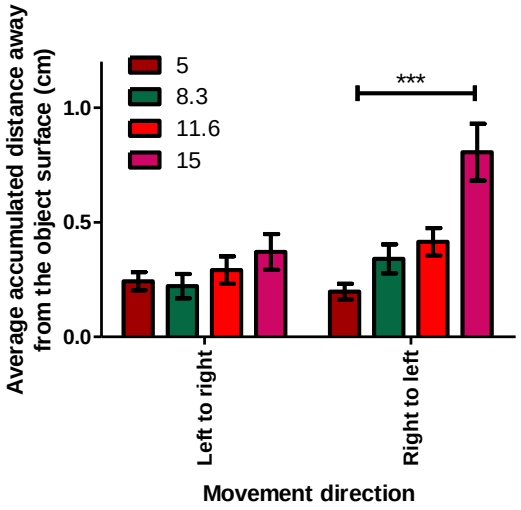

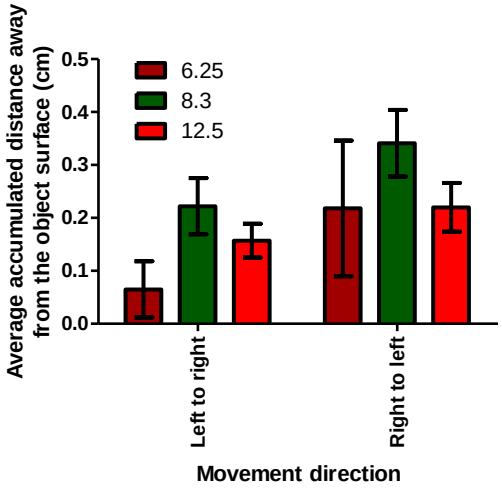

(a) (b)

Figure 76 – Results for 'average accumulated distance away from the object surface' Dependent Variable on 'Horizontal' movement direction. 3D image (a) length and (b) width change results. In both figures, green column (Ratio: 8.3 for 'Horizontal' and 'Vertical' and 26.17 for 'Torus') is used as benchmark.

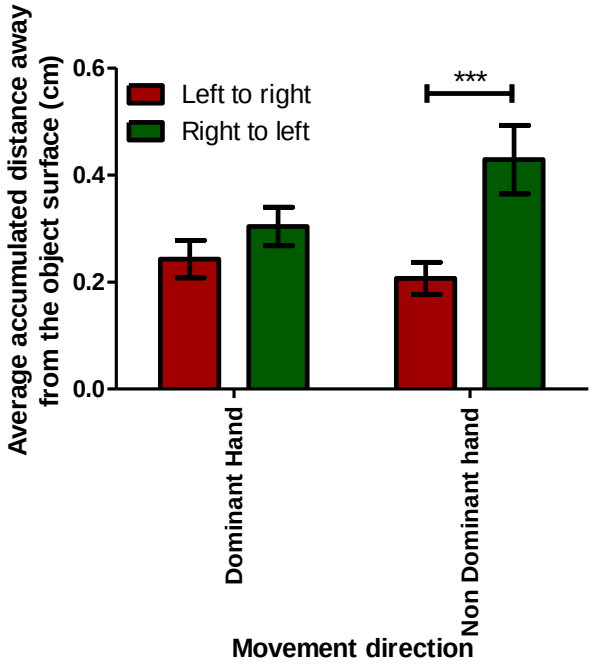

Figure 77 – Results for Handedness and movement direction condition for 'average accumulated distance away from the object surface' in 'Torus'

‘Steering law’ analysis on ‘Horizontal’, ‘Vertical’ and ‘Torus’ object parts

As explained in the study goal hypotheses section, the results can be expressed with the “Steering Law”. The results for time analysis with the “Steering Law“ are shown in Figure 78 and Table 3.

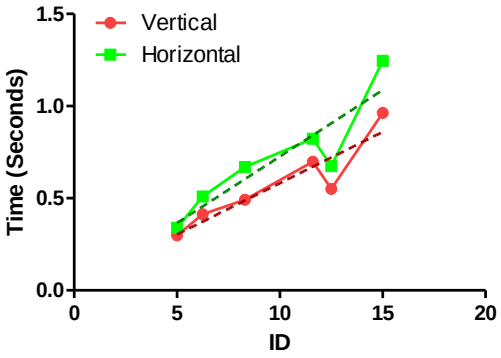

(a)

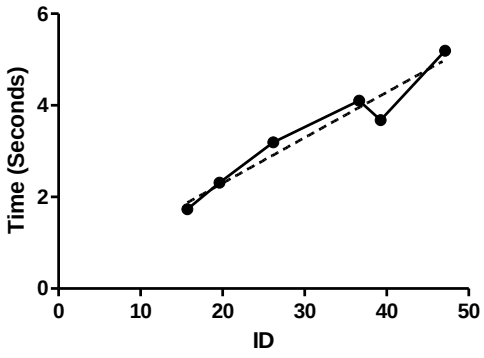

(b)

Figure 78 – Index of difficulty and execution ‘time’ for (a) ‘Vertical’ and ‘Horizontal’, (b) ‘Torus’

Table 3 – “Steering Law” results for ‘Vertical’, ‘Horizontal’ and ‘Torus’

Vertical	Time = 0.05566 x ID + 0.0250 r^2= 0.847 F(1,4) = 22.16; p<0.01
Horizontal	Time = 0.07215 x ID + 0.0046 r^2= 0.818 F(1,4) = 18.01; p<0.05
Torus	Time = 0.31860 x ID + 0.0992 r^2= 0.942 F(1,4) = 65.11; p<0.01

The results in Figure 78 and Table 3 show that “Steering Law” is also valid in VR environments with manual operations for ‘Vertical’, ‘Horizontal’ and ‘Torus’. Furthermore, an additional analysis was done for the ‘Torus’ because the shape of the results resembles polynomial function. This result is shown in Figure 79(a) with 0.3142 + 0.09948 x ID -0.005264 ID^2 with r^2= 0.9421. When “Steven’s Law” (7) was applied to Figure 79(a), the results in Figure 79(b) with -0.8264 + 0.9108 x ID with r^2= 0.957 F(1,4) = 89.12; p<0.001 were obtained.

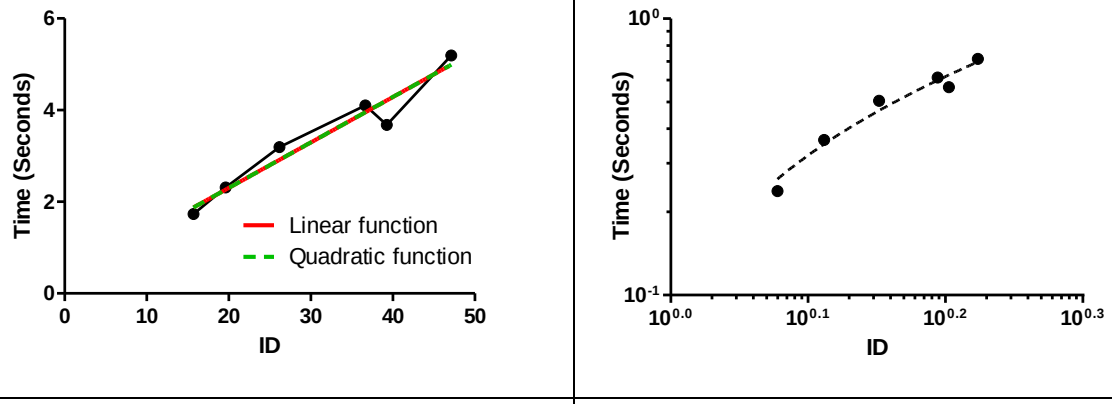

(a) (b)

Figure 79 – Index of difficulty and execution time results with (a) Linear and Quadratic functions and (b) Steven's law results for 'Torus'

In further analysis, each precision dependent variable result is also given here with the index of difficulty term. It is important to keep in mind that "Fitts's law" uses error rate to calculate the throughput. For this error rate, the number of unsuccessful task executions was divided into the successful task executions. In this study here, each trial was counted as successfully executed.

The significant correlations among the results of Figure 78 is found at Figure 78(b) with 'Torus' in 'average number of finger outs' result with -0.00114 - 0.1254 x ID r^2= 0.8694 F(1,4)= 26.63; p<0.01 and in Figure 78(f) with 'Torus' in 'average accumulated distance away from the object surface(cm)' result with 1.193 - 0.01109 x ID r^2= 0.9380 F(1,4)= 60.47; p<0.01.

Discussion

In this study, different length and width of the virtual objects were investigated in manual hand operations using a head-mounted VR. A motion sensor was used as an input device and subjects were asked to retrace 'Vertical', 'Horizontal' and "Torus' in different sizes. Subjects used "NoTouch" system to interact with the virtual objects. Time and precision of the results were studied with ANOVA and "Steering Law".

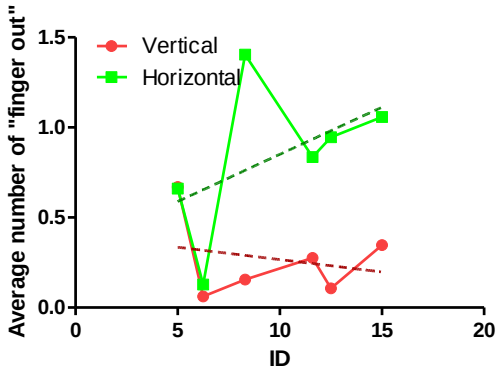

(a)

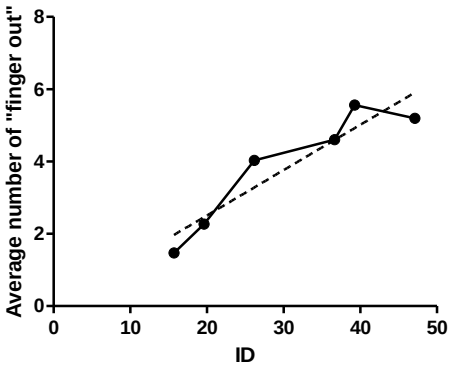

(b)

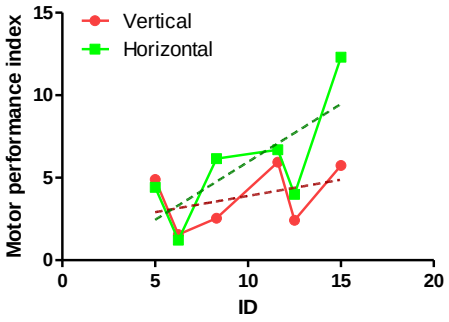

(c)

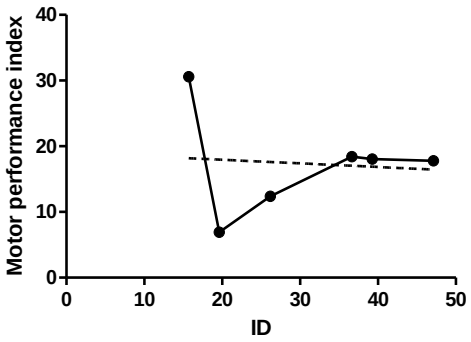

(d)

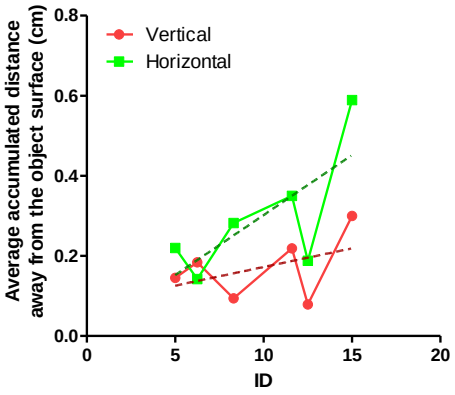

(e)

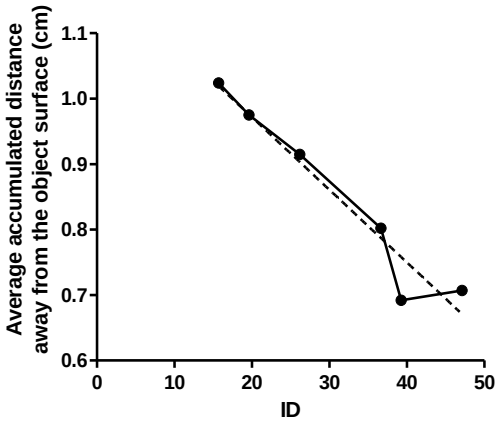

(f)

Figure 80 – Index of difficulty for ‘average number of finger outs’ for (a) ‘Vertical’ and ‘Horizontal’ and (b) ‘Torus’, for ‘motor performance index’ (c) ‘Vertical’ and ‘Horizontal’ and (d) ‘Torus’, for ‘average accumulated distance away from the object surface’ for (e) ‘Vertical’ and ‘Horizontal’ and (f) ‘Torus’.

In the “Steering Law” results for ‘Time’ in Figure 78, ID=12.5 for ‘Vertical’ and ‘Horizontal’, and ID= 39.25 for ‘Torus’, a small spike in these results was observed. These results occurred when the length of the object was 25 cm and the width of the object was 2 cm for ‘Horizontal’ and ‘Vertical’ and when the inner diameter of the ‘Torus’ was 25 cm and the outer diameter of the ‘Torus’ was 2 cm. In literature, two different explanations were used to validate these results: First, according to Zhai et al [209], the depth perception in VR scene is always more difficult to perceive than other dimensions. When virtual fingertip was inside the object, the 2cm cross-sectional diameter was not perceived well and the subject moved freely within these objects. This theory is not valid for this study. In this case, one could expect lower precision results, but Figure 78 shows no major sudden decrease in the precision results for ID= 39.25 or ID=12.5. The other explanation is that muscles used in this ID are different than adjacent ID’s [210]. ID=15 for ‘Vertical’ and ‘Horizontal’, and ID= 47.12 for ‘Torus’ is the virtual object with the length of 45 cm, and ID=11.6 for ‘Vertical’ and ‘Horizontal’, and ID= 39.25 for ‘Torus’ is the virtual object with the length of 35 cm. In these virtual objects, subjects had to use their shoulder muscles while the objects with ID=12.5 for ‘Vertical’ and ‘Horizontal’, and ID= 39.25 for ‘Torus’ were much easier to execute with the smaller arm movements. To further understand these results, there is a need to perform more experiments with small cross-sectional areas in a VR environment.

The other interesting result is the quadratic and logarithmic function result for the ‘Torus’ analysis. As seen in Figure 79, quadratic function (r^2= 0.9421) and logarithmic function (r^2= 0.957) give no better correlation results than linear function (r^2= 0.9421) for the time results of ‘Torus’. In the previous VR “Steering Law” research (e.g. [209]), researchers found linear r^2 correlations higher than the results in here for ‘Horizontal’ and ‘Vertical’ (r^2 between 0.985 and 0.999) with higher ID terms (up to 4000). On the other hand, Liu’s research in VR [208] had similar ID terms as this study here for long path steering and Liu used Steven’s power law to explain his results with equation (7). In Liu’s research, subjects had to retrace objects in VR with headsets while they were holding a pointer, which is close to the experimental method here. Liu also concludes that 2D “Steering Law” is not suitable to describe 3D steering task in a VR environment. The results of this study do not support this theory. Pearson correlation result for linear function and quadratic function r^2 results are very close. The logarithmic function gives

a slightly better r^2 result, but this difference is not noteworthy. As a conclusion, “Steering Law” is also valid for the manual hand operations in VR environments.

In the slope results for the ‘Horizontal’ (0.007215), ‘Vertical’ (0.05566) and ‘Torus’ (0.31860) in Table 3 for “Steering Law”, it can be seen that each object part has a different slope. The time and precision differences of three virtual objects are investigated in the last study of this chapter in detail, but this result also reveals the importance of the object orientation. Even though the same length and width used for ‘Horizontal’ and ’Vertical’, the execution times were different for the same ID’s. In this case, the positioning of an object in the VR scene also has an effect on the performance evaluation of the individuals.

In the “Steering Law” analysis for precision results, it can be observed that there is no direct linear correlation between the ID and ‘average number of finger outs’, ‘motor performance index’ and ‘average accumulated distance away from the object surface’ dependent variables. When the ID and precision results were combined with the complex movement direction and handedness factors’ interaction, it is difficult to come to a general conclusion in order to determine a correlation between different widths and lengths of the objects and the precision. At this point, designers, engineers, and psychologists should work together to determine the precision assessment methods in the VR environments with the “NoTouch” system.

In the second study of this chapter, length and width of the virtual objects in the “NoTouch” system were investigated for the time and precision. Results showed that the “Steering Law”, which is derived from “Fitts’s law”, supports the time results in the VR environment. Furthermore, complex precision results show that individuals precision results are non-linear in VR and should be assessed according to each particular target object to be interacted with.

Study 3 – Ipsilateral versus Contralateral Hand Movements

In the second study of this chapter, how the object length and width affected the human motor performance were explored. The results show that height and width of the designed object can alter the time and precision analysis. Apart from the height and width of the object, there is a third aspect which should be considered in 3-dimensional space; depth. In the third chapter, the third dimension of the Cartesian space, the depth is studied as ipsilateral and contralateral hand movements.

Study Goal and Hypotheses

In the first study of second chapter, the differences between *VR* headset interactions, *2D view screen* interactions and *2D screen view with motion sensor (MS)* interactions were studied. The results showed the worst motor performance for time and precision on the *2D screen view with MS* interactions, which are mostly used in operating rooms as a touchless input application.

The *2D screen view with MS* had the third-dimensional visual feedback disadvantage: subjects had to move their hand in the three-dimensional space when they were looking at a two-dimensional screen which did not provide the depth perception. To understand the depth perception effect, one can look at the results of *2D screen view* condition and *VR* condition in the first study. In the *2D screen view* condition*,* subjects were slower but more precise, which did not allow 3D movements. The more precise task execution could be explained by the small muscle movements and expertise of the subjects on the monitor screen interactions in their daily life. In *VR,* subjects were faster when compared to the two-dimensional visual feedback systems, but the precision of the subjects was between the *2D screen view* and *2D screen view with MS* conditions. In the previous “NoTouch” studies (study 1 and study 2 of this chapter), a significant amount of depth movements was not required to execute the task, and all the targets were placed in the same position. To understand the effects of depth perception in VR, there is still a need for more detailed studies.

In the three-dimensional real world, individuals can interact with the real objects in depth perception. On the other hand, goal-directed hand movements such as grabbing, reaching or extending cannot be executed in the two-dimensional visual feedback systems, such as tv monitors, screens, and projectors. This limitation affects the movements of the subjects [86,87]. Immersive Virtual Reality systems can provide this depth perception and the movement information using the depth cues such as perception, relative motion, occlusion, shadows, etc.[88,89].

The current research for the skill assessment in the VR environments is still not enough to understand how the ipsilateral and contralateral movements in depth perception varies. Most of the upper limb movement studies usually focused on the VR headset's usage for the rehabilitation of patients e.g. [211–214]. This study aims to investigate motor performance of the subjects during the object interaction in the depth and how it effects the training skills of the novices for the surgical simulations. 16 Subjects followed 28 sticks in a VR scene with their dominant and non-dominant hand to understand the effects of fingertip target interactions within the VR scene. The main goal of this study was to understand how target position variation in depth affects the motor performance of the subjects.

Materials and Methods

Subjects

Sixteen right-handed subjects (9 female) ranging in ages between 20 and 33 (average = 26.93) participated in this study. None had any experience in VR and image-guided activities such as laparoscopic surgery training or other. Before starting experiments, each subject's index fingertip width was measured as an average of 1.66 cm with the maximum of 2 cm. To be able to follow the objects in the virtual reality, the minimum distance between the shoulder and the fingertip was calculated as 55 cm. Before starting the experiments, each subject's shoulder to fingertip distance was measured and the minimum distance was 62 cm.

Objects viewed in VR Scene

In this study, the “NoTouch” system was used with additional enhancements in the virtual environment. Instead of ‘Horizontal’, ‘Vertical’ and ‘Torus’, subjects saw 28 virtual objects. These objects had the similar shapes as ‘Horizontal’ or ‘Vertical’ in the “NoTouch” System, but they were rotated 90 degrees through to the depth. 22 cm long and 3 cm wide targets, were placed on a grid to create five columns and six rows in the virtual space. These objects can be seen in Figure 81(a). Each virtual object was attached to a ‘start point’ and a ‘finish point’. These ‘start point’ and ‘finish point’ had the same function as the ‘start point’ and ‘finish point’ described in the Materials and Method section of this chapter.

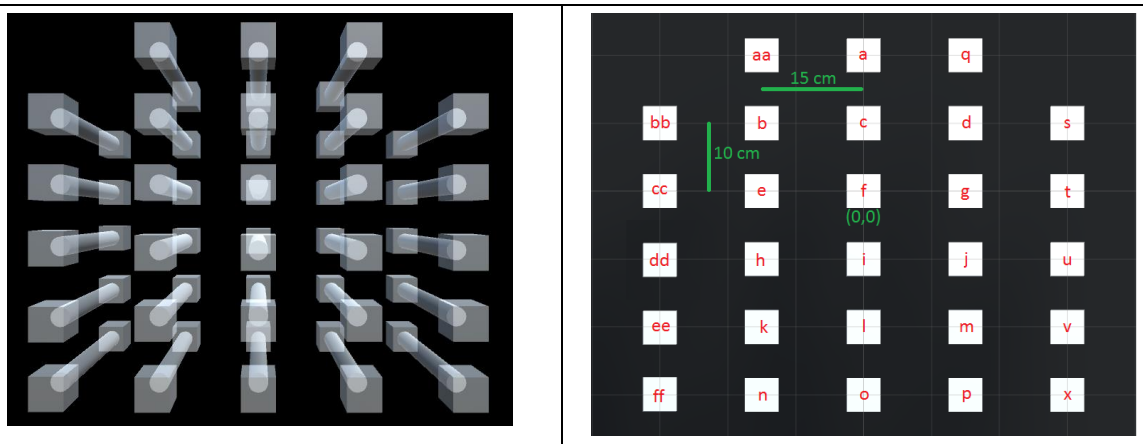

(a) (b)

Figure 81 – VR scene in the third study. (a) subjects left eye vision in VR scene, (b) isometric view of the VR scene with labeled sticks.

In Figure 81, the stick F was placed at the eye level of the subjects and it was centered between their two eyes. The other virtual objects were placed as seen in Figure 81(b). There was 10 cm between each row of sticks and 15 cm between each column of sticks. Subjects were not able to reach upper end of the extreme left and extreme right columns so virtual objects were not placed at these positions.

Procedure

The same procedure in the “NoTouch” system was used in this study, except for movement direction. Subjects had to move their index fingertip from front-to-back and back-to-front. The ‘finish point’ and ‘start point’ at the end of each column was changed

with the movement direction. The subjects followed each target individually while the other targets were disabled and invisible.

Subjects were not able to reach all the stick with their right and left hand. Therefore, objects in VR scene were separated into two groups as seen in Figure 82. Sticks inside the blue lines were followed by the subjects' left hands. Likewise, sticks inside the green lines were followed by the subjects' right hands. In total, subjects followed 22 sticks either with their right hand or left hands.

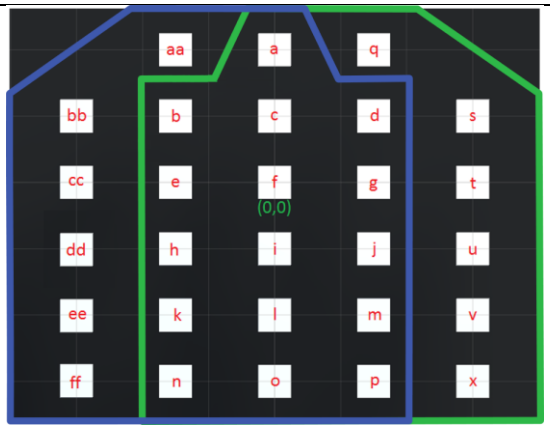

Figure 82 – Stick followed by left and right hand in the VR scene. Subjects followed sticks inside the blue lines with their left hand and followed sticks inside the green line with their right hand.

The sticks that can be reached by both hands are named from a-to-p starting from the top. The sticks that can be only reached by the right hand are named from q to x and the sticks that can be only reached by the left hand are named from aa to ff.

Cartesian Design Plan and Data Generation

Experimental design

Each experiment consisted of 10 successive trial sets per experimental condition for 16 subjects (P_{16}) and there were 88 experimental conditions: each subject followed 22 virtual sticks (S_{22}), with two conditions of handedness (H_2: dominant-hand and non-dominant hand) and with two conditions of finger movements direction for each individual object part (D_2: front to back and back to front). The order of 16 sticks from a-to-p was counterbalanced between subjects and structures to avoid specific

habituation effects. For the same reason, the order of the handedness and direction of finger movement conditions were also counterbalanced between subjects. Each subject performed 880 trials. In total 19360 trials were performed. The Cartesian design plan of the experiment can be presented as S_{22} x D_2 x H_2 x P_{16} x 10 trial sets.

Data generation

The data recorded from each of the subjects were analyzed as a function of the different experimental conditions, for each of the four dependent variables ('time', 'average number of finger outs', 'motor performance index' and 'average accumulated distance away from the object surface'). In this study, all experimental conditions were applied to ANOVA without exception.

Because subjects were not able to perform retracing targets with their both hands on all the sticks, it was not possible to perform a full factorial ANOVA analysis including all the sticks. For this reason, data analysis was performed with two three-way ANOVAs. In the first ANOVA analysis, extreme regions were analyzed. In this analysis, all four sticks at each corner of the VR scene were grouped together, and these four corners were analyzed as extreme regions. In the second ANOVA analysis, 16 sticks followed by both hands were analyzed as the central region. These sticks and their positions are shown in Figure 83(a) for the extreme regions and Figure 83(b) for the central region. During the task execution, while subjects were performing experiments with their right hand on the upper right or lower right region or with their left hand on the upper left or lower left region, it was called a "Ipsilateral" movement. Similarly, while subjects were performing experiments with their right hand on the upper left or lower right left or with their left hand on the upper right or lower right region, it was called a "contralateral" movement.

In the extreme regions three-way ANOVA, the average data for each 'time', 'average number of finger outs', 'motor performance index' and 'average accumulated distance away from the object surface' dependent variables were analyzed with four levels of extreme regions (S_6 = Upper Left, Lower Left, Upper Right and Lower Right), with two levels of handedness (H_2 = Dominant hand and non-dominant hand), with two levels of movement direction (D_2 =Front to back and back to Front) for 16 subjects P_{16}, yielding 4x256 data points for R_4 x D_2 x H_2 for 16 subject P_{16} Cartesian design plan. In

the central region three-way ANOVA, the same dependent variables were analyzed with 16 levels of sticks (S_{16} = from stick a-to-p), with two levels of handedness (H_2 = Dominant hand and non-dominant hand), with two levels of movement direction (D_2 =Front to back and back to Front) for 16 subjects P_{16}, yielding 4x1024 data points for S_{16} x D_2 x H_2 for 16 subject P_{16} Cartesian design plan.

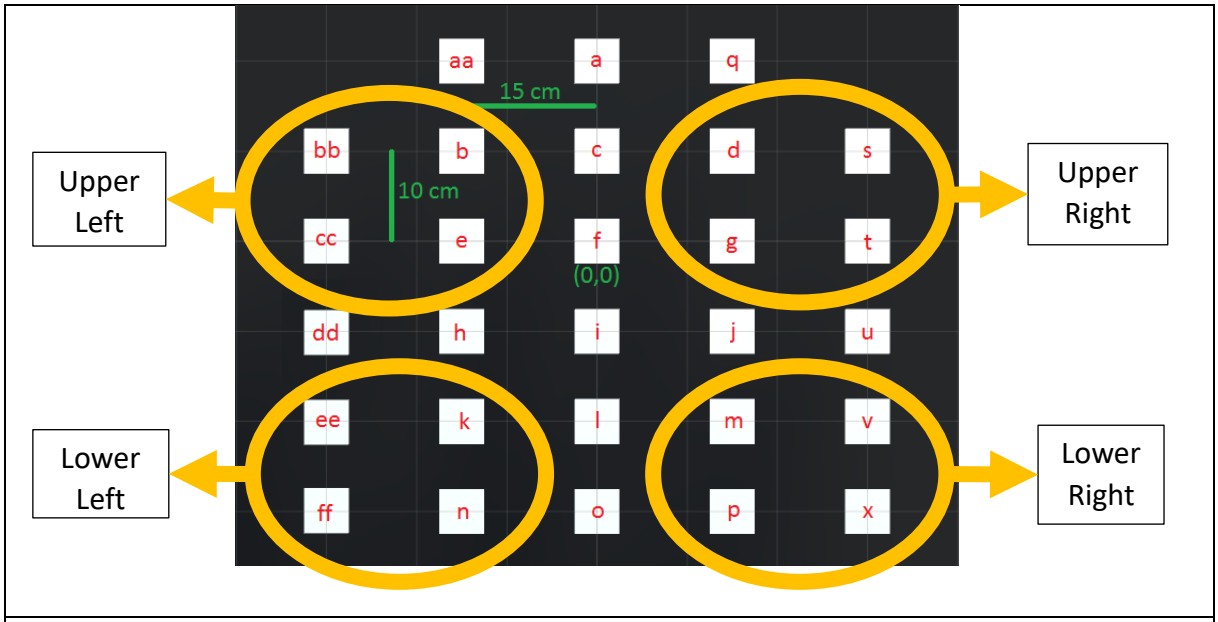

(a)

(b)

Figure 83 – Data analysis regions used in the third study of chapter 2. (a) Extreme regions and (b) central region sticks which are inside the yellow lines.

Results

Medians and extremes of the individual data relative ‘time’, ‘average number of finger outs’, ‘motor performance index’ and ‘average accumulated distance away from the object surface’ for each stick were analyzed first. The results of these analyses are represented graphically as box-and-whiskers plots in Figure 84 for ‘time’, in Figure 85 for ‘average number of finger outs’, in Figure 86 for ‘motor performance index’ and in Figure 87 for ‘average accumulated distance away from the object surface’.

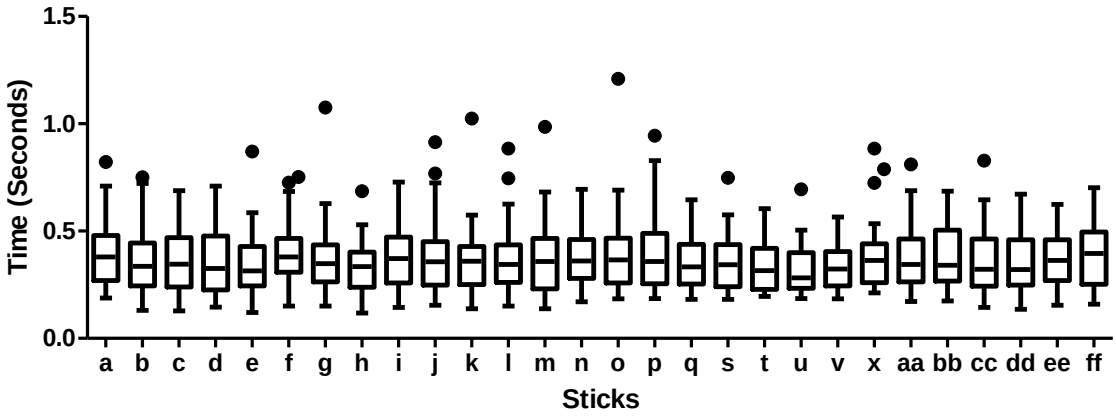

Figure 84 – Tukey’s Box and-whiskers plots with medians and extremes of the individual distributions for ‘time’ dependent variable.

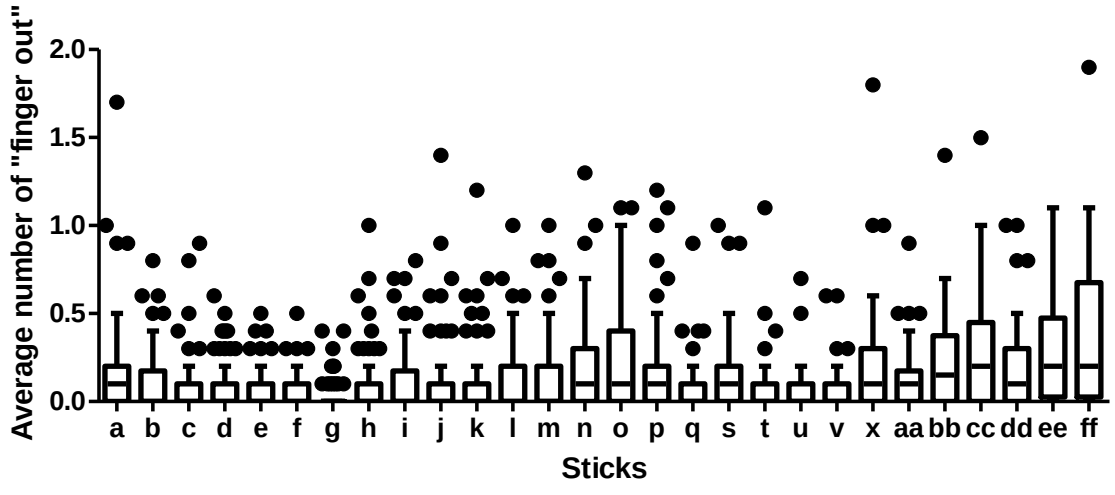

Figure 85 – Tukey’s Box and-whiskers plots with medians and extremes of the individual distributions for ‘average number of finger outs’ dependent variable.

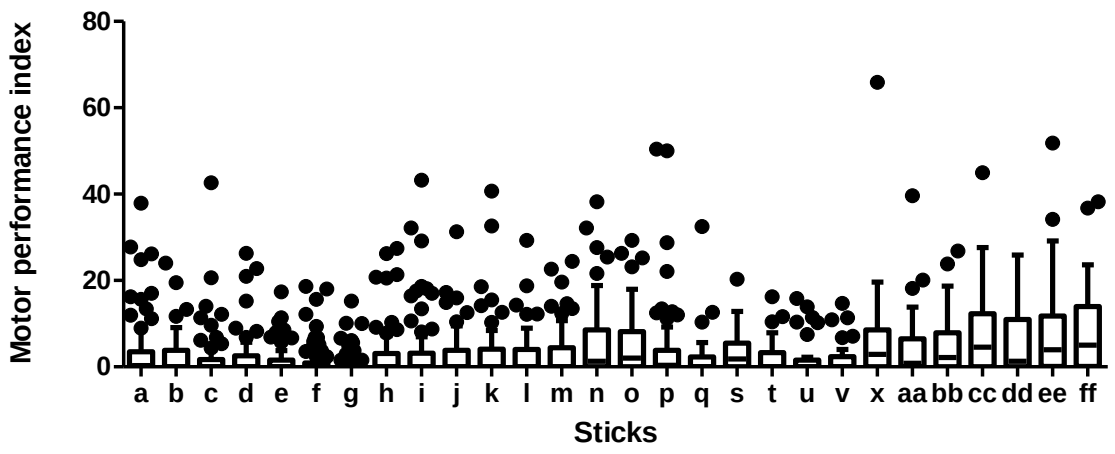

Figure 86 – Tukey's Box and-whiskers plots with medians and extremes of the individual distributions for 'motor performance index' dependent variable.

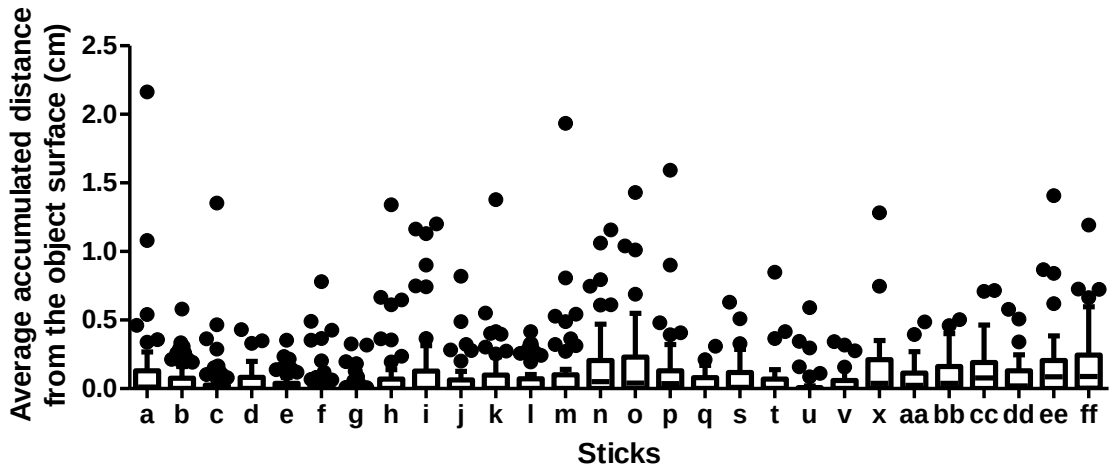

Figure 87 – Tukey's Box and-whiskers plots with medians and extremes of the individual distributions for 'average accumulated distance away from the object surface' dependent variable.

Extreme regions analysis

The data recorded from each subject was analyzed as a function of the different experimental conditions, for each of the four dependent variables: ('time', 'average number of finger outs', 'motor performance index' and 'average accumulated distance away from the object surface').

‘Time’ analysis on extreme regions

Extreme regions three-way ANOVA ‘time’ results are shown in Annex 2-Figure 27. According to the results, none of the independent variables were significantly different.

‘Average number of finger outs’ analysis on extreme regions

Extreme regions three-way ANOVA ‘average number of finger outs’ results are shown in Annex 2-Figure 28. ANOVA results showed that there were significant differences between regions $F(3,255) = 3.16$; $p<0.05$ and handedness $F(1,255)=25.32$; $p<0.0001$. The results of these significant differences are shown in Annex 4-Table 51. There was also a significant interaction between region and handedness factors $F(1,255)=5.07$; $p<0.01$. Means and SEMs of this interaction are shown in Figure 52 and Annex 4-Table 52.

According to results of Annex 4-Table 51, subjects were more precise with their dominant hand and in the upper right region. On the other hand, interaction results in Figure 52 and Annex 4-Table 52 show that subjects were more precise in the lower left region with their dominant hand and precision was significantly less precise with their non-dominant hand in both lower regions with the ‘average number of finger outs’ dependent variable.

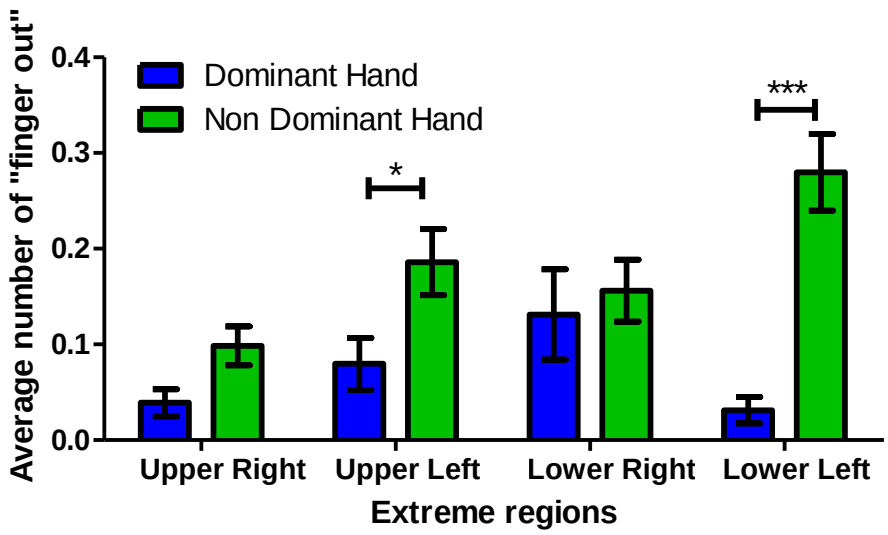

Figure 88 – Handedness and extreme region interaction on ‘average number of finger out’ dependent variable.

‘Motor performance index’ analysis on extreme regions

Extreme regions three-way ANOVA ‘motor performance index’ results are shown in Annex 2-Figure 29. ANOVA results showed that there were significant differences between “regions” $F(3,255) = 3.32$; $p<0.05$ and handedness $F(1,255)=21.87$; $p<0.0001$. Results of these significant differences are shown in Annex 4-Table 53. There was also a significant interaction between region and handedness factors $F(1,255)=6.71$; $p<0.001$. Means and SEMs of this interaction are shown in Figure 89 and Annex 4-Table 54.

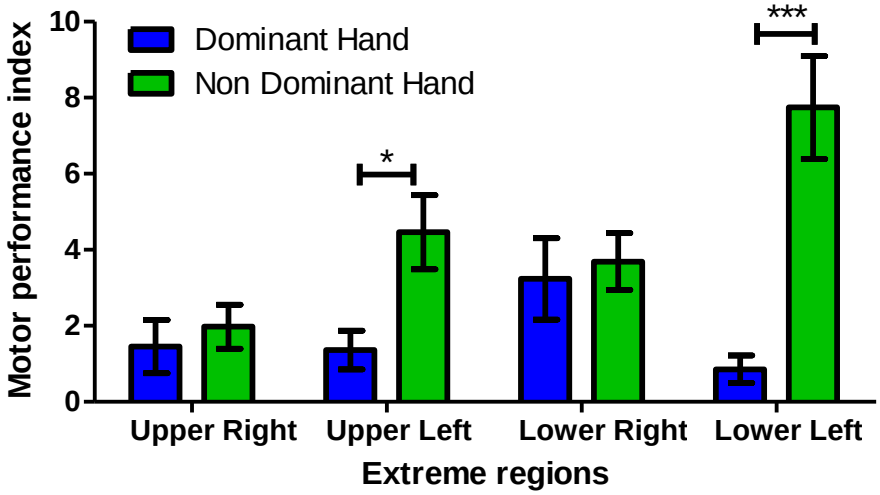

Figure 89 – Handedness and extreme region interaction on ‘motor performance index’ dependent variable

According to results of Annex 4-Table 53, subjects were more precise with their dominant hand and in the upper right region. On the other hand, interaction results in Annex 4-Table 54 and Figure 89, show that subjects were more precise in the lower left region with their dominant hand and precision was significantly less precise with their non-dominant hand in both lower regions with ‘motor performance index’ dependent variable. These results show similarity with the ‘average number of finger outs’ results.

‘Average accumulated distance away from the object surface’ analysis on extreme regions

Extreme regions three-way ANOVA ‘average accumulated distance away from the object surface’ results are shown in Annex 2-Figure 30. ANOVA results showed that there were significant differences between regions $F(3,255) = 2.7$; $p<0.05$ and handedness $F(1,255)=5.74$; $p<0.05$. The results of these significant differences are shown in Annex 4-Table 55. There was also a significant interaction between region and handedness factors $F(1,255)=4.8$; $p<0.01$. Means and SEMs of this interaction are shown in Figure 90 and Annex 4-Table 56.

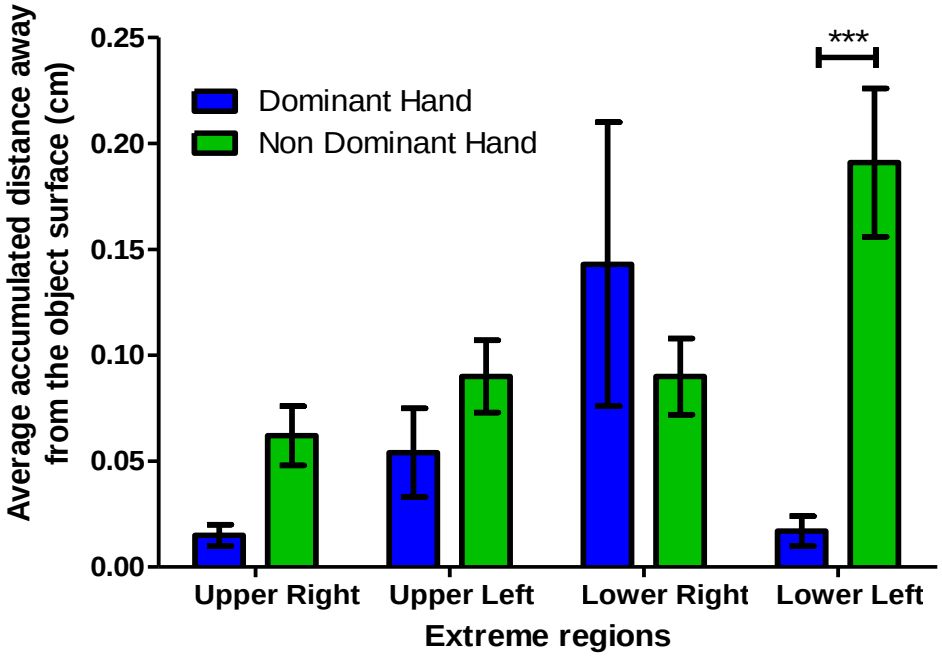

Figure 90 – Handedness and extreme region interaction on ‘average number of finger out’ dependent variable.

According to results of Annex 4-Table 55, subjects were more precise with their dominant hand and in the upper right region. On the other hand, interaction results in Annex 4-Table 56 and Figure 90 show that subjects were more precise in the lower left region with their dominant hand and precision was significantly less precise with their non-dominant hand in both lower regions with ‘average number of finger outs’ and ‘motor performance index’ dependent variables. In the lower right region, results show

that subjects were more precise with their non-dominant hand. In the detailed analysis of the lower right region, each subject's dominant and non-dominant hand results are shown in Figure 91.

According to the results in Figure 91, 5 subjects (Subject 1,8,10,11,13) were more precise with their non-dominant hand. A two-way ANOVA was performed over 16 subjects' lower right region, dominant and non-dominant hand data with a Cartesian plan of $P_{16}xH_2$, 16 participants (P_{16}) and two levels of handedness factor (H_2) for left-to-right and right-to-left data, yielding a total of 64 data points. There was no significant difference in the two-way interactions F(15,63)= 1.58; NS and only Subject 10's data was significantly different. Subject 10's extreme results occurred due to the dominant hand back to front precision result with 1.93cm.

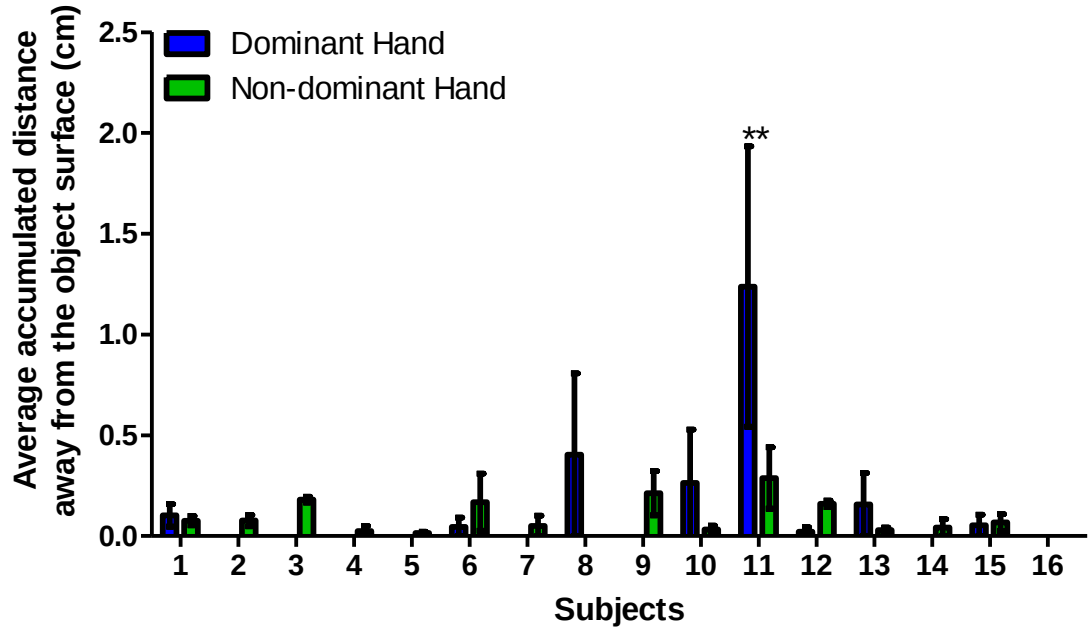

Figure 91 – 16 Subject 'average accumulated away from the object surface' data on lower right region with dominant and non-dominant hand.

Inner region analysis

The data recorded on inner region sticks was analyzed as a function of the different experimental conditions, for each of the four dependent variables: ('time', 'average number of finger outs', 'motor performance index' and 'average accumulated distance away from the object surface').

‘Time’ analysis on inner regions

Inner regions three-way ANOVA ‘time’ results are shown in Annex 2-Figure 32. According to the results, none of the independent variables were significant. ANOVA results showed that there was a significant difference between the factor levels of the movement direction F(1,1023)= 9.34; p< 0.01. This result is shown in Annex 4-Table 57. According to the results in Annex 4-Table 57, subjects were faster in the front-to-back movement direction.

‘Average number of finger outs’ analysis on inner region

Inner region three-way ANOVA ‘average number of finger outs’ results are shown in Annex 2-Figure 32. ANOVA results show differences between sticks F(15,1023) = 4.78; p<0.0001 (Figure 92) and handedness F(1,1023)=7.38; p<0.05. Results of these significant differences are shown in Annex 4-Table 58. There was also a significant interaction between stick and handedness factors F(15,1023)=1.87; p<0.05. Means and SEMs of this interaction are shown in Figure 93 and Annex 4-Table 59.

According to results of Figure 92, Annex 4-Table 58, Figure 93 and Annex 4-Table 59, subjects were more precise with their dominant hand and in the eye level operations compared to targets further away. Interactions show that subjects were more precise with their dominant hand in the lower left sticks (Stick k and n) which shows similarity with the extreme regions analysis, and on the Stick a.

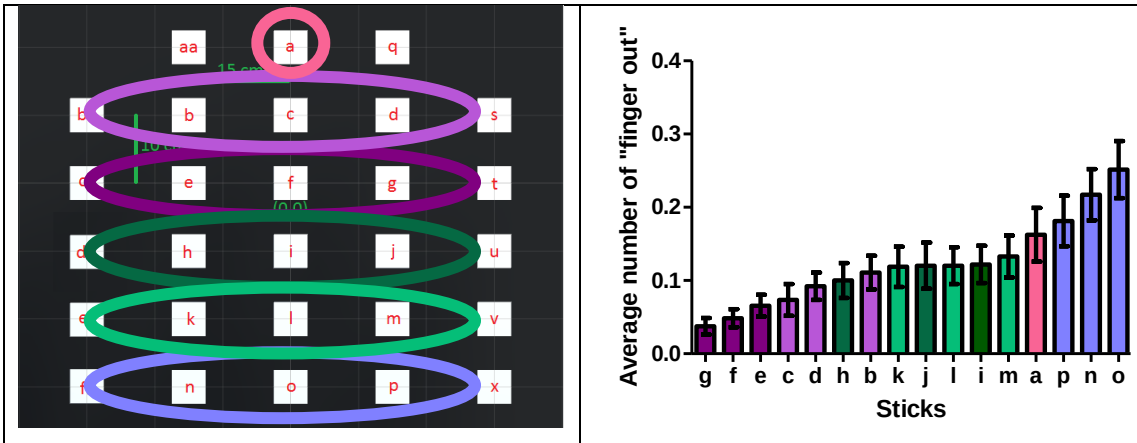

(a) (b)

Figure 92 – Means and SEMs for 'average number of finger outs’. (a) Stick positions and (b) 16 stick 'average number of finger outs’ data.

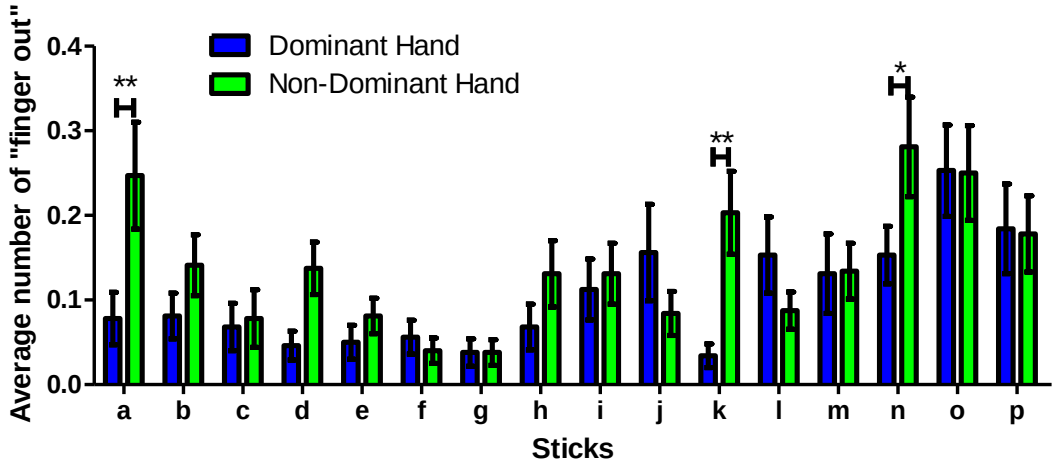

Figure 93 – Handedness and sticks interaction on ‘average number of finger outs” dependent variable.

‘Motor performance index’ analysis on inner region

Inner region three-way ANOVA ‘motor performance index’ results are shown in Annex 2-Figure 33. ANOVA results showed that there were significant differences between sticks $F(15,1023) = 2.53$; $p<0.01$ (Figure 94) and handedness $F(15,1023)=7.61$; $p<0.01$. The results of these significant differences are shown in Annex 4-Table 60.

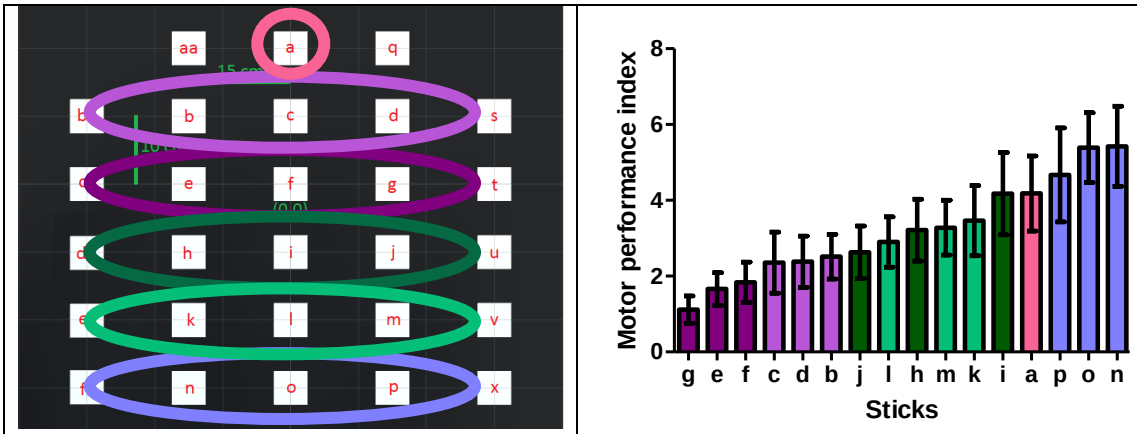

(a) (b)

Figure 94 – Means and SEMs for motor performance index’. (a) Stick positions and (b) 16 stick ‘motor performance index’ data.

According to results of Annex 4-Table 60 and Figure 94, subjects were more precise with their dominant hand and during the eye level operations compared to targets that

were further away. These results show similarity with the ‘average number of finger out’ results.

‘Average accumulated distance away from the object surface’ analysis on inner region

The extreme regions three-way ANOVA ‘average accumulated distance away from the object surface’ results are shown in Annex 2-Figure 34. ANOVA results showed that there were significant differences on sticks $F(15,1023) = 3.02$; $p<0.0001$ (Figure 95) and handedness $F(1,1023)=6.83$; $p<0.001$. The results of these significant differences are shown in Annex 4-Table 61. There was also a significant interaction between stick and handedness factors $F(15,1023)=1.9$; $p<0.05$. Means and SEMs of this interaction are shown in Figure 96 and Annex 4-Table 62.

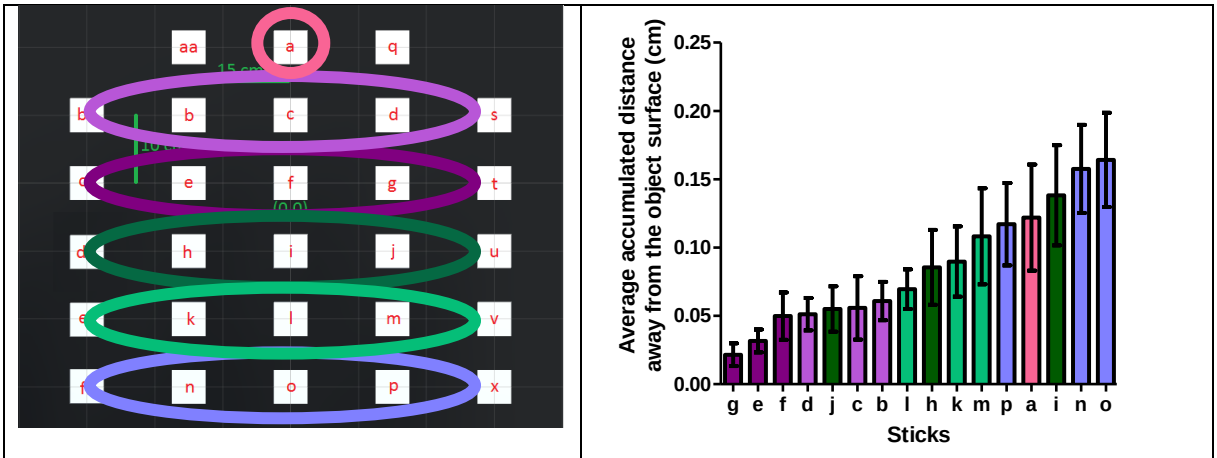

(a) (b)

Figure 95 – Means and SEMs for ‘average accumulated distance away from the object surface’. (a) Stick positions and (b) 16 stick ‘average accumulated distance away from the object surface’ data.

According to results of Figure 95, Figure 96, Annex 4-Table 61, and Annex 4-Table 62 subjects were more precise with their dominant hand and during the eye level operations compared to targets that were further away. Interactions show that subjects were more precise with their dominant hand in the lower left sticks (Stick h, k, and n) which shows similarity with the extreme regions analysis, and on the Stick a.

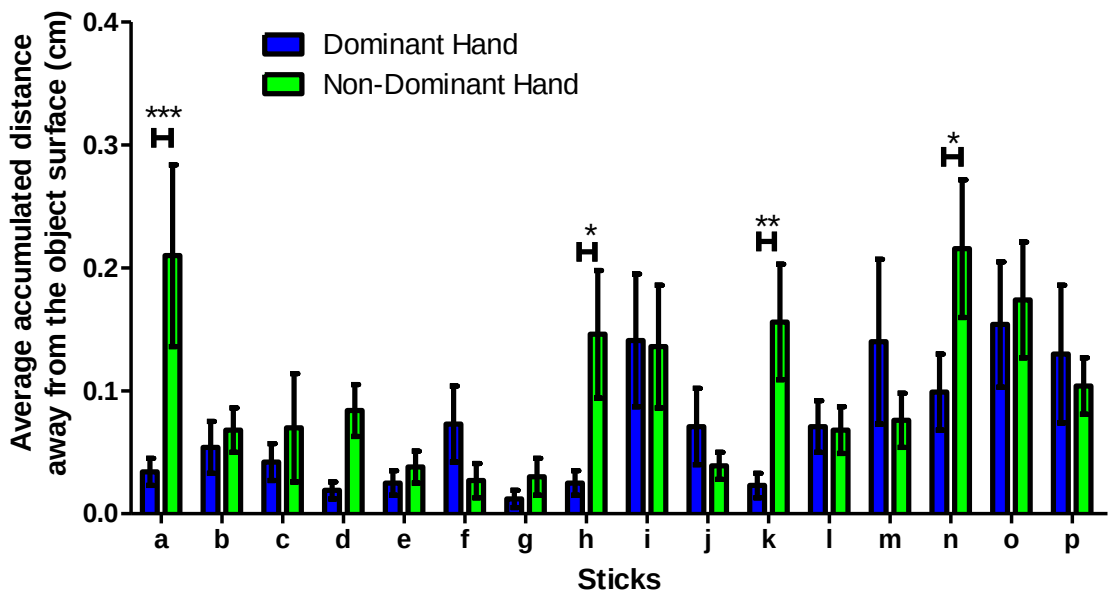

Figure 96 – Handedness and sticks interaction on ‘average accumulated distance away from the object surface” dependent variable.

Discussion

In the third study of this chapter, ipsilateral and contralateral manual hand movements were studied in a virtual environment as extreme regions and inner region with time and three different precision dependent variables.

An important point to be taken into account during the experimental analysis is that all the subjects who performed the experiments in the study here were right-handed. This was not caused by the experimental design parameter selection; right-handed subjects were not deliberately selected amongst the volunteers; all the volunteers who wanted to participate in the experiments were right-handed. This creates a limitation in the interpretation of the results of the study as these results are only valid for right-handed subjects.

In the extreme region analysis, hand movements of the subjects were analyzed with a depth perception in four different regions. According to the results, subjects were more precise with their dominant hand and there was no time difference between each extreme region. However, subjects were significantly more precise in the upper right

region with all three precision dependent variables. On the left side of the extreme regions in the virtual scene, there are significant differences in handedness factor for both the upper and lower left regions. Subjects were more precise with their dominant hand in both the upper and lower left regions. In other words, right-hand contralateral movements were more precise compared to the left-hand ipsilateral movements in the extreme regions. Furthermore, subjects were least precise in the lower left region in general, but in the handedness and the region interactions, it was observed that subjects were more precise with their dominant hand in the lower left region in all three dependent variables and more precise with their non-dominant hand in the upper right region among all extreme regions.

In the inner region analysis, subjects were faster with the front-to-back operation when compared to the back-to-front operations. In the individual stick results, all three-precision dependent variables, ‘average number of finger outs’, ‘motor performance index’ and ‘average accumulated distance away from the object surface’ variables had the similar results: subjects were more precise during the eye-level interactions and they were getting less precise with target location placed further away from the eye level. In the interaction results between handedness and sticks in ’average number of finger outs’ and ‘average accumulated distance away from the object surface’, subjects were least precise with their non-dominant hand on the stick n, which was positioned at the lower left among the targets and subjects were more precise with their non-dominant hand during the eye level interactions. On the other hand, subjects were more precise with their dominant hand during the eye level interactions and with the stick k, which was 10 cm above the stick n and subjects were less precise with their dominant hand with the stick n, which was at the bottom of the virtual scene. In the handedness and stick interactions, it was observed that sticks on the lower left side of the regions (h, k and n) were significantly different for handedness levels. Furthermore, stick a, which was at the top of the virtual scene, was also significantly different for handedness levels.

Another important point to be taken into account in this research is that the current VR headset does not provide a full depth visual feedback information to the individuals. This is because of the 2D screens in the VR headsets. Subjects still needed to look at two 2D screens in the VR headset for visual cues to plan their movements and perceive

the target [215,216]. Current technology can only provide this pseudo depth data with the perspective renderings. The results found in this study need further research to apply to real-world tasks and skill transfer.

In conclusion, these results show the importance of the placing an object in the virtual scene. When a target placed in egocentric space for task execution, handedness, movement direction, and the position of the object should be considered for a better task or training assessment [68].

Study 4 – Effects of Virtual Object Shape Complexity and Size

In the first study of second chapter, the effects of VR on time and precision among the other visual feedback used as simulator environments were studied. In the second study of second chapter, the first two aspects of three-dimensional space, variations of length, and the width of virtual objects were studied. In the third study of second chapter, depth, the third dimension of the three-dimensional space was studied as ipsilateral and contralateral manual hand operations. In the fourth study, effects of shape complexity and the object size are studied. Two medical objects; one is reconstructed from an MRI sequence and one is crafted for medical teaching, are used in this study to investigate time and precision variations in the “NoTouch” system.

Study goal and hypotheses

In the last three studies, different aspects of VR environments were studied, such as the virtual object length, width and depth. In this study, all three of these features are inspected together in one experiment.

The success criteria of a VR simulator can be measured with the individuals skill transfer from VR tasks to the real-life tasks and dexterity within these tasks [217]. Previous research on the skill transfer from the virtual environment to a real task shows the importance of the assessment criteria selection (more information about the sensorimotor training in VR can be found in Adamovich et al [218]). To be able to choose the accurate assessment criteria, the motor performance of the individuals has to studied and examined with different independent variables. To fully understand human motor behavior in VR applications, several complementary behavioral indicators should be taken into consideration, operationalized experimentally in terms of different related dependent variables.

Also, among the independently variable factors which should be taken into account in the case of surgical simulators or virtual reality applications as pre-clinical test

environments, for example, is structural complexity of the virtual image or object. Several studies have previously been conducted on virtual object size [219–221]. It was noticed that subjects were performing better with bigger objects compared to smaller objects [222]. On the other hand, structural complexity of the objects should also be considered, as it may affect human skills and motor performance depending on the context. Although previous authors have addressed the problem of structural complexity and its possible effects on reaching for objects in virtual reality environments (e.g. [90,91]), there still is a need for deeper research into the effects of structural complexity on the time and the precision of hand movements towards or along the borders of virtual objects and other motor skill indicators.

In research on surgical simulators, it was found that active learning (when a subject interacts with the object) leads to better motor performance in VR than passive learning (when a subject just observes the virtual scene) [92]. Moreover, the motor skills of subjects increase when they are provided with tactile [93] or auditory feedback [94]. For example, Swapp and his colleagues [95] showed that tactile feedback improved the speed of subjects in a 3D VR stereo environment. Furthermore, handedness which is affiliated with touch information among other primary somatosensory cortex functions also affects the motor performance of subjects [223]. For instance Batmaz and his colleagues [101] showed that while an inexperienced subject performed the task slower with his dominant hand to pay attention to complete the task, an experienced subject performed the experiment faster with his dominant hand because of individual motor learning. Consequently, the effects of handedness with beginners in virtual environments need further investigation.

To that effect, time and precision of finger movements along the axis of alignment of virtual objects as a function of their size, structural complexity, hand movement direction, and handedness in an interactive virtual reality application using Leap Motion and Oculus DK2 is studied in the last study of this chapter. Understanding how subject’s performance is affected by the object complexity was the main goal of this study.

Materials and Methods

Subjects

Eighteen right handed subjects (7 female) ranging in age between 20 and 33 (average = 26.33) participated in this study. None had any experience in VR and image-guided activities such as laparoscopic surgery training or other. Before starting the experiments, each subject's index fingertip width was measured as average of 1.7 cm with maximum of 2 cm. To be able to follow the objects in the virtual reality, the minimum distance between the shoulder and the fingertip was calculated as 55 cm. Before starting the experiments, each subject's shoulder to fingertip distance was measured and the minimum distance was 62 cm. All the subjects performed the both experiments on object size and object complexity.

Objects in VR Scene

In fourth study of chapter 2, subjects saw two different objects in the "NoTouch" VR scene; their virtual skeleton hand and medical images to follow.

During the experiments, two different rendered representations of human body parts were used. The first one was a femur bone, which was made by computer graphic artists for medical usage. The femur bone was called "simple structure" for this experiment, because while the subject followed the object with the fingertip, one-way movement in horizontal plane was enough to finish the experiment. The second one was a part of a Willis circle, which was generated by computer software via MRI data. The Willis circle was called "complex structure", because subjects had to move their index finger tip in the three-dimensional space; not just on one plane but on all three dimensions. They also had to be careful at the curves, curls and other natural forms on the object to complete the experiment.

According to study of Dankedar and colleagues [180], average human index finger tip width varies between 1.6 cm and 2 cm. For this reason, narrowest cross-sectional area of the simple structure was scaled to the maximum average human index finger tip width, to 2 cm. This size was called as "small" (Figure 97 (a)). For the "medium" (Figure 97 (c)) and the "large" (Figure 97 (e)), the narrowest cross-sectional areas were 3 cm

and 4 cm respectively. The simple structure was uniformly scaled in order not to distort the shape of the femur bone.

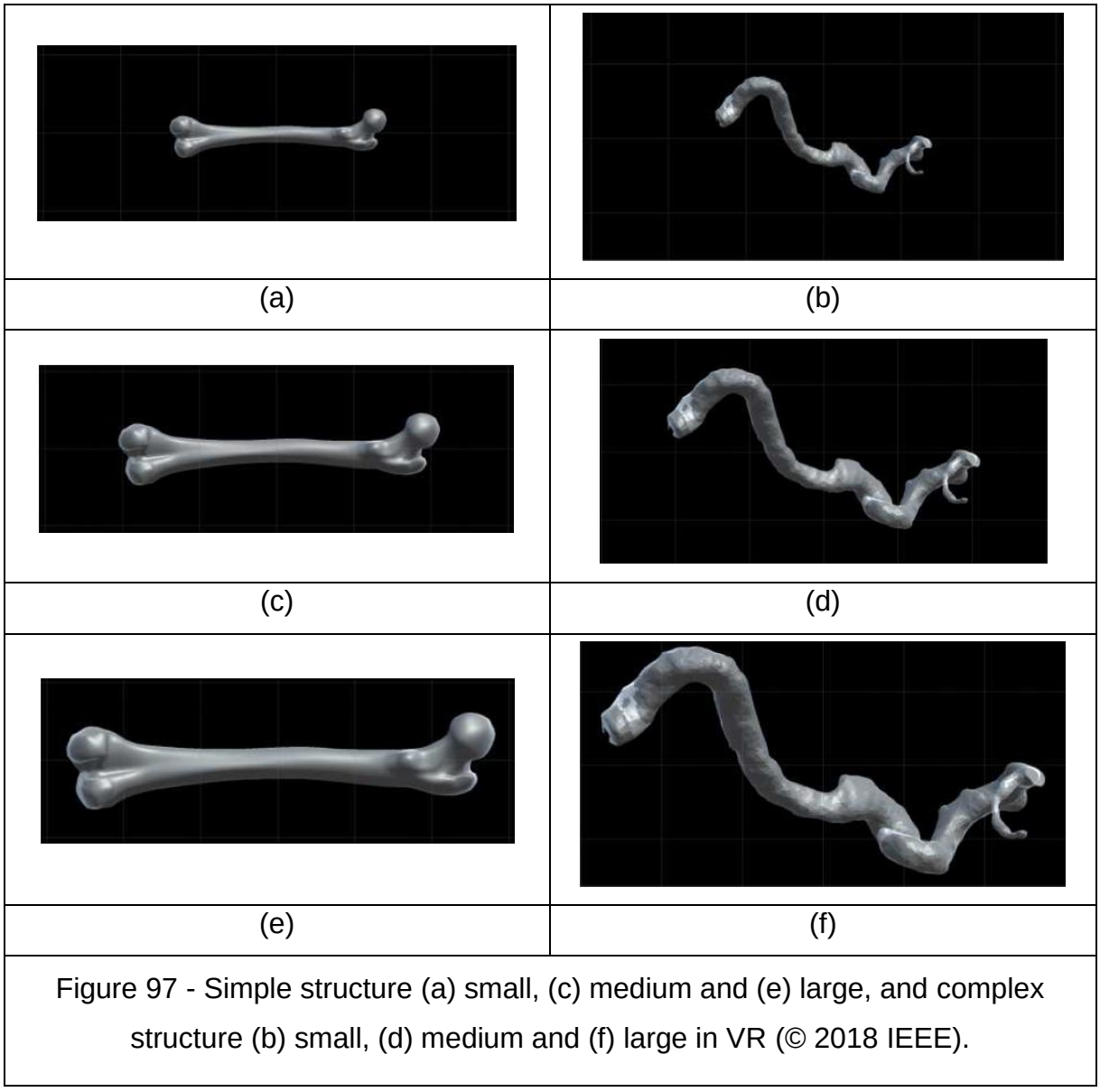

Figure 97 - Simple structure (a) small, (c) medium and (e) large, and complex structure (b) small, (d) medium and (f) large in VR (© 2018 IEEE).

“Small” (Figure 97 (b)), “medium” (Figure 97 (d)) and “large” (Figure 97 (f)) complex structures were the same length as the small, medium and large sized simple structures. All complex structure sizes were also uniformly scaled in order not to distort the shape of the Willis circle. Lengths of simple and complex structures were: for small 28 cm, medium 42 cm and for large 55 cm. This design aimed to observe the effects of complex structure on the motor behavior; subjects had to follow the same distance as they did for the simple structure, but they had to move their hands in VR without tactile feedback.

Two cubes were also placed on each side of the simple object. These cubes were called the `starting point' and the `finishing point', according to the direction of the hand movement.

The center of the complex and simple objects was placed 30 cm in front of the eye level of the subjects. Both structures were placed parallel to screen and subject.

Procedure

For the simple structure, subjects had to start from the `starting point' and follow the structure with their index fingertip until the `finishing point'. The `starting point' turned green when subject's index fingertip was placed at the `starting point'. At the same time the simple structure turned gray. Data collection started when the tip of the subject's index finger left the `starting point' which then turned back to red.

When the index fingertip of the subject reached to the `finishing point', the given structure turned red and the `finishing point' turned green to indicate the end of the trial set.

For trials on the complex structure, a similar approach was used. At the beginning of the experiment, all 52-sub parts of the complex structure were gray. `Starting' and `finishing' points of the complex structure turned green when the subject's index fingertip was inside and turned red when it was outside. During the experiment, if the tip of the subject's index finger left the object’s surface, that individual sub-part, not the whole object, turned red. Likewise, when the tip of the subject's index finger remained inside the sub-part, only that sub-part of the object remained green.

Cartesian Design Plan and Data Generation

Experimental design

Each experiment consisted of 10 successive trial sets per experimental condition for 18 subjects and there were 24 experimental conditions: each subject followed two different structures (Structural Complexity condition - SC_2), with their dominant-hand and their non-dominant hand (Hand condition - H_2), in left-to-right and right-to-left

directions (Direction condition - D_2) for small, medium and large sizes (Size condition – S_3). The order of size conditions was counterbalanced between subjects and structures to avoid specific habituation effects. For the same reason, the order of the handedness and direction of finger movement conditions were also counterbalanced between subjects. Factorial design was properly counterbalanced excluding any systematic effect of order. Each subject performed 240 trials. In total 4320 trials were performed. The full factorial plan of the experiment can be presented as SC_2 x S_3 x D_2 x H_2 x 10 trial sets x 18 subject.

Data generation

Subjects had to perform the experiment starting at the `starting point' and ending at the `finishing point'. Data relative to time and precision of finger movements were recorded in real time between these two points. There was no trial abortion or repetition in case of any errors. Subjects had to fully complete ten trial sets to validate the sets for each condition.

A four-way ANOVA was run on the raw data for ‘time' and ‘average number of finger outs'. The two other variables, ‘motor performance index’ and ‘average accumulated distance away from the object surface’ were not used in this study analysis because it was not possible to measure de these variables in the complex structure. In the four-way analysis design there was two levels of the structural complexity factor ($SC_{2),}$ three levels of the size factor (S_3), two levels of the handedness factor (H_2), and two levels of the direction of finger movement factor (D_2). The full factorial design plan for four-way ANOVA SC_2 x S_3 x D_2 x H_2 with 18 subjects and 10 repetitive trials produced a total of 2 x 4320 data for the dependent variables `execution time' and ‘average number of finger outs’.

Results

In the Pearson's correlation analysis between ‘time' and ‘average number of finger outs’, there was a positive correlation between the two dependent variables $r=0.448$; $p<0.001$ (N=4320).

Medians and extremes of the individual data relative `execution time' and ‘average number of finger outs’ for the different experimental conditions were analyzed first. The results of this analysis are represented graphically as box-and-whiskers plots in (Batmaz et al. [70] Figure3 ) for (a) simple structure and (b) complex object `execution time', and (c) simple object and (d) complex object ‘average number of finger outs’.

Outliers in the Batmaz et al. [70] Figure3 data were indeed rare and given the large amount of data collected for each condition, correcting these few by replacing them by averages would not have changed the statistical analyses. Two outliers at the upper extremes of the distributions around the medians relative to ‘average number of finger outs’ of complex structure medium object size dominant hand right-to-left movement direction, and one outlier at the upper extremes of the distributions around the medians relative to ‘average number of finger outs’ of complex structure medium object size non-dominant hand left-to-right movement direction were corrected by replacing them by the mean of the distribution.

One-way effects

ANOVA revealed a significant difference between simple and complex structures for ‘time' $F(1,4319)= 9886.38$; $p<0.001$ (Figure 98(a)) and ‘average number of finger outs’ $F(1,4319)= 557.49$; $p<0.001$ (Figure 98(b)). Significant differences in two levels of the handedness was observed for `execution time' $F(1,4319)= 5.81$; $p<0.001$ (Figure 98 (c)) and in ‘average number of finger outs’ $F(1,4319)= 21.64$; $p<0.001$ (Figure 98 (d)). Three levels of the size condition was significantly different for `execution time' $F(2,4319)= 13.04$; $p<0.001$ (Figure 98 (e)) and in ‘average number of finger outs’ $F(1,4319)= 63.83$; $p<0.001$ (Figure 98 (f)). The data are shown in Batmaz et al. [70] Table1. According to the results, subjects were faster and more precise with the simple structure compared to complex structure, were slower and less precise with their dominant hand, and produced more errors and faster movements on the small objects compared with the medium and large objects. Neither the `execution time' nor the ‘average number of finger outs’ was significant for the direction of the fingertip movements.

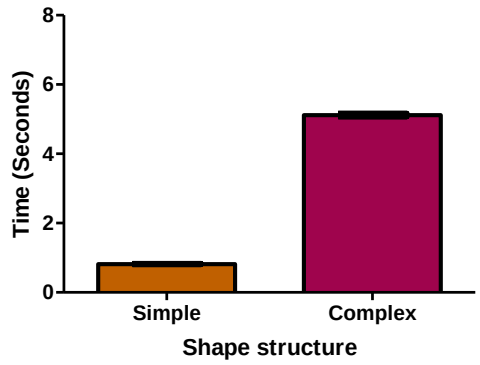

(a)

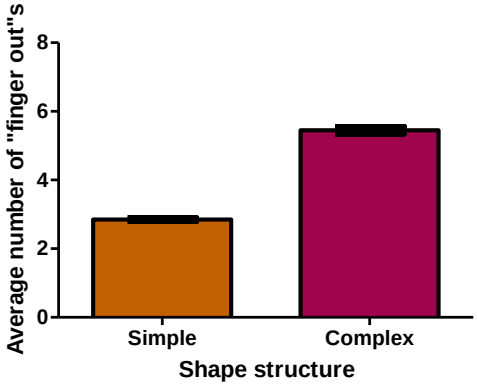

(b)

(c)

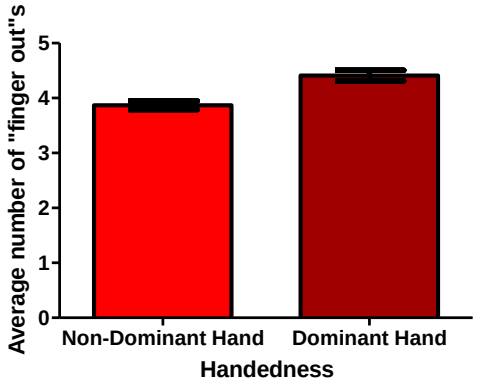

(d)

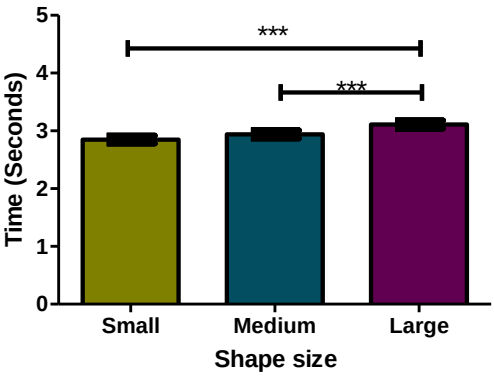

(e)

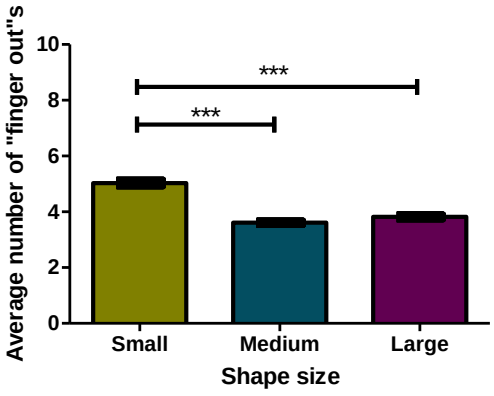

(f)

Figure 98 - Significant effects of object complexity on (a) ‘execution time’ and (b) ‘task error’, of handedness on (c) ‘execution time’ and (d) ‘task error’, of object size on (e) ‘execution time’ and (f)‘task error’ (© 2018 IEEE).

Two-way interactions

Significant interactions were found between the factors structural complexity and handedness on `execution time' $F(1,4319)=10.729$; $p<0.001$ (Figure 99 (a)) and ‘average number of finger outs’ $F(1,4319)=20.3104$; $p<0.001$ (Figure 99 (b)), between the factors object size and handedness on 'execution time' $F(2,4319)=4.40$; $p<0.05$ (Figure 99 (c)) and ‘average number of finger outs’ $F(2,4319)=7.33$; $p<0.001$ (Figure 99 (d)) and factors size and structural complexity on ‘average number of finger outs’ $F(2,4319)=295$; $p<0.001$ (Figure 99 Figure5(e)). Means and SEMs of these results are given in Batmaz et al. [70] Table2.

Figure 99 (a) and Figure 99 (b) results on complex structure showed a speed and precision trade-off: subjects were faster but less precise with their dominant hand on the complex structure. Besides, participants were slower (Figure 99 (c)) and less precise (Figure 99 (d)) with their dominant hand on small object size. Subjects were also getting more precise when the complex structure was getting larger and they were less precise when the simple structure size was getting smaller (Figure 99 (e)).

Detailed handedness results exploration

Subject were both faster and less precise in complex objects, and slower and less precise in small object size with their dominant hand. Structural complexity, handedness and object size three-way ANOVA interaction was not significant for ` time' $F(2,4319)= 2.63$; NS and ‘average number of finger outs’ $F(2,4319)= 2.74$; NS.

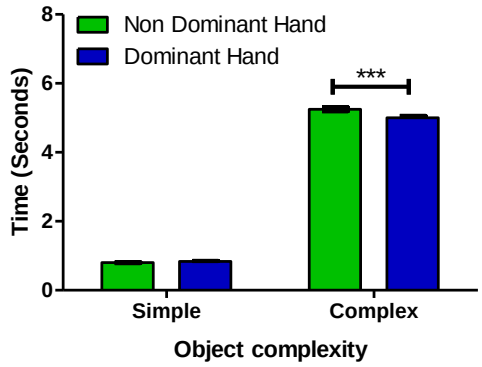

(a)

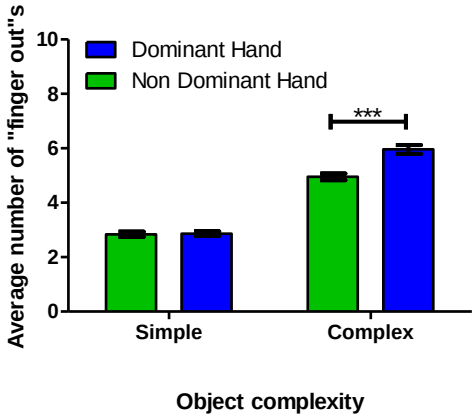

(b)

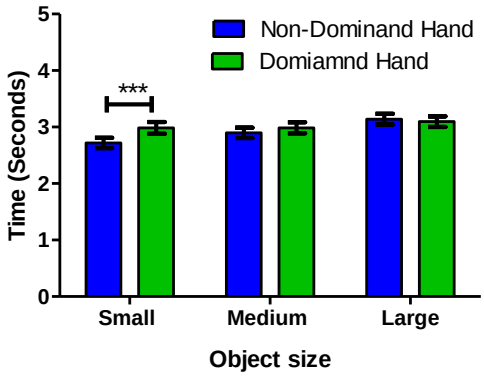

(c)

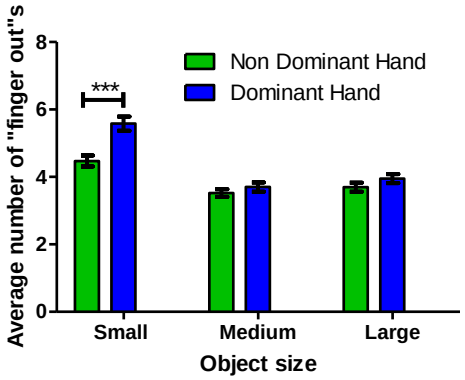

(d)

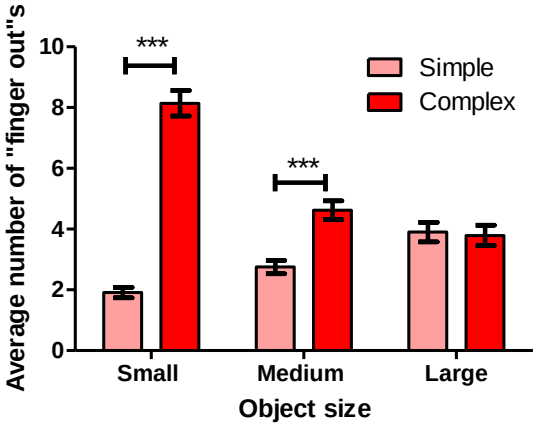

(e)

Figure 99 - Significant two-way interactions between object complexity and handedness on (a) ‘execution time’ and (b) ‘task error’, and between object size and handedness on (c) ‘execution time’ and (d) task error’, and between structural complexity and size on (e) ‘task error’ (© 2018 IEEE).

In the detailed analysis of complex structure and handedness (Figure 99 (a)) and (Figure 99 (b)), a two-way ANOVA was performed over 18 subjects' complex structure, dominant and non-dominant hand data with a Cartesian plan of P_{18} x H_2, 18 participants (P_{18}) and two levels of handedness factor (H_2) over 60 trials (including object size S_3 x index fingertip movement direction D_2 x 10 repetitive trials), yielding a total of 2x2160 data for ` time' and ‘average number of finger outs’. In two-way interactions, twelve subjects (Subject 1,3,5,6,8,9,10,11,13,14,16,18) were slower with their dominant hand and eight of these results (Subject 1,3,5,9,10,11,14,18) were significantly different $F(17,2159)=9.38$; $p<0.001$ (Batmaz et al. [70] Figure6 (a)). Thirteen subjects (Subject 1,2,3,5,6,8,9,10,11,13,16,17,18) were less precise with their dominant hand and seven of these results (Subject 1,3,5,10,13,17,18) were significantly different $F(17,2159)=4.92$; $p<0.001$ (Batmaz et al. [70] Figure6 (b)). Eleven subjects (Subject 1,3,5,6,8,9,10,11,13,16,18) were both slower and less precise with their dominant hand and in total, five of these results (Subject 1,3,5,10,18) were significantly different for both dependent variables.

In the detailed analysis of small object size and handedness (Figure 99 (c)) and (Figure 99 (d)), a two-way ANOVA was performed over 18 subjects' small object size, dominant and non-dominant hand data with a Cartesian plan of P_{18} x H_2, 18 participants (P_{18}) and two levels of handedness factor (H_2) over 40 trials (including structural complexity SC_3 x index fingertip movement direction D_2 x 10 repetitive trials), yielding a total of 2x1440 data for ‘ time' and ‘average number of finger outs’. In two-way interactions, thirteen subjects (Subject 1, 3, 5, 6, 8, 9, 11, 12, 13, 14, 16, 17,18) were slower with their dominant hand and only one of these results (Subject 3) was significantly different $F(17,1440)=0.7$; NS (Batmaz et al. [70] Figure7 (a)). Besides, thirteen subjects (Subject 1, 2, 3, 4, 5, 6, 8, 9, 10, 13, 16, 17, 18) were less precise with their dominant hand and five of these results (Subject 3,5,13,17,18) were significant $F(17,1440)=2.08$; $p<0.01$ (Batmaz et al. [70] (b)). Ten subjects (Subject 1,3,5,6,8,9,13,16,17,18) were both slower and less precise with their dominant hand and only one of these results (Subject 3) was significantly different for both dependent variables.

In both Batmaz et al. [70] Figure6 and Batmaz et al. [70] Figure7, Subject 3 (female, 25 years old, index fingertip width 1.7 cm, distance between shoulder to index finger

tip 66 cm) was slower and less precise with her dominant hand compared to non-dominant hand in small object size and complex object structure. Individual execution time-precision curves of the subject 3 is given in Batmaz et al. [70] Figure8. On the contrary, Subject 15 (female, 26 years old, index fingertip width 1.8 cm, distance between shoulder to index finger tip 73 cm) was faster and more precise with her dominant hand compared to non-dominant hand in small object size and complex object structure. Subject 15 is selected for comparison with Subject 3 because both subjects were female, had similar ages, fingertip widths, shoulder to index finger tip distance and contradicting handedness results on Batmaz et al. [70] Figure6 and Batmaz et al. [70] Figure7. Individual time-precision curves of the Subject 15 is given in Batmaz et al. [70] Figure9.

Subject 3 was getting faster in right-to-left movements in both simple (Batmaz et al. [70] Figure8 (c)) and complex (Batmaz et al. [70] Figure8 (g)) structures, yet she was not getting any precise in ‘average number of finger outs’(Batmaz et al. [70] Figure8 (d) and Batmaz et al. [70] Figure8 (h), respectively). She was getting more precise in left-to-right movements in simple structure (Batmaz et al. [70] Figure8 (b)), however she was not getting any faster (Batmaz et al. [70] Figure8 (a)). She was getting faster (Batmaz et al. [70] Figure8 (e)) and more precise (Batmaz et al. [70] Figure8 (f)) in right-to-left movement in complex structure except for dominant hand small object size: she was getting slower and her precision results were oscillating. Subject 15 was getting faster only in left-to-right movements in complex object (Batmaz et al. [70] Figure9 (e)). Her time results were stable for simple (Batmaz et al. [70] Figure9 (c)) and complex (Batmaz et al. [70] Figure9 (g)) structure left-to-right movements except for simple structure small size dominant hand results (blue line in Batmaz et al. [70] Figure9 (c)). She was getting slightly slower (Batmaz et al. [70] Figure9 (a)), but more precise (Batmaz et al. [70] Figure9 (b)) in left-to-right movement direction in simple structure. Her precision results were oscillating for left-to-right hand movements on simple structure (Batmaz et al. [70] Figure9 (d)) and right-to-left hand movements on complex structure (Batmaz et al. [70] Figure9 (f)). Her precision was also oscillating in right-to-left movement direction for complex structure (Batmaz et al. [70] Figure9 (h)) except for large objects. In both subject results, simple structure showed far less change than the complex structure for ‘time' and ‘average number of finger outs’.

Subject 3 was getting slower (Batmaz et al. [70] Figure8 (e)) and less precise (Batmaz et al. [70] (f)) in complex structure small size dominant hand right-to-left movement. Likewise, Subject 15 was getting less precise in complex structure large object size dominant and non-dominant hand results on right-to-left movement direction (Batmaz et al. [70] Figure9 (h)). These rare task results were not the first or the last trials of subjects. Furthermore, in the figures of 18 subjects' individual ‘time' and ‘average number of finger outs’ data (not shown here due to the space limitations), there was no sudden or obvious increase in the ‘time' or decrease in the ‘average number of finger outs’ that might represent task fatigue or rushing.

Pearson's correlation analysis in these rare result conditions between 18 subjects' ‘time', ‘average number of finger outs’, index fingertip width and shoulder to index fingertip length data showed only correlations between ‘time' and ‘average number of finger outs’. In complex structure small size dominant hand right-to-left movement, there was a positive correlation between ‘time' and ‘average number of finger outs’ with $r=0.690$; $p<0.01$ ($N=18$). Similarly, complex structure small size dominant hand right-to-left movement, there was a positive correlation between ‘time' and ‘average number of finger outs’ with $r=0.686$; $p<0.01$ ($N=18$).

Discussion

Positioning an object in a VR scene without controlling for size and complexity may cause a conflict between design and task demands and mislead conclusions about individual progress or performance evolution during training. When subjects were retracing a simple structure in VR with the tip of their index finger, they were more precise with small size objects. When the image size was increased, motor performance of the subjects decreased. On the other hand, when subjects were retracing a complex structure, they were more precise with large size objects. When the object size increased, motor performance of the subjects also increased. These seemingly contradictory results show that virtual object size and complexity are interdependent and need to be controlled when assessing motor performances with VR training applications or simulators. Besides, when the task environment is simple, the size of the display should be kept small. However, if the virtual object space is complex, then the display size should be large enough to minimize errors. In practical

use, beginners should start training on larger representations of complex objects in VR. For skill assessment in VR, object size may need to be individually calibrated for complex actions [31,36] such as knot tying in laparoscopic surgery, for example. More generally, in the absence of prior data or knowledge, virtual objects should be displayed at a medium size for optimal motor performance as a thumb rule. The results here highlight the importance of the object complexity in VR and lead to conclude that, whenever possible, a simple structure should be preferred over a complex structure.

It was known already that handedness can affect performance in VR displays [224] especially for beginners. Significant differences between dominant and non-dominant hand were observed for the complex structure and small object size with a better precision score for the non-dominant hand. This may seem surprising in the light of previous studies (e.g. [223]). In the detailed analyses here with dominant hand and non-dominant hand, possible reasons can cause this difference were inspected. In individual ‘time' and ‘average number of finger outs’ results over 10 repeated trials of 18 subjects, no task fatigue or rushing was observed that could affect the results. Furthermore, the distance from shoulder to index fingertip and index fingertip width showed no correlation with ‘time' and ‘average number of finger outs’. Several explanations may account for the handedness results here.

Majority of the subjects (11 out of 18) were both slower and less precise with their dominant hand in complex structures. Besides, majority of the subjects (10 out of 18) were both slower and less precise with their dominant hand in small object size. These non-dominant hand speed and precision results could be explained by the fact that subjects were more attentive to task constrains when forced to use the hand they do not use preferentially. This is related to the feeling of agency during motor control [32,122,126]. When subjects use the hand they prefer using, they feel more in control and may become less attentive to contains.

Besides, subjects were asked to retrace the objects in VR while their fingers were wide open, and the outer side of the active hand was facing the motion sensor. This method was particularly selected to acquire stable data from the motion sensor and to overcome the lack of hand visualization. Complex structure was not a symmetrical object. Retracing different curvature segments of the complex object from different

angles with dominant and non-dominant hand with the limited hand gesture could explain these results. Although subjects did not indicate any fatigue or ergonomic comments, motor performance of participants could be affected by the hand movement restrictions.

Another explanation of the handedness results can be the fact that the finger movements of the subjects were controlled through visual feedback only, not tactile or auditory feedback. Color change alone might not be enough to provide ‘average number of finger outs’ feedback in specific object designs to guide the subject to correct his/her errors. From previous studies [94,95,225], it is known that additional feedback can provide useful information during task execution and lead to improve the motor performance of the subjects. Moreover, previous studies on handedness also shows the unexpected results can acquire due to the inexperience of the subjects on the task [101] The results here point towards potentially intricate links between handedness effects and feedback conditions in VR environments and deserve to be studied further.

The other important result here is the significant difference between subjects' task dependent individual performance strategies. This strategy difference occurs spontaneously and in the absence of performance feedback [57,82,85,204]. In this case, it is important to monitor subjects' speed-precision curves, which reveals their choice between speed and precision strategy goals. For instance, Subject 15 was getting slower (Batmaz et al. [70] Figure8 (a)), but more precise (Batmaz et al. [70] Figure8 (b)) in simple structure. On the other hand, in the same conditions, Subject 3 had the similar time results after 10 trials (Batmaz et al. [70] Figure8 (b)), but she was getting more precise (Batmaz et al. [70] Figure8 (b)). Instead of using unsupervised learning, instructing subjects to prioritize precision at the begging of their training [32] would help them optimize their motor performance learning in VR and eliminate unexpected results.

Study 5 – Sound Frequency Effects in Virtual Space

In the first four studies of chapter 2, time and precision of novices in VR were studied with only one error feedback. When the subjects made an error, the color of the virtual object was turned into red to indicate the error. In the last study of chapter 2, an additional feedback, auditory feedback is included to investigate motor performance alteration of the subjects. From the previous research on sonification, it is known that auditory feedback significantly increases the motor performance of the subjects in VR. In this study, the effects of different sound frequencies in VR are explored with the "NoTouch" system.

Study Goal and Hypotheses

The motion sensor in front of the VR headset has a significant drawback: it can only provide a visual feedback. However on the air systems like the Leap Motion any additional feedback to the user is not provided in the current technology. Subjects have to look at a visual feedback resource to understand their spatial position in the virtual scene. This creates two major performance problems for the hand movements in virtual scene: one is static and the other one is dynamic.

In the static hand actions, the motion sensor can provide a robust hand position data to the user as a visual feedback. However, motor performance of the subject decreases due to muscle fatigue after a while. Stationary hands or fingers in the air need a physical feedback to support them. The "NoTouch" system or any other similar human-computer interaction system that uses cameras as a digital input, do not provide any physical feedback support, which leads to muscle fatigue and a decrease in motor performance [226,227]. In this case, additional feedback can be provided to the subjects in order to improve their results [228].

In the dynamic hand movements, subjects have to focus on their maneuvers and adjust their actions to avoid making errors. This avoidance is based only on the visual feedback provided by the screen because no touch or haptic feedback is provided to

support the user. This lack of support also creates a disadvantage of the task fatigue [227,229,230] but more importantly, it creates confusion of the complex structure movements as seen in the fourth study. During a complex task execution, subjects needed more information about the environment to successfully execute the tasks due to the complicated requirements of hand movements. Therefore, an additional feedback can be helpful to increase subject's motor performance results.

In both static and dynamic movements in the virtual scene, subjects need additional feedback to support their movements and increase their performance [231]. Apart from the haptic feedback, auditory feedback is another feedback option that can be used in the VR environments as additional information about the environment to enhance the motor performance of the individuals [232]. The "NoTouch" system can be improved with an auditory feedback to provide this additional feedback in the virtual scene.

While haptic feedback is a larger research area, auditory feedback also increases the motor performance of subjects in the virtual reality environment [96,97]. The positive effect of additional feedback and positive effect of auditory feedback has been studied by different researchers and has started to be used in different applications [98–100]. In this study, the effect of the auditory feedback on the motor performance of the individuals was inspected in a virtual scene. The aim of this study was to explore the effects of the different C frequencies on human motor performance with the manual operations in the virtual reality environment.

In the last experiment of chapter 2, an experiment with the "NoTouch" system is performed to understand the positive effect of the auditory feedback. In this experiment, the main objective was to understand in which extent multisensory feedback improves subjects time and precision results. For this purpose, eight different sound frequency error feedbacks were played to subjects while they were performing the "NoTouch" experiment (explained in the materials and methods of this chapter). Their time and precision results were compared to their results when only the color feedback was provided.

Materials and Methods

Subjects

Eighteen subjects (ten female and four left-handed male) ranging in ages between 20 and 32 (average = 27.94) participated in this study. None had any experience in VR and image-guided activities such as laparoscopic surgery training or other. Before starting the experiments, each subject's index fingertip width was measured as an average of 1.67 cm with the maximum of 1.9 cm. To be able to follow the objects in the virtual reality, the minimum distance between the shoulder and the fingertip was calculated as 40 cm. Before starting the experiments, each subject's shoulder to fingertip distance was measured and the minimum distance was 64 cm. All subjects were normally hearing.

Procedure

In the last experiment of the second chapter, the "NoTouch" System was used with 8 different sound feedbacks. Each feedback was designed according to the 88-key piano keyboard's fundamental C frequencies. These frequencies and their scientific names are given in Table 4. These frequencies are converted to electronical sound by using equation 8.

$Sound = Asin(2\pi ft)$	(8)

In equation 8, A is the amplitude of the sound, f is the frequency and t is the duration of the sound. For this study, A was selected as 1, t was 2.5 seconds and f values were the frequencies shown in Table 4.

During the experiments, whenever an error occurred in 'Horizontal', 'Vertical' and 'Torus', a color feedback was provided to the subject for a visual feedback in the previous studies of the second chapter. In this study with the visual feedback, whenever an error occurred, these sounds were played to the subjects as the auditory feedback through a "Liberty Black" headphone. The sound output of the computer was at %30 so not to disturb subjects during the experiments which was about 70dB. This measurement was done with a Galaxy S6 phone and the SoundMeter application,

which was also approved by Kardous and Shaw [233] study. Before starting the experiments, each subject listened to each sound feedback and it was assured that participants had normal hearing and they were able to hear the sounds and move comfortably in the VR environment.

Table 4 – Frequencies and their scientific names used as auditory feedback

Scientific Name	**Frequency**
C8 Eighth Octave	4186.01 Hz
C7 Double High C	2093 Hz
C6 Soprano C	1046.5 Hz
C5 Tenor C	523.251 Hz
C4 Middle C	261.63 Hz
C3	130.18 Hz
C2 Deep C	65.41 Hz
C1 Pedal C	32.70 Hz

Cartesian Design Plan and Data Generation

Experimental design

Each experiment consisted of 10 successive trial sets per experimental condition for 18 subjects (P_{18}) and there were 108 experimental conditions: each subject followed 'Vertical', 'Horizontal' and 'Torus' in nine different sound feedbacks (S_9: No sound (benchmark condition), C1, C2, C3, C4, C5, C6, C7, C8), with three conditions of object parts (OP_3: 'Vertical', 'Horizontal' and 'Torus), with two conditions of handedness (H_2: dominant-hand and their non-dominant hand) and with two conditions of finger movements direction for each individual object part (D_2: up to down-down to up for 'Vertical', left to right-right to left for 'Horizontal' and clockwise and counterclockwise for 'Torus'. The order of auditory feedback condition was counterbalanced between subjects and structures to avoid specific habituation effects. For the same reason, the order of the handedness and direction of finger movement conditions were also counterbalanced between subjects. Each subject performed 1080 trials. In total 19440

trials were performed. The Cartesian design plan of the experiment can be presented as S_9 x OP_3 x D_2 x H_2 x P_{18} x 10 trial sets.

Data generation

The data recorded from each of the subjects were analyzed as a function of the different experimental conditions, for each of the four dependent variables (‘time’, ‘average number of finger outs’, ‘motor performance index’ and ‘average accumulated distance away from the object surface’).

Because of different movement directions, it was not possible to perform a full-factorial ANOVA including all three objects parts and all movement directions. For this reason, three three-way ANOVA was performed for each object part, separately for each dependent variable: ‘time’, ‘average number of finger outs’, ‘motor performance index’ and ‘average accumulated distance away from the object’ dependent variables. S_9 x D_2 x H_2 x P_{18} Cartesian design plan was used with average of ten repeated trial sets for each combination of conditions within a session, yielding a total of 648 experimental observations for each Object part (OP_3.), ‘Horizontal’, Vertical and ‘Torus’ for each ‘time’, ‘average number of finger outs’, ‘motor performance index’ and ‘average accumulated distance away from the object’.

In detailed sound feedback analysis, the movement direction condition was not included in the data analysis to have a full factorial analysis and a three-way ANAVO performed with a S_9 x S_3 x H_2 x P_{18} *x 10 trials* Cartesian design plan, yielding a total of 19440 data points including the movement direction condition for each dependent variable: ‘time’, ‘average number of finger outs’, ‘motor performance index’ and ‘average accumulated distance away from the object’.

Results

‘Time’ ANOVA results on ‘Horizontal’, ‘Vertical’ and ‘Torus’ object parts

Object parts three-way ANOVA ‘time’ results are shown in Annex 2-Figure 41 for ‘Horizontal’, in Annex 2-Figure 42 for ‘Vertical’ and in Annex 2-Figure 43 for ‘Torus’.

ANOVA results showed that there were significant differences in sound feedback ($F(8,647) = 2.09$; $p<0.05$) and handedness ($F(1,647) = 8.61$; $p<0.01$) for 'Torus'. Means and SEMs are shown in Annex 4-Table 63 and Figure 100.

According to these results, subjects were faster with C4 frequency and slower with the no-sound feedback. Furthermore, subjects were faster with their dominant hand.

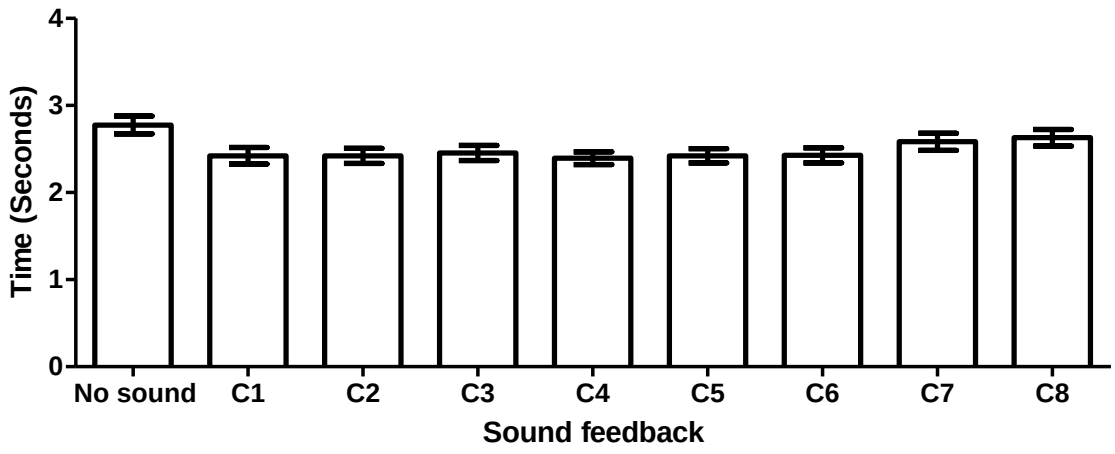

Figure 100 – Sound feedback results on 'time' on 'Torus'.

'Average number of finger outs' ANOVA results on 'Horizontal', 'Vertical' and 'Torus' object parts

Object parts three-way ANOVA 'average number of finger outs' results are shown in Annex 2-Figure 44 for 'Horizontal', in Annex 2-Figure 45 for 'Vertical' and in Annex 2-Figure 46 for 'Torus'.

ANOVA results showed that there were significant differences on sound feedback ($F(8,647) = 2.61$; $p<0.01$), handedness ($F(1,647) = 9.81$; $p<0.01$) and movement direction ($F(1,647) = 6.26$; $p<0.05$) for 'Vertical'. Furthermore, movement direction ($F(1,647) = 15.78$; $p<0.001$) and handedness and movement direction interaction ($F(1,647) = 4.34$; $p<0.05$) were significantly different for 'Horizontal'. Means and SEMs are shown in Annex 4-Table 64, Annex 4-Table 65 and Figure 101 for 'Horizontal' and in Annex 4-Table 66 and Figure 102 for 'Vertical'.

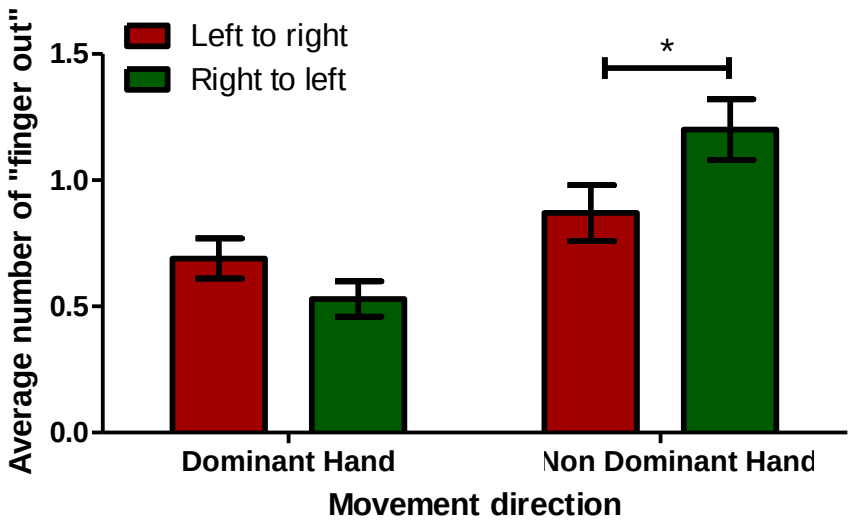

Figure 101 – Movement direction and handedness interaction on 'Horizontal' for 'average number of finger outs' dependent variable

Results of Annex 4-Table 64, Annex 4-Table 65 and Figure 101 show that subjects were more precise with left-to-right movements and they were more precise with their left-to-right movement compared to the right-to-left movements with their non-dominant hand in 'Horizontal'.

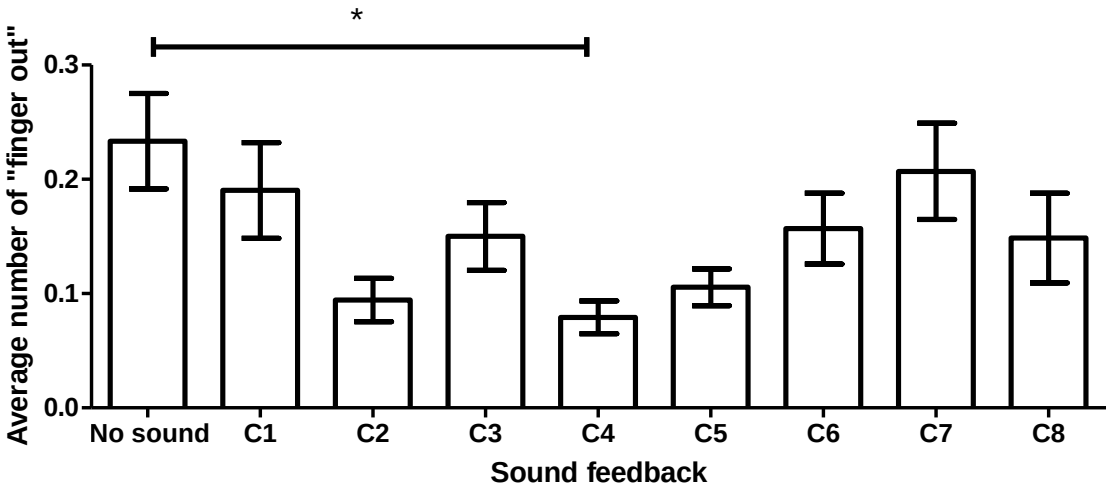

Figure 102 – Sound feedback results on 'average number of finger outs' on 'Vertical'.

Results on Figure 102 and Annex 4-Table 66 show that subjects were more precise in C4 sound compared to other sound feedbacks and they were more precise with their dominant hand and bottom to up movement.

‘Motor performance index’ ANOVA results on ‘Horizontal’, ‘Vertical’ and ‘Torus’ object parts

Object parts three-way ANOVA ‘motor performance index’ results are shown in Annex 2-Figure 47 for ‘Horizontal’, in Annex 2-Figure 48 for ‘Vertical’ and in Annex 2-Figure 49 for ‘Torus’.

ANOVA results showed that there were significant differences in sound feedback ($F(8,647) = 1.97$; $p<0.05$), handedness ($F(1,647) = 19.36$; $p<0.0001$) and movement direction ($F(1,647) = 12.79$; $p<0.001$) for ‘Vertical’. Besides, movement direction condition ($F(1,647) = 12.79$; $p<0.001$) and the interaction between handedness and movement direction ($F(1,647) = 9.84$; $p<0.01$) were significantly different for ‘Horizontal’. Means and SEMs are shown in Annex 4-Table 66 and Figure 103 for ‘Vertical’ and in Annex 4-Table 68, Annex 4-Table 69 and Figure 104 for ‘Horizontal’.

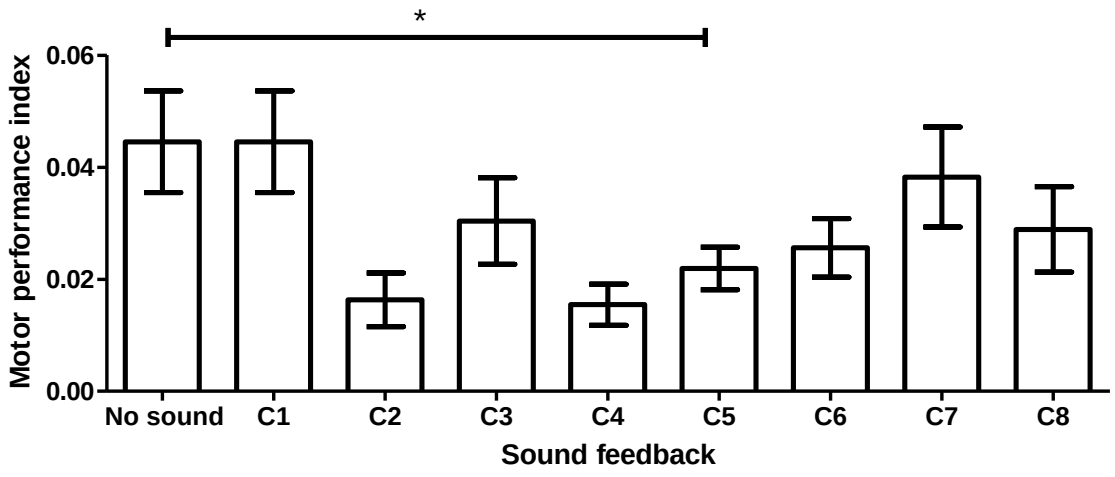

Figure 103 – Sound feedback results on ‘motor performance index’ dependent variable

Results on Annex 4-Table 68, Figure 103, and Annex 4-Table 68 show that subjects were more precise in C4 sound compared to sound feedback in 'Vertical' and on Annex 4-Table 69 and Figure 104 show that they were more precise with their left-to-right movement compared to the right-to-left movements with their non-dominant hand in 'Horizontal'.

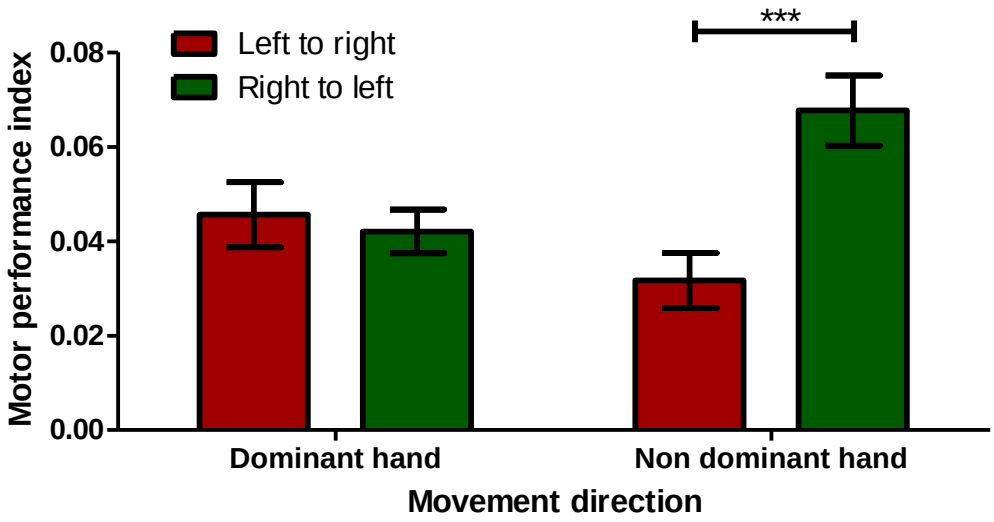

Figure 104 – Movement direction and handedness interaction on 'Horizontal' for 'motor performance index' dependent variable

'Average accumulated distance away from the object surface' ANOVA results on 'Horizontal', 'Vertical' and 'Torus' object parts

Object parts three-way ANOVA 'average accumulated distance away from the object surface' results are shown in Annex 2-Figure 50 for 'Horizontal', in Annex 2-Figure 51 for 'Vertical' and in Annex 2-Figure 52 for 'Torus'.

ANOVA results showed that there were significant differences in sound feedback ($F(8,647) = 2.54$; $p<0.01$), handedness ($F(1,647) = 11.12$; $p<0.0001$) and movement direction ($F(1,647) = 8.09$; $p<0.01$) for 'Vertical'. Means and SEMs are shown in Annex 4-Table 70 and Figure 105 for 'Vertical'.

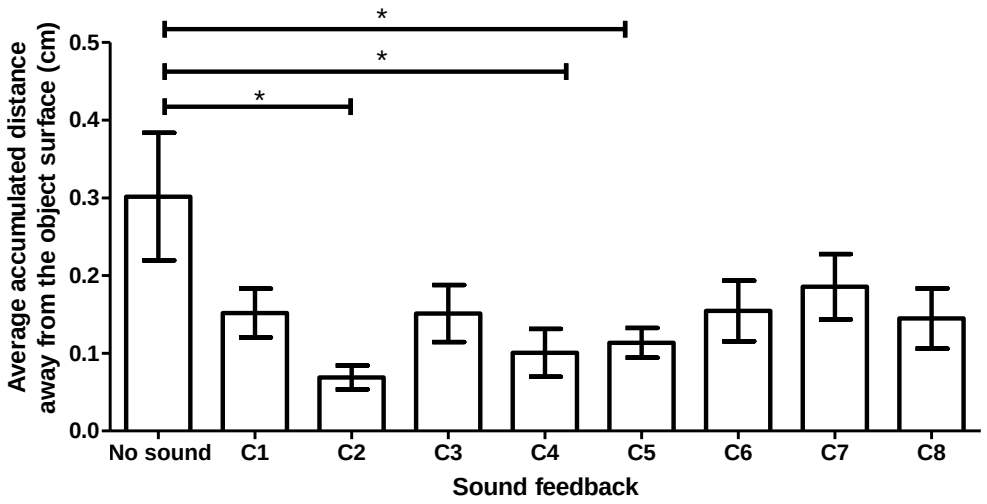

Figure 105 – Sound feedback results on 'average accumulated distance away from the object surface' dependent variable

The results in Annex 4-Table 70 and Figure 105 show that subjects were more precise in C4 sound compared to sound feedback in 'Vertical' and they were more precise with their dominant hand and bottom to up movement.

Detailed ANOVA results on the sound feedback, handedness and object parts

Detailed three-way ANOVA results are shown in Annex 2-Figure 53 for 'time', in Annex 2-Figure 54 for 'average number of finger outs', in Annex 2-Figure 55 for 'motor performance index' and in Annex 2-Figure 56 for 'average accumulated distance away from the object surface'. These results are shown in Annex 4-Table 71, Figure 106, Figure 107, Figure 108, Figure 109, and Figure 110.

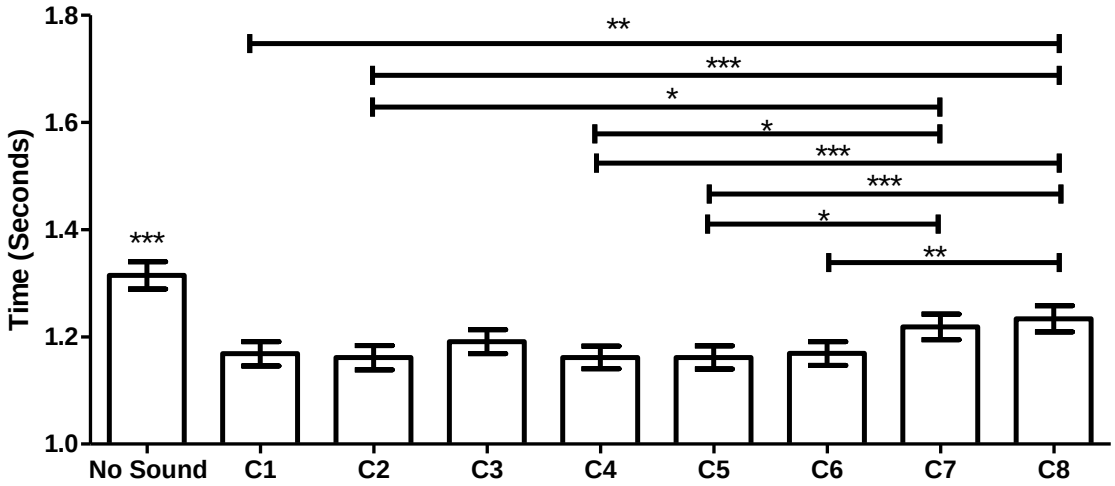

Figure 106 – Sound feedback results on ‘time’ dependent variable for raw data

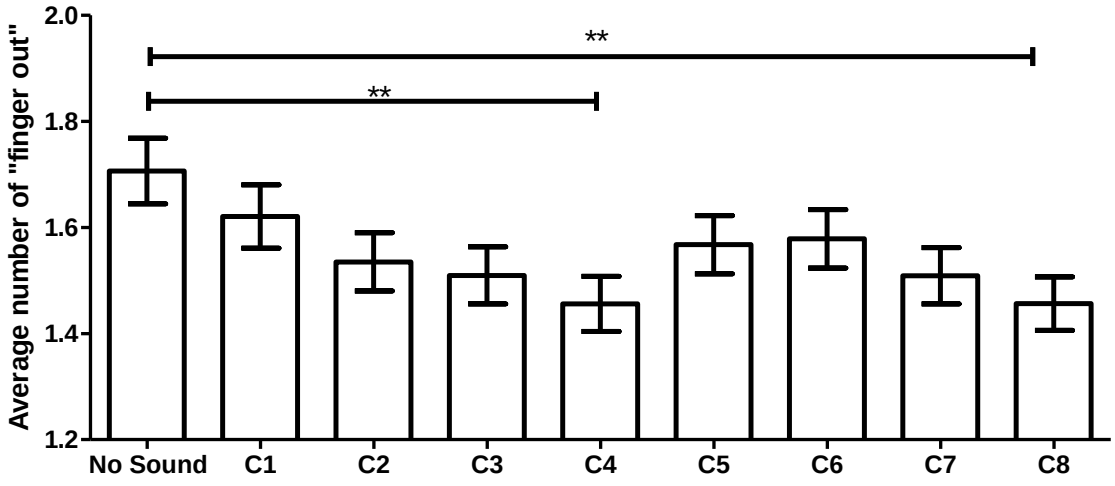

Figure 107 – Sound feedback results on ‘average number of finger outs’ dependent variable for raw data

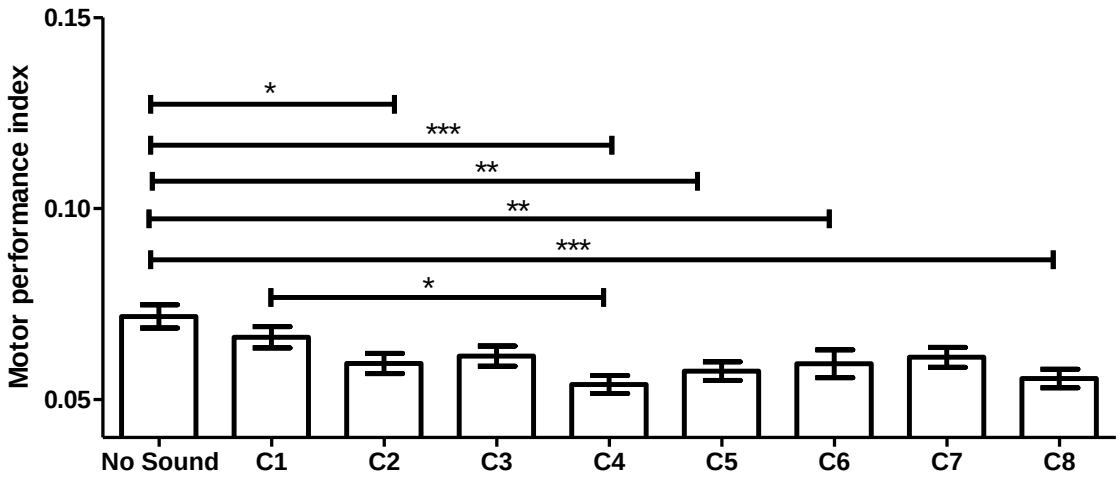

Figure 108 – Sound feedback results on 'motor performance index' dependent variable for raw data

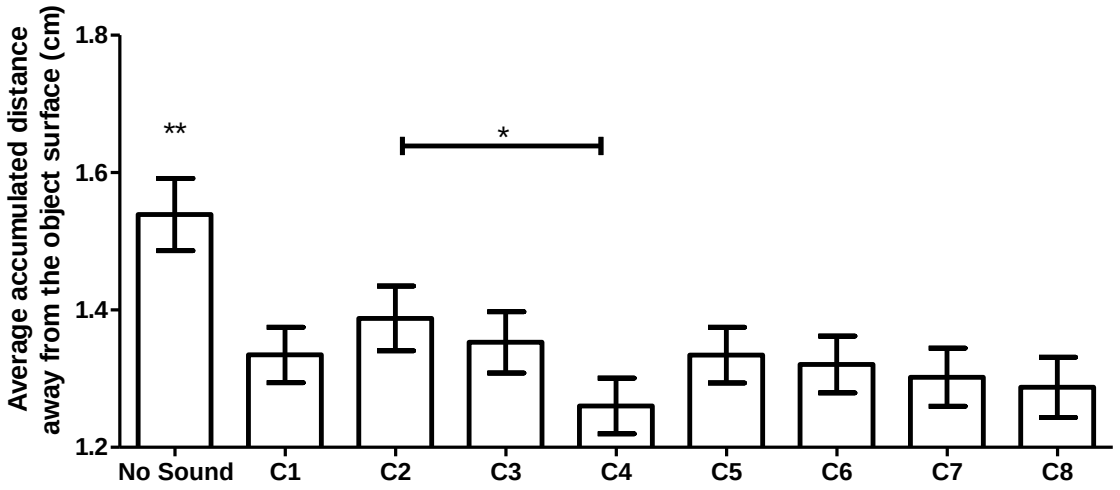

Figure 109 – Sound feedback results on 'average accumulated distance away from the object surface' dependent variable for raw data

According to results of Annex 4-Table 71, Figure 106, Figure 107, Figure 108, and Figure 109, subjects were faster and more precise with C4 sound when compared to other sounds. When the frequency increased to C7 and C8, subjects made fewer mistakes, but at the same time they were getting slower. When no sound feedback

was provided, subjects were slower and less precise compared to the auditory feedback. Furthermore, subjects were faster and more precise with their dominant hand. Annex 4-Table 71 and Figure 110 show that subjects were faster and more precise in 'Vertical' and were slower and less precise in 'Torus' among all object parts.

Handedness and movement direction results for left-handed subjects

In the first and second studies of this chapter, it was found that subjects were more precise with left-to-right movement. In this study, the same result was found: subjects were more precise with their dominant hand in the left-to-right movements in 'Horizontal'. To explore these further, a detailed analysis was done for the left-handed subjects of this experiments. Their results from the experiment were used in a two-way ANOVA for handedness (H_2) and movement direction (D_2) including all nine-sound feedback of four left-handed subjects for ten trials only for 'Horizontal' 'time', 'number of finger outs', 'motor performance index' and 'average accumulated distance away from the object surface' dependent variables. The Cartesian experimental plan can be presented as following: H_2 x D_2 x 9 sound feedback x 4 subjects x 10 trials. In total, 1440 x 4 data points were used for the analyses of 'time', 'number of finger outs', 'motor performance index' and 'average accumulated distance away from the object surface' dependent variables.

The results of this analysis are shown in Annex 2-Figure 57 for 'time', Annex 2-Figure 58 for 'number of finger outs', Annex 2-Figure 59 for 'motor performance index' and Annex 2-Figure 60 for 'average accumulated distance away from the object surface'. The results revealed that there were significant differences in handedness for 'number of finger outs' ($F(1,1439)=19.99$; $p<0.001$) and 'motor performance index' ($F(1,1439)=15.08$; $p<0.001$), and in movement direction for handedness for 'number of finger outs' ($F(1,1439)=4.62$; $p<0.001$), 'motor performance index' ($F(1,1439)=22.08$; $p<0.001$) and 'average accumulated distance away from the object surface' ($F(1,1439)=20.41$; $p<0.001$). Furthermore, handedness and movement direction interaction was significantly different for 'number of finger outs' ($F(1,1439)=7.88$; $p<0.01$) and ' motor performance index' ($F(1,1439)=6.37$; $p<0.05$). The results of means and SEMs are given in the Annex 4-Table 72, Annex 4-Table 73and Figure 111.

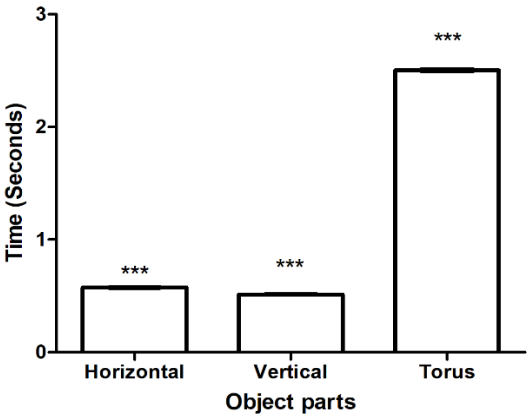

(a)

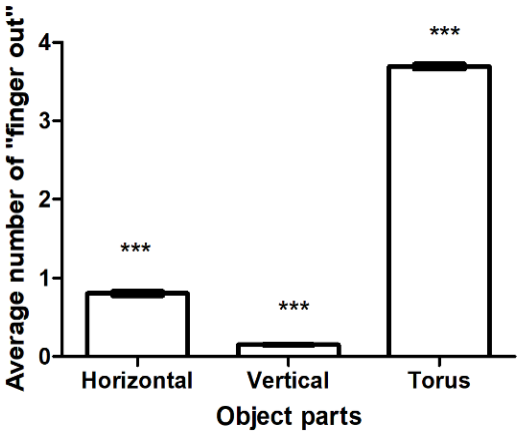

(b)

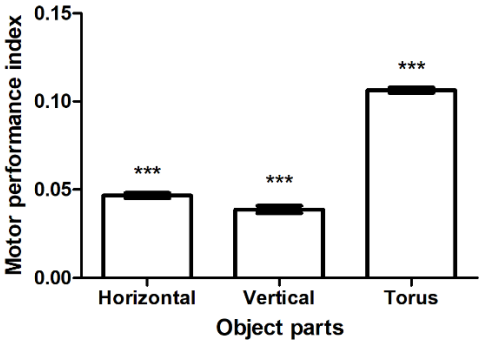

(c)

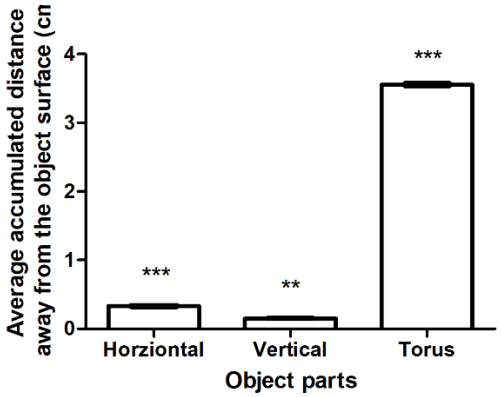

(d)

Figure 110 – Object part results for (a) 'time', (b) 'average number of finger outs', (c) 'motor performance index' (d) 'average accumulated distance away from the object surface' dependent variables for raw data.

According to results of Annex 4-Table 72, left-handed subjects were less precise with their dominant hand and right-to-left movements. The results of Annex 4-Table 73 and Figure 111 show that left-handed subjects were less precise with their dominant hand in the right-to-left manual hand operations.

Discussion

In the last study of this chapter, the effects of eight different sound frequencies on human motor performance and how they affect the time and precision of individual's movement were studied.

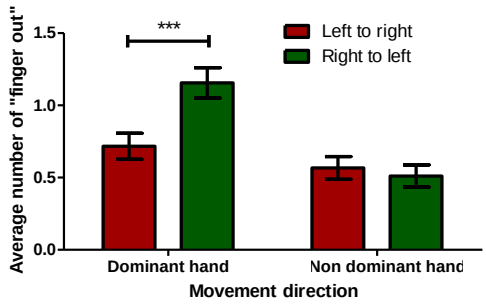

(a)

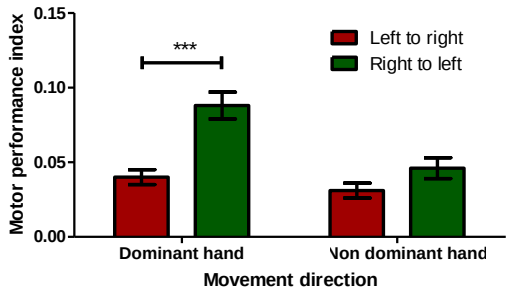

(b)

Figure 111 – Movement direction and handedness interaction on 'Horizontal' for (a) 'average number of finger out' and (b) 'motor performance index' dependent variables for left-handed subjects.

According to detailed results of auditory and visual feedback, subjects were faster and more precise when an auditory feedback was used as a source of additional information from the environment. Previous research on the multi-sensory feedback showed similar results compared to uni-modal signals [234]. Between these 8 different sounds, subjects were faster and more precise, especially when hearing the C4 sound. The C4 sound is known as the Middle C, which is 261.63 Hz. This note also lies in the middle of the piano keyboard and most songs start around this frequency.

The sound feedback used in this experiment did not have any frequency, speed, rhythm or melodic structure variations, but as auditory stimuli, subjects were often used to hearing middle-frequency sounds in their daily lives. This increased subjects' awareness to these sound feedbacks, which leads to faster and more precise movements. A further research on the auditory and multisensory feedback (audiovisual) with altering spectral and temporal characteristics of the sound can provide more information about this study.

Previous research on the human auditory cortex showed that different sounds evoke the human brain [235,236] and a selection of movements are related to these sensory stimuli [237–239]. High frequency sounds usually correspond to 'fast' and 'loud' actions such as a baby crying or excitement, which is correlated to the faster movements [228,240]. On the other hand, in time and precision results of this study, subjects got slower but more precise during higher (C7 and C8) frequencies. In this experiment

here, subjects took their time being more precise so not to cause an auditory error feedback in higher frequencies, which affected their movement time that created a time-precision trade-off.

In the individual object results for ‘Horizontal’, ‘Vertical’ and ‘Torus’, it was found that subjects were faster and significantly more precise with ‘Vertical’ for all three precision dependent variables. Previous studies on ”Steering Law” [85,241] and the second study of this chapter show the similar results and several explanations can be found in the literature to explain these results. For example, while Young et al. [242] study explains these results due to ‘direct mapping between hand and pointer’, Teather and Stuerzlinger [243] relate their results to muscle groups used during the movement of the subjects. Another explanation can be attributed to the gravity force; while the subjects move in ‘Vertical’, gravity has a constant parallel effect on the subject’s hand movement direction. This vertical additional force with the same direction as the movement direction accelerates the task execution duration and helps to stabilize the movement. A similar result was also observed in Murata and Iwase [76], study for upward movements. In ‘Horizontal’, this force is perpendicular to hand movement direction and disturbs the trajectory. Similarly, in ’Torus’, this force is not constant for the direction of the hand movement.

In the individual virtual object results, subjects were significantly more precise in C4 frequency compared to no sound and other sound feedbacks, especially in ‘Vertical’. These complex results between the motor performance of the subjects and the frequencies need further and detailed research especially in the field of neuropsychology, related to the sensory motor-cross talk between the auditory and motor cortex.

Complex interactions between handedness and movement direction were also further investigated with this study. In the previous studies, subjects were all right-handed and results were analyzed according to the right hand dominant subjects. In this experiment, four left-handed subjects participated, and their results were analyzed separately for handedness and movement direction interaction. According to the left-handed subject results, participants were more precise with left-to-right movements and they were less precise with their dominant hand. In further interaction analyses,

left-handed subjects were less precise with their dominant hand in the right-to-left movements compared to the left-to-right movements. In the comparison between left-handed subject results and all of the subject results, it was observed that subjects were more precise with their left-to-right manual operations with their left-hand. The experiment results can be further investigated with the more left-handed subjects to understand the complex interactions between handedness and movement direction.

In conclusion, subjects were faster and more precise with auditory and visual feedback compared to only visual feedback provided to the subjects. To optimize the subjects' performance on time and precision, middle frequency tones should be used. An unpleasant auditory feedback can create time-and-precision tradeoffs. Moreover, multi-sensory cross-talk between human visual cortex, auditory cortex, and motor cortex should be inspected further under the light of these findings.

Conclusions

In this chapter, VR with its different features was studied with human computer interactions. In the first study, different simulation environments were compared, and it was shown that individuals were faster and more precise using their natural view and direct touch. Furthermore, there was no significant major differences between VR, AR and MR in terms of time and precision. In the second study, experiments were performed to understand the effects of the size and width variations of virtual objects in VR and proved the “Steering law” in VR with the “NoTouch” system. In the third study, the ipsilateral and contralateral manual hand movement performance in depth in VR environment was explored. With this experiment, the optimal object position was found to place a target in VR according to the active hand. In the fourth study, an experiment combining the second and third studies of this chapter was performed and the effects of object complexity and size on time and precision of the individuals was studied. According to this study, object complexity must be considered as a dependent variable for the individual assessment. In the last study, experiments with auditory feedback in VR were performed and the best frequency to obtain the optimal motor performance results was found to be the middle tones of a piano keyboard.

Apart from these results, experiments revealed the importance of precision measurement and assessment in VR environments. Precision dependent variables revealed similar results for the third, fourth and fifth study. However, in the first and second studies, each precision variable showed different characteristics. In the detailed interaction results of this chapter, significant interaction results related to the handedness and movement direction dependent variables were found. These complex results show that, not only one, but several precision methods should be used to evaluate the subjects in VR environments and assessment feedbacks should be given according to the task design.

In short, these results [68–70] would be helpful for designers and engineers to develop better surgical simulation applications using optimized human-computer interactions and eye-hand coordination in virtual environments.

Chapter 3
Grip-Force Analysis in Tele-Manipulated Operations

Introduction

In the third chapter of the thesis, hand grip force analysis is performed on human manual operations. In the first two chapters, visual and tactile feedbacks used in medical training applications were analyzed together with the motor performance measurements of the individuals. In the last chapter of the thesis, the research is expanded into a minimally invasive surgical robot system, STRAS. To be able to measure the grip force variations on STRAS, a special glove was designed to collect data. The aim of this glove was to record grip-force signals from different *loci* of measurement in the palm, the fingers, and the fingertips of the dominant and non-dominant hand.

When the surgeon loses haptic information caused by reduced-access conditions in robot-assisted surgery, it may compromise the safety of the procedure. This limitation must be overcome through practice and, in particular, surgical simulation training for specific hand-tool interactions. Using biosensors for the measurement of grip force variations during surgical simulation training with hand-tool interaction provides valuable insight into surgical skill evolution. Biosensor systems for measuring hand and finger grip force intensities need to be calibrated for the specific purpose as they are to serve in the context of surgical tool manipulation with sensory feed-back interaction. Using a tool effectively requires sufficient grip force to prevent it from dropping or slipping and, at the same time, avoiding excessive force that could damage the tool or the tissue it is applied to. Visually guided somatosensory learning is particularly important to the fine-tuning of fingertip forces applied to specific shapes of specific objects or tools.

In the last chapter of the thesis, task execution time and grip forces variations are analyzed by using a biosensor system on STRAS robot-assisted surgical system with a novice user and an expert user [101].

Materials and Methods

Handedness

Like previous chapters, handedness was assessed using the Edinburgh inventory for handedness designed by [107] to confirm that they were all true right-handers.

Research ethics

The study was conducted in conformity with the Helsinki Declaration relative to scientific experiments on human individuals with the full approval of the ethics board of the corresponding author's host institution (CNRS). All participants were volunteers and provided written informed consent. Their identity is not revealed.

Experimental platform

A pair of special gloves were designed for the third chapter to measure applied hand grip force. Force Sensitive Resistors (FSR) are used in the glove design to measure the force applied on the tools in twelve different *loci* of the inner left and right hands.

The glove designed for the experiment contained twelve flexible force sensors, which are shown in Figure 112 (a) and (b). The exact positions of the different force sensitive sensors are given in Table 5. Two layered cloth gloves were used and FSRs were inserted between these two layers. Thus, the FSRs did not interact with the subjects' skin and generated a more comfortable feel for manipulating the handles. The FSRs were inserted into the glove with needle and thread. Each FSR was sewn around the surface of the conductor (active area). The gussets of the sensors were placed on top. The two different types of sensors had a six 12.7mm diameter for the palm and finger tips, and a 5mm diameter for the other finger regions. Each FSR was soldered to a pull-down resistor to create a voltage divider (9).

(a)

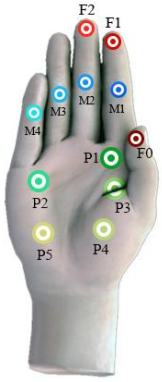

(b)

Figure 112 – Glove hardware design: (a) locations of the Force Sensitive Sensors and (b) locations of the Force Sensitive Sensors on the glove (© 2017 IEEE)

Table 5 – Force Sensitive Resistor (FSR) positions on hand (© 2017 IEEE)

Sensor	Region	Exact Position
F0	Thumb	Distal Phalanges
F1	Index	Distal Phalanges
F2	Middle	Distal Phalanges
M1	Index	Middle Phalanges
M2	Middle	Middle Phalanges
M3	Ring	Middle Phalanges
M4	Pinky	Middle Phalanges
P1	Palm	Head Metacarpal
P2	Palm	Head Metacarpal
P3	Palm	Shaft Metacarpal
P4	Palm	Base Metacarpal
P5	Palm	Base Metacarpal

$$V_{out} = \frac{R_{PD}V_{3.3}}{(R_{PD} + R_{FSR})}$$	(9)

In (9) R_{PD} is the resistance of the pull-down resistor and R_{FSR} is the FSR resistance. $V_{3.3}$ is the supply voltage and the V_{out} is the value read by the analog input. Voltages were transformed into Newton by (10):

$$F_{FSR} = \frac{V_{out}}{(V_{3.3V} - V_{out})R_{PD}} x80$$	(10)

In equation (10), $V_{3.3V}$ represents 3.3V supply voltage and F_{FSR} is the Force of the FSR. This equation can be found in the FSR Integration Guide and Evaluation Catalog of the FSR manufacturer.

The general design of the glove's hardware is shown in Figure 113. Accordingly, 12 FSRs (shown as `sensor_n") are connected to an Arduino Micro with Analog communication. Regulated 3.3V was provided from the power source of the Arduino to the Sensors and the change in the voltage is measured by the Arduino. A 3.7V Li-Po battery was connected to the single cell Li-Po USB charger. This allowed charging and re-using the glove system without any cable driven connections. The battery voltage level was controlled during the research by the Arduino and shown to the user via the user interface.

The glove system was also connected to a Bluetooth circuit to enable wireless communication. The baud rate of the communication from glove to computer was 115200 bits-per-second (bps), and 9600 bps between Arduino and Bluetooth.

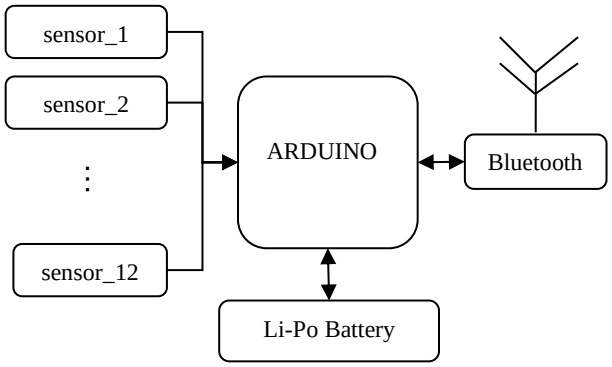

Figure 113 – Sensor glove hardware design chart (© 2017 IEEE)

Software design in experiments

The software of the glove was divided into two parts: one running the glove and one running the computer algorithm for data collection. Both gloves were sending data to the computer separately, and the software read and recorded the input values according to their headers.

The glove is designed to acquire analog voltages provided by the FSR every 20 milliseconds (50Hz). In every loop of the Arduino running software, input voltages were merged with time stamps and voltage levels. This data package was sent to the computer via Bluetooth, which was decoded by the computer software. The voltages were saved in a text file for each sensor, with their time stamps and identifications. Furthermore, the computer software monitored the voltage values received from the gloves via a user interface showing the battery level. If the battery level was below 3.4V, the system did not automatically shut down, but warned the user to change or charge the battery.

Study – Effects of Training Level and Handedness on Grip Force Intensity in a Robot-Controlled Surgical Environment

STRAS (Single access Transluminal Robotic Assistant for Surgeons) is a flexible robotic system based on the Anubis® platform of Karl Storz for application to intraluminal procedures. It consists of three cable-driven systems, one endoscope serving as guide and two inserted instruments. The flexible and bendable instruments have three degrees of freedom and can be teleoperated by a single user via two specially designed master interfaces. In this study, designed gloves which ergonomically fit to the master handles of the system are used to compare forces applied by one expert and one novice user during system-specific task execution.

Study Goal and Hypotheses

Flexible systems such as endoscopes are now used for performing complete minimally invasive surgical procedures, for instance in intraluminal operations. Many surgical platforms have been developed by companies and by laboratories to improve the capability of these flexible systems, for instance by providing additional Degrees of Freedom (DoFs) and triangulation configurations [244,245]. However, the high number of DoF to be controlled requires several surgeons to work together in a very cluttered environment. Robotics has been identified as a tool for improving the use of flexible systems in minimally invasive surgery [246]. This was the motivation to develop a telemanipulated robotic system for assisting surgeons in minimally invasive procedures [104]. This system is based on the Anubis® platform invented by Karl Storz. Previous studies on the STRAS were focused on the system architecture and the control theory of the application [104–106].

In minimally invasive teleoperation systems, surgeons need to operate master interfaces to manipulate the endoscope. Subjects need to master the system and its user interface to fully dominate the slave system because of the remote control and

the complexity of the design. Such expertise can only be reached by getting used to the control mechanism, by practicing in vivo or using robotic surgical systems [102]. Previous studies were more focused on the tool-tip pressure and tactile feedback than the force applied on the grab sticks [103]. The system used in this article is designed without force feedback and the control is therefore based on the visual feedback from the endoscope only.

Dynamic changes in cognitive hand and body schema representations take place especially after repeated tool use to manipulate a physical object [111,112], reflecting the process which highly trained surgeons go through in order to able to ultimately adapt to the visual and tactile constraints of laparoscopic interventions. Experts perform tool-mediated image-guided tasks significantly quicker than trainees, with significantly fewer tool movements, shorter tool paths, and fewer grasp attempts [120]. Also, an expert tends to focus attention mainly on target locations, while novices split their attention between trying to focus on the targets and, at the same time, trying to track the surgical tools. This reflects a common strategy for controlling goal-directed hand movements in non-trained operators [151] and may considerably affect task execution times and the force applied to the control sticks.

Materials and Methods

Subjects

One expert user, who was practicing with the system since its construction and one novice user who had never used the system and had no knowledge on a similar surgical system participated in the experiments. Before the experiment started, the novice user was made familiar with the buttons and the running of the system. The expert user was left-handed and the novice user was right-handed.

STRAS Experimental platform

Slave robotic system

The slave robotic system is built on the Anubis® platform of Karl Storz. This system consists of three flexible, cable-driven sub-systems (for more information, [104]): one

main endoscope and two lateral flexible instruments. The endoscope carries the endoscopic camera at its tip and has two lateral channels which are deviated from the main direction by two flaps at the distal extremity. The instruments have bending extremities (one direction) and can be inserted inside the channels of the endoscope.

This system has a tree-like architecture and the motions of the endoscope act also upon the position and orientation of the instruments. Two kinds of instruments are available: electrical instruments and mechanical instruments. The aim is to teleoperate the robot once the system is initially brought to the operation area manually. Overall, the slave system has 10 motorized DoF. The main endoscope, which is equipped with the endoscopic camera can be bended in two orthogonal directions. This allows moving the endoscopic view respectively from left to right and from up to down, as well as forward / backward. Each instrument has three DoF: translation (t_z) and rotation (θ_z) in the endoscope channel, and deflection of the active extremity (angle β). The deflection is actuated by cables running through the instrument body from the proximal part up to the distal end. Moreover, the mechanical instruments can be opened and closed.

Master/Slave control

The slave robot is controlled at the joint level only by a position loop running at 1000 Hz on a central controller. The master side consists of two specially designed interfaces. These interfaces have 3 DoFs: they can translate for controlling instrument insertion, rotate around a horizontal axis for controlling instrument rotation, and rotate around a last axis (moving with the previous DoF) for controlling instrument bending (Figure 114). Since there is no force measurement on the slave side, no force effects are reproduced on the master side.

The master interfaces have a hemispheric workspace spanned by the two rotations, which can be moved by the first translation, hence creating a cylindrical workspace.

A high-level controller running on a computer under a real-time Linux OS communicates with the master interfaces and provides reference joint positions to the slave central controller (Figure 115).

Figure 114 – Wireless gloves were used on STRAS during the task execution (© 2017 IEEE)

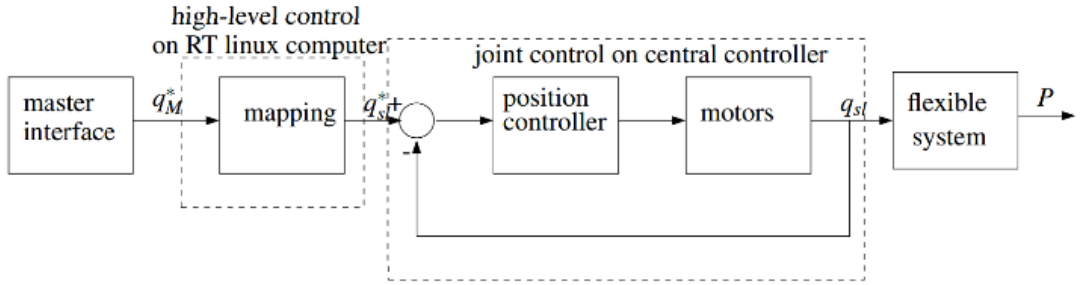

Figure 115 – Master/Slave instrument control chart (© 2017 IEEE)

Procedure

For the study, a simple pick-and-place task (Figure 116) was used. During the research, only the motions of the instruments were used (the endoscope, remained still). This study demonstrated that a single user could perform a complex task involving the whole slave system.

The experiment started with the right or left (changing according to the experimentally defined order) gripper being pulled back (Figure 116 (a)). The user had to approach the object with the distal tool extremity by using the sticks of the master system (Figure 116 (b)). Then, the user had to grip the object and to position it on top of the target box when the distal extremity is in the correct position (Figure 116 (c)). To finish the experiment, the user needed to release the object from the gripper (Figure 116 (d)).

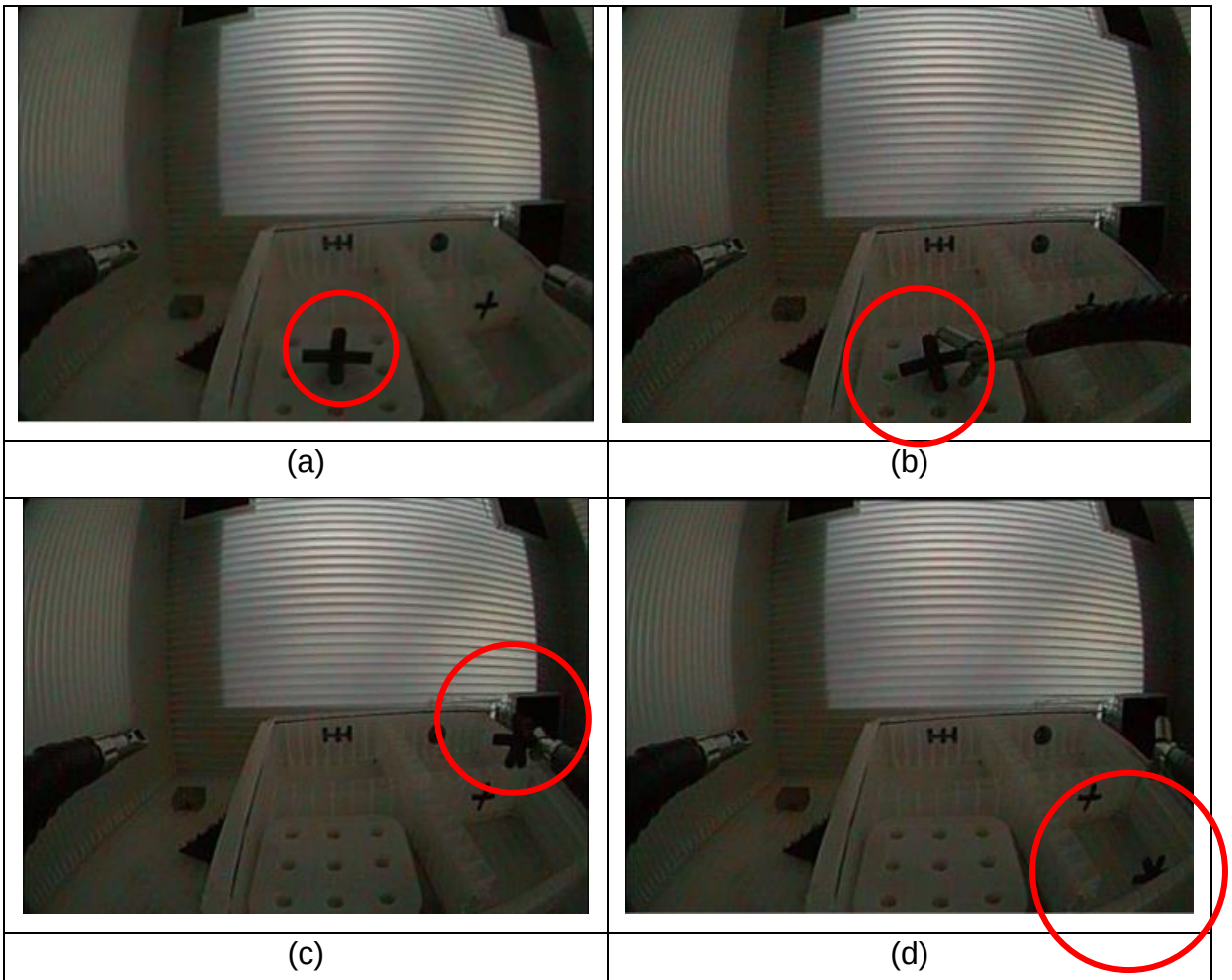

(a) (b) (c) (d)

Figure 116 – Pick-and-place task used in the experiment with the right-hand instrument (a) initial condition, (b) grabbing object, (c) positioning gripper on target box, (d) dropping the object at the end of the experiment (© 2017 IEEE).

Cartesian Design Plan and Data Generation

Experimental design

Experiment consisted of 10 successive trial sets per experimental condition for two subjects (S_2) and they performed the pick-and-place task with their dominant and dominant hand (H_2) which yields 20 trials per subject. In total, 40 trials were performed. The Cartesian design plan of the experiment can be presented as S_2 x H_2 x 10 trial sets.

Data generation

The data recorded from each of the subjects were analyzed as a ‘time’ and for each 12 FSRs (FSR_{12}). Data collection was started when the subject moved the handles of the STRAS (Figure 116 (c)) and stopped when the subject pushed the release button of the gripper from the master system (Figure 116 (d)). For ‘time’ analysis, the number of collected data rows were counted and multiplied with the data acquisition frequency (50 Hz or 20 milliseconds) for each individual trial. The Cartesian design plan can be presented as S_2 x H_2 x 10 trials for ‘time’ analysis for two-way ANOVA. In the meantime, each data raw had 12 FSR data and each of these 12 FSR’s data was used for sensors data analysis. In the force results data analysis, the total number of applied forces during 10 consecutive trials are collected and a three-way ANOVA was performed over S_2 x H_2 x FSR_{12}. In the separate ANOVA analysis, 4 FSR are not used in further data analysis because of their near-zero results. Therefore, 8 FSR’s average collected force data was used in the data analysis in separate FSR ANOVA results with three-way ANOVA, S_2 x H_2 x FSR_8 for each 10 consecutive trials.

Results

‘Time’ results

‘Time’ results for the ANOVA are showed in Figure 117 and Annex 3-Figure 2. In the ANOVA analysis, subjects and their dominant hands were used as major factor levels and the dependent variable was ‘time’. Two-Way ANOVA results show that there is a significant difference between the novice and expert users ($F(1,39)=24.031$; $p<0.001$) and there is no significant difference between dominant and non-dominant hands ($F(1,39)=0.264$, NS). Based on these results, Figure 117 (a) shows the left hand execution times, Figure 117 (b) shows right hand execution times and Figure 117 (c) shows the total amount of time it took to complete the experiment for each session. These results also show similarities with previous researches such as [247]. Moreover, an interaction between the subject and the hand was found ($F(1,39) =43.47$; $p<0.05$) which indicates that both expert and novice user execution times depended on the hand they used (Figure 117 (d)). In the post-hoc test, there is a significant difference between the expert user and the novice user in the dominant hand, with unadjusted

p<0.001. According to cd), the novice user is slower with his dominant hand which indicates that, in this extremely constrained environment, the novice user was more hesitant in maneuvering (Batmaz et al [101] Table 2).

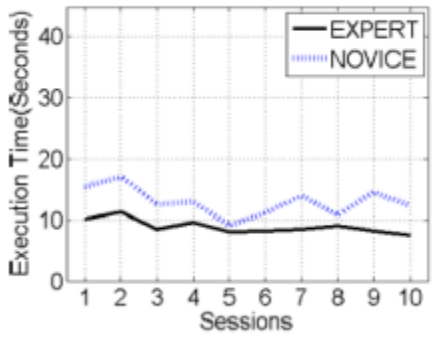

(a)

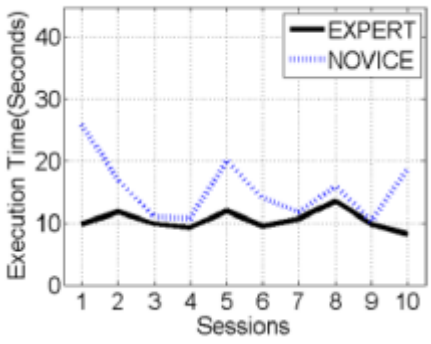

(b)

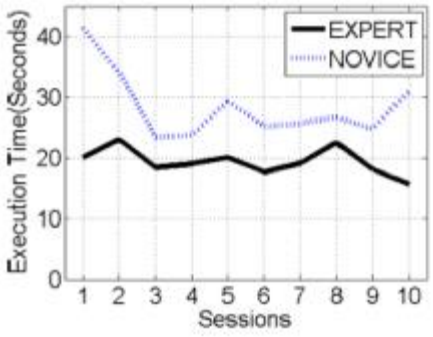

(c)

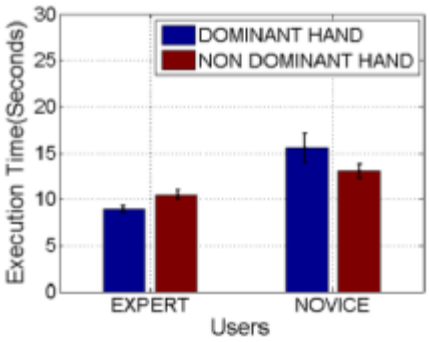

(d)

Figure 117 – ANOVA results on time (a) left hand (b) right hand (c) both hands and (d) time differences between users (© 2017 IEEE).

‘Force’ results

Total force of the subjects is measured as the sum of all forces applied during the ten sessions of the study. Even though gloves are designed to record the whole data during the stick use, users did not need to apply force to some points on particular FSRs. Total number of forces (in Newton) applied by each subject and each hand is given in Batmaz et al [101] Table 3 with excluding the first session of the novice with a further session.

According to Batmaz et al [101] Table 3, applied force by expert and novice users can change according to the handedness of the user. It is also shown that some sensors were not used specially during certain task maneuvers, such as M1. Also, handedness is a determining factor that can affect a particular applied force point. For instance, while the tasks were the same and symmetric for left and the right hands, P2, P4 and P5 force points were not used by the subjects. Furthermore, the One-Way Kruskal-Wallis ANOVA results show that the novice subject was grabbing the sticks significantly harder than the expert user ($H=5.117$; $p<0.024$), in Batmaz et al [101] Table 3. The novice subject, for example, applied a significantly higher total force on the F2 sensor during right hand manipulation of the device.

ANOVA analysis on the total force with the user ($F(1,47)=3.181$;NS), handedness ($F(1,47)=2.419$;NS) and sensor ($F(11,47)=1.191$;NS) major factors gives no significant results.

Separate FSR ANOVA results

By using results in Force Results section, F0, F1, F2 and M1 sensor values were subtracted from the evaluation. For the rest of the research, the average force from each session is used as a dependent variable to discriminate between users, handedness and FSRs.

These three-Way ANOVA (shown in Annex 3-Figure 3) results are summarized in Batmaz et al [101] Table 4, which shows the factor levels and their means and SEMS. Figure 6 shows more detailed results of the ANOVA analysis. Figure 118(a) indicates that the expert user applied a significantly less grip force ($F(1,319)=232.17$; $p<0.001$), and Figure 118 (b) shows that both users applied more force with their dominant right hands ($F(1,319)=142.03$; $p<0.001$). In further analysis in Figure 118 (d), an interaction between the user and hand factors are shown. This figure illustrates a similarity with Figure 117 (d). Moreover, different sensors were gripped with statistically different local forces ($F(7,319)=17.17$; $p<0.001$). For example, sensor M3 was gripped with the strongest, sensor P1 with the weakest force.

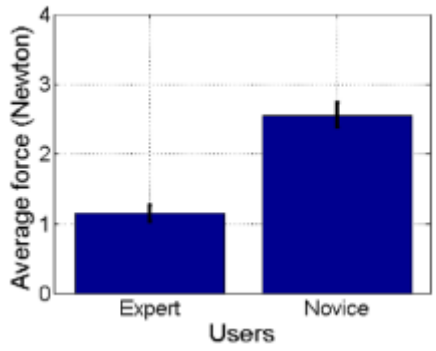

(a)

(b)

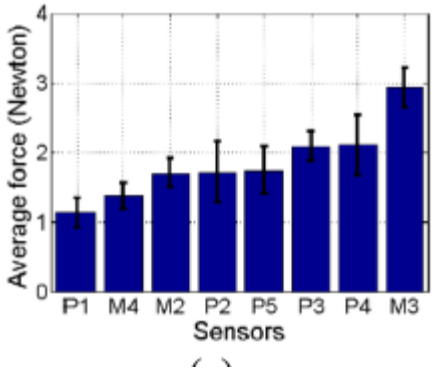

(c)

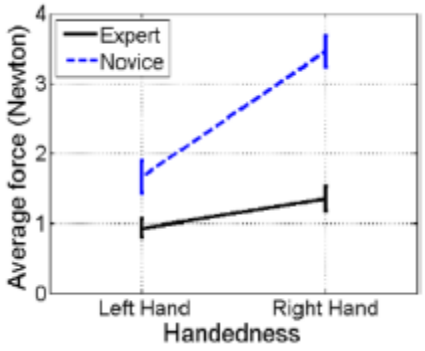

(d)

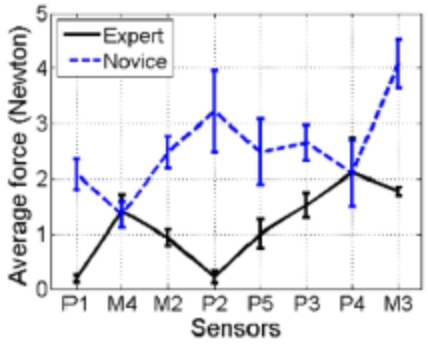

(e)

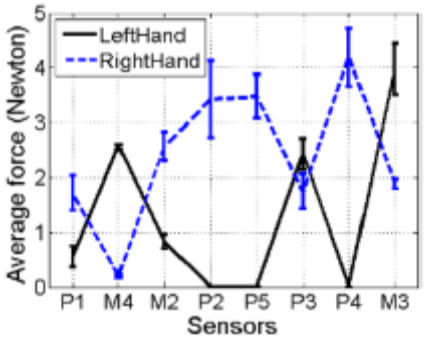

(f)

Figure 118– FSR ANOVA results (a) user differences, (b) handedness differences, (c) FSR differences, (d) user-hand differences, (e) user-sensor differences and (f) hand-sensor differences (© 2017 IEEE).

Another result of the 3 Way ANOVA analysis shows that there is a significant interaction between the user factor and the sensor factor ($F(7,319)=16.43;p<0.001$) conditions (Figure 118(e)). Accordingly, the expert user applied less force than the novice user to all sensors except for M4 and P4. This indicates that the novice operator does not control the forces applied on some of the points as well as the expert. Ergonomics can help to limit the force applied by users in general, but specific forces applied locally can only be optimized through training.

Figure 118 (f) indicates that there is a significant interaction between handedness and the sensors ($F(7,319)=95.98$; $p<0.001$). Users do not apply the same amount of force by their two hands on particular points. This result is also coherent with the data displayed in Batmaz et al [101] Table 3.

Conclusions

In the last chapter of the thesis, touch feedback was investigated during a surgical robot manipulation by a specially designed glove. The glove design was specially made for the handles of the STRAS robotic system to measure the grip force of the users. The sensors on the glove were placed at the specific locations with the tests on the STRAS by the help and feedback of the surgical robotic system users.

In this chapter, tactile grip force on the handles of the STRAS was investigated with a novice and an expert and how the expertise can variate the applied grip force on the handless of a robotic system was explored. As expected, it took longer for the novice to execute the task but more importantly, the novice and the expert were applying different amount of forces to the different regions of the hand. These specific forces applied locally to different regions of the hand can be optimized through training.

This experiment was a preliminary research on the applied grip forces of STRAS robot assisted surgical system. These results can be studied further with different experimental tasks, more subjects and more experimental groups.

This technology and the results of this chapter [101] could be effectively exploited in simulator training for image-guided interventions, and in training programs on robot-assisted surgical systems.

General Discussion

Technology and medicine are two inseparable fields these days. The research on medical applications to enhance the procedures with the help of different technologies is one of the most famous research topic in our era. Surgeons and engineers, software developers, physicists, chemists, etc. are working together to create faster and easier solutions for patients' medical treatment. While there are lots of research on technological support in the medical applications, this study highlights the importance of the human cognitive neuroscience in image guided surgical operations for novices. Even though there is an important scientific progress in robotics and engineering in medicine, the medical operations and surgeries are still performed by the surgeons, not yet by computers. This situation soon can change for basic operations and later for complex operations, but the current circumstances require judgments and decisions of a surgeon in the operation room. In this case, human cognitive neuroscience and its close relationship with medical technologies have to be studied, as technological developments create new sensorial challenges in which surgeons are not accustomed. If new technologies are affecting surgeons' perception and performance cannot be understood well, these developments can be a disadvantage in the operating room.

Another important outcome of these new technologies is their effect on the skills of surgeons. Apart from the conventional surgical skill training and learning, surgeons have to spend additional time and effort on their technological device skill training and learning. While research on technological device development is a large field of study, skill training process and the effects of this technology on the surgeons' motor performance are still not well studied. If the effects of these new technological devices on surgeons' performance and perception are explored, it would be possible to create optimal training systems to assess surgeons. This would help to train surgeons efficiently and increase their success rate.

In short, this thesis has been written within the two main frames of the surgical environment: to which extent does the human perceptual system adapt to conditions of multisensorial constraints for planning, control and execution of complex tasks in a surgical environment and what can be suggested for surgeons' skill training during the task execution.

In the first chapter of this thesis, different visual feedback mechanisms used in the operation room were studied. This research topic was also extended with the tool manipulation, task repetition, glove wearing, expertise level, and color cues effects. In the second chapter, VR and its utilization as a surgical training system in the manual operations were explored with human-computer interactions. Virtual object features were investigated in VR, such as length, width, object size, object complexity, object position and object orientation variations, and the additional auditory feedback variations with the frequency change in the sound. In the third chapter, a special glove was designed for the handles of the STRAS. With this glove, the tactile grip force difference between a novice and an expert was studied.

The first and one of the most vital results obtained from these studies is the importance of the precision in the surgical skill assessment. The expert surgeon was the most precise subject amongst all the participants in the third study of chapter one. When years of experience and skill training with different medical applications and technologies is combined with decision making, strategy and planning in task execution, placing the object at the center of the TA was the priority for the expert surgeon. Batmaz et al. [31,32,36] showed the importance of the precision and why it has to be used as an assessment criterion. It was concluded that to develop motor performance of subjects with a better visuo-motor experience in an image guided visual feedback and to reach the level of an expert surgeon, precision should be taken into account as an assessment criterion. For instance, in the latest review on 2D vs 3D Laparoscopic Cholecystectomy review [159], writers focused on the execution time as the primary outcome, but not on the precision. The precision criterion should be included as an assessment method for future studies on image guided surgical skill evaluation.

Similarly, precision was used as an assessment criterion in the second chapter with three different methods. For each of these precision criteria results, different outcomes were highlighted in each study of chapter two. When different visual feedbacks were compared in the first study of chapter two, different results were obtained for precision criteria for ‘average number of finger outs’ and ‘motor performance index’, and ‘average accumulated distance away from the object surface’ for *2D screen view*. For example, while subjects perform better in ‘average number of finger outs’ with *2D*

screen view compared to the other visual feedbacks (except *real world view with direct touch* condition), this difference vanished in the 'motor performance index' and 'average accumulated distance away from the object surface'. Furthermore, in the second study, the length and width change in each virtual object affected precision criteria diversely. In the "Steering Law" analyses, while 'average number of finger outs' dependent variable gave positive slope sign, 'motor performance index' and 'average accumulated distance away from the object surface' dependent variables gave negative slope sign for 'Torus'. Moreover, in the 'average number of finger outs' dependent variable, 'Horizontal' and 'Vertical' gave different slope signs. These variations show the importance of the different precision criteria measurements and evaluations in the individual assessment. There is no single major 'the' precision criteria that can be used as a dependent variable in head-mounted display-based environments. Each task and the requirements of that task should be precisely defined, and eligible precision criterion or criteria should be selected as assessment criteria during the task evaluation and skill training along with the task execution time.

Experimental studies in the last century have proposed procedures for controlling a trainee's speed-accuracy trade-off in tasks where both time and precision matter critically. These procedures either aim at selectively rewarding either speed or precision during learning (e.g. [123]; for a more recent review see [132]). This can be achieved by providing adequate feed-back to the trainee, especially in the first training sessions. Making sure that the trainee gets as precise as possible before getting faster should be a priority in surgical simulator training. This can be achieved by instructing him/her to privilege accuracy rather than speed. Execution times then become faster automatically with training. Once a desired level of precision is reached by a trainee, time deadlines for task execution can be introduced, and progressively reduced during further training, to ensure the trainee gets as fast as possible without losing precision (e. g. [147,148]). A major goal identified in recent analyses [43] is to ensure that the experimental evaluation of skills in surgical simulator scenarios is not subject to the development of a single observer bias over time, as may easily be the case in fully automated (unsupervised) skill rating procedures. Yet, these represent economy in manpower and are therefore likely to become the adopted standard, which result in trainees not being coached individually and receiving no proper guidance on how to optimize their learning strategies. Supervised learning in small groups, in training loops

with regular and adaptive skill assessment, as shown here in Figure 119, represents a better and not necessarily more costly alternative in the light of the findings reported here, especially in surgical simulator training, where reliable performance standards are urgently needed.

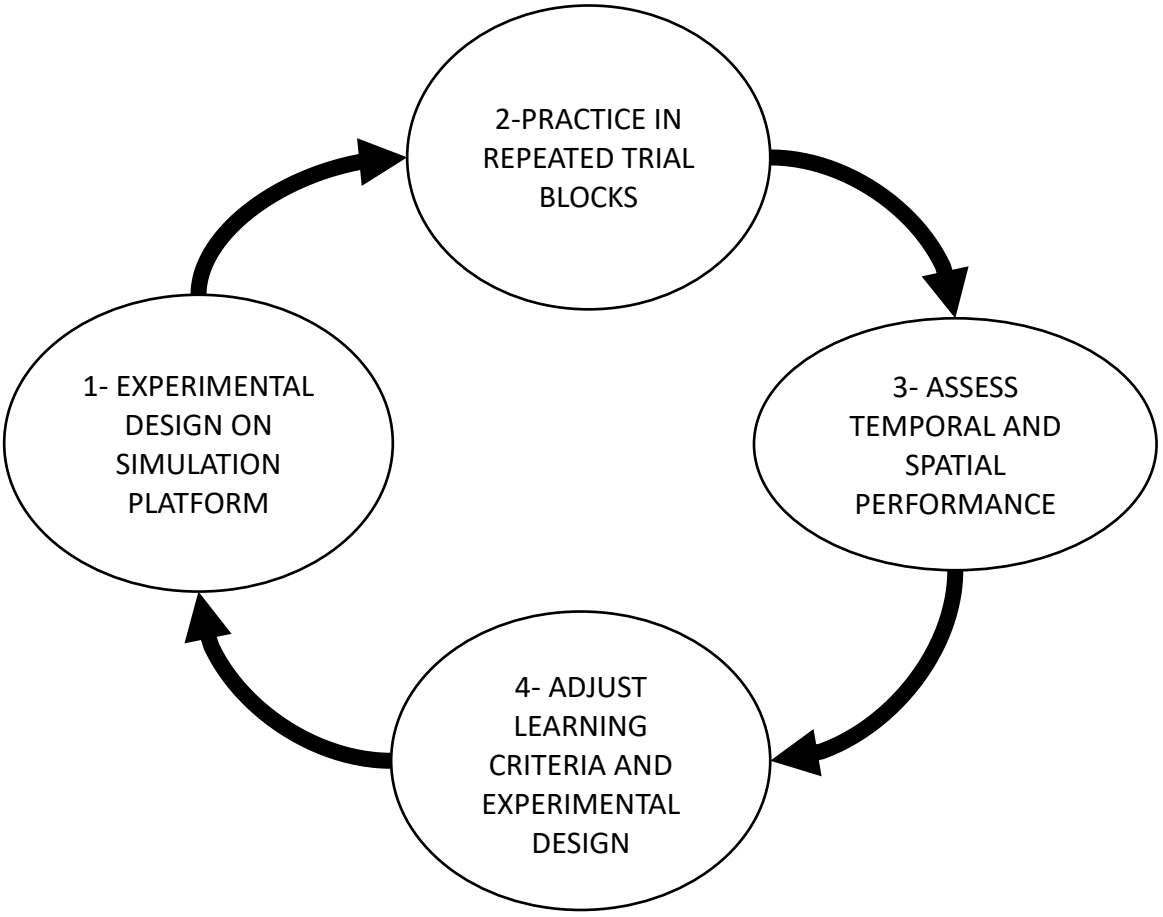

Figure 119 – A closed loop model for adaptive skill assessment as shown here needs to be considered to ensure that evaluation of desired behaviors is appropriate and not subject to the development of a single observer bias over time. Adjustment of learning criteria and test design (step 3 of the loop) may be necessary in the light of data relative to temporal and spatial aspects of tested performance (step 2 of the loop)

The close loop model proposed in Figure 119 also shows the importance of the strategy differences between subjects during the performance assessments. In all three chapters, it was shown that individuals generate different preferences. In the first

study and the last study of first chapter and fourth study of second chapter, time-precision tradeoffs and individual preference differences were investigated in detail. These differences are reflected by strategy specific trade-offs between speed of task execution and the precision with which the object is placed on the targets. As predicted, these trade-offs occur spontaneously and without performance feedback (e.g. [57]). The observations lead to understand why monitoring only execution times for learning curve analysis in simulator training is not a viable option. Some trainees may get faster, but not necessarily better in the task. Yet, in a majority of simulator training programs, the relative precision of image-guided hand maneuvers based on a conditional pixel-by-pixel analysis of hand or tool-movements from the video image data is not taken into account in the individual's learning curve.

Another important result obtained from this work is the significance of the feedback selection. In this thesis, three perceptual feedbacks, visual, tactile and auditory feedbacks were investigated. The visual feedback was one of the major research topics in the first chapter. When the direct vision was compared to 2D image guidance and stereoscopic 3D vision, it was always concluded that the natural direct view was superior to the other image guidance systems. On the other hand, all the subjects were less precise in stereoscopic 3D vision compared to the 2D image guidance.

In the first study of second chapter, the *real-world view with direct touch* condition was compared to other visual feedback systems used in the surgical simulator environments. The results were similar with the first chapter; subjects were faster and more precise with the *real-world view with direct touch* condition. At this point, it is important to keep in mind that subjects followed the objects with their fingertips on a piece of cardboard that provided physical support when they were executing the task with the *real-world view with direct touch*. To understand the relation between visual and haptic feedback effects further, there is a need to perform another experiment that can provide real-world view with natural direct view (a see-through glass system can be used for this purpose) to interact with the real-world objects and 3D computer generated images. The experiments here were done with an immersive 3D stereoscopic head-mounted virtual reality headset, which does not provide the natural real-world view. This new experiment can answer these two questions: does the 2D cardboard interaction compared to 3D free space interaction provide better

performance results with the direct natural view and does natural direct view provide better performance results when it is compared to 3D stereoscopic displays. Although there was a superiority of the direct vision over 3D stereo vision in the first chapter, the effects of the fixed camera position on the motor performance of the subjects during the task execution and task variation has to be taken into account, as mentioned in the first chapter. This additional experiment would help us to further understand the results of the direct vision and direct touch comparison.

In the 2D screen view vs stereoscopic 3D vision comparisons in the first chapter studies, it is concluded that time and precision results of the individuals are affected by visual feedback selection and the expertise of the user. While the execution time was slower in stereoscopic 3D vision compared to the 2D vision in novices, surgeons moved faster in stereoscopic 3D vision which is coherent with the previous image-guided surgery studies. There was no difference between 2D screen view and stereoscopic 3D vision in the expert surgeon time results. The expert surgeon's years of experience on the 2D screen view affected the motor performance measurement results. Furthermore, surgeons made less task errors during the task execution and after the experiments. They highlighted that they were trained to be careful and pay attention to make less task errors during the surgical procedures. These results show the importance of the subjects' background homogeneity selection in the experiments for image guidance research. The competence level in the image guided procedures has to be considered as an independent variable, but more importantly, this research shows that referring to results of the studies without considering the background of the participants is not enough to explain the results. Each experimental task should be designed according to the homogeneity of the target study group background [160] to overcome this problem and experimenter should choose the visual feedback according to the competence of the user. This requires a close collaboration between the surgeons and engineers, operation room designers and cognitive neuroscientists.

The other result obtained from this research was about the tactile feedback. Different tactile feedbacks used in the image-guided interventions are included as independent variables to experimental designs. In each chapter, how the motor performance of the individuals was affected by the variations of the tactile feedback was studied in detail. As shown in the first chapter, the tool manipulation was significantly affecting the time

and precision of the individuals. In short, while the subjects were faster in no tool manipulation, they were more precise with the tool manipulation in straight ahead monitor position. The effects of the tool manipulation have been studied by previous research (e.g. Brown and Stuerzlinger [248], Longo and Lourenco [133], etc.) and showed similar results. The space around one's own body within arm's reach and its perceived extent affects performance by drawing attention to regions of space that are not paid attention to when the same task is performed with the hands directly [132]. Similarly, subjects moved with the cube more stability during tool manipulation when compared to the bare hand manipulation in the trajectory analyses of the first chapter.

In the third chapter, the grip force differences between the expert and the novice were analyzed. Two specially designed gloves were used to understand how the different levels of expertise can create variations in the applied grip force of each individual's *loci*. In this experiment, it is important to keep in mind that each *locus* on the glove was specially positioned according to the trials of the handles of the STRAS and each handle of the STRAS was ergonomically designed to fit the hands of the user. The whole hand of the user was in contact with the handles during the task execution, thus the sensor positions were selected according to the maximum applied force locations. Furthermore, these positions were not selected according to one special task, but for all the possible hand gestures and rotations during a general task execution. Therefore, in the STRAS experiments, subjects did not apply force to all the sensor positions: some of the sensor positions were not used to apply force in that specific pick-and-drop task. For instance, in the pick-and-drop experiment of the STRAS, subjects did not have to pull the handles towards them, which is used to retract the instruments at the tip of the endoscope. Similarly, the index fingertip was only used to open and close the grippers. The sensors which did not produce any significant grip force data were not used in the data analysis section of the third chapter.

Effects of the group homogeneity on different visual and tactile feedback systems were analyzed for time and precision between novices, surgeons and the expert surgeon. Similarly, in the first chapter, there were significant differences for segment traverse duration, dispersion and average distance away from the reference trajectory between surgeons, expert surgeon, and novices when they were using a tool. The third chapter results showed that there was a grip force difference between the novice and the

expert, which was a condition related to the haptic feedback. In the last chapter, both novice and the expert surgeon had to look at a 2D screen monitor to execute the whole task. The expertise effect on the tactile feedback results show the importance of the system application design for the target users. The novice subjects in this study had no training in image-guided procedures, with the above-average spatial abilities necessary for surgery. Such beginners are bound to have more heterogeneous general training backgrounds than expert surgeons. They still need to get used to the image views when monitoring their hands moving across peri-personal space [142]. Effective eye-hand coordination under image guidance can only be considered near-optimal once it produces performance scores with stable speed-precision trade-offs in one and the same individual [31]. Getting there involves complex processes of perceptual learning for motor control and action that deserve to be investigated further.

In the second chapter, the sound feedback in VR was explored. Previous research on the human auditory cortex showed that different sounds evoke the human brain [235,236] and selection of the movements are related to the sensory stimulus [237–239]. In this research, a similar result was found on the motor performance of the subjects for the sound feedback. Subjects were faster and more precise compared to the no-sound feedback, but the optimal sound feedback was found with the middle-C frequency. In lower and higher frequencies, subjects were either slower or less precise compared to the middle-frequency pitch. Especially in the higher frequencies, subjects took their time to be more careful so not to make mistakes and to avoid the unpleasant and uncomfortable sound effect. This trade-off concludes the importance of the sound feedback selection, such as context sensitivity [249] or loudness [250]. For the future research, different aspects of sound, including loudness, context sensitivity, and different pitches can be included as the dependent variables. Moreover, the research on the auditory feedback is still missing a systematic evaluation of auditory feedback in motor learning [99]. A single-frequency alarm tone used in this experiment and the interpretation of the results can be used to map the relation between the movement and performance of the subject while an auditory feedback is present.

In the third chapter, handedness was investigated in detail with the expertise level during the surgical-robotic system operations. In the second chapter studies, the handedness factor was studied in immersive head-mounted display systems. In both

chapters, it was shown that handedness affects the motor performance of the individuals and each subject has to be monitored individually during the skill assessment. It was already known that handedness can affect the motor performance of the individuals [224], especially the beginners. In the fourth study of second chapter, significant differences between dominant and non-dominant hand were observed for the complex structure and small object size with a better precision score for the non-dominant hand. This may seem surprising in the light of previous studies (e.g. [223]) thus, handedness results were investigated further for the non-dominant hand precision results in the fourth study of second chapter. In the further research, after the task fatigue and rushing were eliminated, four different explanations were highlighted for this result: agency, muscular constrains, insufficient error feedback, and absence of performance feedback. The more precise results of the left-handed subjects' with their non-dominant hand in the fourth study can also be explained by the agency; when subjects retrace the object with the hand they prefer using, they feel more in control and may become less attentive to contains [122,126,251].

In the first study of chapter two, subjects were faster whilst using the *2D screen view* with their dominant hand when they were using a mouse with a 2D monitor screen as a visual feedback. Subjects were already used to use a mouse and a 2D screen from their daily lives and this affected the results. Furthermore, handedness and movement direction interactions in the first, second and the fifth studies showed that subjects were more precise with their dominant hand in the counter-clockwise movement direction compared to their non-dominant hand. These results were explained with the research on upper extremity on continuous steering movement experiments for clockwise and counter-clockwise directions [197] and research on shoulder muscles can explain this differences. For example, the Lee et al. [197] study showed that even torque of the steering direction varies with the clockwise and counter-clockwise direction and they relate these results to intra-limb and inter-limb coordination.

As previously mentioned, all the subjects were right-handed in the second chapter studies but not including the fifth study. By using data of the left-handed subjects from the fifth study of chapter two, handedness and movement direction interaction was investigated further in VR. According to results, both right-handed and left-handed subjects were more precise with the left-to-right movements in the fifth study. In the

fourth study, when the structural complexity and object size were investigated, there was no effect on the movement direction factor. In the further analysis of the first and second study, all the right-handed subjects were more precise with left-to-right movements compared to the right-to-left movements with their non-dominant hand. Similarly, left-handed subjects were also more precise with left-to-right movements compared to the right-to-left movements with their dominant hand in the fifth study. When the two results were merged, it appeared that subjects were more precise with left-to-right movements compared to the right-to-left movements with their left hands. This conclusion here can be explained by three different theories; the muscles usage as the clockwise-counterclockwise discussion in the previous paragraph, with the dominant and non-dominant brain hemispheres, and the cultural effects. The previous research on the closed loop movement showed that brain hemispheres can affect the time and the precision of the individuals [252,253] during task execution. For instance, Haaland and Harrington showed that movement speed of the subjects varies between left and right hemispace [252]. Additionally, all the subjects in all three chapters were from western countries in which left-to-right reading and writing is commonplace. This cultural effect can be an explanation for this result; subjects were writing a text from left-to-right. Furthermore, when they learn to read a text during their youth; they would have initially followed the manuscript with their fingertips. This could lead them to practice precise fingertip retracing in left-to-right movement direction with their left hand. Again, it is important to keep in mind that, in the fourth study of second chapter, there was no handedness and movement direction interaction for both complex and simple object structure, so this movement direction difference vanishes with the complex movements. The symmetrical movements in the first, second and fifth studies of the second chapter affects all the individuals with a more precise left-to-right movement and this result should be investigated further in detail with more left-handed subjects and with subjects that have ability to read the text from right-to-left.

In second chapter studies, human-computer interactions in VR was investigated in detail. Apart from the object width and length in the “Steering Law” [85,204,254], the importance of the object complexity was highlighted. Virtual object size and complexity were interdependent and need to be controlled when assessing motor performances with VR training applications and simulators. Furthermore, when the targeted object for interaction is simple, the size of the display should be kept small. However, if the

virtual object space is complex, then the display size should be large enough to minimize errors. In practical use, beginners should start training on larger representations of complex objects in VR. For skill assessment in VR, object size may need to be individually calibrated for complex actions [31,36] such as knot tying in laparoscopic surgery.

Apart from the surgical simulators and surgical skill evaluation, the results and conclusions found in this study can be applied to other image guided systems and tool based manual operations. For example, teleoperation systems using a 2D monitor and handles (such as handling dangerous substances with a robot inspected environment [255], pilot training [256], underwater applications [257], medical applications in space missions [258], aerial vehicle training [259], etc.) can apply results of this thesis to their studies. In VR environments, near-body space research uses different approaches (such as Fitts's law and Steering Law, [260], air pointing studies [248], etc.) can explore further their results in the VR environments by using results of this thesis. The results of this thesis can be also useful for simulation environment research (such as minimally invasive surgical trainer systems [261], robotic surgical system research [262], etc.).

Conclusions and Perspectives

In this thesis, the effects of the multisensorial constraints on time, precision and grip force of the individuals were explored during a complex task execution.

In the first chapter studies, the results reveal complex and spontaneously occurring trade-offs between time and precision in the performance of individuals, in visual spatial learning of an image-guided object positioning task. These trade-offs reflect cognitive strategy variations that need to be monitored individually to ensure effective skill learning. Collecting only time data to establish learning curves is not an option, as getting faster does not straightforwardly imply getting better at the task. Training procedures should include skill evaluation by expert psychologists and procedures for the adaptive control of speed-accuracy trade-offs in the performances of novices. In consistency with earlier findings, image-guidance significantly slows down, and significantly reduces the precision of, goal-directed manual operations of novices, all non-surgeons scoring high in spatial ability. 3D viewing systems do not straightforwardly produce better surgical eye-hand coordination in image-guided procedures. The relative effectiveness of 3D technology for the precision and timing of surgical hand movements depends on the type and direction of hand movement required for the intervention, the flexibility of the camera system generating the image views across target locations in the surgeon's peri-personal space, and on the surgeon's individual training level. The complex interactions between viewing, tool-use, and individual strategy factors open new and important perspectives for further research on novices in image-guided eye-hand coordination.

In the second chapter studies, results show that subjects were faster and more precise in the real-world view with direct touch and there were no major differences between augmented reality, mixed reality, and virtual reality in terms of motor performance of the participants. Object width and height, orientation, position, complexity, and size determined the time and the precision of human hand and finger movements along axes of alignment of object borders. Virtual objects need to be calibrated for optimal tracking of individual performance evaluation in VR environments and simulators. Individual speed precision curves should be monitored from the outset to optimize motor performance during learning. Subjects were more precise at eye-level interactions, and less precise at further away targets. The optimal location for interaction with extreme regions is above the eye level, for both ipsilateral and

contralateral operations. The object's position in virtual depth affects motor performance, suggesting optimal interaction to be at eye level position for close targets, and above eye level position for further away targets. Handedness in no touch systems is a discriminative performance factor. Sound feedback can be used to improve motor performance of the individuals, but a middle-C frequency optimizes the time and precision of the subjects.

In the last chapter, study results show a difference between haptic forces applied by a novice and an expert user. These differences can be compensated for by selective training in specific task sequences. Even though the whole inner surface of the hand is in contact with the grabbers, not all of it is used when applying force to the maneuver sticks. The technology could be effectively exploited in simulator training for image-guided interventions with a tool, and in training programs with a larger number of users, and with a larger variety of different tasks on robot-assisted surgical systems.

Overall, the results of this thesis explored how the sensory feedback mechanism of the human perceptual system is affected during the planning, control, and execution of a complex task. Image-guided surgery, simulators, remote control of wireless robots, and other domains can use the results of this study for their future applications.

Bibliography

1. Studeli T, Freudenthal A, De Ridder H. Evaluation framework of ergonomic requirements for iterative design development of computer systems and their user interfaces for minimal invasive therapy. Proceedings WWCS. 2007. pp. 21–24.
2. Wallen RD. Human Error in Medicine. Biomed Instrum Technol. 2006;40: 290. doi:10.2345/i0899-8205-40-4-290.1
3. Gallagher AG, Ritter EM, Lederman AB, McClusky DA, Smith CD. Video-assisted surgery represents more than a loss of three-dimensional vision. Am J Surg. 2005;189: 76–80. doi:10.1016/j.amjsurg.2004.04.008
4. Luger T, Bosch T, Hoozemans M, de Looze M, Veeger D. Task variation during simulated, repetitive, low-intensity work – influence on manifestation of shoulder muscle fatigue, perceived discomfort and upper-body postures. Ergonomics. 2015;58: 1851–1867. doi:10.1080/00140139.2015.1043356
5. Jalote-Parmar A, Badke-Schaub P, Ali W, Samset E. Cognitive processes as integrative component for developing expert decision-making systems: A workflow centered framework. J Biomed Inform. 2010;43: 60–74. doi:10.1016/j.jbi.2009.07.001
6. Schout BMA, Hendrikx AJM, Scheele F, Bemelmans BLH, Scherpbier AJJA. Validation and implementation of surgical simulators: A critical review of present, past, and future. Surgical Endoscopy and Other Interventional Techniques. 2010. pp. 536–546. doi:10.1007/s00464-009-0634-9
7. Verdaasdonk EGG, Dankelman J, Lange JF, Stassen LPS. Incorporation of proficiency criteria for basic laparoscopic skills training: How does it work? Surg Endosc Other Interv Tech. 2008;22: 2609–2615. doi:10.1007/s00464-008-9849-4
8. Guler O, Yaniv Z. Image-guided navigation: A cost effective practical introduction using the image-guided surgery toolkit (IGSTK). Proceedings of the Annual International Conference of the IEEE Engineering in Medicine and Biology Society, EMBS. 2012. pp. 6056–6059. doi:10.1109/EMBC.2012.6347375
9. Linte CA, Yaniv ZR. Image-guided interventions: We've come a long way, but are we there? IEEE Pulse. 2016;7: 46–50. doi:10.1109/MPUL.2016.2606466
10. Drouin S, Kersten-Oertel M, Chen SJS, Collins DL. A realistic test and development environment for mixed reality in neurosurgery. Lecture Notes in Computer Science (including subseries Lecture Notes in Artificial Intelligence and Lecture Notes in Bioinformatics). 2012. pp. 13–23. doi:10.1007/978-3-642-32630-1_2
11. Abboud M, Orentlicher G. An open system approach for surgical guide production. J Oral Maxillofac Surg. 2011;69. doi:10.1016/j.joms.2011.07.027
12. Kumar AN, Pheiffer TS, Simpson AL, Thompson RC, Miga MI, Dawant BM. Phantom-based comparison of the accuracy of point clouds extracted from stereo cameras and laser range scanner. In: Holmes DR, Yaniv ZR, editors. International Society for Optics and Photonics; 2013. p. 867125. doi:10.1117/12.2008036
13. Napalkova L, Rozenblit JW, Hwang G, Hamilton AJ, Suantak L. An optimal motion planning method for computer-assisted surgical training. Appl Soft Comput. 2014;24: 889–899. doi:10.1016/j.asoc.2014.08.054
14. Rozenblit JW. Models and techniques for computer aided surgical training.

Lecture Notes in Computer Science (including subseries Lecture Notes in Artificial Intelligence and Lecture Notes in Bioinformatics). 2012. pp. 233–241. doi:10.1007/978-3-642-27579-1_30
15. Li M, Hansen C, Rose G. A software solution to dynamically reduce metallic distortions of electromagnetic tracking systems for image-guided surgery. Int J Comput Assist Radiol Surg. 2017;12: 1621–1633. doi:10.1007/s11548-017-1546-0
16. Dawson-Elli A, Potter M, Bensch A, Linte CA. An integrated “plug & play” 3D Slicer module for image-guided navigation for training, simulation and guidance. 2014 IEEE Western New York Image and Signal Processing Workshop, WNYISPW 2014 - Proceedings. 2014. pp. 23–26. doi:10.1109/WNYIPW.2014.6999479
17. Feng C, Rozenblit JW, Hamilton AJ, Wytyczak-Partyka A. Defining spatial regions in computer-assisted laparoscopic surgical training. Proceedings of the International Symposium and Workshop on Engineering of Computer Based Systems. 2009. pp. 176–183. doi:10.1109/ECBS.2009.18
18. Keus F, de Jong J, Gooszen H, van Laarhoven C. Laparoscopic versus open cholecystectomy for patients with symptomatic cholecystolithiasis. Cochrane Database Syst Rev. 2006;18: CD006231. doi:http://dx.doi.org/10.1002/14651858.CD006231
19. Laine S, Rantala A, Gullichsen R, Ovaska J. Laparoscopic vs conventional Nissen fundoplication: A prospective randomized study. Surg Endosc. 1997;11: 441–444. doi:10.1007/s004649900386
20. Medeiros LR, Stein AT, Fachel J, Garry R, Furness S. Laparoscopy versus laparotomy for benign ovarian tumor: A systematic review and meta-analysis. International Journal of Gynecological Cancer. 2008. pp. 387–399. doi:10.1111/j.1525-1438.2007.01045.x
21. Pulijala Y, Ma M, Ayoub A. VR Surgery: Interactive Virtual Reality Application for Training Oral and Maxillofacial Surgeons using Oculus Rift and Leap Motion. Serious Games Edutainment Appl. 2017;Volume II: pp 187-202. doi:10.1007/978-3-319-51645-5
22. Sampogna G, Pugliese R, Elli M, Vanzulli A, Forgione A. Routine clinical application of virtual reality in abdominal surgery. Minim Invasive Ther Allied Technol. 2017;0: 1–12. doi:10.1080/13645706.2016.1275016
23. Zakirova AA, Ganiev BA, Mullin RI. Using virtual reality technology and hand tracking technology to create software for training surgical skills in 3D game. AIP Conference Proceedings. 2015. doi:10.1063/1.4936044
24. Riddle RS, Wasser DE, McCarthy M. Touching The Human Neuron: User-Centric Augmented Reality Viewing and Interaction of in-vivo Cellular Confocal Laser Scanning Microscopy (CLSM) Utilizing High Resolution zStack Data Sets for Applications in Medical Education and Clinical Medicine Using GLASS and Motion Tracking Technology. J Biocommun. Biological Photographic Association; 2017;41. Available: http://firstmonday.org/ojs/index.php/jbc/article/view/7563/6066
25. Farahani N, Post R, Duboy J, Ahmed I, Kolowitz B, Krinchai T, et al. Exploring virtual reality technology and the Oculus Rift for the examination of digital pathology slides. J Pathol Inform. 2016;7: 22. doi:10.4103/2153-3539.181766
26. Beattie N, Horan B, McKenzie S. Taking the LEAP with the Oculus HMD and CAD - Plucking at thin Air? Procedia Technol. 2015;20: 149–154.

doi:10.1016/j.protcy.2015.07.025
27. Pamungkas DS, Ward K. Electro-Tactile Feedback System to Enhance Virtual Reality Experience. Int J Comput Theory Eng. 2016;8: 465–470. doi:10.7763/IJCTE.2016.V8.1090
28. Sanders B., Vincenzi D., Shen Y. Scale and spatial resolution guidelines for the design of virtual engineering laboratories. Adv Intell Syst Comput. 2017;498: 373–382. doi:10.1007/978-3-319-42070-7_34
29. Hoyet L, Argelaguet F, Nicole C, Lécuyer A. "Wow! I Have Six Fingers!": Would You Accept Structural Changes of Your Hand in VR? Front Robot AI. Frontiers; 2016;3: 27. doi:10.3389/frobt.2016.00027
30. Batmaz AU, de Mathelin M, Dresp-Langley B. Effects of 2D and 3D image views on hand movement trajectories in the surgeon's peri-personal space in a computer controlled simulator environment. Cogent Med. 2018; 1426232. doi:10.1080/2331205X.2018.1426232
31. Batmaz AU, de Mathelin M, Dresp-Langley B. Seeing virtual while acting real: Visual display and strategy effects on the time and precision of eye-hand coordination. Buckingham G, editor. PLoS One. Springer Business Media E-book; 2017;12: e0183789. doi:10.1371/journal.pone.0183789
32. Batmaz AU, de Mathelin M, Dresp-Langley B. Getting nowhere fast: trade-off between speed and precision in training to execute image-guided hand-tool movements. BMC Psychol. 2016;
33. Dresp-Langley B. Principles of perceptual grouping: Implications for image-guided surgery. Frontiers in Psychology. Frontiers Media SA; 2015. doi:10.3389/fpsyg.2015.01565
34. Kumler JJ, Bauer ML. Fisheye lens designs and their relative performance. Int Symp Opt Sci Technol. 2000; 360–369. doi:10.1117/12.405226
35. Kanhere A, Aldalali B, Greenberg JA, Heise CP, Zhang L, Jiang H. Reconfigurable micro-camera array with panoramic vision for surgical imaging. J Microelectromechanical Syst. 2013;22: 989–991. doi:10.1109/JMEMS.2013.2262604
36. Batmaz AU, de Mathelin M, Dresp-Langley B. Effects of indirect screen vision and tool-use on the time and precision of object positioning on real-world targets. ECVP. Barcelona; 2016. p. 196.
37. Perkins N, Starkes JL, Lee TD, Hutchison C. Learning to use minimal access surgical instruments and 2-dimensional remote visual feedback: How difficult is the task for novices? Adv Heal Sci Educ. 2002;7: 117–131. doi:10.1023/A:1015700526954
38. Taffinder N, Smith SGT, Huber J, Russell RCG, Darzi A. The effect of a second-generation 3D endoscope on the laparoscopic precision of novices and experienced surgeons. Surg Endosc. 1999;13: 1087–1092. doi:10.1007/s004649901179
39. Bhayani SB, Andriole GL. Three-Dimensional (3D) Vision: Does It Improve Laparoscopic Skills? An Assessment of a 3D Head-Mounted Visualization System. Rev Urol. 2005;7: 211–214.
40. van Bergen P, Kunert W, Bessell J, Buess GF. Comparative study of two-dimensional and three-dimensional vision systems for minimally invasive surgery. Surg Endosc. 1998;12: 948–954. doi:10.1007/s004649900754
41. Votanopoulos K, Brunicardi FC, Thornby J, Bellows CF. Impact of three-dimensional vision in laparoscopic training. World J Surg. 2008;32: 110–118.

doi:10.1007/s00268-007-9253-6
42. Storz P, Buess GF, Kunert W, Kirschniak A. 3D HD versus 2D HD: Surgical task efficiency in standardised phantom tasks. Surg Endosc Other Interv Tech. 2012;26: 1454–1460. doi:10.1007/s00464-011-2055-9
43. Tanagho YS, Andriole GL, Paradis AG, Madison KM, Sandhu GS, Varela JE, et al. 2D Versus 3D Visualization: Impact on Laparoscopic Proficiency Using the Fundamentals of Laparoscopic Surgery Skill Set. J Laparoendosc Adv Surg Tech. 2012;22: 865–870. doi:10.1089/lap.2012.0220
44. Sakata S, Grove PM, Hill A, Watson MO, Stevenson ARL. Impact of simulated three-dimensional perception on precision of depth judgements, technical performance and perceived workload in laparoscopy. Br J Surg. 2017; doi:10.1002/bjs.10528
45. Jones DB, Brewer JD, Soper NJ. The influence of three-dimensional video systems on laparoscopic task performance. Surg Laparosc Endosc. 1996;6: 191–197. Available: http://www.ncbi.nlm.nih.gov/pubmed/8743361
46. Chan ACW, Chung SCS, Yim APC, Lau JYW, Ng EKW, Li AKC. Comparison of two-dimensional vs three-dimensional camera systems in laparoscopic surgery. Surgical Endoscopy. 1997. pp. 438–440. doi:10.1007/s004649900385
47. Hanna GB, Shimi SM, Cuschieri A. Task performance in endoscopic surgery is influenced by location of the image display. Ann Surg. 1998;227: 481–484. doi:10.1097/00000658-199804000-00005
48. Mueller MD, Camartin C, Dreher E, Hänggi W. Three-dimensional laparoscopy: Gadget or progress? A randomized trial on the efficacy of three-dimensional laparoscopy. Surg Endosc. 1999;13: 469–472. doi:10.1007/s004649901014
49. Blavier A, Nyssen AS. The effect of 2D and 3D visual modes on surgical task performance: role of expertise and adaptation processes. Cogn Technol Work. 2014;16: 509–518. doi:10.1007/s10111-014-0281-3
50. Silvestri C, Motro R, Maurin B, Dresp-Langley B. Visual spatial learning of complex object morphologies through the interaction with virtual and real-world data. Des Stud. 2010;31: 363–381. doi:http://dx.doi.org/10.1016/j.destud.2010.03.001
51. Gallace A, Spence C. The cognitive and neural correlates of “tactile consciousness”: A multisensory perspective. Consciousness and Cognition. 2008. pp. 370–407. doi:10.1016/j.concog.2007.01.005
52. Jenmalm P, Dahlstedt S, Johansson RS. Visual and tactile information about object-curvature control fingertip forces and grasp kinematics in human dexterous manipulation. J Neurophysiol. 2000;84: 2984–2997.
53. Graziano MS, Gross CG. The representation of estrapersonal space: A possible role for bimodal, visual-tactile neurons. The cognitive neurosciences. 1995. pp. 1021–1034.
54. Zangaladze A, Epstein CM, Grafton ST, Sathian K. Involvement of visual cortex in tactile discrimination of orientation. Nature. 1999;401: 587–590. doi:10.1038/44139
55. Stein BE, Wallace MW, Stanford TR, Jiang W. Cortex governs multisensory integration in the midbrain. Neuroscientist. 2002;8: 306–314. doi:10.1177/107385840200800406
56. Held R. Visual-haptic mapping and the origin of cross-modal identity. Optom Vis Sci. 2009;86: 595–598. doi:10.1097/OPX.0b013e3181a72999
57. Fitts PM. The information capacity of the human motor system in controlling the

amplitude of movement. J Exp Psychol. 1954;47: 381–391. doi:10.1037/h0055392
58. Ollman R. Choice reaction time and the problem of distinguishing task effects from strategy effects. Atten Perform VI. 1977; 99--113.
59. Luce RD. Response Times: Their Role in Inferring Elementary Mental Organization. Response Times: Their Role in Inferring Elementary Mental Organization. Oxford University Press; 1986.
60. Meyer DE, Irwin DE, Osman AM, Kounois J. The dynamics of cognition and action: Mental processes inferred from speed-accuracy decomposition. Psychol Rev. 1988;95: 183. doi:10.1037/0033-295X.95.2.183
61. Spille J, Wenners A, von Hehn U, Maass N, Pecks U, Mettler L, et al. 2D Versus 3D in Laparoscopic Surgery by Beginners and Experts: A Randomized Controlled Trial on a Pelvitrainer in Objectively Graded Surgical Steps. J Surg Educ. 2017;74: 867–877. doi:10.1016/j.jsurg.2017.01.011
62. Parikh SP, Szczech EC, Castillo RC, Moskowitz R, Zuberi J, Sori A, et al. Prospective Analysis of Laparoscopic Cholecystectomies Based on Postgraduate Resident Level. Surg Laparosc Endosc Percutan Tech. Wolters Kluwer; 2015;25: 487–491.
63. Park YS, Oo AM, Son SY, Shin DJ, Jung DH, Ahn SH, et al. Is a robotic system really better than the three-dimensional laparoscopic system in terms of suturing performance?: comparison among operators with different levels of experience. Surg Endosc Other Interv Tech. 2016;30: 1485–1490. doi:10.1007/s00464-015-4357-9
64. Mashiach R, Mezhybovsky V, Nevler A, Gutman M, Ziv A, Khaikin M. Three-dimensional imaging improves surgical skill performance in a laparoscopic test model for both experienced and novice laparoscopic surgeons. Surg Endosc. 2014;28: 3489–3493. doi:10.1007/s00464-014-3635-2
65. Currò G, La Malfa G, Lazzara S, Caizzone A, Fortugno A, Navarra G. Three-Dimensional Versus Two-Dimensional Laparoscopic Cholecystectomy: Is Surgeon Experience Relevant? J Laparoendosc Adv Surg Tech. 2015;25: 566–570. doi:10.1089/lap.2014.0641
66. Leite M, Carvalho AF, Costa P, Pereira R, Moreira A, Rodrigues N, et al. Assessment of Laparoscopic Skills Performance: 2D Versus 3D Vision and Classic Instrument Versus New Hand-Held Robotic Device for Laparoscopy. Surg Innov. SAGE Publications Inc; 2015;23: 52–61. doi:10.1177/1553350615585638
67. El Boghdady M, Ramakrishnan G, Tang B, Alijani A. A Comparative Study of Generic Visual Components of Two-Dimensional Versus Three-Dimensional Laparoscopic Images. World Journal of Surgery. 2017: 1–7. doi:10.1007/s00268-017-4220-3
68. Batmaz AU, de Mathelin M, Dresp-Langley B. Effect of relative tartget position on ipsilateral and contraleteral manual operations in head-mounted virtual reality. Perception. 2018;
69. Batmaz AU, de Mathelin M, Dresp-Langley B. Inside the virtual brain: using OCULUS DK2 for surgical planing. NeuroTalk. Barcelona Spain; 2017.
70. Batmaz AU, de Mathelin M, Dresp-Langley B. Effects of Image Size And Structural Complexity On Time And Precision Of Hand Movements in Head Mounted Virtual Reality. IEEE VR. Reutlingen, Germany; 2018. (© 2018 IEEE)
71. Vogel JJ, Vogel DS, Cannon-Bowers J, Bowers CA, Muse K, Wright M.

Computer Gaming and Interactive Simulations for Learning: A Meta-Analysis. J Educ Comput Res. 2006;34: 229–243. doi:10.2190/FLHV-K4WA-WPVQ-H0YM
72. Sitzmann T. A meta-analytic examination of the instructional effectiveness of computer-based simulation games. Pers Psychol. 2011;64: 489–528. doi:10.1111/j.1744-6570.2011.01190.x
73. Seymour NE, Gallagher AG, Roman SA, O'Brien MK, Bansal VK, Andersen DK, et al. Virtual Reality Training Improves Operating Room Performance. Ann Surg. 2002;236: 458–464. doi:10.1097/00000658-200210000-00008
74. Jagacinski RJ, Monk DL. Fitts' law in two dimensions with hand and head movements movements. J Mot Behav. 1985;17: 77–95. doi:10.1080/00222895.1985.10735338
75. Boritz J, Booth KS, Cowan WB. Fitts's Law Studies of Directional Mouse Movement. Graph Interface '91. 1991; 216–223.
76. Murata A, Iwase H. Extending fitts' law to a three-dimensional pointing task. Hum Mov Sci. 2001;20: 791–805. doi:10.1016/S0167-9457(01)00058-6
77. Grossman T, Balakrishnan R. Pointing at Trivariate Targets in 3D Environments. Proc 2004 Conf Hum factors Comput Syst - CHI '04. 2004;6: 447–454. doi:10.1145/985692.985749
78. Scheme E, Englehart K. Validation of a selective ensemble-based classification scheme for myoelectric control using a three dimensional Fitts' law test. Neural Syst Rehabil Eng IEEE Trans. 2013;21: 616–623. doi:10.1109/tnsre.2012.2226189
79. Mathur AS. Low cost virtual reality for medical training. 2015 IEEE Virtual Real Conf VR 2015 - Proc. 2015; 345–346. doi:10.1109/VR.2015.7223437
80. Kleven NF, Prasolova-Førland E, Fominykh M, Hansen A, Rasmussen G, Sagberg LM, et al. Training nurses and educating the public using a virtual operating room with Oculus Rift. Proceedings of the 2014 International Conference on Virtual Systems and Multimedia, VSMM 2014. 2014. pp. 206–213. doi:10.1109/VSMM.2014.7136687
81. Carol SK, English WK, Burr BYJ. Evaluation of mouse, rate-controlled isometric joystick, step keys, text keys for text selection on a crt. Ergonomics. 1978;21: 601–613. doi:10.1080/00140137808931762
82. MacKenzie CL, Marteniuk RG, Dugas C, Liske D, Eickmeier B. Three-dimensional Movement Trajectories in Fitts' task: Implications for control. Q J Exp Psychol Sect A. 1987;39: 629–647. doi:10.1080/14640748708401806
83. MacKenzie IS. Fitts' Law as a Research and Design Tool in Human-Computer Interaction. Human–Computer Interact. 1992;7: 91–139. doi:10.1207/s15327051hci0701_3
84. MacKenzie IS, Sellen A, Buxton W. A comparison of input devices in elemental pointing and dragging tasks. Proc SIGCHI Conf Hum factors Comput Syst Reach through Technol. 1991; 161–166. doi:10.1145/108844.108868
85. Accot J, Zhai S. Performance evaluation of input devices in trajectory-based tasks. Proceedings of the SIGCHI conference on Human factors in computing systems the CHI is the limit - CHI '99. 1999. pp. 466–472. doi:10.1145/302979.303133
86. Wittmann F, Held JP, Lambercy O, Starkey ML, Curt A, Höver R, et al. Self-directed arm therapy at home after stroke with a sensor-based virtual reality training system. J Neuroeng Rehabil. 2016;13. doi:10.1186/s12984-016-0182-1
87. Klamroth-Marganska V, Blanco J, Campen K, Curt A, Dietz V, Ettlin T, et al.

Three-dimensional, task-specific robot therapy of the arm after stroke: A multicentre, parallel-group randomised trial. Lancet Neurol. 2014;13: 159–166. doi:10.1016/S1474-4422(13)70305-3
88. Sveistrup H. Motor rehabilitation using virtual reality. Journal of NeuroEngineering and Rehabilitation. 2004. doi:10.1186/1743-0003-1-10
89. Calabrò RS, Naro A, Russo M, Leo A, De Luca R, Balletta T, et al. The role of virtual reality in improving motor performance as revealed by EEG: a randomized clinical trial. J Neuroeng Rehabil. 2017;14. doi:10.1186/s12984-017-0268-4
90. Wingrave CA, Bowman DA. Baseline Factors for Raycasting Selection. Virtual Real Int. 2004;
91. Mine M. ISAAC: A virtual environment tool for the interactive construction of virtual worlds. UNC Chapel Hill Comput Sci Tech Rep TR95-020. Citeseer; 1995;
92. James KH, Humphrey GK, Vilis T, Corrie B, Baddour B, Goodale MA. “Active” and “passive” learning of three-dimensional object structure within an immersive virtual reality environment. Behav Res Methods, Instruments, Comput. 2002;34: 383–390. doi:10.3758/BF03195466
93. Jang S, Vitale JM, Jyung RW, Black JB. Direct manipulation is better than passive viewing for learning anatomy in a three-dimensional virtual reality environment. Comput Educ. 2017;106: 150–165. doi:10.1016/j.compedu.2016.12.009
94. Zhang Y, Fernando T, Xiao H, Travis A. Evaluation of auditory and visual feedback on task performance in a virtual assembly environment. Presence. 2006;15: 613–626. doi:10.1162/pres.15.6.613
95. Swapp D, Pawar V, Loscos C. Interaction with co-located haptic feedback in virtual reality. Virtual Real. 2006;10: 24–30. doi:10.1007/s10055-006-0027-5
96. Fluet GG, Qiu Q, Saleh S, Ramirez D, Adamovich S, Kelly D, et al. Robot-assisted virtual rehabilitation (NJIT-RAVR) system for children with upper extremity hemiplegia. 2009 Virtual Rehabilitation International Conference, VR 2009. 2009. pp. 189–192. doi:10.1109/ICVR.2009.5174230
97. Zhou ZY, Cheok AD, Qiu Y, Yang X. The role of 3-D sound in human reaction and performance in augmented reality environments. IEEE Trans Syst Man, Cybern Part ASystems Humans. 2007;37: 262–272. doi:10.1109/TSMCA.2006.886376
98. Sigrist R, Rauter G, Marchal-Crespo L, Riener R, Wolf P. Sonification and haptic feedback in addition to visual feedback enhances complex motor task learning. Exp Brain Res. 2014;233: 909–925. doi:10.1007/s00221-014-4167-7
99. Sigrist R, Rauter G, Riener R, Wolf P. Augmented visual, auditory, haptic, and multimodal feedback in motor learning: A review. Psychon Bull Rev. 2013;20: 21–53. doi:10.3758/s13423-012-0333-8
100. Burke JL, Prewett MS, Gray AA, Yang L, Stilson FRB, Coovert MD, et al. Comparing the effects of visual-auditory and visual-tactile feedback on user performance. Proceedings of the 8th international conference on Multimodal interfaces - ICMI ’06. 2006. p. 108. doi:10.1145/1180995.1181017
101. Batmaz AU, Dresp-Langley B, de Mathelin M. Novice and expert haptic behaviours while using a robot controlled surgery system. BioMed2017. Innsbruck: IEEE; 2017. doi:10.2316/P.2017.852-022 (© 2017 IEEE)
102. Chitwood WR, Nifong LW, Chapman WH, Felger JE, Bailey BM, Ballint T, et al. Robotic surgical training in an academic institution. Ann Surg. 2001;234: 475. doi:10.1097/00000658-200110000-00007

103. King CH, Culjat MO, Franco ML, Lewis CE, Dutson EP, Grundfest WS, et al. Tactile feedback induces reduced grasping force in robot-assisted surgery. IEEE Trans Haptics. 2009;2: 103–110. doi:10.1109/TOH.2009.4
104. De Donno A, Zorn L, Zanne P, Nageotte F, De Mathelin M. Introducing STRAS: A new flexible robotic system for minimally invasive surgery. International Conference on Robotics and Automation. Karlsruhe; 2013. pp. 1213–1220. doi:10.1109/ICRA.2013.6630726
105. De Donno A, Nageotte F, Zanne P, Zorn L, de Mathelin M. Master/slave control of flexible instruments for minimally invasive surgery. International Conference on Intelligent Robots and Systems. Tokyo: IEEE; 2013. pp. 483–489. doi:10.1109/IROS.2013.6696395
106. de Donno A, Zorn L, Zanne P, Nageotte F, de Mathelin M. First Evaluations in the Control of a Novel Flexible Surgical Robot. The Hamlyn Symposium on Medical Robotics. 2013. p. 31.
107. Oldfield RC. The assessment and analysis of handedness: The Edinburgh inventory. Neuropsychologia. 1971;9: 97–113. doi:10.1016/0028-3932(71)90067-4
108. Hegarty M, Waller D. A dissociation between mental rotation and perspective-taking spatial abilities. Intelligence. 2004;32: 175–191. doi:10.1016/j.intell.2003.12.001
109. Det MJ, Mijerink WJHJ, Hoff C, Totté ER PJ. Optimal ergonomics for laparoscopic surgery in minimally invasive surgery suites: A review and guidelines. Surg Endosc. Springer; 2009;23: 1279–1285. doi:10.1007/s00464-008-0148-x
110. Maithel SK, Villegas L, Stylopoulos N, Dawson S, Jones DB. Simulated laparoscopy using a head-mounted display vs traditional video monitor: An assessment of performance and muscle fatigue. Surg Endosc Other Interv Tech. 2005;19: 406–411. doi:10.1007/s00464-004-8177-6
111. Farnè A, Làdavas E. Dynamic size-change of hand peripersonal space following tool use. Neuroreport. 2000;11: 1645–1649. doi:10.1097/00001756-200006050-00010
112. Maravita A, Husain M, Clarke K, Driver J. Reaching with a tool extends visual-tactile interactions into far space: Evidence from cross-modal extinction. Neuropsychologia. 2001;39: 580–585. doi:10.1016/S0028-3932(00)00150-0
113. Maravita A, Iriki A. Tools for the body (schema). Trends in Cognitive Sciences. 2004. pp. 79–86. doi:doi:10.1016/j.tics.2003.12.008
114. Krakauer JW, Mazzoni P. Human sensorimotor learning: Adaptation, skill, and beyond. Current Opinion in Neurobiology. 2011. pp. 636–644. doi:10.1016/j.conb.2011.06.012
115. Huang VS, Haith A, Mazzoni P, Krakauer JW. Rethinking Motor Learning and Savings in Adaptation Paradigms: Model-Free Memory for Successful Actions Combines with Internal Models. Neuron. 2011;70: 787–801. doi:10.1016/j.neuron.2011.04.012
116. Henriques DYP, Cressman EK. Visuomotor adaptation and proprioceptive recalibration. Journal of Motor Behavior. 2012. pp. 435–444. doi:10.1080/00222895.2012.659232
117. Salomonczyk D, Cressman EK, Henriques DYP. The role of the cross-sensory error signal in visuomotor adaptation. Exp Brain Res. 2013;228: 313–325. doi:10.1007/s00221-013-3564-7

118. Spence C, Nicholls MER, Driver J. The cost of expecting events in the wrong sensory modality. Percept Psychophys. 2001;63: 330–336. doi:10.3758/BF03194473
119. McClelland JL. On the time relations of mental processes: An examination of systems of processes in cascade. Psychol Rev. 1979;86: 287. Available: http://content.apa.org/journals/rev/86/4/287
120. Wilson MR, McGrath JS, Vine SJ, Brewer J, Defriend D, Masters RSW. Perceptual impairment and psychomotor control in virtual laparoscopic surgery. Surg Endosc Other Interv Tech. 2011;25: 2268–2274. doi:10.1007/s00464-010-1546-4
121. Desai S KS. Tactile Inspection Performance with and without Gloves. Proc Hum Factors Soc Annu Meet. SAGE Publications; 1983;27: 782–785. doi:10.1177/154193128302700906
122. Balslev D, Cole J, Miall RC. Proprioception Contributes to the Sense of Agency during Visual Observation of Hand Movements: Evidence from Temporal Judgments of Action. J Cogn Neurosci. 2007;19: 1535–1541. doi:10.1162/jocn.2007.19.9.1535
123. Folegatti A, de Vignemont F, Pavani F, Rossetti Y, Farné A. Losing one's hand: Visual-proprioceptive conflict affects touch perception. PLoS One. 2009;4: e6920. doi:10.1371/journal.pone.0006920
124. Emam TA, Hanna G, Cuschieri A. Ergonomic principles of task alignment, visual display, and direction of execution of laparoscopic bowel suturing. Surg Endosc Other Interv Tech. 2002;16: 267–271. doi:10.1007/s00464-001-8152-4
125. Slachevsky A, Pillon B, Fourneret P, Pradat-Diehl P, Jeannerod M, Dubois B. Preserved adjustment but impaired awareness in a sensory-motor conflict following prefrontal lesions. J Cogn Neurosci. 2001;13: 332–340. doi:10.1162/08989290151137386
126. Preston C, Newport R. Self-denial and the role of intentions in the attribution of agency. Conscious Cogn. 2010;19: 986–998. doi:10.1016/j.concog.2010.04.005
127. Schall JD, Stuphorn V, Brown JW. Monitoring and control of action by the frontal lobes. Neuron. 2002. pp. 309–322. doi:10.1016/S0896-6273(02)00964-9
128. Gibson JJ. Observations on active touch. Psychol Rev. 1962;69: 477. doi:10.1037/h0046962
129. Di Pellegrino G, Ladavas E FA. Seeing where your hands are [11]. Nature. 1997. p. 730. doi:10.1038/41921
130. LaMotte RH, Friedman RM, Lu C, Khalsa PS, Srinivasan M a. Raised object on a planar surface stroked across the fingerpad: responses of cutaneous mechanoreceptors to shape and orientation. J Neurophysiol. 1998;80: 2446–2466.
131. Fogassi, Leonardo and Gallese V. Action as a binding key to multisensory integration. The handbook of multisensory processes. MIT Press Cambridge, MA; 2004.
132. Humphreys GW, Riddoch MJ, Forti S, Ackroyd K. Action influences spatial perception: Neuropsychological evidence. Visual Cognition. 2004. pp. 401–427. doi:10.1080/13506280344000310
133. Longo MR, Lourenco SF. On the nature of near space: Effects of tool use and the transition to far space. Neuropsychologia. 2006;44: 977–981.
134. Sommer R, McCann GC, Sommer R. Personal Space: The Behavioral Basis of Design. American Sociological Review. 1969. p. 164. doi:10.2307/2093905

135. Bogner MSE. Human error in medicine. Lawrence Erlbaum Associates, Inc; 1994.
136. Derossis, Anna M and Antoniuk, Maureen and Fried GM. Evaluation of laparoscopic skills: A 2-year follow-up during residency training. Can J Surg. 1999;42: 293–296.
137. Breedveld P, Wentink M. Eye-hand coordination in laparoscopy - An overview of experiments and supporting aids. Minim Invasive Ther Allied Technol. 2001;10: 155–162. doi:10.1080/136457001753192277
138. Hubber JW, Taffinder N, Russell RC, Darzi A. The effects of different viewing conditions on performance in simulated minimal access surgery. Ergonomics. 2003;46: 999–1016. doi:10.1080/0014013031000109197
139. Sakata S, Watson MO, Grove PM, Stevenson ARL. The Conflicting Evidence of Three-dimensional Displays in Laparoscopy: a review of systems old and new. Ann Surg. 2016;263: 234–239. doi:10.1097/SLA.0000000000001504
140. Uhrich ML, Underwood RA, Standeven JW, Soper NJ, Engsberg JR. Assesment of fatigue, monitor placement, and surgical experience during simulated laparoscopic surgery. Surg Endosc Other Interv Tech. 2002;16: 635–639. doi:10.1007/s00464-001-8151-5
141. Haveran LA, Novitsky YW, Czerniach DR, Kaban GK, Taylor M, Gallagher-Dorval K, et al. Optimizing laparoscopic task efficiency: The role of camera and monitor positions. Surg Endosc Other Interv Tech. Springer-Verlag; 2007;21: 980–984. doi:10.1007/s00464-007-9360-3
142. Masia L, Casadio M, Sandini G, Morasso P. Eye-hand coordination during dynamic visuomotor rotations. PLoS One. 2009;4. doi:10.1371/journal.pone.0007004
143. Boumenir Y, Georges F, Rebillard G, Valentin J, Dresp-Langley B. Wayfinding through an unfamiliar environment. Percept Mot Skills. 2010;111: 829–847.
144. Davare M, Zénon A, Desmurget M, Olivier E. Dissociable contribution of the parietal and frontal cortex to coding movement direction and amplitude. Front Hum Neurosci. 2015;9. doi:10.3389/fnhum.2015.00241
145. Desmurget M, Jordan MI, Prablanc C, Jeannerod M. Constrained and unconstrained movements involve different control strategies. J Neurophysiol. 1997;77: 1644–1650.
146. van der Graaff MCW, Brenner E, Smeets JBJ. Differences in curvature between constrained and unconstrained goal-directed movements to haptic targets. Exp Brain Res. Springer Berlin Heidelberg; 2014;232: 3445–3451. doi:10.1007/s00221-014-4030-x
147. Bonnet C. Psychophysical Approaches, Contextual Effects and Response BIAS. Adv Psychol. 1990;68: 221–242. doi:10.1016/S0166-4115(08)61326-6
148. Bonnet C, Dresp B. A fast procedure for studying conditional accuracy functions. Behav Res Methods, Instruments Comput. 1993;25: 2–8. doi:10.3758/BF03204443
149. Guthrie JP, Ash RA, Stevens CD. Are women “better” than men? J Manag Psychol. 2003;18: 229–243. doi:10.1108/02683940310465243
150. Stoet G, O’Connor DB, Conner M, Laws KR. Are women better than men at multi-tasking? BMC Psychol. 2013;1: 18.
151. Sarlegna F, Blouin J, Bresciani JP, Bourdin C, Vercher JL, Gauthier GM. Target and hand position information in the online control of goal-directed arm movements. Exp Brain Res. 2003;151: 524–535. doi:10.1007/s00221-003-1504-

7
152. Haggard P, Richardson J. Spatial patterns in the control of human arm movement. J Exp Psychol Hum Percept Perform. 1996;22: 42–62. doi:10.1037/0096-1523.22.1.42
153. Kersten-Oertel M, Chen SJS, Collins DL. An evaluation of depth enhancing perceptual cues for vascular volume visualization in neurosurgery. IEEE Trans Vis Comput Graph. 2014;20: 391–403. doi:10.1109/TVCG.2013.240
154. Sanchez-Margallo JA, Sanchez-Margallo FM, Pagador Carrasco JB, Oropesa Garcia I, Gomez Aguilera EJ, Moreno del Pozo J. Usefulness of an optical tracking system in laparoscopic surgery for motor skills assessment. Cir Esp. 2014;92: 421–428. doi:10.1016/j.ciresp.2013.01.006
155. Boppart SA, Deutsch TF, Rattner DW. Optical imaging technology in minimally invasive surgery: Current status and future directions. Surg Endosc. 1999;13: 718–722. doi:10.1007/s004649901081
156. Shimotsu RT, Cao CGL. The effect of color-contrasting shadows on a dynamic 3-D laparoscopic surgical task. IEEE Trans Syst Man, Cybern Part ASystems Humans. 2007;37: 1047–1053. doi:10.1109/TSMCA.2007.904738
157. Svakhine N, Ebert DS, Stredney D. Illustration motifs for effective medical volume illustration. IEEE Comput Graph Appl. 2005;25: 31–39. doi:10.1109/MCG.2005.60
158. Speidel S, Kuhn E, Bodenstedt S, Röhl S, Kenngott H, Müller-Stich B, et al. Visual tracking of da Vinci instruments for laparoscopic surgery. Proc SPIE Med Imaging 2014 Image-Guided Proced Robot Interv Model Med Imaging 2014 Image-Guided Proced Robot Interv Model. 2014;9036: 903608. doi:10.1117/12.2042483
159. Komaei I, Navarra G, Currò G. Three-Dimensional Versus Two-Dimensional Laparoscopic Cholecystectomy: A Systematic Review. J Laparoendosc Adv Surg Tech. Mary Ann Liebert, Inc. 140 Huguenot Street, 3rd Floor New Rochelle, NY 10801 USA; 2017;
160. Ercikan K, Roth W-M. Limits of generalizing in education research: Why criteria for research generalization should include population heterogeneity and uses of knowledge claims. Teach Coll Rec. 2014;116: 1–15. Available: http://search.ebscohost.com/login.aspx?direct=true&db=psyh&AN=2014-16788-004&site=ehost-live&scope=site
161. Ebelhäuser J. Through a surgeon's eyes: the influence of visual-spatial ability and different camera positions on laparoscopic simulator task performance, among novices. University of Twente; 2017.
162. Gallagher AG, Al-Akash M, Seymour NE, Satava RM. An ergonomic analysis of the effects of camera rotation on laparoscopic performance. Surg Endosc Other Interv Tech. 2009;23: 2684–2691. doi:10.1007/s00464-008-0261-x
163. DeLucia PR, Griswold JA. Effects of Camera Arrangement on Perceptual-Motor Performance in Minimally Invasive Surgery. J Exp Psychol Appl. 2011;17: 210–232. doi:10.1037/a0024041
164. Franzeck FM, Rosenthal R, Muller MK, Nocito A, Wittich F, Maurus C, et al. Prospective randomized controlled trial of simulator-based versus traditional in-surgery laparoscopic camera navigation training. Surg Endosc Other Interv Tech. 2012;26: 235–241. doi:10.1007/s00464-011-1860-5
165. Korndorffer JR, Hayes DJ, Dunne JB, Sierra R, Touchard CL, Markert RJ, et al. Development and transferability of a cost-effective laparoscopic camera

navigation simulator. Surgical Endoscopy and Other Interventional Techniques. 2005. pp. 161–167. doi:10.1007/s00464-004-8901-2
166. Hicheur H, Vieilledent S, Richardson MJE, Flash T, Berthoz A. Velocity and curvature in human locomotion along complex curved paths: A comparison with hand movements. Exp Brain Res. 2005;162: 145–154. doi:10.1007/s00221-004-2122-8
167. Viviani P, Terzuolo C. Trajectory determines movement dynamics. Neuroscience. 1982;7: 431–437. doi:10.1016/0306-4522(82)90277-9
168. Bootsma RJ, Boulard M, Fernandez L, Mottet D. Informational constraints in human precision aiming. Neurosci Lett. 2002;333: 141–145. doi:10.1016/S0304-3940(02)01003-0
169. Grosjean M, Shiffrar M, Knoblich G. Fitts's law holds for action perception. Psychological Science. 2007. pp. 95–99. doi:10.1111/j.1467-9280.2007.01854.x
170. Decety J, Jeannerod M. Mentally simulated movements in virtual reality: does Fitt's law hold in motor imagery? Behav Brain Res. 1995;72: 127–134. doi:10.1016/0166-4328(96)00141-6
171. Wolpert DM, Ghahramani Z, Jordan MI. Perceptual distortion contributes to the curvature of human reaching movements. Exp Brain Res. 1994;98: 153–156. doi:10.1007/BF00229120
172. Osu R, Uno Y, Koike Y, Kawato M. Possible explanations for trajectory curvature in multijoint arm movements. J Exp Psychol Hum Percept Perform. 1997;23: 890–913. Available: http://www.ncbi.nlm.nih.gov/pubmed/9180049
173. Miall RC, Haggard PN. The curvature of human arm movements in the absence of visual experience. Exp Brain Res. 1995;103: 421–428. doi:10.1007/BF00241501
174. Saunders JA, Knill DC. Humans use continuous visual feedback from the hand to control fast reaching movements. Exp Brain Res. 2003;152: 341–352. doi:10.1007/s00221-003-1525-2
175. Sergio LE, Scott SH. Hand and joint paths during reaching movements with and without vision. Exp Brain Res. 1998;122: 157–164. doi:10.1007/s002210050503
176. Wolpert DM, Ghahramani W-Z, Jordan MI, Ghahramani Z, Jordan MI. Are arm trajectories planned in kinematic or dynamic coordinates? An adaptation study. Exp Brain Res. 1995;103: 460–470. doi:10.1007/BF00241505
177. Berthier NE. Learning to reach: A mathematical model. Dev Psychol. 1996;32: 811–823. doi:10.1037/0012-1649.32.5.811
178. Gallagher AG, O'Sullivan GC, Gallagher AG, O'Sullivan GC. Fundamentals of Surgical Simulation: Principles and Practice. Fundamentals of Surgical Simulation: Principles and Practice. Springer-Verlag London; 2012. doi:10.1007/978-0-85729-763-1
179. Motion L. VR Developer Mount Setup [Internet]. [cited 2 Jan 2018]. Available: https://www.youtube.com/watch?v=yS64FYRCyw0
180. Dandekar K, Raju BI, Srinivasan MA. 3-D Finite-Element Models of Human and Monkey Fingertips to Investigate the Mechanics of Tactile Sense. J Biomech Eng. 2003;125: 682. doi:10.1115/1.1613673
181. Mine M. Virtual environment interaction techniques [Internet]. UNC Chapel Hill Computer Science Technical Report. 1995. doi:10.1.1.38.1750
182. MacKenzie IS, Kauppinen T, Silfverberg M. Accuracy measures for evaluating computer pointing devices. Proceedings of the SIGCHI conference on Human factors in computing systems - CHI '01. 2001. pp. 9–16.

doi:10.1145/365024.365028
183. Williams CK, Tremblay L, Carnahan H. It pays to go off-track: Practicing with error-augmenting haptic feedback facilitates learning of a curve-tracing task. Front Psychol. 2016;7: 2010. doi:10.3389/fpsyg.2016.02010
184. Krichenbauer M, Yamamoto G, Taketomi T, Sandor C, Kato H. Augmented Reality vs Virtual Reality for 3D Object Manipulation. IEEE Trans Vis Comput Graph. 2017; 1–1. doi:10.1109/TVCG.2017.2658570
185. Seixas MCB, Cardoso JCS, Dias MTG. The Leap Motion Movement for 2D Pointing Tasks - Characterisation and Comparison to Other Devices. Proc 5th Int Conf Pervasive Embed Comput Commun Syst. 2015; 15–24. doi:10.5220/0005206100150024
186. Palter VN, Grantcharov TP. Virtual reality in surgical skills training. Surg Clin North Am. 2010;90: 605–617. doi:10.1016/j.suc.2010.02.005
187. Dong X. An overall solution of Virtual Reality classroom. Proceedings - 2016 IEEE International Conference on Service Operations and Logistics, and Informatics, SOLI 2016. 2016. pp. 119–123. doi:10.1109/SOLI.2016.7551672
188. Arora A, Swords C, Khemani S, Awad Z, Darzi A, Singh A, et al. Virtual reality case-specific rehearsal in temporal bone surgery: A preliminary evaluation. Int J Surg. 2014;12: 141–145. doi:10.1016/j.ijsu.2013.11.019
189. Willaert WIM, Aggarwal R, Herzeele I Van, Cheshire NJ, Vermassen FE. Recent advancements in medical simulation: Patient-specific virtual reality simulation. World J Surg. 2012;36: 1703–1712. doi:10.1007/s00268-012-1489-0
190. Arora A, Swords C, Khemani S, Darzi A, Singh A, Tolley NS. Case-Specific Simulation in Temporal Bone Surgery. Otolaryngol Neck Surg. 2012;147: P81–P82. doi:10.1177/0194599812451438a142
191. Argelaguet F, Andujar C. A survey of 3D object selection techniques for virtual environments. Comput Graph. 2013;37: 121–136. doi:10.1016/j.cag.2012.12.003
192. Milgram P, Takemura H, Utsumi A, Kishino F. Augmented reality: A class of displays on the reality-virtuality continuum. Telemanipulator Telepresence Technol. 1994;2351: 282–292. doi:10.1.1.83.6861
193. Morris D, Hong T, Barbagli F, Chang T, Salisbury K. Haptic feedback enhances force skill learning. Proceedings - Second Joint EuroHaptics Conference and Symposium on Haptic Interfaces for Virtual Environment and Teleoperator Systems, World Haptics 2007. 2007. pp. 21–26. doi:10.1109/WHC.2007.65
194. Luo Y, Vogel D. Crossing-based Selection with Direct Touch Input. CHI. 2014. pp. 2627–2636. doi:10.1145/2556288.2557397
195. Blanch R, Guiard Y, Beaudouin-Lafon M. Semantic Pointing - Improving Target Acquisition with Control-display Ratio Adaptation. Proc Int Conf Hum Factors Comput Syst. 2004;6: 519–526. doi:10.1145/985692.985758
196. Casiez G, Vogel D, Balakrishnan R, Cockburn A. The impact of control-display gain on user performance in pointing tasks. Human-Computer Interact. 2008;23: 215–250. doi:10.1080/07370020802278163
197. Lee HM, Li PC, Wu SK, You JY. Analysis of continuous steering movement using a motor-based quantification system. Sensors (Switzerland). 2012;12: 16008–16023. doi:10.3390/s121216008
198. Stucchi N, Viviani P. Cerebral Dominance and Asynchrony Between Bimanual Two-Dimensional Movements. J Exp Psychol Hum Percept Perform. 1993;19: 1200–1220. doi:10.1037/0096-1523.19.6.1200

199. Semjen A, Summers JJ, Cattaert D. Hand coordination in bimanual circle drawing. J Exp Psychol Hum Percept Perform. 1995;21: 1139–1157. doi:10.1037/0096-1523.21.5.1139
200. Sainburg RL, Kalakanis D. Differences in control of limb dynamics during dominant and nondominant arm reaching. J Neurophysiol. 2000;83: 2661–2675. doi:10.1152/jn.2000.83.5.2661
201. Hore J, Watts S, Tweed D, Miller B. Overarm throws with the nondominant arm: kinematics of accuracy. J Neurophysiol. 1996;76: 3693–3704. doi:10.1152/jn.1996.76.6.3693
202. Drascic D. Skill Acquisition and Task Performance in Teleoperation Using Monoscopic and Stereoscopic Video Remote Viewing. Proc Hum Factors Ergon Soc Annu Meet. 1991;35: 1367–1371. doi:10.1177/154193129103501906
203. Ware C, Lowther K. Selection using a one-eyed cursor in a fish tank VR environment. ACM Trans Comput Interact. 1997;4: 309–322. doi:10.1145/267135.267136
204. Accot J, Zhai S. Beyond Fitts' law: models for trajectory-based HCI tasks. Proc ACM SIGCHI Conf …. 1997; 295–301. doi:10.1145/258549.258760
205. Accot J, Zhai S. Refining Fitts' law models for bivariate pointing. Proceedings of the conference on Human factors in computing systems - CHI '03. 2003. p. 193. doi:10.1145/642611.642646
206. Accot J, Zhai S. More than dotting the i's --- foundations for crossing-based interfaces. Proceedings of the SIGCHI conference on Human factors in computing systems Changing our world, changing ourselves - CHI '02. 2002. p. 73. doi:10.1145/503376.503390
207. Stevens SS. On the psychophysical law. Psychol Rev. 1957;64: 153–181. doi:10.1037/h0046162
208. Liu L. Modeling three-dimensional interaction tasks for desktop virtual reality.
209. Zhai S, Accot J, Woltjer R. Human Action Laws in Electronic Virtual Worlds: An Empirical Study of Path Steering Performance in VR. Presence Teleoperators Virtual Environ. 2004;13: 113–127. doi:10.1162/1054746041382393
210. Roberts JW, Blinch J, Elliott D, Chua R, Lyons JL, Welsh TN. The violation of Fitts' Law: an examination of displacement biases and corrective submovements. Exp Brain Res. 2016;234: 2151–2163. doi:10.1007/s00221-016-4618-4
211. Ustinova KI, Leonard WA, Cassavaugh ND, Ingersoll CD. Development of a 3D immersive videogame to improve arm-postural coordination in patients with TBI. J Neuroeng Rehabil. 2011;8. doi:10.1186/1743-0003-8-61
212. Subramanian SK, Levin MF. Viewing medium affects arm motor performance in 3D virtual environments. J Neuroeng Rehabil. 2011;8. doi:10.1186/1743-0003-8-36
213. Subramanian S, Beaudoin C, Levin MF. Arm pointing movements in a three dimensional virtual environment: Effect of two different viewing media. 2008 Virtual Rehabilitation, IWVR. 2008. pp. 181–185. doi:10.1109/ICVR.2008.4625157
214. Subramanian S, Knaut LA, Beaudoin C, McFadyen BJ, Feldman AG, Levin MF. Virtual reality environments for post-stroke arm rehabilitation. J Neuroeng Rehabil. 2007;4. doi:10.1186/1743-0003-4-20
215. Gerig N, Mayo J, Baur K, Wittmann F, Riener R, Wolf P. Missing depth cues in virtual reality limit performance and quality of three dimensional reaching

movements. PLoS One. 2018;13. doi:10.1371/journal.pone.0189275
216. Riener R, Harders M. Virtual reality in medicine. Virtual Reality in Medicine. 2012. doi:10.1007/978-1-4471-4011-5
217. Torkington J, Smith SGT, Rees BI, Darzi A. Skill transfer from virtual reality to a real laparoscopic task. Surg Endosc. 2001;15: 1076–1079. doi:10.1007/s004640000233
218. Adamovich S V., Fluet GG, Tunik E, Merians AS. Sensorimotor training in virtual reality: A review. NeuroRehabilitation. 2009. pp. 29–44. doi:10.3233/NRE-2009-0497
219. Boustila S, Capobianco A, Bechmann D. Evaluation of factors affecting distance perception in architectural project review in immersive virtual environments. Proc 21st ACM Symp Virtual Real Softw Technol - VRST '15. 2015; 207–216. doi:10.1145/2821592.2821595
220. Heineken E, Schulte FP. Seeing Size and Feeling Weight: The Size-Weight Illusion in Natural and Virtual Reality. Hum Factors J Hum Factors Ergon Soc. 2007;49: 136–144. doi:10.1518/001872007779598028
221. Lederman SJ, Jones LA. Tactile and Haptic Illusions. IEEE Trans Haptics. 2011;4: 273–294. doi:10.1109/TOH.2011.2
222. Argelaguet F, Andujar C. Improving 3D selection in VEs through expanding targets and forced disocclusion. Lecture Notes in Computer Science (including subseries Lecture Notes in Artificial Intelligence and Lecture Notes in Bioinformatics). 2008. pp. 45–57. doi:10.1007/978-3-540-85412-8_5
223. Coren S. Sensorimotor performance as a function of eye dominance and handedness. Percept Mot Skills. 1999;88: 424–426. doi:10.2466/PMS.88.2.424-426
224. Rahm S, Wieser K, Wicki I, Holenstein L, Fucentese SF, Gerber C. Performance of medical students on a virtual reality simulator for knee arthroscopy: an analysis of learning curves and predictors of performance. BMC Surg. 2016;16: 1–8. doi:10.1186/s12893-016-0129-2
225. Just M, Stapley P, Ros M, Naghdy F, Stirling D. Effects of reintroducing haptic feedback to virtual-reality systems on movement profiles when reaching to virtual targets. 11th International Conference on Disability, Virtual Reality and Associated Technologies (ICDVRAT 2016). 2016. pp. 319–322. Available: http://ro.uow.edu.au/eispapers1/373
226. Vosinakis S, Koutsabasis P. Evaluation of visual feedback techniques for virtual grasping with bare hands using Leap Motion and Oculus Rift. Virtual Reality. 2017: 1–16. doi:10.1007/s10055-017-0313-4
227. Travaglini TA, Swaney PJ, Weaver KD, Webster RJ. Initial experiments with the leap motion as a user interface in robotic endonasal surgery. Mechanisms and Machine Science. 2016. pp. 171–179. doi:10.1007/978-3-319-22368-1_17
228. Bevilacqua F, Boyer E, Francoise J, Houix O, Susini P, Roby-Brami A, et al. Sensori-motor Learning With Movement Sonification: A Perspective From Recent Interdisciplinary Studies. Front Neurosci. 2016;10: 385. doi:10.3389/fnins.2016.00385
229. Mauser S, Burgert O. Touch-free, gesture-based control of medical devices and software based on the leap motion controller. Studies in Health Technology and Informatics. 2014. pp. 265–270. doi:10.3233/978-1-61499-375-9-265
230. Rosa GM, Elizondo ML. Use of a gesture user interface as a touchless image navigation system in dental surgery: Case series report. Imaging Sci Dent.

2014;44: 155–160. doi:10.5624/isd.2014.44.2.155
231. Sherman WR, Craig AB. Understanding Virtual Reality. Journal of Documentation. 2003. doi:10.1108/00220410310485776
232. Zhao Y, Bennett CL, Benko H, Cutrell E, Holz C, Morris MR, et al. Enabling People with Visual Impairments to Navigate Virtual Reality with a Haptic and Auditory Cane Simulation. 2018;
233. Kardous CA, Shaw PB. Evaluation of smartphone sound measurement applications. J Acoust Soc Am. 2014; doi:10.1121/1.4865269
234. Calvert G, Spence C, Stein BE. The handbook of multisensory processes. Handb multisensory Process. 2004; 933. doi:nicht verfügbar?
235. Santoro R, Moerel M, De Martino F, Goebel R, Ugurbil K, Yacoub E, et al. Encoding of Natural Sounds at Multiple Spectral and Temporal Resolutions in the Human Auditory Cortex. PLoS Comput Biol. 2014;10. doi:10.1371/journal.pcbi.1003412
236. Moerel M, De Martino F, Santoro R, Ugurbil K, Goebel R, Yacoub E, et al. Processing of Natural Sounds: Characterization of Multipeak Spectral Tuning in Human Auditory Cortex. J Neurosci. 2013;33: 11888–11898. doi:10.1523/JNEUROSCI.5306-12.2013
237. Schluter ND, Rushworth MFS, Passingham RE, Mills KR. Temporary interference in human lateral premotor cortex suggests dominance for the selection of movements. A study using transcranial magnetic stimulation. Brain. 1998;121: 785–799. doi:10.1093/brain/121.5.785
238. Passingham RE. Premotor cortex: Sensory cues and movement. Behav Brain Res. 1985;18: 175–185. doi:10.1016/0166-4328(85)90073-7
239. Halsband U, Ito N, Tanji J, Freund H-J. The role of premotor cortex and the supplementary motor area in the temporal control of movement in man. Brain. 1993;116: 243–266. doi:10.1093/brain/116.1.243
240. Zatorre RJ, Chen JL, Penhune VB. When the brain plays music: Auditory-motor interactions in music perception and production. Nature Reviews Neuroscience. 2007. pp. 547–558. doi:10.1038/nrn2152
241. Ram S, Mahadevan A, Rahmat-Khah H, Turini G, Young JG. Effect of Control-Display Gain and Mapping and Use of Armrests on Accuracy in Temporally Limited Touchless Gestural Steering Tasks. Proc Hum Factors Ergon Soc Annu Meet. 2017;61: 380–384. doi:10.1177/1541931213601577
242. Young J, Lin M, Bick A, Sarwar A, Dennerlein J. Gestural workspaces for computer interaction: Configuration and performance. Proceedings of the Human Factors and Ergonomics Society. 2013. pp. 424–428. doi:10.1177/1541931213571092
243. Teather RJ, Stuerzlinger W. Assessing the effects of orientation and device on (constrained) 3D movement techniques. 3DUI - IEEE Symposium on 3D User Interfaces 2008. 2008. pp. 43–50. doi:10.1109/3DUI.2008.4476590
244. Thompson CC, Ryou M, Soper NJ, Hungess ES, Rothstein RI, Swanstrom LL. Evaluation of a manually driven, multitasking platform for complex endoluminal and natural orifice transluminal endoscopic surgery applications (with video). Gastrointest Endosc. 2009;70: 121–125. doi:10.1016/j.gie.2008.11.007
245. Swanstrom LL, Kozarek R, Pasricha PJ, Gross S, Birkett D, Park PO, et al. Development of a new access device for transgastric surgery. J Gastrointest Surg. 2005;9: 1129–1137. doi:10.1016/j.gassur.2005.08.005
246. Phee SJ, Low SC, Huynh VA, Kencana AP, Sun ZL, Yang K. Master and slave

transluminal endoscopic robot (MASTER) for natural orifice transluminal endoscopic surgery (NOTES). Engineering in Medicine and Biology Society, 2009 EMBC 2009 Annual International Conference of the IEEE. 2009. pp. 1192–1195. doi:10.1109/IEMBS.2009.5333413
247. Pereira R, Moreira AHJ, Leite M, Rodrigues PL, Queirós S, Rodrigues NF, et al. Hand-held robotic device for laparoscopic surgery and training. 3nd International Conference on Serious Games and Applications for Health (SeGAH). IEEE; 2014. pp. 1–8. doi:10.1109/SeGAH.2014.7067079
248. Brown MA, Stuerzlinger W. Exploring the throughput potential of in-air pointing. Lecture Notes in Computer Science (including subseries Lecture Notes in Artificial Intelligence and Lecture Notes in Bioinformatics). 2016. pp. 13–24. doi:10.1007/978-3-319-39516-6_2
249. Aravena P, Delevoye-Turrell Y, Deprez V, Cheylus A, Paulignan Y, Frak V, et al. Grip Force Reveals the Context Sensitivity of Language-Induced Motor Activity during “Action Words” Processing: Evidence from Sentential Negation. PLoS One. 2012;7. doi:10.1371/journal.pone.0050287
250. Beattie RC, Svihovec D a, Carmen RE, Kunkel H a. Loudness discomfort level for speech: comparison of two instructional sets for saturation sound pressure level selection. Ear Hear. 1980;1: 197–205.
251. Synofzik M, Vosgerau G, Lindner A. Me or not me - An optimal integration of agency cues? Conscious Cogn. Elsevier Inc.; 2009;18: 1065–1068. doi:10.1016/j.concog.2009.07.007
252. Haaland KY, Harrington D. The role of the hemispheres in closed loop movements. Brain Cogn. 1989;9: 158–180. doi:10.1016/0278-2626(89)90027-4
253. Wyke M. The effect of brain lesions in the performance of an arm-hand precision task. Neuropsychologia. 1968;6: 125–134. doi:10.1016/0028-3932(68)90054-7
254. Grasso R, Prévost P, Ivanenko YP, Berthoz A. Eye-head coordination for the steering of locomotion in humans: An anticipatory synergy. Neurosci Lett. 1998;253: 115–118. doi:10.1016/S0304-3940(98)00625-9
255. Luk BL, Liu KP, Collie AA, Cooke DS, Chen S. Tele-operated climbing and mobile service robots for remote inspection and maintenance in nuclear industry. Industrial Robot. 2006. pp. 194–204. doi:10.1108/01439910610659105
256. Villacis C, Navarrete M, Rodriguez I, Romero F, Escobar L, Fuertes W, et al. Real-time flight simulator construction with a network for training pilots using mechatronics and cyber-physical system approaches. 2017 IEEE International Conference on Power, Control, Signals and Instrumentation Engineering (ICPCSI). IEEE; 2017. pp. 238–247. doi:10.1109/ICPCSI.2017.8392169
257. Park JY, Jun B huan, Lee P mook, Oh J. Experiments on vision guided docking of an autonomous underwater vehicle using one camera. Ocean Eng. 2009;36: 48–61. doi:10.1016/j.oceaneng.2008.10.001
258. Otto C, Comtois JM, Sargsyan A, Dulchavsky A, Rubinfeld I, Dulchavsky S. The Martian chronicles: Remotely guided diagnosis and treatment in the arctic circle. Surg Endosc Other Interv Tech. 2010;24: 2170–2177. doi:10.1007/s00464-010-0917-1
259. Garcia R, Barnes L. Multi-UAV simulator utilizing x-plane. J Intell Robot Syst Theory Appl. 2010;57: 393–406. doi:10.1007/s10846-009-9372-4
260. Yamanaka S, Stuerzlinger W. Steering Through Sequential Linear Path Segments. Acm Chi. 2017; 232–243. doi:10.1145/3025453.3025836
261. Mccloy R, Stone R. Virtual reality in surgery. BMJ. 2001;323: 912–915.

doi:10.1136/bmj.323.7318.912
262. Morris B. Robotic surgery: applications, limitations, and impact on surgical education. MedGenMed. WebMD/Medscape Health Network; 2005;7: 72. Available: http://www.ncbi.nlm.nih.gov/pubmed/16369298

Annexes

Annex 1 – ANOVA results for Chapter 1

Analysis of Variance

Source	Sum Sq.	d.f.	Mean Sq.	F	Prob>F
TOUCH	0	1	0.02	0.05	0.8309
VISION	8695	2	4347.5	9953.73	0
MANIPULATION	1824.1	1	1824.1	4176.32	0
SESSION	4440	7	634.29	1452.22	0
SUBJECT	13085.8	3	4361.93	9986.77	0
TOUCH*VISION	9.6	2	4.81	11.01	0
TOUCH*MANIPULATION	93.4	1	93.43	213.92	0
TOUCH*SESSION	5.4	7	0.77	1.77	0.0891
TOUCH*SUBJECT	5.2	3	1.73	3.96	0.0078
VISION*MANIPULATION	99.1	2	49.53	113.4	0
VISION*SESSION	640	14	45.71	104.67	0
VISION*SUBJECT	701.6	6	116.94	267.74	0
MANIPULATION*SESSION	22.6	7	3.23	7.4	0
MANIPULATION*SUBJECT	319.9	3	106.64	244.15	0
SESSION*SUBJECT	1494	21	71.14	162.88	0
TOUCH*VISION*MANIPULATION	10.1	2	5.06	11.58	0
TOUCH*VISION*SESSION	12.8	14	0.91	2.09	0.0098
TOUCH*VISION*SUBJECT	7.8	6	1.3	2.97	0.0068
TOUCH*MANIPULATION*SESSION	20.3	7	2.9	6.64	0
TOUCH*MANIPULATION*SUBJECT	11.3	3	3.78	8.65	0
TOUCH*SESSION*SUBJECT	23.2	21	1.11	2.53	0.0001
VISION*MANIPULATION*SESSION	34.3	14	2.45	5.61	0
VISION*MANIPULATION*SUBJECT	14.6	6	2.43	5.56	0
VISION*SESSION*SUBJECT	413.6	42	9.85	22.55	0
MANIPULATION*SESSION*SUBJECT	131.4	21	6.26	14.33	0
TOUCH*VISION*MANIPULATION*SESSION	36.5	14	2.61	5.97	0
TOUCH*VISION*MANIPULATION*SUBJECT	9.4	6	1.56	3.58	0.0015
TOUCH*VISION*SESSION*SUBJECT	27.4	42	0.65	1.49	0.0214
TOUCH*MANIPULATION*SESSION*SUBJECT	28.5	21	1.36	3.11	0
VISION*MANIPULATION*SESSION*SUBJECT	69.6	42	1.66	3.79	0
TOUCH*VISION*MANIPULATION*SESSION*SUBJECT	30.5	42	0.73	1.66	0.0047
Error	1509.5	3456	0.44		
Total	33826.7	3839			

Constrained (Type III) sums of squares.

Annex 1- Figure 1– ‘Time’ ANOVA results for study 1.

Analysis of Variance

Source	Sum Sq.	d.f.	Mean Sq.	F	Prob>F
TOUCH	498864	1	498864	5.86	0.0156
VISION	86765205.3	2	43382602.6	509.26	0
MANIPULATION	24240.6	1	24240.6	0.28	0.5938
SESSION	33865067.7	7	4837866.8	56.79	0
SUBJECT	167117084.3	3	55705694.8	653.91	0
TOUCH*VISION	195360.8	2	97680.4	1.15	0.3178
TOUCH*MANIPULATION	613929.9	1	613929.9	7.21	0.0073
TOUCH*SESSION	749667.4	7	107095.3	1.26	0.2677
TOUCH*SUBJECT	1565070	3	521690	6.12	0.0004
VISION*MANIPULATION	2218672.9	2	1109336.4	13.02	0
VISION*SESSION	4608464.9	14	329176.1	3.86	0
VISION*SUBJECT	41691232.6	6	6948538.8	81.57	0
MANIPULATION*SESSION	1847681.6	7	263954.5	3.1	0.0029
MANIPULATION*SUBJECT	8105884.4	3	2701961.5	31.72	0
SESSION*SUBJECT	62991501.4	21	2999595.3	35.21	0
TOUCH*VISION*MANIPULATION	417925.5	2	208962.8	2.45	0.0862
TOUCH*VISION*SESSION	2846721.6	14	203337.3	2.39	0.0026
TOUCH*VISION*SUBJECT	1407983.8	6	234664	2.75	0.0113
TOUCH*MANIPULATION*SESSION	1327990.1	7	189712.9	2.23	0.0294
TOUCH*MANIPULATION*SUBJECT	59772.4	3	19924.1	0.23	0.8728
TOUCH*SESSION*SUBJECT	2431075.4	21	115765.5	1.36	0.1266
VISION*MANIPULATION*SESSION	3374392.5	14	241028	2.83	0.0003
VISION*MANIPULATION*SUBJECT	2417454.7	6	402909.1	4.73	0.0001
VISION*SESSION*SUBJECT	21985500.4	42	523464.3	6.14	0
MANIPULATION*SESSION*SUBJECT	12887871.5	21	613708.2	7.2	0
TOUCH*VISION*MANIPULATION*SESSION	2104539	14	150324.2	1.76	0.0381
TOUCH*VISION*MANIPULATION*SUBJECT	593699.8	6	98950	1.16	0.324
TOUCH*VISION*SESSION*SUBJECT	2794727.8	42	66541.1	0.78	0.8434
TOUCH*MANIPULATION*SESSION*SUBJECT	2868633.2	21	136601.6	1.6	0.0399
VISION*MANIPULATION*SESSION*SUBJECT	8150713	42	194064.6	2.28	0
TOUCH*VISION*MANIPULATION*SESSION*SUBJECT	4260408	42	101438.3	1.19	0.1871
Error	294410057.8	3456	85188.1		
Total	777197394.4	3839			

Constrained (Type III) sums of squares.

Annex 1- Figure 2 – ‘Precision’ ANOVA results for study 1.

Analysis of Variance

Source	Sum Sq.	d.f.	Mean Sq.	F	Prob>F
TOUCH	77.1	1	77.11	1.89	0.169
VISION	3958.4	2	1979.19	48.6	0
MANIPULATION	1157.7	1	1157.67	28.43	0
SESSION	436	7	62.28	1.53	0.1528
SUBJECT	1208.8	3	402.95	9.89	0
TOUCH*VISION	20	2	9.98	0.24	0.7828
TOUCH*MANIPULATION	0	1	0	0	0.9924
TOUCH*SESSION	42	7	6	0.15	0.9943
TOUCH*SUBJECT	10.4	3	3.47	0.09	0.9682
VISION*MANIPULATION	273.9	2	136.94	3.36	0.0349
VISION*SESSION	314	14	22.43	0.55	0.9035
VISION*SUBJECT	358.3	6	59.72	1.47	0.1859
MANIPULATION*SESSION	39.2	7	5.6	0.14	0.9954
MANIPULATION*SUBJECT	47	3	15.68	0.38	0.7638
SESSION*SUBJECT	728.9	21	34.71	0.85	0.6552
TOUCH*VISION*MANIPULATION	1.5	2	0.75	0.02	0.9817
TOUCH*VISION*SESSION	96.1	14	6.87	0.17	0.9998
TOUCH*VISION*SUBJECT	40.7	6	6.79	0.17	0.9856
TOUCH*MANIPULATION*SESSION	32.2	7	4.6	0.11	0.9975
TOUCH*MANIPULATION*SUBJECT	23.7	3	7.9	0.19	0.9006
TOUCH*SESSION*SUBJECT	107.4	21	5.11	0.13	1
VISION*MANIPULATION*SESSION	102.9	14	7.35	0.18	0.9997
VISION*MANIPULATION*SUBJECT	161.8	6	26.97	0.66	0.6802
VISION*SESSION*SUBJECT	686.9	42	16.36	0.4	0.9998
MANIPULATION*SESSION*SUBJECT	268.2	21	12.77	0.31	0.9988
TOUCH*VISION*MANIPULATION*SESSION	67.3	14	4.81	0.12	1
TOUCH*VISION*MANIPULATION*SUBJECT	12.2	6	2.03	0.05	0.9995
TOUCH*VISION*SESSION*SUBJECT	180.9	42	4.31	0.11	1
TOUCH*MANIPULATION*SESSION*SUBJECT	88	21	4.19	0.1	1
VISION*MANIPULATION*SESSION*SUBJECT	349.8	42	8.33	0.2	1
TOUCH*VISION*MANIPULATION*SESSION*SUBJECT	255.9	42	6.09	0.15	1
Error	78195.8	1920	40.73		
Total	89343	2303			

Constrained (Type III) sums of squares.

Annex 1- Figure 3- ‘Average distance from the reference trajectory’ raw data ANOVA results without segment condition for Study 1.

Analysis of Variance

Source	Sum Sq.	d.f.	Mean Sq.	F	Prob>F
TOUCH	0	1	0	0	0.9931
VISION	146.052	2	73.0262	416.44	0
MANIPULATION	29.576	1	29.5762	168.66	0
SESSION	70.932	7	10.1331	57.78	0
SUBJECT	208.145	3	69.3817	395.65	0
TOUCH*VISION	0.114	2	0.057	0.33	0.7224
TOUCH*MANIPULATION	2.395	1	2.3954	13.66	0.0002
TOUCH*SESSION	0.144	7	0.0205	0.12	0.9972
TOUCH*SUBJECT	0.134	3	0.0446	0.25	0.8583
VISION*MANIPULATION	1.78	2	0.8901	5.08	0.0063
VISION*SESSION	10.789	14	0.7706	4.39	0
VISION*SUBJECT	10.365	6	1.7274	9.85	0
MANIPULATION*SESSION	0.513	7	0.0734	0.42	0.8914
MANIPULATION*SUBJECT	6.514	3	2.1714	12.38	0
SESSION*SUBJECT	23.735	21	1.1303	6.45	0
TOUCH*VISION*MANIPULATION	0.132	2	0.0658	0.38	0.6873
TOUCH*VISION*SESSION	0.328	14	0.0234	0.13	0.9999
TOUCH*VISION*SUBJECT	0.3	6	0.0501	0.29	0.944
TOUCH*MANIPULATION*SESSION	0.652	7	0.0932	0.53	0.8114
TOUCH*MANIPULATION*SUBJECT	0.801	3	0.2671	1.52	0.2065
TOUCH*SESSION*SUBJECT	0.928	21	0.0442	0.25	0.9998
VISION*MANIPULATION*SESSION	1.202	14	0.0859	0.49	0.9398
VISION*MANIPULATION*SUBJECT	0.344	6	0.0574	0.33	0.923
VISION*SESSION*SUBJECT	8.549	42	0.2036	1.16	0.2231
MANIPULATION*SESSION*SUBJECT	3.02	21	0.1438	0.82	0.6969
TOUCH*VISION*MANIPULATION*SESSION	0.812	14	0.058	0.33	0.9902
TOUCH*VISION*MANIPULATION*SUBJECT	0.356	6	0.0594	0.34	0.9167
TOUCH*VISION*SESSION*SUBJECT	0.73	42	0.0174	0.1	1
TOUCH*MANIPULATION*SESSION*SUBJECT	1.37	21	0.0652	0.37	0.9958
VISION*MANIPULATION*SESSION*SUBJECT	2.133	42	0.0508	0.29	1
TOUCH*VISION*MANIPULATION*SESSION*SUBJECT	1.387	42	0.033	0.19	1
Error	336.691	1920	0.1754		
Total	870.927	2303			

Constrained (Type III) sums of squares.

Annex 1- Figure 4- ‘from-target-to-target duration’ raw data ANOVA results without segment condition for Study 1.

Analysis of Variance

Source	Sum Sq.	d.f.	Mean Sq.	F	Prob>F
TOUCH	77.1	1	77.11	1.89	0.169
VISION	3958.4	2	1979.19	48.6	0
MANIPULATION	1157.7	1	1157.67	28.43	0
SESSION	436	7	62.28	1.53	0.1528
SUBJECT	1208.8	3	402.95	9.89	0
TOUCH*VISION	20	2	9.98	0.24	0.7828
TOUCH*MANIPULATION	0	1	0	0	0.9924
TOUCH*SESSION	42	7	6	0.15	0.9943
TOUCH*SUBJECT	10.4	3	3.47	0.09	0.9682
VISION*MANIPULATION	273.9	2	136.94	3.36	0.0349
VISION*SESSION	314	14	22.43	0.55	0.9035
VISION*SUBJECT	358.3	6	59.72	1.47	0.1859
MANIPULATION*SESSION	39.2	7	5.6	0.14	0.9954
MANIPULATION*SUBJECT	47	3	15.68	0.38	0.7638
SESSION*SUBJECT	728.9	21	34.71	0.85	0.6552
TOUCH*VISION*MANIPULATION	1.5	2	0.75	0.02	0.9817
TOUCH*VISION*SESSION	96.1	14	6.87	0.17	0.9998
TOUCH*VISION*SUBJECT	40.7	6	6.79	0.17	0.9856
TOUCH*MANIPULATION*SESSION	32.2	7	4.6	0.11	0.9975
TOUCH*MANIPULATION*SUBJECT	23.7	3	7.9	0.19	0.9006
TOUCH*SESSION*SUBJECT	107.4	21	5.11	0.13	1
VISION*MANIPULATION*SESSION	102.9	14	7.35	0.18	0.9997
VISION*MANIPULATION*SUBJECT	161.8	6	26.97	0.66	0.6802
VISION*SESSION*SUBJECT	686.9	42	16.36	0.4	0.9998
MANIPULATION*SESSION*SUBJECT	268.2	21	12.77	0.31	0.9988
TOUCH*VISION*MANIPULATION*SESSION	67.3	14	4.81	0.12	1
TOUCH*VISION*MANIPULATION*SUBJECT	12.2	6	2.03	0.05	0.9995
TOUCH*VISION*SESSION*SUBJECT	180.9	42	4.31	0.11	1
TOUCH*MANIPULATION*SESSION*SUBJECT	88	21	4.19	0.1	1
VISION*MANIPULATION*SESSION*SUBJECT	349.8	42	8.33	0.2	1
TOUCH*VISION*MANIPULATION*SESSION*SUBJECT	255.9	42	6.09	0.15	1
Error	78195.8	1920	40.73		
Total	89343	2303			

Constrained (Type III) sums of squares.

Annex 1- Figure 5– ‘Average distance from the reference trajectory’ raw data ANOVA results without segment condition for study 1.

Analysis of Variance

Source	Sum Sq.	d.f.	Mean Sq.	F	Prob>F
TOUCH	160.3	1	160.28	6.16	0.0132
VISION	2236	2	1118.01	42.96	0
MANIPULATION	1973.4	1	1973.37	75.83	0
SESSION	1097.4	7	156.77	6.02	0
SUBJECT	1870.1	3	623.37	23.95	0
TOUCH*VISION	69.2	2	34.61	1.33	0.2647
TOUCH*MANIPULATION	2.2	1	2.24	0.09	0.7692
TOUCH*SESSION	50.7	7	7.25	0.28	0.9625
TOUCH*SUBJECT	39	3	13.01	0.5	0.6824
VISION*MANIPULATION	88.3	2	44.17	1.7	0.1835
VISION*SESSION	239.2	14	17.08	0.66	0.8182
VISION*SUBJECT	252.9	6	42.14	1.62	0.1378
MANIPULATION*SESSION	17.6	7	2.51	0.1	0.9985
MANIPULATION*SUBJECT	540.3	3	180.1	6.92	0.0001
SESSION*SUBJECT	464.2	21	22.11	0.85	0.6589
TOUCH*VISION*MANIPULATION	1.7	2	0.87	0.03	0.9672
TOUCH*VISION*SESSION	153.5	14	10.96	0.42	0.9688
TOUCH*VISION*SUBJECT	137.7	6	22.95	0.88	0.5073
TOUCH*MANIPULATION*SESSION	105	7	15.01	0.58	0.7755
TOUCH*MANIPULATION*SUBJECT	24.6	3	8.2	0.32	0.8145
TOUCH*SESSION*SUBJECT	174.4	21	8.31	0.32	0.9986
VISION*MANIPULATION*SESSION	226	14	16.14	0.62	0.8503
VISION*MANIPULATION*SUBJECT	179	6	29.83	1.15	0.3328
VISION*SESSION*SUBJECT	576.1	42	13.72	0.53	0.9947
MANIPULATION*SESSION*SUBJECT	332	21	15.81	0.61	0.9162
TOUCH*VISION*MANIPULATION*SESSION	77.6	14	5.55	0.21	0.9991
TOUCH*VISION*MANIPULATION*SUBJECT	10.1	6	1.69	0.06	0.9989
TOUCH*VISION*SESSION*SUBJECT	287.9	42	6.85	0.26	1
TOUCH*MANIPULATION*SESSION*SUBJECT	264.4	21	12.59	0.48	0.9765
VISION*MANIPULATION*SESSION*SUBJECT	582	42	13.86	0.53	0.9942
TOUCH*VISION*MANIPULATION*SESSION*SUBJECT	396	42	9.43	0.36	0.9999
Error	49968.2	1920	26.03		
Total	62597.1	2303			

Constrained (Type III) sums of squares.

Annex 1- Figure 6– ‘Dispersion in trajectory’ raw data ANOVA results without segment condition for study 1.

Analysis of Variance

Source	Sum Sq.	d.f.	Mean Sq.	F	Prob>F
VISION	146.052	2	73.0262	2269.2	0
SESSION	70.932	7	10.1331	314.87	0
SUBJECT	208.145	3	69.3817	2155.95	0
SEGMENT	207.69	5	41.538	1290.74	0
MANIPULATION	29.576	1	29.5762	919.04	0
VISION*SESSION	10.789	14	0.7706	23.95	0
VISION*SUBJECT	10.365	6	1.7274	53.68	0
VISION*SEGMENT	18.285	10	1.8285	56.82	0
VISION*MANIPULATION	1.78	2	0.8901	27.66	0
SESSION*SUBJECT	23.735	21	1.1303	35.12	0
SESSION*SEGMENT	3.516	35	0.1005	3.12	0
SESSION*MANIPULATION	0.513	7	0.0734	2.28	0.0262
SUBJECT*SEGMENT	33.524	15	2.2349	69.45	0
SUBJECT*MANIPULATION	6.514	3	2.1714	67.47	0
SEGMENT*MANIPULATION	5.652	5	1.1303	35.12	0
VISION*SESSION*SUBJECT	8.549	42	0.2036	6.33	0
VISION*SESSION*SEGMENT	2.568	70	0.0367	1.14	0.2067
VISION*SESSION*MANIPULATION	1.202	14	0.0859	2.67	0.0007
VISION*SUBJECT*SEGMENT	4.71	30	0.157	4.88	0
VISION*SUBJECT*MANIPULATION	0.344	6	0.0574	1.78	0.0993
VISION*SEGMENT*MANIPULATION	1.023	10	0.1023	3.18	0.0005
SESSION*SUBJECT*SEGMENT	8.263	105	0.0787	2.45	0
SESSION*SUBJECT*MANIPULATION	3.02	21	0.1438	4.47	0
SESSION*SEGMENT*MANIPULATION	1.971	35	0.0563	1.75	0.0047
SUBJECT*SEGMENT*MANIPULATION	1.84	15	0.1227	3.81	0
VISION*SESSION*SUBJECT*SEGMENT	8.087	210	0.0385	1.2	0.0401
VISION*SESSION*SUBJECT*MANIPULATION	2.133	42	0.0508	1.58	0.0115
VISION*SESSION*SEGMENT*MANIPULATION	1.964	70	0.0281	0.87	0.7638
VISION*SUBJECT*SEGMENT*MANIPULATION	1.425	30	0.0475	1.48	0.0478
SESSION*SUBJECT*SEGMENT*MANIPULATION	3.297	105	0.0314	0.98	0.5515
VISION*SESSION*SUBJECT*SEGMENT*MANIPULATION	6.386	210	0.0304	0.94	0.6933
Error	37.073	1152	0.0322		
Total	870.927	2303			

Constrained (Type III) sums of squares.

Annex 1- Figure 7- ‘from-target-to-target duration’ raw data ANOVA results including Segment condition for study 1.

Analysis of Variance

Source	Sum Sq.	d.f.	Mean Sq.	F	Prob>F
VISION	2236	2	1118.01	140.53	0
SESSION	1097.4	7	156.77	19.7	0
SUBJECT	1870.1	3	623.37	78.35	0
SEGMENT	14556.8	5	2911.37	365.94	0
MANIPULATION	1973.4	1	1973.37	248.04	0
VISION*SESSION	239.2	14	17.08	2.15	0.0081
VISION*SUBJECT	252.9	6	42.14	5.3	0
VISION*SEGMENT	994.5	10	99.45	12.5	0
VISION*MANIPULATION	88.3	2	44.17	5.55	0.004
SESSION*SUBJECT	464.2	21	22.11	2.78	0
SESSION*SEGMENT	1127.2	35	32.2	4.05	0
SESSION*MANIPULATION	17.6	7	2.51	0.32	0.9473
SUBJECT*SEGMENT	10593.7	15	706.25	88.77	0
SUBJECT*MANIPULATION	540.3	3	180.1	22.64	0
SEGMENT*MANIPULATION	1207.8	5	241.56	30.36	0
VISION*SESSION*SUBJECT	576.1	42	13.72	1.72	0.0031
VISION*SESSION*SEGMENT	910	70	13	1.63	0.001
VISION*SESSION*MANIPULATION	226	14	16.14	2.03	0.0134
VISION*SUBJECT*SEGMENT	2193.7	30	73.12	9.19	0
VISION*SUBJECT*MANIPULATION	179	6	29.83	3.75	0.0011
VISION*SEGMENT*MANIPULATION	287.4	10	28.74	3.61	0.0001
SESSION*SUBJECT*SEGMENT	1943.7	105	18.51	2.33	0
SESSION*SUBJECT*MANIPULATION	332	21	15.81	1.99	0.0051
SESSION*SEGMENT*MANIPULATION	326.6	35	9.33	1.17	0.2269
SUBJECT*SEGMENT*MANIPULATION	2135.4	15	142.36	17.89	0
VISION*SESSION*SUBJECT*SEGMENT	1957.3	210	9.32	1.17	0.0615
VISION*SESSION*SUBJECT*MANIPULATION	582	42	13.86	1.74	0.0026
VISION*SESSION*SEGMENT*MANIPULATION	582.9	70	8.33	1.05	0.3764
VISION*SUBJECT*SEGMENT*MANIPULATION	728.4	30	24.28	3.05	0
SESSION*SUBJECT*SEGMENT*MANIPULATION	1407.8	105	13.41	1.69	0
VISION*SESSION*SUBJECT*SEGMENT*MANIPULATION	1804	210	8.59	1.08	0.2255
Error	9165.3	1152	7.96		
Total	62597.1	2303			

Constrained (Type III) sums of squares.

Annex 1- Figure 8- ‘Dispersion in trajectory’ raw data ANOVA results including Segment condition for study 1.

Analysis of Variance

Source	Sum Sq.	d.f.	Mean Sq.	F	Prob>F
VISION	21.5	1	21.46	2.36	0.125
MANIPULATION	710	1	709.97	77.95	0
SESSION	1987	1	1987.01	218.15	0
POSITION	2896.5	1	2896.51	318	0
GENDER	106.8	1	106.8	11.73	0.0006
VISION*MANIPULATION	8.7	1	8.67	0.95	0.3294
VISION*SESSION	56.3	1	56.28	6.18	0.0131
VISION*POSITION	27.1	1	27.1	2.98	0.0848
VISION*GENDER	8.4	1	8.38	0.92	0.3376
MANIPULATION*SESSION	0.1	1	0.11	0.01	0.9141
MANIPULATION*POSITION	4.4	1	4.42	0.49	0.4863
MANIPULATION*GENDER	0	1	0	0	0.9935
SESSION*POSITION	282.5	1	282.52	31.02	0
SESSION*GENDER	91.2	1	91.19	10.01	0.0016
POSITION*GENDER	105.4	1	105.36	11.57	0.0007
VISION*MANIPULATION*SESSION	2.9	1	2.88	0.32	0.5737
VISION*MANIPULATION*POSITION	15.7	1	15.74	1.73	0.1889
VISION*MANIPULATION*GENDER	7.9	1	7.91	0.87	0.3515
VISION*SESSION*POSITION	18	1	17.97	1.97	0.1604
VISION*SESSION*GENDER	19.2	1	19.15	2.1	0.1473
VISION*POSITION*GENDER	12	1	12.02	1.32	0.2509
MANIPULATION*SESSION*POSITION	0	1	0.02	0	0.9589
MANIPULATION*SESSION*GENDER	0.1	1	0.06	0.01	0.9359
MANIPULATION*POSITION*GENDER	65.2	1	65.17	7.15	0.0076
SESSION*POSITION*GENDER	1.2	1	1.2	0.13	0.717
VISION*MANIPULATION*SESSION*POSITION	10.1	1	10.14	1.11	0.2915
VISION*MANIPULATION*SESSION*GENDER	5.7	1	5.65	0.62	0.4309
VISION*MANIPULATION*POSITION*GENDER	0.4	1	0.44	0.05	0.827
VISION*SESSION*POSITION*GENDER	2.8	1	2.79	0.31	0.5802
MANIPULATION*SESSION*POSITION*GENDER	11.5	1	11.51	1.26	0.2612
VISION*MANIPULATION*SESSION*POSITION*GENDER	4.6	1	4.57	0.5	0.4788
Error	11367.4	1248	9.11		
Total	17850.4	1279			

Constrained (Type III) sums of squares.

Annex 1- Figure 9- ‘Time’ raw data ANOVA results for study 2.

Analysis of Variance

Source	Sum Sq.	d.f.	Mean Sq.	F	Prob>F
VISION	3825063.1	1	3825063.1	22.97	0
MANIPULATION	243708	1	243708	1.46	0.2267
SESSION	105342.6	1	105342.6	0.63	0.4266
POSITION	3967400.5	1	3967400.5	23.82	0
GENDER	121953.2	1	121953.2	0.73	0.3923
VISION*MANIPULATION	28200.1	1	28200.1	0.17	0.6808
VISION*SESSION	449325.3	1	449325.3	2.7	0.1007
VISION*POSITION	1532641.6	1	1532641.6	9.2	0.0025
VISION*GENDER	784872.2	1	784872.2	4.71	0.0301
MANIPULATION*SESSION	358182.6	1	358182.6	2.15	0.1428
MANIPULATION*POSITION	3901315.3	1	3901315.3	23.42	0
MANIPULATION*GENDER	1686498	1	1686498	10.13	0.0015
SESSION*POSITION	108412.8	1	108412.8	0.65	0.4199
SESSION*GENDER	145180.8	1	145180.8	0.87	0.3507
POSITION*GENDER	390391.7	1	390391.7	2.34	0.126
VISION*MANIPULATION*SESSION	582343.1	1	582343.1	3.5	0.0617
VISION*MANIPULATION*POSITION	328320.3	1	328320.3	1.97	0.1606
VISION*MANIPULATION*GENDER	175687.5	1	175687.5	1.05	0.3046
VISION*SESSION*POSITION	270572	1	270572	1.62	0.2027
VISION*SESSION*GENDER	1690856.6	1	1690856.6	10.15	0.0015
VISION*POSITION*GENDER	10465.3	1	10465.3	0.06	0.8021
MANIPULATION*SESSION*POSITION	1786226.5	1	1786226.5	10.72	0.0011
MANIPULATION*SESSION*GENDER	4089.8	1	4089.8	0.02	0.8755
MANIPULATION*POSITION*GENDER	25974	1	25974	0.16	0.693
SESSION*POSITION*GENDER	1835877	1	1835877	11.02	0.0009
VISION*MANIPULATION*SESSION*POSITION	110149.9	1	110149.9	0.66	0.4162
VISION*MANIPULATION*SESSION*GENDER	3544.5	1	3544.5	0.02	0.884
VISION*MANIPULATION*POSITION*GENDER	125215.3	1	125215.3	0.75	0.3861
VISION*SESSION*POSITION*GENDER	1212658.1	1	1212658.1	7.28	0.0071
MANIPULATION*SESSION*POSITION*GENDER	231125	1	231125	1.39	0.239
VISION*MANIPULATION*SESSION*POSITION*GENDER	577405.2	1	577405.2	3.47	0.0629
Error	207864366.1	1248	166558		
Total	234483363.8	1279			

Constrained (Type III) sums of squares.

Annex 1- Figure 10- ‘Precision’ raw data ANOVA results for study 2.

Analysis of Variance

Source	Sum Sq.	d.f.	Mean Sq.	F	Prob>F
VISION	5707.5	3	1902.49	321.62	0
MANIPULATION	482.2	1	482.19	81.51	0
SESSION	427.6	1	427.65	72.29	0
GENDER	7.5	1	7.5	1.27	0.2603
VISION*MANIPULATION	36.5	3	12.17	2.06	0.1041
VISION*SESSION	73.7	3	24.58	4.16	0.0061
VISION*GENDER	64.9	3	21.65	3.66	0.0121
MANIPULATION*SESSION	2.9	1	2.88	0.49	0.4858
MANIPULATION*GENDER	13.9	1	13.87	2.34	0.126
SESSION*GENDER	51.8	1	51.83	8.76	0.0031
VISION*MANIPULATION*SESSION	15.8	3	5.26	0.89	0.446
VISION*MANIPULATION*GENDER	25.1	3	8.37	1.42	0.2366
VISION*SESSION*GENDER	21.5	3	7.18	1.21	0.3034
MANIPULATION*SESSION*GENDER	6.7	1	6.69	1.13	0.2876
VISION*MANIPULATION*SESSION*GENDER	11.4	3	3.8	0.64	0.5873
Error	7382.5	1248	5.92		
Total	14331.6	1279			

Constrained (Type III) sums of squares.

Annex 1- Figure 11- ‘Time’ raw data ANOVA results for straight ahead monitor position for study 2.

Analysis of Variance

Source	Sum Sq.	d.f.	Mean Sq.	F	Prob>F
VISION	138703235.5	3	46234411.8	200.86	0
MANIPULATION	8528996.3	1	8528996.3	37.05	0
SESSION	531746.8	1	531746.8	2.31	0.1288
GENDER	132580.3	1	132580.3	0.58	0.448
VISION*MANIPULATION	5040947	3	1680315.7	7.3	0.0001
VISION*SESSION	683906.9	3	227969	0.99	0.3965
VISION*GENDER	1996997.2	3	665665.7	2.89	0.0343
MANIPULATION*SESSION	1714124.4	1	1714124.4	7.45	0.0064
MANIPULATION*GENDER	380776.5	1	380776.5	1.65	0.1986
SESSION*GENDER	101335.4	1	101335.4	0.44	0.5071
VISION*MANIPULATION*SESSION	1235630.9	3	411877	1.79	0.1473
VISION*MANIPULATION*GENDER	1025243.1	3	341747.7	1.48	0.217
VISION*SESSION*GENDER	3395183.6	3	1131727.9	4.92	0.0021
MANIPULATION*SESSION*GENDER	68606	1	68606	0.3	0.5852
VISION*MANIPULATION*SESSION*GENDER	1079259.4	3	359753.1	1.56	0.1966
Error	287265666.8	1248	230180.8		
Total	451884236	1279			

Constrained (Type III) sums of squares.

Annex 1- Figure 12- ‘Precision’ raw data ANOVA results for straight ahead monitor position for study 2.

Analysis of Variance

Source	Sum Sq.	d.f.	Mean Sq.	F	Prob>F
VISION	8840.1	3	2946.71	321.9	0
MANIPULATION	864.9	1	864.94	94.49	0
SESSION	1788.9	1	1788.88	195.42	0
GENDER	317.9	1	317.87	34.72	0
VISION*MANIPULATION	169.5	3	56.5	6.17	0.0004
VISION*SESSION	454.8	3	151.62	16.56	0
VISION*GENDER	186.2	3	62.07	6.78	0.0002
MANIPULATION*SESSION	0.3	1	0.3	0.03	0.8554
MANIPULATION*GENDER	47.1	1	47.15	5.15	0.0234
SESSION*GENDER	58.3	1	58.25	6.36	0.0118
VISION*MANIPULATION*SESSION	1.9	3	0.64	0.07	0.976
VISION*MANIPULATION*GENDER	15.5	3	5.17	0.56	0.6382
VISION*SESSION*GENDER	52.7	3	17.55	1.92	0.1249
MANIPULATION*SESSION*GENDER	0.1	1	0.07	0.01	0.9321
VISION*MANIPULATION*SESSION*GENDER	9.8	3	3.26	0.36	0.7848
Error	11424.2	1248	9.15		
Total	24232.2	1279			

Constrained (Type III) sums of squares.

Annex 1- Figure 13- ‘Time’ raw data ANOVA results for side way monitor position for study 2.

Analysis of Variance

Source	Sum Sq.	d.f.	Mean Sq.	F	Prob>F
VISION	69388227.8	3	23129409.3	166.06	0
MANIPULATION	584178.9	1	584178.9	4.19	0.0408
SESSION	115539	1	115539	0.83	0.3626
GENDER	2057370.7	1	2057370.7	14.77	0.0001
VISION*MANIPULATION	2153500.7	3	717833.6	5.15	0.0015
VISION*SESSION	921470.5	3	307156.8	2.21	0.0858
VISION*GENDER	5565910.9	3	1855303.6	13.32	0
MANIPULATION*SESSION	3078.3	1	3078.3	0.02	0.8818
MANIPULATION*GENDER	320582.9	1	320582.9	2.3	0.1295
SESSION*GENDER	605824.5	1	605824.5	4.35	0.0372
VISION*MANIPULATION*SESSION	1113960	3	371320	2.67	0.0465
VISION*MANIPULATION*GENDER	2357665.6	3	785888.5	5.64	0.0008
VISION*SESSION*GENDER	1433545.5	3	477848.5	3.43	0.0165
MANIPULATION*SESSION*GENDER	746669.7	1	746669.7	5.36	0.0208
VISION*MANIPULATION*SESSION*GENDER	413650.5	3	137883.5	0.99	0.3967
Error	173830115.5	1248	139287		
Total	261611291	1279			

Constrained (Type III) sums of squares.

Annex 1- Figure 14- ‘Precision’ raw data ANOVA results for side way monitor position for study 2.

Analysis of Variance

Source	Sum Sq.	d.f.	Mean Sq.	F	Prob>F
VISION	2.15	1	2.146	0.25	0.6159
MANIPULATION	71	1	70.997	8.38	0.0047
SESSION	198.7	1	198.701	23.45	0
POSITION	289.65	1	289.651	34.18	0
GENDER	10.68	1	10.68	1.26	0.2644
VISION*MANIPULATION	0.87	1	0.867	0.1	0.7498
VISION*SESSION	5.63	1	5.628	0.66	0.4171
VISION*POSITION	2.71	1	2.71	0.32	0.573
VISION*GENDER	0.84	1	0.838	0.1	0.7538
MANIPULATION*SESSION	0.01	1	0.011	0	0.9718
MANIPULATION*POSITION	0.44	1	0.442	0.05	0.8199
MANIPULATION*GENDER	0	1	0	0	0.9979
SESSION*POSITION	28.25	1	28.252	3.33	0.071
SESSION*GENDER	9.12	1	9.119	1.08	0.3022
POSITION*GENDER	10.54	1	10.536	1.24	0.2676
VISION*MANIPULATION*SESSION	0.29	1	0.288	0.03	0.854
VISION*MANIPULATION*POSITION	1.57	1	1.574	0.19	0.6674
VISION*MANIPULATION*GENDER	0.79	1	0.791	0.09	0.7606
VISION*SESSION*POSITION	1.8	1	1.797	0.21	0.6462
VISION*SESSION*GENDER	1.92	1	1.915	0.23	0.6355
VISION*POSITION*GENDER	1.2	1	1.202	0.14	0.7073
MANIPULATION*SESSION*POSITION	0	1	0.002	0	0.9866
MANIPULATION*SESSION*GENDER	0.01	1	0.006	0	0.979
MANIPULATION*POSITION*GENDER	6.52	1	6.517	0.77	0.3827
SESSION*POSITION*GENDER	0.12	1	0.12	0.01	0.9056
VISION*MANIPULATION*SESSION*POSITION	1.01	1	1.014	0.12	0.7301
VISION*MANIPULATION*SESSION*GENDER	0.57	1	0.565	0.07	0.7967
VISION*MANIPULATION*POSITION*GENDER	0.04	1	0.044	0.01	0.943
VISION*SESSION*POSITION*GENDER	0.28	1	0.279	0.03	0.8564
MANIPULATION*SESSION*POSITION*GENDER	1.15	1	1.151	0.14	0.7133
VISION*MANIPULATION*SESSION*POSITION*GENDER	0.46	1	0.457	0.05	0.8168
Error	813.48	96	8.474		
Total	1461.78	127			

Constrained (Type III) sums of squares.

Annex 1- Figure 15- ‘Time’ mean data ANOVA results for study 2

Analysis of Variance

Source	Sum Sq.	d.f.	Mean Sq.	F	Prob>F
VISION	382265.8	1	382265.8	3.87	0.0522
MANIPULATION	24392.9	1	24392.9	0.25	0.6205
SESSION	10603.3	1	10603.3	0.11	0.744
POSITION	397497.6	1	397497.6	4.02	0.0478
GENDER	12109.6	1	12109.6	0.12	0.7271
VISION*MANIPULATION	2784.4	1	2784.4	0.03	0.8671
VISION*SESSION	44962.5	1	44962.5	0.45	0.5017
VISION*POSITION	153250.3	1	153250.3	1.55	0.2162
VISION*GENDER	78457.5	1	78457.5	0.79	0.3753
MANIPULATION*SESSION	35744.7	1	35744.7	0.36	0.5491
MANIPULATION*POSITION	390175.7	1	390175.7	3.95	0.0498
MANIPULATION*GENDER	168417.6	1	168417.6	1.7	0.195
SESSION*POSITION	10859.7	1	10859.7	0.11	0.741
SESSION*GENDER	14386.3	1	14386.3	0.15	0.7037
POSITION*GENDER	38815.9	1	38815.9	0.39	0.5324
VISION*MANIPULATION*SESSION	58610.3	1	58610.3	0.59	0.4432
VISION*MANIPULATION*POSITION	32736	1	32736	0.33	0.5664
VISION*MANIPULATION*GENDER	17554.7	1	17554.7	0.18	0.6744
VISION*SESSION*POSITION	26941	1	26941	0.27	0.6029
VISION*SESSION*GENDER	169143.8	1	169143.8	1.71	0.194
VISION*POSITION*GENDER	1052.3	1	1052.3	0.01	0.918
MANIPULATION*SESSION*POSITION	178727.3	1	178727.3	1.81	0.1819
MANIPULATION*SESSION*GENDER	424.1	1	424.1	0	0.9479
MANIPULATION*POSITION*GENDER	2583	1	2583	0.03	0.8719
SESSION*POSITION*GENDER	183845.3	1	183845.3	1.86	0.1759
VISION*MANIPULATION*SESSION*POSITION	11081.9	1	11081.9	0.11	0.7385
VISION*MANIPULATION*SESSION*GENDER	328.3	1	328.3	0	0.9542
VISION*MANIPULATION*POSITION*GENDER	12620.6	1	12620.6	0.13	0.7217
VISION*SESSION*POSITION*GENDER	121339.7	1	121339.7	1.23	0.2707
MANIPULATION*SESSION*POSITION*GENDER	23193.2	1	23193.2	0.23	0.6292
VISION*MANIPULATION*SESSION*POSITION*GENDER	57502.9	1	57502.9	0.58	0.4476
Error	9491382.8	96	98868.6		
Total	12153791.1	127			

Constrained (Type III) sums of squares.

Annex 1- Figure 16- ‘Precision’ mean data ANOVA results for study 2.

Analysis of Variance

Source	Sum Sq.	d.f.	Mean Sq.	F	Prob>F
VISION	570.75	3	190.249	29.83	0
MANIPULATION	48.22	1	48.219	7.56	0.0071
SESSION	42.76	1	42.765	6.71	0.0111
GENDER	0.75	1	0.75	0.12	0.7323
VISION*MANIPULATION	3.65	3	1.217	0.19	0.9024
VISION*SESSION	7.37	3	2.458	0.39	0.7637
VISION*GENDER	6.49	3	2.165	0.34	0.7969
MANIPULATION*SESSION	0.29	1	0.288	0.05	0.8323
MANIPULATION*GENDER	1.39	1	1.387	0.22	0.6421
SESSION*GENDER	5.18	1	5.183	0.81	0.3696
VISION*MANIPULATION*SESSION	1.58	3	0.526	0.08	0.9694
VISION*MANIPULATION*GENDER	2.51	3	0.837	0.13	0.9413
VISION*SESSION*GENDER	2.15	3	0.718	0.11	0.9526
MANIPULATION*SESSION*GENDER	0.67	1	0.669	0.1	0.7466
VISION*MANIPULATION*SESSION*GENDER	1.14	3	0.38	0.06	0.9808
Error	612.25	96	6.378		
Total	1307.17	127			

Annex 1- Figure 17- ‘Time’ mean data ANOVA results for straight ahead monitor position for study 2.

Analysis of Variance

Source	Sum Sq.	d.f.	Mean Sq.	F	Prob>F
VISION	13869642.3	3	4623214.1	26.62	0
MANIPULATION	852654.8	1	852654.8	4.91	0.0291
SESSION	53097.3	1	53097.3	0.31	0.5816
GENDER	13101.8	1	13101.8	0.08	0.7842
VISION*MANIPULATION	503949.5	3	167983.2	0.97	0.4115
VISION*SESSION	68377.6	3	22792.5	0.13	0.9413
VISION*GENDER	199169.1	3	66389.7	0.38	0.766
MANIPULATION*SESSION	171478.3	1	171478.3	0.99	0.3229
MANIPULATION*GENDER	37778.1	1	37778.1	0.22	0.642
SESSION*GENDER	10278.2	1	10278.2	0.06	0.8083
VISION*MANIPULATION*SESSION	123997.3	3	41332.4	0.24	0.8697
VISION*MANIPULATION*GENDER	102778.2	3	34259.4	0.2	0.898
VISION*SESSION*GENDER	339682.8	3	113227.6	0.65	0.5836
MANIPULATION*SESSION*GENDER	6888.4	1	6888.4	0.04	0.8426
VISION*MANIPULATION*SESSION*GENDER	107662.8	3	35887.6	0.21	0.8916
Error	16672761.3	96	173674.6		
Total	33133297.6	127			

Annex 1- Figure 18- ‘Precision’ mean data ANOVA results for straight ahead monitor position for study 2.

Analysis of Variance

Source	Sum Sq.	d.f.	Mean Sq.	F	Prob>F
VISION	884.01	3	294.671	34.75	0
MANIPULATION	86.49	1	86.494	10.2	0.0019
SESSION	178.89	1	178.888	21.1	0
GENDER	31.79	1	31.787	3.75	0.0558
VISION*MANIPULATION	16.95	3	5.65	0.67	0.5748
VISION*SESSION	45.48	3	15.162	1.79	0.1546
VISION*GENDER	18.62	3	6.207	0.73	0.5354
MANIPULATION*SESSION	0.03	1	0.03	0	0.9524
MANIPULATION*GENDER	4.71	1	4.715	0.56	0.4577
SESSION*GENDER	5.83	1	5.825	0.69	0.4093
VISION*MANIPULATION*SESSION	0.19	3	0.064	0.01	0.9991
VISION*MANIPULATION*GENDER	1.55	3	0.517	0.06	0.9802
VISION*SESSION*GENDER	5.27	3	1.755	0.21	0.8913
MANIPULATION*SESSION*GENDER	0.01	1	0.007	0	0.9777
VISION*MANIPULATION*SESSION*GENDER	0.98	3	0.326	0.04	0.9899
Error	814.06	96	8.48		
Total	2094.87	127			

Annex 1- Figure 19- ‘Time’ mean data ANOVA results for side way monitor position for study 2.

Analysis of Variance

Source	Sum Sq.	d.f.	Mean Sq.	F	Prob>F
VISION	6939027.8	3	2313009.3	33.87	0
MANIPULATION	58396.5	1	58396.5	0.86	0.3574
SESSION	11552	1	11552	0.17	0.6818
GENDER	205761.1	1	205761.1	3.01	0.0858
VISION*MANIPULATION	215278.1	3	71759.4	1.05	0.3738
VISION*SESSION	92038.8	3	30679.6	0.45	0.7184
VISION*GENDER	555972.4	3	185324.1	2.71	0.0491
MANIPULATION*SESSION	312.5	1	312.5	0	0.9462
MANIPULATION*GENDER	32131.1	1	32131.1	0.47	0.4944
SESSION*GENDER	60639	1	60639	0.89	0.3484
VISION*MANIPULATION*SESSION	111839.8	3	37279.9	0.55	0.6521
VISION*MANIPULATION*GENDER	235891.1	3	78630.4	1.15	0.3324
VISION*SESSION*GENDER	143082.8	3	47694.3	0.7	0.5552
MANIPULATION*SESSION*GENDER	74981.3	1	74981.3	1.1	0.2973
VISION*MANIPULATION*SESSION*GENDER	41401.6	3	13800.5	0.2	0.8947
Error	6555364.5	96	68285		
Total	15333670.5	127			

Annex 1- Figure 20- ‘Precision’ mean data ANOVA results for side way monitor position in study 2.

RM ANOVA TIME ANALYSIS

Measure:Time

Source		Type III Sum of Squares	df	Mean Square	F	Sig.	Partial Eta Squared	Noncent. Parameter	Observed Power
Vision	Sphericity Assumed	285,374	3	95,125	59,288	,000	,894	177,863	1,000
	Greenhouse-Geisser	285,374	1,276	223,566	59,288	,000	,894	75,679	1,000
	Huynh-Feldt	285,374	1,435	198,904	59,288	,000	,894	85,062	1,000
	Lower-bound	285,374	1,000	285,374	59,288	,000	,894	59,288	1,000
Error(Vision)	Sphericity Assumed	33,694	21	1,604					
	Greenhouse-Geisser	33,694	8,935	3,771					
	Huynh-Feldt	33,694	10,043	3,355					
	Lower-bound	33,694	7,000	4,813					
Manipulation	Sphericity Assumed	24,115	1	24,115	26,345	,001	,790	26,345	,992
	Greenhouse-Geisser	24,115	1,000	24,115	26,345	,001	,790	26,345	,992
	Huynh-Feldt	24,115	1,000	24,115	26,345	,001	,790	26,345	,992
	Lower-bound	24,115	1,000	24,115	26,345	,001	,790	26,345	,992
Error(Manipulation)	Sphericity Assumed	6,408	7	,915					
	Greenhouse-Geisser	6,408	7,000	,915					
	Huynh-Feldt	6,408	7,000	,915					
	Lower-bound	6,408	7,000	,915					
Vision * Manipulation	Sphericity Assumed	1,825	3	,608	2,269	,110	,245	6,808	,493
	Greenhouse-Geisser	1,825	2,122	,860	2,269	,136	,245	4,817	,398
	Huynh-Feldt	1,825	3,000	,608	2,269	,110	,245	6,808	,493
	Lower-bound	1,825	1,000	1,825	2,269	,176	,245	2,269	,257
Error (Vision*Manipulation)	Sphericity Assumed	5,628	21	,268					
	Greenhouse-Geisser	5,628	14,857	,379					
	Huynh-Feldt	5,628	21,000	,268					
	Lower-bound	5,628	7,000	,804					

Annex 1- Figure 21- ‘Time’ two-way RM ANOVA results for straight ahead monitor position in study 2.

RM ANOVA PRECISION ANALYSIS

Measure:Precision

Source		Type III Sum of Squares	df	Mean Square	F	Sig.	Partial Eta Squared	Noncent. Parameter	Observed Power
Vision	Sphericity Assumed	6935161,774	3	2311720,591	27,997	,000	,800	83,991	1,000
	Greenhouse-Geisser	6935161,774	2,023	3427488,779	27,997	,000	,800	56,649	1,000
	Huynh-Feldt	6935161,774	2,851	2432733,209	27,997	,000	,800	79,813	1,000
	Lower-bound	6935161,774	1,000	6935161,774	27,997	,001	,800	27,997	,994
Error(Vision)	Sphericity Assumed	1733981,728	21	82570,558					
	Greenhouse-Geisser	1733981,728	14,164	122423,819					
	Huynh-Feldt	1733981,728	19,955	86892,915					
	Lower-bound	1733981,728	7,000	247711,675					
Manipulation	Sphericity Assumed	426449,813	1	426449,813	30,807	,001	,815	30,807	,997
	Greenhouse-Geisser	426449,813	1,000	426449,813	30,807	,001	,815	30,807	,997
	Huynh-Feldt	426449,813	1,000	426449,813	30,807	,001	,815	30,807	,997
	Lower-bound	426449,813	1,000	426449,813	30,807	,001	,815	30,807	,997
Error(Manipulation)	Sphericity Assumed	96899,011	7	13842,716					
	Greenhouse-Geisser	96899,011	7,000	13842,716					
	Huynh-Feldt	96899,011	7,000	13842,716					
	Lower-bound	96899,011	7,000	13842,716					
Vision * Manipulation	Sphericity Assumed	252047,349	3	84015,783	7,278	,002	,510	21,834	,959
	Greenhouse-Geisser	252047,349	1,992	126546,554	7,278	,007	,510	14,496	,872
	Huynh-Feldt	252047,349	2,782	90593,487	7,278	,002	,510	20,249	,948
	Lower-bound	252047,349	1,000	252047,349	7,278	,031	,510	7,278	,640
Error (Vision*Manipulation)	Sphericity Assumed	242419,163	21	11543,770					
	Greenhouse-Geisser	242419,163	13,942	17387,498					
	Huynh-Feldt	242419,163	19,475	12447,546					
	Lower-bound	242419,163	7,000	34631,309					

Annex 1- Figure 22- ‘Precision’ RM ANOVA results for straight ahead monitor position in study 2.

Analysis of Variance

Source	Sum Sq.	d.f.	Mean Sq.	F	Prob>F
VISION	5707.5	3	1902.49	298.56	0
MANIPULATION	482.2	1	482.19	75.67	0
VISION*MANIPULATION	36.5	3	12.17	1.91	0.1261
Error	8105.4	1272	6.37		
Total	14331.6	1279			

Annex 1- Figure 23- 'Time' two-way ANOVA results for straight ahead monitor position in study 2.

Analysis of Variance

Source	Sum Sq.	d.f.	Mean Sq.	F	Prob>F
VISION	1.38703e+08	3	46234411.8	196.29	1.31961e-104
MANIPULATION	8.529e+06	1	8528996.3	36.21	2.3134e-09
VISION*MANIPULATION	5.04095e+06	3	1680315.7	7.13	9.4235e-05
Error	2.99611e+08	1272	235543.3		
Total	4.51884e+08	1279			

Annex 1- Figure 24- 'Precision' two-way ANOVA results for straight ahead monitor position in study 2.

Analysis of Variance

Source	Sum Sq.	d.f.	Mean Sq.	F	Prob>F
VISION	95.399	3	31.7996	157.79	0
MANIPULATION	7.852	1	7.8522	38.96	0
SESSION	7.367	1	7.3665	36.55	0
SEGMENT	65.414	5	13.0829	64.92	0
VISION*MANIPULATION	0.589	3	0.1962	0.97	0.4046
VISION*SESSION	1.325	3	0.4418	2.19	0.0877
VISION*SEGMENT	9.407	15	0.6271	3.11	0.0001
MANIPULATION*SESSION	0.063	1	0.0633	0.31	0.5754
MANIPULATION*SEGMENT	0.968	5	0.1936	0.96	0.4412
SESSION*SEGMENT	0.456	5	0.0911	0.45	0.8119
VISION*MANIPULATION*SESSION	0.205	3	0.0682	0.34	0.7977
VISION*MANIPULATION*SEGMENT	1.062	15	0.0708	0.35	0.9893
VISION*SESSION*SEGMENT	0.769	15	0.0513	0.25	0.9982
MANIPULATION*SESSION*SEGMENT	0.119	5	0.0237	0.12	0.9885
VISION*MANIPULATION*SESSION*SEGMENT	0.43	15	0.0286	0.14	1
Error	135.425	672	0.2015		
Total	326.849	767			

Annex 1- Figure 25- 'from-target-to-target duration' trajectory mean data ANOVA results for direct, fisheye, undistorted and Oculus vision for study 2.

Analysis of Variance

Source	Sum Sq.	d.f.	Mean Sq.	F	Prob>F
VISION	89.013	2	44.5066	238.16	0
MANIPULATION	5.403	1	5.4026	28.91	0
SESSION	3.748	1	3.7484	20.06	0
SEGMENT	42.975	5	8.595	45.99	0
VISION*MANIPULATION	0.547	2	0.2734	1.46	0.2325
VISION*SESSION	0.638	2	0.3192	1.71	0.1823
VISION*SEGMENT	8.186	10	0.8186	4.38	0
MANIPULATION*SESSION	0.171	1	0.1707	0.91	0.3397
MANIPULATION*SEGMENT	0.612	5	0.1224	0.65	0.6579
SESSION*SEGMENT	0.28	5	0.0559	0.3	0.9133
VISION*MANIPULATION*SESSION	0.052	2	0.026	0.14	0.87
VISION*MANIPULATION*SEGMENT	0.832	10	0.0832	0.45	0.9239
VISION*SESSION*SEGMENT	0.634	10	0.0634	0.34	0.9702
MANIPULATION*SESSION*SEGMENT	0.104	5	0.0209	0.11	0.9898
VISION*MANIPULATION*SESSION*SEGMENT	0.272	10	0.0272	0.15	0.999
Error	94.188	504	0.1869		
Total	247.655	575			

Annex 1- Figure 26 - ‘from-target-to-target duration’ trajectory mean data ANOVA results for direct, undistorted and Oculus vision for study 2.

Analysis of Variance

Source	Sum Sq.	d.f.	Mean Sq.	F	Prob>F
VISION	13398.6	3	4466.19	80.62	0
MANIPULATION	773.3	1	773.25	13.96	0.0002
SESSION	186.7	1	186.75	3.37	0.0668
SEGMENT	9206	5	1841.19	33.23	0
VISION*MANIPULATION	97.4	3	32.48	0.59	0.6241
VISION*SESSION	200.5	3	66.83	1.21	0.3065
VISION*SEGMENT	4763.1	15	317.54	5.73	0
MANIPULATION*SESSION	194.7	1	194.68	3.51	0.0613
MANIPULATION*SEGMENT	1103.3	5	220.67	3.98	0.0014
SESSION*SEGMENT	186.5	5	37.3	0.67	0.6439
VISION*MANIPULATION*SESSION	135.9	3	45.28	0.82	0.4845
VISION*MANIPULATION*SEGMENT	1506.7	15	100.45	1.81	0.0294
VISION*SESSION*SEGMENT	669.7	15	44.65	0.81	0.6717
MANIPULATION*SESSION*SEGMENT	47.4	5	9.48	0.17	0.9733
VISION*MANIPULATION*SESSION*SEGMENT	531.4	15	35.43	0.64	0.8431
Error	37229	672	55.4		
Total	70230.2	767			

Annex 1- Figure 27- ‘Dispersion in trajectory’ mean data ANOVA results for direct, fisheye, undistorted and Oculus vision for study 2.

Analysis of Variance

Source	Sum Sq.	d.f.	Mean Sq.	F	Prob>F
VISION	24261.5	3	8087.16	192.6	0
MANIPULATION	292	1	292	6.95	0.0086
SESSION	403.2	1	403.18	9.6	0.002
SEGMENT	21541.6	5	4308.31	102.61	0
VISION*MANIPULATION	48.2	3	16.05	0.38	0.7658
VISION*SESSION	89.1	3	29.7	0.71	0.5479
VISION*SEGMENT	6504.3	15	433.62	10.33	0
MANIPULATION*SESSION	67.5	1	67.46	1.61	0.2054
MANIPULATION*SEGMENT	252.2	5	50.43	1.2	0.307
SESSION*SEGMENT	741.1	5	148.23	3.53	0.0037
VISION*MANIPULATION*SESSION	24.6	3	8.21	0.2	0.8994
VISION*MANIPULATION*SEGMENT	355.3	15	23.69	0.56	0.9026
VISION*SESSION*SEGMENT	327.8	15	21.85	0.52	0.9302
MANIPULATION*SESSION*SEGMENT	119.9	5	23.98	0.57	0.7223
VISION*MANIPULATION*SESSION*SEGMENT	113.4	15	7.56	0.18	0.9998
Error	28216.1	672	41.99		
Total	83357.7	767			

Annex 1- Figure 28 - ‘Average distance from the reference trajectory’ mean data ANOVA results for direct, fisheye, undistorted and Oculus vision for study 2.

Analysis of Variance

Source	Sum Sq.	d.f.	Mean Sq.	F	Prob>F
VISION	23678.4	2	11839.2	268.57	0
MANIPULATION	140.3	1	140.3	3.18	0.075
SESSION	319.3	1	319.3	7.24	0.0074
SEGMENT	17000.6	5	3400.1	77.13	0
VISION*MANIPULATION	13.3	2	6.6	0.15	0.8601
VISION*SESSION	88.2	2	44.1	1	0.3686
VISION*SEGMENT	6207.6	10	620.8	14.08	0
MANIPULATION*SESSION	43.2	1	43.2	0.98	0.3224
MANIPULATION*SEGMENT	357.3	5	71.5	1.62	0.1527
SESSION*SEGMENT	499.7	5	99.9	2.27	0.0467
VISION*MANIPULATION*SESSION	23.5	2	11.7	0.27	0.7663
VISION*MANIPULATION*SEGMENT	222.4	10	22.2	0.5	0.8871
VISION*SESSION*SEGMENT	307	10	30.7	0.7	0.7282
MANIPULATION*SESSION*SEGMENT	72.4	5	14.5	0.33	0.8957
VISION*MANIPULATION*SESSION*SEGMENT	87.4	10	8.7	0.2	0.9964
Error	22217.2	504	44.1		
Total	71277.9	575			

Annex 1- Figure 29 - ‘‘Average distance from the reference trajectory’ mean data ANOVA results for direct, undistorted and Oculus vision for study 2.

Analysis of Variance

Source	Sum Sq.	d.f.	Mean Sq.	F	Prob>F
VISION	5207.8	3	1735.94	223.07	1.03917e-121
MANIPULATION	1713.7	1	1713.71	220.21	6.82743e-47
VISION*MANIPULATION	237.3	3	79.1	10.16	1.23622e-06
Error	13011.7	1672	7.78		
Total	20726.3	1679			

Annex 1- Figure 30 - Novice visual feedback ‘time’ raw data ANOVA results for direct, fisheye, undistorted and Oculus vision for study 3.

Analysis of Variance

Source	Sum Sq.	d.f.	Mean Sq.	F	Prob>F
VISION	153.2	2	76.59	8.98	0.0001
MANIPULATION	2447.2	1	2447.16	287	0
COLOR	3.8	1	3.79	0.44	0.5053
VISION*MANIPULATION	35.9	2	17.96	2.11	0.1221
VISION*COLOR	42.1	2	21.04	2.47	0.0851
MANIPULATION*COLOR	3.4	1	3.37	0.39	0.5299
VISION*MANIPULATION*COLOR	20.4	2	10.22	1.2	0.3019
Error	12176.3	1428	8.53		
Total	14882.3	1439			

Annex 1- Figure 31 - Novice color feedback ‘time’ raw data ANOVA results for fisheye, undistorted and Oculus vision for study 3.

Analysis of Variance

Source	Sum Sq.	d.f.	Mean Sq.	F	Prob>F
VISION	71096786.5	3	23698928.8	78.96	0
MANIPULATION	123811.9	1	123811.9	0.41	0.5208
VISION*MANIPULATION	2024691.8	3	674897.3	2.25	0.0809
Error	501816112.1	1672	300129.3		
Total	574941397.4	1679			

Annex 1- Figure 32 - Novice visual feedback ‘precision’ raw data ANOVA results for direct, fisheye, undistorted and Oculus vision for study 3.

Analysis of Variance

Source	Sum Sq.	d.f.	Mean Sq.	F	Prob>F
VISION	48734271.7	2	24367135.8	79.1	0
MANIPULATION	103022.5	1	103022.5	0.33	0.5632
COLOR	303979.2	1	303979.2	0.99	0.3207
VISION*MANIPULATION	1023998.5	2	511999.3	1.66	0.1901
VISION*COLOR	888955.4	2	444477.7	1.44	0.2366
MANIPULATION*COLOR	114739.8	1	114739.8	0.37	0.5418
VISION*MANIPULATION*COLOR	615542	2	307771	1	0.3685
Error	439920284.4	1428	308067.4		
Total	491704793.5	1439			

Annex 1- Figure 33 - Novices *color feedback* 'precision' raw data ANOVA results for fisheye, undistorted and Oculus vision for study 3.

Analysis of Variance

Source	Sum Sq.	d.f.	Mean Sq.	F	Prob>F
VISION	6798.6	3	2266.2	78.09	0
MANIPULATION	236.8	1	236.83	8.16	0.0044
VISION*MANIPULATION	26.1	3	8.71	0.3	0.8254
Error	24144	832	29.02		
Total	31277.5	839			

Annex 1- Figure 34 – Six surgeons *visual feedback* 'time' raw data ANOVA results for direct, fisheye, undistorted and Oculus vision for study 3.

Analysis of Variance

Source	Sum Sq.	d.f.	Mean Sq.	F	Prob>F
VISION	539.2	2	269.608	8.47	0.0002
MANIPULATION	327.2	1	327.241	10.28	0.0014
COLOR	958.4	1	958.42	30.11	0
VISION*MANIPULATION	2.9	2	1.435	0.05	0.9559
VISION*COLOR	20.4	2	10.207	0.32	0.7258
MANIPULATION*COLOR	0.7	1	0.739	0.02	0.879
VISION*MANIPULATION*COLOR	12.4	2	6.191	0.19	0.8233
Error	22535.2	708	31.829		
Total	24396.5	719			

Annex 1- Figure 35- Six surgeons *color feedback* 'time' raw data ANOVA results for fisheye, undistorted and Oculus vision for study 3.

Analysis of Variance

Source	Sum Sq.	d.f.	Mean Sq.	F	Prob>F
VISION	38967622.54	3	12989207.5	51.49	0
MANIPULATION	3773.65	1	3773.7	0.01	0.9027
VISION*MANIPULATION	3972507.04	3	1324169	5.25	0.0014
Error	209901811.45	832	252285.8		
Total	252847413.33	839			

Annex 1- Figure 36 – Six surgeons *visual feedback* ‘precision’ raw data ANOVA results for direct, fisheye, undistorted and Oculus vision for study 3.

Analysis of Variance

Source	Sum Sq.	d.f.	Mean Sq.	F	Prob>F
VISION	29897581.7	2	14948790.9	53.7	0
MANIPULATION	57173.7	1	57173.7	0.21	0.6506
COLOR	207332.7	1	207332.7	0.74	0.3884
VISION*MANIPULATION	3768722.5	2	1884361.2	6.77	0.0012
VISION*COLOR	3002822.4	2	1501411.2	5.39	0.0047
MANIPULATION*COLOR	211219.8	1	211219.8	0.76	0.384
VISION*MANIPULATION*COLOR	2112.8	2	1056.4	0	0.9962
Error	197096659.2	708	278385.1		
Total	234243624.7	719			

Annex 1- Figure 37 – Six surgeons *color feedback* ‘precision’ raw data ANOVA results for fisheye, undistorted and Oculus vision for study 3.

Analysis of Variance

Source	Sum Sq.	d.f.	Mean Sq.	F	Prob>F
VISION	586.99	3	195.662	37.74	0
MANIPULATION	49.47	1	49.469	9.54	0.0024
VISION*MANIPULATION	28.81	3	9.604	1.85	0.1408
Error	684.29	132	5.184		
Total	1379.68	139			

Annex 1- Figure 38 - Expert surgeon *visual feedback* ‘time’ raw data ANOVA results for direct, fisheye, undistorted and Oculus vision for study 3.

Analysis of Variance

Source	Sum Sq.	d.f.	Mean Sq.	F	Prob>F
VISION	399.7	2	199.848	71.88	0
MANIPULATION	103.9	1	103.9	37.37	0
COLOR	218.21	1	218.214	78.49	0
VISION*MANIPULATION	2.65	2	1.326	0.48	0.622
VISION*COLOR	119.66	2	59.831	21.52	0
MANIPULATION*COLOR	0.66	1	0.656	0.24	0.6281
VISION*MANIPULATION*COLOR	0.8	2	0.402	0.14	0.8656
Error	300.27	108	2.78		
Total	1145.85	119			

Annex 1- Figure 39 - Expert surgeon *color feedback* 'time' raw data ANOVA results for fisheye, undistorted and Oculus vision for study 3.

Analysis of Variance

Source	Sum Sq.	d.f.	Mean Sq.	F	Prob>F
VISION	1951284	3	650428	10.3	0
MANIPULATION	484324.8	1	484324.8	7.67	0.0064
VISION*MANIPULATION	472947.4	3	157649.1	2.5	0.0626
Error	8335728.3	132	63149.5		
Total	11103291.9	139			

Annex 1- Figure 40 - Expert surgeon visual feedback 'precision' raw data ANOVA results for direct, fisheye, undistorted and Oculus vision for study 3.

Analysis of Variance

Source	Sum Sq.	d.f.	Mean Sq.	F	Prob>F
VISION	910490.5	2	455245.2	8.15	0.0005
MANIPULATION	134938.1	1	134938.1	2.41	0.1231
COLOR	824357.6	1	824357.6	14.75	0.0002
VISION*MANIPULATION	258227.3	2	129113.7	2.31	0.1041
VISION*COLOR	263767.1	2	131883.6	2.36	0.0993
MANIPULATION*COLOR	207667.2	1	207667.2	3.72	0.0565
VISION*MANIPULATION*COLOR	284006.5	2	142003.2	2.54	0.0835
Error	6035825.4	108	55887.3		
Total	8919279.7	119			

Annex 1- Figure 41- Expert surgeon color feedback 'precision' raw data ANOVA results for fisheye, undistorted and Oculus vision for study 3.

Analysis of Variance

Source	Sum Sq.	d.f.	Mean Sq.	F	Prob>F
EXPERTISE	12331.3	2	6165.66	429.51	0
VISION	3900.3	3	1300.11	90.57	0
MANIPULATION	510.7	1	510.71	35.58	0
EXPERTISE*VISION	1716.5	6	286.08	19.93	0
EXPERTISE*MANIPULATION	137.2	2	68.59	4.78	0.0085
VISION*MANIPULATION	101.1	3	33.72	2.35	0.0707
EXPERTISE*VISION*MANIPULATION	33.6	6	5.6	0.39	0.8859
Error	37840	2636	14.36		
Total	68452.1	2659			

Annex 1- Figure 42 - Novices, surgeons and expert surgeon *visual feedback* ‘time’ raw data ANOVA results for direct, fisheye, undistorted and Oculus 3D vision for study 3.

Analysis of Variance

Source	Sum Sq.	d.f.	Mean Sq.	F	Prob>F
EXPERTISE	14889.3	2	7444.63	477.15	0
VISION	361.7	2	180.83	11.59	0
MANIPULATION	812	1	811.98	52.04	0
COLOR	626	1	625.96	40.12	0
EXPERTISE*VISION	1052.1	4	263.02	16.86	0
EXPERTISE*MANIPULATION	193.2	2	96.61	6.19	0.0021
EXPERTISE*COLOR	681.7	2	340.85	21.85	0
VISION*MANIPULATION	1.2	2	0.58	0.04	0.9635
VISION*COLOR	156	2	77.99	5	0.0068
MANIPULATION*COLOR	0.3	1	0.32	0.02	0.8864
EXPERTISE*VISION*MANIPULATION	12.6	4	3.16	0.2	0.9371
EXPERTISE*VISION*COLOR	88.3	4	22.07	1.41	0.2265
EXPERTISE*MANIPULATION*COLOR	4.1	2	2.07	0.13	0.8758
VISION*MANIPULATION*COLOR	1	2	0.48	0.03	0.9695
EXPERTISE*VISION*MANIPULATION*COLOR	29.3	4	7.33	0.47	0.7579
Error	35011.8	2244	15.6		
Total	55313.9	2279			

Annex 1- Figure 43 - Novices, surgeons and expert surgeon *color feedback* ‘time’ raw data ANOVA results for fisheye, undistorted and Oculus vision for study 3.

Analysis of Variance

Source	Sum Sq.	d.f.	Mean Sq.	F	Prob>F
EXPERTISE	39116649.5	2	19558324.7	71.6	0
VISION	31166352.9	3	10388784.3	38.03	0
MANIPULATION	541322.3	1	541322.3	1.98	0.1593
EXPERTISE*VISION	4722355.7	6	787059.3	2.88	0.0084
EXPERTISE*MANIPULATION	387408.5	2	193704.2	0.71	0.4922
VISION*MANIPULATION	2084694	3	694898	2.54	0.0545
EXPERTISE*VISION*MANIPULATION	2566051.5	6	427675.2	1.57	0.1531
Error	720053651.8	2636	273161.5		
Total	882974975.4	2659			

Annex 1- Figure 44 - Novices, surgeons and expert surgeon visual feedback ‘precision’ raw data ANOVA results for direct, fisheye, undistorted and Oculus 3D vision for study 3.

Analysis of Variance

Source	Sum Sq.	d.f.	Mean Sq.	F	Prob>F
EXPERTISE	39309601.1	2	19654800.6	68.59	0
VISION	20712868	2	10356434	36.14	0
MANIPULATION	25082	1	25082	0.09	0.7674
COLOR	1255990	1	1255990	4.38	0.0364
EXPERTISE*VISION	4563686.7	4	1140921.7	3.98	0.0032
EXPERTISE*MANIPULATION	202001.3	2	101000.7	0.35	0.703
EXPERTISE*COLOR	521457.5	2	260728.8	0.91	0.4027
VISION*MANIPULATION	1383146.5	2	691573.3	2.41	0.0898
VISION*COLOR	1063775.4	2	531887.7	1.86	0.1565
MANIPULATION*COLOR	107084.9	1	107084.9	0.37	0.5411
EXPERTISE*VISION*MANIPULATION	2480832.9	4	620208.2	2.16	0.0706
EXPERTISE*VISION*COLOR	1128528	4	282132	0.98	0.4147
EXPERTISE*MANIPULATION*COLOR	520291.6	2	260145.8	0.91	0.4036
VISION*MANIPULATION*COLOR	360511.4	2	180255.7	0.63	0.5332
EXPERTISE*VISION*MANIPULATION*COLOR	401250.5	4	100312.6	0.35	0.8441
Error	643052769	2244	286565.4		
Total	774177298.9	2279			

Annex 1- Figure 45 - Novices, surgeons and expert surgeon color feedback ‘precision’ raw data ANOVA results for fisheye, undistorted and Oculus 3D vision for study 3.

Analysis of Variance

Source	Sum Sq.	d.f.	Mean Sq.	F	Prob>F
EXPERTISE	6.149	2	3.07467	5.35	0.0053
VISION	3.115	3	1.03829	1.81	0.1465
MANIPULATION	1.174	1	1.17361	2.04	0.1542
EXPERTISE*VISION	6.39	6	1.06493	1.85	0.0895
EXPERTISE*MANIPULATION	1.1	2	0.55011	0.96	0.3853
VISION*MANIPULATION	1.362	3	0.45417	0.79	0.5002
EXPERTISE*VISION*MANIPULATION	5.962	6	0.99371	1.73	0.1147
Error	139.042	242	0.57455		
Total	162.406	265			

Annex 1- Figure 46 - Novices, surgeons and expert surgeon vision feedback ‘error’ raw data ANOVA results for direct, fisheye, undistorted and Oculus vision for study 3.

Analysis of Variance

Source	Sum Sq.	d.f.	Mean Sq.	F	Prob>F
EXPERTISE	2.576	2	1.28819	2.15	0.119
VISION	2.915	2	1.45741	2.44	0.0903
MANIPULATION	1.023	1	1.02269	1.71	0.1927
COLOR	0.938	1	0.9375	1.57	0.2123
EXPERTISE*VISION	4.3	4	1.07493	1.8	0.1312
EXPERTISE*MANIPULATION	0.509	2	0.25457	0.43	0.6542
EXPERTISE*COLOR	2.573	2	1.28673	2.15	0.1193
VISION*MANIPULATION	1.359	2	0.67963	1.14	0.3234
VISION*COLOR	1.078	2	0.53889	0.9	0.4081
MANIPULATION*COLOR	0.704	1	0.70417	1.18	0.2794
EXPERTISE*VISION*MANIPULATION	5.577	4	1.39437	2.33	0.0575
EXPERTISE*VISION*COLOR	4.417	4	1.10417	1.84	0.1219
EXPERTISE*MANIPULATION*COLOR	0.161	2	0.08059	0.13	0.8741
VISION*MANIPULATION*COLOR	1.878	2	0.93889	1.57	0.211
EXPERTISE*VISION*MANIPULATION*COLOR	2.654	4	0.66338	1.11	0.3539
Error	114.917	192	0.59852		
Total	145	227			

Annex 1- Figure 47 - Novices, surgeons and expert surgeon color feedback ‘error’ raw data ANOVA results for fisheye, undistorted and Oculus 3D vision for study 3.

Analysis of Variance

Source	Sum Sq.	d.f.	Mean Sq.	F	Prob>F
EXPERTISE	165.63	2	82.8167	147.79	0
VISION	62.17	3	20.7234	36.98	0
MANIPULATION	8.39	1	8.3919	14.98	0.0001
SEGMENT	221.8	5	44.3607	79.16	0
EXPERTISE*VISION	33.32	6	5.5533	9.91	0
EXPERTISE*MANIPULATION	1.3	2	0.6516	1.16	0.3129
EXPERTISE*SEGMENT	31.99	10	3.1989	5.71	0
VISION*MANIPULATION	2.46	3	0.821	1.47	0.2223
VISION*SEGMENT	17	15	1.1332	2.02	0.0114
MANIPULATION*SEGMENT	1.24	5	0.2485	0.44	0.8182
EXPERTISE*VISION*MANIPULATION	0.72	6	0.1196	0.21	0.9727
EXPERTISE*VISION*SEGMENT	8.25	30	0.2751	0.49	0.9909
EXPERTISE*MANIPULATION*SEGMENT	1.79	10	0.1787	0.32	0.9765
VISION*MANIPULATION*SEGMENT	1.31	15	0.0874	0.16	0.9999
EXPERTISE*VISION*MANIPULATION*SEGMENT	2.87	30	0.0958	0.17	1
Error	813.67	1452	0.5604		
Total	1962.47	1595			

Annex 1- Figure 48 - Novices, surgeons and expert surgeon *visual feedback* 'from-target-to-target duration' data ANOVA results for direct, fisheye, undistorted and Oculus 3D vision for study 3.

Analysis of Variance

Source	Sum Sq.	d.f.	Mean Sq.	F	Prob>F
EXPERTISE	216.8	2	108.4	170.47	0
VISION	5.77	2	2.886	4.54	0.0109
MANIPULATION	14.63	1	14.633	23.01	0
SEGMENT	262.12	5	52.424	82.44	0
COLOR	11.74	1	11.736	18.46	0
EXPERTISE*VISION	19.17	4	4.793	7.54	0
EXPERTISE*MANIPULATION	1.72	2	0.86	1.35	0.259
EXPERTISE*SEGMENT	40.38	10	4.038	6.35	0
EXPERTISE*COLOR	13.74	2	6.872	10.81	0
VISION*MANIPULATION	0.08	2	0.041	0.07	0.937
VISION*SEGMENT	9.69	10	0.969	1.52	0.1255
VISION*COLOR	2.19	2	1.095	1.72	0.1793
MANIPULATION*SEGMENT	1.21	5	0.243	0.38	0.8616
MANIPULATION*COLOR	0.02	1	0.018	0.03	0.8674
SEGMENT*COLOR	0.98	5	0.196	0.31	0.9086
EXPERTISE*VISION*MANIPULATION	0.59	4	0.148	0.23	0.9197
EXPERTISE*VISION*SEGMENT	5.13	20	0.256	0.4	0.9912
EXPERTISE*VISION*COLOR	2.16	4	0.541	0.85	0.4932
EXPERTISE*MANIPULATION*SEGMENT	3.17	10	0.317	0.5	0.8922
EXPERTISE*MANIPULATION*COLOR	0.07	2	0.035	0.05	0.9468
EXPERTISE*SEGMENT*COLOR	3.08	10	0.308	0.48	0.9006
VISION*MANIPULATION*SEGMENT	1.15	10	0.115	0.18	0.9976
VISION*MANIPULATION*COLOR	0.07	2	0.035	0.06	0.9459
VISION*SEGMENT*COLOR	0.69	10	0.069	0.11	0.9997
MANIPULATION*SEGMENT*COLOR	0.19	5	0.038	0.06	0.9977
EXPERTISE*VISION*MANIPULATION*SEGMENT	1.51	20	0.075	0.12	1
EXPERTISE*VISION*MANIPULATION*COLOR	0.55	4	0.137	0.22	0.9297
EXPERTISE*VISION*SEGMENT*COLOR	2.6	20	0.13	0.2	0.9999
EXPERTISE*MANIPULATION*SEGMENT*COLOR	1.91	10	0.191	0.3	0.9813
VISION*MANIPULATION*SEGMENT*COLOR	0.22	10	0.022	0.03	1
EXPERTISE*VISION*MANIPULATION*SEGMENT*COLOR	1.11	20	0.055	0.09	1
Error	732.54	1152	0.636		
Total	1720.94	1367			

Annex 1- Figure 49 - Novices, surgeons and expert surgeon *color feedback* ‘from-target-to-target duration’ data ANOVA results for fisheye, undistorted and Oculus 3D vision for study 3.

Analysis of Variance

Source	Sum Sq.	d.f.	Mean Sq.	F	Prob>F
EXPERTISE	29.6	2	14.81	0.45	0.6382
VISION	10514.6	3	3504.86	106.3	0
MANIPULATION	652.6	1	652.59	19.79	0
SEGMENT	11095.3	5	2219.05	67.3	0
EXPERTISE*VISION	652.4	6	108.73	3.3	0.0032
EXPERTISE*MANIPULATION	343.2	2	171.59	5.2	0.0056
EXPERTISE*SEGMENT	1779.4	10	177.94	5.4	0
VISION*MANIPULATION	89.4	3	29.79	0.9	0.4387
VISION*SEGMENT	4433	15	295.54	8.96	0
MANIPULATION*SEGMENT	180.4	5	36.09	1.09	0.3614
EXPERTISE*VISION*MANIPULATION	413.7	6	68.95	2.09	0.0515
EXPERTISE*VISION*SEGMENT	1193.7	30	39.79	1.21	0.2047
EXPERTISE*MANIPULATION*SEGMENT	1222.2	10	122.22	3.71	0.0001
VISION*MANIPULATION*SEGMENT	486.1	15	32.41	0.98	0.4706
EXPERTISE*VISION*MANIPULATION*SEGMENT	743.3	30	24.78	0.75	0.8319
Error	47874.1	1452	32.97		
Total	127411.8	1595			

Annex 1- Figure 50 - Novices, surgeons and expert surgeon *visual feedback* ‘average distance from the reference trajectory’ data ANOVA results for direct, fisheye, undistorted and Oculus 3D vision for study 3.

Analysis of Variance

Source	Sum Sq.	d.f.	Mean Sq.	F	Prob>F
EXPERTISE	196.3	2	98.16	2.8	0.061
VISION	9730.7	2	4865.35	138.95	0
MANIPULATION	713.5	1	713.47	20.38	0
SEGMENT	12669.2	5	2533.84	72.37	0
COLOR	139.4	1	139.41	3.98	0.0462
EXPERTISE*VISION	470.4	4	117.61	3.36	0.0096
EXPERTISE*MANIPULATION	529.9	2	264.95	7.57	0.0005
EXPERTISE*SEGMENT	2078.8	10	207.88	5.94	0
EXPERTISE*COLOR	123.3	2	61.66	1.76	0.1723
VISION*MANIPULATION	80.5	2	40.23	1.15	0.3174
VISION*SEGMENT	3669.7	10	366.97	10.48	0
VISION*COLOR	386	2	192.99	5.51	0.0041
MANIPULATION*SEGMENT	191.7	5	38.34	1.1	0.3613
MANIPULATION*COLOR	1.1	1	1.08	0.03	0.8606
SEGMENT*COLOR	31.9	5	6.38	0.18	0.9693
EXPERTISE*VISION*MANIPULATION	336.4	4	84.11	2.4	0.0482
EXPERTISE*VISION*SEGMENT	901.6	20	45.08	1.29	0.1772
EXPERTISE*VISION*COLOR	331	4	82.74	2.36	0.0514
EXPERTISE*MANIPULATION*SEGMENT	1271.1	10	127.11	3.63	0.0001
EXPERTISE*MANIPULATION*COLOR	19.5	2	9.73	0.28	0.7575
EXPERTISE*SEGMENT*COLOR	154.9	10	15.49	0.44	0.9258
VISION*MANIPULATION*SEGMENT	404.1	10	40.41	1.15	0.3181
VISION*MANIPULATION*COLOR	97	2	48.5	1.39	0.2507
VISION*SEGMENT*COLOR	161.5	10	16.15	0.46	0.9151
MANIPULATION*SEGMENT*COLOR	182.3	5	36.47	1.04	0.3916
EXPERTISE*VISION*MANIPULATION*SEGMENT	499.3	20	24.96	0.71	0.8159
EXPERTISE*VISION*MANIPULATION*COLOR	43.5	4	10.88	0.31	0.8709
EXPERTISE*VISION*SEGMENT*COLOR	330	20	16.5	0.47	0.9769
EXPERTISE*MANIPULATION*SEGMENT*COLOR	135.1	10	13.51	0.39	0.9533
VISION*MANIPULATION*SEGMENT*COLOR	76.5	10	7.65	0.22	0.9947
EXPERTISE*VISION*MANIPULATION*SEGMENT*COLOR	329.6	20	16.48	0.47	0.9771
Error	40336.6	1152	35.01		
Total	114194.9	1367			

Annex 1- Figure 51 - Novices, surgeons and expert surgeon color feedback ‘average distance from the reference trajectory’ data ANOVA results for fisheye, undistorted and Oculus 3D vision for study 3.

Analysis of Variance

Source	Sum Sq.	d.f.	Mean Sq.	F	Prob>F
EXPERTISE	624.3	2	312.13	7.84	0.0004
VISION	6254.7	3	2084.91	52.37	0
MANIPULATION	877.7	1	877.67	22.05	0
SEGMENT	4442.3	5	888.45	22.32	0
EXPERTISE*VISION	818.1	6	136.36	3.43	0.0023
EXPERTISE*MANIPULATION	357.9	2	178.95	4.5	0.0113
EXPERTISE*SEGMENT	1634.2	10	163.42	4.11	0
VISION*MANIPULATION	142.7	3	47.56	1.19	0.3104
VISION*SEGMENT	3211.2	15	214.08	5.38	0
MANIPULATION*SEGMENT	599.7	5	119.95	3.01	0.0103
EXPERTISE*VISION*MANIPULATION	656.8	6	109.47	2.75	0.0116
EXPERTISE*VISION*SEGMENT	1700.9	30	56.7	1.42	0.0646
EXPERTISE*MANIPULATION*SEGMENT	1388.1	10	138.81	3.49	0.0001
VISION*MANIPULATION*SEGMENT	804.7	15	53.65	1.35	0.1657
EXPERTISE*VISION*MANIPULATION*SEGMENT	2151	30	71.7	1.8	0.0051
Error	57801.7	1452	39.81		
Total	105540.8	1595			

Annex 1- Figure 52 - Novices, surgeons and expert surgeon visual feedback ‘dispersion in trajectory’ data ANOVA results for direct, fisheye, undistorted and Oculus 3D vision for study 3.

Analysis of Variance

Source	Sum Sq.	d.f.	Mean Sq.	F	Prob>F
EXPERTISE	196.6	2	98.32	2.48	0.0844
VISION	6003.7	2	3001.84	75.64	0
MANIPULATION	1063.1	1	1063.15	26.79	0
SEGMENT	6199.6	5	1239.91	31.24	0
COLOR	180.7	1	180.74	4.55	0.033
EXPERTISE*VISION	467.2	4	116.81	2.94	0.0195
EXPERTISE*MANIPULATION	430.1	2	215.06	5.42	0.0045
EXPERTISE*SEGMENT	1388.3	10	138.83	3.5	0.0001
EXPERTISE*COLOR	124.1	2	62.05	1.56	0.2098
VISION*MANIPULATION	107.5	2	53.76	1.35	0.2584
VISION*SEGMENT	2304.2	10	230.42	5.81	0
VISION*COLOR	410.1	2	205.06	5.17	0.0058
MANIPULATION*SEGMENT	988.9	5	197.77	4.98	0.0002
MANIPULATION*COLOR	15.8	1	15.85	0.4	0.5276
SEGMENT*COLOR	58.1	5	11.62	0.29	0.917
EXPERTISE*VISION*MANIPULATION	617.2	4	154.3	3.89	0.0038
EXPERTISE*VISION*SEGMENT	916.6	20	45.83	1.15	0.2865
EXPERTISE*VISION*COLOR	530.7	4	132.68	3.34	0.0099
EXPERTISE*MANIPULATION*SEGMENT	1355.1	10	135.51	3.41	0.0002
EXPERTISE*MANIPULATION*COLOR	48.6	2	24.3	0.61	0.5422
EXPERTISE*SEGMENT*COLOR	278	10	27.8	0.7	0.7246
VISION*MANIPULATION*SEGMENT	352.3	10	35.23	0.89	0.544
VISION*MANIPULATION*COLOR	235.6	2	117.79	2.97	0.0518
VISION*SEGMENT*COLOR	288.3	10	28.83	0.73	0.7
MANIPULATION*SEGMENT*COLOR	66.5	5	13.31	0.34	0.8917
EXPERTISE*VISION*MANIPULATION*SEGMENT	804.7	20	40.24	1.01	0.4419
EXPERTISE*VISION*MANIPULATION*COLOR	232.3	4	58.08	1.46	0.2111
EXPERTISE*VISION*SEGMENT*COLOR	562.3	20	28.12	0.71	0.8206
EXPERTISE*MANIPULATION*SEGMENT*COLOR	217.6	10	21.76	0.55	0.8562
VISION*MANIPULATION*SEGMENT*COLOR	257.4	10	25.74	0.65	0.7725
EXPERTISE*VISION*MANIPULATION*SEGMENT*COLOR	447.1	20	22.36	0.56	0.9381
Error	45715.9	1152	39.68		
Total	89869.7	1367			

Annex 1- Figure 53 - Novices, surgeons and expert surgeon color feedback ‘dispersion in trajectory’ data ANOVA results for fisheye, undistorted and Oculus 3D vision for study 3.

Annex 2 – ANOVA results for Chapter 2

Analysis of Variance

Source	Sum Sq.	d.f.	Mean Sq.	F	Prob>F
VisualFeedback	63.922	5	12.7844	79.62	0
Handedness	0.206	1	0.2063	1.28	0.2577
Direction	0.002	1	0.0019	0.01	0.9134
VisualFeedback*Handedness	2.139	5	0.4277	2.66	0.022
VisualFeedback*Direction	0.376	5	0.0752	0.47	0.7999
Handedness*Direction	0.07	1	0.0704	0.44	0.5083
VisualFeedback*Handedness*Direction	0.144	5	0.0289	0.18	0.9702
Error	65.516	408	0.1606		
Total	132.389	431			

Annex 2-Figure 1– 'Horizontal' 'time' mean data ANOVA results for study 1

Analysis of Variance

Source	Sum Sq.	d.f.	Mean Sq.	F	Prob>F
VisualFeedback	49.323	5	9.86466	30.97	0
Handedness	0.105	1	0.1048	0.33	0.5666
Direction	0.811	1	0.8106	2.54	0.1114
VisualFeedback*Handedness	2.791	5	0.5583	1.75	0.1215
VisualFeedback*Direction	0.255	5	0.05102	0.16	0.9768
Handedness*Direction	0	1	0.00047	0	0.9695
VisualFeedback*Handedness*Direction	0.61	5	0.12195	0.38	0.8605
Error	129.955	408	0.31852		
Total	183.851	431			

Annex 2-Figure 2 – 'Vertical' 'time' mean data ANOVA results for study 1

Analysis of Variance

Source	Sum Sq.	d.f.	Mean Sq.	F	Prob>F
VisualFeedback	530.7	5	106.14	39.46	0
Handedness	10.18	1	10.185	3.79	0.0524
Direction	5.75	1	5.751	2.14	0.1445
VisualFeedback*Handedness	13.46	5	2.691	1	0.4171
VisualFeedback*Direction	4.55	5	0.91	0.34	0.8896
Handedness*Direction	2.12	1	2.124	0.79	0.3747
VisualFeedback*Handedness*Direction	1.88	5	0.376	0.14	0.9829
Error	1097.51	408	2.69		
Total	1664.41	431			

Annex 2-Figure 3 – 'Torus' 'time' mean data ANOVA results for study 1

Analysis of Variance

Source	Sum Sq.	d.f.	Mean Sq.	F	Prob>F
VisualFeedback	197.77	5	39.5547	8.77	0
Handedness	31.47	1	31.4712	6.98	0.0086
Direction	37.45	1	37.4533	8.31	0.0042
VisualFeedback*Handedness	49	5	9.7992	2.17	0.0563
VisualFeedback*Direction	74.07	5	14.8146	3.29	0.0064
Handedness*Direction	1.79	1	1.789	0.4	0.5291
VisualFeedback*Handedness*Direction	30.21	5	6.0419	1.34	0.2464
Error	1839.84	408	4.5094		
Total	2261.61	431			

Annex 2-Figure 4 – 'Horizontal' 'average number of finger outs' mean data ANOVA results

Analysis of Variance

Source	Sum Sq.	d.f.	Mean Sq.	F	Prob>F
VisualFeedback	9.7545	5	1.95089	12.56	0
Handedness	0.8211	1	0.82107	5.29	0.022
Direction	0.1101	1	0.11006	0.71	0.4004
VisualFeedback*Handedness	1.3698	5	0.27396	1.76	0.1191
VisualFeedback*Direction	1.207	5	0.2414	1.55	0.172
Handedness*Direction	0.1412	1	0.14115	0.91	0.341
VisualFeedback*Handedness*Direction	0.1773	5	0.03546	0.23	0.9501
Error	63.3695	408	0.15532		
Total	76.8966	431			

Annex 2-Figure 5 – 'Vertical' 'average number of finger outs' mean data ANOVA results

Analysis of Variance

Source	Sum Sq.	d.f.	Mean Sq.	F	Prob>F
VisualFeedback	1856.4	5	371.279	152.13	0
Handedness	17.71	1	17.71	7.26	0.0074
Direction	6.78	1	6.78	2.78	0.0963
VisualFeedback*Handedness	20.9	5	4.181	1.71	0.1304
VisualFeedback*Direction	7.35	5	1.469	0.6	0.6984
Handedness*Direction	31.3	1	31.299	12.82	0.0004
VisualFeedback*Handedness*Direction	20.89	5	4.177	1.71	0.1307
Error	995.73	408	2.441		
Total	2982.31	431			

Annex 2-Figure 6 – 'Torus' 'Average number of finger outs' mean data ANOVA results

Analysis of Variance

Source	Sum Sq.	d.f.	Mean Sq.	F	Prob>F
VisualFeedback	2948.5	4	737.134	14.02	0
Handedness	1.6	1	1.564	0.03	0.8632
Direction	377.2	1	377.161	7.18	0.0077
VisualFeedback*Handedness	947.7	4	236.918	4.51	0.0015
VisualFeedback*Direction	481.7	4	120.433	2.29	0.0594
Handedness*Direction	129.3	1	129.269	2.46	0.1177
VisualFeedback*Handedness*Direction	950	4	237.496	4.52	0.0014
Error	17870.4	340	52.56		
Total	23540.4	359			

Annex 2-Figure 7 – ‘Horizontal’ ‘motor performance index’ mean data ANOVA results

Analysis of Variance

Source	Sum Sq.	d.f.	Mean Sq.	F	Prob>F
VisualFeedback	7959.1	4	1989.78	9.65	0
Handedness	456	1	456.05	2.21	0.1379
Direction	78.3	1	78.28	0.38	0.5382
VisualFeedback*Handedness	441.2	4	110.3	0.54	0.7101
VisualFeedback*Direction	906.3	4	226.57	1.1	0.357
Handedness*Direction	37.4	1	37.42	0.18	0.6704
VisualFeedback*Handedness*Direction	30.9	4	7.72	0.04	0.9973
Error	70096.3	340	206.17		
Total	80005.5	359			

Annex 2-Figure 8 – ‘Vertical’ ‘motor performance index’ mean data ANOVA results

Analysis of Variance

Source	Sum Sq.	d.f.	Mean Sq.	F	Prob>F
VisualFeedback	18595.7	4	4648.91	46.97	0
Handedness	234.8	1	234.78	2.37	0.1244
Direction	48.1	1	48.06	0.49	0.4864
VisualFeedback*Handedness	1080.5	4	270.12	2.73	0.0292
VisualFeedback*Direction	376.2	4	94.05	0.95	0.435
Handedness*Direction	72.2	1	72.17	0.73	0.3937
VisualFeedback*Handedness*Direction	292.3	4	73.07	0.74	0.5664
Error	33650.2	340	98.97		
Total	54302.4	359			

Annex 2-Figure 9 – ‘Torus’ ‘motor performance index’ mean data ANOVA results

Analysis of Variance

Source	Sum Sq.	d.f.	Mean Sq.	F	Prob>F
VisualFeedback	10.1197	4	2.52992	15.04	0
Handedness	0.0189	1	0.01892	0.11	0.7375
Direction	2.1643	1	2.16432	12.87	0.0004
VisualFeedback*Handedness	2.6401	4	0.66002	3.92	0.004
VisualFeedback*Direction	0.4131	4	0.10328	0.61	0.6527
Handedness*Direction	1.0841	1	1.08409	6.45	0.0116
VisualFeedback*Handedness*Direction	2.896	4	0.724	4.31	0.0021
Error	57.1787	340	0.16817		
Total	76.0751	359			

Annex 2-Figure 10 – 'Horizontal' part 'average accumulated distance away from the object surface' mean data ANOVA results

Analysis of Variance

Source	Sum Sq.	d.f.	Mean Sq.	F	Prob>F
VisualFeedback	22.407	4	5.6018	4.36	0.0019
Handedness	0.583	1	0.58277	0.45	0.5013
Direction	3.517	1	3.51701	2.73	0.0991
VisualFeedback*Handedness	1.882	4	0.47041	0.37	0.833
VisualFeedback*Direction	2.527	4	0.63175	0.49	0.7422
Handedness*Direction	0.332	1	0.33215	0.26	0.6116
VisualFeedback*Handedness*Direction	1.012	4	0.25299	0.2	0.94
Error	437.255	340	1.28604		
Total	469.514	359			

Annex 2-Figure 11 – 'Vertical' 'average accumulated distance away from the object surface' mean data ANOVA results

Analysis of Variance

Source	Sum Sq.	d.f.	Mean Sq.	F	Prob>F
VisualFeedback	73.48	4	18.37	35.93	0
Handedness	0.326	1	0.3257	0.64	0.4253
Direction	0	1	0.0002	0	0.9839
VisualFeedback*Handedness	4.75	4	1.1875	2.32	0.0565
VisualFeedback*Direction	0.138	4	0.0346	0.07	0.9916
Handedness*Direction	4.984	1	4.9839	9.75	0.0019
VisualFeedback*Handedness*Direction	5.482	4	1.3704	2.68	0.0316
Error	173.839	340	0.5113		
Total	255.605	359			

Annex 2-Figure 12 – 'Torus' 'average accumulated distance away from the object surface' mean data ANOVA results

Analysis of Variance

Source	Sum Sq.	d.f.	Mean Sq.	F	Prob>F
ObjectSize	34.6859	5	6.93718	49.74	0
Handedness	0.0326	1	0.03263	0.23	0.6289
Direction	0.7962	1	0.79616	5.71	0.0173
ObjectSize*Handedness	0.2603	5	0.05206	0.37	0.867
ObjectSize*Direction	0.4833	5	0.09666	0.69	0.629
Handedness*Direction	0.1782	1	0.17821	1.28	0.259
ObjectSize*Handedness*Direction	0.2577	5	0.05153	0.37	0.8695
Error	56.9078	408	0.13948		
Total	93.602	431			

Annex 2-Figure 13 – 'Horizontal' Object 'time' mean data ANOVA results for second study

Analysis of Variance

Source	Sum Sq.	d.f.	Mean Sq.	F	Prob>F
ObjectSize	19.8509	5	3.97018	50.94	0
Handedness	0.0023	1	0.00229	0.03	0.8639
Direction	0.5118	1	0.51179	6.57	0.0107
ObjectSize*Handedness	0.0538	5	0.01075	0.14	0.9834
ObjectSize*Direction	0.1112	5	0.02224	0.29	0.921
Handedness*Direction	0.1693	1	0.16927	2.17	0.1413
ObjectSize*Handedness*Direction	0.0868	5	0.01737	0.22	0.9526
Error	31.7964	408	0.07793		
Total	52.4992	431			

Annex 2-Figure 14 – 'Vertical' Object part 'time' mean data ANOVA results for second study

Analysis of Variance

Source	Sum Sq.	d.f.	Mean Sq.	F	Prob>F
ObjectSize	582.67	5	116.533	68.97	0
Handedness	4.82	1	4.822	2.85	0.0919
Direction	4.9	1	4.9	2.9	0.0894
ObjectSize*Handedness	0.75	5	0.149	0.09	0.9941
ObjectSize*Direction	3.86	5	0.772	0.46	0.8083
Handedness*Direction	5.71	1	5.71	3.38	0.0667
ObjectSize*Handedness*Direction	0.43	5	0.086	0.05	0.9984
Error	689.38	408	1.69		
Total	1292.51	431			

Annex 2-Figure 15 – 'Torus' Object part 'time' mean data ANOVA results for second study

Analysis of Variance

Source	Sum Sq.	d.f.	Mean Sq.	F	Prob>F
ObjectSize	65.98	5	13.1965	5.23	0.0001
Handedness	0.4	1	0.4033	0.16	0.6895
Direction	21.78	1	21.7801	8.63	0.0035
ObjectSize*Handedness	19.37	5	3.8742	1.54	0.1777
ObjectSize*Direction	27.8	5	5.5593	2.2	0.0532
Handedness*Direction	4.28	1	4.2801	1.7	0.1935
ObjectSize*Handedness*Direction	6.92	5	1.3831	0.55	0.7398
Error	1029.6	408	2.5235		
Total	1176.13	431			

Annex 2-Figure 16 – 'Horizontal' Object part 'average number of finger outs' mean data ANOVA results for second study

Analysis of Variance

Source	Sum Sq.	d.f.	Mean Sq.	F	Prob>F
ObjectSize	17.746	5	3.54916	11.25	0
Handedness	0.074	1	0.07383	0.23	0.6288
Direction	0.095	1	0.09494	0.3	0.5836
ObjectSize*Handedness	0.434	5	0.08676	0.28	0.9267
ObjectSize*Direction	0.335	5	0.06709	0.21	0.9571
Handedness*Direction	0.067	1	0.06701	0.21	0.6451
ObjectSize*Handedness*Direction	0.292	5	0.05838	0.19	0.9682
Error	128.711	408	0.31547		
Total	147.873	431			

Annex 2-Figure 17 – 'Vertical' Object part 'average number of finger outs' mean data ANOVA results for second study

Analysis of Variance

Source	Sum Sq.	d.f.	Mean Sq.	F	Prob>F
ObjectSize	1050.2	5	210.04	69.22	0
Handedness	11.57	1	11.571	3.81	0.0515
Direction	4.67	1	4.667	1.54	0.2157
ObjectSize*Handedness	6.05	5	1.21	0.4	0.8497
ObjectSize*Direction	15.56	5	3.112	1.03	0.4021
Handedness*Direction	24.51	1	24.51	8.08	0.0047
ObjectSize*Handedness*Direction	17.83	5	3.567	1.18	0.3205
Error	1238.11	408	3.035		
Total	2368.5	431			

Annex 2-Figure 18 – 'Torus' Object part 'average number of finger outs' mean data ANOVA results for second study

Analysis of Variance

Source	Sum Sq.	d.f.	Mean Sq.	F	Prob>F
ObjectSize	5041.2	5	1008.24	15.18	0
Handedness	274.3	1	274.34	4.13	0.0427
Direction	1217	1	1217.01	18.33	0
ObjectSize*Handedness	334.5	5	66.91	1.01	0.4128
ObjectSize*Direction	1281	5	256.19	3.86	0.002
Handedness*Direction	145.3	1	145.32	2.19	0.1398
ObjectSize*Handedness*Direction	128.9	5	25.78	0.39	0.8569
Error	27095	408	66.41		
Total	35517.3	431			

Annex 2-Figure 19 – ‘Horizontal’ Object part ‘motor performance index’ mean data ANOVA results for second study

Analysis of Variance

Source	Sum Sq.	d.f.	Mean Sq.	F	Prob>F
ObjectSize	1254.1	5	250.826	4.7	0.0004
Handedness	224.4	1	224.39	4.2	0.041
Direction	4.1	1	4.068	0.08	0.7827
ObjectSize*Handedness	205.8	5	41.16	0.77	0.5713
ObjectSize*Direction	237.7	5	47.535	0.89	0.4876
Handedness*Direction	8.2	1	8.159	0.15	0.6961
ObjectSize*Handedness*Direction	235.6	5	47.129	0.88	0.4927
Error	21789.2	408	53.405		
Total	24005.5	431			

Annex 2-Figure 20 – ‘Vertical’ Object part ‘motor performance index’ mean data ANOVA results for second study

Analysis of Variance

Source	Sum Sq.	d.f.	Mean Sq.	F	Prob>F
ObjectSize	22315.2	5	4463.03	33.49	0
Handedness	116.9	1	116.86	0.88	0.3496
Direction	1185.6	1	1185.61	8.9	0.003
ObjectSize*Handedness	238.2	5	47.64	0.36	0.8774
ObjectSize*Direction	7179.3	5	1435.86	10.77	0
Handedness*Direction	992.3	1	992.28	7.45	0.0066
ObjectSize*Handedness*Direction	362.9	5	72.58	0.54	0.7424
Error	54374.8	408	133.27		
Total	86765.1	431			

Annex 2-Figure 21 – ‘Torus’ Object part ‘motor performance index’ mean data ANOVA results for second study

Analysis of Variance

Source	Sum Sq.	d.f.	Mean Sq.	F	Prob>F
ObjectSize	9.375	5	1.87499	10.41	0
Handedness	0.2135	1	0.21345	1.19	0.2769
Direction	2.1608	1	2.16083	12	0.0006
ObjectSize*Handedness	0.7614	5	0.15228	0.85	0.5179
ObjectSize*Direction	2.3036	5	0.46071	2.56	0.027
Handedness*Direction	0.7079	1	0.70793	3.93	0.0481
ObjectSize*Handedness*Direction	0.9312	5	0.18623	1.03	0.3969
Error	73.4643	408	0.18006		
Total	89.9176	431			

Annex 2-Figure 22 – 'Horizontal' Object part 'average accumulated distance away from the object surface' mean data ANOVA results for second study

Analysis of Variance

Source	Sum Sq.	d.f.	Mean Sq.	F	Prob>F
ObjectSize	2.441	5	0.48823	1.68	0.1384
Handedness	0.438	1	0.43825	1.51	0.2203
Direction	0.299	1	0.29916	1.03	0.311
ObjectSize*Handedness	2.146	5	0.42927	1.48	0.1964
ObjectSize*Direction	1.482	5	0.29634	1.02	0.4058
Handedness*Direction	0.107	1	0.10692	0.37	0.5446
ObjectSize*Handedness*Direction	1.879	5	0.37576	1.29	0.2662
Error	118.628	408	0.29075		
Total	127.24	431			

Annex 2-Figure 23 – 'Vertical' Object part 'average accumulated distance away from the object surface' mean data ANOVA results for second study

Analysis of Variance

Source	Sum Sq.	d.f.	Mean Sq.	F	Prob>F
ObjectSize	7.0515	5	1.4103	9.86	0
Handedness	0.0814	1	0.08137	0.57	0.4511
Direction	1.7842	1	1.7842	12.48	0.0005
ObjectSize*Handedness	0.3699	5	0.07398	0.52	0.7631
ObjectSize*Direction	0.9363	5	0.18727	1.31	0.2588
Handedness*Direction	0.2656	1	0.26562	1.86	0.1737
ObjectSize*Handedness*Direction	0.4224	5	0.08449	0.59	0.707
Error	58.3394	408	0.14299		
Total	69.2508	431			

Annex 2-Figure 24 – 'Torus' Object part 'average accumulated distance away from the object surface' mean data ANOVA results for second study

Analysis of Variance

Source	Sum Sq.	d.f.	Mean Sq.	F	Prob>F
StructureComplexity	1999.58	1	1999.58	1174.87	0
Handedness	1.17	1	1.17	0.69	0.4066
Direction	0.08	1	0.08	0.05	0.8306
Size	5.27	2	2.64	1.55	0.2136
StructureComplexity*Handedness	2.17	1	2.17	1.28	0.2595
StructureComplexity*Direction	0.02	1	0.02	0.01	0.9195
StructureComplexity*Size	0.79	2	0.39	0.23	0.7934
Handedness*Direction	0	1	0	0	0.9708
Handedness*Size	1.78	2	0.89	0.52	0.5935
Direction*Size	1.25	2	0.62	0.37	0.6937
StructureComplexity*Handedness*Direction	0	1	0	0	0.9889
StructureComplexity*Handedness*Size	1.06	2	0.53	0.31	0.7318
StructureComplexity*Direction*Size	1.47	2	0.74	0.43	0.6492
Handedness*Direction*Size	1.75	2	0.88	0.51	0.598
StructureComplexity*Handedness*Direction*Size	1.54	2	0.77	0.45	0.6367
Error	694.4	408	1.7		
Total	2712.33	431			

Annex 2-Figure 25 – Structural complexity ‘time’ mean data ANOVA results for second study

Analysis of Variance

Source	Sum Sq.	d.f.	Mean Sq.	F	Prob>F
StructureComplexity	768.27	1	768.267	113.57	0
Handedness	32.29	1	32.286	4.77	0.0295
Direction	3.54	1	3.539	0.52	0.4699
Size	154.58	2	77.292	11.43	0
StructureComplexity*Handedness	30.14	1	30.136	4.45	0.0354
StructureComplexity*Direction	6.04	1	6.044	0.89	0.3451
StructureComplexity*Size	757.27	2	378.635	55.97	0
Handedness*Direction	0.03	1	0.025	0	0.9514
Handedness*Size	17.27	2	8.634	1.28	0.2802
Direction*Size	0.6	2	0.3	0.04	0.9566
StructureComplexity*Handedness*Direction	0.59	1	0.585	0.09	0.7688
StructureComplexity*Handedness*Size	12.38	2	6.188	0.91	0.4014
StructureComplexity*Direction*Size	5.92	2	2.961	0.44	0.6458
Handedness*Direction*Size	5.81	2	2.903	0.43	0.6514
StructureComplexity*Handedness*Direction*Size	0.2	2	0.098	0.01	0.9856
Error	2760.01	408	6.765		
Total	4554.92	431			

Annex 2-Figure 26 – Structural complexity ‘average number of finger outs’ mean data ANOVA results for second study

Analysis of Variance

Source	Sum Sq.	d.f.	Mean Sq.	F	Prob>F
Region	0.01283	3	0.00428	0.22	0.8797
Handedness	0.00514	1	0.00514	0.27	0.6044
Direction	0.04099	1	0.04099	2.15	0.1443
Region*Handedness	0.06295	3	0.02098	1.1	0.3505
Region*Direction	0.04434	3	0.01478	0.77	0.5097
Handedness*Direction	0.00234	1	0.00234	0.12	0.7266
Region*Handedness*Direction	0.01779	3	0.00593	0.31	0.8178
Error	4.58434	240	0.0191		
Total	4.77072	255			

Annex 2-Figure 27 –Extreme regions ‘time’ mean data ANOVA results for third study

Analysis of Variance

Source	Sum Sq.	d.f.	Mean Sq.	F	Prob>F
Region	0.28831	3	0.0961	3.16	0.0255
Handedness	0.7711	1	0.7711	25.32	0
Direction	0.01129	1	0.01129	0.37	0.5432
Region*Handedness	0.46347	3	0.15449	5.07	0.002
Region*Direction	0.02918	3	0.00973	0.32	0.8113
Handedness*Direction	0.00004	1	0.00004	0	0.9715
Region*Handedness*Direction	0.19543	3	0.06514	2.14	0.0959
Error	7.30867	240	0.03045		
Total	9.06749	255			

Annex 2-Figure 28 – Extreme regions ‘average number of finger outs’ mean data ANOVA results for third study

Analysis of Variance

Source	Sum Sq.	d.f.	Mean Sq.	F	Prob>F
Region	221.97	3	73.989	3.32	0.0206
Handedness	487.68	1	487.68	21.87	0
Direction	1.5	1	1.495	0.07	0.7959
Region*Handedness	449.06	3	149.687	6.71	0.0002
Region*Direction	93.01	3	31.002	1.39	0.2463
Handedness*Direction	1	1	1.004	0.05	0.8322
Region*Handedness*Direction	203.41	3	67.803	3.04	0.0297
Error	5351.4	240	22.297		
Total	6809.02	255			

Annex 2-Figure 29 – Extreme regions ‘motor performance index’ mean data ANOVA results for third study

Analysis of Variance

Source	Sum Sq.	d.f.	Mean Sq.	F	Prob>F
Region	0.23467	3	0.07822	2.7	0.0465
Handedness	0.16653	1	0.16653	5.74	0.0173
Direction	0.00788	1	0.00788	0.27	0.6027
Region*Handedness	0.41795	3	0.13932	4.8	0.0029
Region*Direction	0.00596	3	0.00199	0.07	0.9766
Handedness*Direction	0.001	1	0.001	0.03	0.8527
Region*Handedness*Direction	0.05398	3	0.01799	0.62	0.6023
Error	6.95884	240	0.029		
Total	7.84681	255			

Annex 2-Figure 30 – Extreme regions ‘‘average accumulated distance away from the object surface’ mean data ANOVA results for third study

Analysis of Variance

Source	Sum Sq.	d.f.	Mean Sq.	F	Prob>F
Region	0.3273	15	0.02182	1.06	0.388
Handedness	0	1	0.00001	0	0.9801
Direction	0.192	1	0.19196	9.34	0.0023
Region*Handedness	0.2249	15	0.015	0.73	0.7553
Region*Direction	0.1274	15	0.00849	0.41	0.9757
Handedness*Direction	0.0049	1	0.00492	0.24	0.6246
Region*Handedness*Direction	0.0858	15	0.00572	0.28	0.997
Error	19.7197	960	0.02054		
Total	20.682	1023			

Annex 2-Figure 31 –Inner regions ‘time’ mean data ANOVA results for third study

Analysis of Variance

Source	Sum Sq.	d.f.	Mean Sq.	F	Prob>F
Region	3.2457	15	0.21638	4.78	0
Handedness	0.3342	1	0.33423	7.38	0.0067
Direction	0.0234	1	0.02345	0.52	0.4721
Region*Handedness	1.2691	15	0.0846	1.87	0.0229
Region*Direction	0.9011	15	0.06007	1.33	0.179
Handedness*Direction	0.0465	1	0.04649	1.03	0.3113
Region*Handedness*Direction	0.5737	15	0.03824	0.84	0.6282
Error	43.4931	960	0.04531		
Total	49.8868	1023			

Annex 2-Figure 32 – Inner regions ‘average number of finger outs’ mean data ANOVA results for third study

Analysis of Variance

Source	Sum Sq.	d.f.	Mean Sq.	F	Prob>F
Region	1582.7	15	105.51	2.53	0.0011
Handedness	317.3	1	317.294	7.61	0.0059
Direction	54.3	1	54.284	1.3	0.254
Region*Handedness	965.4	15	64.36	1.54	0.0832
Region*Direction	1027.8	15	68.519	1.64	0.0568
Handedness*Direction	110.8	1	110.797	2.66	0.1033
Region*Handedness*Direction	633.7	15	42.248	1.01	0.4378
Error	40004.2	960	41.671		
Total	44696.2	1023			

Annex 2-Figure 33 – Inner regions ‘motor performance index’ mean data ANOVA results for third study

Analysis of Variance

Source	Sum Sq.	d.f.	Mean Sq.	F	Prob>F
Region	1.8633	15	0.12422	3.02	0.0001
Handedness	0.281	1	0.28096	6.83	0.0091
Direction	0.0111	1	0.01112	0.27	0.6033
Region*Handedness	1.1705	15	0.07803	1.9	0.0202
Region*Direction	0.7904	15	0.05269	1.28	0.2073
Handedness*Direction	0.0271	1	0.02705	0.66	0.4177
Region*Handedness*Direction	0.3443	15	0.02295	0.56	0.9074
Error	39.5085	960	0.04115		
Total	43.9961	1023			

Annex 2-Figure 34 – Inner regions ‘‘average accumulated distance away from the object surface’ mean data ANOVA results for third study

Analysis of Variance

Source	Sum Sq.	d.f.	Mean Sq.	F	Prob>F
Structure	19995.8	1	19995.8	9886.38	0
Size	52.7	2	26.4	13.04	0
Handedness	11.7	1	11.7	5.81	0.016
Direction	0.8	1	0.8	0.39	0.5347
Structure*Size	7.9	2	3.9	1.95	0.1427
Structure*Handedness	21.7	1	21.7	10.73	0.0011
Structure*Direction	0.2	1	0.2	0.09	0.7692
Size*Handedness	17.8	2	8.9	4.4	0.0124
Size*Direction	12.5	2	6.2	3.08	0.0461
Handedness*Direction	0	1	0	0.01	0.9154
Structure*Size*Handedness	10.6	2	5.3	2.63	0.0722
Structure*Size*Direction	14.7	2	7.4	3.64	0.0264
Structure*Handedness*Direction	0	1	0	0	0.9678
Size*Handedness*Direction	17.5	2	8.8	4.33	0.0132
Structure*Size*Handedness*Direction	15.4	2	7.7	3.8	0.0224
Error	8688.9	4296	2		
Total	28868.3	4319			

Annex 2-Figure 35 – ‘Time’ raw data ANOVA results for shape structure, object size, handedness and movement direction

Analysis of Variance

Source	Sum Sq.	d.f.	Mean Sq.	F	Prob>F
Structure	7321.6	1	7321.61	557.49	0
Size	1676.7	2	838.34	63.83	0
Handedness	284.2	1	284.18	21.64	0
Direction	49.8	1	49.84	3.79	0.0515
Structure*Size	7748.8	2	3874.38	295.01	0
Structure*Handedness	264	1	264.03	20.1	0
Structure*Direction	78.9	1	78.95	6.01	0.0143
Size*Handedness	192.4	2	96.21	7.33	0.0007
Size*Direction	0.1	2	0.03	0	0.9978
Handedness*Direction	2.5	1	2.5	0.19	0.6624
Structure*Size*Handedness	72	2	36	2.74	0.0646
Structure*Size*Direction	36.1	2	18.03	1.37	0.2536
Structure*Handedness*Direction	20.3	1	20.28	1.54	0.214
Size*Handedness*Direction	65.9	2	32.96	2.51	0.0814
Structure*Size*Handedness*Direction	8.6	2	4.31	0.33	0.7201
Error	56420	4296	13.13		
Total	74241.9	4319			

Annex 2-Figure 36 – ‘Average number of finger outs’ raw data ANOVA results for shape structure, object size, handedness and movement direction

Analysis of Variance

Source	Sum Sq.	d.f.	Mean Sq.	F	Prob>F
Subject	5599.16	17	329.363	255.42	0
Handedness	32.69	1	32.688	25.35	0
Subject*Handedness	205.56	17	12.092	9.38	0
Error	2738.86	2124	1.289		
Total	8576.27	2159			

Annex 2-Figure 37 – ‘Time’ raw data ANOVA results on complex structure with 18 subject and handedness data

Analysis of Variance

Source	Sum Sq.	d.f.	Mean Sq.	F	Prob>F
Subject	7393.8	17	434.931	24.03	3.25476e-69
Handedness	548	1	548.03	30.27	4.20297e-08
Subject*Handedness	1320.9	17	77.698	4.29	9.75407e-09
Error	38449	2124	18.102		
Total	47711.7	2159			

Annex 2-Figure 38 – ‘Average number of finger outs’ raw data ANOVA results on complex structure with 18 subject and handedness data

Analysis of Variance

Source	Sum Sq.	d.f.	Mean Sq.	F	Prob>F
Subject	944.55	17	55.5618	8.81	0
Handedness	25.87	1	25.8748	4.1	0.043
Subject*Handedness	74.77	17	4.3981	0.7	0.8077
Error	8850.8	1404	6.304		
Total	9895.99	1439			

Annex 2-Figure 39 – ‘Time’ raw data ANOVA results on small object size with 18 subject and handedness data

Analysis of Variance

Source	Sum Sq.	d.f.	Mean Sq.	F	Prob>F
Subject	2844	17	167.295	7.08	0
Handedness	442.2	1	442.225	18.72	0
Subject*Handedness	836.5	17	49.206	2.08	0.0059
Error	33164.3	1404	23.621		
Total	37287	1439			

Annex 2-Figure 40 – ‘Average number of finger outs’ raw data ANOVA results on small object size with 18 subject and handedness data

Analysis of Variance

Source	Sum Sq.	d.f.	Mean Sq.	F	Prob>F
SoundFeedback	0.2718	8	0.03397	0.63	0.7544
Handedness	0.0454	1	0.04537	0.84	0.36
Direction	0.1115	1	0.11151	2.06	0.1515
SoundFeedback*Handedness	0.0481	8	0.00601	0.11	0.9988
SoundFeedback*Direction	0.0968	8	0.0121	0.22	0.9866
Handedness*Direction	0.0408	1	0.04077	0.75	0.3856
SoundFeedback*Handedness*Direction	0.0531	8	0.00664	0.12	0.9983
Error	33.09	612	0.05407		
Total	33.756	647			

Annex 2-Figure 41– ‘Horizontal’ Object part ‘Time’ mean data ANOVA results

Analysis of Variance

Source	Sum Sq.	d.f.	Mean Sq.	F	Prob>F
SoundFeedback	0.1916	8	0.02395	0.62	0.7591
Handedness	0.0726	1	0.07257	1.89	0.17
Direction	0.0397	1	0.03969	1.03	0.31
SoundFeedback*Handedness	0.0533	8	0.00666	0.17	0.9944
SoundFeedback*Direction	0.0853	8	0.01067	0.28	0.9733
Handedness*Direction	0.0072	1	0.00717	0.19	0.666
SoundFeedback*Handedness*Direction	0.0267	8	0.00333	0.09	0.9995
Error	23.5337	612	0.03845		
Total	24.0099	647			

Annex 2-Figure 42– ‘Vertical’ Object part ‘Time’ mean data ANOVA results

Analysis of Variance

Source	Sum Sq.	d.f.	Mean Sq.	F	Prob>F
SoundFeedback	9.82	8	1.22749	2.09	0.0344
Handedness	5.047	1	5.04747	8.61	0.0035
Direction	1.837	1	1.83742	3.14	0.0771
SoundFeedback*Handedness	0.306	8	0.03821	0.07	0.9998
SoundFeedback*Direction	0.798	8	0.0997	0.17	0.9947
Handedness*Direction	3.909	1	3.90918	6.67	0.01
SoundFeedback*Handedness*Direction	0.372	8	0.04647	0.08	0.9997
Error	358.591	612	0.58593		
Total	380.68	647			

Annex 2-Figure 43– ‘Torus’ Object part ‘Time’ mean data ANOVA results

Analysis of Variance

Source	Sum Sq.	d.f.	Mean Sq.	F	Prob>F
SoundFeedback	19.74	8	2.468	1.58	0.1273
Handedness	0.31	1	0.3086	0.2	0.6568
Direction	24.64	1	24.6356	15.78	0.0001
SoundFeedback*Handedness	13.02	8	1.6278	1.04	0.4026
SoundFeedback*Direction	12.07	8	1.5093	0.97	0.4612
Handedness*Direction	6.77	1	6.7732	4.34	0.0377
SoundFeedback*Handedness*Direction	7.08	8	0.8852	0.57	0.8054
Error	955.69	612	1.5616		
Total	1037.95	647			

Annex 2-Figure 44 – 'Horizontal' object part 'Average number of finger outs' mean data ANOVA results

Analysis of Variance

Source	Sum Sq.	d.f.	Mean Sq.	F	Prob>F
SoundFeedback	1.5777	8	0.19721	2.61	0.0081
Handedness	0.7401	1	0.74014	9.81	0.0018
Direction	0.4726	1	0.47261	6.26	0.0126
SoundFeedback*Handedness	0.38	8	0.0475	0.63	0.7534
SoundFeedback*Direction	0.2981	8	0.03726	0.49	0.8611
Handedness*Direction	0.0313	1	0.03125	0.41	0.5202
SoundFeedback*Handedness*Direction	0.2678	8	0.03347	0.44	0.8949
Error	46.1906	612	0.07547		
Total	49.9581	647			

Annex 2-Figure 45 – 'Vertical' object part 'Average number of finger outs' mean data ANOVA results

Analysis of Variance

Source	Sum Sq.	d.f.	Mean Sq.	F	Prob>F
SoundFeedback	13.49	8	1.68643	0.48	0.8695
Handedness	7.78	1	7.77932	2.22	0.1366
Direction	0.43	1	0.42525	0.12	0.7276
SoundFeedback*Handedness	6.1	8	0.76252	0.22	0.9878
SoundFeedback*Direction	3.61	8	0.45073	0.13	0.998
Handedness*Direction	8.96	1	8.96056	2.56	0.1102
SoundFeedback*Handedness*Direction	1.87	8	0.23403	0.07	0.9998
Error	2142.85	612	3.50139		
Total	2185.09	647			

Annex 2-Figure 46 – 'Torus' object part 'Average number of finger outs' mean data ANOVA results

Analysis of Variance

Source	Sum Sq.	d.f.	Mean Sq.	F	Prob>F
SoundFeedback	0.07749	8	0.00969	1.49	0.1562
Handedness	0.00587	1	0.00587	0.9	0.342
Direction	0.04535	1	0.04535	6.99	0.0084
SoundFeedback*Handedness	0.03416	8	0.00427	0.66	0.7284
SoundFeedback*Direction	0.02862	8	0.00358	0.55	0.8176
Handedness*Direction	0.0638	1	0.0638	9.84	0.0018
SoundFeedback*Handedness*Direction	0.00932	8	0.00116	0.18	0.9936
Error	3.96945	612	0.00649		
Total	4.23333	647			

Annex 2-Figure 47 – ‘Horizontal’ object part ‘motor performance index’ mean data ANOVA results

Analysis of Variance

Source	Sum Sq.	d.f.	Mean Sq.	F	Prob>F
SoundFeedback	0.05503	8	0.00688	1.97	0.0475
Handedness	0.06749	1	0.06749	19.36	0
Direction	0.04461	1	0.04461	12.79	0.0004
SoundFeedback*Handedness	0.02205	8	0.00276	0.79	0.6112
SoundFeedback*Direction	0.01676	8	0.0021	0.6	0.7773
Handedness*Direction	0.00218	1	0.00218	0.63	0.4292
SoundFeedback*Handedness*Direction	0.01962	8	0.00245	0.7	0.6885
Error	2.13367	612	0.00349		
Total	2.36142	647			

Annex 2-Figure 48 – ‘Vertical’ object part ‘motor performance index’ mean data ANOVA results

Analysis of Variance

Source	Sum Sq.	d.f.	Mean Sq.	F	Prob>F
SoundFeedback	0.02122	8	0.00265	0.34	0.9481
Handedness	0.00147	1	0.00147	0.19	0.6625
Direction	0.00007	1	0.00007	0.01	0.9214
SoundFeedback*Handedness	0.01176	8	0.00147	0.19	0.9921
SoundFeedback*Direction	0.00692	8	0.00086	0.11	0.9988
Handedness*Direction	0.00732	1	0.00732	0.95	0.3297
SoundFeedback*Handedness*Direction	0.00818	8	0.00102	0.13	0.9978
Error	4.70687	612	0.00769		
Total	4.76381	647			

Annex 2-Figure 49 – ‘Torus’ object part ‘motor performance index’ mean data ANOVA results

Analysis of Variance

Source	Sum Sq.	d.f.	Mean Sq.	F	Prob>F
SoundFeedback	13.894	8	1.73676	1.93	0.0528
Handedness	0.162	1	0.1621	0.18	0.6712
Direction	0.145	1	0.14495	0.16	0.6881
SoundFeedback*Handedness	2.059	8	0.25743	0.29	0.9705
SoundFeedback*Direction	12.723	8	1.59043	1.77	0.0801
Handedness*Direction	0.953	1	0.95305	1.06	0.3035
SoundFeedback*Handedness*Direction	1.106	8	0.13821	0.15	0.9963
Error	549.989	612	0.89868		
Total	582.375	647			

Annex 2-Figure 50 – 'Horizontal' object part 'average accumulated distance away from the object surface' mean data ANOVA results

Analysis of Variance

Source	Sum Sq.	d.f.	Mean Sq.	F	Prob>F
SoundFeedback	2.4915	8	0.31143	2.54	0.01
Handedness	1.3631	1	1.36309	11.12	0.0009
Direction	0.9914	1	0.99142	8.09	0.0046
SoundFeedback*Handedness	1.0232	8	0.1279	1.04	0.4017
SoundFeedback*Direction	0.1457	8	0.01821	0.15	0.9967
Handedness*Direction	0.0583	1	0.0583	0.48	0.4906
SoundFeedback*Handedness*Direction	0.2735	8	0.03418	0.28	0.9728
Error	75.0049	612	0.12256		
Total	81.3516	647			

Annex 2-Figure 51 – 'Vertical' object part 'average accumulated distance away from the object surface' mean data ANOVA results

Analysis of Variance

Source	Sum Sq.	d.f.	Mean Sq.	F	Prob>F
SoundFeedback	3.896	8	0.48698	0.38	0.9303
Handedness	0.226	1	0.22628	0.18	0.6736
Direction	0.74	1	0.74008	0.58	0.4463
SoundFeedback*Handedness	1.026	8	0.12831	0.1	0.9992
SoundFeedback*Direction	2.507	8	0.31333	0.25	0.9818
Handedness*Direction	1.953	1	1.95338	1.53	0.2162
SoundFeedback*Handedness*Direction	2.004	8	0.2505	0.2	0.9913
Error	779.911	612	1.27436		
Total	792.263	647			

Annex 2-Figure 52 – 'Torus' object part 'average accumulated distance away from the object surface' mean data ANOVA results

Analysis of Variance

Source	Sum Sq.	d.f.	Mean Sq.	F	Prob>F
SoundFeedback	4.56	8	0.57	2.55	0.0092
Handedness	2.48	1	2.476	11.08	0.0009
Object	1659.65	2	829.823	3711.3	0
SoundFeedback*Handedness	0.12	8	0.015	0.07	0.9998
SoundFeedback*Object	5.73	16	0.358	1.6	0.061
Handedness*Object	2.69	2	1.344	6.01	0.0025
SoundFeedback*Handedness*Object	0.28	16	0.018	0.08	1
Error	422.59	1890	0.224		
Total	2098.09	1943			

Annex 2-Figure 53 – Detailed ‘Time’ mean data ANOVA results on auditory feedback including all object parts and their movement directions.

Analysis of Variance

Source	Sum Sq.	d.f.	Mean Sq.	F	Prob>F
SoundFeedback	11.38	8	1.42	1.88	0.0588
Handedness	0.49	1	0.49	0.64	0.4229
Object	4752.52	2	2376.26	3143.94	0
SoundFeedback*Handedness	1.02	8	0.13	0.17	0.9949
SoundFeedback*Object	10.07	16	0.63	0.83	0.6487
Handedness*Object	1.29	2	0.65	0.86	0.425
SoundFeedback*Handedness*Object	3.24	16	0.2	0.27	0.9983
Error	1428.5	1890	0.76		
Total	6208.51	1943			

Annex 2-Figure 54 – Detailed ‘average number of finger outs’ mean data ANOVA results on auditory feedback including all object parts and their movement directions.

Analysis of Variance

Source	Sum Sq.	d.f.	Mean Sq.	F	Prob>F
SoundFeedback	0.0529	8	0.00661	1.13	0.3398
Handedness	0.0458	1	0.04584	7.83	0.0052
Object	2.1565	2	1.07826	184.21	0
SoundFeedback*Handedness	0.0047	8	0.00059	0.1	0.9992
SoundFeedback*Object	0.1007	16	0.00629	1.07	0.3737
Handedness*Object	0.0284	2	0.01421	2.43	0.0886
SoundFeedback*Handedness*Object	0.0632	16	0.00395	0.68	0.8208
Error	11.0628	1890	0.00585		
Total	13.5151	1943			

Annex 2-Figure 55 – Detailed ‘motor performance index’ mean data ANOVA results on auditory feedback including all object parts and their movement directions.

Analysis of Variance

Source	Sum Sq.	d.f.	Mean Sq.	F	Prob>F
SoundFeedback	11.38	8	1.42	1.88	0.0588
Handedness	0.49	1	0.49	0.64	0.4229
Object	4752.52	2	2376.26	3143.94	0
SoundFeedback*Handedness	1.02	8	0.13	0.17	0.9949
SoundFeedback*Object	10.07	16	0.63	0.83	0.6487
Handedness*Object	1.29	2	0.65	0.86	0.425
SoundFeedback*Handedness*Object	3.24	16	0.2	0.27	0.9983
Error	1428.5	1890	0.76		
Total	6208.51	1943			

Annex 2-Figure 56 – Detailed ‘average accumulate distance away from the object surface’ mean data ANOVA results on auditory feedback including all object parts and their movement directions.

Analysis of Variance

Source	Sum Sq.	d.f.	Mean Sq.	F	Prob>F
Handedness	0.0033	1	0.00328	0.11	0.7347
MovementDirection	0.0024	1	0.00239	0.08	0.7723
Handedness*MovementDirection	0.0486	1	0.04865	1.7	0.1921
Error	41.0134	1436	0.02856		
Total	41.0677	1439			

Annex 2-Figure 57 – Detailed ‘time’ data ANOVA results on left-handed movement direction and handedness interaction

Analysis of Variance

Source	Sum Sq.	d.f.	Mean Sq.	F	Prob>F
Handedness	56.41	1	56.4062	19.99	0
MovementDirection	13.03	1	13.034	4.62	0.0318
Handedness*MovementDirection	22.25	1	22.2507	7.88	0.0051
Error	4052.61	1436	2.8222		
Total	4144.3	1439			

Annex 2-Figure 58 – Detailed ‘average number of finger out’ data ANOVA results on left-handed movement direction and handedness interaction

Analysis of Variance

Source	Sum Sq.	d.f.	Mean Sq.	F	Prob>F
Handedness	0.2399	1	0.23994	15.08	0.0001
MovementDirection	0.3512	1	0.35123	22.08	0
Handedness*MovementDirection	0.1013	1	0.10128	6.37	0.0117
Error	22.8426	1436	0.01591		
Total	23.5351	1439			

Annex 2-Figure 59 – Detailed ‘motor performance index’ data ANOVA results on left-handed movement direction and handedness interaction

Analysis of Variance

Source	Sum Sq.	d.f.	Mean Sq.	F	Prob>F
Handedness	2.67	1	2.6656	1.04	0.3084
MovementDirection	52.4	1	52.4047	20.41	0
Handedness*MovementDirection	1.05	1	1.0521	0.41	0.5222
Error	3686.6	1436	2.5673		
Total	3742.72	1439			

Annex 2-Figure 60 – Detailed ‘average accumulated distance away from the object surface’ data ANOVA results on left-handed movement direction and handedness interaction

Annex 3 – ANOVA results for Chapter 3

Analysis of Variance

Source	Sum Sq.	d.f.	Mean Sq.	F	Prob>F
Grip	28.42	1	28.4239	59.69	0
Hand	7.51	1	7.5071	15.76	0.0001
Music	5.21	3	1.7369	3.65	0.0121
Sensor	518.95	11	47.1771	99.07	0
Vision	4.15	1	4.1523	8.72	0.0032
Grip*Hand	0.24	1	0.2411	0.51	0.4768
Grip*Music	0.5	3	0.1663	0.35	0.7897
Grip*Sensor	15.36	11	1.3968	2.93	0.0007
Grip*Vision	0.25	1	0.2546	0.53	0.4647
Hand*Music	0.29	3	0.096	0.2	0.8953
Hand*Sensor	79.41	11	7.2195	15.16	0
Hand*Vision	2.12	1	2.1195	4.45	0.0349
Music*Sensor	11.02	33	0.3338	0.7	0.8987
Music*Vision	0.38	3	0.1263	0.27	0.8505
Sensor*Vision	10.63	11	0.9663	2.03	0.0223
Grip*Hand*Music	0.16	3	0.052	0.11	0.9548
Grip*Hand*Sensor	3.88	11	0.3525	0.74	0.7004
Grip*Hand*Vision	0.01	1	0.0084	0.02	0.8944
Grip*Music*Sensor	1.46	33	0.0442	0.09	1
Grip*Music*Vision	0.09	3	0.0296	0.06	0.9798
Grip*Sensor*Vision	0.32	11	0.0294	0.06	1
Hand*Music*Sensor	5.28	33	0.16	0.34	0.9999
Hand*Music*Vision	0.2	3	0.0671	0.14	0.9355
Hand*Sensor*Vision	5.26	11	0.4782	1	0.4397
Music*Sensor*Vision	1.95	33	0.0592	0.12	1
Grip*Hand*Music*Sensor	1.16	33	0.0352	0.07	1
Grip*Hand*Music*Vision	0.03	3	0.0088	0.02	0.9966
Grip*Hand*Sensor*Vision	0.42	11	0.0383	0.08	1
Grip*Music*Sensor*Vision	0.7	33	0.0213	0.04	1
Hand*Music*Sensor*Vision	1.26	33	0.0382	0.08	1
Grip*Hand*Music*Sensor*Vision	0.49	33	0.0147	0.03	1
Error	1828.6	3840	0.4762		
Total	2535.71	4223			

Annex 3-Figure 1- Five-way grip force ANOVA results for first study of third chapter

Analysis of Variance

Source	Sum Sq.	d.f.	Mean Sq.	F	Prob>F
SUBJECT	210.773	1	210.773	24.03	0
HAND	2.314	1	2.314	0.26	0.6107
SUBJECT*HAND	43.472	1	43.472	4.96	0.0323
Error	315.746	36	8.771		
Total	572.304	39			

Annex 3-Figure 2- Subject and handedness ANOVA Time results for second study of third chapter

Analysis of Variance

Source	Sum Sq.	d.f.	Mean Sq.	F	Prob>F
HANDEDNESS	98.11	1	98.107	142.03	6.87806e-27
USER	160.37	1	160.366	232.17	7.46193e-39
FSR	83.03	7	11.861	17.17	5.81548e-19
HANDEDNESS*USER	37.69	1	37.687	54.56	1.63492e-12
HANDEDNESS*FSR	464.08	7	66.297	95.98	1.6481e-71
USER*FSR	79.46	7	11.351	16.43	3.37573e-18
HANDEDNESS*USER*FSR	123.26	7	17.609	25.49	5.01476e-27
Error	198.93	288	0.691		
Total	1244.92	319			

Annex 3-Figure 3- Subject, Hand and Sensor ANOVA Force results for second study of third chapter

Annex 4 Tables

Annex 4-Table 1 - Trajectory movement ANOVA summary for trajectory analysis for study 1

Factor	**Factor Level**	**'from-target-to-target duration'**		**'average distance from the reference trajectory'**		**'dispersion in trajectory'**	
		Mean	**SEM**	**Mean**	**SEM**	**Mean**	**SEM**
Vision	Direct	0.86	0.012	11.31	0.207	10	0.185
	Fisheye	1.40	0.023	14.52	0.239	12.41	0.194
	Undistorted	1.38	0.022	13.05	0.212	11.20	0.175
Manipulation	No Tool	1.10	0.015	13.66	0.198	12.13	0.170
	Tool	1.33	0.020	12.25	0.165	10.28	0.130
Session	Session 1	1.56	0.047	13.99	0.399	12.53	0.353
	Session 2	1.40	0.039	12.88	0.371	11.81	0.305
	Session 3	1.31	0.037	13.16	0.387	11.63	0.342
	Session 4	1.12	0.031	12.85	0.339	11.14	0.335
	Session 5	1.14	0.034	12.55	0.330	10.91	0.302
	Session 6	1.03	0.030	12.50	0.318	10.28	0.250
	Session 7	1.11	0.028	12.81	0.371	10.71	0.272
	Session 8	1.07	0.028	12.94	0.407	10.62	0.262
Participant	Subject 1	1.66	0.030	13.74	0.403	12.50	0.306
	Subject 2	1.32	0.024	13.60	0.185	11.58	0.157
	Subject 3	1.00	0.019	12.05	0.187	10.21	0.185
	Subject 4	0.88	0.012	12.45	0.186	10.53	0.176
Segment	X1	0.55	0.016	21.97	0.442	15.30	0.312
	X2	1.39	0.031	9.73	0.179	9.09	0.245
	X3	1.28	0.027	10.41	0.158	8.01	0.185
	X4	1.38	0.030	11.98	0.186	12.81	0.274
	X5	1.34	0.029	11.36	0.169	9.64	0.133
	X0	1.35	0.029	12.30	0.158	12.38	0.206

Annex 4-Table 2 - Interactions between the factors ‘Vision’ and ‘Segment’ in the data from Subject 1 on ‘from-target-to-target duration’

		D Means	**T**	**P**
Subject 1				
X1	Direct vs Fisheye	0.124	1.643	NS
	Fisheye vs Undistorted	0.024	1.322	NS
	Direct vs Undistorted	0.010	0.320	NS
X2	Direct vs Fisheye	0.805	10.687	p<0.001
	Fisheye vs Undistorted	0.0568	0.754	NS
	Direct vs Undistorted	0.862	11.441	p<0.01
X3	Direct vs Fisheye	0.728	9.664	p<0.01
	Fisheye vs Undistorted	0.034	0.456	NS
	Direct vs Undistorted	0.762	10.119	p<0.01
X4	Direct vs Fisheye	0.968	12.589	p<0.01
	Fisheye vs Undistorted	0.135	1.974	NS
	Direct vs Undistorted	0.833	11.064	p<0.01
X5	Direct vs Fisheye	0.850	11.285	p<0.01
	Fisheye vs Undistorted	0.003	0.042	NS
	Direct vs Undistorted	0.853	11.327	p<0.01
X0	Direct vs Fisheye	0.806	10.706	p<0.01
	Fisheye vs Undistorted	0.080	1.063	NS
	Direct vs Undistorted	0.886	11.769	p<0.01

Annex 4-Table 3 - Interactions between the factors ‘Vision’ and ‘Segment’ in the data from Subject 2 on ‘from-target-to-target duration’

		D Means	**T**	**P**
Subject 2				
X1	Direct vs Fisheye	0.07	1.014	NS
	Fisheye vs Undistorted	0.053	0.789	NS
	Direct vs Undistorted	0.122	1.803	NS
X2	Direct vs Fisheye	0.782	11.586	p<0.001
	Fisheye vs Undistorted	0.075	1.116	NS
	Direct vs Undistorted	0.707	10.469	p<0.01
X3	Direct vs Fisheye	0.647	9.573	p<0.001
	Fisheye vs Undistorted	0.004	0.058	NS
	Direct vs Undistorted	0.650	9.633	p<0.01
X4	Direct vs Fisheye	0.731	10.830	p<0.001
	Fisheye vs Undistorted	0.076	1.127	NS
	Direct vs Undistorted	0.655	9.703	p<0.01
X5	Direct vs Fisheye	0.722	10.694	p<0.001
	Fisheye vs Undistorted	0.022	0.332	NS
	Direct vs Undistorted	0.745	11.026	p<0.01
X0	Direct vs Fisheye	0.706	10.460	p<0.001
	Fisheye vs Undistorted	0.067	0.9988	NS
	Direct vs Undistorted	0.774	11.458	p<0.01

Annex 4-Table 4 - Interactions between the factors ‘Vision’ and ‘Segment’ in the data from Subject 3 on ‘from-target-to-target duration’

		D Means	**T**	**P**
Subject 3				
X1	Direct vs Fisheye	0.0685	1.014	NS
	Fisheye vs Undistorted	0.0532	0.789	NS
	Direct vs Undistorted	0.122	1.803	NS
X2	Direct vs Fisheye	0.782	11.586	p<0.001
	Fisheye vs Undistorted	0.075	1.116	NS
	Direct vs Undistorted	0.707	10.469	p<0.01
X3	Direct vs Fisheye	0.647	9.575	p<0.001
	Fisheye vs Undistorted	0.004	0.058	NS
	Direct vs Undistorted	0.650	9.633	p<0.01
X4	Direct vs Fisheye	0.731	10.830	p<0.001
	Fisheye vs Undistorted	0.076	1.127	NS
	Direct vs Undistorted	0.655	9.703	p<0.01
X5	Direct vs Fisheye	0.722	10.694	p<0.001
	Fisheye vs Undistorted	0.022	0.332	NS
	Direct vs Undistorted	0.745	11.026	p<0.01
X0	Direct vs Fisheye	0.706	10.460	p<0.001
	Fisheye vs Undistorted	0.067	0.998	NS
	Direct vs Undistorted	0.774	11.458	p<0.01

Annex 4-Table 5 - Interactions between the factors ‘Vision’ and ‘Segment’ in the data from Subject 4 on ‘from-target-to-target duration’

		D Means	**T**	**P**
Subject 4				
X1	Direct vs Fisheye	0.068	1.014	NS
	Fisheye vs Undistorted	0.053	0.789	NS
	Direct vs Undistorted	0.122	1.803	NS
X2	Direct vs Fisheye	0.782	11.586	p<0.001
	Fisheye vs Undistorted	0.075	1.116	NS
	Direct vs Undistorted	0.707	10.469	p<0.01
X3	Direct vs Fisheye	0.647	9.575	p<0.001
	Fisheye vs Undistorted	0.004	0.058	NS
	Direct vs Undistorted	0.650	9.633	p<0.01
X4	Direct vs Fisheye	0.731	10.830	p<0.001
	Fisheye vs Undistorted	0.076	1.127	NS
	Direct vs Undistorted	0.655	9.703	p<0.01
X5	Direct vs Fisheye	0.722	10.694	p<0.001
	Fisheye vs Undistorted	0.022	0.332	NS
	Direct vs Undistorted	0.745	11.026	p<0.01
X0	Direct vs Fisheye	0.706	10.460	p<0.001
	Fisheye vs Undistorted	0.067	0.998	NS
	Direct vs Undistorted	0.774	11.458	p<0.01

Annex 4-Table 6 - Interactions between the factors ‘Vision’ and ‘Segment’ in the data from Subject 1 on ‘dispersion in trajectory’

		D Means	T	P
Subject 1				
X1	Direct vs Fisheye	4.234	3.648	p<0.0001
	Fisheye vs Undistorted	1.230	1.00	NS
	Direct vs Undistorted	3.004	2.588	p<0.001
X4	Direct vs Fisheye	11.447	9.863	p<0.0001
	Fisheye vs Undistorted	2.591	2.233	p<0.05
	Direct vs Undistorted	8.856	7.630	p<0.0001

Annex 4-Table 7 - Interactions between the factors ‘Vision’ and ‘Segment’ in the data from Subject 2 on ‘dispersion in trajectory’

		D Means	t	P
Subject 2				
X1	Direct vs Fisheye	4.042	5.272	p<0.0001
	Fisheye vs Undistorted	2.136	2.486	p<0.05
	Direct vs Undistorted	1.906	2.785	p<0.01
X2	Direct vs Fisheye	5.223	6.182	p<0.0001
	Fisheye vs Undistorted	3.907	4.040	p<0.001
	Direct vs Undistorted	2.126	2.772	p<0.01
X3	Direct vs Fisheye	4.445	4.493	p<0.0001
	Fisheye vs Undistorted	1.036	1.352	NS
	Direct vs Undistorted	2.409	3.142	p<0.01
X4	Direct vs Fisheye	3.042	3.97	p<0.0001
	Fisheye vs Undistorted	2.108	2.750	NS
	Direct vs Undistorted	0.933	1.217	p<0.01
X5	Direct vs Fisheye	0.448	0.584	NS
	Fisheye vs Undistorted	1.971	2.570	p<0.05
	Direct vs Undistorted	1.523	1.986	NS
X0	Direct vs Fisheye	3.359	4.381	p<0.0001
	Fisheye vs Undistorted	1.143	1.491	NS
	Direct vs Undistorted	2.216	2.890	p<0.01

Annex 4-Table 8 - Interactions between the factors ‘Vision’ and ‘Segment’ in the data from Subject 3 on ‘dispersion in trajectory’

		D Means	T	P
Subject 3				
X1	Direct vs Fisheye	4.763	5.950	p<0.0001
	Fisheye vs Undistorted	2.239	2.787	p<0.01
	Direct vs Undistorted	2.525	3.154	p<0.01
X2	Direct vs Fisheye	5.567	6.955	p<0.0001
	Fisheye vs Undistorted	2.162	2.701	p<0.01
	Direct vs Undistorted	3.405	4.254	p<0.0001
X4	Direct vs Fisheye	4.061	5.074	p<0.0001
	Fisheye vs Undistorted	0.934	1.166	NS
	Direct vs Undistorted	3.128	3.907	p<0.0001

Annex 4-Table 9 - Interactions between the factors ‘Vision’ and ‘Segment’ in the data from Subject 4 on ‘dispersion in trajectory’

		D Means	T	P
Subject 4				
X2	Direct vs Fisheye	2.032	2.747	p<0.01
	Fisheye vs Undistorted	1.319	1.784	NS
	Direct vs Undistorted	0.712	0.963	NS
X3	Direct vs Fisheye	2.240	3.028	p<0.01
	Fisheye vs Undistorted	1.204	1.627	NS
	Direct vs Undistorted	1.036	1.401	NS
X4	Direct vs Fisheye	2.017	2.727	p<0.01
	Fisheye vs Undistorted	1.576	2.130	NS
	Direct vs Undistorted	0.441	0.597	NS

Annex 4-Table 10 – Means and SEMs for trajectory analysis of study 2

Factor	Level	Segment traverse duration (seconds)		Average distance from the reference trajectory (pixel)		Dispersion in trajectory (pixel)	
		Mean	SEM	Mean	SEM	Mean	SEM
Vision	Direct	1.006	0.025	13.53	0.43	11.96	0.53
	Fisheye	1.767	0.045	16.78	0.56	13.63	0.51
	Undistorted	1.769	0.042	15.01	0.48	12.88	0.55
	Oculus 3D	1.897	0.044	27.81	0.94	22.38	0.84
Manipulation	No Tool	1.509	0.030	18.9	0.54	16.22	0.49
	Tool	1.711	0.036	17.67	0.52	14.21	0.48
Session	Session 1	1.708	0.035	19.01	0.58	15.71	0.51
	Session 2	1.512	0.031	17.56	0.48	14.72	0.46
Segment	X1	0.984	0.032	29.59	1.34	20.74	0.90
	X2	1.607	0.048	14.16	0.60	12.90	0.78
	X3	1.657	0.053	14.36	0.60	12.12	0.87
	X4	1.839	0.059	18.51	0.85	19.28	1.03
	X5	1.818	0.058	17.52	0.65	13.88	0.54
	X0	1.755	0.056	15.57	0.41	12.36	0.50

Annex 4-Table 11 - Novice ‘time’ and ‘precision’ results for Study 3

Factor	Level	‘Time’		‘Precision’	
		Mean	SEM	Mean	SEM
Vision	Direct	6.560	0.117	1142	33
	Fisheye	11.17	0.148	1332	25
	Undistorted	11.42	0.144	1351	23
	Oculus	11.96	0.147	1732	28
Manipulation	No Tool	9.646	0.095	1423	21
	Tool	11.97	0.131	1436	20
Color	Color	11.57	0.109	1486	23
	Gray Scale	11.47	0.130	1457	21

Annex 4-Table 12 - Surgeon ‘time’ and ‘precision’ results for study 3

Factor	Level	‘Time’		‘Precision’	
		Mean	SEM	Mean	SEM
Vision	Direct	9.259	0.209	1135	26
	Fisheye	17.37	0.389	1392	36
	Undistorted	17.93	0.405	1205	33
	Oculus	15.88	0.318	1699	35
Manipulation	No Tool	15.34	0.301	1392	27
	Tool	16.55	0.293	1387	27
Color	Color	18.21	0.323	1449	32
	Gray Scale	15.91	0.276	1415	28

Annex 4-Table 13 - Expert surgeon ‘time’ and ‘precision’ results for Study 3

Factor	Level	‘Time’		‘Precision’	
		Mean	SEM	Mean	SEM
Vision	Direct	11.17	0.350	630	55
	Fisheye	17.05	0.571	811	38
	Undistorted	13.32	0.277	818	32
	Oculus	13.06	0.275	999	51
Manipulation	No Tool	13.25	0.338	791	39
	Tool	14.76	0.394	890	27
Color	Color	15.82	0.455	959	32
	Gray Scale	13.13	0.234	739	35

Annex 4-Table 14 - Novice, Surgeon and expert surgeon ‘error’ results for Study 3

Factor	Level	‘Error’	
		Mean	SEM
Expertise	Novice	0.548	0.061
	Surgeons	0.298	0.073
	Expert Surgeon	0.786	0.261
Vision	Direct	0.368	0.109
	Fisheye	0.605	0.101
	Undistorted	0.566	0.100
	Oculus	0.329	0.069
Manipulation	No Tool	0.429	0.058
	Tool	0.533	0.077
Color	Color	0.535	0.077
	Gray Scale	0.465	0.071

Annex 4-Table 15 - Novice, Surgeon and expert surgeon trajectory results for Study 3

Factor	Level	‘from-target-to-target duration’		‘average distance from the reference trajectory’		‘dispersion in trajectory’	
		Mean	SEM	Mean	SEM	Mean	SEM
Expertise	Novice	1.879	0.027	17.25	0.27	14.18	0.25
	Surgeons	2.67	0.617	17.62	0.43	14.63	0.37
	Expert Surgeon	2.297	0.096	16.61	1.01	16.50	1.06
Vision	Direct	1.359	0.038	13.80	0.44	11.48	0.51
	Fisheye	2.264	0.053	16.45	0.37	13.88	0.34
	Undistorted	2.349	0.058	14.26	0.27	12.19	0.28
	Oculus	2.231	0.046	23.07	0.50	18.74	0.43
Manipulation	No Tool	1.992	0.038	17.83	0.32	15.13	0.29
	Tool	2.307	0.040	16.84	0.31	13.75	0.28
Color	Color	2.369	0.045	18.13	0.36	15.22	0.33
	Gray Scale	2.194	0.041	17.72	0.34	14.65	0.29
Segment	X1	0.809	0.023	27.71	0.73	20.23	0.55
	X2	2.411	0.059	12.50	0.29	12.31	0.40
	X3	2.288	0.062	13.42	0.40	11.28	0.51
	X4	2.526	0.62	15.76	0.46	16.92	0.55
	X5	2.488	0.064	18.59	0.38	14.53	0.36
	X0	2.377	0.063	16.04	0.32	11.38	0.32

Annex 4-Table 16 - Means and SEMs for ‘time’ on ‘Vertical’, ‘Horizontal’ and ‘Torus’ for visual feedback

Visual feedback	Vertical		Horizontal		Torus	
	Mean	SEM	Mean	SEM	Mean	SEM
Real world view with direct touch	0.295	0.004	0.333	0.0047	1.623	0.025
Augmented reality (AR)	0.576	0.036	0.718	0.0014	3.182	0.057
Virtual reality (VR)	0.649	0.046	0.804	0.022	3.142	0.055
Mixed reality (MR)	0.586	0.030	0.781	0.021	3.590	0.073
2D Screen view	1.397	0.055	1.295	0.019	4.043	0.046
2D Screen view+ MS	1.201	0.075	1.296	0.042	5.324	0.103

Annex 4-Table 17 - Means and SEMs for ‘time’ on ‘Horizontal’ for handedness

Handedness	Mean	SEM
Dominant Hand	3.313	0.095
Non-Dominant Hand	3.655	0.136

Annex 4-Table 18 - Means and SEMs for ‘time’ on ‘Horizontal’ for handedness and visual feedback interaction

Visual feedback	Handedness	Mean	SEM
Real world view with direct touch	Dominant Hand	0.281	0.014
	Non-dominant Hand	0.309	0.016
Augmented reality (AR)	Dominant Hand	0.589	0.059
	Non-dominant Hand	0.563	0.045
Virtual reality (VR)	Dominant Hand	0.669	0.070
	Non-dominant Hand	0.630	0.061
Mixed reality (MR)	Dominant Hand	0.595	0.04
	Non-dominant Hand	0.579	0.042
2D Screen view	Dominant Hand	1.213	0.068
	Non-dominant Hand	1.581	0.079
2D Screen view+ MS	Dominant Hand	1.220	0.113
	Non-dominant Hand	1.182	0.102

Annex 4-Table 19 - Means and SEMs for ‘average number of finger outs’ on ‘Horizontal’, ‘Vertical’ and ‘Torus’ for visual feedback and handedness interaction

	Vertical		**Horizontal**		**Torus**	
	Mean	**SEM**	**Mean**	**SEM**	**Mean**	**SEM**
Visual Feedback						
Real world view with direct touch	0.0125	0.0039	0.0111	0.0037	0.0722	0.011
Augmented reality (AR)	0.191	0.046	1.229	0.218	3.819	0.223
Virtual reality (VR)	0.183	0.038	1.096	0.196	3.615	0.211
Mixed reality (MR)	0.209	0.054	1.871	0.539	4.675	0.239
2D Screen view	0.261	0.029	0.1833	0.028	1.182	0.096
2D Screen view+ MS	0.518	0.075	1.532	0.160	6.289	0.23
Handedness						
Dominant Hand	0.182	0.023	1.257	0.199	3.06	3.48
Non-Dominant Hand	0.277	0.032	0.717	0.091	0.17	0.18

Annex 4-Table 20 - Means and SEMs for ‘average number of finger outs’ on ‘Horizontal’ for movement direction

	Mean	**SEM**
Left to right	0.693	0.077
Right to left	1.281	0.205

Annex 4-Table 21 - Means and SEMs for ‘average number of finger outs’ on ‘Vertical’ for handedness and visual feedback interaction

Visual feedback	Handedness	Mean	SEM
Real world view with direct touch	Dominant Hand	0.0111	0.005
	Non-dominant Hand	0.0139	0.006
Augmented reality (AR)	Dominant Hand	0.158	0.053
	Non-dominant Hand	0.225	0.077
Virtual reality (VR)	Dominant Hand	0.161	0.046
	Non-dominant Hand	0.206	0.062
Mixed reality (MR)	Dominant Hand	0.239	0.093
	Non-dominant Hand	0.181	0.057
2D Screen view	Dominant Hand	0.0972	0.019
	Non-dominant Hand	0.425	0.042
2D Screen view+ MS	Dominant Hand	0.425	0.063
	Non-dominant Hand	0.611	0.136

Annex 4-Table 22 - Means and SEMs for ‘average number of finger outs’ on ‘Horizontal’ for movement direction and visual feedback interaction

Visual feedback	Movement direction	Mean	SEM
Real world view with direct touch	Left to right	0.005	0.003
	Right to left	0.016	0.04
Augmented reality (AR)	Left to right	0.672	0.922
	Right to left	1.786	0.391
Virtual reality (VR)	Left to right	0.533	0.0159
	Right to left	1.658	0.336
Mixed reality (MR)	Left to right	0.953	0.196
	Right to left	2.789	1.045
2D Screen view	Left to right	0.178	0.04
	Right to left	0.189	0.04
2D Screen view+ MS	Left to right	1.814	0.264
	Right to left	1.25	0.175

Annex 4-Table 23 - Means and SEMs for ‘average number of finger outs’ on ‘Torus’ for movement direction and handedness interaction

Movement direction	Handedness	Mean	SEM
Clockwise	Dominant Hand	3.199	0.256
	Non-dominant Hand	3.120	0.23
Counter-Clockwise	Dominant Hand	2.921	0.245
	Non-dominant Hand	3.855	0.274

Annex 4-Table 24 - Means and SEMs for ‘motor performance index’ variable on ‘Vertical’, ‘Horizontal’ and ‘Torus’ for visual feedback

Visual feedback	‘Vertical’		‘Horizontal’		‘Torus’	
	Mean	SEM	Mean	SEM	Mean	SEM
Augmented reality (AR)	4.692	1.805	5.253	0.946	11.503	1.100
Virtual reality (VR)	4.716	1.454	3.648	0.616	9.974	0.954
Mixed reality (MR)	4.184	1.308	4.585	0.692	14.148	1.085
2D Screen view	4.827	0.743	3.841	0.880	13.383	1.384
2D Screen view+ MS	16.346	2.541	11.12	1.239	29.791	1.415

Annex 4-Table 25 - Means and SEMs for ‘motor performance index’ on ‘Horizontal’ for movement direction

	Mean	SEM
Left to right	4.63	0.557
Right to left	6.748	0.639

Annex 4-Table 26 - Means and SEMs for ‘motor performance index’ on ‘Horizontal’ for visual feedback and handedness

Visual feedback	Handedness	Mean	SEM
Augmented reality (AR)	Dominant Hand	5.021	0.963
	Non-Dominant Hand	5.484	1.643
Virtual reality (VR)	Dominant Hand	4.373	0.584
	Non-Dominant Hand	2.923	0.884
Mixed reality (MR)	Dominant Hand	5.518	1.117
	Non-Dominant Hand	3.652	0.803
2D Screen view	Dominant Hand	1.058	0.462
	Non-Dominant Hand	6.623	1.578
2D Screen view+ MS	Dominant Hand	13.618	1.894
	Non-Dominant Hand	8.622	1.511

Annex 4-Table 27 - Means and SEMs for ‘motor performance index’ on ‘Horizontal’ for movement direction and handedness interaction

Handedness	Movement direction	Mean	SEM
Dominant Hand	Left to Right	4.798	0.826
	Right to Left	5.065	0.639
Non-Dominant Hand	Left to right	2.919	0.470
	Right to left	6.182	0.918

Annex 4-Table 28 - Means and SEMs for ‘motor performance index’ on ‘Torus’ for handedness

Handedness	Mean	SEM
Dominant Hand	14.372	0.891
Non-Dominant Hand	17.148	0.933

Annex 4-Table 29 - Means and SEMs for ‘motor performance index’ on ‘Torus’ for visual feedback and handedness interaction

Visual feedback	Handedness	Mean	SEM
Augmented reality (AR)	Dominant Hand	11.602	1.428
	Non-Dominant Hand	11.406	1.421
Virtual reality (VR)	Dominant Hand	9.638	1.327
	Non-Dominant Hand	10.309	1,387
Mixed reality (MR)	Dominant Hand	13.109	1.283
	Non-Dominant Hand	15.187	1.752
2D Screen view	Dominant Hand	7.096	0.935
	Non-Dominant Hand	19.669	2.155
2D Screen view+ MS	Dominant Hand	30.412	2.047
	Non-Dominant Hand	29.169	1.979

Annex 4-Table 30 - Means and SEMs for ‘motor performance index’ on ‘Torus’ for handedness and movement direction interaction

Handedness	Movement direction	Mean	SEM
Dominant Hand	Clockwise	15.291	1.318
	Counter Clockwise	13.452	1.197
Non-Dominant Hand	Clockwise	15.971	1.284
	Counter Clockwise	18.325	1.350

Annex 4-Table 31 - Means and SEMs for ‘average accumulated distance away from the object surface’ variable on ‘Vertical’, ‘Horizontal’ and ‘Torus’ for visual feedback

Visual feedback	Vertical		Horizontal		Torus	
	Mean	SEM	Mean	SEM	Mean	SEM
Augmented reality (AR)	5.25	2.54	4.97	2.12	30.88	2.52
Virtual reality (VR)	8.86	5.16	2.65	0.739	25.67	1.99
Mixed reality (MR)	4.62	2.24	1.98	0.5	41.90	4.14
2D Screen view	4.85	0.87	5.57	2.59	86.83	12.58
2D Screen view+ MS	54.25	17.56	32.014	6.95	130.14	11.49

Annex 4-Table 32 - Means and SEMs for ‘average accumulated distance away from the object surface’ on ‘Horizontal’ for movement direction

Movement direction	Mean	SEM
Left to right	0.231	0.025
Right to left	0.391	0.041

Annex 4-Table 33 - Means and SEMs for ‘average accumulated distance away from the object surface’ variable on ‘Horizontal’ for visual feedback and handedness interaction

Visual feedback	Handedness	Mean	SEM
Augmented reality (AR)	Dominant Hand	0.234	0.037
	Non-Dominant Hand	0.321	0.111
Virtual reality (VR)	Dominant Hand	0.288	0.046
	Non-Dominant Hand	0.155	0.035
Mixed reality (MR)	Dominant Hand	0.285	0.048
	Non-Dominant Hand	0.189	0.045
2D Screen view	Dominant Hand	0.0272	0.011
	Non-Dominant Hand	0.349	0.098
2D Screen view+ MS	Dominant Hand	0.696	0.096
	Non-Dominant Hand	0.568	0.102

Annex 4-Table 34 - Means and SEMs for ‘average accumulated distance away from the object surface’ on ‘Torus’ for handedness and movement direction interaction

Handedness	Movement direction	‘Torus’	
		Mean	SEM
Dominant Hand	Left to right	0.290	0.045
	Right to left	0.322	0.038
Non-Dominant Hand	Left to right	0.172	0.021
	Right to left	0.460	0.072

Annex 4-Table 35 - Means and SEMs for ‘average accumulated distance away from the object surface’ on ‘Torus’ for visual feedback and handedness interaction

Visual feedback	**Handedness**	**‘Horizontal’**	
		Mean	**SEM**
Augmented reality (AR)	Dominant Hand	0.969	0.066
	Non-Dominant Hand	0.899	0.058
Virtual reality (VR)	Dominant Hand	0.931	0.077
	Non-Dominant Hand	0.958	0.060
Mixed reality (MR)	Dominant Hand	0.892	0.054
	Non-Dominant Hand	0.793	0.037
2D Screen view	Dominant Hand	1.556	0.219
	Non-Dominant Hand	2.396	0.254
2D Screen view+ MS	Dominant Hand	0.942	0.057
	Non-Dominant Hand	0.869	0.056

Annex 4-Table 36 - Means and SEMs for ‘average distance from the object surface’ on ‘Torus’ for handedness and movement direction interaction

Handedness	**Movement direction**	**Mean**	**SEM**
Dominant Hand	Clockwise	1.178	0.095
	Counter Clockwise	0.938	0.046
Non-Dominant Hand	Clockwise	1.089	0.09
	Counter Clockwise	1.277	0.109

Annex 4-Table 37 - Means and SEMs for ‘time’ on ‘Vertical’, ‘Horizontal’ and ‘Torus’ for object size

Ratio	‘Vertical’		‘Horizontal’		Ratio	‘Torus’	
	Mean	SEM	Mean	SEM		Mean	SEM
5	0.298	0.015	0.339	0.017	15.7	1.73	0.699
12.5	0.550	0.026	0.674	0.032	39.26	3.676	1.393
8.3	0.492	0.023	0.669	0.064	26.17	3.1940	0.196
6.25	0.413	0.021	0.509	0.027	19.63	2.3141	0.935
11.6	0.698	0.036	0.823	0.036	36.65	4.101	0.150
15	0.963	0.055	1.245	0.022	47.12	5.193	0.211

Annex 4-Table 38 - Means and SEMs for ‘time’ on ‘Vertical’ and ‘Horizontal’ for movement direction

Movement direction	‘Vertical’		‘Horizontal’	
	Mean	SEM	Mean	SEM
Left to Right	-	-	0.668	0.028
Right to Left	-	-	0.754	0.035
Up to Bottom	0.536	0.022	-	-
Bottom to Up	0.570	0.017	-	-

Annex 4-Table 39 - Means and SEMs for ‘average number of finger outs’ on ‘Vertical’, ‘Horizontal’ and ‘Torus’ for object size

Ratio	‘Vertical’		‘Horizontal’		Ratio	‘Torus’	
	Mean	SEM	Mean	SEM		Mean	SEM
5	0.669	0.139	0.661	0.114	15.7	1.471	0.057
12.5	0.107	0.019	0.946	0.163	39.26	5.560	0.194
8.3	0.156	0.029	1.404	0.378	26.17	4.028	0.319
6.25	0.062	0.026	0.128	0.046	19.63	2.269	0.139
11.6	0.276	0.039	0.836	0.124	36.65	4.606	0.193
15	0.347	0.05	1.058	0.128	47.12	5.193	0.241

Annex 4-Table 40 - Means and SEMs for ‘average number of finger outs’ on ‘Horizontal’ for movement direction

Movement direction	Mean	SEM
Left to Right	0.614	0.065
Right to Left	1.063	0.14

Annex 4-Table 41 - Means and SEMs for ‘average number of finger outs’ on ‘Torus’ for movement direction and handedness interaction

Handedness	Movement direction	Mean	SEM
Dominant Hand	Clockwise	3.875	0.211
	Counter-Clockwise	3.606	0.25
Non-Dominant Hand	Clockwise	3.726	0.204
	Counter-Clockwise	4.410	0.230

Annex 4-Table 42 – Means and SEMs for ‘motor performance index’ on ‘Vertical’, ‘Horizontal’ and ‘Torus’ for object size

Ratio	‘Vertical’		‘Horizontal’		Ratio	‘Torus’	
	Mean	SEM	Mean	SEM		Mean	SEM
5	4.892	0.881	4.415	0.735	15.7	30.568	2.35
12.5	2.418	0.604	3.998	0.787	39.26	18.05	1.091
8.3	2.549	0.536	6.155	1.047	26.17	12.387	1.274
6.25	1.5592	1.107	1.216	0.495	19.63	6.920	0.623
11.6	5.943	1.028	6.969	0.967	36.65	18.414	1.370
15	5.748	0.855	12.308	1.590	47.12	17.782	1.417

Annex 4-Table 43 - Means and SEMs for ‘motor performance index’ on ‘Vertical’ and ‘Horizontal’ for handedness

Handedness	**‘Vertical’**		**‘Horizontal’**	
	Mean	**SEM**	**Mean**	**SEM**
Dominant Hand	3.1243	0.362	5.047	0.541
Non-Dominant Hand	4.579	0.6179	6.64	0.682

Annex 4-Table 44 - Means and SEMs for ‘motor performance index’ on ‘Horizontal’ and ‘Torus’ for movement direction

Movement direction	**‘Horizontal’**		**‘Torus’**	
	Mean	**SEM**	**Mean**	**SEM**
Left to Right	4.165	0.459	-	-
Right to Left	7.522	0.726	-	-
Clockwise	-	-	15.697	0.863
Counter-clockwise	-	-	19.010	1.048

Annex 4-Table 45 - Means and SEMs for ‘motor performance index’ on ‘Horizontal’ and ‘Torus’ for movement direction

Ratio	Movement direction	‘Horizontal’		‘Torus’	
		Mean	SEM	Mean	SEM
5	Left to Right	4.722	0.988	-	-
	Right to Left	4.108	1.102	-	-
12.5	Left to Right	2.844	0.679	-	-
	Right to Left	5.152	1.405	-	-
8.3	Left to Right	4.349	1.222	-	-
	Right to Left	7.961	1.663	-	-
6.25	Left to Right	0.386	0.239	-	-
	Right to Left	2.046	0.948	-	-
11.6	Left to Right	5.627	1.339	-	-
	Right to Left	8.312	1.376	-	-
15	Left to Right	7.063	1.494	-	-
	Right to Left	17.55	2.54	-	-
15.7	Clockwise	-	-	19.841	2.937
	Counter-clockwise	-	-	41.294	2.684
39.26	Clockwise	-	-	17.767	1.645
	Counter-clockwise	-	-	18.333	1.454
26.17	Clockwise	-	-	12.369	1.775
	Counter-clockwise	-	-	12.406	1.853
19.63	Clockwise	-	-	7.471	0.997
	Counter-clockwise	-	-	6.371	0.751
36.65	Clockwise	-	-	18.128	1.999
	Counter-clockwise	-	-	18.699	1.901
47.12	Clockwise	-	-	18.604	2.166
	Counter-clockwise	-	-	16.959	1.848

Annex 4-Table 46 - Means and SEMs for ‘motor performance index’ on ‘Torus’ for handedness and movement direction

Handedness	Movement direction	Mean	SEM
Dominant Hand	Clockwise	16.69	1.23
	Counter-Clockwise	14.70	1.209
Non-Dominant Hand	Clockwise	16.97	1.938
	Counter-Clockwise	21.05	1.544

Annex 4-Table 47 - Means and SEMs for ‘average accumulated distance away from the object surface’ on ‘Vertical’, ‘Horizontal’ and ‘Torus’ for object size

Ratio	Vertical		Horizontal		Ratio	Torus	
	Mean	SEM	Mean	SEM		Mean	SEM
5	0.145	0.029	0.220	0.026	15.7	1.024	0.061
12.5	0.079	0.019	0.188	0.028	39.26	0.692	0.037
8.3	0.094	0.017	0.282	0.041	26.17	0.915	0.049
6.25	0.184	0.141	0.142	0.069	19.63	0.975	0.050
11.6	0.219	0.031	0.35	0.043	36.65	0.802	0.036
15	0.300	0.044	0.589	0.030	47.12	0.707	0.030

Annex 4-Table 48 - Means and SEMs for ‘average accumulated distance away from the object surface’ on ‘Horizontal’ and ‘Torus’ for movement direction

Movement Direction	‘Horizontal’		‘Torus’	
	Mean	SEM	Mean	SEM
Left to Right	0.225	0.023	-	-
Right to Left	0.366	0.037	-	-
Clockwise	-	-	0.788	0.027
Counter-clockwise	-	-	0.917	0.266

Annex 4-Table 49 - Means and SEMs for ‘average accumulated distance away from the object surface’ on ‘Horizontal’ for object size and movement direction interaction

Ratio	Movement direction	Mean	SEM
5	Left to Right	0.243	0.040
	Right to Left	0.198	0.034
12.5	Left to Right	0.157	0.032
	Right to Left	0.22	0.046
8.3	Left to Right	0.222	0.053
	Right to Left	0.341	0.063
6.25	Left to Right	0.065	0.053
	Right to Left	0.218	0.128
11.6	Left to Right	0.292	0.060
	Right to Left	0.415	0.060
15	Left to Right	0.371	0.078
	Right to Left	0.806	0.124

Annex 4-Table 50 - Means and SEMs for ‘average accumulated distance away from the object surface’ on ‘Horizontal’ for handedness and movement direction interaction

Handedness	Movement direction	Mean	SEM
Dominant Hand	Left to Right	0.243	0.035
	Right to Left	0.304	0.036
Non-Dominant Hand	Left to Right	0.207	0.030
	Right to Left	0.429	0.064

Annex 4-Table 51 – Means and SEMs for ‘average number of finger outs’ on extreme regions and handedness

	Mean	**SEM**
Regions		
Lower Left	0.156	0.026
Lower Right	0.143	0.028
Upper Left	0.133	0.023
Upper Right	0.069	0.013
Handedness		
Dominant Hand	0.070	0.015
Non-Dominant Hand	0.180	0.017

Annex 4-Table 52 - Means and SEMs for ‘average number of finger outs’ for extreme regions and handedness interaction

Extreme Region	**Handedness**	**Mean**	**SEM**
Upper Right	Dominant Hand	0.039	0.014
	Non-Dominant Hand	0.098	0.020
Upper Left	Dominant Hand	0.080	0.027
	Non-Dominant Hand	0.186	0.035
Lower Right	Dominant Hand	0.131	0.047
	Non-Dominant Hand	0.156	0.032
Lower Left	Dominant Hand	0.031	0.014
	Non-Dominant Hand	0.280	0.040

Annex 4-Table 53 - Means and SEMs for ‘motor performance index’ on extreme regions and handedness

	Mean	**SEM**
Regions		
Lower Left	4.299	0.819
Lower Right	3.413	0.646
Upper Left	3.002	0.583
Upper Right	1.713	0.452
Handedness		
Dominant Hand	1.727	0.360
Non-Dominant Hand	4.487	0.509

Annex 4-Table 54 - Means and SEMs for ‘motor performance index’ for extreme regions and handedness interaction

Extreme Region	**Handedness**	**Mean**	**SEM**
Upper Right	Dominant Hand	1.453	0.70
	Non-Dominant Hand	1.975	0.579
Upper Left	Dominant Hand	1.363	0.511
	Non-Dominant Hand	4.642	0.973
Lower Right	Dominant Hand	3.235	1.069
	Non-Dominant Hand	3.591	0.743
Lower Left	Dominant Hand	0.857	0.362
	Non-Dominant Hand	7.742	1.355

Annex 4-Table 55 - Means and SEMs for ‘average accumulated distance away from the object surface’ on extreme regions and handedness

	Mean	**SEM**
Regions		
Lower Left	0.104	0.021
Lower Right	0.117	0.035
Upper Left	0.072	0.014
Upper Right	0.039	0.008
Handedness		
Dominant Hand	0.057	0.018
Non-Dominant Hand	0.108	0.012

Annex 4-Table 56 - Means and SEMs for ‘average accumulated distance away from the object surface’ for extreme regions and handedness interaction

Extreme Region	**Handedness**	**Mean (cm)**	**SEM**
Upper Right	Dominant Hand	0.015	0.005
	Non-Dominant Hand	0.062	0.014
Upper Left	Dominant Hand	0.054	0.021
	Non-Dominant Hand	0.090	0.017
Lower Right	Dominant Hand	0.143	0.067
	Non-Dominant Hand	0.090	0.018
Lower Left	Dominant Hand	0.017	0.007
	Non-Dominant Hand	0.191	0.035

Annex 4-Table 57 - Means and SEMs for ‘time’ on inner regions for movement direction

Movement direction	Mean	SEM
Front to back	0.354	0.005
Back to front	0.382	0.007

Annex 4-Table 58 - Means and SEMs for ‘average number of finger outs’ for inner regions and handedness

	Mean	SEM
Sticks		
a	0.162	0.036
b	0.110	0.022
c	0.073	0.021
d	0.092	0.018
e	0.065	0.148
f	0.048	0.012
g	0.037	0.011
h	0.100	0.024
I	0.122	0.025
j	0.120	0.031
k	0.119	0.027
l	0.120	0.025
m	0.133	0.029
n	0.217	0.035
o	0.251	0.039
p	0.181	0.034
Handedness		
Dominant Hand	0.104	0.009
Non-Dominant Hand	0.140	0.010

Annex 4-Table 59 - Means and SEMs for ‘average number of finger outs’ on extreme regions and handedness interaction

Extreme Region	**Handedness**	Mean	SEM
a	Dominant Hand	0.078	0.031
	Non-Dominant Hand	0.247	0.063
b	Dominant Hand	0.0812	0.027
	Non-Dominant Hand	0.141	0.036
c	Dominant Hand	0.068	0.028
	Non-Dominant Hand	0.078	0.034
d	Dominant Hand	0.046	0.017
	Non-Dominant Hand	0.1375	0.031
e	Dominant Hand	0.05	0.02
	Non-Dominant Hand	0.081	0.021
f	Dominant Hand	0.056	0.020
	Non-Dominant Hand	0.04	0.015
g	Dominant Hand	0.038	0.016
	Non-Dominant Hand	0.038	0.015
h	Dominant Hand	0.068	0.027
	Non-Dominant Hand	0.131	0.039
I	Dominant Hand	0.1125	0.036
	Non-Dominant Hand	0.131	0.036
j	Dominant Hand	0.156	0.057
	Non-Dominant Hand	0.084	0.026
k	Dominant Hand	0.034	0.014
	Non-Dominant Hand	0.203	0.049
l	Dominant Hand	0.153	0.045
	Non-Dominant Hand	0.0875	0.022
m	Dominant Hand	0.131	0.047
	Non-Dominant Hand	0.134	0.033
n	Dominant Hand	0.153	0.034
	Non-Dominant Hand	0.281	0.059
o	Dominant Hand	0.253	0.054
	Non-Dominant Hand	0.25	0.056
p	Dominant Hand	0.184	0.053
	Non-Dominant Hand	0.178	0.045

Annex 4-Table 60 - Means and SEMs for ‘motor performance index’ on sticks and handedness

	Mean	SEM
Sticks		
a	4.180	0.991
b	2.513	0.589
c	2.357	0.808
d	2.380	0.678
e	1.661	0.428
f	1.839	0.534
g	1.115	0.361
h	3.215	0.817
I	4.175	1.086
j	2.631	0.693
k	3.465	0.927
l	2.900	0.661
m	3.278	0.723
n	5.424	1.056
o	5.391	0.921
p	4.668	1.241
Handedness		
Dominant Hand	2.643	0.272
Non-Dominant Hand	3.756	0.308

Annex 4-Table 61 – Means and SEMs for ‘average accumulated distance away from the object surface’ on sticks and handedness

	Mean(cm)	SEM
Sticks		
a	1.213	0.038
b	0.061	0.014
c	0.058	0.023
d	0.051	0.011
e	0.031	0.008
f	0.049	0.017
g	0.021	0.008
h	0.085	0.027
I	0.138	0.036
j	0.055	0.016
k	0.089	0.026
l	0.069	0.014
m	0.108	0.035
n	0.157	0.032
o	0.164	0.035
p	0.117	0.030
Handedness		
Dominant Hand	0.070	0.008
Non-Dominant Hand	0.103	0.010

Annex 4-Table 62 – Means and SEMs for ‘average accumulated distance away from the object surface’ for sticks and handedness interaction

Sticks	Handedness	Mean (cm)	SEM
a	Dominant Hand	0.034	0.011
	Non-Dominant Hand	0.210	0.074
b	Dominant Hand	0.054	0.021
	Non-Dominant Hand	0.068	0.018
c	Dominant Hand	0.042	0.015
	Non-Dominant Hand	0.070	0.044
d	Dominant Hand	0.019	0.007
	Non-Dominant Hand	0.084	0.021
e	Dominant Hand	0.025	0.010
	Non-Dominant Hand	0.038	0.013
f	Dominant Hand	0.073	0.031
	Non-Dominant Hand	0.027	0.014
g	Dominant Hand	0.012	0.007
	Non-Dominant Hand	0.030	0.015
h	Dominant Hand	0.025	0.010
	Non-Dominant Hand	0.146	0.052
I	Dominant Hand	0.141	0.054
	Non-Dominant Hand	0.136	0.050
j	Dominant Hand	0.071	0.031
	Non-Dominant Hand	0.039	0.011
k	Dominant Hand	0.023	0.010
	Non-Dominant Hand	0.156	0.047
l	Dominant Hand	0.071	0.021
	Non-Dominant Hand	0.068	0.019
m	Dominant Hand	0.140	0.067
	Non-Dominant Hand	0.076	0.022
n	Dominant Hand	0.099	0.031
	Non-Dominant Hand	0.2156	0.056
o	Dominant Hand	0.154	0.051
	Non-Dominant Hand	0.174	0.047
p	Dominant Hand	0.130	0.056
	Non-Dominant Hand	0.104	0.023

Annex 4-Table 63 - Means and SEMs for ‘time’ on ‘Torus’ for sound feedback and handedness

	Mean	**SEM**
Sound Feedback		
No Sound	2.776	0.102
C1	2.422	0.095
C2	2.422	0.087
C3	2.455	0.088
C4	2.395	0.074
C5	2.423	0.081
C6	2.428	0.087
C7	2.584	0.097
C8	2.630	0.095
Handedness		
Dominant Hand	2.416	0.040
Non-Dominant Hand	2.592	0.044

Annex 4-Table 64 - Means and SEMs for ‘average number of finger out’ on ‘Horizontal’ for movement direction

Movement direction	**Mean**	**SEM**
Left to Right	0.613	0.056
Right to Left	0.997	0.081

Annex 4-Table 65 – Means and SEMs for ‘average number of finger out’ on ‘Horizontal’ for movement direction and handedness interaction

Movement direction	**Handedness**	Mean	SEM
Left to right	Dominant Hand	0.695	0.083
	Non-Dominant Hand	0.531	0.073
Right to left	Dominant Hand	0.874	0.107
	Non-Dominant Hand	1.120	0.122

Annex 4-Table 66 - Means and SEMs for ‘average number of finger outs’ on ‘Vertical’ for sound feedback and handedness

	Mean	**SEM**
Sound Feedback		
No Sound	0.233	0.042
C1	0.190	0.042
C2	0.094	0.019
C3	0.150	0.029
C4	0.079	0.015
C5	0.106	0.016
C6	0.157	0.022
C7	0.207	0.042
C8	0.149	0.039
Handedness		
Dominant Hand	0.118	0.011
Non-Dominant Hand	0.186	0.019
Movement Direction		
Bottom to Up	0.125	0.014
Up to Bottom	0.179	0.016

Annex 4-Table 67 - Means and SEMs for ‘motor performance index’ on ‘Vertical for sound feedback, handedness and movement direction

	Mean	**SEM**
Sound Feedback		
No Sound	0.445	0.009
C1	0.035	0.0096
C2	0.016	0.0048
C3	0.030	0.0078
C4	0.016	0.0036
C5	0.022	0.0039
C6	0.026	0.0052
C7	0.038	0.0089
C8	0.0289	0.0076
Handedness		
Dominant Hand	0.0182	0.0019
Non-Dominant Hand	0.0387	0.0042
Movement Direction		
Bottom to Up	0.0202	0.0024
Up to Bottom	0.0367	0.0041

Annex 4-Table 68 - Means and SEMs for ‘motor performance index’ on ‘Vertical’ for movement direction

Movement direction	**Mean**	**SEM**
Left to right	0.039	0.0045
Right to left	0.054	0.0044

Annex 4-Table 69 - Means and SEMs for ‘motor performance index’ on ‘Horizontal’ for movement direction and handedness interaction

Movement direction	**Handedness**	Mean	SEM
Left to right	Dominant Hand	0.046	0.0069
	Non-Dominant Hand	0.032	0.006
Right to left	Dominant Hand	0.042	0.0046
	Non-Dominant Hand	0.068	0.007

Annex 4-Table 70 - Means and SEMs for ‘average accumulated distance away from the object surface’ on ‘Vertical’ for sound feedback, handedness and movement direction

	Mean	**SEM**
Sound Feedback		
No Sound	0.3016	0.0822
C1	0.1517	0.0313
C2	0.069	0.0154
C3	0.1512	0.0367
C4	0.1005	0.0307
C5	0.1134	0.0192
C6	0.1544	0.0391
C7	0.1855	0.0421
C8	0.1447	0.0387
Handedness		
Dominant Hand	0.1066	0.0108
Non-Dominant Hand	0.1983	0.0255
Movement Direction		
Bottom to Up	0.1133	0.0160
Up to Bottom	0.1916	0.0226

Annex 4-Table 71 - Means and SEMs for sound feedback, handedness and object part for each dependent variable

	Time		**Number of finger out**		**Motor performance index**		**Accumulated distance away from the object surface**	
	Mean	**SEM**	**Mean**	**SEM**	**Mean**	**SEM**	**Mean**	**SEM**
Sound Feedback	F(8,19440)= 20.710; p<0.0001		F(8,19440)= 3.32; p<0.0001		F(8,19440)= 4.859; p<0.0001		F(8,19440)= 8.363; p<0.0001	
No Sound	1.314	0.025	1.706	0.061	0.071	0.003	1.539	0.052
C1	1.169	0.022	1.621	0.060	0.007	0.003	1.335	0.040
C2	1.161	0.022	1.535	0.055	0.059	0.027	1.388	0.047
C3	1.191	0.022	1.510	0.054	0.061	0.003	1.353	0.045
C4	1.161	0.021	1.456	0.052	0.054	0.002	1.260	0.040
C5	1.161	0.022	1.568	0.055	0.057	0.002	1.334	0.041
C6	1.169	0.021	1.579	0.055	0.058	0.003	1.321	0.041
C7	1.219	0.024	1.509	0.053	0.061	0.003	1.302	0.042
C8	1.234	0.025	1.457	0.051	0.055	0.002	1.287	0.044
Handedness	F(1,19440)= 90.216; p<0.0001		F(1,19440)= 13.72; p<0.0001		F(1,19440)= 33.714; p<0.0001		F(1,19440)= 2.86; NS	
Dominant Hand	1.162	0.010	1.494	0.026	0.055	0.001	1.331	0.021
Non-Dominant Hand	1.233	0.011	1.603	0.026	0.065	0.001	1.362	0.021
Object Part	F(2,19440)= 30181; p<0.0001		F(2,19440)= 5466; p<0.0001		F(2,19440)= 972; p<0.0001		F(2,19440)= 13974; p<0.0001	
Horizontal	0.575	0.003	0.804	0.028	0.047	0.002	0.332	0.015
Vertical	0.514	0.003	0.152	0.006	0.028	0.001	0.152	0.009
Torus	2.503	0.011	3.691	0.034	0.106	0.001	3.556	0.022

Annex 4-Table 72 – Means and SEMs for movement direction and handedness for each precision dependent variable for left-handed subjects

	Average number of finger out		**Motor performance index**		**Average accumulated distance away from the object surface**	
	Mean	**SEM**	**Mean**	**SEM**	**Mean**	**SEM**
Movement Direction						
Left to right	0.643	0.60	0.036	0.003	0.228	0.019
Right to left	0.833	0.066	0.067	0.006	0.610	0.082
Handedness						
Dominant Hand	0.936	0.070	0.064	0.005	0.462	0.052
Non-Dominant Hand	0.738	0.045	0.0514	0.003	0.419	0.042

Annex 4-Table 73 - Means and SEMs for movement direction and handedness interaction for each precision dependent variable for left-handed subjects

Movement direction	**Handedness**	**Average number of finger out**		**Motor performance index**	
		Mean	**SEM**	**Mean**	**SEM**
Left to right	Dominant Hand	0.717	0.090	0.040	0.005
	Non-Dominant Hand	0.567	0.079	0.031	0.005
Right to left	Dominant Hand	1.156	0.1053	0.088	0.009
	Non-Dominant Hand	0.511	0.077	0.046	0.007

Annex 5 Data, Code and Publications

For the data and the code of the thesis, please follow the following link below:

https://osf.io/avyk6/

Publications :

1. Batmaz AU, de Mathelin M, Dresp-Langley B (2018) Effects of 2D and 3D image views on hand movement trajectories in the surgeon's peri-personal space in a computer-controlled simulator environment *Cogent Medicine,* 5(1), 1426232. https://doi.org/10.1080/2331205X.2018.1426232
2. Batmaz AU, de Mathelin M, Dresp-Langley B (2017) Seeing virtual while acting real: Visual display and strategy effects on the time and precision of eye-hand coordination. *PLoS ONE* 12(8): e0183789. https://doi.org/10.1371/journal.pone.0183789
3. Batmaz AU, de Mathelin M, Dresp-Langley B (2016) Getting nowhere fast: trade-off between speed and precision in training to execute image-guided hand-tool movements. *BMC Psychology*, 4(1), 55. https://doi.org/10.1186/s40359-016-0161-0
4. Batmaz AU, de Mathelin M, Dresp-Langley B (2018) Effects of image size and structural complexity on time and precision of hand movements in head mounted virtual reality. *IEEE VR* Reutlingen Germany.
5. Batmaz AU, de Mathelin M, Dresp-Langley B (2017) Effects of relative target position on ipsilateral and contralateral manual operations in head-mounted virtual reality. *European Conference on Visual Perception (ECVP),* Berlin Germany. http://journals.sagepub.com/page/pec/collections/ecvp-abstracts/index/ecvp-2017
6. Batmaz AU, Falek MA, Zorn L, Nageotte F, Zanne P, de Mathelin M, Dresp-Langley B (2017) Novice and expert haptic behaviours while using a robot-controlled surgery system. In *13th IASTED International Conference on Biomedical Engineering (BioMed)* (pp. 94-99). IEEE. https://doi.org/10.2316/P.2017.852-022

7. Batmaz AU, de Mathelin M, Dresp-Langley B (2016). Effects of indirect screen vision and tool-use on the time and precision of object positioning on real-world targets. *Perception*, 45(ECVP Supplement), 196. http://journals.sagepub.com/doi/full/10.1177/0301006616671273
8. Batmaz AU, de Mathelin M, Dresp-Langley B (2017). Inside the Virtual Brain: using Oculus Dk2 for Surgical Planning. *NeuroTalk*, Barcelona Spain
9. Batmaz AU, de Mathelin M, Dresp-Langley B (Submitted in March 2018) Effects of different sound frequencies on time and precision of manual operations in head-mounted virtual reality. *ECVP 2018.*

Annex 6 French abstract

Introduction

L’émergence des technologies contrôlées par ordinateur, dans les domaines de la santé et du biomédical, a engendré de nouveaux besoins en matière de recherche sur les interactions intuitives et le contrôle de conception, à la lumière des stratégies comportementales humaines. Rassembler les points de vue des utilisateurs sur les configurations requises peut-être, une première étape pour comprendre, combien la conception et les procédures proposées doivent être adaptées pour correspondre aux besoins des utilisateurs. Cependant, cela sera insuffisant tant que les experts n’auront pas une complète compréhension de l’ensemble des aspects relatifs aux contraintes spécifiques liées à la réalisation des tâches. Des études interdisciplinaires centrées sur la conception d’interfaces, privilégiant un affichage ergonomique et plus encore, qui tiennent compte de la psychophysique humaine, sont nécessaires pour comprendre complètement, les contraintes propres à des environnements de tâches et à des domaines de travail spécifiques. Etre capable de décider ce qui devrait être amélioré, en terme de développement et concernant les applications dédiées aux technologies émergentes, requiert d’être capable d’évaluer comment les modifications conceptuelles et les modes d’affichage peuvent faciliter le traitement de l’information par l’Homme lors de l’exécution des tâches. L’erreur humaine pose ici une question critique en ce qu’elle est en partie contrôlée par les propriétés de l’affichage qui lui-même, peut être plus ou moins optimal selon les conditions mises en place. Bien qu’il existe un consensus sur le fait que les processus cognititifs de l’homme soient une composante intégrative des technologies d'intervention assistées par ordinateur, savoir ; comment les performances et les prises de décision humaines sont affectées par ces technologies, n’est pas encore assez maitrisé. Le besoin urgent de recherche dans ce domaine dépasse de loin la sphère d’analyse du flux de travail et des modèles de tâches, comme le montreront clairement ici, les différentes situations expérimentales qui soulignent le problème de la variation des performances

individuelles, de novices apprenant à exécuter des mouvements de la main guidés par l'image, dans un simulateur d'environnement contrôlé par ordinateur.

Dans le premier chapitre de cette thèse, différentes méthodes utilisées dans le milieu chirurgical pour créer de meilleurs systèmes de formation et pour comprendre dans quelle mesure, ils affectent les performances motrices des sujets ont été étudiées Dans cet objectif, la plateforme expérimentale « EXCALIBUR » a été conçue et équipée de composant matériels et logiciels spécifiques à l'attention de novices. Plus loin dans ce premier chapitre, l'hétérogénéité d'expertise des sujets, les repères de couleur, l'hétérogénéité d'expérience des sujets et la position de la caméra sont examinés en détail pour, comprendre les effets induits par la vision stéréoscopique 3D chez les chirurgiens et les experts en chirurgie.

Dans le second chapitre de la thèse, les performances motrices des novices dans le domaine des applications VR de formation en chirurgie virtuelle (VR), ont été étudiées au niveau des opérations manuelles et des interactions hommes-machine, (HCI). Différents objets médicaux et non médicaux ont été examinés par le système « NoTouch ». Cette plateforme expérimentale est équipée, d'un capteur de mouvement et d'un casque à réalité virtuelle immersive pour collecter les données des participants.

Le troisième chapitre de la thèse est consacré, à l'analyse des forces de préhension mises en œuvre lors l'exécution d'une tâche réalisée par robot chirurgical. Dans les deux précédents chapitres, les effets des différents retours visuels et tactiles utilisés ont été étudiés. Dans le dernier chapitre de la thèse, la recherche a été étendue au robot chirurgical STRAS, un système robotisé et flexible pour la chirurgie minimalement invasive. Afin de pouvoir mesurer les variations de la force de préhension (saisie), un gant a spécifiquement été conçu pour la collecte des données. L'objectif de ce gant a été d'enregistrer les signaux exprimant la force de préhension à partir de différents points de mesures positionnés sur la paume, les doigts et les extrémités des doigts ; à la fois de la main dominante et de la main non-dominante.

L'ensemble des trois chapitres ne sont pas seulement centrés, sur la durée d'exécution des tâches mais aussi, sur les critères de précision qui affectent la performance motrice des sujets et sur leur évaluation durant l'acquisition des compétences pour

des tâches déterminées. Au travers de l'ensemble des études traitées dans ces trois chapitres, différents retours visuels, tactiles et auditifs utilisés dans le domaine chirurgical et dans celui des simulations d'acquisition des compétences ont été examinés En conséquence, ce sont également, les zones du cortex visuel, soma-sensoriel et auditif ainsi que, les échanges complexes entre ces zones qui ont été examinés, au travers des résultats de chaque étude.

Dans le premier chapitre, les effets de l'imagerie 2D et 3D, ainsi que la manipulation des outils seront étudiés grâce à un dispositif d'entrainement à la chirurgie. Le second chapitre étudiera les interactions homme-machine, lors de l'utilisation d'un casque à réalité virtuelle immersive. Le dernier chapitre analysera les différences de forces de préhension appliquées soit, par des novices soit, par des experts, durant l'exécution de tâches, en utilisant un robot chirurgical. D'une manière générale, les résultats et les conclusions rapportés dans chacun des chapitres peuvent être utilisé pour améliorer les environnements d'entrainement et de simulation.

Chapitre 1

Comparaison des opérations manuelles dans le monde réel sous guidance 2D et 3D

Dans ce premier chapitre, les analyses de la vitesse et de la précision des opérations manuelles, en milieu réel, ont été examinées sous l'angle des différentes rétroactions visuelles et tactiles. Quand un chirurgien exécute une chirurgie minimalement invasive, il/elle doit regarder une autre source de retour visuel, fournie par une caméra digital. L'information fournie par la vue naturelle avec les yeux n'est pas la même chose que de regarder à travers un écran 2D. Cette limitation affecte également la perception des utilisateurs et perturbe les actions et les mouvements dans le monde réel. Une précédente recherche sur ce sujet, montre que les sujets sont plus lents, moins précis et commettent plus d'erreurs en utilisant un écran 2D.

En outre, lors d'une procédure chirurgicale, le chirurgien utilise un outil pour réaliser la tâche. La manipulation de cet outil désactive le retour haptique direct. Dans cette

situation, le chirurgien doit exécuter des mouvements, des manœuvres et des actions, d'après les informations transférées par l'outil chirurgical.

Pour surmonter ces principaux défis posés par des rétroactions visuelles et tactiles modifiées, différentes approches ont déjà été tentées : entrainer les débutants sur simulateur chirurgical, essayer de définir la position de l'écran la plus adaptée pour réaliser la chirurgie, utiliser différents retours visuels, inclure la stéréovision pour créer un retour visuel artificiel. Ce sont quelques unes des solutions actuellement mises en place pour répondre à ces inconvénients.

Dans le premier chapitre de cette thèse, différentes méthodes utilisées dans le milieu chirurgical pour créer le meilleur système d'apprentissage de la chirurgie sont étudiées, avec la plateforme expérimentale « EXCALIBUR ».

Etude 1 – Les compromis individuels Vitesse-Précision en sessions d'apprentissage

Dans cette première étude du chapitre 1, le processus d'apprentissage des participants est analysé, pour comprendre l'effet rétroactif engendré par l'image guidé en ce qui concerne : 'la durée', la 'précision' et la 'trajectoire. Les sujets deviennent plus lents et commettent plus d'erreurs avec un retour visuel guidé par l'image. Dans cette étude, la manipulation des outils et la progression ont été examinés, pour des débutants complets, afin de comprendre l'évaluation de la performance motrice lors de tâches exécutées avec un retour par imagerie 2D.

Les résultats des Figure 12, Figure 13, Figure 14 et de la Figure 15 confirment, que la vision vidéo 2D affecte négativement, la durée d'exécution, la précision et les mouvements, sur des trajectoires orientées sur objectif comparativement, à une vision en action directe (contrôle). Cette baisse de la performance est statistiquement significative. Bien que ce désavantage de la guidance par imagerie puisse diminuer grâce à la formation et éventuellement se stabiliser, aucun des individus ne parvient à réussir aussi bien que dans les conditions de vision directe, des dernières séances de formation.

Etude 2 Les effets de la position des moniteurs 2D et des conditions de visualisation de l'image

La première étude de ce chapitre nous a permis d'étudier, dans le cadre de différentes modalités de manipulation, les effets sur l'apprentissage selon que l'on soit en condition de vision directe ou, dans une situation d'exécution par image guidée. En résumé, les résultats ont montré que l'image guidée rend les sujets plus lents et moins précis. Que même après huit sessions d'apprentissage, les sujets guidés par l'image ne deviennent pas aussi précis et rapides que lors d'une exécution en vision directe. Pour surmonter les désavantages de l'exécution guidée par l'image, plusieurs méthodes, à mettre en place sur les lieux dédiés à la chirurgie, sont proposées. L'une d'entre elles est d'améliorer l'ergonomie des salles d'opération. L'autre est de développer de nouvelles façons de représenter le monde réel dans les dispositifs d'imagerie chirurgicale guidée (Oculus 3D stéréovision).

Au sein du groupe "moniteur droit devant", il n'y a pas eu d'interactions significatives entre le mode de visualisation et l'utilisation d'un outil et leurs effets sur le temps d'exécution. Au sein du groupe « moniteur sur les cotés », Nous avons trouvé une telle interaction, par ailleurs indépendante d'un changement de position du moniteur. Cette interaction n'apparait que dans des conditions de vision avec casque de réalité virtuelle 3D, dans lesquelles, l'utilisation d'un outil engendre les effets les plus préjudiciables sur le temps d'exécution que dans toute autre condition de visualisation. Pour les deux groupes d'étude, nous avons trouvé des interactions significatives entre les conditions de visualisation et l'utilisation d'un outil et leurs effets sur la précision (dans le groupe moniteur droit devant et le groupe moniteur sur les cotés), impliquant des conditions d'utilisation du casque de réalité virtuelle 3D ou dans des conditions de vision Fisheye 2D, (Figure 27).

Etude 3 les effets des indicateurs de couleurs localisés intégrés aux images

La première étude de ce chapitre nous a permis d'étudier dans le cadre de différentes modalités de manipulation, les effets sur l'apprentissage selon que l'on soit en condition de vision directe ou dans une situation d'exécution par image guidée. En résumé, les résultats ont montré, que l'image guidée rend les sujets plus lents et moins

précis. Que même après huit sessions d'apprentissage, les sujets guidés par l'image ne deviennent pas aussi précis que lors d'une exécution en vision directe. La seconde étude de ce chapitre 1 nous a permis d'étudier : les deux techniques que sont la stéréoscopie 3D et le positionnement du moniteur. Ces méthodes sont utilisées pour améliorer les performances motrices des chirurgiens en salle d'opération. Les modalités de positionnement du moniteur affectent les performances des débutants, comme cela a été montré par des études antérieures. D'un autre coté, de précédentes recherches ont montré que le retour visuel de la stéréovision 3D n'apportait aucune supériorité par rapport à l'image guidée en 2D. Quatre explications sont développées dans l'article de Batmaz et al. Étude pour expliquer les raisons possibles de cette différence. Dans la dernière et troisième étude du chapitre 1 ces différentes raisons ont été étudiées avec le dispositif expérimental EXCALIBUR.

Les résultats relatifs au temps (en temps) présentés dans la Figure 44(a) montrent une interaction significative entre les conditions de l'expertise et les conditions de visionnage et, que les novices ont été plus rapides pour chacune des conditions de retour visuel. Le chirurgien expert a été plus lent en vision directe et plus rapide dans les conditions de vue non déformée et en en Oculus 3D comparativement à l'ensemble des chirurgiens. Le groupe des chirurgiens a été le plus lent dans les conditions de vue non déformée et en en Oculus 3D.

Les résultats relatifs à la précision, présentés dans la Figure 44 (b), montrent une interaction spécifique entre les conditions de l'expertise et les conditions de visionnage, et que le chirurgien expert, a été le plus précis pour chacun des niveaux de condition de vue .Qu'il n'y a eu aucune différence de précision entre les novices et les chirurgiens dans les retours visuels excepté, en vision non déformée où les chirurgiens ont été plus précis comparativement aux novices.

Les résultats relatifs aux erreurs, présentés Figure 44 (c) montrent que les chirurgiens ont commis moins d'erreurs comparativement aux novices et, qu'il n'y a pas de différence d'erreur entre les novices et le chirurgien expert, pour la variable dépendante 'erreur'.

Conclusions

Les résultats de ce chapitre révèlent les compromis complexes et spontanés qui se produisent entre la rapidité et la précision, au niveau des performances individuelles des débutant complets, dans l'apprentissage visuo-spatial d'une tâche de positionnement d'un objet par image guidé. Ces compromis reflètent la variation des stratégies cognitives qui doivent être contrôlées individuellement, pour assurer un développement effectif et efficace des compétences. Collecter uniquement les données temps afin, d'établir une courbe d'apprentissage n'est pas suffisant, tout comme devenir plus rapide, n'implique pas directement de devenir meilleur dans la réalisation de la tâche. Les procédures de formation doivent inclure une évaluation des compétences par des psychologues experts et des procédures pour un contrôle adaptatif des compromis vitesse-précision, s'agissant de la performance des novices.

En cohérence avec les précédentes études, l'imagerie guidée ralentit significativement et réduit significativement la précision des opérations manuelles orientées sur un objectif des novices, tous ces non-chirurgiens ayant un très bon score concernant leur habileté spatiale. Cela semble être en contradiction avec certains des résultats que nous avons rapportés précédemment ; les systèmes de visualisation 3D ne génèrent pas directement une meilleure coordination œil-main pour réaliser un acte, lors de procédures guidées par l'image. L'efficacité relative de la technologie 3D, en ce qui concerne la rapidité et la précision du mouvement de la main dépend du type et de la direction du mouvement de la main requis pour l'intervention, du niveau individuel de formation du chirurgien et des participants ainsi que, de leur intégration à des groupes homogènes, de la présence d'indicateurs de couleur, et de la flexibilité du dispositif caméra générant les vues des espaces cibles dans l'espace peripersonnel du chirurgien.

Les interactions complexes entre la visualisation, l'utilisation de l'outil, les facteurs ergonomiques et individuels ouvrent de nouvelles et d'importantes perspectives pour des recherches plus poussées sur les novices, dans la coordination œil-main guidée par l'image.

CHAPITRE 2

Les interactions Homme - Machine lors de l'utilisation d'un casque de réalité virtuelle

Dans le second chapitre, l'analyse de la vitesse et de la précision des opérations manuelles réelles ont été étudiées en réalité virtuelle (VR).

Le développement récent de technologies proposant différents systèmes de retour visuel a permis aux chirurgiens de s'entrainer par eux-mêmes dans différents environnements. La réalité virtuelle s'est popularisée et s'est développée, au cours de la dernière décennie, grâce à l'apport de la technologie et de l'industrie. Des nouvelles applications pour simulateur dans le domaine de la formation chirurgicale commencent à se développer mais, le principal inconvénient de ces applications est leur technique d'évaluation. Ces applications n'effectuent aucune expérience d'évaluation cognitive ou psychomotrice et n'intègrent pour l'évaluation de la performance que la durée d'exécution. Cette limitation présente un inconvénient pour comprendre la psychophysique sous-jacente à ces applications et la réalité virtuelle, elle même.

L'un des plus grands avantages des dispositifs de réalité virtuelle est leur capacité à créer des objets virtuels de toutes tailles, d'aspects ou d'échelles et, de nous offrir la possibilité de pouvoir interagir avec ces objets en utilisant différents périphériques d'entrée. Différentes tailles, l'orientation, l'échelle et même la position des objets virtuels conçus peuvent affecter les performances motrices des personnes et les effets de ces caractéristiques, sur la cognition humaine, doivent être étudiés avec l'aide de la psychophysique. D'un autre coté, les interactions humaines avec ces objets virtuels dans la réalité virtuelle, ne sont pas équivalentes à celles des interactions réalisées dans le monde réel car les rétroactions sont artificielles. Pour surmonter ce problème, les concepteurs et les ingénieurs augmentent les retours visuels, tactiles et auditif pour améliorer la perception et aider les utilisateurs, à se concentrer dans la réalité virtuelle, ce qui cause des variations de la performance et dans la prise de décision humaine. Les effets de ces feed-back qui ne sont pas réels et des pseudos feed-back, sur les performances motrices de l'homme, ne sont pas encore assez bien connus.

Dans le premier chapitre ont été étudiés l'importance de l'évaluation de la précision dans le domaine de la formation chirurgicale ainsi que, les effets des différentes stratégies et méthodes visant à améliorer les performances motrices des novices, en dispositifs d'imagerie guidée. Dans le second chapitre, la performance motrice de débutants complets en applications de formation médicale virtuelle sera analysée lors d'opérations manuelles en examinant les interactions Hommes-Machine. Dans cet objectif, le système « NoTouch » a été développé pour collecter les données des complets débutants.

Etude - 1 Les effets de différents rendus virtuels

Dans cette première étude du chapitre deux, différents niveaux de rendu virtuel seront étudiés. Nous verrons comment, avant de travailler en réalité virtuelle, cela affecte les performances motrices des sujets et, les différences existantes entre plusieurs simulations d'environnement chirurgicaux seront examinées. Les précédentes études ont effectué plusieurs comparaisons entre différents environnements de simulateur. Dans cette étude, ces environnements de simulation ont été analysés, de manière approfondie, à l'aide de variables dépendantes en fonction du temps et de la précision. L'étude porte spécifiquement sur la comparaison entre des environnements immersifs utilisant le casque de réalité virtuelle et les environnements de simulation conventionnels.

Les résultats présentés en Figure 52 indiquent que les sujets ont été plus rapides et plus précis en vision monde réel avec toucher direct comparativement aux autres différents types de retour visuel utilisés dans cette expérimentation. L'autre résultat qui ressort des Figure 52, Figure 54, Figure 58 et Figure 63 est qu'il n'y a pas de différence majeure en VR, AR et MR, en ce qui concerne le temps et la précision. Ce résultat était valide pour chaque objet (Horizontal, Vertical et Torus) pour les 4 quatre variables dépendantes.

Etude 2 - Les effets de la longueur et de la largeur de l'objet virtuel

Dans la première étude du chapitre 2, six différentes rétroactions visuelles et leurs effets sur les opérations manuelles dans les plans horizontaux, verticaux et toroïdaux ont été analysées. En résumé, les résultats ont montré que les sujets ont été plus

rapides et plus précis quand ils étaient en interaction avec l'objet, en visualisation du monde réel et avec toucher direct, et, qu'il n'y avait aucune différence majeure de performance motrice entre VR, AR, et MR. Dans la seconde étude du chapitre 2, les effets de la longueur, de la largeur des objets virtuels seront examinés avec le dispositif « NoTouch ». Les résultats sont analysés avec la loi de Steering qui est une dérivation de la loi de Fitts.

Les résultats du Tableau 3 et de la Figure 78 montrent que la loi de Steering est également valide dans les environnements VR avec opérations manuelles pour la Verticale, l'Horizontale et en Torus.

Lorsque nous regardons l'analyse de la loi de Steering, concernant les résultats de la précision dans la Figure 80, nous pouvons observer qu'il n'existe pas de corrélation linéaire entre l'ID (la indice de difficulté) et les variables dépendantes (nombre moyen de doigts en dehors, l'indice de performance motrice, la distance d'éloignement des objets moyenne cumulée)

Lorsque nous combinons l'ID et les résultats de la précision avec l'interaction complexe des facteurs liés à la direction du mouvement et la dominance manuelle, il est difficile de parvenir à une conclusion générale pour déterminer une corrélation entre les largeurs et les longueurs différentes des objets et la précision.

Etude 3 - Mouvements de la main, Ipsilatéralité par opposition à la Contra-latéralité

Dans la seconde étude de ce chapitre, il s'agissait d'explorer comment la longueur et la largeur de l'objet affectent les performances motrices. Les résultats montrent que la hauteur et la largeur de l'objet conçu peut altérer l'analyse de la durée et la précision.

Hormis la hauteur et la largeur de l'objet, s'ajoute un troisième aspect, la profondeur, qui devrait être considéré dans un espace tridimensionnel. La troisième dimension de l'espace cartésien, la profondeur, au travers de mouvements de la main ipsilateraux et de mouvements contralatéraux, est étudié dans le troisième chapitre de la thèse, lors de la réalisation de mouvements de la main. Ipsilatéraux et contra-latéraux en zones centrale ou en zones extrêmes (Figure 83).

D’après les résultats obtenus dans les régions extrêmes présentés dans la Figure 88, Figure 89 et Figure 90, les sujets ont été plus précis avec leur main dominante et il n’y a pas eu de différence en temps entre chacune des régions extrêmes mais ; les sujets ont été significativement plus précis dans la région supérieure droite d’après trois variables dépendantes de précision. L’analyse des régions intérieures, montrent que les sujets ont été plus précis pour les interactions positionnées aux niveaux des yeux et sont devenus moins précis au fur et à mesure de l’éloignement des cibles Figure 92, Figure 94 et Figure 95.

Etude 4 - Les effets liés à la taille et à la complexité de la forme des objets virtuels

Dans la première étude du second chapitre, les effets de la réalité virtuelle sur le temps et la précision ont été étudiés ainsi que les rétroactions visuelles, en utilisant un environnement de simulation. Dans la seconde étude du deuxième chapitre deux aspects, dans l’espace en trois dimensions, ont d’abord été étudiés : les variations de longueur et de largeur de l’objet virtuel. Dans la troisième étude du second chapitre, la profondeur, troisième dimension de l’espace tridimensionnel est étudiée lors de la réalisation de mouvements ipsilatéraux et contra-latéraux de la main. Dans cette quatrième étude, nous allons détailler les effets de la taille des objets et de la complexité de leur forme. Deux objets médicaux (Figure 97) sont utilisés dans cet objectif avec le système «NoTouch» afin, d’analyser les variations en termes de temps et de précision. Le premier objet a été reconstruit à partir d’une séquence MRI et le deuxième avait été élaboré pour l’enseignement médical.

Les résultats de la Figure 98 ont montré que les sujets ont été plus rapides et plus précis sur des structures simples, comparativement à des structures complexes ; qu’ils ont été plus lents et moins précis avec leur main dominante et ont commis plus d’erreurs et produit des mouvements plus rapides, avec les petits objets qu’avec des objets, de taille moyenne ou grande.

Etude 5 – Les effets de la fréquence sonore dans l’espace virtuel

Dans la première étude du chapitre 2, nous avons étudié les temps et la précision des novices en réalité virtuelle, en utilisant uniquement la rétroaction visuelle. Quand les sujets commettaient une erreur, la couleur de l’objet virtuel virait au rouge pour

matérialiser une erreur et aider les sujets, à corriger cette erreur. Dans cette dernière étude du chapitre 2, un feedback audio additionnel a été inclus pour analyser l'altération de la performance motrice des sujets. De précédentes recherches sur la sonorisation en réalité virtuelle ont montré qu'un retour audio augmentait les performances motrices des sujets. Dans cette étude, nous explorons les effets de l'utilisation de différences fréquences sonores en réalité virtuelle, dans l'environnement du dispositif « NoTouch ».

D'après les résultats des Figure 106, Figure 107, Figure 108 et de la Figure 109, les sujets ont été plus rapides et plus précis avec un son C4 comparativement à d'autres sons. Lorsque la fréquence augmentait à C7 et C8, les sujets commettaient moins d'erreurs mais devenaient, dans le même temps, plus lents.

Conclusions

Dans ce chapitre, la réalité virtuelle a été étudiée sous ses différentes caractéristiques lors d'interaction Homme-Machine. Dans la première étude, différents environnements de simulation ont été comparés et il a été montré que les sujets ont été plus rapides et plus précis en vision naturelle et en contact direct ; qu'il n'y avait par ailleurs, aucune différence significative en termes de temps et de précision entre VR, AR et MR.

Dans la seconde étude de ce chapitre, des expérimentations ont été réalisées pour comprendre les effets des variations de la longueur et de la largeur des objets virtuels dans la VR et vérifier, que la loi de Steering en VR avec le dispositif « NoTouch » est valide. Dans la troisième étude, ce sont les performances des mouvements en profondeur de la main ipsilatéraux et contralatéraux qui ont été analysées dans un environnement virtuel. Cette expérimentation a permis de déterminer, en fonction de la main active, la position optimale de l'objet pour placer une cible en VR. La quatrième étude nous a permis d'expérimenter les effets de la taille et de la complexité de l'objet sur les temps de réalisation et la précisions des sujets, en combinant la deuxième étude et la troisième étude de ce chapitre. Cette étude nous a montré que la complexité de l'objet doit être considérée comme une variable dépendante pour l'évaluation individuelle. Dans la dernière étude des expérimentations, incluant un retour auditif dans la réalité virtuelle, ont été réalisées et nous avons déterminé que la fréquence

optimale pour obtenir les meilleurs résultats en termes de performance motrice est dans les tons moyens d'un clavier de piano.

En dehors de ces résultats, les expérimentations ont révélé l'importance des mesures et de l'évaluation de la précision dans les environnements virtuels. Les variables dépendantes de précision révèlent des résultats similaires dans la troisième, quatrième et cinquième étude. Cependant, dans la première et la seconde étude, chaque variable dépendante a montré différentes caractéristiques sans corrélation linéaire avec une fonction. Ces résultats montrent non seulement, que plusieurs méthodes d'analyse de la précision devraient être utilisées pour évaluer les sujets dans un environnement immersif virtuel mais aussi, que les retours d'évaluation doivent être donnés en fonction de la conception des tâches.

En résumé, ces résultats peuvent être utiles aux ingénieurs et concepteurs pour de meilleures applications de simulation chirurgicales, destinées à optimiser les interactions homme machine et la coordination oeil-main dans un environnement virtuel.

Chapitre 3

L'analyse de la force de préhension dans les opérations télé manipulées

Dans Le troisième chapitre de la thèse, l'analyse de la force de préhension a été étudiée lors d'opérations manuelles humaines. Dans les deux premiers chapitres, les rétroactions visuelles et tactiles utilisées dans les applications de formation médicale ont été analysées au moyen de mesures de la performance motrice des individus. Dans le dernier chapitre de la thèse, la recherche a été étendue au robot chirurgical STRAS, un système robotisé et flexible pour la chirurgie minimalement invasive. Afin de pouvoir mesurer les variations de la force de préhension, une paire de gants a spécifiquement été conçu pour la collecte des données. L'objectif de cette paire de gants a été d'enregistrer les signaux exprimant la force de préhension à partir de différents points de mesures positionnés sur la paume, les doigts et les extrémités des

doigts ; à la fois de la main dominante et de la main non-dominante (vue du gant: Figure 112).

Lorsque le chirurgien perd l'information haptique du fait des conditions d'accès réduits en chirurgie assistée par un robot, cela peut compromettre la sécurité de la procédure. Cette limitation doit être surmontée par la pratique, et en particulier au travers d'un entrainement en simulateur chirurgical, pour les interactions main-outil spécifiques.

L'utilisation de capteurs pour la mesure des variations de la force de préhension lors d'un apprentissage en simulateur chirurgical avec interactions main-outil fournit de précieux renseignements sur l'évolution des compétences chirurgicales. Pour mesurer l'intensité des forces de préhension des mains et des doigts et être utilisés dans un contexte de manipulation d'outils chirurgicaux, intégrant des interactions de retour sensoriel, les dispositifs bio capteurs doivent être calibrés dans cet objectif

L'utilisation d'un outil requiert l'application d'une force de préhension appropriée pour prévenir tous risques de le lâcher ou de déraper et dans le même temps, pour éviter une force excessive qui pourrait en endommager l'outil ou les tissus sur lesquels elle est exercée. L'apprentissage somatosensoriel guidé visuellement est particulièrement important pour un réglage fin des forces du bout des doigts, appliquées à des formes particulières d'objets ou d'outils spécifiques.

Dans le dernier chapitre de la thèse, la durée d'exécution de la tâche et les variations des forces de préhension mises en œuvre, par un utilisateur novice et un utilisateur expert du système robotisé chirurgical STRAS, ont été analysées en en utilisant un dispositif de capteurs.

D'après les résultats présentés dans la Figure 117, le sujet expert a été plus rapide et la dominance manuelle a affecté les temps d'exécution de la tâche. En outre, les résultats de la Figure 28, montrent que l'expert appliquait moins de forces de préhension sur les poignées de STRAS et que tant l'expert que le novice appliquaient des valeurs différentes de force de préhension aux différents points de la paume.

Conclusions

Dans le dernier chapitre de la thèse, le retour tactile a été étudié au cours de la manipulation d'un robot chirurgical avec une paire de gants développés spécialement. La conception des gants a été spécifiquement adaptée, aux poignées du système robotisé STRAS, afin de pouvoir mesurer les forces de préhension des utilisateurs. Les capteurs ont été positionnés sur les gants après des tests sur STRAS et avec l'aide et les retours des utilisateurs du système chirurgical robotisé.

Dans ce chapitre, les forces de préhension tactiles, exercées sur les poignées du robot STRAS, ont été étudiées avec un novice et un expert. Nous avons analysé comment le degré d'expertise peut faire varier les forces de préhensions appliquées au système robotique Comme cela était attendu, le novice a mis plus longtemps pour exécuter la tâche mais plus important, le novice et l'expert ont appliqué des forces de valeurs différentes aux manettes avec des régions différentes de la main. Les forces spécifiques exercées localement sur les différentes zones de la main peuvent être optimisées grâce à l'entrainement

Cette expérience a constitué une recherche préliminaire sur les forces de préhension appliquées avec le système robotisé chirurgical STRAS. Ces résultats peuvent être étudiés plus en avant, avec des tâches expérimentales différentes, un nombre de participants plus important et plus de groupes expérimentaux.

Cette technologie et les résultats de ce chapitre pourraient être efficacement exploités dans les formations en simulateur, dédiés aux interventions guidées par l'image et dans les programmes d'apprentissage aux systèmes de chirurgie assistés.

Discussion générale

Au cours du siècle dernier, des études expérimentales ont proposé des procédures permettant de contrôler les compromis vitesse précision d'un stagiaire, dans des tâches où, le temps et la précision ont une importance critique. Ces procédures visent à récompenser soit la vitesse soit la précision au cours de l'apprentissage. Cela peut être atteint en fournissant un retour d'action adéquat à l'apprenant, particulièrement, lors des premières séances d'apprentissage. Faire en sorte que l'apprenant devienne

le plus précis possible avant de chercher à être le plus rapide devrait être une priorité des formations en simulateur chirurgical. Cet objectif peut être atteint en lui donnant pour instruction, de privilégier la précision plutôt que la vitesse. La durée d'exécution se raccourcissant alors automatiquement avec l'entrainement. Une fois que le niveau de précision désiré est atteint par un apprenant, des limites de temps dans l'exécution d'une tâche peuvent être introduites et réduites progressivement, au fur et à mesure des séance d'entrainement suivantes afin de s'assurer que l'apprenant, devienne le plus rapide possible sans perdre en précision. L'objectif majeur des analyses récentes est de s'assurer que les évaluations experimentales des compétences, dans les scenari de simulateur chirurgical,ne dépendent pas de la seule observation du facteur temps. Ce qui peut être facilement le cas des procedure d'évaluation des compétences entièrement automatisées, (qui ne sont pas supervisées). Cependant, ces procédures offrent une économie de main d'œuvre et pourraient devenir la norme adoptée avec pour résultat : des stagiaires qui ne seront qui ne seront pas suivis individuellement et ne recevront aucun conseil pour optimiser leurs stratégies d'apprentissage. A la lumière des résultats rapportés ici, des apprentissages supervisés en petit groupes et en cycles d'apprentissage, avec une évaluation régulière et adaptative des compétences, comme présenté dans la Figure 119, constituent une meilleure alternative, pas nécessairement plus onéreuse. Ceci, particulièrement, dans les formations en simulateur chirurgical pour lesquelles : des standards de performance fiables sont immédiatement nécessaires. Le modèle de cycle proposé dans la Figure 119 montre également l'importance des différences de stratégie entre les sujets pendant les évaluations des performances.

Dans l'ensemble des 3 chapitres, il a été montré que les individus génèrent des préférences différentes. Dans la première étude et dans la dernière étude du premier chapitre, ainsi que, dans la quatrième étude du second chapitre, les compromis temps – précision et les préférences individuelles ont été analysés en détail. Ces différences sont reflétées par les compromis stratégiques spécifiques, entre la vitesse d'exécution de la tâche et la précision avec laquelle l'objet est placé sur les cibles. Comme attendu, ces compromis apparaissent spontanément et sans retours d'information sur la performance. Ces observations permettent de comprendre pourquoi le seul contrôle des temps d'exécution, pour une analyse de la courbe d'apprentissage, n'est pas une option acceptable. Quelques élèves peuvent devenir plus rapides mais pas forcément

meilleurs dans la réalisation de la tâche. Pourtant, dans une majorité de programmes d'entrainement sur simulateur, basés sur une analyse conditionnelle pixel par pixel de la main ou des mouvements de l'outil à partir des données d'images vidéo, la précision relative des manœuvres manuelles guidées par l'image n'est pas prise en compte dans les courbes d'apprentissage individuelles.

Conclusions

Dans cette thèse, les effets des contraintes multi sensorielles, sur le temps, la précision et la force de préhension des individus, ont été explorées pendant la réalisation de tâches complexes. Dans les études du premier chapitre, les résultats révèlent que des compromis complexes et spontanés se produisent entre le temps et la précision dans les performances individuelles, lors de l'apprentissage visuo-spatial et dans une tâche de positionnement d'objets guidée par l'image. Ces compromis reflètent des variations de stratégies cognitives qui doivent être surveillés individuellement pour assurer un apprentissage effectif des compétences. Ne collecter que les données relatives aux temps de réalisation pour établir une courbe d'apprentissage n'est pas une option acceptable car devenir plus rapide n'implique pas, directement, de devenir meilleur dans la réalisation d'une tache. Les procédures d'apprentissage devraient inclure une évaluation des compétences par des psychologues experts ainsi que des procédures pour un contrôle adaptatif des compromis vitesse-précisions, au niveau des performances réalisées par des novices. En cohérence avec des conclusions antérieures, la guidance par l'image ralentit significativement les novices et abaissent leur niveau de précision dans les opérations manuelles centrées sur objectif alors même, que les non-chirurgiens ont un score en habileté spatiale élevé. Les systèmes de visualisation 3D n'apportent pas une meilleure coordination chirurgicale œil-main dans les procédures guidées par l'image. L'effectivité relative de la technologie 3D, en ce qui concerne la précision et le chronométrage des mouvements chirurgicaux manuels, dépend du type et de la direction des mouvements de la main requis pour une intervention, de la flexibilité du système caméra générant les vues images dans les espaces cibles, positionnés dans l'espace peripersonnel du chirurgien et du niveau individuel de formation. Les interactions complexes entre la visualisation, l'utilisation d'un outil et les facteurs des stratégies individuelles ouvrent de nouvelles et

d’importantes perspectives pour un développement de la recherche sur les débutants dans la coordination œil main par image guidée.

Dans les études du second chapitre, les résultats montrent que les sujets ont été plus rapides et plus précis, en vision monde réel avec toucher direct, et qu’il n’y avait pas de différences majeures chez les participants, en termes de performances motrices, entre la réalité augmentée, la réalité mixte et la réalité virtuelle. La longueur et la largeur, l’orientation, la position, la complexité et la taille ont déterminé les temps d’exécution, la précision des mouvements de la main humaine et les mouvements des doigts le long des axes d’alignement des bords des objets. Les objets virtuels doivent être calibrés pour un suivi optimal de l’évaluation des performances individuelles dans les environnements VR et les simulateurs. Les courbes vitesse-précision individuelles devraient être surveillées dès le départ, pour optimiser la performance motrice lors des apprentissages Les sujets ont été plus précis lorsque les interactions se situaient au niveau des yeux et moins précis pour des cibles plus éloignées. La localisation optimale pour des interactions avec les régions extrêmes se situe au dessus du niveau de l’œil, ceci, pour les opérations ipsilaterales et contralaterales. La position en profondeur virtuelle des objets affecte les performances motrices, suggérant pour une interaction optimale, une position au niveau des yeux pour les cibles proches et au dessus du niveau des yeux pour les cibles plus éloignées. La dominance manuelle dans les dispositifs sans toucher est un facteur de performance discriminatif. Un retour son (audio) peut être utilisé pour améliorer la performance individuelle des individus, les fréquences moyennes C optimisent le temps d’exécution et la précision des sujets.

Dans le dernier chapitre, les résultats des études montrent une différence entre les forces haptiques appliquées par un novice et celles appliquées par un utilisateur expert. Ces différences peuvent être compensées par un entrainement sélectif en séquences de tâches spécifiques. Bien que toute la surface intérieure de la main soit en contact avec les poignées, seules certaines parties de cette surface sont utilisées pour appliquer une force sur les manettes de manœuvre. La technologie pourrait être exploitée, efficacement, dans les apprentissages en simulateur pour les interventions guidées par l’image avec outil, ainsi que, dans les programmes de formation aux systèmes chirurgicaux à assistance robotisé destinés à un nombre important d’utilisateurs et qui incluent une grande variété de tâches différentes.

D’une manière générale, les résultats de cette thèse ont exploité la manière dont le mécanisme de rétroaction sensorielle du système perceptif humain est affecté pendant la planification, le contrôle et l’exécution d’une tâche complexe. La chirurgie guidée par l’image, les simulateurs, les dispositifs de commande à distance des robots sans fils et d’autres domaines peuvent utiliser les résultats de cette étude pour leurs futures applications.

Anil Ufuk BATMAZ

Speed, precision and grip force analysis of human manual operations with and without direct visual input

Résumé

Le système perceptif d'un chirurgien doit s'adapter aux contraintes multisensorielles liées à la chirurgie guidée par l'image. Trois expériences sont conçues pour explorer ces contraintes visuelles et haptiques pour l'apprentissage guidé par l'image. Les résultats montrent que les sujets sont plus rapides et plus précis avec une vision directe. La stéréoscopie 3D n'améliore pas les performances des débutants complets. En réalité virtuelle, la variation de la longueur, largeur, position et complexité de l'objet affecte les performances motrices. La force de préhension appliquée sur un système robotique chirurgical dépend de l'expérience de l'utilisateur. En conclusion, le temps et la précision sont importants, mais la précision doit rester une priorité pour un apprenti. L'homogénéité des groupes d'étude est important pour la recherche sur la formation chirurgicale. Les résultats ont un impact direct sur le suivi des compétences individuelles pour les applications guidées par l'image.

Mots-clés:
Formation en chirurgie guidée par l'image, formation sur simulateur, guidage par l'image 2D/3D, temps et précision, rétroaction visuelle, rétroaction haptique, interactions homme-machine, réalité virtuelle, manipulation d'outils.

Résumé en anglaise

Perceptual system of a surgeon must adapt to conditions of multisensorial constrains regard to planning, control, and execution of the image-guided surgical operations. Three experimental setups are designed to explore these visual and haptic constraints in the image-guided training. Results show that subjects are faster and more precise with direct vision compared to image guidance. Stereoscopic 3D viewing does not represent a performance advantage for complete beginners. In virtual reality, variation in object length, width, position, and complexity affect the motor performance. Applied grip force on a surgical robot system depends on the user experience level. In conclusion, both time and precision matter critically, but trainee gets as precise as possible before getting faster should be a priority. Study group homogeneity and background play key role in surgical training research. The findings have direct implications for individual skill monitoring for image-guided applications.

Keywords:
Image-guided surgery training, simulator training, 2D/3D image guidance, time and precision, visual feedback, haptic feedback, human-computer interactions, virtual reality, object manipulation.